UNIVERSITY OF READING

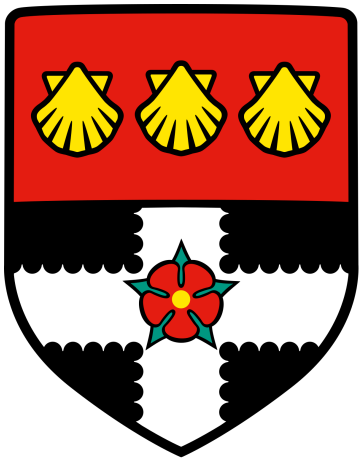

The relationship between the metabolites of the dietary flavonoid quercetin, and haemostasis and thrombosis: an integrated systems approach

A thesis submitted for the degree of Doctor of Philosophy

By Alexander Stainer

Institute for Cardiovascular and Metabolic Research

School of Biological Sciences

September 2017

Declaration

I confirm that this is my own work and the use of all material from other sources has been properly and fully acknowledged.

Signed: Alexander Stainer

Date: September 2017

Abstract

Quercetin is one of the most widely consumed flavonoids worldwide, and exerts numerous effects protective against cardiovascular disease, including the inhibition of platelet function. However, quercetin is extensively metabolised, and current data is limited regarding these metabolites. In this study, the anti-platelet effects of quercetin, and two methylated metabolites, tamarixetin and isorhamnetin, were investigated, to examine how anti-platelet efficacy is altered upon metabolism. Quercetin, tamarixetin and isorhamnetin inhibited collagen-stimulated platelet aggregation, and aggregation stimulated by ADP, thrombin and the thromboxane A_2 mimetic U46619, at physiologically achievable concentrations. Granule secretion, integrin $\alpha_{IIb}\beta_3$ activation and outside-in signalling, adhesion and spreading and calcium mobilisation were inhibited in a concentration-dependent manner; metabolism of quercetin can enhance or reduce anti-platelet effect. Due to high plasma binding, anti-platelet effects in platelet rich plasma and whole blood were investigated; significant inhibitory effects were maintained, with inhibition of clot retraction and thrombus formation under arterial flow conditions. The potential pharmacological importance of quercetin intake was investigated, with *in vitro* anti-platelet effects of novel quercetin formulations and an *in vivo* anti-thrombotic effect of an isoquercetin formulation after oral administration being demonstrated for the first time, and the identification of an interaction between the methylated metabolites and aspirin. To identify and predict important flavonoid interactions and potential inhibitory mechanisms, mathematical models of platelet aggregation and thrombus formation were developed, as was a pharmacokinetic/pharmacodynamic model of the dynamic anti-thrombotic actions of quercetin, which predicted optimal dosing regimens and highlighted the potential for increased anti-thrombotic effects upon altering quercetin metabolism. In summary, this study provided evidence for the potential of quercetin and its methylated metabolites in the inhibition of platelet function and thrombus formation, and identified interactions with aspirin, highlighting the potential of quercetin as an anti-platelet dietary compound or supplement, and identified some of the mechanisms underlying these actions.

Acknowledgements

First and foremost, I would like to express my gratitude to my supervisor Prof. Jon Gibbins for his advice and support throughout the past four years, and for giving me the opportunity to advance my career through a PhD. I truly appreciate all the help and support you have given me. Thanks also to my supervisor Dr. Marcus Tindall for all the advice regarding the mathematical modelling, and to my supervisor Prof. Julie Lovegrove for the advice and support throughout. Thanks to the BBSRC for the funding, without which this research would not have been possible.

Thank you to all the members of the laboratory for your support and expertise. Thanks to Alex Bye for the hours spent explaining proper data analysis and for discussing the best way to approach experiments, and science in general, and for the daily lunch runs and pints at the SCR. Thanks to Lisa for the laughs, and for sitting in the microscope room for hours on end staring at thrombi, and thanks to Amanda for supporting me from day one; thanks to both of you for all the cake. Thank you Paru for all the help with the mouse work, and for consistently brightening the office with your conversation and stories. Thanks to Tanya and Neline for their technical help, and thanks to Mike Fry, Francoise and Tasha for the help and support. Thanks also to previous members of the lab – Sakthi, Leo, Marilena and Mike Schenk – for your advice and technical help, and thanks to the other PhD students Gagan and Khaled for their support. Thanks to Sophie, Sarah and Jo for keeping me company in the office and providing some truly excellent humour. Also, a big thank you to all my blood donors.

A huge thank you to Luke Crumplin, without whose help and support throughout the years I may not have ended up in such a position as this, and thank you to Jack Sullivan and Stephen Venning; you three are the best friends a guy could ever ask for. Here's to many new adventures. Thanks to Simon for the Japanese exploration, and to Kat for the love and support.

Most importantly, thanks to mum and dad for absolutely everything. Without you I'd have nothing - I hope it was worth it throughout the years! Thanks to Nanny and Grampy, and to Marm and Pops; you guys were great, and I dedicate this thesis to you as well as my parents. Thanks to Auntie Cyd and Uncle Stu, and to Uncle David, Auntie Sue, Little David and Sammy. I couldn't ask for a better family. Big thanks to Max for keeping me company throughout the years, and to Musky and Mimi for doing the same. Love you all.

Publications

Manuscripts in preparation

Stainer, A.R., Sasikumar, P., Bye, A.P., Holbrook, L-M., Unsworth, A.J. & Gibbins, J.M. Quercetin and its metabolites inhibit thrombus formation *in vitro* and *in vivo*, and interact with aspirin to enhance anti-platelet effects.

Stainer, A.R., Gibbins, J.M. & Tindall, M. Mathematical modelling of the effects of quercetin and its metabolites on platelet aggregation.

Stainer, A.R., Holbrook L-M., Gibbins, J.M. & Tindall, M. A pharmacokinetic / pharmacodynamic model of the metabolism and anti-thrombotic effect of quercetin.

Published

Lovegrove, J.A., **Stainer, A.** & Hobbs, D.A. (2016). Role of flavonoids and nitrates in cardiovascular health. *Proc. Nutr. Soc.,* 1-13.

Vaiyapuri S., Sage T., Rana, R.H., Schenk, M.P., Ali, M.S., Unsworth, A.J., Jones, C.I., **Stainer, A.R.,** Kriek, N., Moraes, L.A. & Gibbins, J.M. (2015). EphB2 regulates contact-dependent and contact-independent signalling to control platelet function. *Blood,* **125**, 720-730.

Vaiyapuri, S., Roweth, H., Ali, M.S., Unsworth, A.J., **Stainer, A.R.,** Flora, G.D., Crescente, M., Jones, C.I., Moraes, L.A. & Gibbins, J.M. (2015). Pharmacological actions of nobiletin in the modulation of platelet function. *Br. J. Pharmacol.,* **172**, 4133-4145.

Ogbechi, J., Thérèse, R., Hall, B.S., Bodman-Smith, K., Vogel, M., Wu, H-L., **Stainer, A.,** Esmon, C.T., Ahnström, J., Pluschke, G. & Simmonds, R.E. (2015). Mycolactone-dependent depletion of endothelial cell thrombomodulin is strongly associated with fibrin deposition in Buruli Ulcer lesions. *PLoS Pathog.,* **11**, e1005011.

Bye, A.P., Unsworth, A.J., Vaiyapuri, S., **Stainer, A.R.,** Fry, M.J., Gibbins, J.M. (2015). Ibrutinib inhibits platelet integrin αIIbβ3 outside-in signalling and thrombus stability but not adhesion to collagen. *Arterioscler. Thromb. Vasc. Biol.,* **35**, 2326-2335.

Presentations

Poster presentation: 2nd EUPLAN (European platelet network) conference, Le Bischenberg, France, 2014. The relationship between the metabolites of the dietary flavonoid quercetin and haemostasis, thrombosis and platelet function.

Poster presentation: British Society for Cardiovascular Research (BSCR) autumn meeting, Reading, UK, 2014. The relationship between the metabolites of the dietary flavonoid quercetin, and haemostasis, thrombosis and platelet function.

Poster presentation: UK platelet meeting, Leicester, UK, 2015. A comparison of quercetin and its *in vivo* metabolites in the inhibition of platelet function.

Oral presentation: International Society on Thrombosis and Haemostasis (ISTH) Congress, Berlin, Germany, 2017. Quercetin and its metabolites inhibit platelet function and thrombus formation both *in vitro* and *in vivo*, and combine with aspirin to increase anti-platelet effects.

Oral presentation: 1st Italian-UK platelet meeting, Bath, UK, 2017. Quercetin and its metabolites inhibit platelet function and thrombus formation both *in vitro* and *in vivo*, and combine with aspirin to increase anti-platelet effects.

Abbreviations

ACD – acid citrate dextrose

ADAP – adhesion and degranulation-promoting adaptor protein

ADP – adenosine diphosphate

ANOVA – analysis of variance

ApoE – apolipoprotein E

APTT – activated partial thromboplastin time

ASA – acetylsalicylic acid / aspirin

ATP – adenosine triphosphate

AU – arbitrary units

BSA – bovine serum albumin

BTK – Bruton's tyrosine kinase

Ca^{2+} – calcium ion

$CaCl_2$ – calcium chloride

CADP – collagen plus ADP cartridge

CalDAG-GEFI – Ca^{2+} and DAG-regulated guanine nucleotide exchange factor I

CAM – cell adhesion molecule

cAMP – cyclic adenosine monophosphate

CCD – charge-coupled device

CD – cluster of differentiation

CD62P – P-selectin

CEACAM-1 – carcinoembryonic antigen cell adhesion molecule-1

CEPI – collagen plus epinephrine cartridge

cGMP – cyclic guanosine monophosphate

CHD – coronary heart disease

CHI – chalcone isomerase

CHS – chalcone synthase

CLEC-2 – C-type lectin-like receptor 2

cm^2 – square centimetre

C_{max} – maximal plasma concentration

CO_2 – carbon dioxide

CoA – coenzyme A

COMT – catechol-*O*-methyl transferase

COX - cyclooxygenase

CPR – cytochrome p450 reductase

CRP-XL – cross-linked collagen-related peptide

Csk – C-terminal Src kinase

CT – closure time

CVD – cardiovascular disease

CYP – cytochrome p450

Cy5 – cyanine 5 dye

C4H – cinnamate 4-hydroxylase

C57BL/6 – C57 Black 6 mice

DAG - diacylglycerol

DIC – disseminated intravascular coagulation

DioC6 – 3,3'-dihexyloxacarbocyanine iodide

DMSO – dimethyl sulfoxide

DNA – deoxyribonucleic acid

DTS – dense tubular system

ECM – extracellular matrix

EGTA – ethylene glycol-bis(β-aminoethyl ether)-N,N,N',N'-tetraacetic acid

eNOS – endothelial NOS

ERK – extracellular signal-regulated kinase

ESAM – endothelial cell specific adhesion molecule

FcR – Fc receptor

FITC – fluorescein isothiocyanate

FLAGG – FLavonoid AGGregation model

FLAT – FLAvonoid Thrombus model

FLS – flavonol synthase

FMO – flavonoid monooxygenase

FSC – forward scatter

Fura-2 AM – Fura-2-acetoxymethyl ester

F3H – flavanone 3-hydroxylase

g – g-force

g – grams

Gads – Grb2 related adaptor protein downstream of Shc

GDP – guanosine diphosphate

GEF – guanine nucleotide exchange factor

GP – glycoprotein

GPCR – G-protein coupled receptor

GPO – Gly-Pro-Hyp

GPRP – Gly-Pro-Arg-Pro

GSK3β - glycogen synthase kinase 3 beta

GTP – guanosine triphosphate

h – hour(s)

HCK – haematopoietic cell kinase

HDL – high density lipoprotein

HDRS – Hamilton depression rating scale

HEPES – 4-(2-hydroxyethyl)-1-piperazineethanesulfonic acid

HIV – human immunodeficiency virus

HLEC – human lens epithelial cell

HLEF – human lung embryonic fibroblast

HSA – human serum albumin

HUVEC – human umbilical vein endothelial cell

I – isorhamnetin

IC_{50} – half maximal inhibitory concentration

ID - identification

Ig – immunoglobulin

iNOS – inducible NOS

IP receptor – prostaglandin receptor

IP_3 – inositol triphosphate

IP3R – inositol triphosphate receptor

IQC950-AN – isoquercetin

Isoblend – isoquercetin plus vitamins B3 and C

ITAM – immunoreceptor tyrosine-based activation motif

ITIM – immunoreceptor tyrosine-based inhibitory motif

IV - intravenous

JAM-A – junctional adhesion molecule A

KCl – potassium chloride

K_D – dissociation constant

kg – kilogram

LAD coronary artery – left anterior descending coronary artery

LAT – linker for activation of T cells

LDL – low density lipoprotein

LD_{50} – median lethal dose

LPH – lactin-phlorizin hydrolase

LTA – light transmission aggregometry

M – molar

MAPK – mitogen-activated protein kinase

MATLAB – matrix laboratory

mg – milligram

Mg^{2+} - magnesium ion

$MgCl_2$ – magnesium chloride

mg/kg – milligrams/kilogram

Min – minute(s)

mL – millilitre

MLC – myosin light chain

mm – millimetre(s)

mmol/L – millimolar

mRNA – messenger RNA

MRP2 – multidrug resistance-associated protein 2

MRSA – methicillin-resistant *Staphylococcus aureus*

μg – microgram

μL – microliter

μM – micro-molar

NaCl – sodium chloride

$NaHCO_3$ – sodium bicarbonate

Na_2HPO_4 – disodium phosphate

NAT2 – N-acetyltransferase 2

nm – nanometre

nM - nanomolar

nNOS – neuronal NOS

NO – nitric oxide

NOAEL – no adverse effect level

NOS – nitric oxide synthase

ns – not significant

OCS – open canalicular system

ODE – ordinary differential equation

OH – hydroxyl group

Orai1 – calcium-release activated calcium modulator 1

PAL – phenylalanine ammonia-lyase

PAR – protease activated receptor

PBS – phosphate buffered saline

PD – pharmacodynamic

PDE - phosphodiesterase

PDGF – platelet derived growth factor

PDI – protein disulphide isomerase

PE – phycoerythrin

PECAM-1 – platelet endothelial cell adhesion molecule 1

PFA – paraformaldehyde / platelet function analyser

PF4 – platelet factor 4

PGI_2 - prostacyclin

PH – pleckstrin homology

PIP2 – phosphatidylinositol 4,5-bisphosphate

PIP3 – phosphatidylinositol 3,4,5-trisphosphate

PI3K – phosphoinositide 3-kinase

PK – pharmacokinetic

PKA – cAMP-dependent protein kinase

PKC – protein kinase C

PKG – cGMP-dependent protein kinase

PK/PD – pharmacokinetic/pharmacodynamic

PLC - phospholipase

PMQ – pentamethylquercetin

PPAR – peroxisome proliferator activated receptor

PRP – platelet rich plasma

PT – prothrombin time

PVDF – polyvinylidene fluoride

Q – quercetin

QB3C – QU995 plus vitamins B3 and C

QU995 – 99.5% pure quercetin aglycone

Q3G – quercetin-3-glucuronide

RBC – red blood cell

RIAM – Rap1-GTP-interacting adaptor molecule

RNA – ribonucleic acid

RPM – revolutions per minute

RR – relative risk

RXR – retinoic X receptor

s – second(s)

s^{-1} – per second (reciprocal second)

SA – salicylic acid

SDS – sodium dodecyl sulphate

SDS-PAGE – sodium dodecyl sulphate polyacrylamide gel electrophoresis

SEM – standard error of the mean

SFK – Src-family kinase

SGA – small for gestational age

sGC – soluble guanylyl cyclase

SGLT1 – sodium-dependant glucose transporter 1

SHP-1 – Src homology 2 domain-containing protein tyrosine phosphatase-1

SHP-2 – Src homology 2 domain-containing protein tyrosine phosphatase-2

SH2 – Src homology 2

SH3 – Src homology 3

SLP-76 – SH2 domain containing leukocyte protein of 76 kDa

SM proteins – Sec1/Munc proteins

SNAREs – soluble NSF attachment protein receptors

SOCE – store operated calcium entry

SSC – side scatter

STIM1 – stromal interaction molecule 1

SULTs - sulphotransferases

Syk – spleen tyrosine kinase

S1P – sphingosine 1-phosphate

T – tamarixetin / thrombin

TBS-T – Tris buffered saline with Tween 20

TGF-β - transforming growth factor β

TGX – Tris-glycine eXtended

T_{max} – time to maximal concentration

TP – thromboxane receptor

TPO - thrombopoietin

TRPC6 – transient receptor potential cation channel subfamily C member 6

tSNAREs – OCS/plasma membrane SNAREs

TULA-2 – T-cell ubiquitin ligand-2

TXA_2 – thromboxane A_2

U/mL – unit/millilitre

UGT – uridine 5'-diphosphate glucuronosyltransferase

UGTs – uridine diphosphoglucuronosyl transferases

UGT1A6 – UDP-glucuronosyltransferase 1A6

U46619 – 9,11-Dideoxy-11α,9α-epoxymethanoprostaglandin

V – volts

Veh - vehicle

vSNAREs – vesicular SNAREs

v/v – volume/volume

vWF – von Willebrand Factor

w/v – weight/volume

Y - tyrosine

^{o}C – degrees centigrade

4CL – 4-coumaroyl-CoA ligase

Table of Contents

Index of Figures

List of Tables

1 – Introduction

1.1 Platelets in haemostasis

Platelets are small, anucleate cells which are critical in the physiological process of haemostasis, first identified and functionally characterised by Schultze (1865) and Bizzozero (1882). Circulating in a resting state under normal physiological conditions, upon vessel injury, platelets adhere to extracellular matrix (ECM) proteins, such as collagen, on the vascular subendothelium. These ECM proteins are recognised by glycoprotein (GP) receptors on the platelet surface, and upon binding platelets become tethered and form a monolayer over the vessel injury, leading to the cessation of bleeding (Moroi *et al.*, 1996; Polanowska-Grabowska *et al.*, 1999; Nuyttens *et al.*, 2011). Through the binding of platelet glycoproteins to ECM proteins, tyrosine kinase signalling cascades are initiated, resulting in the mobilisation of calcium, secretion of platelet granule contents, and the activation of platelet integrins. The mobilisation of calcium is a rapid process, driving granule secretion as well as integrin activation. Platelet granule contents contain a multitude of activatory molecules, leading to the positive feedback loop of activation seen in platelets, with the activation of surrounding platelets and their incorporation into the aggregate. The activation of integrin $\alpha_{IIb}\beta_3$ is common to all of the platelet activation pathways, with activation of this platelet and megakaryocyte-specific fibrinogen receptor resulting in an increase in affinity for fibrinogen (and other ligands), fibrinogen binding and the formation of divalent cross links of fibrinogen between platelets and development of a stable platelet aggregate (Ma *et al.*, 2007; Sánchez-Cortés and Mrksich, 2009).

Platelets, in addition to their activation, aggregation and role in sealing the wound, are also involved in coagulation, leading to the development of a stable thrombus. Platelets provide a charged phospholipid surface, and procoagulant platelets, defined by sustained cytosolic calcium elevation and exposure of phosphatidylserine on the cell surface, are produced upon strong stimulation of platelets, typically with thrombin and collagen (Heemskerk *et al.*, 2002; Keuren *et al.*, 2005). These procoagulant platelets facilitate the assembly and activation of the tenase and prothrombinase complexes, resulting in the activation of coagulation factor X and prothrombin into factor Xa and

thrombin (a potent platelet agonist in itself), respectively, and platelets also provide binding sites for factor XI and prothrombin (Heemskerk *et al.*, 2002). A recent study by Podoplelova *et al.* (2016) demonstrated procoagulant 'cap' regions in platelets; in procoagulant platelets, coagulation factors were found to distribute non-homogenously, with concentrations in the cap an order of magnitude higher than the rest of the platelet. Platelets also release microparticles upon activation, which have shown extensive procoagulant activity, binding to factor VIII and factor Va, and facilitate prothrombinase complex formation (Sims *et al.*, 1988; Gilbert *et al.*, 1991). These microparticles have demonstrated procoagulant activity 50-100X greater than that of activated platelets (Sinauridze *et al.*, 2007). This involvement of platelets in the coagulation process leads to the efficient production of thrombin and subsequent cleavage of fibrinogen to fibrin, which is deposited at the vessel injury, forming a large part of the developing clot and acting to 'trap' blood cells, incorporating them into a stable thrombus, which retracts upon healing of the injury (Falati *et al.*, 2002; Ariëns, 2013).

Although platelet function is regulated by various physiological mechanisms to prevent inappropriate activation, thrombi can form in the absence of a traditional vessel injury. This process is called thrombosis, and is one of the leading causes of mortality worldwide, in both the developed and developing world (Gaziano *et al.*, 2010). Indeed, thrombosis can occur in relation to atherosclerosis (with plaque rupture being the major cause of coronary thrombosis), coronary heart disease, stroke, and even cancer, as well as through complications in pregnancy and surgery (Elyamany *et al.*, 2014; Otsuka *et al.*, 2016; Khan *et al.*, 2017). In 2014, coronary heart disease (CHD) was the single biggest cause of death in the UK (69,000 deaths), accounting for 15 and 10% of male and female deaths, respectively. A total of 155,000 deaths in 2014 were reported due to wider cardiovascular disease (CVD), with 1.7 million CVD-related episodes recorded in UK hospitals, and over 313 million prescriptions dispensed for CVD in 2014 alone (Townsend *et al.*, 2015). The pathology of thrombosis, therefore, clearly has a significant human and economic cost.

1.2 Platelet production

Platelets are produced from megakaryocytes, bone marrow cells produced from hematopoietic stem cells, through the process of thrombopoiesis. Megakaryocytes constitute approximately 0.05-0.1% of nucleated cells in the bone marrow, and are also found in the lungs and circulating in the blood (Levine *et al.*, 1993; Huang *et al.*, 2016a). It is estimated that between 10^3 and 10^4 platelets are produced per megakaryocyte (Kaufman *et al.*, 1965). The production of platelets from megakaryocytes is primarily driven by the cytokine thrombopoietin (TPO) and its megakaryocyte specific receptor, c-Mpl (de Sauvage *et al.*, 1994; Kaushansky *et al.*, 1994). Thrombopoietin stimulates endomitosis, a process in which megakaryocytes undergo cycles of DNA replication without the associated cell division, resulting in a polyploid cell; indeed, this process can result in a cell with a DNA content of up to 128n, all within a single polylobulated nucleus (Gurney *et al.*, 1994; Zimmet and Ravid, 2000; Sim *et al.*, 2016). It is thought that the purpose of endomitosis is to allow for the production of significant levels of mRNA and protein, to be included into platelets, as well as to drive formation of the invaginated membrane system, which supplies membrane for the production of proplatelets (Zimmet and Ravid, 2000; Schulze *et al.*, 2006; Machlus *et al.*, 2014). This production of proplatelets, elongated branching processes from the megakaryocyte, is hypothesised to be primarily regulated by cytoskeletal changes; Thon *et al.* (2010) demonstrated a role for microtubule based twisting forces in the elongation of proplatelets, with roles for actin also demonstrated (Patel *et al.*, 2005). Microtubules are also hypothesised to be crucial to the transport of organelles and granules into proplatelets, for incorporation into budding platelets (Richardson *et al.*, 2005). These proplatelet processes extend into bone marrow sinusoidal blood vessels, where the flow of blood results in the shearing of platelets from the proplatelet in a biophysical process (Junt *et al.*, 2007). Whilst the biomolecular processes regulating this are not fully understood, Zhang *et al.* (2012) have demonstrated a critical role for sphingosine 1-phosphate (S1P), with mice lacking its receptor exhibiting thrombocytopenia, with defective shedding of proplatelets within sinusoidal blood vessels.

The production of platelets in the lung has also been long recognised (Howell and Donahue, 1937). However, only recently has the potential significance of this been recognised. A recent study by Lefrançais *et al.* (2017) demonstrated the migration of murine bone marrow megakaryocytes into the lungs, where populations of these cells, mature and immature, as well haematopoietic progenitor cells were observed in the lung extravascular spaces. These lung megakaryocytes produced platelets at a substantial level, accounting for approximately 50% of platelet production in the mouse. Indeed, lung-resident progenitor cells were able to migrate out of the lungs and back into the bone marrow under thrombocytopenic conditions, restoring platelet counts (Lefrançais *et al.*, 2017). The lungs are thus a key site of platelet production, with the significance of this only now being recognised.

1.3 Platelet ultrastructure

Platelets are small, anucleate cells, with a diameter of between 1 and 3.5μm, and a volume of 7-10.5μm^3, with a circulating count of 150-450 x 10^9 platelets per litre (Giles, 1981; Martin *et al.*, 1982). Approximately 10^{11} platelets are produced per day, and they have a relatively short life-span; upon entering the circulation, they circulate for approximately 8-10 days before removal and clearance (Stuart *et al.*, 1975; Grozovsky *et al.*, 2015). The mechanisms underlying platelet clearance are not fully understood, but a role has been shown for the Ashwell-Morrell receptor-mediated recognition and removal of senescent, desialylated platelets in the liver, with a role for clearance linked to apoptotic signals also indicated (Mason *et al.*, 2007; Grewal *et al.*, 2008; Grozovsky *et al.*, 2015). In addition to this, the spleen, through antibody-mediated clearance, is a major site of platelet clearance (Kaplan and Saba, 1978; Grozovsky *et al.,* 2010). Auto-antibodies directed against platelet membrane glycoproteins are produced in the spleen, and upon binding to glycoproteins, platelets coated with immunoglobulin G (IgG) are recognised and phagocytosed by spleen-resident macrophages; the importance of this mechanism is demonstrated by the high antibody concentrations found in the spleen (Sandler, 2000; Crow and Lazarus, 2003; Chan *et al.,* 2003). Indeed, splenectomy results in the restoration of platelet count in most immune thrombocytopenia patients, further highlighting the importance of the spleen in platelet clearance (Kühne *et. al.,* 2007).

The platelet plasma membrane contains a multitude of cell surface receptors critical to their activation and aggregation. These include adhesion receptors, G-protein coupled receptors, and integrins, discussed in more detail in Section 1.4. The platelet plasma membrane is structurally supported by an intricate cytoskeleton (Shin *et al.*, 2017), seen in Figure 1-1. Composed primarily of microtubules and actin filaments (as well as spectrin networks), this cytoskeleton is crucial in the maintenance of their characteristic, resting discoid shape; upon activation, this cytoskeletal network is dynamically rearranged through depolymerisation, reorganisation and polymerisation, resulting in the shape change observed upon platelet activation (Hartwig, 1992; Kaushansky *et al.*, 2015; Sandmann and

Koster, 2016). As described by Behnke (1967), platelets contain two membrane channel structures; the open canalicular system (OCS) and the dense tubular system (DTS) (Figure 1-1). The open canalicular system is comprised of plasma membrane invaginations which act as a site of platelet granule release, as well as a site of substance entry into the platelet (Escolar and White, 1991; Fogelson and Wang, 1996). The dense tubular system is a series of channels derived from megakaryocyte smooth endoplasmic reticulum, with wide distribution throughout the platelet (White, 1972). Quiescent platelets actively sequester calcium ions (Ca^{2+}) in the dense tubular system, and upon activation, calcium is rapidly released; this mobilisation of calcium leads to rapid rises in cytoplasmic Ca^{2+} levels which is vital for further activation, discussed in Section 1.4.3.2 (Gerrard *et al.*, 1978; Ware *et al.*, 1986; Ebbeling *et al.*, 1992). ATPases are also stored in the DTS, which are important for adenylate cyclase activity involved in the regulation of GPCR downstream signalling (Cutler *et al.*, 1978).

Found within the platelet are numerous secretory granules, defined by their contents and ultrastructure; α-granules, dense granules, and lysosomes (Figure 1-1). Alpha granules appear as spherical granules, approximately 200-500nm in diameter, and are the primary secretory granule within the platelet, with 40-80 per platelet (Italiano and Battinelli, 2009). They contain a multitude of molecules crucial to platelet adhesion and aggregation; proteins such as von Willebrand Factor (vWF), fibronectin, fibrinogen and coagulation factors, growth factors such as transforming growth factor β (TGF-β) and platelet derived growth factor (PDGF) and chemokines including platelet factor 4 (PF4) (Stenberg *et al.*, 1984; Harrison and Cramer, 1993; Maynard *et al.*, 2007). They also contain several transmembrane receptors such as integrin $\alpha_{IIb}\beta_3$, PECAM-1, and GPIb-V-IX complex, the levels of which therefore increase on the cell surface upon activation (Cramer *et al.*, 1994; Berger *et al.*, 1996). There is evidence that α-granules may be divided into different types, each containing different cargo. Italiano *et al.* (2008) demonstrated the presence of different subtypes of α-granules, containing pro and anti-angiogenic products; these were differentially secreted by platelets. This is supported by Sehgal and Storrie (2007), who observed differential packaging and release of fibrinogen and vWF in α-granules.

Dense granules, of which there are only 3-5 per platelet, contain lower molecular weight components key to the regulation of the activation process, including ADP, ATP, Mg^{2+}, Ca^{2+} and serotonin (Gear and Burke, 1982; Meyers *et al.*, 1982; Jonnalagadda *et al.*, 2012; Golebiewska and Poole, 2015). Upon platelet activation, α-granules and dense granules secrete their contents through the open canalicular system (α- and dense granules are differentially released), or through the surface (non-OCS) plasma membrane, whereupon these contents act to further stimulate and activate platelets, be it the same platelet (autocrine) or surrounding platelets (paracrine), leading to the positive feedback activatory loop characteristic of platelets (Goggs *et al.*, 2013; Golebiewska and Poole, 2015). This granule secretion process is discussed in Section 1.4.3.1. Significantly less work has focused on platelet lysosomes, which are defined by their acidic nature and the presence of contents such as acid hydrolases, and are also released *in vivo* upon platelet activation (Ciferri *et al.*, 2000; Polasek, 2005). Platelets also contain glycogen particles, serving as a crucial energy source, and mitochondria, for energy generation, with other suggested roles for platelet mitochondria in pro-thrombotic redox signalling and in apoptosis; a diagram of platelet ultrastructure is presented in Figure 1-1(Zharikov and Shiva, 2013; Rocha *et al.*, 2014).

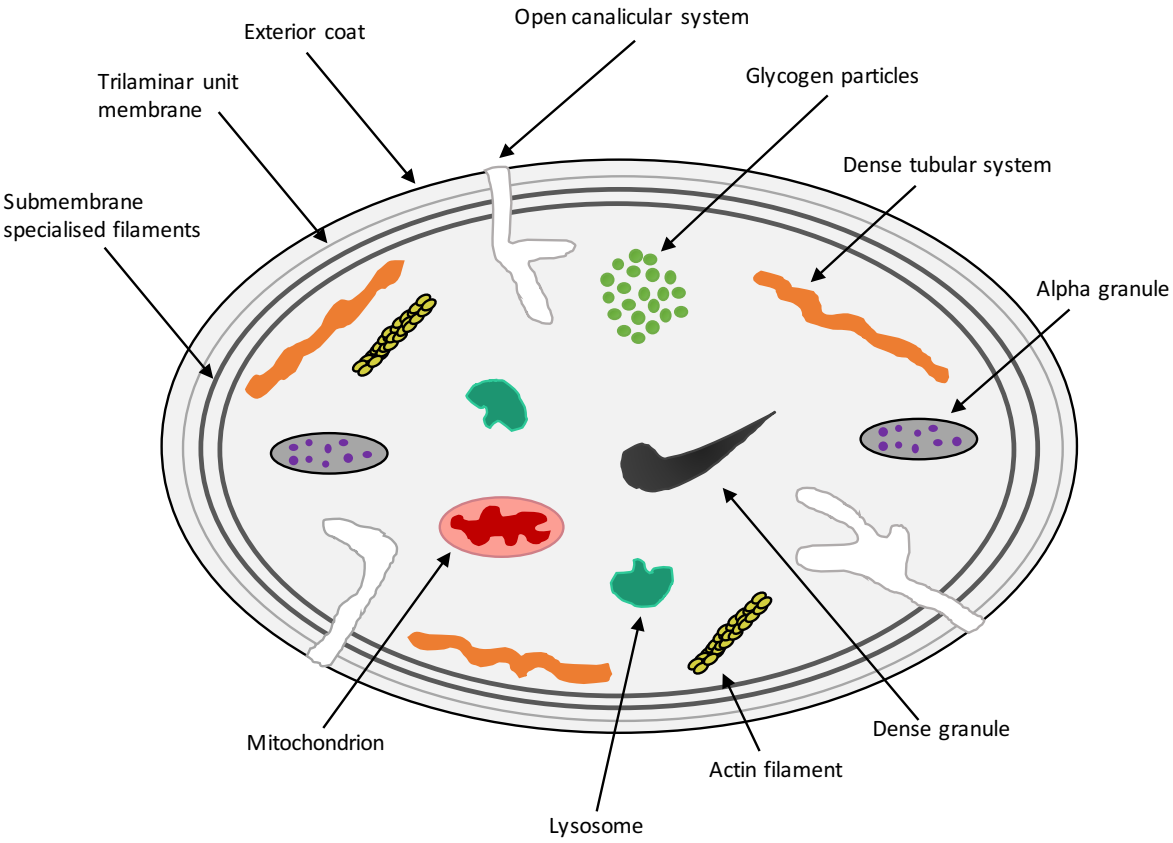

Figure 1-1 Human platelet ultrastructure

The external membranes of a platelet are comprised of an external glycoprotein coat, with a trilaminar unit membrane as well as specialised filaments such as actin in the submembrane area, forming the wall of the platelet. The external membranes, with the band of microtubules and microfilaments around the circumference of the platelet, are key to maintaining the resting platelet shape, as well as driving the shape change initiated by platelet activation. The open canalicular system (OCS) and the dense tubular system (DTS) are membrane systems, with the OCS acting as a site of platelet granule release and substance entry into the platelet, and the DTS having roles as a store of calcium (with associated release into the cytosol) and ATPases, amongst other substances. Platelets contain α and dense granules as well as lysosomes, all released upon activation, as well as glycogen particles as an energy source and mitochondria for energy generation.

1.4 The role of platelets upon vascular injury

1.4.1 Platelet activation: platelet-collagen interactions

As stated previously, upon vessel injury, the blood becomes exposed to subendothelial extracellular matrix proteins. One such protein is collagen, considered to be the most thrombogenic of these ECM proteins (Baumgartner and Haudenschild, 1972). There are 28 types of collagen in the collagen family, each containing one or more triple helical domain; types I, II, III, IV, V, VI, VIII, XII, XIII and XIV are found in human blood vessel walls (Barnes and Farndale, 1999; Ricard-Blum, 2011). Upon damage to the vessel wall, platelets adhere and spread on this exposed collagen to prevent blood loss from the vessel. This initial response to vascular injury is largely mediated through the interactions between platelet glycoprotein (GP)Ib-V-IX complex and integrin α2β1 with ECM collagen (Cole *et al.*, 2003; Nuyttens *et al.*, 2011). Initial tethering of platelets to the exposed ECM occurs through collagen-vWF-GPIb-V-IX interactions. Upon vessel injury, von Willebrand Factor is released from Wiebel Palade bodies (and is also present in α-granules) in endothelial cells (as well as through a constitutive secretory mechanism), and adheres to exposed subendothelial collagen though its A3 domain (Jaffe *et al.*, 1974; Alevriadou *et al.*, 1993; Peyvandi *et al.*, 2011). This now immobilised vWF binds the platelet GPIb-V-IX complex through its A1 domain; through this interaction, platelets are slowed and roll along the injured vessel wall, facilitating the direct interaction between collagen and glycoprotein VI (GPVI), as well as integrin α2β1, supporting firm platelet adhesion (Emsley *et al.*, 1998; Knight *et al.*, 1999; Cole *et al.*, 2003). This leads to the stimulation of intracellular tyrosine kinase signalling, resulting in platelet calcium mobilisation, granule secretion, integrin $\alpha_{IIb}\beta_3$ activation and the formation of a platelet aggregate. Whilst tyrosine kinase signalling associated with GPIb-V-IX and integrin α2β1 has been demonstrated, it is the signalling through GPVI that is the major contributor, resulting in full platelet activation and aggregation (Gibbins *et al.*, 1997; Wu *et al.*, 2003; Inoue *et al.*, 2003).

1.4.1.1 GPIb-V-IX complex

The platelet glycoprotein Ib-V-IX receptor is the receptor involved in initial contact between platelets and the extracellular matrix upon vessel wall injury. Expressed only in platelets and megakaryocytes, the GPIb-V-IX complex contains four transmembrane subunits; GPIbα, GPIbβ, GPV and GPIX (Luo *et al.*, 2007). It is an abundant complex, with approximately 25,000 copies of GPIbα per platelet (Du *et al.*, 1987). The extracellular portion (N terminal) of GPIbα contains binding sites for many substances, primarily vWF, but including thrombin, P-Selectin and coagulation factor XII (Berndt *et al.*, 2001). The cytoplasmic tail (C terminal) comprises 96 amino acids, with binding sites for associated proteins including 14-3-3ζ (Feng *et al.*, 2000).

As stated previously, the primary function of the GPIb-V-IX complex involves the initial tethering of platelets to the exposed ECM collagen through its interaction with vWF. The vWF thus acts as a bridge between collagen and GPIb-V-IX, with this transient interaction causing platelets to roll on the exposed ECM, leading to the formation of more stable interactions (Emsley *et al.*, 1998; Savage *et al.*, 2002). Gitz *et al.* (2013) demonstrated glycoprotein Ibα clustering upon platelet adhesion to vWF at an arterial shear rate; this clustering was associated with improved platelet-vWF interactions, with the interaction strengthened under the unique shear conditions of flowing blood. Interestingly, this clustering process required the translocation of GPIbα to lipid rafts, and was dependent on 14-3-3ζ binding to its cytoplasmic tail (Gitz *et al.*, 2013). Overall, however, the GPIb-V-IX interaction with vWF and associated collagen is not sufficient for the stable adhesion of platelets, with the rapid dissociation rate instead resulting in platelet rolling, a process which has been observed *in vitro* by Savage *et al.* (2002); this supports the formation of more stable interactions with integrin α2β1, and signalling through binding of collagen to GPVI (Gibbins *et al.*, 1997; Nuyttens *et al.*, 2011). The GPIb-V-IX complex also binds other substances, including thrombspondin-1, which Jurk *et al.* (2003) demonstrated resulted in firm adhesion via a vWF-independent mechanism, and α-thrombin, which

upon binding to GPIbα, results in accelerated cleavage of the thrombin receptor PAR-1 (De Candia *et al.*, 2001).

Whilst the above physical interaction between vWF and the GPIb-V-IX complex is of primary importance in platelet recruitment to the site of vessel injury, evidence suggests that this complex can also stimulate tyrosine kinase signalling (Wu *et al.*, 2001). Upon binding of vWF, the GPIb-V-IX complex becomes increasingly localised in lipid rafts; the importance of this association was demonstrated by Shrimpton *et al.* (2002), who observed that upon depletion of platelet lipid rafts, the GPIb-V-IX dependent adhesion of platelets to a vWF surface was inhibited, as was vWF-stimulated aggregation under static and shear conditions. Upon localisation to lipid rafts, binding of VWF to the complex results in tyrosine phosphorylation of the Fc Receptor (FcR) γ-chain and adaptor molecule ADAP (adhesion and degranulation-promoting adaptor protein), in a Src kinase-dependent manner; this in turn leads to calcium mobilisation, phosphatidylinositol 3-kinase (PI3K) and protein kinase C (PKC) activity, ultimately leading to the activation of integrin $\alpha_{IIb}\beta_3$ (Falati *et al.*, 1999; Kasirer-Friede *et al.*, 2004). Upon stimulation with vWF and botrocetin (which enhances vWF affinity for GPIbα), Wu *et al.* (2001) also observed phosphorylation of FcRγ-chain (complexed with Src and Lyn), with downstream activation of spleen tyrosine kinase (Syk), linker for activation of T cells (LAT) and phospholipase Cγ2 (PLCγ2)(Fukuda *et al.*, 2005). Stimulation of FcRγ-chain deficient platelets with vWF plus botrocetin in this study demonstrated its role in this signalling cascade linked to the GPIb-V-IX complex, with an impairment in aggregation also observed (Wu *et al.*, 2001). The similarities between this signalling cascade and that downstream of GPVI upon collagen stimulation (discussed later) must be noted; indeed, Arthur *et al.* (2005) demonstrated an association of the GPIb-V-IX complex and GPVI via an interaction between the GPIbα and GPVI ectodomains. There may therefore be cross-talk between the platelet responses regulated by these two receptors, with further studies needed to elucidate this. The GPIbα cytoplasmic tail also associates with 14-3-3ζ, calmodulin and filamin, opening potential links to other signalling pathways; the pathways downstream of GPIb-V-IX have not been fully defined and elucidated, and further work is required to understand the full

contribution of this signalling to platelet activation and aggregation (Feng *et al.*, 2000; Andrews *et al.*, 2001; Williamson *et al.*, 2002).

1.4.1.2 Integrin α2β1

Integrins are a family of large transmembrane adhesion receptors, and are heterodimers comprised of non-covalently associated α and β subunits. Whilst most of the receptor extends into the extracellular region, there is a single pass transmembrane domain, with both subunits ending in short cytoplasmic domains (Campbell and Humphries, 2011). This structure allows for the interaction of integrins with extracellular matrix components as well as cytosolic proteins, with either interaction capable of initiating signalling events (Shattil and Newman, 2004). There are 18 integrin α subunits and 8 β subunits in humans; in platelets, α_{IIb}, α_v, α_2, α_5 and α_6 are the identified α subunits, and β_1 and β_3 are the identified β subunits (Ginsberg *et al.*, 1993). Integrin α2β1 is a collagen receptor in platelets, and integrin $\alpha_{IIb}\beta_3$ is a fibrinogen receptor; both are of critical importance to the platelet activation and aggregation process.

Integrin α2β1 was the first collagen receptor identified in platelets (Kunicki *et al.*, 1988). There are 2000-4000 copies per platelet, and it is able to bind collagen types I, II, III, IV and XI (Varga-Szabo *et al.*, 2008; Nuyttens *et al.*, 2011). Collagen binding occurs at the α2 subunit through binding to the I domain in a Mg^{2+}-dependent fashion, with a conformational change in the domain associated with collagen-binding (Jokinen *et al.*, 2004). Integrin α2β1 binds collagen through high affinity interactions with GFOGER sequences, with binding to other G*XX'*GER sequences also occurring with a lower affinity (Emsley *et al.*, 2000; Siljander *et al.*, 2004; Munnix *et al.*, 2008).

Upon GPVI signalling (discussed next), integrin α2β1 undergoes 'inside-out' signalling, resulting in a rapid conformational change of the extracellular domains from a bent, closed conformation to an open conformation in which the extracellular domains extend upwards and outwards (Nuyttens *et al.*, 2011). This 'open' state of the integrin then readily binds collagen through the aforementioned sequences, resulting in firm platelet adhesion and strengthening the physical bond of the platelet to the exposed ECM of the injured vessel wall. Whilst the GPIb-V-IX complex:vWF interaction is

critical under high shear conditions, integrin α2β1-collagen interactions are important under intermediate to low shear conditions (Farndale *et al.*, 2007). Indeed, there is evidence suggesting that the interaction of vWF with the GPIb-V-IX can mediate the conformation change and activation of integrin α2β1 independent of GPVI signalling (Cruz *et al.*, 2005). In addition to this, there is also evidence that high affinity binding of the integrin to collagen GFOGER motifs can occur when integrin α2β1 is in its resting state; it is hypothesised by Farndale *et al.* (2007) that this may lead to collagen:GPVI binding and subsequent increased affinity of integrin α2β1 for collagen.

As well as supporting firm physical adhesion of the platelet to the ECM of the injured vessel wall, there is evidence that integrin α2β1 undergoes 'outside-in' tyrosine kinase signalling. Interaction of α2β1 with collagen stimulates the tyrosine phosphorylation of Src, Syk, SLP-76 and PLCγ2, leading to the formation of filopodia and lamellipodia upon adhesion to collagen; this occurred in the absence of the GPVI-FcRγ-chain complex, specifically indicating α2β1 in this process (Inoue *et al.*, 2003). This activation of PLCγ downstream of α2β1 leads to the activation of integrin $\alpha_{IIb}\beta_3$, through two independent pathways; a Src-kinase dependent pathway and a Rac GTPase-mediated pathway (Guidetti *et al.*, 2009). There is therefore significant evidence of a role of integrin α2β1 in tyrosine kinase signalling; interesting to note here is the similarity of the signalling proteins involved with that of the GPVI-mediated pathway of platelet activation. Indeed, this sharing of signalling molecules (also shared to a degree with GPIb-V-IX dependent signalling) is hypothesised to constitute a cooperative interaction, with signalling through one pathway reinforcing the others (Farndale *et al.*, 2007).

The importance of integrin α2β1 to the platelet activatory process is demonstrated by the observation that, in β1 deficient platelets, GPVI signalling is diminished, with looser thrombi forming upon flow of blood over collagen coated surfaces, with increased embolism also observed (Kuijpers *et al.*, 2003). α2β1 deficient platelets also displayed delayed and inhibited collagen-stimulated aggregation, as well as a lack of adhesion to collagen under static and flowing conditions (Chen *et al.*, 2002).

1.4.1.3 GPVI

GPVI is a platelet and megakaryocyte specific 62kDa type I transmembrane collagen receptor belonging to the immunoglobulin (Ig) superfamily (Clemetson *et al.*, 1999; Moroi *et al.*, 1996). It contains two Ig-like extracellular domains, with a mucin-like stalk and a transmembrane region terminating in a cytoplasmic tail 51 amino acids in length, with approximately 3000-6000 copies per platelet (Nieswandt and Watson, 2003; Dütting *et al.*, 2012; Ozaki *et al.*, 2013). GPVI binds collagen through recognition of specific Gly-Pro-Hyp (GPO) sequences (Munnix *et al.*, 2008). The transmembrane region of GPVI contains a positively charged arginine that allows non-covalent association with FcRγ-chain; one GPVI receptor is associated with one FcRγ-chain dimer (Gibbins *et al.*, 1997; Nieswandt and Watson, 2003). These FcRγ-chains contain an immunoreceptor tyrosine-based activation motif, or ITAM, which is responsible for signal transduction after collagen binding to GPVI (Gibbins *et al.*, 1997). Platelet activation upon collagen binding to GPVI results in strong platelet activation, leading to calcium mobilisation, granule secretion and integrin activation; the strength of this activation is demonstrated by the GPVI-specific ligand, collagen related peptide (cross-linked, CRP-XL), which potently activates and aggregates platelets (Smethurst *et al.*, 2007; Dütting *et al.*, 2012).

Protein kinase signalling is heavily involved in platelet function, with particularly strong roles downstream of collagen:GPVI binding; kinases phosphorylate target proteins through the transfer of a phosphoryl group from ATP (which binds to the ATP-binding site) to specific amino acids (tyrosine or serine/threonine) with a free hydroxyl group on the target protein, occurring in the kinase active site (Krebs and Beavo, 1979; Knighton *et al.,* 1991; Wang and Cole, 2014). This leads to activation of the substrate, for example via conformational changes allowing substrate access to the active site, or the alignment of critical catalytic residues (Cheng *et. al.,* 2011). Due to their critical involvement in platelet activation, these kinases are tightly regulated, with associated activator and inhibitor proteins, and regulation via phosphatases (Millward *et al.,* 1999).

The Src kinases Fyn and Lyn bind, through their Src homology 3 (SH3) domain, to a proline-rich region on the cytosolic tail of GPVI (Ezumi *et al.*, 1998). Upon binding of collagen to GPVI, crosslinking of the receptor occurs, bringing the GPVI-associated Fyn and Lyn into contact with the FcRγ-chain; the ITAM region of FcRγ-chain is then phosphorylated by these kinases (Ezumi *et al.*, 1998; Quek *et al.*, 2000)(Figure 1-2). Fyn and Lyn are held in an inactive conformation, and upon platelet activation, are converted into their active confirmation via the dephosphorylation of an inhibitory tyrosine residue by the protein tyrosine phosphatase CD148 (Senis *et al.*, 2009).

The phosphorylation of the FcRγ-chain ITAM results in the binding of Syk via its Src Homology 2 (SH2) domains, which is subsequently autophosphorylated and phosphorylated by Src kinases (Gibbins *et al.*, 1997; Grucza *et al.*, 1999; Watson *et al.*, 2005). This phosphorylation of Syk has recently shown to be regulated by the protein phosphatase TULA-2 (T-cell ubiquitin ligand-2) via dephosphorylation of tyrosine 346, which may act to prevent aberrant activation (Dunster *et al.*, 2015; Reppschlager *et al.*, 2016). Syk proceeds to phosphorylate linker for activation of T cells (LAT), which leads to the formation of a signalosome structure composed of adaptor and effector proteins, bringing the effectors of downstream signalling into contact with their substrates (Pasquet *et al.*, 1999a; Judd *et al.*, 2002) (Figure 1-2). Two such adaptor proteins key to the activatory process are Gads (Grb2 related adaptor protein downstream of Shc), and SLP-76 (SH2-domain containing leukocyte protein of 76kDa), which are crucial in the downstream recruitment and activation of phospholipase Cγ2 (PLCγ2) (Gross *et al.*, 1999; Asazuma *et al.*, 2000; Leo *et al.*, 2002; Hughes *et al.*, 2008). The guanine nucleotide exchange factors Vav1 and Vav3 are also recruited to the LAT signalosome; their functional role is less clear, but it has been observed that Vav1+Vav3 deficient platelets displayed a substantial reduction in collagen-stimulated PLCγ2 phosphorylation (Pearce *et al.*, 2004).

The LAT signalosome also recruits phosphatidylinositol 3-kinase (PI3K), resulting in the PI3K-mediated conversion of phosphatidylinositol-4,5-bisphosphate (PIP2) to phosphatidylinositol-3,4,5-

trisphosphate (PIP3) (Pasquet *et al.*, 1999b; Gilio *et al.*, 2009). Through interaction with their pleckstrin homology (PH) domains, PIP3 facilitates the recruitment of PLCγ2 and Tec family kinases, key activatory proteins of this cascade, to the plasma membrane; this leads to the Tec and Bruton's tyrosine kinase (BTK)-mediated phosphorylation of PLCγ2 (Quek *et al.*, 1998; Pasquet *et al.*, 1999b; Atkinson *et al.*, 2003) (Figure 1-2). Activated PLCγ2 cleaves PIP2 into inositol-1,4,5-trisposphate (IP_3) and diacylglycerol (DAG). This IP_3 binds IP_3 receptor and stimulates the mobilisation of calcium from intracellular stores (in the dense tubular system), whilst DAG activates protein kinase C (PKC) (Brass and Joseph, 1985; Daniel *et al.*, 1994; Nakashima *et al.*, 1997). Both calcium mobilisation and protein kinase C activation leads to platelet granule release and the alteration of integrin $\alpha_{IIb}\beta_3$ to its active, 'open' conformation, leading to platelet activation and aggregation (Shattil and Brass, 1987; Yacoub *et al.*, 2006; Konopatskaya *et al.*, 2011)(Figure 1-2). A diagram of tyrosine kinase signalling stimulated by collagen binding to GPVI is presented in Figure 1-2.

Figure 1-2 The GPVI signalling pathway of platelet activation

The binding of collagen to GPVI results in receptor clustering, and tyrosine phosphorylation of the Fc Receptor (FcR) γ-chain by Fyn and Lyn, two Src family kinases. This causes spleen tyrosine kinase (Syk) to bind and become phosphorylated. Syk then phosphorylates the transmembrane adaptor protein linker for activation of T cells (LAT), causing the formation of the LAT signalosome, with the assembly of Gads (Grb2 related adaptor protein downstream of Shc), SLP-76 and Vav. Recruitment of phosphatidylinositol 3-kinase (PI3K) to the signalosome results in the conversion of phosphatidylinositol-4,5-bisphosphate (PIP2) to phosphatidylinositol-3,4,5-trisphosphate (PIP3). Tec kinase and BTK interact with this PIP3 via their pleckstrin homology (PH) domains, facilitating recruitment and phosphorylation of phospholipase Cγ2 (PLCγ2). The activated PLCγ cleaves PIP2 into inositol-1,4,5-trisphosphate (IP_3) and diacylglycerol (DAG), with IP_3 stimulating intracellular calcium mobilisation and DAG activating protein kinase C (PKC), leading to platelet granule release, integrin αIIbβ3 activation and ultimately, platelet aggregation.

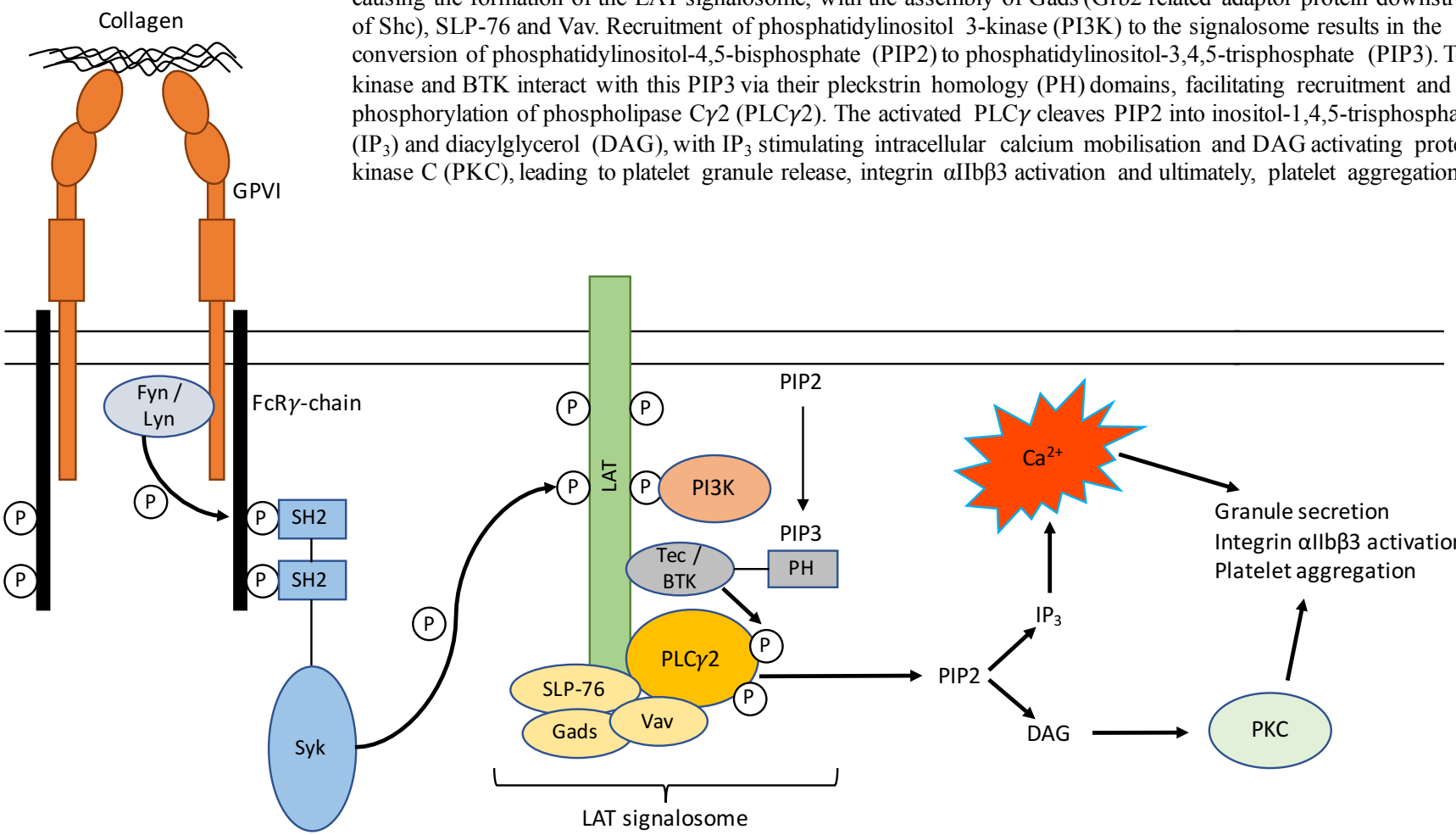

1.4.2 G-protein coupled receptor mediated platelet activation

As mentioned above, the activation of platelets through collagen binding to GPVI results in the secretion of platelet granules; these granules contain numerous soluble agonists that act to drive the activatory process forward, leading to aggregate and thrombus formation. Such soluble agonists include adenosine diphosphate (ADP), thrombin, thromboxane A2 and epinephrine. These soluble agonists stimulate platelet activation via binding to G-protein coupled receptors, or GPCRs.

GPCRs are a large family of membrane receptors; over 800 have been identified in the human genome (Fredriksson and Schiöth, 2005). They comprise an extracellular N-terminus, seven transmembrane domains, and an intracellular C-terminus. Ligand binding occurs at the N-terminus, with the extracellular and transmembrane domains also forming binding pockets for some ligands (Dohlman *et al.*, 1987; Lerner *et al.*, 1996; Verrall *et al.*, 1997). Upon the binding of agonist to GPCRs, conformational changes occur in the transmembrane and intracellular segments, resulting in the interaction with, and activation of, G proteins. G proteins are heterotrimeric proteins consisting of Gα, Gβ and Gγ subunits, and in their resting, inactive state, guanosine diphosphate (GDP) is bound to the α subunit. Upon activation, this GDP is released, and replaced by guanosine triphosphate (GTP), leading to the dissociation of the activated Gα subunit from the Gβγ dimer (Sondek *et al.*, 1996; Oldham and Hamm, 2008). These subunits then transduce intracellular signals leading to platelet activation through numerous mechanisms. Upon hydrolysis of Gα-bound GTP to GDP, the Gα subunit re-associates with Gβγ, and the trimeric G protein re-associates with the GPCR (Kleuss *et al.*, 1994). Figure 1-3 shows an overview of activatory platelet GPCR signalling.

1.4.2.1 Thrombin

Thrombin is a serine protease, generated in the intrinsic pathway of coagulation through conversion of the zymogen prothrombin by Factor Xa (Esmon and Jackson, 1974; Krishnaswamy, 2013). As discussed in Section 1.1, thrombin acts to cleave fibrinogen into fibrin monomers; these polymerise at the vessel injury site, trapping passing blood cells into the developing clot, and leading to the development of a stable, fibrin-rich clot (Heemskerk *et al.*, 2002). As well as its well-established role in the coagulation cascade, thrombin is one of the most potent platelet agonists, inducing calcium mobilisation, granule secretion and aggregation, and prothrombin is contained within platelet α-granules (McNicol and Gerrard, 1993; Chen *et al.*, 2004; Maynard *et al.*, 2007).

On the platelet surface, thrombin binds to the protease activated receptor (PAR) GPCRs (Figure 1-3). There are two PAR receptor isoforms on human platelets: PAR1 and PAR4 (Vu *et al.*, 1991; Xu *et al.*, 1998; Kahn *et al.*, 1999). PAR1 is a higher affinity receptor for thrombin, with approximately 1500-2500 copies per platelet, with PAR4 contributing to the activatory process at higher thrombin concentrations (Kahn *et al.*, 1999; Quinn *et al.*, 2007). It has been demonstrated that PAR1 and PAR4 form heterodimers, enhancing thrombin-stimulated signalling and activation (Leger *et al.*, 2006). PAR1 and PAR4 are coupled to $G\alpha_q$ and $G\alpha_{12/13}$ (Figure 1-3)(Offermanns *et al.*, 1994; Coughlin, 2000). Thrombin does not bind to PAR1/4 in a typical receptor-ligand manner; instead, thrombin acts to cleave the extracellular N-terminus of the receptor, which serves to unmask a new N-terminal sequence. This new N-terminal sequence acts as a tethered ligand, binding to the receptor's second extracellular loop; this binding results in the activation of $G\alpha_q$ and $G\alpha_{13}$ subunits of the receptor-associated G proteins (Vu *et al.*, 1991; Nanevicz *et al.*, 1995). $G\alpha_q$ subunits activate phospholipase C β isoforms – this leads to the PLCβ-mediated cleavage of PIP2 into IP3 and DAG, leading to the release of Ca^{2+} from intracellular stores and the activation of PKC, respectively (Brass and Joseph, 1985; Rhee, 2001; Lian *et al.*, 2005). This Ca^{2+} mobilisation and PKC activation results in granule secretion and the activation of integrin $\alpha_{IIb}\beta_3$, leading to further platelet activation and aggregation

(Figure 1-3)(Shattil and Brass, 1987; Yacoub *et al.*, 2006; Konopatskaya *et al.*, 2011). This demonstrates well the positive feedback activatory mechanisms associated with platelets; upon stimulation with collagen, platelets secrete their granule contents, including prothrombin, which is converted to thrombin and serves to further activate the platelet (as well as surrounding platelets). PARs are also coupled to $G\alpha_{12/13}$, with $G\alpha_{13}$ demonstrating a distinct functional role (Offermanns *et al.*, 1994; Li *et al.*, 2010). $G\alpha_{13}$ activates guanine nucleotide exchange factors (GEFs) for RhoA; RhoA releases GDP and binds GTP and becomes activated (Kozasa *et al.*, 1998). This activated RhoA subsequently activates Rho kinase, leading to the phosphorylation and inhibition of myosin light chain (MLC) phosphatase. MLC phosphorylation thereby increases, resulting in an increase in MLC-dependent contraction, platelet shape change and granule secretion (Figure 1-3)(Klages *et al.*, 1999). It was historically thought that PAR1 may also be coupled to $G\alpha_i$; it has been demonstrated, however, that thrombin-stimulated reductions in cyclic adenosine monophosphate (cAMP) concentrations are a result of signalling through ADP released as a result of thrombin-stimulation (Jantzen *et al.*, 2001; Kim *et al.*, 2002).

The importance of PAR receptors in the overall platelet activatory response is demonstrated by the phenotype of mice deficient in PAR4. PAR4 knockout mice demonstrated a significantly extended tail bleeding time, with a complete lack of aggregatory response to thrombin. The same mice were protected against thrombosis in a thromboplastin-induced model of pulmonary embolism (Hamilton *et al.*, 2004). Single nucleotide polymorphisms of PAR4 have been identified in humans that correlate to differential platelet reactivity, offering evidence for a role for altered thrombin/PAR4 signalling in the heritable variation in inter-individual platelet reactivity, which has been identified as a genetic risk factor for CVD (Bray *et al.*, 2007; Edelstein *et al.*, 2013; Edelstein *et al.*, 2014).

1.4.2.2 ADP

Adenosine diphosphate was recognised as a platelet agonist in 1961 by Gaarder *et al.* (1961), who observed ADP in red blood cells as a molecule that could influence the adhesiveness of platelets. This was built upon in 1962 by work from Born (1962), who observed ADP could stimulate platelet aggregation. In addition to red blood cells, platelet dense granules are a store of ADP, which upon platelet activation, is secreted and acts in an autocrine and paracrine fashion to drive a secondary wave of platelet activation (D'Souza and Glueck, 1977; Fogelson and Wang, 1996).

There are two purinergic G-protein coupled receptors for ADP on the platelet; P2Y1 and P2Y12; P2Y1 couples to $G\alpha_q$, whilst P2Y12 is coupled to $G\alpha_i$ (Figure 1-3)(Ohlmann *et al.*, 1995; Jin *et al.*, 1998; Hollopeter *et al.*, 2001). ADP binding to P2Y1 causes dissociation of the G-protein into α and $\beta\gamma$ dimer subunits and activation of the $G\alpha_q$ subunit. This activated $G\alpha_q$ subunit, as described in the previous section, activates PLCβ, which acts to cleave PIP2 into IP_3 and DAG, with the downstream mobilisation of Ca^{2+} and activation of PKC and associated activation of integrin $\alpha_{IIb}\beta_3$ (Brass and Joseph, 1985; Rhee, 2001; Lian *et al.*, 2005). ADP binding to P2Y12 causes activation of the $G\alpha_i$ subunit; signalling through this subunit occurs via the inhibition of the enzyme adenylyl cyclase (Taussig *et al.*, 1993; Yang *et al.*, 2002). This enzyme produces cyclic adenosine monophosphate (cAMP) from adenosine triphosphate (ATP), which activates cAMP-dependent protein kinase (PKA); PKA phosphorylates a broad range of substrates, resulting in their inactivation and subsequent inhibition of Ca^{2+} mobilisation, granule release and aggregation (Figure 1-3) (Smolenski, 2012; Subramanian *et al.*, 2013; Beck *et al.*, 2014). The inhibition of adenylyl cyclase by activated $G\alpha_i$ subunits results in the inhibition of this inhibitory pathway, aiding in platelet activation. Signalling through P2Y12 also occurs through the dissociated $\beta\gamma$ dimer, which can also interact with adenylyl cyclase, as well as regulate the activation of PI3K β/γ isoforms (Leopoldt *et al.*, 1998; Garcia *et al.*, 2010). The activation of PI3Ks leads to the production of PIP3, resulting in the downstream activation of Akt, a serine/threonine kinase, as well as the activation of Rap1B, resulting in the activation of

integrin $\alpha_{IIb}\beta_3$ and promotion of granule secretion (Figure 1-3) (Murga *et al.*, 1998; Kauffenstein *et al.*, 2001; Lova *et al.*, 2003). It has been observed that upon stimulation of platelets with ADP, platelets become unresponsive to subsequent ADP stimulation; this is thought to be due to receptor desensitization and/or internalisation (Hardy *et al.*, 2005; Mundell *et al.*, 2006; Reiner *et al.*, 2009). Further work is needed to elucidate the mechanisms responsible for this.

Whilst P2Y1 and P2Y12 signal through different Gα subunits, it has been demonstrated that co-activation of both is required for ADP-stimulated platelet activation (Jin and Kunapuli, 1998; Jantzen *et al.*, 1999; Pulcinelli *et al.*, 1999). Jin and Kunapuli (1998) demonstrated through use of specific antagonists that blocking signalling through one receptor is sufficient to prevent ADP-stimulated aggregation. This requirement for concomitant activation is also demonstrated by the use of pharmaceutical drugs such as clopidogrel, which selectively inhibits P2Y12, demonstrating significant anti-platelet effects as one of the most commonly prescribed anti-platelet medications (Savi *et al.*, 2001; Hollopeter *et al.*, 2001; Foster *et al.*, 2001; Katsanos *et al.*, 2015; Park *et al.*, 2016). Indeed, the focus on the development of novel P2Y12 receptor antagonists such as prasugrel, ticagrelor and cangrelor demonstrates the importance of ADP as a platelet agonist (Testa *et al.*, 2010; Bednar *et al.*, 2016).

This importance is also demonstrated by mice deficient in ADP receptors. Fabre *et al.* (1999) observed that P2Y1-deficient mice demonstrated reduced ADP-stimulated aggregation, prolonged bleeding times, and were protected against thromboembolism in a collagen and ADP-induced model. P2Y12-null mice also demonstrated severely prolonged tail bleeding times, and significantly reduced ADP-stimulated aggregation, as well as decreased sensitivity to collagen and thrombin, demonstrating the interplay between the mechanisms underlying platelet activation through these receptors (Foster *et al.*, 2001).

1.4.2.3 Thromboxane A_2

As well as a potent vasoconstrictor, thromboxane A_2 (TXA_2) is a platelet agonist that is produced within the platelet (Gryglewski *et al.*, 1978). Upon mobilisation of Ca^{2+} from intracellular stores upon activation, platelet phospholipase A_2 becomes activated; through the actions of this enzyme, membrane phospholipids are hydrolysed, liberating arachidonic acid (Balsinde *et al.*, 2002). This is converted through the actions of the aspirin-sensitive cyclooxygenase-1 (COX-1) and thromboxane synthase to produce thromboxane A_2 (Tazawa *et al.*, 1996). TXA_2 diffuses across the plasma membrane where, due to its short half-life, it acts in an autocrine or paracrine manner to provide positive-feedback activation and aggregation (FitzGerald, 1991; Schrör, 2016). Due to its instability, TXA_2 is converted to thromboxane B_2, an inactive, more stable lipid (Hamberg *et al.*, 1975; FitzGerald, 1991).

Thromboxane A_2 binds to the thromboxane receptor (TP), of which two splice variants have been identified; TPα and TPβ, which are the product of a single gene and differ only in the sequence of their C-terminus (Hirata *et al.*, 1991; Raychowdhury *et al.*, 1995; Habib *et al.*, 1999). Thromboxane receptors are coupled to $G\alpha_q$ and $G\alpha_{12/13}$ G-proteins (Knezevic *et al.*, 1993; Djellas *et al.*, 1999). Binding of TXA_2 to TP therefore stimulates the activation of PLCβ and associated downstream mobilisation of calcium and activation of PKC through $G\alpha_q$ subunit action, and stimulates the activation of RhoA, Rho kinase and resultant increase in phosphorylation of myosin light chain through $G\alpha_{12/13}$ subunit action, leading to shape change, granule secretion, activation of integrin $\alpha_{IIb}\beta_3$ and downstream platelet aggregation (Figure 1-3) (Kozasa *et al.*, 1998; Klages *et al.*, 1999; Konopatskaya *et al.*, 2011).

The importance of thromboxane A_2 in platelet activation is demonstrated by Thomas *et al.* (1998), who observed prolonged tail bleeding times, a lack of TXA_2-stimulated aggregation, and delayed collagen-stimulated aggregation in TP knockout mice. On a macroscopic scale, Kobayashi *et al.*

(2004) observed significantly delayed progression of atherosclerosis in ApoE-deficient mice (prone to atherosclerosis) also deficient in TP. In the same mice, *ex vivo* thrombin-induced platelet activation was also reduced. Another way in which the importance of thromboxane A_2 is demonstrated is through the efficacy of the most widely used anti-platelet agent globally, aspirin (Lanas and Scheiman, 2007; Srivastava, 2010). Aspirin binds and irreversibly inhibits cyclooxygenase-1 (COX-1), an enzyme involved in the production of thromboxane A_2. Through acetylation of COX-1, aspirin prevents the binding of arachidonic acid, thus inhibiting platelet thromboxane formation (Burch *et al.,* 1978; Jaffe and Weksler, 1979; Schrör, 1997). The anti-platelet efficacy of this approach is demonstrated by the reduction in total strokes, non-fatal myocardial infarctions and serious vascular events upon aspirin use observed in a meta-analysis of randomised trials by Baigent *et al* (2009).

1.4.2.4 Epinephrine

As well as being a vasoconstrictor, epinephrine is also a platelet agonist (Floras *et al.*, 1988). Stimulation of platelets by epinephrine is, however, weak, with aggregation observed upon epinephrine stimulation in platelet rich plasma (PRP) but not washed platelets in some studies, and a lack of epinephrine-induced calcium mobilisation and shape change also observed; as such, many argue that it is a potentiating agent rather than an agonist in its own right (Lanza *et al.*, 1988; Steen *et al.*, 1993; Nieuwland *et al.*, 1993). Nonetheless, epinephrine is capable of potentiating the platelet response to other agonists, and functions through the actions of a GPCR (Keularts *et al.*, 2000).

Epinephrine binds the α_{2A} adrenergic receptor, which is coupled to $G\alpha_z$, a member of the $G\alpha_i$ family (Newman *et al.*, 1978; Smith and Limbird, 1981; Yang *et al.*, 2000). As a $G\alpha_i$ family member, platelet stimulation with epinephrine results in the $G\alpha_z$-mediated inhibition of adenylyl cyclase, as well as $\beta\gamma$ dimer-stimulated activation of PI3K, production of PIP3, and activation of Akt and Rap1B, leading to promotion of granule secretion and activation of integrin $\alpha_{IIb}\beta_3$ (Figure 1-3) (Wong *et al.*, 1992; Woulfe *et al.*, 2002).

A study by Yang *et al.* (2000) investigated the effect of deletion of $G\alpha_z$, and observed reduced epinephrine-induced platelet responses as well as protection from thromboembolism in a collagen/epinephrine induced model. Pozgajova *et al.* (2006) generated α_{2A}-deficient mice, and also observed protection against pulmonary thromboembolism, as well as a significant reduction in thrombus stability, implying a role for epinephrine in the stabilization of thrombi.

Figure 1-3 An overview of activatory platelet G-protein coupled receptor signalling

A range of soluble agonists stimulate platelets through G-protein coupled receptor (GPCR) signalling. Thrombin receptors protease-activated receptor 1/4 (PAR1/4), the ADP receptor P2Y1 and the thromboxane receptor (TP) couple to the $G\alpha_q$ signalling pathway, leading to the activation of phospholipase Cβ (PLCβ) and the downstream mobilisation of calcium and activation of protein kinase C (PKC), leading to granule secretion and activation of integrin αIIbβ3, and driving aggregation. Ca^{2+} mobilisation also drives the activation of phospholipase A_2 (PLA_2), leading to the production of thromboxane A_2. TP and PAR1/4 couple to $G\alpha_{13}$, signalling through which leads to activation of Rho kinase and increased phosphorylation of myosin light chain (MLC), driving platelet shape change and granule secretion. The ADP receptor P2Y12 is coupled to $G\alpha_i$ and the epinephrine α_{2A} adrenergic receptor is coupled to $G\alpha_z$, which signal through the inhibition of adenylyl cyclase, removing protein kinase A (PKA) inhibition of pro-activatory substrates. The $\beta\gamma$ subunits from these two G-proteins also contain signalling capacity, activating phosphatidylinositol 3-kinase β/γ (PI3Kβ/γ), resulting in the activation of Akt and Rap1B, driving granule secretion and integrin αIIbβ3 activation, leading to positive feedback activation and aggregation.

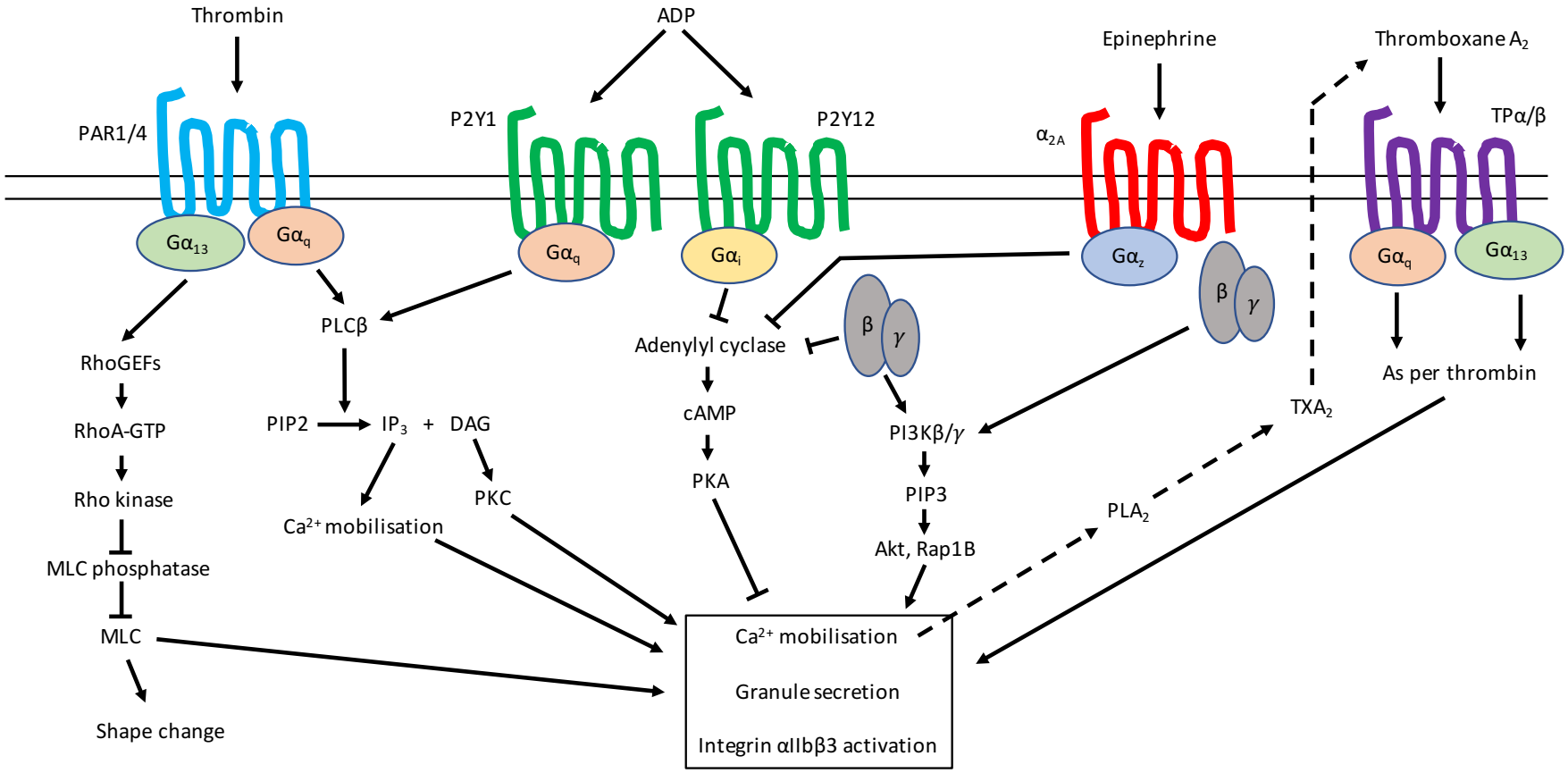

1.4.3 Common platelet activatory processes

The process of platelet activation and aggregation, regardless of agonist, primarily converges on three common mechanisms; calcium mobilisation, granule secretion, and integrin $\alpha_{IIb}\beta_3$ activation. These three processes are discussed next.

1.4.3.1 Calcium mobilisation

Platelet stimulation by agonists leads to the rapid (0.2-0.3 seconds) mobilisation of calcium from intracellular stores, as well as entry of Ca^{2+} from the extracellular compartment (Sage and Rink, 1986; Jardín *et al.*, 2009). This mobilisation of calcium drives the platelet activatory process, resulting in granule release and the activation of integrin $\alpha_{IIb}\beta_3$ (Hathaway and Adelstein, 1979; Shattil and Brass, 1987; Varga-Szabo *et al.*, 2009).

The release of calcium from intracellular stores occurs through the actions of IP_3 (Brass and Joseph, 1985). Numerous platelet agonists activate different isoforms of phospholipase C (see Figures 1-2 and 1-3), leading to the cleavage of PIP2 into IP_3 and DAG (Rhee, 2001). This IP_3 binds to the IP_3 receptor, IP_3R, which is a Ca^{2+}-permeable ion channel, leading to the release of Ca^{2+} from the intracellular platelet stores, largely within the dense tubular system (DTS) (Gerrard *et al.*, 1978; Maeda *et al.*, 1991; Varga-Szabo *et al.*, 2009).

As well as the release into the cytosol of intracellular stores, extracellular Ca^{2+} entry further drives the activatory process. One way in which this entry occurs is through store-operated calcium entry, or SOCE. A transmembrane protein named stromal interaction molecule 1 (STIM1) is situated in the membrane of the DTS, with a Ca^{2+}-binding EF hand domain within the lumen of the DTS (Zhang *et al.*, 2005; Stathopulos *et al.*, 2008). Upon binding of IP_3 and release of calcium from this intracellular store, this calcium binding is disturbed, STIM1 becomes activated, and redistributes to the plasma

membrane (Liou *et al.*, 2005; Grosse *et al.*, 2007). Also found in the plasma membrane is calcium-release activated calcium modulator 1, also known as Orai1 (Vig *et al.*, 2006). This calcium-selective ion channel is opened by the activated STIM1, allowing calcium entry into the cell (Tolhurst *et al.*, 2008). Calcium entry into the platelet can also occur via SOCE-independent mechanisms; evidence suggests that the canonical transient receptor potential cation channel subfamily C member 6 (TRPC6) protein is a store-independent nonselective cation entry channel, with thrombin inducing calcium entry through this channel via a store-independent mechanism (Hassock *et al.*, 2002; Vemana *et al.*, 2015). Another method of Ca^{2+} entry into the platelet is through direct, receptor-operated mechanisms; for example, the $P2X_1$ purinoceptor binds ATP, and can form homomeric, nonselective cation channels (Vial *et al.*, 1997; Sage *et al.*, 2000). All of these mechanisms serve to increase platelet cytosolic Ca^{2+} levels upon platelet activation.

The elevation of cytosolic calcium levels leads to the activation of platelets largely through the actions of Ca^{2+} and DAG-regulated guanine nucleotide exchange factor I (CalDAG-GEFI). Ca^{2+} is a crucial regulator of this molecule, which activates Rap1, a small GTPase, directly activating integrin $\alpha_{IIb}\beta_3$ in a rapid manner, promoting quick adhesion of platelets to the site of vessel injury (Stefanini *et al.*, 2009). CalDAG-GEFI activity also stimulates the production of TXA_2 via the MAPK/ERK (mitogen-activated protein kinase/extracellular signal-regulated kinases) signalling pathway, providing positive feedback, through granule secretion and further integrin activation, to the activatory process (Stefanini and Bergmeier, 2010).

1.4.3.2 Granule secretion

As described previously, platelets contain alpha and dense granules, which contain numerous activatory molecules (Section 1.3). Upon platelet activation, these granules fuse with membranes of the open canalicular system (OCS) or the plasma membrane, secreting their contents into the extracellular environment where they act in an autocrine or paracrine manner to further drive platelet activation (Golebiewska and Poole, 2015).

The molecular mechanisms underlying platelet granule secretion are focussed on SNAREs – soluble NSF attachment protein receptors (Sollner *et al.*, 1993; Blair and Flaumenhaft, 2009). These membrane associated proteins are associated with platelet granules (vesicular SNAREs or vSNAREs) or the OCS/plasma membrane (tSNAREs) (Duman and Forte, 2003; Sudhof and Rothman, 2009). Granule secretion is driven by the association of these two groups of SNAREs. vSNAREs and tSNARES contain coiled-coil domains; the interaction of these domains brings the granule and OCS/plasma membranes into close proximity, generates energy, and leads to membrane fusion and the formation of pores, leading to secretion of alpha and dense granule contents (Harbury, 1998; Antonin *et al.*, 2002). These SNAREs are associated with numerous chaperone proteins that aid in the granule secretion process, and a large role for the actin cytoskeleton (specifically actin polymerisation and the interaction of actin with SNARE proteins) has also been demonstrated (Polgar and Reed, 1999; Woronowicz *et al.*, 2010). The mechanisms for α- and dense granule release are largely similar, with different SNAREs implicated (Flaumenhaft *et al.*, 1999; Golebiewska *et al.*, 2015). Regulatory SM (Sec1/Munc) proteins are also associated with SNAREs, with a hypothesised role in the prevention of inappropriate granule secretion (Shirakawa *et al.*, 2004).

1.4.3.3 Integrin $\alpha_{IIb}\beta_3$ activation

Integrin $\alpha_{IIb}\beta_3$, also known as CD41/CD61, is a receptor for fibrinogen (as well as other adhesive proteins such as vWF, vitronectin and fibronectin) found mostly on platelets and megakaryocytes (Ma *et al.*, 2007; Li and Cong, 2009). It is a heterodimer consisting of an αIIb subunit and a β3 subunit, linked via noncovalent coupling (Bennett, 2005). At 60,000-80,000 copies per platelet, it is the most abundant platelet receptor, and is also found in α-granules where, upon activation, fusion of the granule and plasma membranes results in an increase in receptor number on the platelet surface (Wencel-Drake *et al.*, 1986; Wagner *et al.*, 1996). This abundance reflects the importance of this integrin; indeed, all platelet activatory signalling pathways converge on the activation of integrin $\alpha_{IIb}\beta_3$, leading to the binding of fibrinogen, platelet aggregation and thrombus formation.

Integrin $\alpha_{IIb}\beta_3$ can transduce signals in two directions. In the resting platelet, interactions between the transmembrane regions of α_{IIb} and β_3, as well as the cytoplasmic domains of α_{IIb} and β_3, result in the integrin being stabilized in a resting state (Hughes *et al.*, 1996; Weljie *et al.*, 2002). Upon platelet activation, these interactions are disrupted via a mechanism surrounding talin, a cytosolic protein. Platelet activation, as described in the previous sections, results in the elevation of cytosolic Ca^{2+} and the production of DAG. This leads to the downstream activation of Rap1, which interacts with the adaptor protein Rap1-GTP-interacting adaptor molecule (RIAM) (Lafuente *et al.*, 2004; Han *et al.*, 2006). This complex interacts with talin, exposing a β3 binding site and recruiting it to the plasma membrane (Lee *et al.*, 2009). This binding site can also be exposed via phosphoinositide binding and cleavage by the calcium-dependent protease, calpain (Martel *et al.*, 2001; Yan *et al.*, 2001). Talin, as part of the Rap1-RIAM-talin complex, binds the cytoplasmic tail of the β3 subunit of integrin $\alpha_{IIb}\beta_3$, disrupting the α_{IIb}/β_3 cytoplasmic tail interaction and driving a conformational change in the integrin extracellular region; a key role for the focal adhesion protein kindlin-3 has also been demonstrated in this process (Ulmer *et al.*, 2003; Han *et al.*, 2006; Moser *et al.*, 2008; Lagarrigue *et al.*, 2016). It must be noted that recent evidence has suggested RIAM is dispensable for $\alpha_{IIb}\beta_3$ activation in mice (instead

regulating β2 integrin activation), suggesting alternate Rap1 interacting molecules also have a role (Stritt *et al.*, 2014; Calderwood, 2015). This conformational change leads to integrin clustering and 'opens' the integrin into a high affinity ligand binding state, and is known as 'inside-out' signalling (Takagi *et al.*, 2002; Buensuceso *et al.*, 2003; Luo *et al.*, 2004).

This high affinity, open state binds fibrinogen, leading to the development of fibrinogen bridges between platelets and the formation of stable platelet aggregates (Bonnefoy *et al.*, 2001). As well as this physical interaction, the binding of fibrinogen to integrin $\alpha_{IIb}\beta_3$ stimulates intracellular signalling events, termed 'outside-in' signalling. Upon fibrinogen binding, $G\alpha_{13}$ interacts with the cytoplasmic tail of β3, activating Src-family kinases (SFKs), specifically c-Src, which also binds β3 (Obergfell *et al.*, 2002; Gong *et al.*, 2010). This results in the tyrosine phosphorylation of the cytoplasmic tail of β3, enhancing the interaction of β3 with cytoskeletal proteins including myosin heavy chain; this drives the cytoskeletal rearrangement characteristic of both platelet aggregation and clot retraction (Jenkins *et al.*, 1998). c-Src activity also leads to the transient inactivation of RhoA, promoting platelet spreading (Arthur *et al.*, 2000). After aggregation and thrombus formation has occurred, this transient inhibition of RhoA is reversed via calpain-mediated cleavage of β3, leading to re-activation of RhoA and retraction of the clot (Flevaris *et al.*, 2007). The Src-family kinases activated upon fibrinogen binding also activate Syk, resulting in the formation of a signalling complex similar to GPVI (with the involvement of LAT, SLP76, Vav and BTK) that activates PLCγ2, with associated downstream activatory signalling (Woodside *et al.*, 2001; Boylan *et al.*, 2008). A role for PKCβ-mediated platelet spreading has also been hypothesised (Buensuceso *et al.*, 2005). Thus, there are many activatory pathways and mechanisms associated with integrin $\alpha_{IIb}\beta_3$ outside-in signalling.

The critical importance of this integrin in platelet function is demonstrated by the phenotype of β3-null mice, which display significantly prolonged tail bleeding times and greatly inhibited thrombus formation, as well as spontaneous gastrointestinal haemorrhage (Hodivala-Dilke *et al.*, 1999). Its importance is also demonstrated by the autosomal recessive condition Glanzmann thrombasthenia,

which results in reduced or defective integrin $\alpha_{IIb}\beta_3$ (Glanzmann, 1918). This condition is associated with symptoms ranging from mild bruising to frequent and serious haemorrhages, which can prove fatal (Nurden, 2006). The central role of this receptor in platelet function has also led to the development of pharmacological agents targeting this integrin. The monoclonal antibody Fab fragment abciximab, as well as the small molecule inhibitors tirofiban and eptifibatide, are effective inhibitors of platelet aggregation, and are used largely in association with a percutaneous coronary intervention, to prevent thrombotic events (EPIC-Investigators, 1994; PRISM-PLUS-Investigators, 1998; PURSUIT-Investigators, 1998; Neumann *et al.*, 2001). (Shen *et al.*, 2013) recently developed a promising anti-thrombotic which acts to inhibit $G\alpha_{13}$ –integrin β3 interaction; this allowed the initial talin-β3 interaction, inside-out signalling, fibrinogen binding and platelet adhesion to sites of injury, but prevented out-side in signalling, thereby inhibiting thrombosis whilst maintaining haemostasis.

1.5 Negative regulation of platelet function

Whilst platelets play a crucial role in the haemostatic process, their inappropriate activation can lead to pathological conditions such as myocardial infarction. Platelet function is therefore tightly regulated to maintain circulating platelets in a quiescent state in the absence of vascular injury. Upon vessel injury and thrombus formation, these negative regulatory mechanisms also function to limit the size of a growing thrombus. As well as the well-characterised functions of the vascular endothelium-derived nitric oxide (NO) and prostacyclin (PGI_2) on platelets, there are numerous negative regulatory mechanisms contained within the platelet itself (Moncada *et al.*, 1977; Radomski *et al.*, 1987a).

1.5.1 Prostacyclin

Prostacyclin is a potent inhibitor of platelet aggregation, produced by endothelial cells from arachidonic acid and secreted into the circulation (Moncada *et al.*, 1977; Mitchell and Warner, 1999). Prostacyclin binds to the platelet prostaglandin receptor (IP receptor), which is a GPCR coupled to $G\alpha_s$ (Dutta-Roy and Sinha, 1987; Nishimura *et al.*, 1995). Activation of this G-protein results in the subsequent activation of adenylyl cyclase, and the production of cyclic adenosine monophosphate (cAMP) (Gorman *et al.*, 1977). This cAMP activates cAMP-dependent protein kinase (PKA), which phosphorylates a wide range of substrates leading to their inhibition. Such substrates include Rap1B, which, as previously described, is crucial to integrin $\alpha_{IIb}\beta_3$ activation, as well as IP_3 receptor, leading to the prevention of intracellular Ca^{2+} mobilisation, and $G\alpha_{13}$, inhibiting adhesion and spreading of platelets (Altschuler and Lapetina, 1993; Smolenski, 2012; Bye *et al.*, 2016). There are many other PKA substrates, including G-proteins and actin binding proteins, the phosphorylation of which maintains the platelet in its quiescent state (Smolenski, 2012).

1.5.2 Nitric Oxide

Nitric oxide is a small gaseous signalling molecule produced from L-arginine by a family of enzymes known as nitric oxide synthases (NOS), of which there is endothelial NOS (eNOS), inducible NOS (iNOS) and neuronal NOS (nNOS) (Ignarro *et al.*, 1987; Förstermann and Sessa, 2012). Nitric oxide produced in endothelial cells via eNOS diffuses passively across the platelet plasma membrane and binds and activates soluble guanylyl cyclase (sGC) (Katsuki *et al.*, 1977; Friebe and Koesling, 2009; Dangel *et al.*, 2010). Activated sGC produces cyclic guanosine monophosphate (cGMP), which in turn activates cGMP-dependent protein kinase, also known as protein kinase G (PKG) (Radomski *et al.*, 1987b; Wall *et al.*, 2003). PKG phosphorylates and inhibits many substrates, and there is significant overlap in the substrates for PKA and PKG, leading to the downstream inhibition of granule secretion, integrin activation and aggregation (Butt *et al.*, 1994; Smolenski, 2012; Bye *et al.*, 2016). cGMP also regulates the activity of phosphodiesterases (PDEs), enzymes that degrade cyclic nucleotides, thereby providing a self-regulated negative feedback loop(Haslam *et al.*, 1999; Feijge *et al.*, 2004; Francis *et al.*, 2005). There is some controversy surrounding the potential presence of NOS in platelets; this ambiguity is largely attributed to analytical problems in the detection and measurement of NOS protein and activity (Gambaryan and Tsikas, 2015). A recent study by Cozzi *et al.* (2015) demonstrated, for the first time, NO production in individual platelets during adhesion to collagen under flowing conditions, with platelet deposition on this surface inversely related to production of nitric oxide. More research is needed to elucidate the role of platelet-derived NO in the overall negative regulation of platelet function.

1.5.3 PECAM-1

Platelet endothelial cell adhesion molecule-1 (PECAM-1) is a 130kDa glycoprotein that spans the platelet membrane and negatively regulates platelet function in response to a number of agonists (Sun

et al., 1996b; Jones *et al.*, 2009). PECAM-1 is a member of the immunoglobulin family of adhesion molecules, and is expressed on endothelial cells, as well as other haematopoietic cells such as natural killer cells and neutrophils (Ohto *et al.*, 1985; Sun *et al.*, 1996a). PECAM-1 contains an immunoreceptor tyrosine-based inhibitory (ITIM) motif; upon platelet activation stimulated by collagen (as well upon stimulation by thrombin, or homophilic ligation), phosphorylation of the ITIM by Src-family kinases occurs (Cicmil *et al.*, 2000). Moraes *et al.* (2010) elucidated the mechanism of inhibition of collagen-stimulated platelet activation by PECAM-1. Src homology 2 domain-containing protein tyrosine phosphatase-2 (SHP-2) is recruited to the phosphorylated ITIM and activated, and interacts with the p85 subunit of PI3K in a PECAM-1 regulated manner. In this way, PI3K is lost from the LAT signalosome, leading to reduced activatory PI3K signalling (Moraes *et al.*, 2010). PECAM-1 clustering has also been shown to inhibit ADP and thrombin-stimulated platelet responses, and a role for PECAM-1 in the inhibition of vWF-GPIb-V-IX-mediated platelet activation has also been demonstrated (Rathore *et al.*, 2003; Jones *et al.*, 2009; Jones *et al.*, 2014). The combined effects of PECAM-1 on multiple platelet activatory pathways leads to greater platelet spreading and thrombus formation on vWF *in vitro* in PECAM-1-deficient platelets (Cicmil *et al.*, 2002). This effect was maintained *in vivo,* with significantly larger and more stable thrombi forming in PECAM-1 deficient mice following laser-injury (Falati *et al.*, 2006). As well as PECAM-1, other members of the cell adhesion molecule (CAM) family have demonstrated an inhibitory effect in platelet function, including carcinoembryonic antigen cell adhesion molecule-1 (CEACAM-1) and endothelial cell specific adhesion molecule (ESAM), which are also implicated in the regulation of thrombus formation and growth (Nasdala *et al.*, 2002; Stalker *et al.*, 2009; Wong *et al.*, 2009).

1.5.4 G6B

The G6B protein is an immunoglobulin receptor, and has been identified on the platelet surface (Macaulay *et al.*, 2007; Senis *et al.*, 2007; Newland *et al.*, 2007). G6B contains two ITIM motifs on the cytoplasmic tail; upon platelet activation, these ITIM motifs become phosphorylated on tyrosine residues, and bind the tyrosine phosphatases SHP-1 and SHP-2 (de Vet *et al.*, 2001; Mori *et al.*, 2008).

The cross-linking of G6B through the use of antibodies resulted in the inhibition of ADP and CRP-XL-stimulated platelet activation and aggregation, as well as an inhibition of collagen and CLEC-2 (C-type lectin-like receptor 2)-induced platelet signalling (Newland *et al.*, 2007; Mori *et al.*, 2008). The mechanism of inhibition downstream of ITIM phosphorylation has not been fully elucidated, but has been demonstrated to be, at least in part, independent of SHP-1 and SHP-2 action (Mori *et al.*, 2008).

1.5.5 JAM-A

Junctional adhesion molecule A (JAM-A) is another platelet receptor recently shown to negatively regulate platelet function. JAM-A inhibits platelet function through an inhibition of integrin $\alpha_{IIb}\beta_3$ outside-in signalling; integrin-associated JAM-A binds C-terminal Src kinase (Csk) (Naik *et al.*, 2012; Naik *et al.*, 2014). This Csk phosphorylates and inactivates c-Src, supressing integrin outside-in signalling and maintaining the integrin in an inactive state. Platelet stimulation results in dephosphorylation of JAM-A and loss of Csk from the $\alpha_{IIb}\beta_3$ complex, allowing the transduction of integrin outside-in signals (Naik *et al.*, 2014). JAM-A deficient mice displayed enhanced thrombus formation, and platelet-specific JAM-A deficiency resulted in increased and more rapid atherosclerotic progression in ApoE-null mice, demonstrating a clear role for this receptor in the negative regulation of platelet function (Naik *et al.*, 2012; Karshovska *et al.*, 2015).

1.5.6 Nuclear receptors

Whilst platelets are anucleate, curiously, they express nuclear receptors, a class of proteins that typically regulate the transcription of genes. Examples found in the platelet include the glucocorticoid receptor, peroxisome proliferator activated receptor (PPAR) β/γ/δ isoforms, and retinoic X receptor (RXR) (Akbiyik *et al.*, 2004; Moraes *et al.*, 2005; Ali *et al.*, 2006; Moraes *et al.*, 2007). Addition of nuclear receptor ligands to platelets has been shown to inhibit platelet activatory signalling and

aggregation upon stimulation with various agonists, including collagen, ADP and thromboxane A_2 (Moraes *et al.*, 2007). For example, RXR binds $G\alpha_q$ subunit, inhibiting the downstream mobilisation of calcium, and recently, Unsworth *et al.* (2017b) demonstrated that PPARγ agonists inhibit integrin $\alpha_{IIb}\beta_3$ outside-in signalling by disrupting the $G\alpha_{13}$-β3 interaction, attributed to increases in the activity of PKA (Moraes *et al.*, 2007; Unsworth *et al.*, 2017a).

1.6 Quercetin structure, production and endogenous function

1.6.1 Flavonoids, flavonols and quercetin

Flavonoids are a diverse class of polyphenols found in plants. They are the most common of all plant phenolic compounds, and are found throughout the plant (Kumar and Pandey, 2013). One of the first descriptions of flavonoids and their biological activity came in 1936, when Rusznyak and Szent-Gyorgyi (1936) observed that a Hungarian red pepper extract increased the permeability of capillary walls. Interest in flavonoids has continued to grow, with over 9000 now identified (Williams and Grayer, 2004). The basic flavonoid structure consists of a fifteen-carbon backbone, comprising two benzene rings (A and B) linked by a heterocyclic, oxygenated middle ring (C), shown in Figure 1-4A (Pinheiro and Justino, 2012). This wide-ranging group of 'flavonoids' is divided into several classes based on common structural features; flavonols, flavones, flavanones, isoflavones, flavan-3-ols and anthocyanins, which are defined by the presence (or absence) of C-ring oxidation and specific hydroxyl (-OH) groups (Tsimogiannis *et al.*, 2007). These are the most common groups of flavonoids, and together make up approximately 80% of all known flavonoids (Pinheiro and Justino, 2012). Flavonols are characterised by the presence of a C-3 hydroxyl group and a C-4 carbonyl group, with their structure shown in Figure 1-4B (Wright *et al.*, 2010b). Examples of flavonols include myricetin, kaempferol and fisetin, with different flavonols distinguished by differential hydroxylation patterns on the A and B rings (Halbwirth, 2010). One of the most common dietary flavonols, and indeed one of the most common dietary flavonoids in general, is quercetin, 3,3',4',5,7-pentahydroxyflavone, the structure of which is presented in Figure 1-4C (Pandey and Rizvi, 2009; Anand David *et al.*, 2016). In nature, quercetin exists as an aglycone (non-conjugated) or in conjugated forms, primarily glycosides (Lozoya *et al.*, 1994; Kwak *et al.*, 2017).

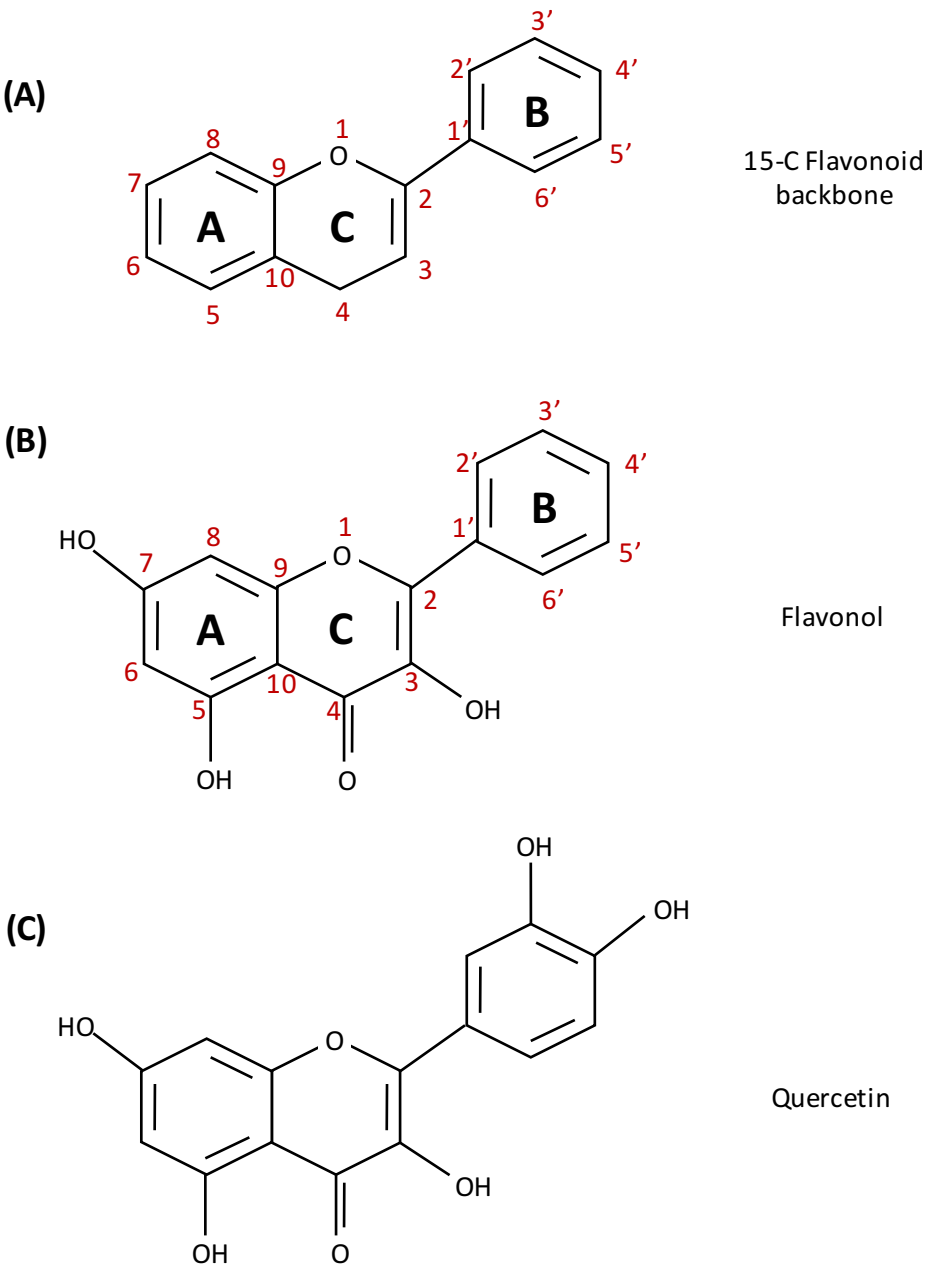

Figure 1-4 The structure of the flavonoid backbone, flavonols and quercetin

The 15-carbon flavonoid backbone (A) consists of two benzene rings, A and B, linked by a heterocyclic, oxygenated middle ring, C. The numbers are included to indicate the positions of modifications/additions to the backbone. The flavonol structure (B) is distinguished from other flavonoid groups by a C-3 hydroxyl group and and C-4 carbonyl group, and also possesses C-5 and C-7 hydroxyl groups. Quercetin (C) is comprised of the flavonol structure, and is defined by the addition of hydroxyl groups at the 3' and 4' position. O, oxygen; OH, hydroxyl group.

1.6.2 Quercetin biosynthesis

Quercetin synthesis in plants is triggered by numerous factors; ultraviolet radiation, temperature extremes, drought, and the presence of heavy metals or microbial infection can all promote the synthesis of quercetin (Tattini *et al.*, 2004; Treutter, 2005; Huang *et al.*, 2016b). Biosynthesis occurs via the phenylpropanoid pathway, as shown in Figure 1-5 (Weisshaar and Jenkins, 1998). This is a complex pathway capable of producing many plant metabolites; quercetin is only one such metabolite. Quercetin is produced from the amino acid L-phenylalanine (or L-tyrosine) through a complex series of reactions. Through the actions of phenylalanine ammonia-lyase (PAL) and cinnamate 4-hydroxylase (C4H), L-phenylalanine is converted to cinnamic acid and *para(p)*-coumaric acid, respectively (Weisshaar and Jenkins, 1998). 4-coumaroyl-CoA ligase (4CL) converts the *p*-coumaric acid into *p*-coumaroyl-coenzyme A (CoA), which, with the addition of three malonyl-CoA molecules, is converted into naringenin chalcone by chalcone synthase (CHS) (Stahlhut *et al.*, 2015). Chalcone isomerase (CHI) then isomerises the naringenin chalcone into naringenin (Stahlhut *et al.*, 2015). Conversion of naringenin into dihydrokaempferol occurs through flavanone 3-hydroxylase (F3H), which is subsequently converted into kaempferol by flavonol synthase (FLS). The final step in quercetin synthesis is the conversion of kaempferol into quercetin, a reaction mediated by cytochrome p450 flavonoid monooxygenase (FMO), which is associated with the electron donor, cytochrome p450 reductase (CPR) (Figure 1-5)(Patschke and Grisebach, 1968; Leonard *et al.*, 2006; Stahlhut *et al.*, 2015). This complex series of metabolic reactions occurs in all parts of the plant, where flavonoids have a variety of endogenous functions, discussed next (Koes *et al.*, 1994; Mierziak *et al.*, 2014).

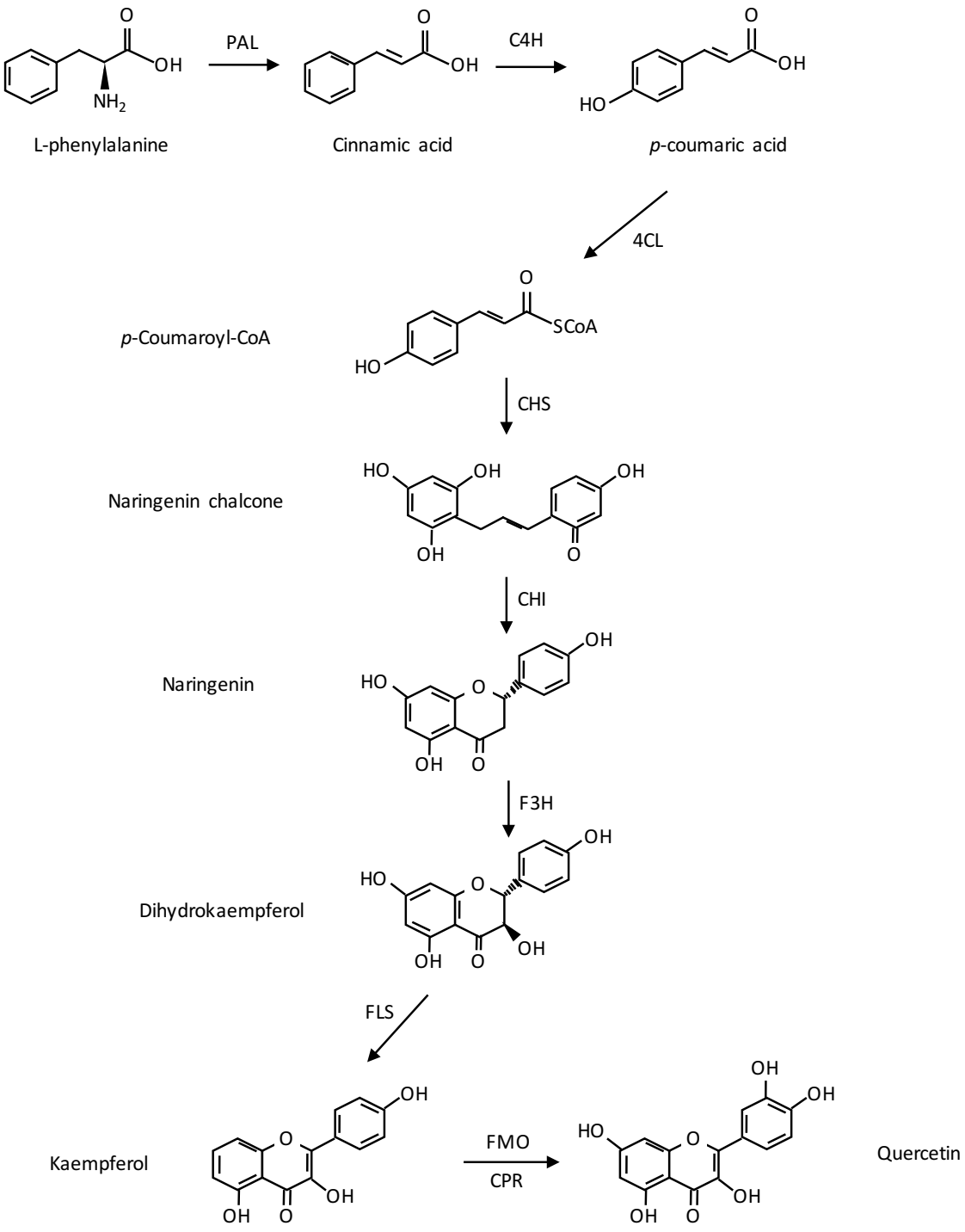

Figure 1-5 The phenylpropanoid pathway of quercetin synthesis

Quercetin is synthesised in plants from the amino acid L-phenylalanine via the phenylpropanoid pathway. A complex pathway, the steps leading to the synthesis of quercetin are shown above (with a full description of the process in the text), with the enzymes responsible for the reactions stated next to the arrows. PAL, phenylalanine ammonia lyase; C4H, cinnamate 4-hydroxylase; 4CL, 4-coumaroyl-CoA ligase; CHS, chalcone synthase; CHI, chalcone isomerase; F3H, flavanone 3-hydroxylase; FLS, flavonol synthase; FMO, flavonoid monooxygenase; CPR, cytochrome p450 reductase.

1.6.3 Endogenous functions of flavonoids

Flavonoids have a wide range of endogenous functions, with many linked to their anti-oxidant capacity (Mierziak *et al.*, 2014). Indeed, quercetin is a potent anti-oxidant, and serves to protect the plant against oxidative stress induced by environmental stresses such as ultraviolet radiation, temperature extremes, drought and heavy metals (Treutter, 2005; Celik and Arinc, 2010). Flavonoid levels increase in response to these factors, with the plant enhancing production in order to cope with the stresses; for example, flavonoids accumulate in the epidermis and hypodermis of plant structures, reducing ultraviolet penetration into vulnerable tissues (Braidot *et al.*, 2008; del Valle *et al.*, 2015). The antioxidant capacity of flavonoids also serves to protect the plant against microbial and fungal infection, and they are also able to inhibit bacterial, fungal and viral enzymes required for their replication (Selway, 1986; Weidenbörner and Jha, 1993; Wu *et al.*, 2013). They can also act to attract beneficial nitrogen-fixing bacteria, with low-nitrogen conditions stimulating the production of flavonoids (Webster *et al.*, 1998; Abdel-Lateif *et al.*, 2012).

Flavonoids are also responsible for some allelopathic functions of plants. Flavonoids can be secreted through plant roots, and in the soil they function to inhibit the germination of seeds from other plants, through the inhibition of ATP production and auxin function (Kong *et al.*, 2007; Weston and Mathesius, 2013). Flavonoids are also involved in plant-animal interactions; they give colour and taste to fruits and seeds, and can protect against herbivorous insects by acting as toxins, altering their growth and behaviour, and preventing their laying of eggs (Tabashnik, 1987; Koes *et al.*, 1994; Simmonds and Stevenson, 2001).

1.7 Quercetin intake, absorption and metabolism in humans

1.7.1 Quercetin intake

The primary method of human intake of quercetin is through the diet. Quercetin is found in many foods, and is most commonly consumed in fruits, vegetables, tea and red wine (Egert *et al.*, 2008). Onions are a particularly good source of quercetin, containing approximately 8-16mg per 100g, as well as cranberries, with approximately 15-20mg per 100g (indeed, many berries are rich sources of quercetin) (Harnly *et al.*, 2006). Red leaf lettuce is a particularly good source, with approximately 30mg per 100g (Nishimuro *et al.*, 2015). A typical western diet will result in a quercetin intake of up to 30mg quercetin per day, with a median intake of 10mg (Egert *et al.*, 2008; Harwood *et al.*, 2007). This level of intake is similar to that found in a study by Nishimuro *et al.* (2015), who observed a median intake of 15.5-16.2mg quercetin per day in Japanese participants consuming a regular diet. Individuals who consume large amounts of fruits and vegetables may intake between 200 and 500mg quercetin per day (Harwood *et al.*, 2007). Quercetin is particularly present in the Mediterranean diet, and it is hypothesised that the reduced incidence of cardiovascular disease associated with this diet may, in part, be explicable by enhanced quercetin intake (de Lorgeril *et al.*, 1999; Crescente *et al.*, 2009; Estruch *et al.*, 2013; Gormaz *et al.*, 2015). Quercetin is also consumed as a supplement, of which there are many available, with a recommended supplemental daily dose of 200-1200mg (Hendler and Rorvik, 2009).

Quercetin exists in foods largely in glycosylated forms, with many different conjugates; for example, onions are rich in quercetin glucosides, whilst buckwheat tea is rich in quercetin-3-*O*-rutinoside (Graefe *et al.*, 2001; Kwak *et al.*, 2017). These different glycosides are differentially absorbed and have differing bioavailabilities; the absorption and metabolism of quercetin is discussed next (Graefe *et al.*, 2001).

1.7.2 Absorption and metabolism of quercetin

Quercetin absorption and its extensive metabolism can occur at many sites in the body; the oral cavity, stomach, small intestine and colon are all sites of metabolism and absorption, with the liver also involved in the metabolism of quercetin. These processes all lead to a plethora of quercetin metabolites in the plasma, with eventual excretion via urine, faeces, or through degradation and exhalation as CO_2 (Nemeth and Piskula, 2007). These processes are summarised below, and the metabolic fate of quercetin is shown in Figure 1-6.

1.7.2.1 Oral cavity

As the first section of the alimentary tract, quercetin in food first comes into contact with the digestive and metabolic systems of the body here. As stated previously, quercetin in foods largely exists as glycosides; these can be hydrolysed in the mouth by enzymes of human or microbial origin, and quercetin can also be oxidated by salivary enzymes (Takahama *et al.*, 2002). For example, glucosidases originating from oral cavity epithelial cells have been demonstrated to hydrolyse onion quercetin glucosides into quercetin aglycone (Hirota *et al.*, 2001). After mastication, food is swallowed and transported to the stomach (Figure 1-6).

1.7.2.2 Stomach

The stomach is not considered to play a large role in the absorption or metabolism or quercetin; for example, non-enzymatic metabolism of flavonoids, through gastric acid hydrolysis, was observed not to occur (Gee *et al.*, 1998). In rats, however, quercetin aglycone was absorbed in the stomach, but quercetin glycosides were not (Crespy *et al.*, 2002). This suggests that the flavonoid aglycones formed after oral cavity metabolism may be absorbed in the stomach. Also in rats, sulphated, methylated and glucuronidated metabolites were identified in stomach tissues, with uridine 5'-diphosphate

glucuronosyltransferase (UGT) activity also identified in the gastric mucosa (Murota and Terao, 2005; Graf *et al.*, 2006). Thus, in humans, the stomach may play a minor role in metabolism and absorption of quercetin (Figure 1-6). The contents of the stomach is emptied into the small intestine.

1.7.2.3 Small intestine

The small intestine is the major site of quercetin absorption, as well as metabolism (Figure 1-6). It is here that the presence or absence of a sugar moiety greatly effects the absorption process; it has been demonstrated in several studies that the absorption of glucosylated quercetin is significantly greater than that of the aglycone, and results in total plasma quercetin levels several times higher (Hollman *et al.*, 1995; Morand *et al.*, 2000). Indeed, the location of the glucose moiety can also have an effect, with a 300mg quercetin-4-O-β-D-glucoside dose resulting in slightly higher peak plasma quercetin levels (9.72μM) than a 1g dose of quercetin-3-glucoside (9.2μM) (Hubbard *et al.*, 2004; Stopa *et al.*, 2017). The food matrix can also influence the absorption of quercetin, with a combination of lipids and emulsifiers increasing significalty the absorption of quercetin in rats in a study by Azuma *et al.* (2002). A study in pigs by Lesser *et al.* (2004) also demonstrated enhanced bioavailability of quercetin from both quercetin aglycone and quercetin-3-glucoside upon administration with a fat-enriched diet, hypothesised to be due to improved quercetin solubility (quercetin aglycone is lipophilic) and absorption via lipid micelles.

Absorption of quercetin glycosides by the small intestine can occur via two mechanisms. Firstly, deglycolsylation can occur in the lumen via the actions of membrane-bound enzymes, followed by passive diffusion of the aglycone across the enterocyte membrane into the cell, where it undergoes phase II metabolism (Depeint *et al.*, 2002; Meskin *et al.*, 2003). One such enzyme is lactin-phlorizin hydrolase (LPH), which is concentrated on the apical enterocyte membrane, allowing efficient hydrolysis of glycosides (Day *et al.*, 2000; Nemeth *et al.*, 2003). Secondly, quercetin glucosides can be actively transported across the membrane through the actions of the sodium-dependant glucose

transporter 1 (SGLT1), allowing entry of quercetin glycosides into the enterocyte without de-glycosylation (Figure 1-6)(Wolffram *et al.*, 2002; Day *et al.*, 2003). Different quercetin glycosides are affected differently by the actions of LPH and SGLT1; for example, Day *et al.* (2003) demonstrated that quercetin-4'-glucoside absorption involved both LPH hydrolysis and active transport via SGLT1, whereas quercetin-3-glucoside was absorbed only after LPH hydrolysis. This could explain the difference in bioavailability of different quercetin glucosides described above. Quercetin glucosides that gain entry into the enterocyte can also be transported back into the intestinal lumen through the actions of multidrug resistance-associated protein 2 (MRP2) (Walgren *et al.*, 2000).

Quercetin glucosides in the enterocyte undergo hydrolysis by cytosolic enterocyte β-glucosidases (Ioku *et al.*, 1998; Day *et al.*, 1998). Following this, quercetin undergoes phase II metabolism in the small intestine, undergoing conjugation reactions, primarily glucuronidation, sulphation and methylation (Figure 1-6)(Manach *et al.*, 1998; Crespy *et al.*, 1999). These reactions are performed by UDP-glucuronyltransferases (UGTs), sulphotransferases (SULTs) and catechol *O*-methyltransferase (COMT), respectively, with quercetin glucuronides, sulphates and methylated metabolites forming the major plasma metabolites (O'Leary *et al.*, 2003; Huang *et al.*, 2009; Chen *et al.*, 2014). Two methylated metabolites of quercetin – tamarixetin and isorhamnetin – are the focus of this study.

Quercetin that is not absorbed or metabolised by the small intestine continues to pass through the body, with colonic absorption and metabolism occurring next.

1.7.2.4 Colon

Flavonoid metabolism in the colon occurs primarily through the actions of the colonic microflora; this is an abundant population, with approximately 10^{12} microorganisms/mL (van Duynhoven *et al.*, 2011). Quercetin glycosides that are not hydrolysed in the small intestine include rutin, quercetin-3-O-rutinoside. These glycosides are hydrolysed by enzymes produced by the colonic microflora, such as

α-rhamnosidase (Amaretti *et al.*, 2015). This releases the flavonoid aglycones; however, in the colon, quercetin aglycone is also cleaved, giving rise to phenolic acids, primarily phenylacetic and phenylpropionic acids (Rechner *et al.*, 2004). Absorption from the colon or further metabolism of these products then occurs; flavonoids and metabolites not absorbed here are excreted through the faeces (Figure 1-6).

1.7.2.5 Liver

Quercetin absorbed from the small intestine enters the liver through the portal vein, where it undergoes further metabolism (Figure 1-6)(DeSesso and Jacobson, 2001). Phase I metabolism results in the introduction or exposure of polar groups, with phase II metabolism, also occurring in the liver, resulting in the conjugation of these polar groups (Williamson *et al.*, 2000; Nemeth and Piskula, 2007). As in the small intestine, conjugation reactions in the liver include glucuronidation, sulphation and methylation, again through the actions of UGTs, SULTs and COMT. From the liver, these quercetin metabolites and conjugates enter the systemic circulation (van Duynhoven *et al.*, 2011). They may also be excreted into the bile, where they re-enter the small intestine, are hydrolysed, and absorbed once more by the enterocyte, creating a cycle of absorption, metabolism, biliary excretion and re-absorption known as enterohepatic cycling (Figure 1-6)(Crespy *et al.*, 1999; Matsukawa *et al.*, 2009).

1.7.2.6 Plasma

Flavonoid glycosides are not found in plasma – instead, it is largely metabolites and conjugated forms of quercetin (Figure 1-6)(Sesink *et al.*, 2001). Many studies have been performed to elucidate the identity of plasma metabolites of quercetin, and pharmacokinetic studies have been performed to investigate the parameters of quercetin absorption, such as maximum concentration achieved (C_{max}) and time to C_{max} (T_{max}). Hubbard *et al.* (2004) investigated the pharmacokinetics of a 300mg dose of quercetin-4'-O-β-D-glucoside, and found a total plasma quercetin C_{max} of 9.72μM at 30 minutes. They

also identified tamarixetin and isorhamnetin, methylated metabolites, at peak concentrations of 0.54μM and 0.44μM at 45 and 30 minutes, respectively. Graefe *et al.* (2001) also supplemented with quercetin-4'-O-glucoside at a dose of 100mg, and observed a peak plasma concentration of 2.3μM at approximately 40 minutes. It was also observed in this study that total concentrations of isorhamnetin, a methylated metabolite, reached approximately one tenth of the total plasma quercetin concentration. A study by Mullen *et al.* (2002) orally administered quercetin-4'-glucoside in rats and identified 18 plasma metabolites, with varying degrees of glucuronidation, methylation and sulphation, demonstrating the extensive metabolism of quercetin. A traditional lack of standards and lack of sensitive techniques led, in many studies, to the identification of quercetin and methylated metabolites after enzyme treatment with sulphatases and glucuronidases. The development of better standards and techniques is changing this; for example, a technique developed by Lee *et al.* (2012b) allowed the identification of specific glucuronide, sulphate and methylated metabolites, as well as metabolites with multiple conjugates, for example methylquercetin diglucuronide. These enhanced techniques have also allowed the identification of (albeit low) levels of quercetin aglycone in plasma, the presence of which was historically a point of some controversy (Sesink *et al.*, 2001; Chen *et al.*, 2005).

Once in the plasma, quercetin (plus metabolites and conjugates) largely binds plasma proteins; it has been demonstrated that quercetin binds human serum albumin (HSA) with high affinity. Indeed, up to 99% of circulating quercetin can be bound to HSA (Boulton *et al.*, 1998; Kaldas *et al.*, 2005). This influences the anti-platelet effect of quercetin, discussed later.

There is also some evidence that platelets can mediate further metabolism of quercetin (Figure 1-6). Wright *et al.* (2010a) demonstrated, using confocal microscopy, that quercetin gained access to the platelet cytosol, where it was transformed into a compound that had an identical mass to tamarixetin. They hypothesise that this was mediated by platelet COMT, opening a potential new avenue for flavonoid metabolism.

From the plasma, quercetin and its metabolites are distributed to the tissues throughout the body, where further metabolism/deconjugation can occur, or are eliminated; elimination occurs through the urine, faeces and through degradation and exhalation as CO_2 (Walle *et al.*, 2001; Bieger *et al.*, 2008). The metabolic fate of quercetin is summarised in Figure 1-6.

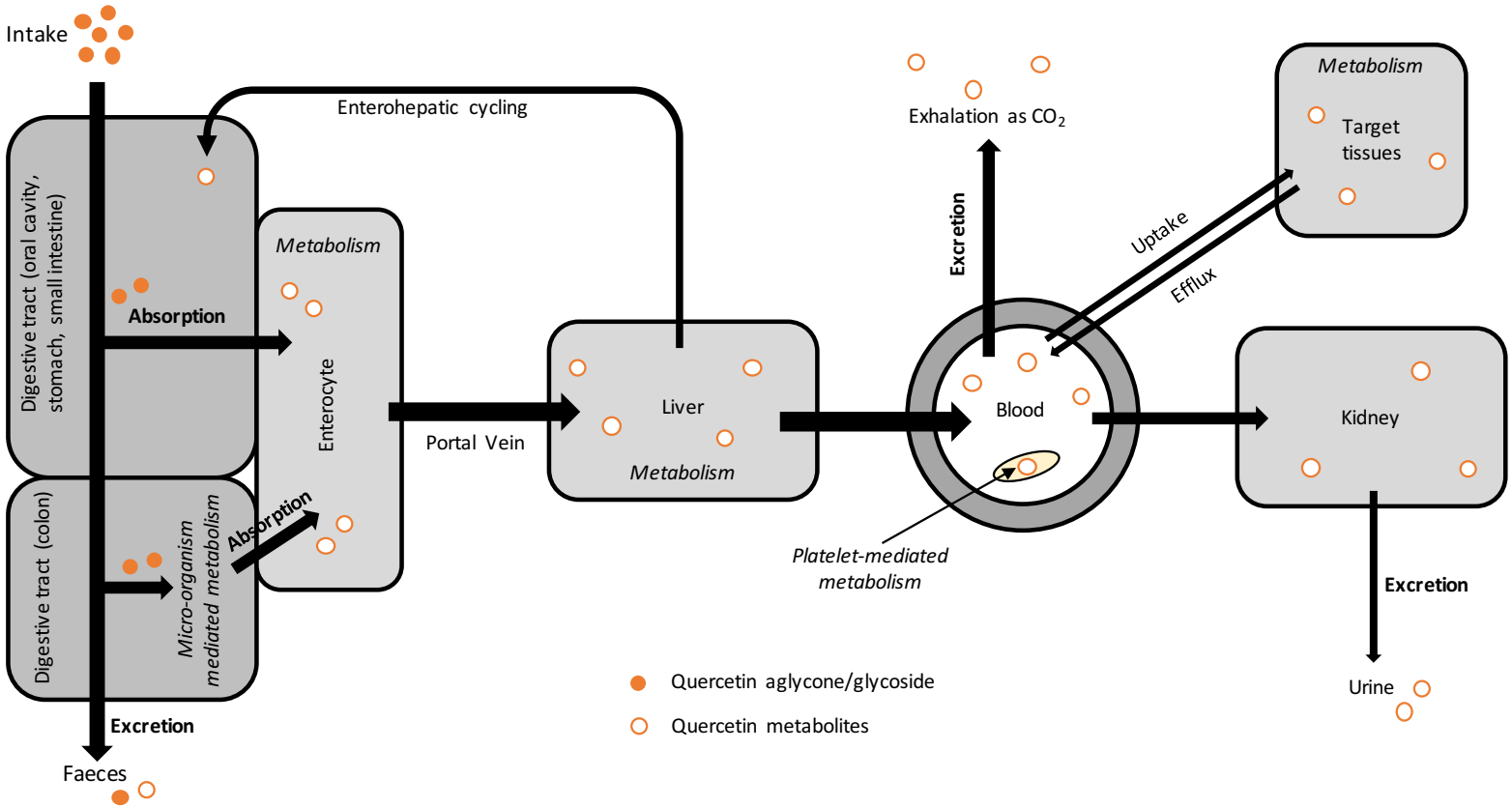

Figure 1-6 The metabolic fate of quercetin

Upon oral intake of quercetin aglycone or quercetin glycosides (solid orange circles), quercetin travels through the digestive tract, from the oral cavity to the stomach, and to the small intestine. Metabolism can occur in the oral cavity, stomach and the small intestine, with metabolism and absorption in the small intestine playing the major role. Quercetin not metabolised and absorbed in these compartments moves through to the colon, where colonic microflora metabolise quercetin. Quercetin that has not been metabolised and absorbed here is excreted in faeces. Absorption into, and further metabolism within enterocytes occurs, and metabolites (hollow orange circles) are transported into the liver through the portal vein. Further metabolism occurs in the liver, from which metabolites enter the systemic circulation or the bile, where they can re-enter the digestive tract through enterohepatic cycling. In the blood, metabolites circulate, and are transported to target tissues, enter platelets where they are further metabolised, or are transported to the kidneys where they are excreted through the urine. Metabolites can also be broken down further and excreted as exhaled carbon dioxide (CO_2).

1.8 Anti-CVD effects of quercetin

In many studies, quercetin has demonstrated a plethora of positive health benefits. These include anticancer activity; quercetin has been shown to induce cytotoxicity in leukaemia cells and breast and lung cancer cells, with no effect on normal cells. Indeed, delayed tumour growth, tumour regression and increased survival in mice following quercetin treatment has been observed in several studies (Zheng *et al.*, 2012; Srivastava *et al.*, 2016; Zhou *et al.*, 2017). Quercetin has also displayed potent antibacterial and antiviral activity; a study by Hirai *et al.* (2010) demonstrated the anti-bacterial effect of quercetin against *Staphylococcus aureus,* including against some clinically relevant methicillin-resistant *Staphylococcus aureus* (MRSA) strains, and studies have also shown quercetin to inhibit the infection of cells with human immunodeficiency virus (HIV) and influenza virus (Nair *et al.*, 2009; Wu *et al.*, 2016). Quercetin has also demonstrated anti-ageing and cell-rejuvenating effects (Chondrogianni *et al.*, 2010). As well as these potential health benefits, quercetin is a potent anti-oxidant, with anti-oxidant activity comparable to Trolox (a commonly used experimental antioxidant) under certain conditions; indeed, this anti-oxidant activity may explain some of the potential health benefits of quercetin (Letan, 1966; Zhang *et al.*, 2011b). These observations have led many to investigate the potential of quercetin as a neutraceutical, or, indeed, as a potential pharmaceutical agent (Boots *et al.*, 2008; Tapas *et al.*, 2008; Maalik *et al.*, 2014).

In addition to these wide-ranging health benefits, quercetin has also demonstrated anti-CVD effects in numerous studies. A randomised, placebo-controlled, double-blinded study by Lee *et al.* (2011) investigated the effects of 100mg quercetin per day for 10 weeks on cardiometabolic biomarkers in male smokers. They observed a significant reduction in total and LDL (low-density lipoprotein) cholesterol, and an increase in HDL (high-density lipoprotein) cholesterol in the quercetin-supplemented group. They also observed significant reductions in systolic and diastolic blood pressure, and a significant decrease in glucose concentration upon 10 weeks of 100mg quercetin supplementation (Lee *et al.*, 2011). Liu *et al.* (2015) demonstrated that 24-week supplementation with

100mg/kg quercetin in Apolipoprotein E (ApoE) knockout mice reduced significantly liver damage induced by a high-fat diet, as well as reducing hepatic oxidised LDL and cholesterol levels. Another randomised, placebo-controlled, double-blinded study performed by Edwards *et al.* (2007), observed a reduction in systolic and diastolic blood pressure, as well as mean arterial pressure, in stage 1 hypertensive subjects following 28 days of 730mg per day quercetin treatment. It must be noted, however, that no significant effects were observed upon the same treatment regimen in pre-hypertensive subjects, and no oxidative stress markers were reduced in either population after treatment. A meta-analysis of randomised control trials performed by Serban *et al.* (2016) demonstrated a significant effect of quercetin doses over 500mg per day in the reduction of both systolic and diastolic blood pressure.

The observation of these beneficial effects of quercetin, and in flavonoids in general, led to the investigation of their potential anti-CVD effect in cohort studies. Many of these studies have focussed on flavonoid or flavonol intake in general, as opposed to focussing in specifically on quercetin. A large prospective cohort study by McCullough *et al.* (2012), including 38,000 men and 60,000 women, reported a relative risk (RR) of fatal CVD of 0.82 in the top quintile of flavonoid intake, compared with the bottom quintile, with beneficial effects also observed in the intermediate intake categories (approximately 150-300mg total flavonoid intake per day). This included a lower risk of stroke and ischemic heart disease mortality in men. Specifically, high flavonol intake was also associated with a lower fatal CVD risk. Hertog *et al.* (1995) reported on data from the Seven Countries Study, and also observed an inverse relationship between flavonoid intake and coronary heart disease mortality. A meta-analysis of 14 prospective cohort studies by Wang *et al.* (2014a) observed a RR of 0.89 for CVD risk when comparing the highest and lowest flavonol intake categories; however, a similar meta-analysis observed no significant association between high flavonol intake and risk of CHD (Wang *et al.*, 2012a). A study of cardiovascular disease in women by Sesso *et al.* (2003) concluded there was no strong association between flavonoid intake and a lower CVD risk in women. Another meta-analysis by Hollman *et al.* (2010), investigating stroke specifically, observed an inverse association between high flavonoid intake and both fatal and non-fatal stroke (pooled RR = 0.8). Investigating

quercetin specifically, the Finnish Mobile Clinic study observed a RR of ischemic heart disease of 0.79 between the highest and lowest quercetin intake quartiles (Knekt *et al.*, 2002). However, the Caerphilly study noted no association between quercetin intake and coronary heart disease incidence (Hertog *et al.*, 1997). Thus, more studies must be undertaken to truly elucidate the relationship between flavonoid, flavonol and quercetin intake and CVD risk.

The potential anti-CVD effects of flavonoids and, specifically, quercetin described above are thought, at least in part, to be due to quercetin's anti-platelet effect.

1.9 The anti-platelet effects of quercetin and its metabolites

As discussed in Section 1.7.2, quercetin is extensively metabolised upon intake. The anti-platelet effect of quercetin aglycone has been the focus of a range of studies, but current data is limited regarding potential anti-platelet effects of its metabolites. Much less data has been gathered on these metabolites, the *in vivo* 'effectors' that accumulate and circulate in plasma following quercetin intake. Thus, in this study, the anti-platelet effects of quercetin as well as two methylated plasma metabolites, tamarixetin and isorhamnetin, are investigated. In addition to this, many studies have focussed on the anti-platelet effects of quercetin in washed platelets, as opposed to platelet rich plasma (PRP) or whole blood; as discussed in Section 1.7.2.6, quercetin binds plasma proteins with a high affinity. Nonetheless, research into the effects of quercetin in washed platelets provides a useful investigation into the mechanisms through which quercetin exerts its anti-platelet effects.

Quercetin aglycone has been demonstrated in several studies to inhibit washed platelet function; Oh *et al.* (2012) observed significant inhibition of collagen (2.5μg/mL), thrombin (0.1U/mL) and ADP (10μM) stimulated aggregation at quercetin concentrations between 12.5 and 100μM, with IC_{50} values of 25, 12.5 and 25μM, respectively. Pignatelli *et al.* (2000) also investigated the anti-aggregatory capacity of quercetin, and observed inhibitory effects of 20μM quercetin when washed platelets were stimulated with 2 and 4μg/mL collagen, and Wright *et al.* (2010b) observed an abolition of washed platelet aggregation upon treatment with 40μM quercetin. Oh *et al.* (2012) also demonstrated an inhibition of collagen-stimulated dense granule release and integrin $\alpha_{IIb}\beta_3$ activation at concentrations of 25μM plus, and Hubbard *et al.* (2003) observed significant inhibition of collagen-stimulated calcium mobilisation upon 15-20μM quercetin aglycone treatment. One of the issues with much of the research done on quercetin aglycone is the high concentrations used; intake of quercetin from a dietary source, or through supplementation, is unlikely to reach such high levels; for example, upon ingestion of a high-quercetin onion soup (containing 69mg total quercetin), plasma total quercetin levels peaked at 2.59μM, and, as described in section 1.7.2.6, supplementation with 300mg-1g of

different quercetin glucosides resulted in peak total plasma quercetin concentrations of 9.2-9.72μM (Hubbard *et al.*, 2004; Hubbard *et al.*, 2006; Stopa *et al.*, 2017). The potential effects of lower concentrations of quercetin aglycone must therefore be investigated.

Significantly less work has focussed on the anti-platelet effects of the metabolites of quercetin. One such study that investigated these effects was from Wright *et al.* (2010b), who observed an inhibitory effect of tamarixetin, the 4'-methylated form of quercetin, and quercetin-3'-sulphate, a sulphated derivative. These metabolites inhibited collagen (5μg/mL) stimulated washed platelet aggregation and dense granule secretion with similar potency, but were less potent than quercetin aglycone; Wright *et al.* (2010b) therefore hypothesised that a C-4 carbonyl and C-3 hydroxyl group, as well as a B ring catechol moiety, are associated with increased inhibitory potency. More data on the anti-platelet effect of quercetin's metabolites is clearly required.

Quercetin and its metabolites also inhibit phosphorylation events associated with collagen-stimulated platelet activatory signalling. Quercetin and tamarixetin inhibited significantly collagen-stimulated total tyrosine phosphorylation and PLCγ2 phosphorylation at concentrations of 20μM, and inhibited Syk phosphorylation at 40μM, in a similar manner, with quercetin proving significantly more inhibitory against Fyn kinase activity compared to tamarixetin (Wright *et al.*, 2010b). In addition to this, quercetin aglycone has been demonstrated to inhibit the collagen-stimulated phosphorylation of PI3K, Akt and LAT at concentrations above 25μM (Hubbard *et al.*, 2003; Oh *et al.*, 2012). These inhibitory effects are through direct kinase inhibition; indeed, quercetin possesses broad direct kinase-inhibitory activity, with evidence for an inhibition of MAPKs, ERK, SFKs, PI3K, Akt, Fyn, PLCγ2 and glycogen synthase kinase 3-beta (GSK3β) (Wright *et al.*, 2010b; Boly *et al.*, 2011; Russo *et al.*, 2014b; Wright *et al.*, 2015). Quercetin binds to the ATP binding site of many kinases; through this competitive binding, ATP-binding is inhibited and the kinase cannot transfer a phosphoryl group to its substrate, thus inhibiting substrate activation (Glossman and Eigenbrodt, 1981; Walker *et. al.,* 2000; Breen and Soellner, 2015). The ATP-binding pocket is highly conserved between kinases, and thus

likely explains the wide array of kinases that quercetin effectively inhibits (Vulpetti and Bosotti, 2004). However, there is evidence to suggest quercetin is also able to bind the catalytic domains/active sites of some kinases, such as protein kinase C (PKC) and Haematopoietic cell kinase (HCK); this may offer evidence into the differing inhibitory potency of quercetin against individual kinases (Anzenbacher and Zanger, 2012; Zappia *et. al.,* 2013).

As stated in section 1.7.2.6, quercetin binds heavily to plasma proteins (up to 99%). This reduces the amount of quercetin available to exert anti-platelet effects; therefore, the potential inhibitory effects of quercetin and its metabolites must be examined in PRP. Data examining quercetin aglycone has demonstrated a much-reduced inhibitory potency in PRP; quercetin inhibited ADP (50μM) stimulated platelet aggregation by only 25% at a concentration of 200μM, and inhibited collagen (5μg/mL) stimulated platelet aggregation by less than 10% at the same concentration (Raghavendra and Naidu, 2009; Wright *et al.*, 2013). Pignatelli *et al.* (2006) observed a lack of inhibitory effect of quercetin up to 20μM on collagen (7μg/mL) stimulated aggregation in PRP; however, Chen and Deuster (2009) observed a 50% inhibition of ADP (10μM) induced aggregation by 10μM quercetin, implying that some inhibitory effects are maintained in the presence of plasma proteins. Again, significantly less work has investigated the effects of the metabolites of quercetin on platelet aggregation; in one of the only studies investigating this, Wright *et al.* (2013) concluded a lack of inhibitory effect of up to 200μM tamarixetin on collagen (5μg/mL) induced platelet aggregation in PRP. Indeed, data for the anti-platelet effect of isorhamnetin in PRP is absent from the literature.

In vivo, quercetin and its metabolites act in the medium of whole blood, where anti-platelet effects observed *in vitro* are potentially translated into anti-thrombotic effects. It is therefore crucial to investigate the potential anti-platelet effects of compounds of interest *in vitro* using whole blood; one way in which this can be done is through an *in vitro* assay of thrombus formation under flow. Interestingly, Wright *et al.* (2013) demonstrated a significantly greater effect of tamarixetin compared to quercetin (5μM) in the inhibition of thrombus formation; the magnitude of effect was low, however,

with tamarixetin inhibiting by approximately 5%, and quercetin not inhibiting the process at all. Upon increasing the concentration to 200μM, only a minor increase in inhibition was observed, with tamarixetin and quercetin inhibiting thrombus formation by approximately 10 and 7%, respectively (Wright *et al.*, 2013). Nonetheless, these results demonstrate that metabolism of quercetin may enhance anti-platelet/anti-thrombotic effect. Data on the effects of quercetin and its metabolites on thrombus formation under flow *in vitro* is largely limited to this study, in which only one intermediate (5μM) and one very high, supraphysiological (200μM) concentration was used.

Testing a compound of interest *in vivo* is one of the best ways to elucidate the presence and magnitude of a true anti-thrombotic effect, as it is *in vivo* that any compound of interest will act upon administration. Several studies have examined the *in vivo* anti-thrombotic effect of different quercetin forms. A recent study by Liang *et al.* (2015) investigated the anti-thrombotic effect of pentamethylquercetin (PMQ), a form of quercetin found in seabuckthorn and identified in dog plasma at levels up to 8μM after intra-gastric administration of a 20mg/kg dose (Hibasami *et al.*, 2005; Chen *et al.*, 2011). Liang *et al.* (2015) observed that an intravenous (IV) dose of 20mg/kg PMQ in mice significantly improved blood flow in a ferric chloride-induced arterial thrombosis model, with anti-thrombotic potency similar to 50mg/kg aspirin. This demonstrates a potent anti-thrombotic efficacy of this quercetin derivative; however, the method of administration (IV) and concentration of flavonoid administered reduces the physiological significance of these findings. Jasuja *et al.* (2012) have demonstrated a potent anti-thrombotic effect of quercetin-3-rutinoside (rutin) using a murine laser injury model of thrombosis. Intravenous administration of 0.5mg/kg rutin prior to injury dramatically inhibited thrombus formation; a recent study by Lin *et al.* (2015) has shown that this inhibition is due to inhibition of protein disulphide isomerase (PDI), an oxidoreductase required for thrombus formation, with Jasuja *et al.* (2012) concluding only quercetin metabolites with a 3-O-glycoside moiety are able to inhibit PDI activity. However, as discussed in Section 1.7.2, during absorption and metabolism, glycoside moieties are cleaved (with rutin undergoing significant colonic metabolism), and quercetin glycosides are not found in plasma following oral quercetin intake. Thus,

the relevance of these findings is limited, and more work must be undertaken to investigate the *in vivo* anti-thrombotic effects of quercetin upon oral intake of quercetin glycosides, the main forms found in foods, allowing for full absorption and metabolism.

Studies of platelet function *ex vivo* following quercetin supplementation have also been undertaken. In a study by Hubbard *et al.* (2004), ingestion of 150mg of quercetin-4-O-β-D-glucoside by human subjects resulted in an inhibition of collagen (0.5μg/mL) stimulated platelet aggregation, as well as an inhibition collagen (25μg/mL) stimulated total tyrosine and Syk tyrosine phosphorylation at both 30 and 120 minutes post-intake. A nutritional study, in which participants consumed onion soup high in quercetin (69mg total), observed an inhibition of collagen (25μg/mL) stimulated Syk tyrosine phosphorylation at 1 hour, and a trend towards inhibited collagen (0.5μg/mL) stimulated aggregation at 1 and 3 hours (Hubbard *et al.*, 2006). Recently, Stopa *et al.* (2017) demonstrated the anti-platelet effects of a 1g isoquercetin (quercetin-3-glucoside) dose; they observed a significant reduction of PDI activity 2 hours after dose administration. Stopa *et al.* (2017) also demonstrated that isoquercetin administration inhibited platelet thrombin and factor Va generation by approximately 50% after 4 hours. It is therefore hypothesised that this quercetin glucoside may demonstrate effective *in vivo* anti-thrombotic action; this hypothesis is tested in this study.

There is also limited evidence that quercetin can interact and synergise with other flavonoids and anti-platelet medications in the inhibition of platelet function. Pignatelli *et al.* (2000) demonstrated that, individually, 5μM quercetin and 25μM catechin were unable to inhibit collagen (4μg/mL) stimulated platelet aggregation; when added together, however, significant inhibition of platelet aggregation was achieved (approximately 60% inhibition). This flavonoid combination also inhibited platelet calcium mobilisation and IP_3 formation (Pignatelli *et al.*, 2000). A study by Crescente *et al.* (2009) demonstrated that a resveratrol, gallic acid and quercetin mixture (as found in red wine) did not inhibit platelet aggregation, but when aspirin was added, also at a sub-inhibitory level, a significant effect on platelet aggregation was observed, providing evidence for a potential interaction between quercetin

and aspirin that warrants further investigation (also performed in this study). The potential interactions between quercetin's metabolites and anti-platelet medications such as aspirin have, however, not been investigated.

1.10 Mathematical modelling of platelet function, haemostasis and thrombosis, and flavonoid pharmacokinetics

In addition to traditional 'wet lab' experimentation, mathematical modelling approaches to scientific questions in cardiovascular and platelet biology are being increasingly utilised to understand and predict the mechanisms through which platelet function and signalling are regulated. The development of mathematical models to describe biological systems is allowing *in silico* experimentation, and combined with *in vitro* and *in vivo* data, allows simulations and predictions describing complex biological phenomenon that may not have been easily elucidated in the laboratory.

On the individual platelet scale, a recent study by Dunster *et al.* (2015) examined GPVI signalling, specifically investigating the regulation of the early steps of this pathway by phosphatases. The development of a series of nonlinear ordinary differential equation (ODE) models, in tandem with the collection of *in vitro* platelet signalling data, allowed them to exclude the possibility of a constitutively active phosphatase in the regulation of this process; instead, model development led to a complex interactive pathway with a key role for the phosphatase T-cell ubiquitin ligand-2 (TULA-2) in the regulation of Syk activity. Model simulations also allowed the prediction that a single TULA-2 molecule would dephosphorylate numerous Syk molecules, thus implying GPVI receptor clustering as a crucial mechanism involved in both activation and the regulation of activation (Dunster *et al.*, 2015). This mathematical modelling study also resulted in the novel hypothesis that the temporal regulation, as opposed to the response magnitude, may be more critical to the GPVI pathway of platelet activation, demonstrating the ability of modelling studies to output novel biological hypotheses (Dunster *et al.*, 2015).

On a more macroscopic scale, numerous mathematical models have been developed to describe the process of thrombus formation and predict important regulatory factors in this process. A multi-scale model of thrombus formation by Xu *et al.* (2008) examined the interaction between platelets, the

coagulation cascade, and the dynamics of blood flow, modelling coagulation reactions on the platelet surface as well as blood flow around the developing thrombus. This quantitative model allowed novel predictions that may not have been obvious from qualitative biological experimentation; from this model, low factor VII levels were predicted to cause a significant delay in the production of thrombin in the early stages of venous thrombus formation (Xu *et al.*, 2008; Xu *et al.*, 2009; Xu *et al.*, 2010). A study by Leiderman and Fogelson (2011) presented a spatial-temporal model of thrombus formation, examining the interactions between coagulation reactions, platelet activation, and blood flow. From the model, they hypothesise that wall shear rate, platelet concentration at the vessel wall, and fluid dynamics within a porous, developing thrombus are crucial to the overall formation of a thrombus (Leiderman and Fogelson, 2011). Again, these novel conclusions may not have easily been elucidated from biological experimentation, and demonstrate the usefulness of mathematical modelling approaches.

As well as platelet function, mathematical modelling approaches can also be utilised to investigate and model flavonoid pharmacokinetics. One example of this comes from Chen *et al.* (2005), which presented a model of quercetin pharmacokinetics in rats. Upon oral administration of quercetin aglycone, pharmacokinetic parameters were obtained, and from this, a mathematical model of the absorption, metabolism and excretion of quercetin and its metabolites in rats was developed. This study highlighted the importance of gut metabolism, with approximately 93% of quercetin metabolised here, with 3.1% metabolised in the liver (Chen *et al.*, 2005). A two-compartment pharmacokinetic model was presented that describes the metabolic fate of quercetin aglycone and its metabolites from administration through to excretion, as well as plasma aglycone and metabolite profiles over time, and matches well biological data gathered in the study (Chen *et al.*, 2005).

Mathematical models presented in the literature have largely focussed on either platelet function and thrombus formation, or flavonoid/quercetin pharmacokinetics. The future development of mathematical models linking these three parameters may therefore prove useful in elucidating the contribution of specific metabolites to pharmacodynamic effects on platelet function and thrombus

formation, specifically in relation to their plasma concentration over time profile, as well as in the development of more complex models including other dietary flavonoids and, potentially, anti-platelet medications.

The models presented in this study include two mathematical models of platelet aggregation, and one model of thrombus formation, developed to include pharmacokinetic equations in a pharmacokinetic/pharmacodynamic model of quercetin metabolism, elimination and anti-thrombotic effect. The aggregation models developed utilised linear ordinary differential equations, describing the change over time in the population of inactive, active and aggregated platelets; this approach was chosen as the aim of the modelling was to develop simple models that could be fitted to *in vitro* data, and developed to incorporate other flavonoids, metabolites or anti-platelet drugs. The thrombus formation model also utilised linear ordinary differential equations describing the growth of a thrombus over time; again, the aim was not to include all the complexities and multiple scales of the underlying biological processes, but to describe in a simple yet accurate manner the overall biological process and its inhibition by quercetin and its methylated metabolites, and to allow for *in silico* experimentation. This was extended in the PK/PD model, to include the metabolism and elimination of quercetin; ordinary differential equations were again utilised in a one-compartment model.

1.11 Hypothesis

Quercetin inhibits thrombosis through anti-platelet mechanisms, the efficacy of which are modulated by its metabolism, and can be mathematically modelled to predict inhibitory mechanisms, interactions, and optimal dosing regimens. The methylated metabolites tamarixetin and isorhamnetin maintain anti-platelet effects in platelet rich plasma and whole blood, and interact with aspirin to enhance anti-platelet effects.

1.12 Research objectives

Previous work on the anti-platelet effects of quercetin has focussed largely on the ability of quercetin aglycone to inhibit washed platelet function. However, it is the metabolites of quercetin that are the final 'effectors' *in vivo*. Methylated metabolites are some of the key metabolites identified in plasma following quercetin intake; however, relatively little is known about their anti-platelet effects. One of the first objectives, therefore, was to initially assess the potency of, and the mechanisms through which, quercetin and its methylated metabolites tamarixetin (4'-methylquercetin) and isorhamnetin (3'-methylquercetin) inhibited *in vitro* washed platelet function, individually and in combination, focussing specifically on physiologically relevant quercetin concentrations as demonstrated in dietary and supplemental intake studies.

It has been demonstrated that quercetin binds heavily to plasma proteins. Having established the potencies and gained mechanistic insight into the anti-platelet effects of quercetin, tamarixetin and isorhamnetin, the next step was to elucidate how anti-platelet efficacy translated from washed platelets to platelet rich plasma and whole blood. Following on from this, research focussed on investigating the anti-platelet effects of novel quercetin formulations in *in vitro* washed platelet functional assays, as well as potential anti-thrombotic effects in an *in vivo* murine laser injury model of thrombosis. Having characterised the efficacy of quercetin and its methylated metabolites in the inhibition of

platelet function, an investigation was also undertaken into their interaction with the most commonly used anti-platelet agent, aspirin.

Furthermore, having established *in vitro* anti-platelet and anti-thrombotic actions of quercetin and its methylated metabolites, as well as an *in vivo* anti-thrombotic effect of isoquercetin, mathematical models were developed describing the effects of quercetin, tamarixetin and isorhamnetin on platelet activation, aggregation and thrombus formation, and incorporated into a pharmacokinetic/pharmacodynamic (PK/PD) model of the anti-thrombotic actions of quercetin. These models were developed with a view to running *in silico* experimentation, investigating the best doses and dosing regimens to achieve optimal anti-thrombotic effect upon quercetin supplementation.

The key questions addressed during this project therefore include:

- What are the mechanisms through which quercetin and its methylated metabolites tamarixetin and isorhamnetin inhibit platelet function *in vitro*, and does methylation modulate the anti-platelet potency?
- How do the anti-platelet effects of quercetin, tamarixetin and isorhamnetin translate from washed platelets to platelet rich plasma and whole blood?
- Does isoquercetin inhibit *in vivo* thrombosis in a murine laser injury model?
- Are there interactions between quercetin, its methylated metabolites, and aspirin in the inhibition of platelet function?
- How can mathematical models describe the anti-activatory, anti-aggregatory and anti-thrombotic effects of quercetin and its metabolites, and what does a PK/PD model of the anti-thrombotic effect of quercetin and its metabolites predict to be the best dose and dosing regimen to achieve consistent effects?

2 – Materials and Methods

2.1 Materials

2.1.1 Flavonoids

Quercetin was purchased from Sigma (Poole, UK) and isorhamnetin, tamarixetin and quercetin-3-glucuronide was from Extrasynthese (Lyon, France). QU995, QU995 plus vitamins B3 and C (QB3C), IQC950AN (isoquercetin) and IQC950AN plus vitamins B3 and C (isoblend) were supplied by Quercegen Pharmaceuticals LLC (Marlborough, MA, USA).

2.1.2 Agonists

Horm-Chemie collagen (collagen fibres from equine tendons) was from Nycomed (Munich, Germany). Thrombin from bovine plasma was from Sigma (Poole, UK) and cross-linked collagen-related peptide (CRP-XL) was provided by Professor Richard Farndale (University of Cambridge, UK). U46619, a thromboxane A2 analog, was from Tocris Biosciences (Bristol, UK). Adenosine diphosphate (ADP) was from Sigma (Poole, UK).

2.1.3 Antibodies

Flourescein isothiocyanate (FITC) conjugated polyclonal rabbit anti-human fibrinogen antibody was from Dako (Glostrup, Denmark; catalog no. F0111), and PE/Cy5 mouse anti-human CD62P monoclonal antibody was from BD Biosciences (New Jersey, USA; catalog no. 551142, clone AK-4). FITC anti-human CD42b mouse monoclonal antibody was from Affymetrix (San Diego, CA, USA)(now Thermo Fisher Scientific, Massachusetts, USA; catalog no. 11-0429-42, clone HIP1). Anti-Syk phospho-tyrosine 525+526 rabbit polyclonal antibody was from Abcam (Cambridge, UK; catalog no. ab58575), and anti-LAT phospho-tyrosine 200 rabbit monoclonal antibody was from Abcam (Cambridge, UK; catalog no. ab68139, clone EP983(2)Y). Anti-β3 integrin (N-20) goat polyclonal antibody was from Santa-Cruz Biotechnology (Dallas, TX, USA; catalog no. sc6627). Alexa Fluor 647 donkey anti-rabbit polyclonal antibody (catalog no. A-31573) and Alexa Fluor 488 donkey anti-goat polyclonal antibody (catalog no. A-11055) were from Life Technologies (Carlsbad,

CA, USA) (now Thermo Fisher Scientific, Massachusetts, USA) . DyLight 649 anti-GPIbα antibody for use in mice was from EMFRET Analytics (Würzburg, Germany; catalog no. M0403, clone Xia.G5).

2.1.4 Animals

C57BL/6 mice were from Envigo (Huntingdon, UK)

2.1.5 Other Reagents

Alexa Fluor 488 annexin V was from Life Tech (Carlsbad, CA, USA)(now Thermo Fisher Scientific, Massachusetts, USA; catalog no. A13201). CHRONO-LUME kit was from Chronolog (PA, USA). Clear and black 96-well flat bottom plates were from Greiner Bio One (Frickenhausen, Germany). Glass microscope slides were from Thermo-Fisher Scientific (Waltham, MA, USA), and ProLong Gold Antifade Mountant was from Life Tech (Carlsbad, CA, USA). Circular coverglasses (13mm) were from Agar Scientific (Essex, UK). Fibrinogen from human plasma was from Sigma (Poole, UK). Paraformaldehyde (16%, methanol-free) was from Agar Scientific (Essex, UK). Alexa Fluor 488 phalloidin was from Thermo-Fisher Scientific (Waltham, MA, USA). GPRP (Gly-Pro-Arg-Pro) was from Sigma (Poole, UK). Protease-free bovine serum albumin (BSA) was from First Link (Wolverhampton, UK). Phosphate-Buffered Saline (PBS) tablets were from Sigma (Poole, UK). Immun-Blot PVDF membrane, 10X Tris/glycine/SDS buffer, Precision Plus Protein dual colour standard and 4-20% Mini-PROTEAN TGX (Tris-Glycine eXtended) precast protein gels (15-well, 15μl) were from Bio-Rad (Hercules, CA, USA). Whatman 3MM Chr chromatography paper was from Thermo Fisher Scientific (Waltham, MA, USA). Fura-2-AM and Tris were from Thermo-Fisher Scientific (Waltham, MA, USA). Digitonin and EGTA were from Sigma (Poole, UK). DioC6(3) (3,3'Dihexyloxacarbocyanine iodide) 98% was from Sigma (Poole, UK). Vena8 Fluoro+ biochips were from Cellix Ltd (Dublin, Ireland). Platelet function analyser (PFA)-100 cartridges were from Sysmex (Milton Keynes, UK). All other reagents were obtained from Sigma (Poole, UK).

2.2 Methods

2.2.1 Human platelet preparation

Human blood was taken from consenting, drug-free volunteers on the day of the experiment according to methodology approved by the University of Reading Research Ethics Committee. Blood was taken using 4% (w/v) sodium citrate and Acid Citrate Dextrose (ACD; 110mmol/L glucose, 80mmol/L citric acid, 120 mmol/L sodium citrate) as anticoagulant. Whole blood was centrifuged at 102*g* for 20 minutes at 20^{o}C to yield platelet rich plasma (PRP). Where washed platelets were required, they were isolated from the PRP by further centrifugation at 1413*g* for 10 minutes at 20^{o}C in the presence of 0.1μg/mL prostacyclin to prevent activation. The supernatant was discarded in Klorsept disinfectant (Medentech, Wexford, Ireland) and the platelet pellet was resuspended in 25mL of modified Tyrodes-HEPES buffer (134mmol/L NaCl, 0.34mmol/L Na_2HPO_4, 2.9mmol/L KCl, 12mmol/L $NaHCO_3$, 20mmol/L HEPES, 5mmol/L glucose, 1mmol/L $MgCl_2$, pH 7.3) and 3mL of ACD in the presence of 0.1μg/mL prostacyclin. Platelets were centrifuged at 1413*g* for 10 minutes at 20^{o}C and resuspended to a density of 2 or 4 X 10^8 cells/mL in modified Tyrodes-HEPES buffer using a platelet count obtained with a Z series Coulter Counter (Beckman Coulter, CA, USA). Washed platelets were rested for at least 30 minutes at 30^{o}C prior to the experiment to allow responses to recover.

ADP-sensitive washed platelets (used in studying the effects of quercetin and its methylated metabolites on platelet aggregation stimulated by soluble agonists, Section 3.7) were prepared by collecting blood into 4% (w/v) sodium citrate and centrifugation at 102*g* for 20 minutes at 20^{o}C to yield PRP (without addition of ACD). Platelets were isolated from the PRP by further centrifugation at 350*g* for 20 minutes. This slower centrifugation protocol prevents receptor desensitisation associated with higher centrifugation speeds. The supernatant was discarded and the platelet pellet was re-suspended to a density of 2 or 4 X 10^8 cells/mL in modified Tyrodes-HEPES buffer.

2.2.2 Platelet aggregometry

Light transmission aggregometry (LTA) was performed in an optical platelet aggregometer (Chrono-Log, PA, USA, and Helena Biosciences Europe, Gateshead, UK), as originally described by Born (1962). Washed platelets or PRP (450µL) were stimulated in the presence of agonist (50µL) with continuous stirring (1200rpm at 37^{o}C) for 5 minutes and aggregation was measured as an increase in light transmittance. The effects of flavonoids on platelet aggregation were measured by incubating washed platelets or PRP with 1µL flavonoid dissolved in 100% DMSO or 100% DMSO alone (final DMSO concentration in sample of 0.2% v/v) for 5 minutes (with an initial 10s stirring to distribute flavonoid) prior to the addition of agonist.

Plate-based aggregometry was performed using a NOVOstar plate reader (BMG Labtech, Ortenberg, Germany), with a modified protocol to that originally described by Lordkipanidzé *et al.* (2014). Washed platelets at a concentration of 2X10^{8} cells/mL or PRP were loaded into 96-well plates and treated with vehicle control (1% DMSO, v/v), flavonoids (for 5 minutes), aspirin (for 30 minutes) or both at 37^{o}C prior to addition of agonist. After agonist addition, plates were then shaken at 1200rpm for 5 minutes at 37^{o}C using a BioShake iQ plate shaker (Quantifoil Instruments, Jena, Germany). Absorption of 405nm light was measured in the plate reader and values converted to percentage aggregation using unstimulated and stimulated (uninhibited) samples to represent 0% and 100% aggregation, respectively.

2.2.3 Flow cytometric analyses

Fibrinogen binding was measured using FITC-conjugated polyclonal rabbit anti-human fibrinogen antibody, and P-Selectin exposure was measured using PE/Cy5 mouse anti-human CD62P antibody in a 96-well flat bottom plate. Washed platelets (2 X 10^{8} cells/mL) were treated with flavonoids or DMSO (0.25% v/v) and incubated for 5 minutes at room temperature with occasional gentle mixing. 1µL anti-fibrinogen and 1µL anti-CD62P antibody were added per sample prior to stimulation with agonists for 20 minutes. Where thrombin was used as an agonist, GPRP (25µg/mL) was added to

prevent fibrin polymerization. Samples were subsequently diluted to 2 X 10^7 cells/mL for flow cytometric analysis.

Annexin V binding (as a marker for phosphatidylserine exposure) and GPIb exposure were also measured by flow cytometry. Alexa Fluor 488 annexin V or FITC anti-human CD42b mouse monoclonal antibody was added to washed platelets (2 X 10^7 cells/mL) in a 96-well flat bottom plate. Quercetin, vehicle (negative) control (DMSO, 0.25% v/v) or positive control were added and incubated for 20 minutes.

Reactions were stopped and samples fixed in 0.2% (w/v) paraformaldehyde. Analyses were performed by flow cytometry using a BD Accuri C6 flow cytometer (BD Biosciences, Oxford, UK), and data were collected from 10,000 events (gated on platelets using FSC (forwards scatter, limited between 1520-16000000) and SSC (side scatter, limited between 152-1600000)) and analysed using inbuilt BD Accuri C6 plus software, version 1.0.264.21.

2.2.4 Dense granule secretion

Dense Granule secretion was measured using a lumi-aggregometer (model 700, Chronolo-Log, PA, USA), to detect ATP secreted from platelet dense granules upon stimulation as first described by Feinman *et al.* (1977). Washed platelets at a density of 4 X 10^8 cells/mL were used. 399µL of washed platelets were added to a glass cuvette and incubated with 50µL of Chronolume reagent for 2 minutes. 2nM ATP was added to this stirred suspension of platelets to set the ATP response baseline. The luminescence increase was observed using the AggroLink 8 software (Chrono-Log, PA, USA), with the luminescent gain adjusted until the ATP response was within the manufacturer-instructed range of 20-60%. These settings were saved and used for the rest of the experiment. Flavonoids or vehicle control (DMSO, 0.25% v/v) were incubated with washed platelets for 5 minutes, with Chronolume reagent (50µL) added after 3 minutes, prior to collagen (5µg/mL) addition and setting the baseline.

Dense granule secretion was measured for 3 minutes following the addition of collagen using the AggroLink 8 software, which calculates ATP secretion levels from the 2nM ATP standard.

2.2.5 Platelet adhesion and spreading

Glass coverslips were coated in 6 well plates with 1μg/mL CRP-XL or 100μg/mL fibrinogen (in modified Tyrodes-HEPES buffer) for 1 hour. 1% BSA was then added onto coverslips and incubated for 1 hour to prevent platelets binding to glass. Coverslips were washed 3 times with PBS (10mmol/L phosphate buffer, 2.7mmol/L KaCl, 137mmol/L NaCl, pH 7.4). Washed platelets at a density of 2 X 10^8 cells/mL were incubated with flavonoid (1μl, 0.33% v/v DMSO) for 5 minutes, diluted to 2 x 10^7 cells/mL and added onto coverslips and incubated for 45 minutes at 37^{o}C. Supernatant was then removed from the coverslips, which were again washed 3 times with PBS. Platelets were then fixed with 0.2% (w/v) PFA for 10 minutes, and the supernatant was removed and coverslips washed 3 times with PBS. Platelets were then permeabilized with 0.2% Triton-X for 5 minutes, and then supernatant was removed and coverslips washed 3 times again with PBS. Alexa-Fluor 488 phalloidin was then added onto the coverslips for 1 hour, incubated in the dark, to label platelet F (filamentous) -actin. Supernatant was removed and coverslips washed 3 times with PBS. Coverslips were then mounted onto slides with addition of Prolong Gold Antifade mountant to preserve fluorescence. Samples were imaged the next day, using a 100X oil immersion lens on a Nikon A1-R confocal microscope (Nikon, Tokyo, Japan). Fluorescence was excited at 488nm with an argon laser and emitted at 500-520nm, with images captured in one focal plane. Platelet adhesion data were obtained by counting the number of platelets on 5 images of each coverslip that were captured randomly. Platelets were scored as adhered (not spread), spreading (defined as extending filopodia) or spread fully (lamellipodia formed), and the relative frequency of each population was determined.

2.2.6 Cytosolic calcium elevation – measurement of $[Ca^{2+}]_i$

PRP was loaded with the fluorescent dye Fura-2, which binds free intracellular calcium, by adding 2μM Fura-2 AM to PRP and incubating for 1 hour at 30^{o}C. After this incubation, PRP was centrifuged

at 350*g* for 20 minutes and the resultant platelet pellet was resuspended in modified Tyrodes-HEPES buffer to yield a platelet density of 4 X 10^8 cells/mL. Fura-2 AM loaded washed platelets were incubated with flavonoid (0.2% v/v DMSO) or vehicle control for 5 minutes at 37°C prior to addition of CRP-XL 1µg/mL. Fluorescence measurements (excitation 340 and 380nm, emission 510nm) were recorded for 5 minutes (1 measurement every 1.5s) using a NOVOstar plate reader. Dual excitation (at 340 and 380nm) allows quantification of $[Ca^{2+}]_i$; free Fura-2 peak excitation occurs at approximately 380nm, whereas calcium-bound Fura-2 peak excitation is at ~340nm (Bootman *et al.*, 2013). $[Ca^{2+}]_i$ was estimated by utilizing the methodology of Grynkiewicz *et al.* (1985) summarized below, using the ratio of the 340nm and 380nm excited signals. In one untreated sample, 50µM digitonin was added to lyse the platelets, releasing the Fura-2 into the Tyrodes buffer, containing 2mM $CaCl_2$, allowing measurement of the maximum fluorescence ratio. To calculate the minimum fluorescence ratio, Ca^{2+} ions were chelated by addition of 10mM ethylene glycol-bis(β-aminoethyl ester)-N,N,N',N'-tetraacetic acid (EGTA) and 10mM TRIS base (added to ensure an alkaline pH for optimal Ca^{2+} chelation by EGTA). Autofluorescence was measured using unloaded platelets at 4 X 10^8 cells/mL. Using the calibration values from above, experimental $[Ca^{2+}]_i$ concentrations were calculated using the following equation:

$$[Ca^{2+}]_i = K_d \times \frac{S_f}{S_b} \times \frac{R - R_{min}}{R_{max} - R}$$

Where K_d is the dissociation constant of Fura-2 (224nM). S_f and S_b are the values of the fluorescence at 380nm excitation (corrected to background autofluorescence), with zero or saturating Ca^{2+} respectively. R is the 340/380nm fluorescence ratio, corrected to background fluorescence. R_{min} and R_{max} are the ratio limits at zero or saturating Ca2+, respectively, adjusted using a viscosity constant of 0.85. This corrects for the effects of the cellular environment on the fluorescence of Fura-2.

2.2.7 SDS-PAGE and Immunoblotting

Washed human platelets were prepared to a density of 4 X 10^8 cells/mL. Platelets (225µL) were treated with flavonoids or vehicle control (DMSO, 0.4% v/v) for 5 minutes after 10 seconds stirring (1200rpm, 37^{o}C) in the aggregometer. Platelets were then stimulated with CRP-XL 1µg/mL (25µL), after which 6X reducing sample buffer (12% (w/v) Sodium Dodecyl Sulphate (SDS), 30% (v/v) glycerol, 0.15M Tris-HCl (pH 6.8), 0.001% (w/v) Brilliant Blue R, 30% (v/v) β-mercaptoethanol) (50µL) was immediately added to samples. Samples were heated and boiled at 95^{o}C for 3 minutes before storing at -20^{o}C until use.

Proteins were separated by SDS-PAGE as previously described by Laemmli (1970), using 4-20% Mini-PROTEAN TGX precast protein gels. Samples were heated to 95^{o}C for 3 minutes again prior to loading into gels, which were submerged in 1X Tris/Glycine/SDS buffer (25mM Tris, 192mM glycine, 0.1% SDS, pH 8.3) within a Mini-PROTEAN tetra vertical electrophoresis cell (Bio-Rad, CA, USA). Electrophoresis was run for 45 minutes at a constant voltage of 150V.

Following protein separation, gels were removed from their plates. Sections of 3MM filter paper were soaked in 3 separate transfer buffers; 4 pieces in anode I (300mM Tris, 20% (v/v) methanol, pH 10.4), 2 pieces in anode II (25mM Tris, 20% (v/v) methanol, pH 10.4), and 6 pieces in cathode buffer (25mM Tris, 20% (v/v) methanol, 40mM 6-amino-n-hexanoic acid, pH 9.4). A section of polyvinylidene difluoride (PVDF) membrane was soaked in methanol. Semi-dry western blotting was performed using a Trans-Blot SD semi-dry transfer cell (Bio-Rad, CA, USA). SDS-PAGE gel was transferred on top of PVDF membrane, on top of anode I and anode II buffer-saturated filter paper. Cathode buffer-saturated filter paper was added onto this and placed between electrodes of the semi-dry blotter. Proteins were then transferred for 2 hours at 15V.

PVDF membranes were then transferred into a 2% (w/v) solution of bovine serum albumin (BSA) dissolved in TBS-T (Tris buffered saline with Tween 20; 20mM Tris, 140mM NaCl, 0.1% Tween, pH

7.6) to block the membrane for 1 hour at room temperature. Primary antibodies were diluted to a concentration of 1:1000 in a 2% (w/v) solution of BSA (dissolved in TBS-T) and membranes were incubated with these solutions overnight at 4^{o}C on a rotator. Primary antibody solutions were removed from the PVDF membranes the next day and membranes were washed 3x10 minutes with TBS-T. Secondary antibodies (Alexa Fluor 647 donkey anti-rabbit polyclonal antibody and Alexa Fluor 488 donkey anti-goat polyclonal antibody) were added 1:4000 to a 1% BSA (dissolved in TBS-T) solution, which was then added to PVDF membranes and incubated in the dark at room temperature for 1 hour. PVDF membranes were washed 3x5 minutes with TBS-T. PVDF membranes were scanned using a Typhoon Trio fluorescence imager (Amersham Biosciences, Buckinghamshire, UK), and levels of fluorescence of individual bands were normalised to loading controls.

2.2.8 Clot retraction

To measure the retraction of a thrombin-stimulated clot, PRP was obtained and prepared as described above. PRP was incubated with flavonoid or vehicle control (0.25% v/v DMSO) for 60 minutes, to mimic approximate peak flavonoid time upon consumption. 745µL of warmed modified Tyrodes-HEPES buffer was added (to make the final volume 1mL) to test tubes, along with 5µL of red blood cells, to allow visualization of the clot. 50µL of thrombin (final concentration 1U/mL) was added to the test tubes, after which 200µL of PRP was added to initiate clot formation. A glass pipette was added to the centre of each test tube, around which the clot would form, and samples were placed in an incubator chamber at 30^{o}C. Photographs were taken every 15 minutes and the assay was terminated at 2 hours, once the vehicle-treated samples' clots had retracted fully. Clots were removed from the glass pipettes and transferred into allocated microfuge tubes, which had been individually pre-weighed. Remaining plasma was transferred into separate allocated microfuge tubes. Clot plus microfuge tube and plasma plus microfuge tube weights were measured, and the weight of the microfuge tubes subtracted to give clot mass and plasma mass for each sample.

2.2.9 Platelet Function Analyser (PFA)-100

The platelet function analyser (PFA)-100 (Siemens, Munich, Germany) utilises citrated (3.2% sodium citrate) human whole blood drawn through cartridges which contain a nitrocellulose membrane (0.45μm pore size) coated with collagen and ADP (CADP, 2μg type I equine fibrillar collagen plus 50μg adenosine 5'-diphosphate) or collagen and epinephrine (CEPI, 2μg type I equine fibrillar collagen plus 10μg epinephrine bitartrate), with a 200μm aperture cut into the membrane, as originally described by Kundu *et al.* (1995). Whole blood flows through the aperture, platelets adhere and aggregate and upon blockage of the aperture a 'closure time' (CT) is reported. Citrated human whole blood was treated with flavonoid, aspirin or vehicle control (0.1% DMSO + 0.1% ethanol, v/v) for 60 minutes at 30^{o}C, after which 800μL whole blood was added into the reservoir of the cartridges (which had been coming to room temperature for 60 minutes). Cartridges were loaded into the PFA-100 analyser carousel and samples were then run; an automated process during which samples were assigned an ID, the carousel is heated to 30^{o}C, and whole blood is drawn through the aperture using the negative pressure of a vacuum at a shear rate between 5000 and 6000s^{-1}. Upon occlusion of the aperture, the test is concluded and the closure time is automatically printed.

2.2.10 **In vitro** *thrombus formation under flow*

Human whole blood was incubated at 30^{o}C with 5μM of the lipophilic dye DiOC6 for 1 hour. Vena8 BioChip microfluidic channels were coated with type I collagen 100μg/mL for one hour and excess collagen washed through with modified Tyrodes-HEPES buffer. Whole blood was incubated with flavonoids or vehicle control (0.2% v/v DMSO) for 10 minutes prior to perfusion through the collagen-coated microfluidic channels at an approximately arteriolar shear rate of 500s^{-1} (shear stress of 20 dyn/cm^{2}). Fluorescence was excited at 488nm with an argon laser and emission detected at 500-520nm. The microfluidic channel was observed on the 20X objective of a Nikon A1-R confocal microscope, with images captured every 1 second for 600 seconds. Mean thrombus fluorescence intensity was calculated using NIS Elements software (Nikon, Tokyo, Japan).

2.2.11 In vivo *thrombus formation*

In vivo thrombus formation was performed as initially described by Falati *et al.* (2002). C57BL/6 mice were dosed twice per day by gavage, once in the morning (9am), and once in the afternoon (5pm), with 200mg/kg of isoblend containing 0.2mg/kg folic acid, or vehicle (100µl distilled water, 39mg/kg ascorbic acid, 3mg/kg niacin, 0.2mg/kg folic acid). This gavage was performed 48 hours or 72-hours before the experiment was initiated (corresponding to 5 or 7 doses, respectively), to mimic a potential method of human supplemental consumption of isoquercetin. On the day of the experiment, mice were anaesthetised by intraperitoneal injection of ketamine (125mg/kg), xylazine (12.5mg/kg) and atropine (0.25mg/kg). Anaesthesia was maintained with 5mg/kg pentobarbital as required, through a carotid artery cannula. The cremaster muscle of the testicle was exteriorized and the connective tissue removed, after which an incision was made, allowing the cremaster muscle to be affixed over a glass slide as a single sheet; the muscle preparation was hydrated throughout with buffer (135mM NaCl, 4.7mM KCl, 2.7mM $CaCl_2$, 18mM NaHCO3, pH 7.4). Platelets were labelled with DyLight 649 anti-GPIbα antibody (0.2µg/g mouse weight), and cremaster arteriole wall injury was performed using a Micropoint Ablation Laser Unit (Andor Technology PLC, Belfast, Northern Ireland). Thrombus formation was observed using an Olympus BX61W1 microscope (Olympus Corporation, Tokyo, Japan), with images captured both prior to and after the injury, using a Hamamatsu digital camera C9300 (Hamamatsu Photonics UK Ltd, Hertfordshire UK) charge-coupled device (CCD) camera in 640 x 480 format. Images were analysed using Slidebook 6 software (Intelligent Imaging Innovations, CO, USA). Isoquercetin preparation and gavage was performed and supervised by myself, with the mouse surgery and data acquisition performed by Dr. Parvathy Sasikumar.

2.2.12 Statistical Analyses and mathematical modelling

Aggregation, fibrinogen binding, P-Selectin exposure, dense granule secretion, adhesion and spreading, intracellular calcium mobilization, quercetin toxicity, clot retraction, PFA-100 closure time and peak protein phosphorylation cell signalling data were analysed by one-way ANOVA with post-hoc Dunnett's multiple comparison test. Aspirin plus flavonoid aggregometry data were analysed by

2-way ANOVA with post-hoc Dunnett's multiple comparison test. *In vitro* thrombus formation under flow data and Syk and LAT phosphorylation data were analysed by 2-way ANOVA with post-hoc Bonferroni multiple comparison correction. *In vivo* thrombus formation analyses were performed by unpaired t-tests. Synergistic effects were analysed by Mann-Whitney U tests (PFA-100 synergy by paired t-tests). All data are presented as means ± SEM, and $P \leq 0.05$ were considered to be statistically significant. All mathematical modelling was performed in MATLAB (version R2015b (MathWorks, 2015)).

3 – Metabolism of quercetin can enhance or reduce its anti-platelet effect

3.1 Metabolism of quercetin can enhance or reduce its anti-platelet effect

Previously, quercetin aglycone has been shown to inhibit human platelet function. Collagen-stimulated aggregation and protein tyrosine phosphorylation, as well as the thrombin and thromboxane A_2-stimulated platelet pathways, are all inhibited by the addition of quercetin aglycone *in vitro* (Hubbard *et al.*, 2003; Guerrero *et al.*, 2007; Navarro-Núñez *et al.*, 2009). Dietary intake also has an effect, with ingestion of quercetin rich onion soup inhibiting collagen-stimulated platelet aggregation *ex vivo* (Hubbard *et al.*, 2006).

Structurally, it has been suggested that a planar, C-4 carbonyl-substituted and a C-3 hydroxylated C ring are important for strong platelet functional inhibition, as well as a B ring catechol group (Wright *et al.*, 2010b). Quercetin aglycone possesses all three of these attributes, whilst its methylated metabolites tamarixetin (4'-methylated) and isorhamnetin (3'-methylated) possess the C ring structures associated with increased potency, but not the B ring catechol moiety. Another metabolite, quercetin-3-glucuronide, possesses the C-4 carbonyl group and B-ring catechol moiety, but not the C-3 hydroxylation. Methylation and glucuronidation are two primary metabolic modifications that flavonoids including quercetin undergo in intestinal enterocytes and liver hepatocytes upon consumption (Hollman, 2004; Wright *et al.*, 2010b; Kumar and Pandey, 2013). Such metabolic changes could have dramatic effects on biological action and resultant anti-platelet effect, but current data is limited due to a paucity of information regarding the actions of these metabolites. Data has largely focused on the aglycone, of which a truly comprehensive picture of *in vitro* anti-platelet function is also incomplete. The aim of this chapter was therefore to investigate the ability of, and the potency with which, quercetin and its metabolites tamarixetin and isorhamnetin (as well as quercetin-3-glucuronide) inhibit human platelet function, in order to understand how metabolic changes to quercetin affects its function.

3.2 Quercetin and its metabolites differentially inhibit collagen-stimulated platelet aggregation

The primary function of platelets is to aggregate at the site of vessel injury; inappropriate formation of aggregates is also important in pathophysiological states such as thrombosis (Andrews and Berndt, 2004; Davì and Patrono 2007; Barrett *et al.*, 2008). Collagen is exposed on the subendothelium upon vessel injury. It was therefore investigated how key metabolic changes to quercetin (methylation and glucuronidation) affected the ability to inhibit collagen-stimulated washed platelet aggregation. A full range of concentrations were tested (1-50μM) to understand potential minimal and maximal effects, as well as to understand the effects at physiologically achievable concentrations. Reported physiological concentrations vary widely according to supplementation/dietary method, dose, and the form of quercetin administered; a range between 0-10μM is used here (and throughout) to represent a feasible physiological concentration (with the upper level of 10μM representing a high, yet fully achievable concentration of total quercetin) (Hubbard *et al.*, 2004; Kashino *et al.*, 2015; Stopa *et al.*, 2017).

Washed human platelets (2 x 10^8 cells/mL) were incubated with quercetin, tamarixetin, isorhamnetin or quercetin-3-glucuronide for 5 minutes at 37^{o}C, following 10s stirring to ensure full mixing of flavonoid into the solution. An incubation period of 5 minutes was chosen for two main reasons. Firstly, data from Wright *et al.* (2013) suggests that at 5, 40 and 120 minutes incubation period, there is not a significant difference in levels of washed platelet aggregation inhibition achieved by quercetin or tamarixetin. The second is a practical reason; in order to keep consistency between washed platelet assays, a fixed incubation time period needed to be chosen. As some assays require a high number of samples, time constraints prevent a longer incubation period. After the incubation period, platelets were stimulated with collagen (5μg/mL; chosen to give strong stimulation) and responses were recorded using an optical aggregometer with continuous stirring (1200rpm) at 37^{o}C for 5 minutes.

This time point was chosen to ensure that any effect seen by the flavonoids were due to true inhibition, and not a delay in the aggregatory response.

Figure 3-1A shows a typical aggregatory response to collagen (5μg/mL); as platelets aggregate, more light passes through the solution, and light transmission increases. Quercetin was able to inhibit this response significantly at concentrations of 5μM (25% inhibition) and above, with concentrations of 7μM plus causing over 90% inhibition of aggregation at this concentration of collagen after 300s (Figure 3-1B). The time point of 5 minutes ensures that any effect seen by quercetin and its metabolites is due to true inhibition, as opposed to a delay in aggregation. The IC_{50}, calculated from a four-parameter nonlinear regression curve, is 5.7 ± 0.49μM (Figure 3-1C); this is lower than previously reported values for inhibition of collagen-stimulated aggregation of ~8.7μM (Hubbard *et al.*, 2003).

As stated previously, quercetin is extensively metabolised upon consumption in the small intestine and liver, and so the abilities of two methylated metabolites, tamarixetin and isorhamnetin, to inhibit collagen-stimulated platelet aggregation, were also investigated. Tamarixetin inhibited significantly aggregation at all concentrations tested (1-50μM), in a concentration-dependent manner (Figure 3-2A/B). An important observation is that of inhibition as low as 1μM, a concentration of flavonoid physiologically achievable through both diet and supplementation. Unlike quercetin, however, full (>90%) inhibition was only seen at concentrations of 20μM and above. Figure 3-2C shows the IC_{50} for tamarixetin of 7.14 ± 0.54μM, slightly higher than that of quercetin (individual donor IC_{50} comparisons demonstrate a statistically significantly lower IC_{50} for quercetin compared to tamarixetin). Isorhamnetin, like quercetin, caused significant inhibition of platelet aggregation at and above 5μM (Figure 3-2D/E). The IC_{50} for isorhamnetin is 4.8 ±1.46 μM (Figure 3-2F), similar to, yet marginally lower than quercetin (not a significant difference when comparing individual donor IC_{50} values). This is caused by increased inhibition seen by isorhamnetin at lower concentrations when compared to quercetin. It may be that *in vivo,* such seemingly small differences are important when considering the relatively low plasma levels of such compounds. IC_{50} values for isorhamnetin were significantly lower

than tamarixetin, demonstrating an interesting difference in potency upon methylation of different residues.

Glucuronidation is another key metabolic modification that occurs *in vivo* upon flavonoid consumption, and so the effect of quercetin-3-glucuronide upon collagen-stimulated platelet aggregation was also tested. At the concentrations tested previously, quercetin-3-glucuronide was unable to significantly inhibit aggregation. The effects of higher concentrations of 100,150 and 200μM were therefore tested (Figure 3-3A). Quercetin-3-glucuronide inhibited significantly platelet aggregation only at 150 and 200μM. Indeed, the magnitude of the effect was still less than seen with quercetin, tamarixetin and isorhamnetin, with 200μM causing ~50% inhibition (Figure 3-3B). This dramatically lower potency is likely due, at least in part, to the cell impermeability of quercetin-3-glucuronide, as discussed later (3-8, 'Discussion of results presented in Chapter 3').

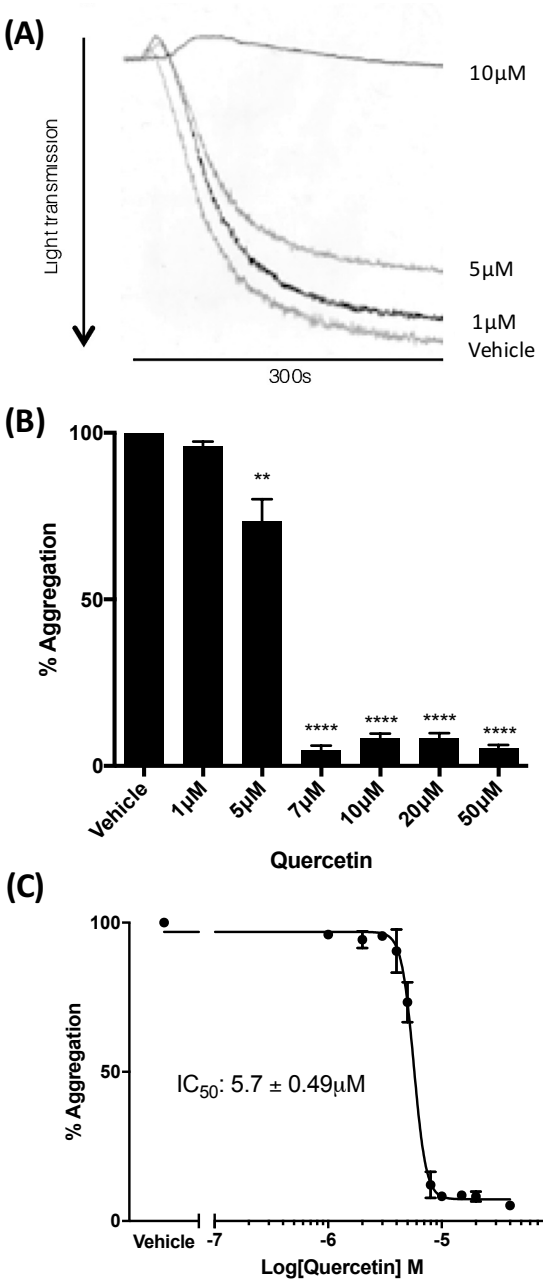

Figure 3-1 Quercetin aglycone inhibits collagen-stimulated washed platelet aggregation

Washed human platelets (2 x 10^8 cells/mL) were incubated with quercetin or vehicle (DMSO, 0.2% v/v) for 5 minutes (with 10 seconds stirring to mix) prior to addition of collagen (5µg/mL). Aggregation was measured for 5 minutes at 37°C under constant stirring (1200rpm) conditions in a Chrono-Log optical platelet aggregometer. (A) Representative traces from aggregation assays. (B) Percentage aggregation of samples at 5 minutes normalised to the level of aggregation in the absence of quercetin (vehicle). (C) Four parameter nonlinear regression curve, used to estimate the IC_{50} of quercetin. N=4, data represent mean ± SEM. ** $p \leq 0.005$, **** $p \leq 0.0001$ compared to vehicle control, analysed by one-way ANOVA with post-hoc Dunnett's test.

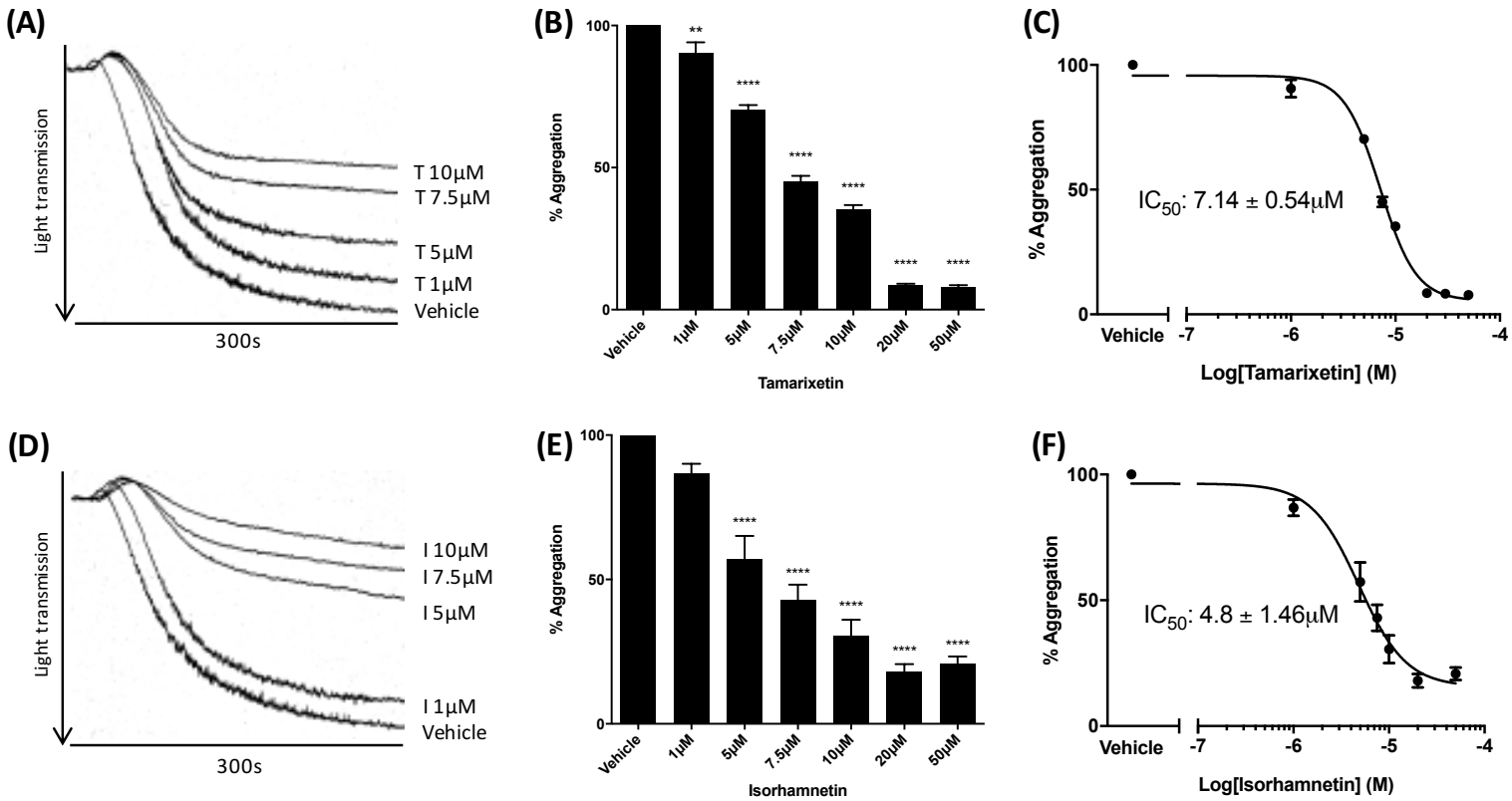

Figure 3-2 Tamarixetin and isorhamnetin inhibit collagen-stimulated washed platelet aggregation

Washed human platelets (2 x 10^8 cells/mL) were incubated with tamarixetin, isorhamnetin or vehicle (DMSO, 0.2% v/v) for 5 minutes (with 10 seconds stirring to mix) prior to addition of collagen (5µg/mL). Aggregation was measured for 5 minutes at 37°C under constant stirring (1200rpm) conditions in a Chrono-Log optical platelet aggregometer. (A/D) Representative traces from aggregation assays for tamarixetin (A) and isorhamnetin (D). (B/E) Percentage aggregation of tamarixetin-inhibited (B) and isorhamnetin-inhibited (D) samples at 5 minutes, normalised to the level of aggregation in the absence of flavonoid (vehicle). (C/F) Four parameter nonlinear regression curve, used to estimate the IC_{50} of tamarixetin (C) and isorhamnetin (F). N=4, data represent mean ± SEM. ** $p \leq 0.005$, **** $p \leq 0.0001$ compared to vehicle control, analysed by one-way ANOVA with post-hoc Dunnett's test. T, tamarixetin; I, isorhamnetin.

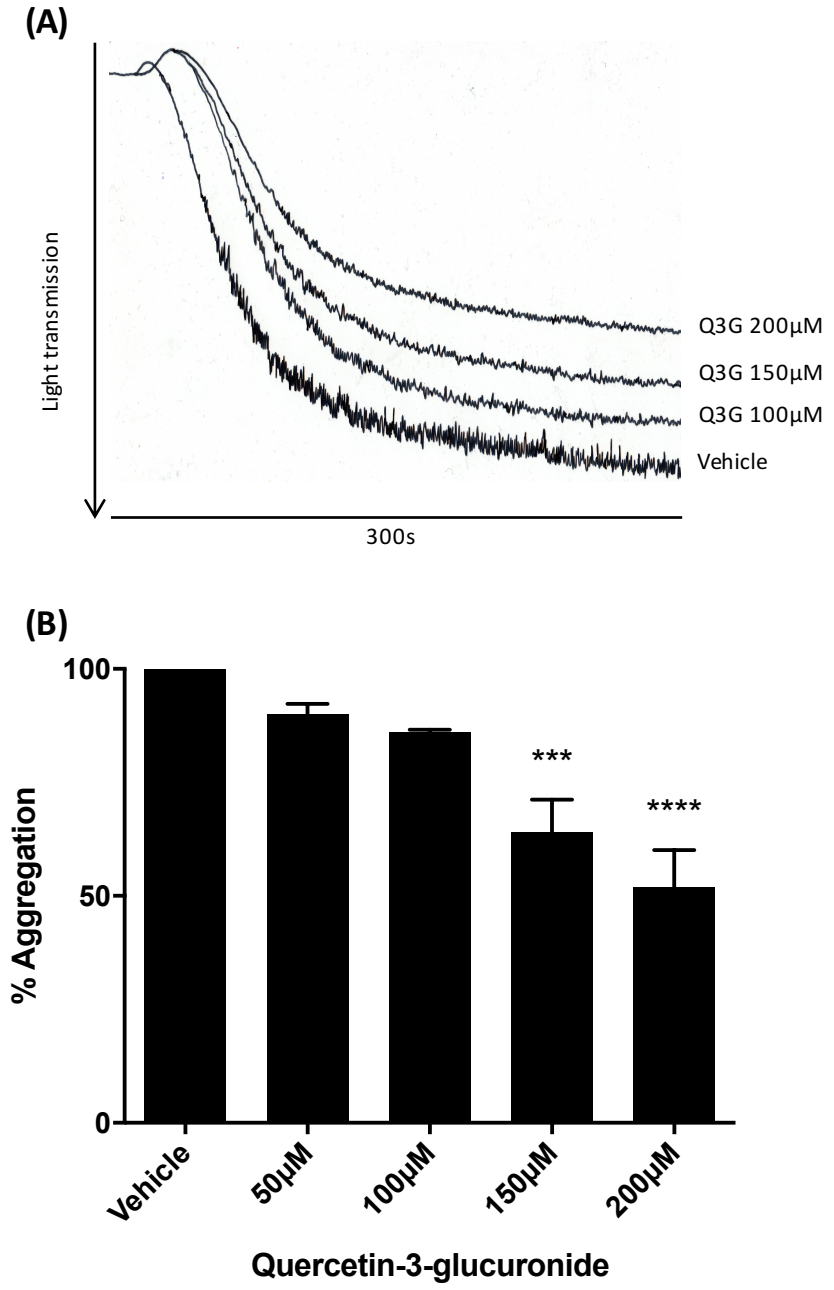

Figure 3-3 Quercetin-3-glucuronide inhibits collagen-stimulated washed platelet aggregation less potently than quercetin, tamarixetin and isorhamnetin

Washed human platelets (2 x 10^8 cells/mL) were incubated with quercetin-3-glucuronide or vehicle (DMSO, 0.2% v/v) for 5 minutes (with 10 seconds stirring to mix) prior to addition of collagen (5µg/mL). Aggregation was measured for 5 minutes at 37°C under constant stirring (1200rpm) conditions in a Chrono-Log optical platelet aggregometer. (A) Representative traces from aggregation assays. (B) Percentage aggregation of samples at 5 minutes normalised to level of aggregation in the absence of quercetin-3-glucuronide (vehicle). N=3, data represent mean ± SEM. ***$p \leq 0.001$, ****$p \leq 0.0001$ compared to vehicle control, analysed by one-way ANOVA with post-hoc Dunnett's test. Q3G, quercetin-3-glucuronide.

3.3 Inhibition of platelet granule secretion by quercetin is altered by its metabolism

3.3.1 Isorhamnetin is a more potent inhibitor of dense granule secretion

A key process driving the positive feedback cycle of platelet activation is the release of stored platelet granules. Dense granules contain many small molecules involved in these early activatory processes, including ATP, ADP and serotonin, and contents are rapidly secreted upon platelet activation (Gear and Burke, 1982; Meyers *et al.*, 1982; Jonnalagadda *et al.*, 2012). It was therefore investigated if dense granule secretion was differentially affected by quercetin and its metabolites. This was performed using lumiaggregometry, as first described by Feinman *et al.* (1977). This assay utilises the firefly luciferin-luciferase reaction. In short, the oxidative enzyme luciferase converts luciferin to oxyluciferin using ATP as energy, and as a result of this reaction, light is emitted (McElroy, 1947). Through the addition of chronolume reagent, which contains luciferin and luciferase, ATP secreted from platelet dense granules is used in this conversion reaction and light is detected in the lumiaggregometer.

Washed human platelets (4 x 10^8 cells/mL) were treated with quercetin, tamarixetin or isorhamnetin or vehicle control for 5 minutes, with chronolume reagent added in the last 2 minutes to allow the luciferin-luciferase reaction to occur. Platelets were used at 4 x 10^8 cells/mL here due to the luciferin-luciferase assay kit and ATP standard being optimised for this platelet concentration as opposed to 2 x 10^8 cells/mL (used for most other assays due to high sample number and being a standard, often-used cell density for *in vitro* experimentation). It must therefore be considered that the effective amount of flavonoid available 'per platelet' may differ here at equivalent concentrations compared to other assays. Platelets were then stimulated with collagen (5μg/mL), and the secretion of ATP was monitored for 3 minutes.

Figure 3-4B shows a typical luminescence trace when vehicle-treated platelets are stimulated; the level of luminescence is proportional to the level of ATP secreted. Quercetin concentration-dependently inhibited the release of dense granules, with significant inhibition achieved at 7.5μM (~50%) and 10μM (~70% inhibition) (Figure 3-4A). There was a trend for increased inhibition from 1μM through to 5μM, which did not reach significance. Tamarixetin affected dense granule secretion very similarly to quercetin (with no significant difference between the two), with significant inhibition also seen at 5μM (Figure 3-4C/D). Isorhamnetin was more potent (statistically significant increased effect compared to quercetin at 5μM and a trend ($p=0.063$) towards increased effect at 2.5μM), with a concentration-dependent response observed from 2.5-10μM (Figure 3-4E/F). Dense granule secretion was reduced to 17% of the level of vehicle-treated platelets at the highest concentration tested (10μM). This order of potency is in agreement with the aggregation data in as much as isorhamnetin displays an increased potency (further work could consolidate this) – the data presented in this section supports an inhibitory hierarchy of isorhamnetin > quercetin = tamarixetin.

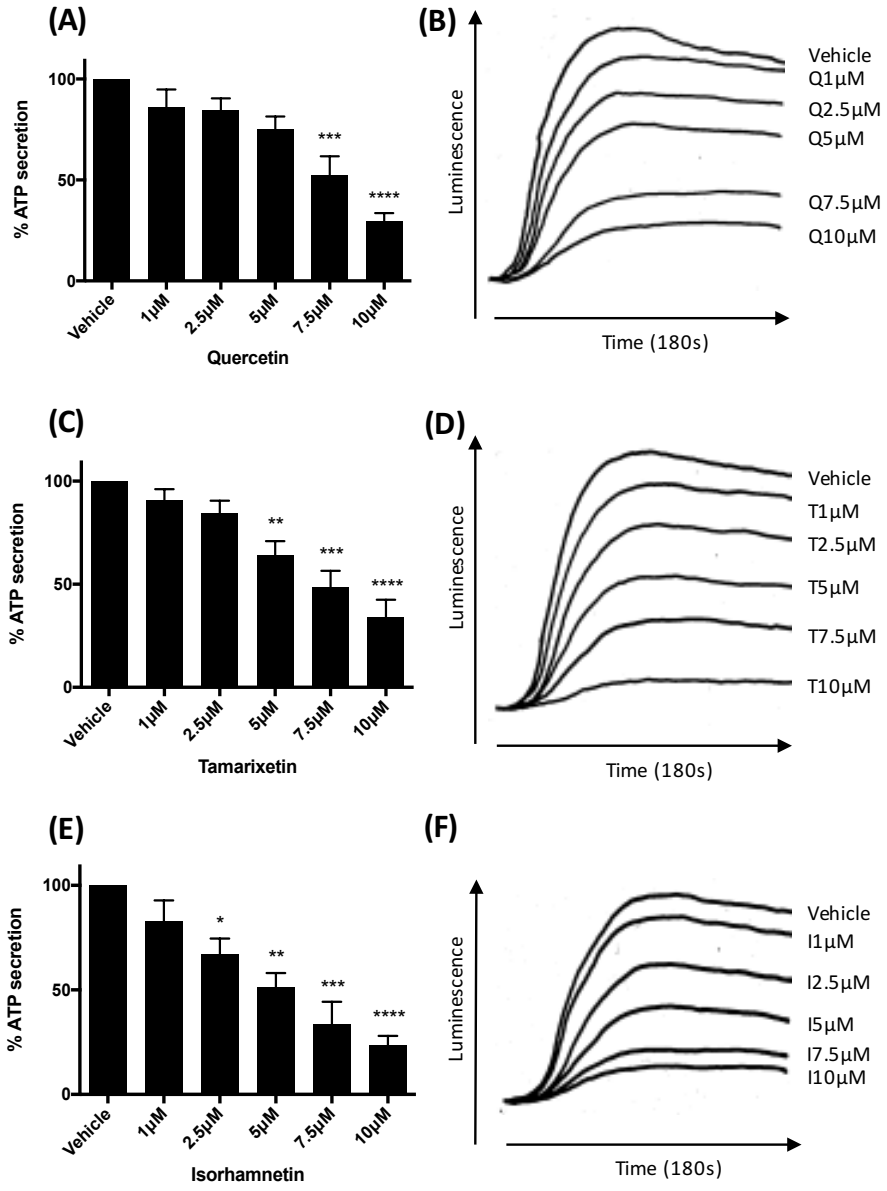

Figure 3-4 Quercetin, tamarixetin and isorhamnetin inhibit dense granule secretion

Using lumiaggregometry, washed platelets (4 x 10^8 cells/mL) were treated with flavonoid or vehicle control (DMSO, 0.25% v/v) for 5 minutes, with 50µl Chronolume luminescent substrate added in 2 minutes prior to stimulation. Collagen (5µg/mL) was added to stimulate platelets and ATP secretion was monitored for 180 seconds under stirring conditions (1200rpm) at 37°C. (A,C,E) ATP secretion as a percentage of the amount secreted in the absence of quercetin, tamarixetin or isorhamnetin (vehicle). (B,D,F) Representative traces showing increase in luminescence upon ATP secretion and inhibition by flavonoids. N=4, data represent mean ± SEM. *p<0.05, **p<0.005, ***p<0.001, ****p<0.0001 compared to vehicle control, analysed by one-way ANOVA with post-hoc Dunnett's test. Q, quercetin; T, tamarixetin; I, isorhamnetin.

3.3.2 Alpha-granule secretion is also inhibited more potently by isorhamnetin

Platelet α-granules, similar to dense granules, also contain many components key to the positive feedback mechanisms that define platelet activation. α-granules are a store of many molecules involved in the critical processes of adhesion, aggregation, and ultimately, thrombus formation. These include proteins such as fibrinogen, von Willebrand Factor, fibronectin and coagulation factors, as well as growth factors including platelet derived growth factor (PDGF) and transforming growth factor β (TGF-β) and chemokines such as platelet factor 4 (PF4) (Stenberg *et al.*, 1984; Harrison and Cramer, 1993; Maynard *et al.*, 2007). P-Selectin (CD62P) is a transmembrane adhesion receptor contained within α-granules, and upon platelet activation and release of granule contents, it is exposed on the platelet cell membrane, where it functions in leukocyte recruitment (Koedam *et al.*, 1992). This exposure of P-Selectin is a useful marker of α-granule secretion, and with the use of fluorescent anti-CD62P antibodies, can be measured using flow cytometry. The effect of quercetin, tamarixetin, isorhamnetin and quercetin-3-glucuronide on the GPVI-stimulated exposure of P-Selectin was therefore investigated as a marker of α-granule secretion.

Washed platelets (2 x 10^8 cells/mL) were incubated with flavonoid or vehicle control for 5 minutes. Anti-CD62 Cy5/PE conjugated antibody was added to platelet samples, which were then stimulated with the GPVI-specific agonist collagen-related peptide (cross-linked) (CRP-XL) (1μg/mL). CRP-XL is a triple helical peptide, with ten glycine-proline-hydroxyproline triplets on each strand, and binds the ectodomain of GPVI causing potent platelet activation (Morton *et al.*, 1995; Smethurst *et al.*, 2007). CRP-XL was used in this assay; collagen is inappropriate for use in flow cytometry as it can coat the tubing of the machinery and cause problematic blockages due to aggregate formation. A concentration of 1μg/mL was chosen to represent strong stimulation, and to elicit a similar response to 5μg/mL collagen. After 20 minutes stimulation with occasional gentle mixing, reactions were terminated and samples fixed with 0.2% (w/v) paraformaldehyde. A 20-minute stimulation time was chosen for flow cytometry based on experiments which showed increasing P-Selectin exposure (and fibrinogen

binding to integrin $\alpha_{IIb}\beta_3$, described later) up to this time point, at which a plateau is reached. This increased reaction time compared to aggregation (where after 5 minutes aggregation is complete) is likely due, at least in part, to a lack of stirring. Samples were subsequently diluted to 2 x 10^7 cells/mL for flow cytometric analysis as described in Section 2.2.3; this was done for all subsequent flow cytometry experiments. Fluorescence was then measured using flow cytometry, gated onto the platelet population (as described in Chapter 2) to ensure only appropriate events were recorded. Experiments were also initially performed with samples minus paraformaldehyde to ensure fixing did not significantly affect results, which was confirmed to not be an issue (as well as this, paraformaldehyde was a consistent factor throughout all samples) (data not shown).

Representative fluorescence histograms are shown in Figure 3-5A/D/G, showing a decrease in fluorescence upon incubation with flavonoid compared to vehicle control (CRP-XL + DMSO, 0.25% v/v), representative of an inhibition of P-Selectin exposure. Quercetin was found to be a potent inhibitor P-Selectin exposure, with 15% inhibition observed at the lowest concentration of 0.5μM, and >90% inhibition at 10μM (Figure 3-5B). Potent inhibition of dense granule release was also observed at 10μM quercetin, suggesting quercetin is an effective inhibitor of granular release. The IC_{50} for quercetin is 2.5 ± 0.23μM, near half the value for inhibition of collagen-stimulated aggregation (Figure 3-5C). This could reflect a more potent inhibitory ability of α-granule secretion, but it must also be considered that differences in assay methodology (and indeed agonist) could influence this as well.

Tamarixetin displayed a similar profile of inhibition to quercetin, with a concentration-dependent effect from 1-10μM (Figure 3-5E). A significant effect was not observed at 0.5μM, and this slightly lower potency is reflected in the higher IC_{50} value of 2.7 ± 0.27μM when compared to quercetin (Figure 3-5F), although the difference is minimal, as also seen in the aggregation data (Figures 3-1 and 3-2). As stated earlier, minimal differences in IC_{50} values could, however, be important *in vivo*. The maximum level of inhibition achieved by tamarixetin is also lower than quercetin; a 77% effect with tamarixetin compared to ~90% with quercetin. Isorhamnetin inhibited significantly P-Selectin

exposure at all concentrations tested (0.5-10μM), with 40% inhibition at 0.5μM and ~85% effect at 10μM (Figure 3-5H). This is a significant result; to achieve such a high level of inhibition at a very low concentration. With a high-quercetin diet or quercetin supplementation, total plasma quercetin concentrations can exceed this (Hubbard *et al.*, 2004; Hubbard *et al.*, 2006; Kashino *et al.*, 2015; Stopa *et al.*, 2017). The IC_{50} for isorhamnetin is 0.89 ± 0.28μM (Figure 3-5I); this reflects the increased effect at lower concentrations when compared to quercetin and tamarixetin (a significantly enhanced inhibition at 1μM compared to both quercetin and tamarixetin). This order of potency, isorhamnetin > quercetin > tamarixetin, is in agreement with data already shown so far (individual donor IC_{50} values are not compared here due to large variability impeding analysis).

Similar to the collagen-stimulated aggregation data, quercetin-3-glucuronide required concentrations an order of magnitude higher to achieve significant levels of inhibition (Figure 3-6B). Representative fluorescence histograms are shown in Figure 3-6A. At 50μM, approximately 50% inhibition was observed. This enhanced effect compared to inhibition of aggregation may reflect, as mentioned above, an increased potency for inhibition of the molecular event of P-Selectin exposure compared to the macro-scale event of platelet aggregation. This again suggests cell impermeability as a mechanism for greatly reduced effect. If quercetin-3-glucuronide is unable to gain entry to the platelet cytosol, it will be unable to interact with the intracellular kinases and molecular mechanisms involved in P-Selectin exposure and aggregation, instead relying solely on extracellular target inhibition. This is discussed further in section 3.8.

The data presented in section 3.3 demonstrate the efficacy of quercetin and its methylated metabolites in the inhibition of platelet granule secretion. A lesser role is indicated for quercetin-3-glucuronide. Taken together, this suggests one of the key mechanisms through which quercetin and its metabolites inhibit aggregation is through an early effect on granule secretion.

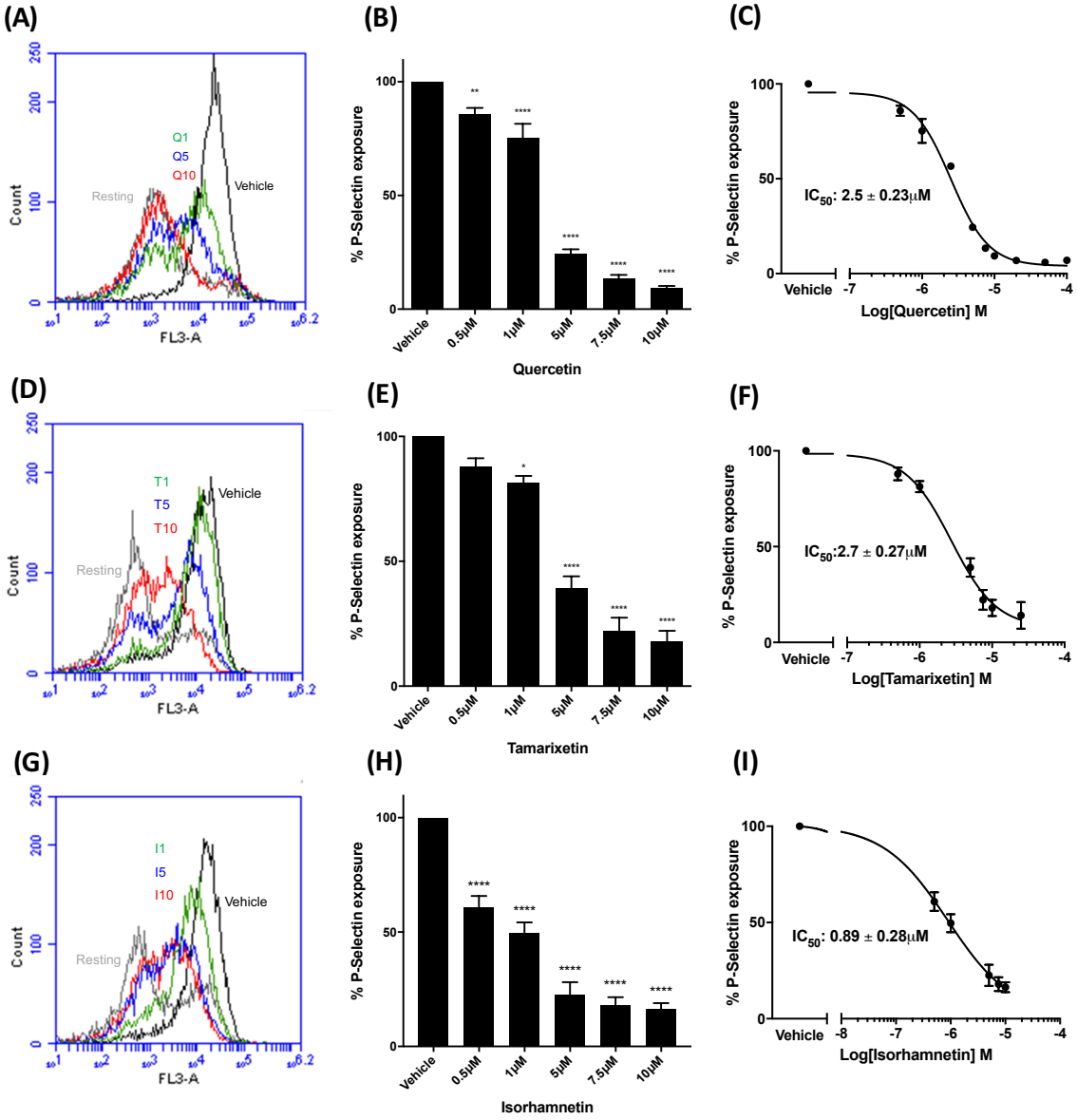

Figure 3-5 Quercetin, tamarixetin and isorhamnetin inhibit platelet α-granule secretion

Washed platelets (2 x 10^8 cells/mL) were incubated with quercetin (A), tamarixetin (D), isorhamnetin (G) or vehicle control (DMSO, 0.25%v/v) for 5 minutes, after which PE/Cy5 anti-human CD62P antibody was added to sample prior to stimulation. Samples were then stimulated with CRP-XL (1μg/mL) for 20 minutes, after which they were fixed in 0.2% paraformaldehyde. P-Selectin exposure on the cell surface was then measured by flow cytometry, with representative fluorescence histograms shown in A,D,G, and data normalized to the level of P-Selectin exposure in the absence of flavonoid (vehicle) (B,E,H). Four parameter nonlinear regression curves were utilised to estimate the IC_{50} of quercetin (C), tamarixetin (F) and isorhamnetin (I). N=3, data represent mean ± SEM. *p<0.05, **p<0.005, ****p<0.0001 compared to vehicle control, analysed by one-way ANOVA with post-hoc Dunnett's test. Q, quercetin; T, tamarixetin; I, isorhamnetin

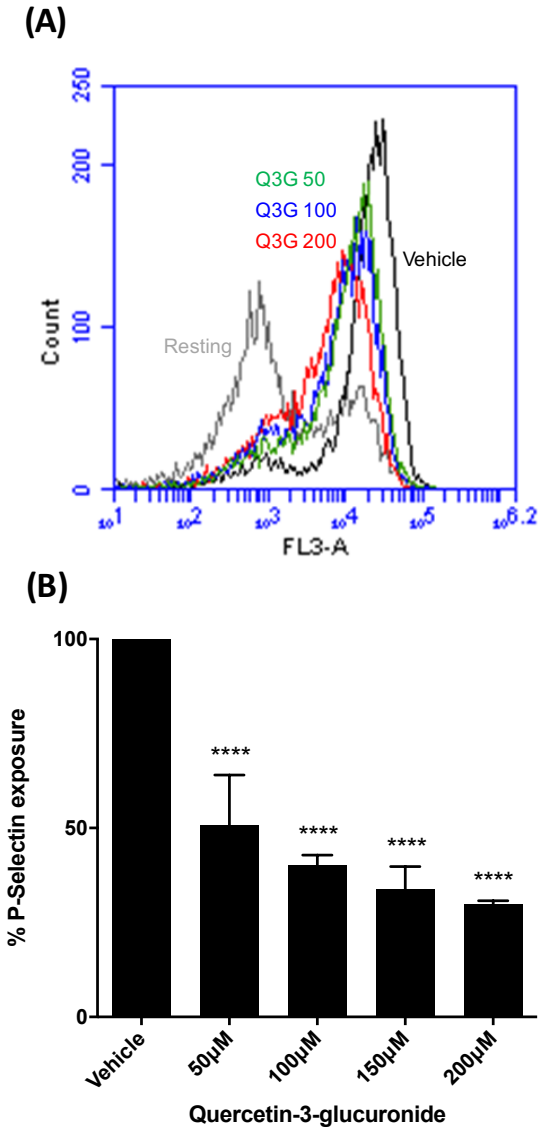

Figure 3-6 Quercetin-3-glucuronide shows reduced potency in the inhibition of α-granule secretion

Washed platelets (2 x 10^8 cells/mL) were incubated with quercetin-3-glucuronide or vehicle control (DMSO, 0.25%v/v) for 5 minutes, after which PE/Cy5 anti-human CD62P antibody was added to sample prior to stimulation. Samples were then stimulated with CRP-XL (1μg/mL) for 20 minutes, after which they were fixed in 0.2% paraformaldehyde. P-Selectin exposure on the cell surface was then measured by flow cytometry, with representative fluorescence histograms shown in (A), and data normalized to the level of P-Selectin exposure in the absence of quercetin-3-glucuronide (vehicle) (B). N=3, data represent mean ± SEM. ****p<0.0001 compared to vehicle control. Data analysed by one-way ANOVA with post-hoc Dunnett's test. Q3G, quercetin-3-glucuronide.

3.4 The effects of quercetin and its metabolites on integrin $\alpha_{IIb}\beta_3$ activation

The activation of integrin $\alpha_{IIb}\beta_3$ is one of the most critical events in platelet aggregation and thrombus formation. This fibrinogen receptor is responsible for the platelet:platelet interactions that drive the aggregatory process; its importance is demonstrated in patients suffering from Glanzmann thrombasthenia, who experience bleeding problems ranging from mild bruising to severe haemorrhage (Glanzmann, 1918; George *et al.*, 1990; D'Andrea *et al.*, 2009). The successful pharmacological antagonism of integrin $\alpha_{IIb}\beta_3$ post-surgery with agents such as abciximab and eptifibatide again prove the pivotal physiological function of this integrin (Genetta and Mauro, 1996; PURSUIT-Investigators, 1998). Upon platelet activation, signals from within the platelet function to upregulate the affinity of the integrin into an 'open' state ('inside-out signalling'), as well as to increase the number of $\alpha_{IIb}\beta_3$ molecules on the platelet surface (Wencel-Drake *et al.*, 1986; Ma *et al.*, 2007). The binding of fibrinogen to integrin $\alpha_{IIb}\beta_3$ and associated receptor clustering then propagates 'outside-in' signalling, leading to adhesion and platelet spreading and eventual aggregate formation (Shattil and Newman, 2004; Li *et al.*, 2010). The comparative ability of quercetin and its metabolites to inhibit the binding of fibrinogen to activated platelet integrin $\alpha_{IIb}\beta_3$ was therefore measured by flow cytometry, and the relative effect of quercetin, tamarixetin and isorhamnetin on the adhesion and spreading of platelets on fibrinogen and CRP-XL was investigated.

3.4.1 Fibrinogen binding to integrin $\alpha_{IIb}\beta_3$ stimulated by GPVI-specific activation is inhibited differentially by quercetin and its methylated metabolites

The effect of quercetin on fibrinogen binding to integrin $\alpha_{IIb}\beta_3$ as a measure of 'inside-out' signalling was measured via flow cytometry. Washed platelets (2 x 10^8 cells/mL) were incubated with flavonoid or vehicle control for 5 minutes prior to addition of FITC-conjugated anti-fibrinogen antibody. Platelets were then stimulated with the GPVI-specific agonist CRP-XL (1μg/mL) for 20 minutes at room temperature, with occasional gentle mixing. CRP-XL was used at a concentration of 1μg/mL to reflect the same conditions used in the α-granule secretion experiments (section 3.3.2), allowing a comparison of the effects. Samples were then fixed in 0.2% (w/v) paraformaldehyde and fluorescence measured by flow cytometry.

Fibrinogen binding to resting platelets was low; this is to be expected as in resting platelets the integrin should be in a 'closed', non-activated state (Figure 3-7A, 'Resting' sample). Upon stimulation, the integrin opens to its 'active' conformation and fibrinogen binds (Figure 3-7A, 'Vehicle' sample). Representative fluorescence histograms are shown in Figure 3-7A/D/G, showing a decrease in fluorescence upon incubation with flavonoid compared to vehicle control (CRP-XL + DMSO, 0.25% v/v, 'Vehicle' samples in the figures), representative of an inhibition of fibrinogen binding. Quercetin inhibited potently this process; >25% inhibition was seen at 0.5μM (Figure 3-7B). At high concentrations, fibrinogen binding was completely inhibited (>95%), suggesting that at levels of quercetin >7.5μM, very little integrin activation is taking place, or fibrinogen is unable to bind to any activated integrin (we cannot exclude the possibility that quercetin may antagonise fibrinogen binding; this is addressed in the discussion of results in Chapter 4). The IC_{50} value for quercetin is 3.2 ± 0.46μM, similar to that for P-Selectin exposure, indicating a comparable potency/role for quercetin in the inhibition of these molecular processes (Figure 3-7C). Indeed, in washed platelets, the release of fibrinogen from platelet α-granules upon stimulation serves as the source of fibrinogen (compared to plasma, where there is a high concentration of non-platelet derived fibrinogen), and as such inhibited

fibrinogen binding may be a result of either a true effect on the binding of fibrinogen to integrin αIIbβ3, or a result of inhibited fibrinogen release from α-granules. However, independent experiments using fluorescently labelled fibrinogen directly displayed very similar results to the data presented in this section, confirming the effect was a true inhibition of fibrinogen binding to the integrin (data not shown).

Tamarixetin inhibited fibrinogen binding at concentrations between 1-10μM. No significant effect was observed at 0.5μM, showing a reduced (although not significant) potency compared to quercetin at lower concentrations (Figure 3-7E). A plateau of effect seems to have been reached at concentrations above 7.5μM, with ~70% inhibition observed at both 7.5 and 10μM, demonstrating a reduced efficacy at higher concentrations compared to quercetin. This is reflected in the higher IC_{50} value of 4.2 ± 0.56μM (Figure 3-7F). A reduced potency at higher concentrations compared to quercetin is also seen with isorhamnetin, which inhibited fibrinogen binding ~70% at 7.5 and 10μM, much like tamarixetin (Figure 3-7H). Consistent with the effects of quercetin and isorhamnetin on α-granule secretion, however, isorhamnetin proved more potent at lower concentrations (35% inhibition at 1μM), paralleled in the lower IC_{50} value of 1.3 ± 0.49μM (Figure 3-7I). Indeed, at 0.5μM and 1μM, isorhamnetin inhibited fibrinogen binding significantly more than both quercetin and tamarixetin.

Quercetin-3-glucuronide demonstrated lower potency for the inhibition of fibrinogen binding to platelet integrin $\alpha_{IIb}\beta_3$ compared to quercetin. Concentrations an order of magnitude higher were required to achieve significant inhibition, with only 36% inhibition at 50μM (Figure 3-8B). Representative fluorescence histograms are shown in Figure 3-8A. At 200μM, similar to aggregation and α-granule secretion, quercetin-3-glucuronide failed to abolish fibrinogen binding, reaching only 60% reduction. Whilst this is a high level of effect, it must be analysed in context with the concentration used; 200μM is unachievable through diet or supplementation. Taken together with the aggregation and granule secretion data, it was concluded that quercetin-3-glucuronide displays low potency compared to quercetin and its methylated metabolites, implying glucuronidation as a

metabolic modification that reduces the anti-platelet effect of quercetin. As such, it was no longer included in experiments. It is likely that the inability to gain access to the platelet cytosolic compartment is dramatically limiting its effect, particularly considering the nature of the assays so far and that they have been performed in washed platelets. There is the potential for quercetin-3-glucuronide to effect platelet function through inhibition of extracellular processes, such as the function of extracellular protein disulphide isomerase (PDI). This will be discussed at the end of the chapter and also in the future work section.

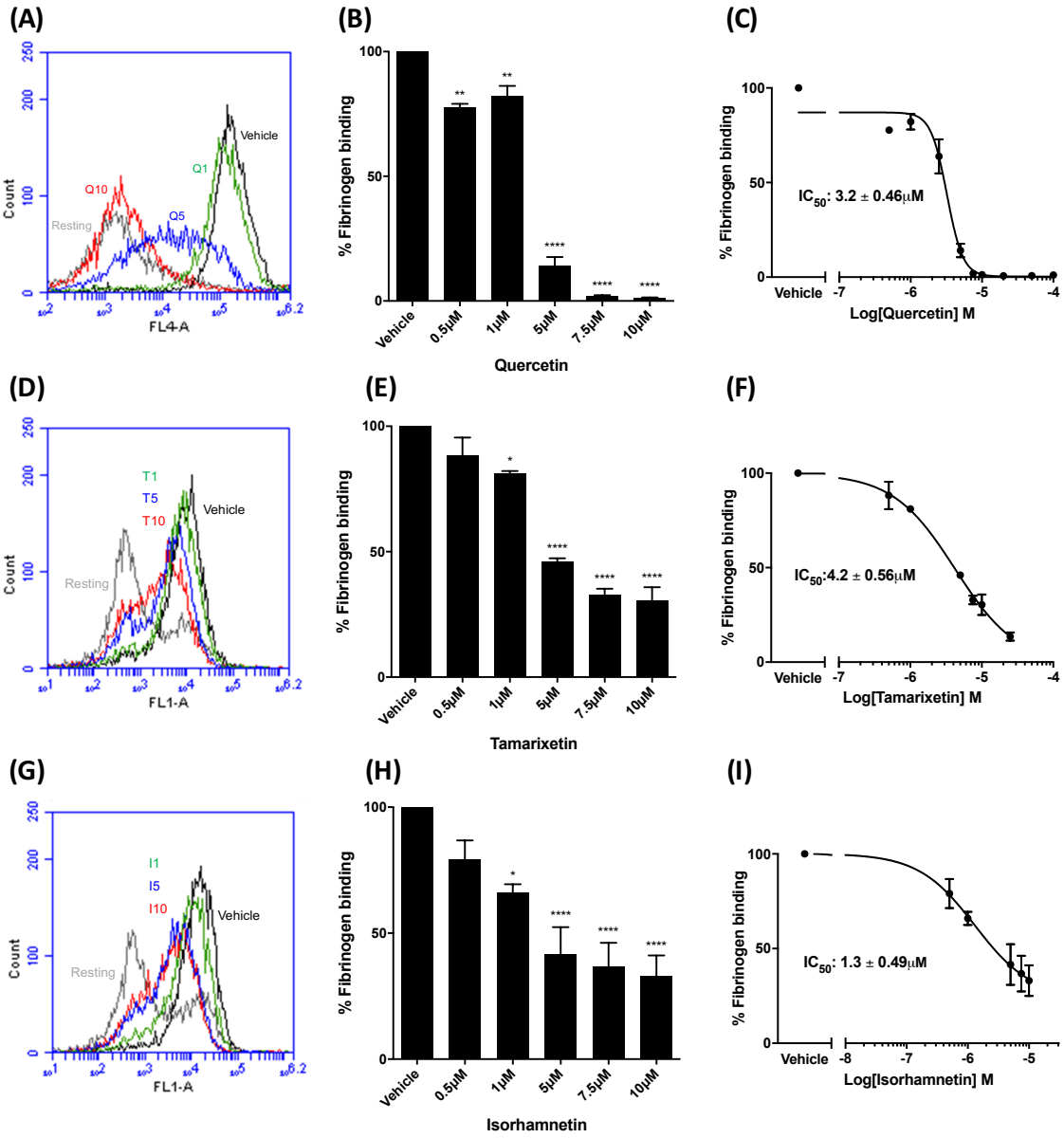

Figure 3-7 Quercetin and its methylated metabolites inhibit fibrinogen binding with similar potency

Washed platelets (2 x 10^8 cells/mL) were incubated with quercetin (A), tamarixetin (D), isorhamnetin (G) or vehicle control (DMSO, 0.25% v/v) for 5 minutes, after which FITC-conjugated anti-fibrinogen antibody was added to samples prior to stimulation. Samples were then stimulated with CRP-XL (1μg/mL) for 20 minutes, after which they were fixed in 0.2% paraformaldehyde. Fibrinogen binding was then measured by flow cytometry, with representative fluorescence histograms shown in A,D,G, and data normalized to the level of fibrinogen binding in the absence of flavonoid (vehicle) (B,E,H). Four parameter nonlinear regression curves were used to estimate the IC_{50} of quercetin (C), tamarixetin (F) and isorhamnetin (I). N=3, data represent mean ± SEM. *p<0.05, **p<0.005, ****p<0.0001 compared to vehicle control, analysed by one-way ANOVA with post-hoc Dunnett's test. Q, quercetin; T, tamarixetin; I, isorhamnetin.

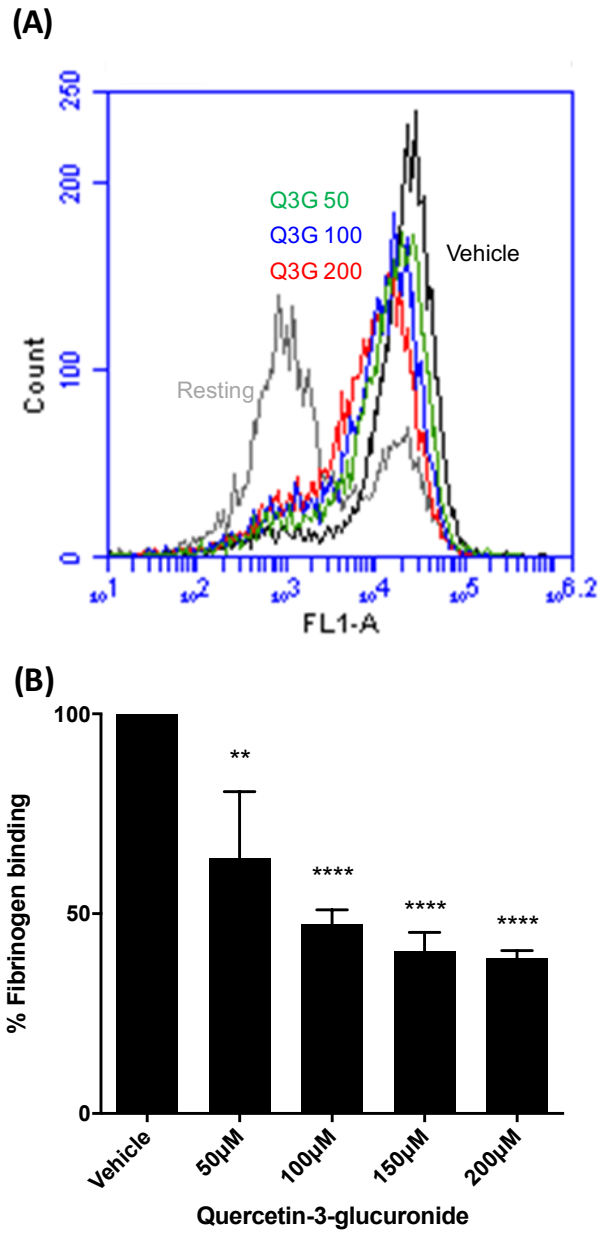

Figure 3-8 Quercetin-3-glucuronide inhibits fibrinogen binding with a much reduced potency

Washed platelets (2 x 10^8 cells/mL) were incubated with quercetin-3-glucuronide or vehicle control (DMSO, 0.25% v/v) for 5 minutes, after which FITC-conjugated anti-fibrinogen antibody was added to samples prior to stimulation. Samples were then stimulated with CRP-XL (1μg/mL) for 20 minutes, after which they were fixed in 0.2% paraformaldehyde. Fibrinogen binding was then measured by flow cytometry, with representative fluorescence histograms shown in (A), and data normalized to the level of fibrinogen binding in the absence of quercetin-3-glucuronide (vehicle) (B). N=3, data represent mean ± SEM. **p<0.005, ****p<0.0001 compared to vehicle control, analysed by one-way ANOVA with post-hoc Dunnett's test. Q3G; quercetin-3-glucuronide.

3.4.2 A comparison and summary of the IC_{50} values of quercetin, tamarixetin and isorhamnetin in the inhibition of aggregation, granule release and fibrinogen binding to activated integrin $\alpha_{IIb}\beta_3$

Table 3-1 compares the IC_{50} values for quercetin, tamarixetin and isorhamnetin in the inhibition of collagen-stimulated aggregation, as well as the GPVI-specific stimulated secretion of α-granules and fibrinogen binding. It demonstrates a consistent order of potency of isorhamnetin > quercetin > tamarixetin. This suggests, therefore, that metabolic modification of quercetin, specifically methylation, can either enhance or reduce its anti-platelet activity, depending on the residue modified. Whilst the differences between some IC_{50} values are small, they must be considered in relation to the absolute value. As an example, the IC_{50} value for the inhibition of fibrinogen binding by isorhamnetin (1.3 ± 0.49μM) represents a ~60% reduction compared to the equivalent value of quercetin (3.2 ± 0.46μM). Such seemingly small differences may translate into interesting differences of effect *in vivo*. It also suggests that quercetin and its metabolites are more potent inhibitors of α-granule release, followed by fibrinogen binding to activated integrin $\alpha_{IIb}\beta_3$ and lastly, aggregation. This must take into account, however, the nature of the methodologies, including the macro- vs micro- scale on which they are performed

Table 3-1 – A comparison of the IC_{50} values (μM) for the inhibition of aggregation, P-Selectin exposure and fibrinogen binding by quercetin, tamarixetin and isorhamnetin

Flavonoid	Aggregation	P-Selectin Exposure	Fibrinogen Binding
Quercetin	5.7 ± 0.49	2.5 ± 0.23	3.2 ± 0.46
Tamarixetin	7.14 ± 0.54	2.7 ± 0.27	4.2 ± 0.56
Isorhamnetin	4.8 ± 1.46	0.89 ± 0.28	1.3 ± 0.49

3.4.3 Fibrinogen binding to integrin $\alpha_{IIb}\beta_3$ upon dual-agonist stimulation is inhibited by quercetin

In vivo, upon vessel wall injury, there are a multitude of activatory substances in the local extracellular milieu. Concentrations that individually may not cause an activatory response, when combined, may synergise to cause a full functional response; it is unclear how flavonoids may act on this (Huang and Detwiler, 1981; Razi *et al.*, 2005; Razi *et al.*, 2009). This was simulated *in vitro* using CRP-XL (to represent GPVI stimulation by collagen) and thrombin dual-stimulation, and the ability of quercetin to inhibit fibrinogen binding to integrin $\alpha_{IIb}\beta_3$ stimulated by this response was investigated.

Washed platelets (2 x 10^8 cells/mL) were stimulated individually with concentrations of CRP-XL ranging from 0.02 - 1μg/mL, and concentrations of thrombin from 0.025 - 0.1U/mL. This was performed for 4 donors independently, in order to define subthreshold concentrations of both agonists for each donor. The reason behind this is the widely differing inter-donor response to agonists. Subthreshold responses were defined as <10% aggregation compared to CRP-XL 1μg/mL and thrombin 0.1U/mL control. Representative traces from this experiment can be seen in Figure 3-9A, demonstrating the ability of individually ineffective agonist concentrations to synergise and cause a full aggregation response (compared to CRP-XL 1μg/mL as a strong agonist). Once agonist concentrations had been defined for each donor, washed platelets (2 x 10^8 cells/mL) from the same donor were incubated with quercetin or vehicle control for 5 minutes, after which FITC-conjugated anti-fibrinogen antibody and GPRP were added and platelets were stimulated for 20 minutes with CRP-XL and thrombin at the donor-specific pre-determined concentrations. GPRP was added to prevent fibrin polymerisation caused by thrombin. Samples were then fixed in 0.2% (w/v) paraformaldehyde and fibrinogen binding levels were determined through fluorescence measurements using flow cytometry.

Figure 3-9A shows representative traces from the defining of subthreshold concentrations of CRP-XL and thrombin. Defined as <10% aggregation compared to strong agonist control, it can be seen that

(for the donor represented in the Figure) concentrations of CRP-XL (0.025μg/mL) and thrombin (0.05U/mL) that individually are subthreshold for aggregation, when combined, can cause a full aggregatory response; indeed, as seen in Figure 3-9A, a greater level of aggregation was achieved than upon stimulation with CRP-XL (1μg/mL) (a concentration of CRP-XL 40X higher). Over 4 donors, the response to individually (per-donor) determined subthreshold agonist combinations was not significantly different from that to CRP-XL 1μg/mL. The ability of quercetin to inhibit fibrinogen binding triggered by this dual-agonist stimulation was then investigated, and was found to be extremely effective; at concentrations between 1-10μM, >90% inhibition was achieved (Figure 3-9B). At 0.5μM quercetin, this dual-agonist fibrinogen binding response was inhibited by an average of 70%. Lower nanomolar concentrations were tested, but significant inhibition was only seen at 0.5μM (data not shown). Such a potent effect on fibrinogen binding at nanomolar concentrations highlights the inhibition of synergistic agonist responses as a potential mechanism through which quercetin and its metabolites may impede activation *in vivo*.

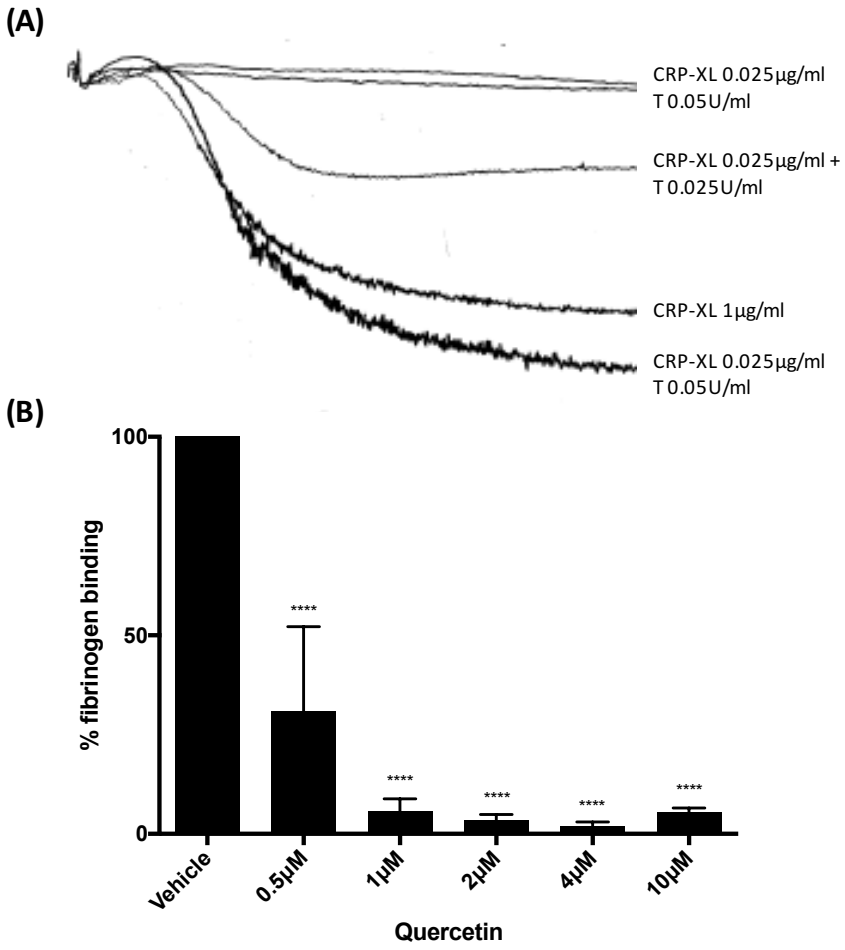

Figure 3-9 Quercetin potently inhibits fibrinogen binding stimulated by a synergistic response to CRP-XL and thrombin

Washed platelets (2 x 10^8 cells/mL) were stimulated with CRP-XL and thrombin and aggregation measured at 37°C under constant stirring (1200rpm) conditions to establish subthreshold and synergistic concentrations, with representative traces shown in (A). Washed platelets (2 x 10^8 cells/mL) were then incubated with quercetin or vehicle control (DMSO, 0.25% v/v) for 5 minutes, after which FITC anti-fibrinogen antibody was added, prior to stimulation for 20 minutes with CRP-XL and thrombin at the concentrations determined in (A). Samples were then fixed in 0.2% paraformaldehyde and fibrinogen binding measured by flow cytometry, with data normalised to the levels of fibrinogen binding in the absence of quercetin (vehicle) (B). N=4, data represent mean ± SEM. ****$p<0.0001$ compared to vehicle control, analysed by one-way ANOVA with post-hoc Dunnett's test. C, collagen; T, thrombin

3.4.4 Platelet adhesion and spreading on fibrinogen and CRP-XL is inhibited by quercetin, tamarixetin and isorhamnetin

Upon ligand binding to integrin $\alpha_{IIb}\beta_3$, a cascade of intracellular 'outside-in' signalling events occurs, resulting in platelet spreading and a dramatic increase in the platelet surface contact area, with the extension of filopodia and subsequently lammelipodia (Furie and Furie 2008; Lee *et al.*, 2012a). Platelets also spread on collagen, with reported roles for GPVI and integrin $\alpha2\beta1$ in this process (Falet *et al.*, 2000; Suzuki-Inoue *et al.*, 2001; Inoue *et al.*, 2003). Platelet spreading on CRP-XL has also been reported, with key roles for GPVI, SLP-76 (lymphocyte cytosolic protein 2), PI3K and gelsolin (Falet *et al.*, 2000). This platelet spreading is of critical importance to both haemostasis and thrombosis, involving both GPVI and integrin $\alpha_{IIb}\beta_3$ function. The data presented thus far has demonstrated the ability of quercetin and its methylated metabolites to inhibit platelet function through these two pathways. In order to confirm an effect on the GPVI pathway and to investigate the ability to inhibit outside-in integrin signalling, the ability of quercetin, tamarixetin and isorhamnetin to inhibit both adhesion to, and spreading on fibrinogen and CRP-XL was investigated.

Glass coverslips were coated with fibrinogen (100μg/mL) or CRP-XL (1μg/mL) for 1 hour, then incubated with BSA for 1 hour to prevent platelet-glass binding. Washed platelets (2×10^8 cells/mL) were incubated with flavonoid or vehicle control for 5 minutes, after which they were diluted to 2×10^7 cells/mL and added onto the coated coverslips. After 45 minutes at 37°C, supernatant was removed from the coverslips, which were washed with PBS. Samples were then fixed with 0.2% (w/v) paraformaldehyde, washed with PBS, and adhered platelets permeabilized with 0.2% Triton-X. After a further wash step, Alexa-Fluor 488 phalloidin was added to stain actin to allow visualisation of the adhered/spread platelets, which was performed using a confocal microscope. Five images were captured of each sample (taken in random locations on the slide to prevent observer bias), and from these images platelets were scored into three categories: adhered (not spread), filopodia/'spreading'

(extending filopodia) or spread (lamellipodia formed), with the percentage of each population under different experimental treatments calculated.

Quercetin, tamarixetin and isorhamnetin inhibited significantly platelet adhesion on fibrinogen at 1, 2.5 and 5μM. A maximal effect is observed, with ~25% inhibition of adhesion at all concentrations test for all flavonoids (Figure 3-10A,C,E). It may therefore be that quercetin and its metabolites have a limited effect on platelet adhesion to fibrinogen, as increasing flavonoid concentration did not result in an increased effect (or it could be that higher concentrations would overcome this). As seen in Figure 3-10(B,D,F), all flavonoids tested affected the spreading process; an increase in platelets in the earlier stages of 'adhered' and 'filopodia', with a corresponding decrease in the number fully extending lamellipodia was observed. This was concentration-dependent for quercetin and isorhamnetin, with 5μM reducing significantly the percentage of platelets fully spreading by 35% and 44%, respectively. Significant inhibition (33% inhibition of lamellipodia formation) was observed as low as 1μM for isorhamnetin. The effect of tamarixetin was different to that of quercetin and isorhamnetin. Much like the % adhesion data, a 'plateau' of effect was seen, with all concentrations tested reducing lamellipodia by approximately 20-25%, with a corresponding 20-25% increase in platelets in the 'filopodia' stage (Figure 3-10D). It may be that at higher concentrations, this would have been overcome. Consistent with the other data presented so far, isorhamnetin was significantly more potent than both quercetin and tamarixetin (defined as a statistically significant decrease in platelets reaching the lamellipodia stage compared to other flavonoid treatment), with a trend (which did not reach significance) for quercetin having an increased effect over tamarixetin. Representative images are shown in Figure 3-11; for reasons of clarity, only images from vehicle-treated and 5μM flavonoid-treated samples are shown.

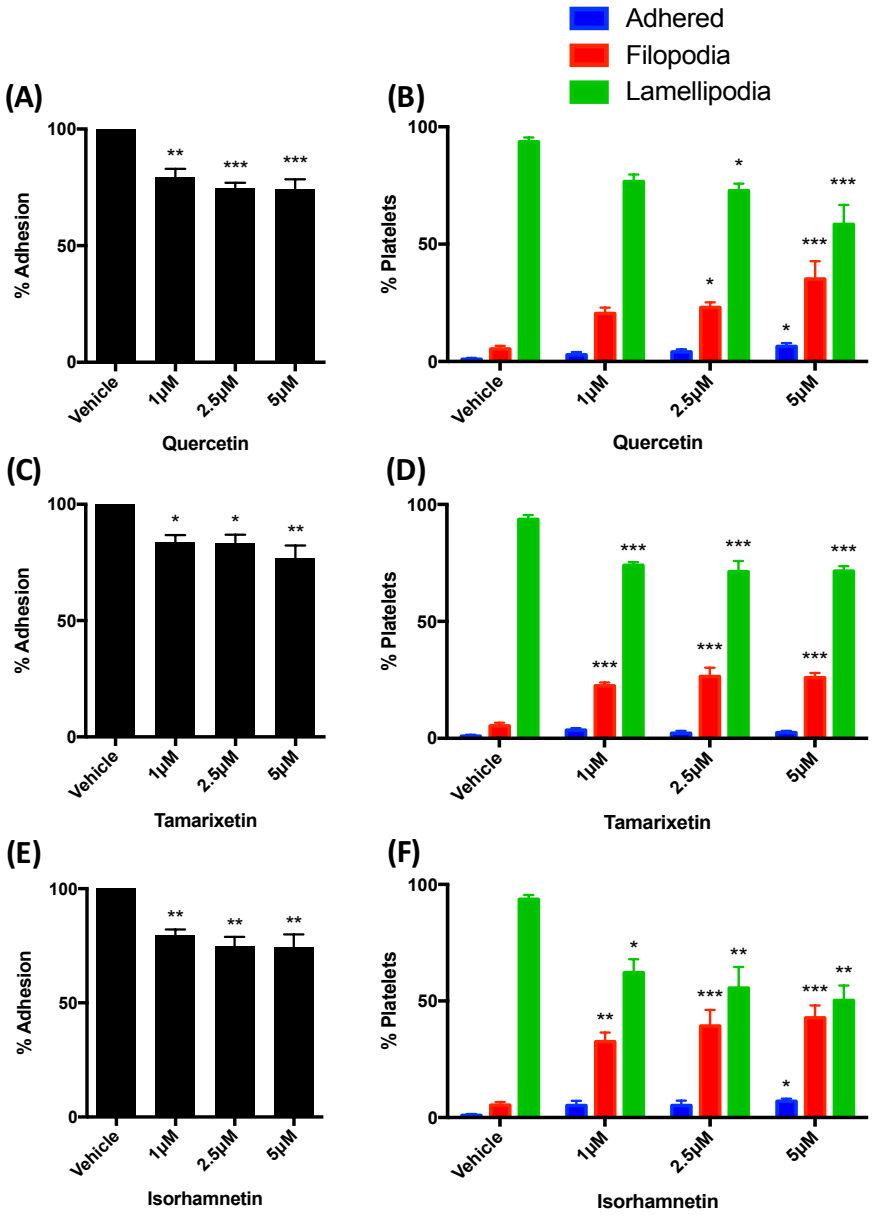

Figure 3-10 Quercetin, tamarixetin and isorhamnetin inhibit adhesion and spreading on fibrinogen

Washed platelets (2 x 10^8 cells/mL) were incubated with quercetin (A/B), tamarixetin (C/D), isorhamnetin (E/F) or vehicle control (DMSO 0.33% v/v) for 5 minutes, diluted to 2 x 10^7 cells/mL, and then added onto fibrinogen (100μg/mL) coated coverslips for 45 minutes at 37°C. Cells were fixed with 0.2% paraformaldehyde for 10 minutes and permeabilized with 0.2% Triton-X for 5 minutes. Alexa-Fluor 488 phalloidin was added for 1 hour and coverslips mounted onto slides with Prolong Gold Antifade mountant. Data represent percentage adhesion normalised to levels of adhesion in the absence of flavonoid (vehicle) (A,C,E) and percentage of platelets in each stage of spreading (B,D,F), mean ± SEM. Data was analysed from 5 separate, randomly taken images from each sample. N=4, data analysed by one way ANOVA with post-hoc Dunnett's test. *p<0.05, **p<0.005, ***p<0.001, compared to vehicle control.

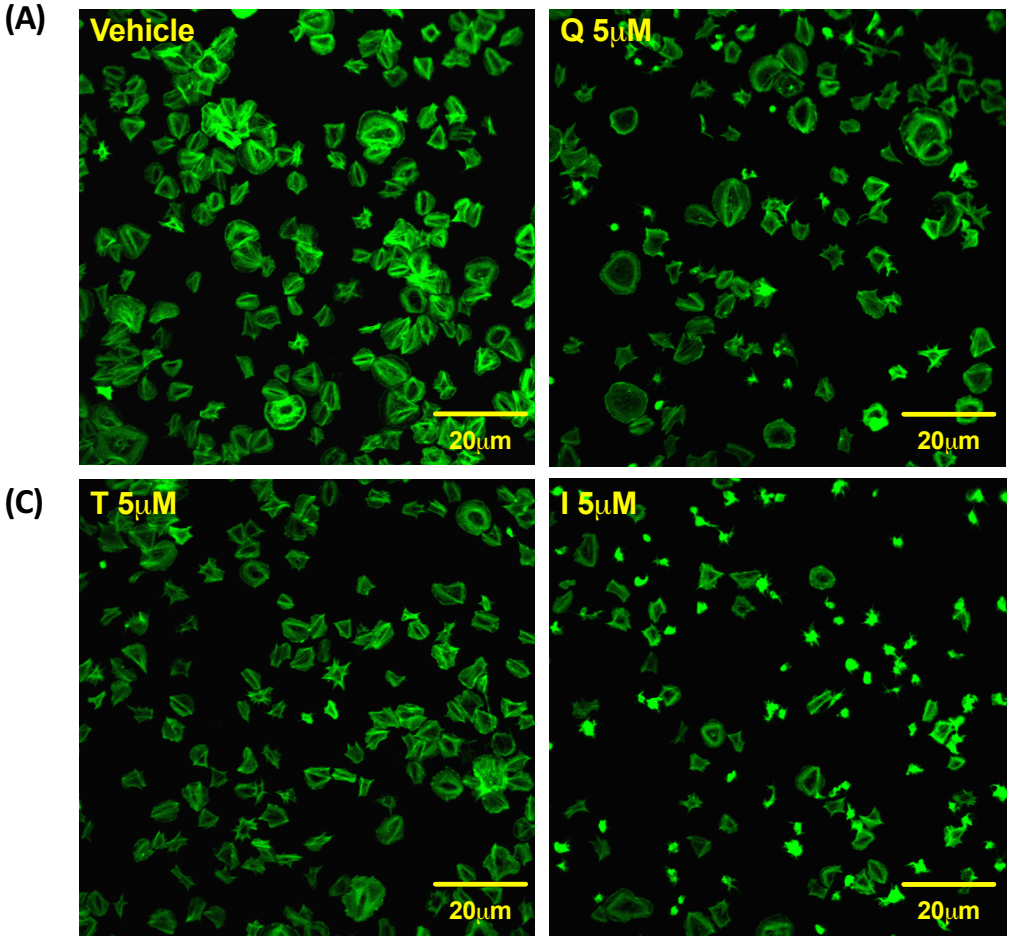

Figure 3-11 Representative images showing quercetin, tamarixetin and isorhamnetin inhibit platelet adhesion and spreading on fibrinogen

Washed platelets (2 x 10^8 cells/mL) were incubated with quercetin (B), tamarixetin (C), isorhamnetin (D) or vehicle control (A) (DMSO, 0.33% v/v) for 5 minutes, diluted to 2 x 10^7 cells/mL, and then allowed to spread on fibrinogen (100μg/mL) coated coverslips for 45 minutes at 37°C. Cells were fixed with 0.2% paraformaldehyde for 10 minutes and permeabilized with 0.2% Triton-X for 5 minutes. Platelets were stained with Alexa-Fluor 488 phalloidin for 1 hour and coverslips mounted. Samples were imaged the next day using a 100X oil immersion lens on a Nikon A1-R confocal microscope, with representative images shown here. Q, quercetin; T, tamarixetin; I, isorhamnetin.

Unlike fibrinogen, platelet adhesion onto CRP-XL was concentration-dependent for quercetin, tamarixetin and isorhamnetin. Quercetin inhibited significantly adhesion onto CRP-XL at 2.5μM and 5μM, with a 53% and 65% average reduction in adhesion, respectively (Figure 3-12A). Tamarixetin inhibited adhesion onto CRP-XL by approximately 30% at 5μM (Figure 3-12C). As seen in other assays, isorhamnetin was statistically significantly more potent compared to tamarixetin at lower concentrations, inhibiting adhesion by an average of 28% at 1μM (Figure 3-12E). This increased potency is not carried through to the higher tested concentrations (5 and 10μM). The increased magnitude of effect in the inhibition of adhesion to CRP-XL compared to fibrinogen implies the initial steps of GPVI signalling leading to platelet adhesion are more potently inhibited by quercetin and its metabolites compared to the initial fibrinogen:integrin signalling interactions. The appearance of the fibrinogen-spread and CRP-XL-spread platelets is different; platelets spread on CRP-XL appear to generally retain a bright actin-rich cell centre, whereas fibrinogen-spread platelets appear to lack this, instead having a more organised lamellipodia structure. The platelet spreading process on CRP-XL is inhibited by quercetin and isorhamnetin in a similar way to spreading on fibrinogen. At 5μM quercetin and isorhamnetin, there is a 30% and a 36% average reduction in platelets reaching the lamellipodia stage (Figure 3-12B,F). However, a significant effect on spreading was not reached at 1μM for any flavonoid tested. Unlike on fibrinogen, a concentration-dependent effect of tamarixetin was observed, with an approximate 20% reduction in platelets extending lamellipodia compared to vehicle control at 5μM (Figure 3-12D). This is consistent with other data presented so far which demonstrate a concentration-dependent effect of quercetin and its methylated metabolites on GPVI-stimulated platelet function. Representative images are shown in Figure 3-13.

The data presented in section 3.4 demonstrates a clear effect of quercetin and its methylated metabolites on integrin $\alpha_{IIb}\beta_3$ function, through a dual effect on 'inside-out' and 'outside-in' signalling. The initial conformational change of integrin $\alpha_{IIb}\beta_3$ to its 'open' state is inhibited, as well as the downstream outside-in signalling leading to functions such as platelet spreading and clot retraction (investigated in Chapter 4). This dual effect on integrin $\alpha_{IIb}\beta_3$ is likely to contribute significantly to

the overall anti-platelet effect of quercetin and its metabolites, as it is a major contributor to the overall platelet activatory process, and is crucial to the development of stable aggregates.

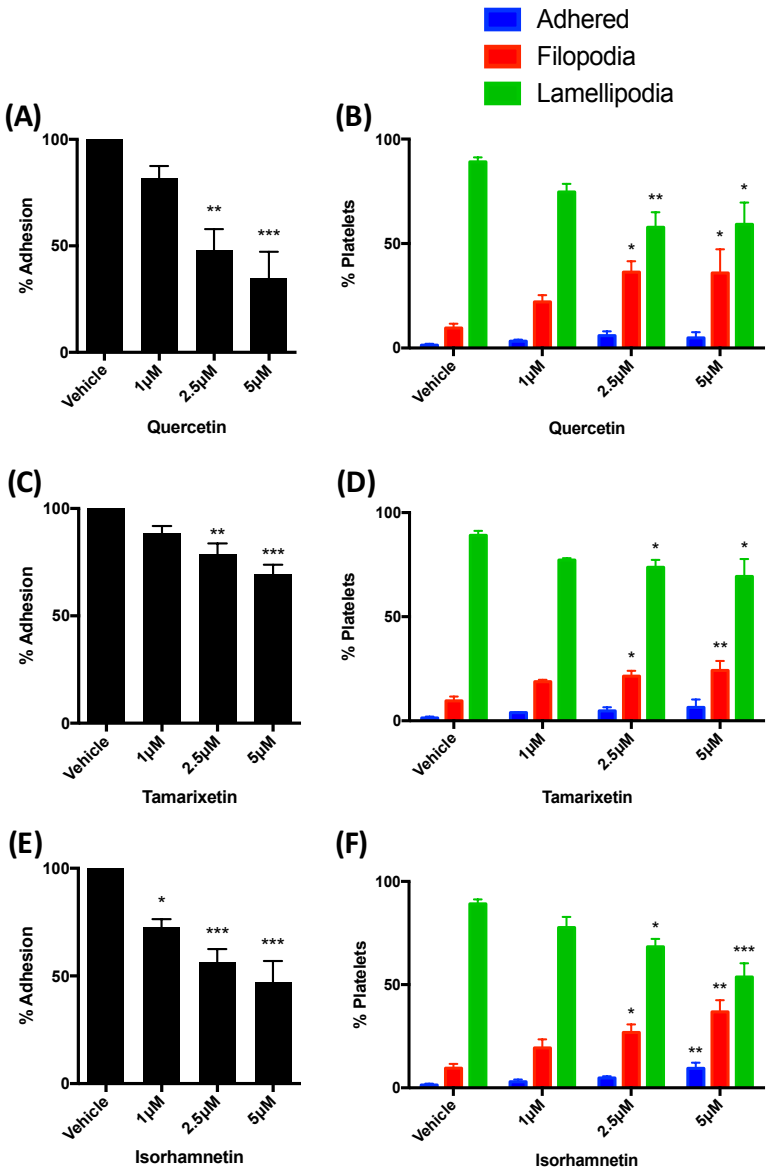

Figure 3-12 Quercetin, tamarixetin and isorhamnetin inhibit adhesion and spreading on CRP-XL

Washed platelets (2 x 10^8 cells/mL) were incubated with quercetin (A/B), tamarixetin (C/D), isorhamnetin (E/F) or vehicle control (DMSO, 0.33% v/v) for 5 minutes, diluted to 2 x 10^7 cells/mL, and then added onto CRP-XL (1μg/mL) coated coverslips for 45 minutes at 37°C. Cells were fixed with 0.2% paraformaldehyde for 10 minutes and permeabilized with 0.2% Triton-X for 5 minutes. Alexa-Fluor 488 phalloidin was added for 1 hour and coverslips mounted onto slides with Prolong Gold Antifade mountant. Data represent percentage adhesion normalised to levels of adhesion in the absence of flavonoid (vehicle) (A,C,E) and percentage of platelets in each stage of spreading (B,D,F), mean ± SEM. Data was analysed from 5 separate, randomly taken images from each sample. N=4, data analysed by one way ANOVA with post-hoc Dunnett's test. *p<0.05, **p<0.005, ***p<0.001, compared to vehicle control.

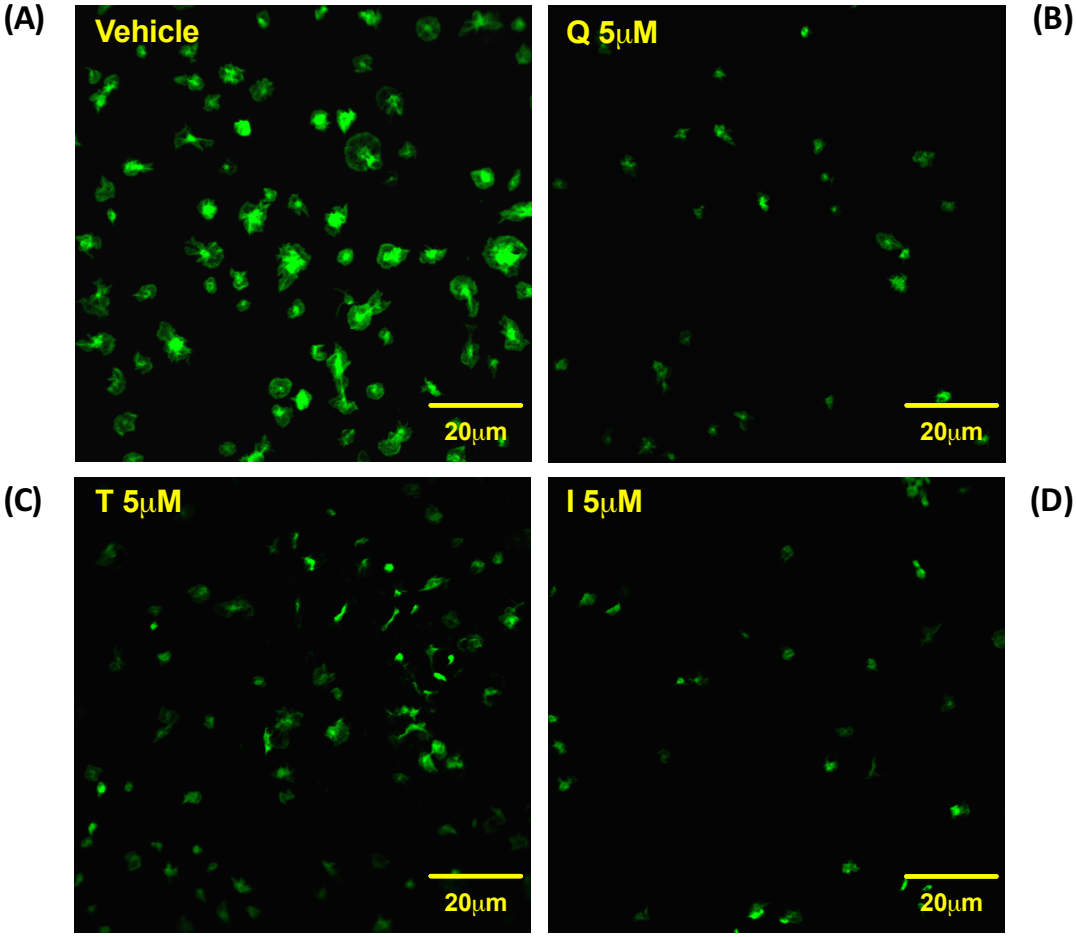

Figure 3-13 Representative images showing quercetin, tamarixetin and isorhamnetin inhibit platelet adhesion and spreading on CRP-XL

Washed platelets (2 x 10^8 cells/mL) were incubated with quercetin (B), tamarixetin (C), isorhamnetin (D) or vehicle control (A) (DMSO, 0.33% v/v) for 5 minutes, diluted to 2 x 10^7 cells/mL, and then allowed to spread on CRP-XL (1μg/mL) coated coverslips for 45 minutes at 37°C. Cells were fixed with 0.2% paraformaldehyde for 10 minutes and permeabilized with 0.2% Triton-X for 5 minutes. Platelets were stained with Alexa-Fluor 488 phalloidin for 1 hour and coverslips mounted. Samples were imaged the next day using a 100X oil immersion lens on a Nikon A1-R confocal microscope, with representative images shown here. Q, quercetin; T, tamarixetin; I, isorhamnetin.

3.5 Cytosolic calcium elevation stimulated by CRP-XL is inhibited by quercetin and its methylated metabolites

The mobilisation of calcium from intracellular platelet stores and the entry of calcium into the cell through membrane channels is a crucial series of events in platelet activation, preceding secretion and integrin activation. It is a very rapid process; indeed, intracellular calcium mobilisation has been reported 0.2-0.3 seconds after thrombin stimulation (Sage and Rink, 1986). Calcium gains entry into the platelet cytosol via release from intracellular stores, store-operated calcium entry (SOCE), and also via store-independent entry mechanisms (discussed in Chapter 1) (Hassock *et al.*, 2002; Stefanini *et al.*, 2009; Prakriya and Lewis, 2015). This increase in cytosolic calcium drives many activatory processes in the platelet, including granule release, TXA_2 formation and integrin $\alpha_{IIb}\beta_3$ activation (Quinton *et al.*, 2002; Stefanini *et al.*, 2009). The activation of phospholipase Cβ/γ is a common factor of platelet stimulation by many agonists; downstream of this activation lies the cleavage of phosphatidylinositol 4,5-bisphosphate (PIP2), resultant generation of inositol triphosphate (IP_3), binding of IP_3 to the IP_3 receptor and the subsequent release of calcium from intracellular stores and the associated activatory mechanisms (Brass and Joseph, 1985; Guillemette *et al.*, 1988; Varga-Szabo *et al.*, 2009). It has been shown previously that dietary flavonoids are able to inhibit collagen-stimulated PLCγ2 phosphorylation, with a planar-hydroxylated C-ring (as present in quercetin) and a methylated B-ring (which tamarixetin and isorhamnetin possess) associated with increased inhibitory potency; at 20μM, quercetin and tamarixetin were reported to inhibit collagen-stimulated PLCγ2 phosphorylation by approximately 30% (Wright *et al.*, 2010b). In the present study it was therefore investigated whether quercetin and its methylated metabolites, tamarixetin and isorhamnetin, directly inhibited the elevation of cytosolic calcium upon CRP-XL stimulation.

PRP was incubated with Fura-2, a fluorescent dye which binds free intracellular calcium, to allow visualisation of calcium in the platelet cytosol. Fura-2 loaded washed platelets (4×10^8 cells/mL) were prepared from the PRP. As described in Section 3.3.1, the different cell density used here (4×10^8

cells/mL) compared to other *in vitro* assays (2 x 10^8 cells/mL) must be considered. Platelets were incubated with quercetin, tamarixetin, isorhamnetin or vehicle control for 5 minutes at 37°C, after which they were stimulated with CRP-XL (1μg/mL)(also at 37°C). Fluorescence was recorded for 5 minutes, and $[Ca^{2+}]_i$ was estimated using the equation described in Chapter 2 (Materials and Methods). Fluorescence values and fluorescence ratios used to calculate $[Ca^{2+}]_i$ were corrected to background autofluorescence (i.e. the fluorescence measurements of unloaded platelets), to ensure accurate calculations.

Stimulation with CRP-XL caused a rise in cytosolic calcium, as seen in Figure 3-14. In vehicle-treated platelets, this peak reached approximately 1500-1800nM. Quercetin inhibited significantly peak cytosolic calcium levels in a concentration dependent manner between 1-10μM. Figure 3-14A shows the cytosolic calcium kinetics for quercetin-inhibited samples compared to vehicle control. Over the 5 minutes of measurement, the calcium concentration of all quercetin-inhibited samples remained lower than the control, showing this is a true inhibitory effect and not a delay in calcium mobilisation. Calculation of peak calcium concentration reached over the 5-minute period (normalised to control) shows that peak calcium levels were inhibited by up to 60% at the highest concentration tested (10μM), with approximately 30% inhibition at a quercetin concentration of 1μM (Figure 3-14B). Tamarixetin inhibited cytosolic calcium elevation similarly to quercetin; at 10μM, an average of 58% reduction in peak cytosolic calcium was observed (Figure 3-14C,D). Significant inhibition was achieved at all isorhamnetin concentrations tested, with the lowest (1μM) decreasing peak cytosolic calcium levels by 35% (Figure 3-14E,F). At 10μM, peak levels were reduced by over 85%, suggesting a role for this methylated metabolite in the potent inhibition of calcium mobilization in platelets upon activation. The overall order of inhibitory potency in the reduction of cytosolic calcium elevation is isorhamnetin > quercetin = tamarixetin, with isorhamnetin inhibiting significantly more than quercetin at 2.5 and 10μM, and no significant difference in effect between quercetin and tamarixetin. All three flavonoids, however, clearly have an effect on this early process in the platelet activation pathway.

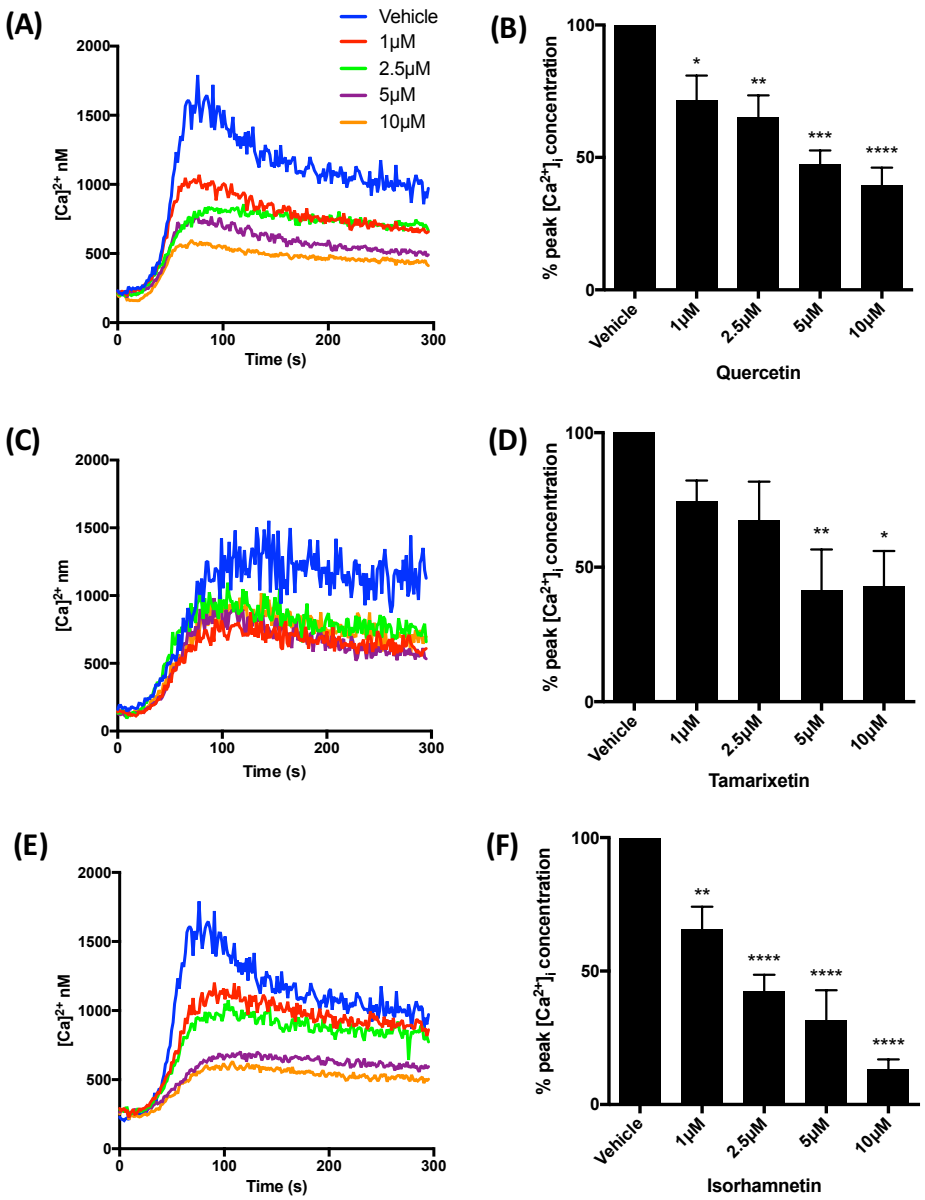

Figure 3-14 Quercetin and its methylated metabolites inhibit CRP-XL-stimulated cytosolic calcium elevation

Fura-2 loaded washed platelets (4 x 10^8 cells/mL) were incubated with quercetin (A,B), tamarixetin (C,D), isorhamnetin (E,F) or vehicle control (DMSO, 0.2% v/v) for 5 minutes at 37°C prior to stimulation with CRP-XL (1μg/mL). Fluorescence (excitation 340 and 380nm, emission 510nm) was recorded for 5 minutes using a NOVOstar plate reader, and $[Ca^{2+}]_i$ was estimated using the equation described in Chapter 2 (A,B,C). Peak $[Ca^{2+}]_i$ was taken as the maximum value reached in the sample over the 5 minute period, and was normalised to peak calcium levels in the absence of flavonoid (vehicle) (B,D,F). N=4, data in B,D,F represent mean ± SEM, analysed by one-way ANOVA with post-hoc Dunnett's test. *p<0.05, **p<0.005, ***p<0.001, ****p<0.0001 compared to vehicle control.

3.6 Combinatorial and more-than-additive inhibitory effects of quercetin, tamarixetin and isorhamnetin

3.6.1 Quercetin and its methylated metabolites can combine to inhibit platelet aggregation in a more than additive way at higher flavonoid concentrations

Quercetin is extensively metabolised *in vivo*, yielding methylated, glucuronidated and sulphated metabolites (Day *et al.*, 2001; Lee *et al.*, 2012b; Nakamura *et al.*, 2014). The presence of the aglycone in plasma is a point of some contention; earlier investigations concluded the aglycone was irrelevant or absent (Gugler *et al.*, 1975; Day *et al.*, 2001). The introduction of new, more sensitive methodologies has, however, confirmed plasma quercetin aglycone, albeit at low levels (for example, 0.2μg/mL 5 minutes after a 10mg/kg dose in rats) (Chen *et al.*, 2005). The importance of the aglycone *in vivo* has also been suggested by Menendez *et al.* (2011), who provide evidence that quercetin-3-O-glucuronide may be deconjugated in target tissues into the aglycone, acting as a plasma 'carrier' for the aglycone, which is suggested as the active substance. In much of the literature, and in the data presented so far, work has largely focussed on the effects of individual flavonoids/metabolites on platelet function. *In vivo*, though, there will be a combination of metabolites as well as, potentially, the aglycone. It was therefore investigated whether quercetin, tamarixetin and isorhamnetin in combination acted in an additive, more than additive, or competitive way on platelet aggregation, fibrinogen binding and P-Selectin exposure.

To test the combined effects of quercetin and its metabolites on platelet aggregation, due to large sample numbers, a plate-based aggregation assay was utilised using a modified version to that originally described by Lordkipanidzé *et al.* (2014). Washed platelets (2×10^8 cells/mL) were added into wells pre-loaded with flavonoids or vehicle control and incubated for 5 minutes at 37°C. Collagen (5μg/mL) was added to wells and the plate was shaken at 1200rpm for 5 minutes using a BioShake iQ heated plate shaker at 37°C. This enabled, as closely as possible, the conditions of light transmission aggregometry (LTA) to be maintained, whilst allowing for high throughput experimentation.

Absorption of 405nm light was measured in a plate reader and absorption values were converted to percentage aggregation, with unstimulated and uninhibited samples acting as 0 and 100% aggregation, respectively. This assay gives an endpoint readout, and as such foregoes the kinetics of platelet aggregation that LTA usefully provides. This is balanced out, however, when considering the increase in throughput it provides, as well as allowing the simultaneous analysis of multiple flavonoids, reducing inter-donor variability.

Figure 3-15 shows the inhibitory effects of combining quercetin with isorhamnetin (A), quercetin with tamarixetin (B), tamarixetin with isorhamnetin (C), and all three together (D). More-than-additive effects were attributed by comparing the effects of individual flavonoids added together (e.g. the inhibitory effect of quercetin 5μM added onto that of isorhamnetin 5μM) to that of dual treatment (quercetin 5μM + isorhamnetin 5μM dual (simultaneous) incubation) from the same donors. A statistically significantly higher response was then denoted by an "S". As can be seen across Figure 3-15, dual or triple flavonoid treatment resulted in significant inhibition of aggregation compared to vehicle control when combining concentrations as low as 2.5μM. In the case of triple flavonoid treatment, 1μM of each inhibited platelet aggregation by 23%. In the circulation, individual flavonoids may reach these low levels that, individually, do not inhibit aggregation, but when combined, have a significant effect. Worthy to note are the differences in the effect of individual flavonoid concentrations in this assay compared to traditional light transmission aggregometry (Figures 3-1 and 3-2), specifically a lack of significant inhibitory effect at individual concentrations except quercetin 5μM. This could be due to assay differences, and is discussed further in section 3.8. Interestingly, tamarixetin and isorhamnetin in combination only inhibited significantly platelet aggregation when dual 5μM treatment was given. This effect in itself was low, reducing aggregation by 30% compared to a ~80% and ~90% effect for quercetin/isorhamnetin and quercetin/tamarixetin dual treatment, respectively. A low inhibitory effect was observed at all isorhamnetin/tamarixetin combinations, as seen in Figure 3-15C.

A more-than-additive effect was observed only at 5μM for quercetin/isorhamnetin dual treatment, inhibiting aggregation by ~80% (Figure 3-15A). Quercetin/tamarixetin dual treatment caused such effects at lower flavonoid concentrations; quercetin 5μM + tamarixetin 1μM reduced aggregation by ~65% (Figure 3-15B). Tamarixetin/isorhamnetin dual treatment did not cause a more than additive inhibitory effect at any tested concentrations; indeed, a general low effect of this combination is observed. Triple treatment resulted in a more-than-additive effect at 5μM (of quercetin, tamarixetin plus isorhamnetin), completely preventing aggregation (Figure 3-15D); however, a total flavonoid concentration of 15μM is high relative to physiologically feasible levels through dietary means. Such more-than-additive effects of flavonoids, on the whole, therefore, appear to be largely confined to higher concentrations, and may be indicative of synergistic effects between flavonoids. These do, however, correspond to concentrations that are physiologically achievable, as discussed in section 3.2.

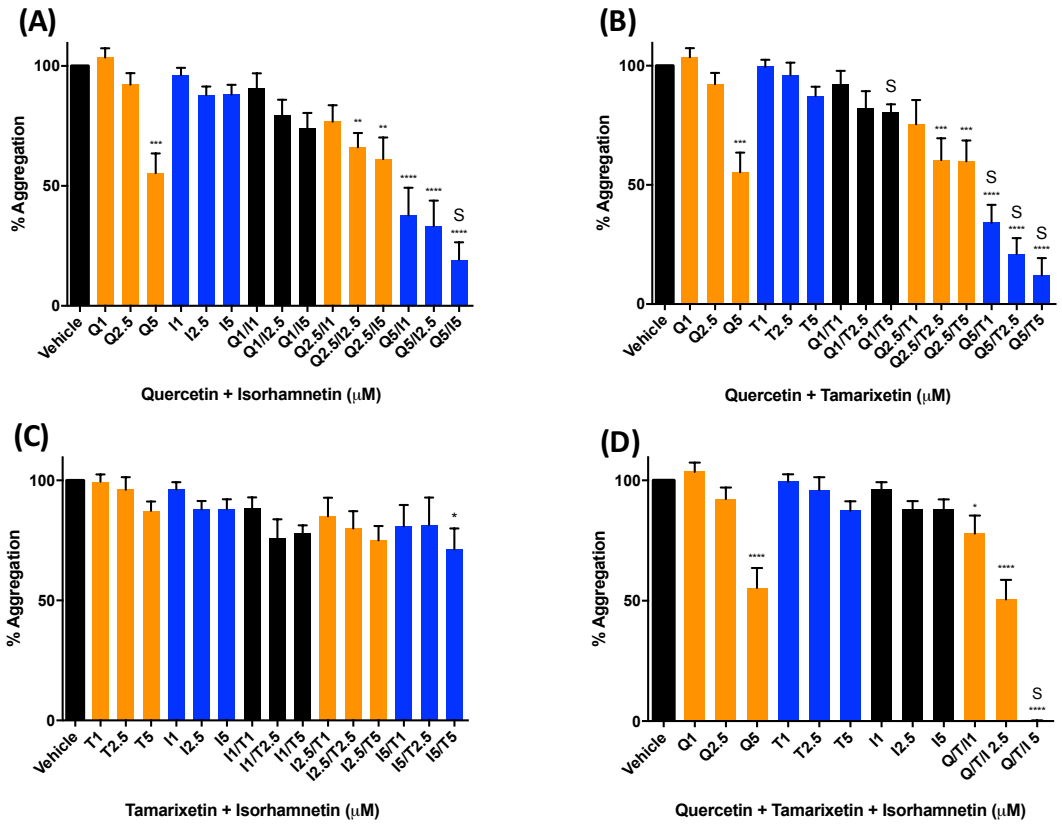

Figure 3-15 The effect of quercetin/metabolite combinations on collagen-stimulated platelet aggregation

Washed platelets (2 x 10^8 cells/mL) were incubated in a 96 well plate with flavonoid combinations or vehicle control (1% DMSO, v/v) for 5 minutes at 37°C on a heated plate shaker. Collagen (5µg/mL) was added to wells and the plate was shaken at 1200rpm for 5 minutes at 37°C. Absorption of 405nm light was then measured on a plate reader, and values converted to percentage aggregation using unstimulated and stimulated (uninhibited) samples to represent 0% and 100%, respectively. (A) quercetin plus isorhamnetin. (B) quercetin plus tamarixetin. (C) tamarixetin plus isorhamnetin. (D) quercetin plus tamarixetin plus isorhamnetin. Data represent percentage aggregation, normalised to levels of aggregation in the absence of flavonoid (vehicle). N=5, data represent mean ± SEM. Data analysed by one-way ANOVA with post-hoc Dunnett's test for effect compared to vehicle control, and by Mann Whitney U-test for test of more-than-additive effects. *p<0.05, **p<0.005, ***p<0.001, ****p<0.0001 compared to vehicle control. "S" indicates a more-than-additive effect of dual treatment compared to the combined effects of individual flavonoid concentrations. Q, Quercetin; I, Isorhamnetin; T, Tamarixetin.

3.6.2 More-than-additive effects on fibrinogen binding and P-Selectin exposure also occur only at higher flavonoid concentrations

The presence of some potentially synergistic interactions between quercetin and its metabolites in the inhibition of platelet aggregation led to the investigation of their combined effects on fibrinogen binding and P-Selectin exposure. As fibrinogen binding and α-granule release are, as previously mentioned in this chapter, key drivers of aggregation, it was hypothesised that more than additive interactions of flavonoids may occur to inhibit these processes, thereby dampening downstream platelet aggregation.

Washed platelets (2 x 10^8 cells/mL) were incubated with flavonoid combinations or vehicle control for 5 minutes. FITC-conjugated anti-fibrinogen antibody and PE/Cy5 anti-human CD62 antibody were added, and platelets were stimulated with CRP-XL (1μg/mL) for 20 minutes, after which they were fixed in 0.2% (w/v) paraformaldehyde. Fibrinogen binding and P-Selectin exposure on the cell surface was then analysed by flow cytometry.

Significant inhibition of both P-Selectin exposure and fibrinogen binding upon treatment with individual flavonoid concentrations was observed at 2.5μM quercetin, and 1 and 2.5μM isorhamnetin. The data presented in Figures 3-5 and 3-7 displays significant inhibition of these molecular processes at slightly lower individual flavonoid concentrations; a lack of significant effect here is attributed to comparatively large standard errors. Every flavonoid combination tested inhibited significantly both fibrinogen binding and P-Selectin exposure (Figure 3-16A/C). Dual flavonoid treatment with quercetin + tamarixetin, quercetin + isorhamnetin, and tamarixetin + isorhamnetin showed similar effects, with 0.5μM dual treatment inhibiting fibrinogen binding by ~45% and P-Selectin exposure by ~50%. Treatment with all three flavonoids, as expected, resulted in increased inhibition, with 0.5μM triple treatment reducing fibrinogen binding by 55% and P-Selectin exposure by 64%. It is interesting to note that the reduced potency of the tamarixetin + isorhamnetin combination as seen in section 3.6.1

is not observed here; this implies that the decreased effect on aggregation is not due to a reduced effect on fibrinogen binding or α-granule secretion, but through action (or lack thereof) on another mechanism driving platelet aggregation. Similar to the aggregation data presented in the previous section, more-than-additive, potentially synergistic interactions between flavonoids are again reserved to the higher concentrations tested. Such an effect on CRP-XL stimulated fibrinogen binding was observed only at 2.5μM quercetin + tamarixetin + isorhamnetin, inhibiting by ~85% (Figure 3-16A). P-Selectin exposure was inhibited in a more than additive manner by quercetin + isorhamnetin 2.5μM (~90% reduction), as well as by quercetin + tamarixetin + isorhamnetin 2.5μM (92% inhibition) (Figure 3-16C). Representative fluorescence histograms for triple flavonoid treatment are shown in Figure 3-16B (fibrinogen binding) and Figure 3-16D (P-Selectin exposure).

Combined with the aggregation data in section 3.6.1, this provides evidence that quercetin and its metabolites can act in a more-than-additive, potentially synergistic way to inhibit platelet function. As multiple metabolites as well as (potentially) the aglycone circulate in plasma following consumption, this may offer an explanation as to how quercetin is able to inhibit platelet function upon dietary or supplemental intake despite its rapid and extensive metabolism.

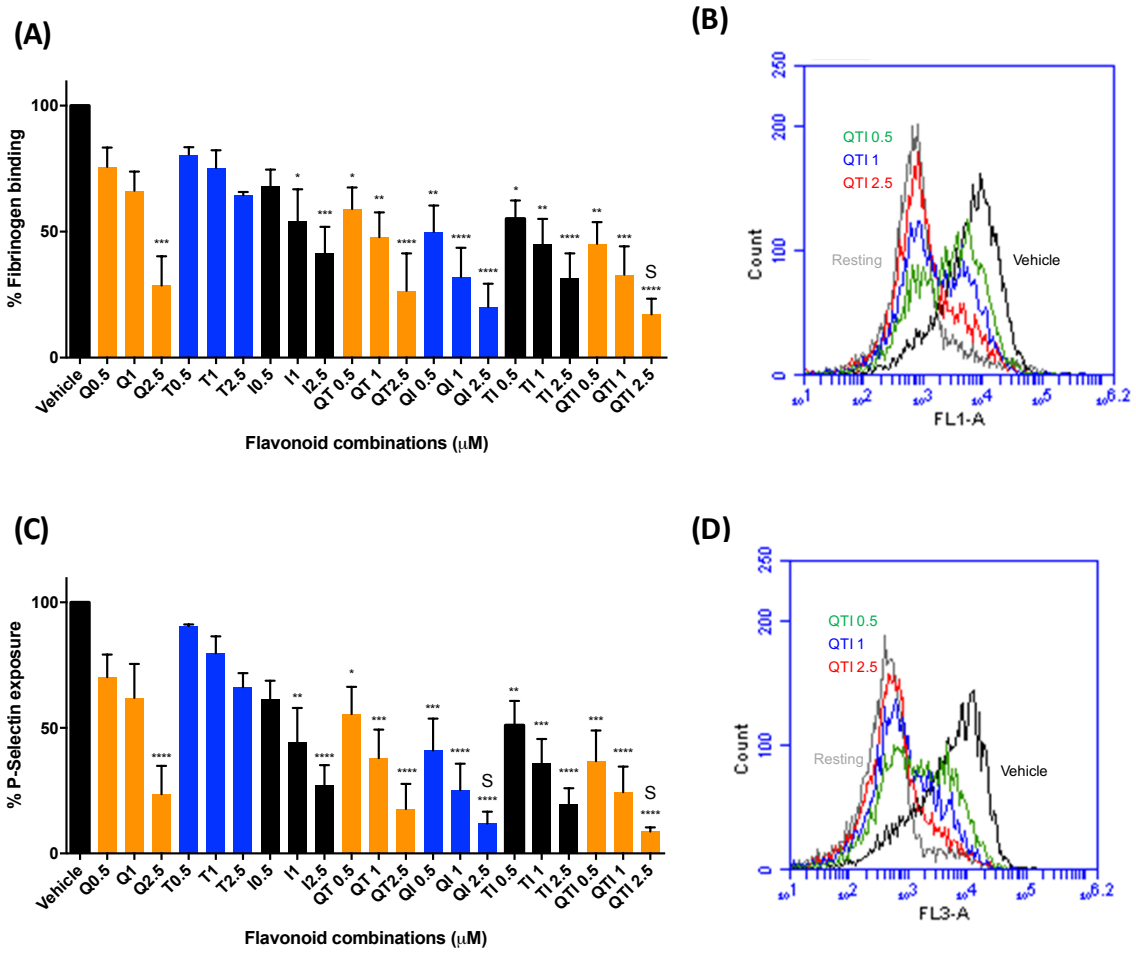

Figure 3-16 The effect of quercetin/metabolite combinations on CRP-XL stimulated fibrinogen binding and P-Selectin exposure

Washed platelets (2 x 10^8 cells/mL) were incubated with flavonoid combinations or vehicle control (DMSO, 1% v/v) for 5 minutes, after which FITC-conjugated anti-fibrinogen antibody and PE/Cy5 anti-human CD62P antibody were added. Samples were then stimulated with CRP-XL (1µg/mL) for 20 minutes, after which they were fixed in 0.2% paraformaldehyde. Fibrinogen binding (A) and P-Selectin exposure (C) on the cell surface was then measured by flow cytometry and data normalised to levels of fibrinogen binding and P-Selectin exposure in the absence of flavonoid (vehicle). Representative fluorescence histograms upon triple flavonoid treatment (B/D). N=4, data represent mean ± SEM. *p<0.05, **p<0.005, ***p<0.001, ****p<0.0001 compared to vehicle control, "S" indicates a more-than-additive effect of dual treatment compared to the combined effects of individual flavonoid concentrations. Data analysed by one-way ANOVA with post-hoc Dunnett's test for effect compared to vehicle control, and by Mann Whitney U-test for test of more-than-additive effects. Q, Quercetin; T, Tamarixetin; I, Isorhamnetin.

3.7 Platelet activation through GPCR pathways is also inhibited by quercetin and its methylated metabolites

The data presented so far has focussed primarily on the GPVI-dependent mechanism of platelet activation, as this is one of the key early processes that drives the system forward. Whilst initial platelet adhesion and interaction with vWF and subendothelial collagen is a process largely independent of GPCR mechanisms, G-protein coupled receptor signalling stimulated by the binding of the soluble ligands ADP, thromboxane A_2 and thrombin are crucial in the propagation of the growing thrombus (Woulfe, 2005; Offermanns, 2006). Adenosine diphosphate binds and signals through the two GPCRs $P2Y_1$ (coupled to G_q) and $P2Y_{12}$ (coupled to G_i) (Jin *et al.*, 1998; Hechler *et al.*, 1998; Hollopeter *et al.*, 2001). Thromboxane A_2, produced in the platelet from arachidonic acid, binds the thromboxane receptor (TP), which is coupled to two G proteins; G_q and G_{13} (Knezevic *et al.*, 1993; Djellas *et al.*, 1999; Paul *et al.*, 1999). Thrombin acts in a different manner, in that it cleaves part of the N-terminus of the GPCRs PAR-1 and PAR-4; this cleavage results in the exposure of a sequence that acts as a tethered ligand for the PARs (Vu *et al.*, 1991; Kahn *et al.*, 1999; Woulfe, 2005). The activation of these GPCRs leads to the transduction of signals resulting in the activation of PLC and associated calcium mobilisation, cytoskeletal remodelling, decrease in cAMP levels, and the activation of Rho and PI3K (Hung *et al.*, 1992; Negrescu *et al.*, 1995; Klages *et al.*, 1999; Kauffenstein *et al.*, 2001; Li *et al.*, 2003). It has been shown that quercetin aglycone can inhibit thrombin-stimulated platelet aggregation and tyrosine phosphorylation (Navarro-Núñez *et al.*, 2009). The aglycone has also demonstrated some ability to inhibit platelet responses to thromboxane A_2 and ADP (Beretz *et al.*, 1982; Guerrero *et al.*, 2007). These data are, however, far from exhaustive, and to a large degree have not considered the effects of the metabolites of quercetin. The ability of quercetin aglycone as well as tamarixetin and isorhamnetin to inhibit platelet aggregation stimulated by a range of ADP, U46619 (9,11-Dideoxy-11α,9α-epoxymethanoprostaglandin F2α, a thromboxane A_2 mimetic) and thrombin concentrations was therefore investigated, in order to understand how GPCR-mediated platelet function is altered by these flavonoids.

To test a range of agonists at varying concentrations, the plate-based aggregometry method was again utilised. ADP-sensitive washed platelets (2 x 10^8 cells/mL) were incubated with flavonoid or vehicle control (DMSO, 0.2% v/v) for 5 minutes at 37^{o}C on a heated plate shaker in a 96-well plate. ADP-sensitive washed platelets were used due to the use of soluble agonists such as ADP in this assay; during the normal platelet preparation described in Section 2.2.1, platelets can become desensitised to ADP due to higher centrifugation speeds. Platelets were stimulated with ADP, U46619 or thrombin over a range of concentrations and the plate was shaken at 1200rpm for 5 minutes at 37^{o}C. Absorption of 405nm light was measured and converted into percentage aggregation as described in section 3.6.1, normalized to levels of aggregation in the absence of flavonoid (vehicle). Percentage aggregation values were plotted, with the coloured stars in Figures 3-17 and 3-18 indicating a significant inhibitory effect at the concentration of agonist represented by the same colour line compared to vehicle control, e.g. if a quercetin concentration caused significant inhibition of aggregation stimulated by 2.5μM ADP, this would be represented by a red star.

Quercetin inhibited significantly ADP-stimulated aggregation in a concentration-dependent manner (Figure 3-17A). This was observed as low as 1μM; when stimulated with 2.5μM ADP, platelet aggregation was inhibited 30%. The maximum effect on platelet aggregation was a 70% reduction, achieved by 10μM quercetin upon stimulation again with 2.5μM ADP. Compared to collagen-stimulated aggregation data as seen in Figures 3-1 and 3-2, it can be seen that whilst inhibition at 1μM was less pronounced upon stimulation of aggregation with collagen, at 10μM it was all but abolished, implying a stronger role for quercetin in the inhibition of collagen-stimulated aggregation at higher concentrations compared to its effect on ADP-mediated aggregation, with perhaps a reversed, weaker role at lower flavonoid concentrations. It must also be considered, however, the difference in assay methodology; LTA vs plate-based aggregometry, which could also be a cause of some variation in results (and as such a direct comparison of results is carried out with appropriate caution). Tamarixetin overall showed a similar potency compared to quercetin. At 1μM it inhibited aggregation >40% when

stimulated with 5μM ADP (Figure 3-17B). At higher concentrations it inhibited similarly to collagen-stimulated aggregation; 10μM tamarixetin reduced aggregation by approximately 60% upon stimulation with 1μM ADP. Isorhamnetin dose-dependently effected ADP-stimulated aggregation in a similar way to quercetin, reaching a maximal inhibitory effect of 65% at 10μM isorhamnetin, with 30% reduction of aggregation at 1μM isorhamnetin upon stimulation with 5μM ADP (Figure 3-17C). Again, this demonstrates a slightly reduced efficacy compared to inhibition of collagen-stimulated aggregation at higher flavonoid concentrations, with increased effect at lower concentrations.

Compared to ADP-stimulation, platelet aggregation induced by U46619 was less effected by quercetin, tamarixetin and isorhamnetin (Figure 3-17D,E,F). Indeed, significant inhibition by quercetin was only achieved at 10μM, with a maximum reduction in aggregation of 45% upon stimulation with 0.1μM U46619 (Figure 3-17D). Tamarixetin decreased aggregation by only ~38% at 10μM, although a significant effect was also seen at 7.5 and 5μM (Figure 3-17E). Isorhamnetin at 10μM inhibited aggregation by an average of 55%, with a significant (40%) effect observed at 7.5μM, upon stimulation with 0.1μM U46619 (Figure 3-17F). Compared to platelet aggregation stimulated through GPVI, however, this is again a less potent effect, as also seen upon stimulation with ADP. This continues to provide evidence for a weaker (yet still high) maximal role for GPCR-mediated pathway inhibition in the effect of quercetin and its methylated metabolites on platelet function compared to GPVI-mediated effects at higher flavonoid concentrations.

Thrombin is one of the, if not arguably the most potent platelet agonist (McNicol and Gerrard, 1993; Chen *et al.*, 2004). It was therefore also of interest how quercetin and its metabolites effected aggregation stimulated by this serine protease. As with ADP and U46619, thrombin-stimulated platelet aggregation was effected by quercetin to a much lesser degree than with collagen-stimulation at higher concentrations; 10μM quercetin inhibited aggregation by up to 45% (Figure 3-18A). It is interesting to note that (again as with ADP and U46619) lower concentrations (i.e. 1μM) reduced platelet aggregation more potently, up to ~37%. As aforementioned, this could imply a narrower range

of effect for flavonoids in GPCR-mediated platelet function, but the difference in assay methodology (plate based aggregation here compared to light transmission aggregometry for the collagen-stimulated aggregation data) must also be kept in mind. Significant inhibition was observed only at 7.5μM tamarixetin (~33% effect upon stimulation with 0.025U/mL thrombin) (Figure 3-18B). Isorhamnetin displayed dose-dependent significant inhibition of 0.025U/mL thrombin-stimulated platelet aggregation as low as 2.5μM (30%), with a maximal effect at 10μM of ~52% (Figure 3-18C).

Overall, the results presented in section 3.7 display a role for quercetin, tamarixetin and isorhamnetin in the inhibition of platelet GPCR pathways. There is a difference in the magnitude of the effect in general, the maximal effect being reduced compared to GPVI-mediated aggregation; this may be unsurprising given the high level of involvement of tyrosine kinases in the critical GPVI pathway of platelet activation and resultant sensitivity to the effects of kinase inhibitors, contrasted to the comparatively lesser (yet still key) roles of GPCRs in the platelet activation process (discussed in Chapter 1). Nonetheless, quercetin, tamarixetin and isorhamnetin do significantly inhibit aggregation stimulated through GPCR-mediated pathways. This is likely due to quercetin's ability to inhibit a broad spectrum of kinases, both in platelets and other cell types (Wright *et al.*, 2010b; Boly *et al.*, 2011; Oh *et al.*, 2012; Russo *et al.*, 2014a).

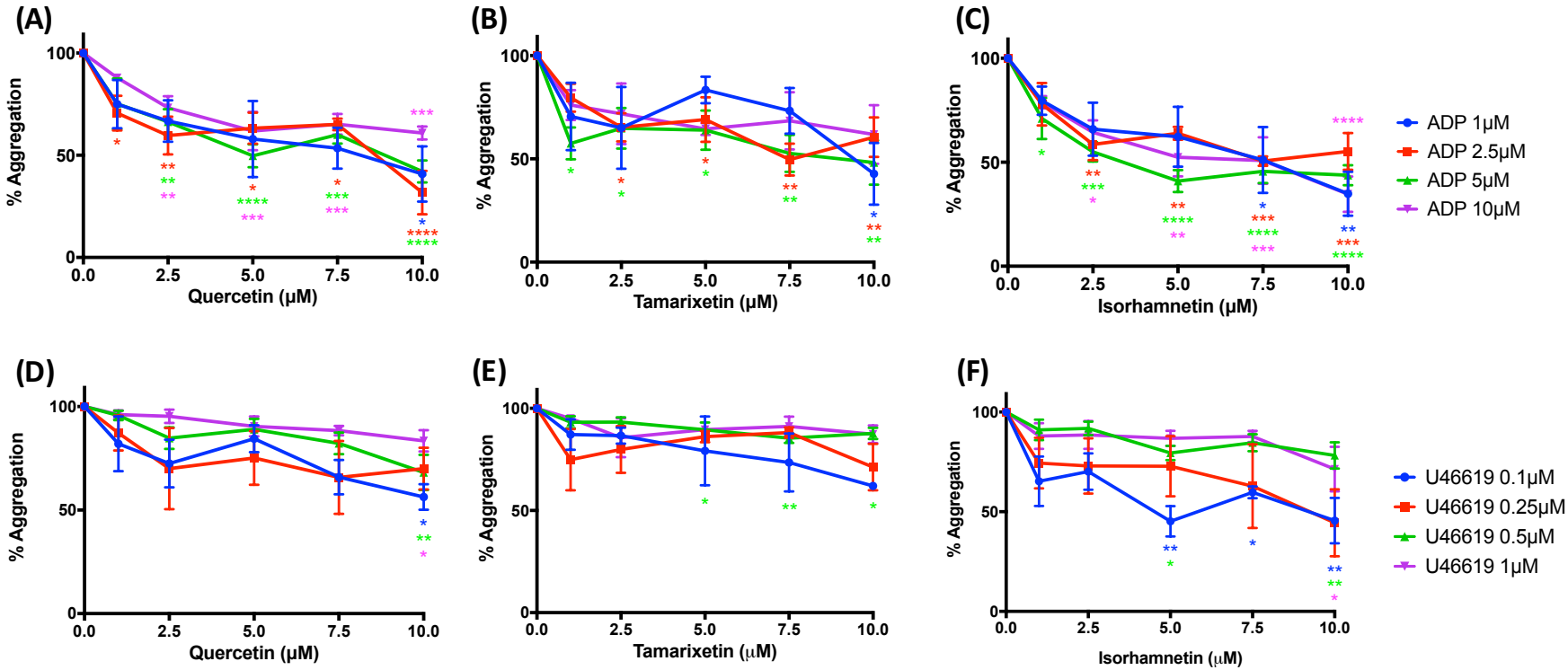

Figure 3-17 Quercetin, tamarixetin and isorhamnetin inhibit platelet aggregation stimulated through G-protein coupled receptors

Washed platelets (2 x 10^8 cells/mL) were incubated in a 96 well plate with quercetin (A,D), tamarixetin (B,E), isorhamnetin (D,F) or vehicle control (DMSO, 0.2% v/v) for 5 minutes at 37°C on a heated plate shaker. ADP or U46619, at concentrations indicated by the legend, were added to wells and the plate was shaken at 1200rpm for 5 minutes at 37°C. Absorption of 405nm light was then measured on a plate reader, and values converted to percentage aggregation using unstimulated and stimulated (uninhibited) samples to represent 0% and 100%, respectively. Data represent percentage aggregation with each agonist concentration normalised to levels of aggregation in the absence of flavonoid (vehicle). N=4, data represent mean ± SEM. Data analysed by one-way ANOVA with post-hoc Dunnett's test, coloured stars refer to statistical significance compared to vehicle control against the agonist indicated by the same colour line in the legend. *p<0.05, **p<0.005, ***p<0.001, ****p<0.0001. ADP, adenosine diphosphate.

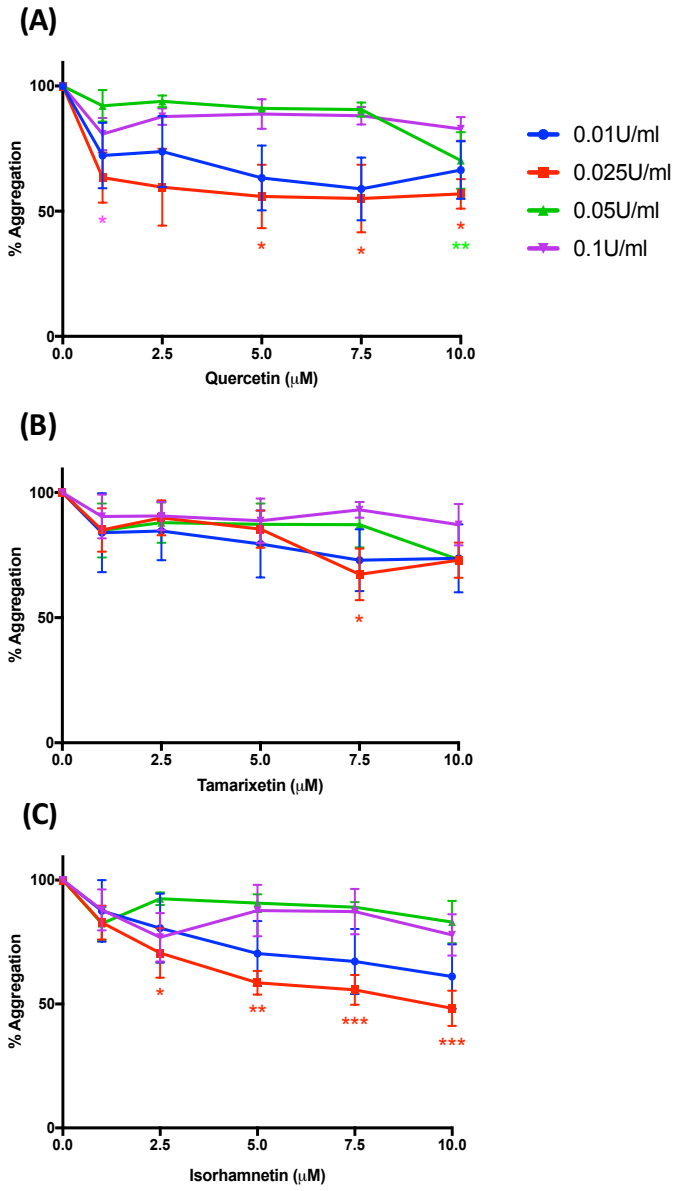

Figure 3-18 – Quercetin and its methylated metabolites inhibit thrombin-stimulated platelet aggregation

Washed platelets (2 x 10^8 cells/mL) were incubated in a 96 well plate with quercetin (A), tamarixetin (B), isorhamnetin (C) or vehicle control (DMSO, 0.2% v/v) for 5 minutes at 37°C on a heated plate shaker. Thrombin, at concentrations indicated by the legend, were added to wells and the plate was shaken at 1200rpm for 5 minutes at 37°C. Absorption of 405nm light was then measured on a plate reader, and values converted to percentage aggregation using unstimulated and stimulated (uninhibited) samples to represent 0% and 100%, respectively. Data represent percentage aggregation with each agonist concentration normalised to levels of aggregation in the absence of flavonoid (vehicle). N=4, data represent mean ± SEM. Data analysed by one-way ANOVA with post-hoc Dunnett's test, coloured stars refer to statistical significance compared to vehicle control against the agonist indicated by the same colour line in the legend. *p<0.05, **p<0.005, ***p<0.001, ****p<0.0001.

3.8 Discussion of results presented in Chapter 3

The purpose of this chapter was to elucidate the mechanisms through which quercetin affects human platelet function, as well as to investigate the efficacy and potency of its metabolites. These aims were addressed using a range of assays in which washed platelets were used, utilising quercetin and its methylated metabolites tamarixetin and isorhamnetin, and to a lesser degree the glucuronidated metabolite quercetin-3-glucuronide. The use of washed platelet removes potentially interfering variables such as plasma proteins and allows effects to be studied in a 'clean' system. As stated in section 3.6.1, there is some contention in the literature regarding the presence of quercetin aglycone in plasma following consumption. Work by Chen *et al.* (2005) has shown the aglycone present in plasma, and Menendez *et al.* (2011) have proposed the de-conjugation of quercetin glucuronide to the aglycone as a mechanism through which quercetin may have a vascular effect *in vivo*. Kawai *et al.* (2008) have also shown de-conjugation of quercetin-3-glucuronide to the aglycone and methylated forms in atherosclerotic plaque-associated macrophages, hypothesised to be through action of the enzymes β-glucuronidase (both plasma and cell-resident) and catechol-*O*-methyl transferase (COMT). Indeed, platelets possess both of these enzymes, and the metabolic activity of platelet COMT in quercetin metabolism has also been suggested (De Luca *et al.*, 1976; Wiley *et al.*, 1976; Stramentinoli *et al.*, 1978; Wright *et al.*, 2010a). For these reasons, and to act as a comparator to metabolites, quercetin aglycone was included in the functional assays.

As the primary function of platelets is to aggregate at the site of vessel injury, initial testing focussed on a collagen-stimulated platelet aggregation assay. Quercetin, tamarixetin and isorhamnetin were found to inhibit platelet aggregation in a similar yet hierarchical manner; isorhamnetin > quercetin > tamarixetin, as indicated by the IC_{50} values. This hierarchy is a consistent observation throughout the results presented in this chapter, and indicates that metabolism could enhance anti-platelet effect; as metabolism is extensive upon consumption of quercetin, this observation may provide some evidence towards the explanation of quercetin's anti-platelet effect *in vivo,* despite plasma aglycone levels being

low. The observed IC_{50} values are lower than previously reported. For example, Hubbard *et al.* (2003) calculated an IC_{50} of 8.69μM for the inhibition of aggregation stimulated by the same concentration of agonist (collagen 5μg/mL). This difference in values may reflect different experimental time points and methodologies. It may also reflect reagent differences, perhaps an improvement in flavonoid preparation and impurity removal with time. Indeed, Hubbard *et al.* (2003) reported a reduced IC_{50} value compared to results reported some decades prior to their publication (Beretz *et al.*, 1982; Landolfi *et al.*, 1984). Quercetin-3-glucuronide required concentrations an order of magnitude higher to achieve a significant effect. It is hypothesised that this could represent an inability of this metabolite to enter the platelet due to the glucuronide moiety; quercetin-3-glucuronide has been previously described as cell impermeable (Shimizu *et al.*, 2015). It is therefore also possible that metabolism, specifically through glucuronidation, can reduce platelet inhibitory effect.

An observation of the anti-aggregatory effect of quercetin and its methylated metabolites led to the investigation of the factors driving this process; granule secretion is one such early event. Dense granule secretion, measured via lumi-aggregometry, was inhibited significantly at a flavonoid range of 2.5-10μM. P-Selectin exposure on the platelet cell surface was used as a marker of α-granule secretion, measured using flow cytometry, and was potently inhibited by quercetin, isorhamnetin and tamarixetin. Inhibition of this process was observed as low as 0.5μM, demonstrating a significant (up to 40%) effect at a sub-micromolar concentration proved easily physiologically achievable. These data support previous observations of quercetin as an inhibitor of granule secretion. However, it demonstrates an increased potency compared to previous reports: for example, Oh *et al.* (2012) observed an anti-secretory effect only at 25μM quercetin or higher concentrations. The difference seen between the magnitude of effect on dense and α-granule secretion likely lies in the different methodologies; dense granule secretion was measured under stirring, aggregating conditions detecting luminescence, and α-granule secretion was measured in a static well detecting fluorescence. Nonetheless, it is clear that quercetin, tamarixetin and isorhamnetin reduce the levels of platelet granule secretion. The inhibition of aggregation is likely explained to a degree by this result; if the

release of pro-activatory molecules (including fibrinogen, which in washed platelets comes primarily from granule secretion as plasma fibrinogen has been removed) is lowered, the aggregatory process they drive will also be dampened. Quercetin-3-glucuronide, as in aggregometry, was much less effective in preventing P-Selectin exposure.

α-granules secrete fibrinogen, which interacts with activated integrin $\alpha_{IIb}\beta_3$, driving signalling inside the platelet and the formation of platelet-platelet interactions and a stable aggregate. As the process of granule release is inhibited by quercetin and its metabolites, it was next investigated if the fibrinogen:integrin $\alpha_{IIb}\beta_3$ interaction is also altered. Inside-out signalling was measured using a fibrinogen binding flow cytometry assay, and was found to be significantly inhibited by quercetin and both methylated metabolites, with >25% inhibition at concentrations as low as 0.5μM. As with granule secretion, inhibition is again lower than previously reported values (Oh *et al.*, 2012). The hierarchy of effect, isorhamnetin > quercetin > tamarixetin, is maintained for the inhibition of inside-out signalling, as seen in Table 1. This suggests that methylation at the 3' position is important for inhibitory potency, whilst 4'-methylation may result in a reduced effect compared to the aglycone. Consistent with aggregation and P-selectin exposure, quercetin-3-glucuronide required much higher concentrations to achieve an inhibitory effect, hypothesised to be due to cell impermeability. As a result of these findings, quercetin-3-glucuronide was excluded from further functional assays. Given its limited effect on platelet function *in vitro,* its inhibitory activity on kinases in a cell free system could also be tested; regardless of the possibility of it not gaining entry into the cytosol (which could be explored further using microscopy), it may be a weak inhibitor. Recent work from other groups has shown that a 3-O glycosidic linkage as found in quercetin-3-glucuronide may result in preferential inhibition of extracellular targets such as extracellular protein disulphide isomerase (PDI), resulting in an inhibition of platelet thrombin generation and thrombus formation (Jasuja *et al.*, 2012; Stopa *et al.*, 2017). As such, it may be an effective metabolite *in vivo,* and the ability of quercetin-3-glucuronide to inhibit PDI activity could also be explored.

The above work demonstrated the ability of quercetin to inhibit fibrinogen binding stimulated by a single agonist. However, *in vivo,* there are numerous activatory factors present. Individually, at low concentrations, they may not cause substantial activation. When combined, though, they cause a greater-than-sum (synergistic) platelet response. This was confirmed, with concentrations of CRP-XL and thrombin that did not aggregate platelets individually, when added together caused a full aggregatory response. In a novel observation, quercetin inhibited significantly fibrinogen binding stimulated by this dual agonist stimulation, with concentrations as low as 0.5μM inhibiting ~70%. This may offer another potential mechanism through which low concentrations of flavonoids achieved through diet are able to inhibit platelet function.

Following inside-out signalling and the binding of fibrinogen to integrin $\alpha_{IIb}\beta_3$, outside-in signalling drives platelet spreading with the extension of filopodia and lamellipodia. As an effect on inside-out signalling was demonstrated, it was investigated whether quercetin, tamarixetin and isorhamnetin also inhibited the signalling of integrin $\alpha_{IIb}\beta_3$ from outside-in. This was tested through static platelet adhesion and spreading on fibrinogen. Quercetin and its methylated metabolites were found to inhibit both adhesion and spreading on fibrinogen, with a reduction in the number of platelets spreading lamellipodia. A plateau of effect was seen on adhesion, with all flavonoids at all concentrations inhibiting adhesion by only 25%; as discussed in section 3.4.3, this may be beneficial, as spreading is important for haemostasis, and so a limited effect could protect this important physiological mechanism, whilst proving protective against thrombosis (Discussed in Chapter 8) (Lee *et. al.,* 2012a). This clearly demonstrates the ability of quercetin, tamarixetin and isorhamnetin to inhibit platelet integrin $\alpha_{IIb}\beta_3$ outside-in signalling. Platelets also spread on collagen, and there is evidence to suggest that GPVI is involved in this (Falet *et al.*, 2000). Thus, platelet spreading on CRP-XL was also investigated. As with fibrinogen, all tested flavonoids inhibited adhesion and spreading onto CRP-XL, with adhesion and spreading affected in a concentration-dependent manner. Adhesion to CRP-XL was more potently affected, implying inhibition of the GPVI signalling pathway is stronger. A specific effect on adhesion and spreading on CRP-XL may point to an inhibition of GPVI dimerization, thereby

reducing the ability of the platelet to bind CRP-XL. It may also be that quercetin and its metabolites affect the clustering of GPVI dimers, demonstrated recently to be important to the GPVI activation pathway (Poulter *et al.*, 2017). Further work could test these hypotheses. These results are in agreement with Navarro-Núñez *et al.* (2010), who showed quercetin at 50μM inhibited platelet spreading on collagen and fibrinogen; the concentrations used here are much lower, however, and also show for the first time the ability of quercetin's methylated metabolites to inhibit this process. Overall, these results demonstrate a clear effect of quercetin and its metabolites on integrin $\alpha_{IIb}\beta_3$ function.

Before platelets secrete their granule contents and integrin $\alpha_{IIb}\beta_3$ becomes activated lies the mobilisation of calcium through release of calcium from intracellular stores and its entry into cells through store-operated and store-independent mechanisms. This calcium mobilisation is driven by the activation-dependent phosphorylation of phospholipase C, production of inositol trisphosphate (IP_3) through hydrolysis of phosphatidylinositol 4,5-bisphosphate (PIP2), and binding of IP_3 to IP_3 receptor (Brass and Joseph, 1985; Guillemette *et al.*, 1988; Varga-Szabo *et al.*, 2009). This series of events occurs rapidly, with thrombin-stimulation causing calcium mobilisation after 0.2-0.3 seconds (Sage and Rink, 1986). As the data presented so far shows the processes regulated by calcium release are inhibited by quercetin and its metabolites, it was investigated whether the upstream elevation of cytosolic calcium stimulated by CRP-XL (1μg/mL) was affected. As calcium was added into the platelet buffer, entry of calcium from extracellular sources as well as release from intracellular stores was taken into account. Quercetin inhibited significantly this calcium response in a concentration dependent manner, as low as 1μM. This is in contrast to Hubbard *et al.* (2003), who observed an inhibitory effect of quercetin on calcium mobilisation only at 15μM plus; this may reflect different experimental methodologies and the use of a different agonist (collagen). Tamarixetin and isorhamnetin also dampened the calcium response, with isorhamnetin also inhibiting as low as 1μM. This data therefore suggests the inhibition of cytosolic calcium elevation as one of the key mechanisms through which these flavonoids inhibit platelet function. Consistent with all other data, isorhamnetin proved more potent than quercetin, which in turn was more potent than tamarixetin. Thus, methylation

as a whole may not imply a strong inhibitory effect, but rather the specific residue on which methylation occurs. Wright *et al.* (2010b) suggested a B ring catechol moiety in increased inhibitory potency, but it may be that a 3' methylation, as in the case of isorhamnetin, is more effective in platelet functional inhibition. This is at least the case in washed platelets; potency in PRP and whole blood is investigated in Chapter 4.

The data presented so far has demonstrated a clear picture of the individual effects of quercetin and its methylated metabolites tamarixetin and isorhamnetin in the inhibition of platelet function, both at a macroscopic scale (e.g. aggregation) and at individual molecular events (mobilisation of calcium, binding of fibrinogen to integrin $\alpha_{IIb}\beta_3$ etc.). *In vivo*, there will be a complex mixture of flavonoid metabolites (as well as likely the aglycone). Indeed, upon consumption of fried onions, Mullen *et al.* (2006) identified 5 plasma quercetin metabolites, with six in trace amounts, and upon consumption of applesauce with added apple peel or onions, Lee *et al.* (2012b) identified 16 plasma quercetin metabolites.

In this study it was investigated whether quercetin, tamarixetin and isorhamnetin, in dual and triple addition, combined to have an additive, more than additive (potentially synergistic), or other effect on platelet aggregation, as well as fibrinogen binding and P-Selectin exposure. There was an observable difference in the individual flavonoid results between this assay (plate based aggregometry) and previously performed light transmission aggregometry. This is likely largely due to the different experimental methodologies. Overall, combinatorial effects were largely confined to the 'additive' category. It was found that more-than-additive effects were largely confined to higher flavonoid concentrations, requiring 5μM of at least one flavonoid for aggregation and 2.5μM for fibrinogen binding and P-Selectin exposure. This is to a degree in agreement with work from Pignatelli *et al.* (2000), who showed 5μM quercetin and 25μM catechin (individually ineffective) could synergise to inhibit collagen-stimulated platelet aggregation, although the concentrations required here are lower. However, significant inhibitory effects were observed when combining flavonoid concentrations as

low as 0.5μM. The degree of anti-platelet effect required for benefit with respect to prevention of thrombosis is difficult to elucidate, but this greater-than-additive effect, as well as the additive effects at lower concentrations, may occur *in vivo* and provide explanation, at least in part, to the seemingly paradoxical observations of low flavonoid bioavailability versus anti-platelet (and by extension anti-CVD) effect. Quercetin and its metabolites, as well as interacting with each other, may also interact with anti-platelet medication such as aspirin to further reduce platelet function; this possibility is investigated in Chapter 5.

Work has primarily focussed on the GPVI-pathway of activation, as the main early driver of the platelet activatory process. Signalling through GPCRs also represents major mechanisms through which positive feedback and the propagation of a growing thrombus occurs, and so it is also important to understand how compounds of interest affect these pathways. Therefore, the effects of quercetin, tamarixetin and isorhamnetin on thrombin, U46619 and ADP-stimulated aggregation were investigated. Overall, a pattern of concentration-dependent inhibition was observed for all flavonoids, with ADP-stimulated aggregation affected at concentrations of quercetin, tamarixetin and isorhamnetin as low as 1μM. ADP-stimulated aggregation was most affected, followed by U46619, with thrombin-stimulated aggregation least inhibited. This could be due to the increased involvement of PI3K in the ADP pathway of platelet activation (Woulfe, 2005). Indeed, the commonly used PI3K inhibitor LY294002 was derived from quercetin, offering evidence for this explanation (Vlahos *et al.*, 1994). These effects on GPCR-mediated platelet function could likely be explained through the ability of quercetin to inhibit protein and lipid kinases. As demonstrated by Navarro-Núñez *et al.* (2009), quercetin is a potent inhibitor of Fyn, Lyn, Src, Syk, AKT, and PI3K. The data presented here demonstrate that the maximal effects on GPCR-stimulated platelet aggregation were, however, lower compared to collagen-stimulated aggregation. The level of inhibition observed at low (1μM) flavonoid concentrations may explain, in part, the *in vivo* effect of quercetin. The modulation of platelet GPCR function is an important therapeutic angle – blockade of $P2Y_{12}$ in combination with aspirin is one of the most widely used therapies in high-risk patients and GPCRs as targets are driving drug discovery,

with the development of novel agents such as cangrelor (Bhatt *et al.*, 2013; Gurbel *et al.*, 2015). Any flavonoid effects on GPCR-mediated platelet function may therefore represent a tractable and clinically useful means to reduce risk of thrombosis.

In summary, the results presented in this chapter demonstrate a clear inhibitory effect of quercetin and its two methylated metabolites, tamarixetin and isorhamnetin, on human washed platelet function. Early processes in the platelet activatory pathway such as cytosolic calcium elevation and granule release are inhibited, as is the function of integrin $\alpha_{IIb}\beta_3$ through an effect on both inside-out and outside-in signalling. This multi-function effect culminates in a potent inhibition of platelet aggregation. It is hypothesised that this is through the general kinase inhibitory effect of quercetin, as GPCR-mediated platelet function is also potently affected. A hierarchy of effect is observed: isorhamnetin > quercetin > tamarixetin. It is thus suggested that a C-4 carbonyl substituted and C-3 hydroxylated C ring (as suggested by Wright *et al.* (2010b)), and methylation at the 3' position, are key inhibitory groups (at least for washed platelet function), with a reduced potency for a B ring catechol moiety, and further reduced potency for 4' methylation. The next chapter will discuss the inhibitory effect of quercetin and its methylated metabolites in the presence of plasma proteins, and in whole blood.

4 – Quercetin and its methylated metabolites maintain a significant anti-platelet effect in platelet rich plasma and whole blood

4.1 Quercetin and its methylated metabolites maintain a significant anti-platelet effect in platelet rich plasma and whole blood

One of the main criticisms of the potential of quercetin, and flavonoids in general, as agents possessing anti-platelet effects is their low bioavailability (Walle, 2004; Cai *et al.*, 2013; Thilakarathna and Rupasinghe, 2013). This is largely due to losses during metabolism, such as excretion from the liver and intestine, with widely reported bioavailabilities ranging from 6-48% (indeed this wide range of reported values is a topic of debate in the field) (Crespy *et al.*, 2003; Graf *et al.*, 2005; Chen *et al.*, 2005; Lesser and Wolffram, 2006). Further to this, the actions of quercetin or any metabolites that do reach the systemic circulation will be limited by its high levels of binding to plasma proteins; it has been shown that quercetin binds to human serum albumin (HSA) with a high affinity, with up to ~99% of circulating quercetin binding to HSA (Boulton *et al.*, 1998; Kaldas *et al.*, 2005). This translates into reduced anti-platelet effects of quercetin in platelet rich plasma. Work by Pignatelli *et al.* (2006) has shown quercetin concentrations of 1.25-20μM to be unable to inhibit collagen-stimulated PRP aggregation, and Raghavendra and Naidu (2009) observed only 25% inhibition of ADP-stimulated PRP aggregation at 200μM quercetin. Quercetin has, however, shown potency in other studies, with Chen and Deuster (2009) showing ADP-stimulated aggregation inhibited 50% by 10μM quercetin. This reduction of effect is mirrored in whole blood assays; Wright *et al.* (2013) concluded that flavonoid effects are drastically reduced in whole blood, with 5μM quercetin ineffective in the inhibition of thrombus formation *in vitro,* and the methylated metabolite tamarixetin inhibiting by only 5%. Indeed, the same study also observed <10% inhibition of collagen-stimulated platelet aggregation in the presence of plasma proteins when treated with 200μM quercetin and tamarixetin (Wright *et al.*, 2013).

The body of work investigating quercetin's anti-platelet effect in plasma and whole blood is clearly limited, with widely varying results, and there is a paucity of information regarding the effect of its metabolites. In addition to this, the high levels of quercetin required for inhibition in plasma and whole

blood may cause cytotoxicity. Whilst low quercetin levels (0.1μM) have proven cytoprotective, high concentrations were cytotoxic in a study by Cao *et al.* (2007), with an LD_{50} of 90.85μM in human lens epithelial cells (HLECs). A similar result was obtained by Matsuo *et al.* (2005), concluding quercetin is cytotoxic in human umbilical vein endothelial cells (HUVECs) and human lung embryonic fibroblasts (HLEFs) with LD_{50} values of 61μM and 303μM, respectively. It is therefore clear that increased concentrations are required to achieve anti-platelet effects in plasma and whole blood, and that in other cell types, these high concentrations may cause adverse, even cytotoxic effects.

The aim of this chapter, therefore, was to investigate how the effects of quercetin and its methylated metabolites in washed platelets transferred into anti-platelet efficacy in platelet rich plasma and whole blood, as well as their relative potencies, and to investigate whether the higher concentrations predicted to be required for anti-platelet effects in the presence of plasma proteins had an impact on the cell viability of resting platelets.

4.2 Quercetin does not cause platelet necrosis or activation of platelets at supraphysiological concentrations

Due to the cytotoxicity of quercetin in other cell types, the effect of high (up to 200μM) quercetin concentrations on markers of platelet necrosis were investigated. Platelet necrosis is marked by an aberrant increase in the exposure of phosphatidylserine on the cell surface (Fadok *et al.*, 1992; Gyulkhandanyan *et al.*, 2012; Leytin, 2012). Mitochondrial injury, as occurs during necrosis, is associated with the shedding of GPIbα (Bergmeier *et al.*, 2004a; Josefsson *et al.*, 2012). Thus, the effect of quercetin (up to 200μM) on the exposure of phosphatidylserine (measured through annexin V binding) and cell surface GPIbα levels were investigated, to clarify whether inhibition observed at high concentrations in previous studies was due to the inhibition of platelet activatory mechanisms or potentially due to a necrotic phenotype. Phosphatidylserine exposure and shedding of GPIbα also occur during normal activation of platelets (Fox, 1994; Lentz, 2003; Gardiner *et al.*, 2007; Schoenwaelder *et al.*, 2009). The effects of an agent at very high, supraphysiological concentrations can be unpredictable, and so to ensure these levels were not causing unpredictable, aberrant activation, the effects of high quercetin concentrations on the exposure of P-selectin and fibrinogen binding to integrin $\alpha_{IIb}\beta_3$ were also investigated.

Phosphatidylserine exposure, GPIbα levels, P-selectin exposure and fibrinogen binding to integrin $\alpha_{IIb}\beta_3$ were all measured using flow cytometry. Alexa Fluor 488-conjugated annexin V, FITC-coupled anti-CD42b antibody, Cy5/PE conjugated anti-CD62P antibody or FITC-labelled anti-fibrinogen antibody were added to washed platelets (2×10^7 cells/mL). Quercetin, vehicle (negative) control or agonist (positive control) were then added to samples and incubated at room temperature for 20 minutes, with occasional gentle mixing. The agonists were CRP-XL (1μg/mL) for P-Selectin exposure, fibrinogen binding and phosphatidylserine exposure experiments and thrombin (0.1U/mL) for GPIbα level assay. Thrombin has previously proven an effective agonist for studying the shedding of GPIbα,

and so was used in this part of the assay (Bergmeier *et al.*, 2004b). In thrombin-stimulated samples, GPRP was added to prevent fibrin polymerisation. Reactions were then terminated with 0.2% paraformaldehyde, and fluorescence was measured by flow cytometry.

Annexin V binding was used as a measure of phosphatidylserine exposure on the platelet surface. CRP-XL stimulation, as expected, caused an increase in binding; due to large a large SEM this did not reach statistical significance ($p=0.083$). As seen in Figure 4-1A, quercetin at 10, 100 and 200μM did not cause an increase in annexin V binding compared to vehicle control. Thrombin stimulation resulted in a significant decrease in the cell surface GPIbα level; quercetin, again at 10, 100 and 200μM did not cause a significant change in levels. It must be noted, however, that there was a trend towards reduced GPIbα levels with 200μM quercetin treatment, but this did not reach significance.

CRP-XL at 1μg/mL as a positive control resulted in a dramatic increase in P-Selectin exposure on the cell surface. Quercetin treatment at a range of 10-200μM did not result in a significant increase, shown in Figure 4-1C. As seen in Figure 4-1D, quercetin did not cause an increase in fibrinogen binding to integrin $\alpha_{IIb}\beta_3$ at concentrations up to 200μM. However, there is a trend towards increased binding which did not reach significance. It was hypothesized that this could be due to quercetin's fluorescent properties interfering with the FITC flow cytometry assay; independent experiments using only quercetin plus buffer showed only minor fluorescence shifts at 100μM and concentrations above this (data not shown). When combined with the observation of a trend towards reduced GPIbα levels upon treatment with 200μM quercetin, it may be that at very high, supraphysiological concentrations above 200μM, undesirable effects in platelets may occur, be they activatory or necrotic. The increase in fibrinogen binding leans the conclusion towards an activatory phenotype, although another marker of activation, P-Selectin exposure, was not affected, implying the fluorescence of quercetin may be a confounding issue. It should be kept in mind, though, that a statistically significant effect was not reached, and thus it is reasonable to conclude that at concentrations up to 200μM, quercetin-induced platelet necrosis or activation is unlikely to occur. The quercetin levels used here were purposefully

supraphysiological, with 10μM added as a high, physiologically achievable comparator quercetin concentration. A lack of any clear adverse effect (as seen in Figure 4-1) at this concentration concludes that undesirable effects on platelets at *in vivo* plasma levels (and indeed in the platelet assays presented so far) are highly unlikely to occur.

In order to investigate the effects of quercetin and its metabolites in platelet rich plasma, in which much flavonoid may bind to plasma proteins, concentrations up to 50μM were chosen in order to determine the viability of inhibitory effects.

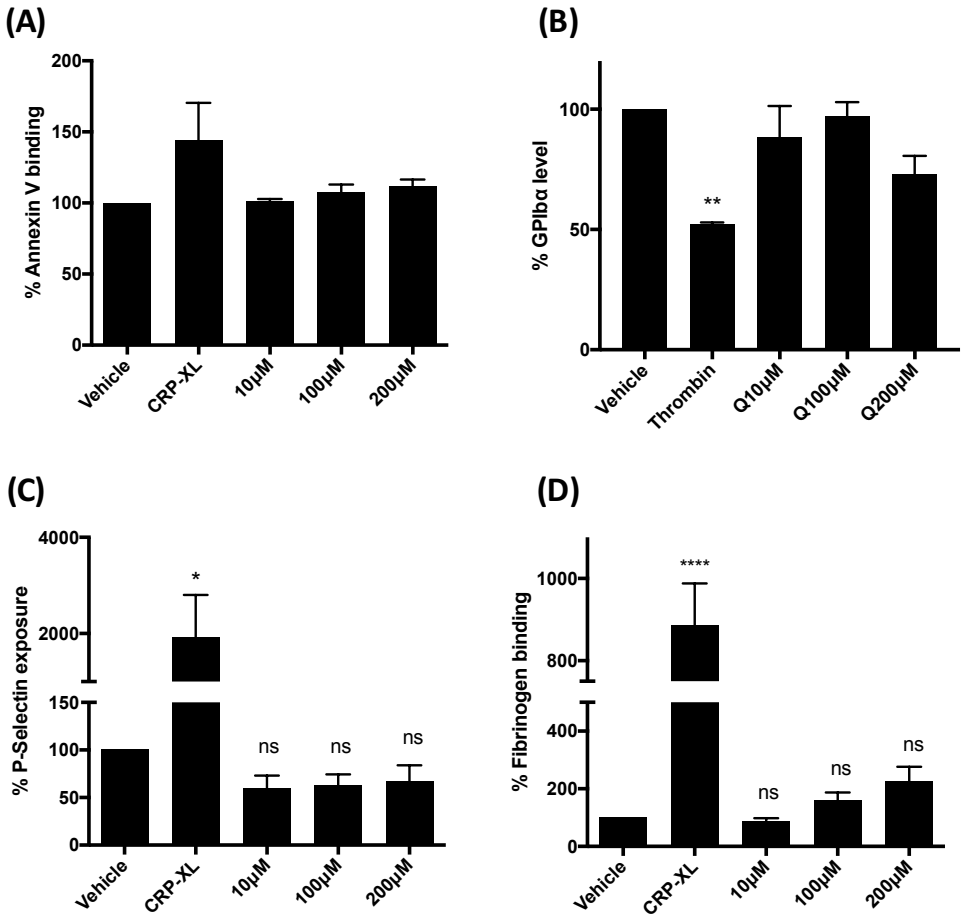

Figure 4-1 High quercetin concentrations do not cause platelet necrosis or activation

Alexa Fluor 488-conjugated annexin V, FITC-coupled anti-CD42b antibody, Cy5/PE conjugated anti-CD62P antibody or FITC-labelled anti-fibrinogen antibody were added to washed platelets (2 x 10^7 cells/mL) to measure annexin V binding (A), GPIbα levels (B), P-selectin exposure (C) and fibrinogen binding to integrin αIIbβ3 (D), respectively. Quercetin, vehicle (DMSO, 0.25% v/v, negative control) or CRP-XL (1µg/mL)/thrombin (0.1U/mL) (positive control) were then added to samples and incubated for 20 minutes, after which they were fixed in 0.2% paraformaldehyde. Samples were then analysed by flow cytometry and data normalised to vehicle (negative) control. N=3, data represent mean ± SEM. *$p<0.05$, **$p<0.005$, ****$p<0.0001$ compared to vehicle control, analysed by one-way ANOVA with post-hoc Dunnett's test.

4.3 Quercetin and tamarixetin inhibit platelet aggregation in PRP with higher potency than isorhamnetin

The washed platelet work presented in chapter 3 allowed the elucidation of key mechanistic effects of quercetin and its metabolites on platelet function. In order to understand if and how these effects may be translated *in vivo*, an understanding of the anti-platelet effects of these flavonoids in platelet rich plasma must be ascertained. This was initially investigated by studying platelet aggregometry using PRP, to provide an indication of the overall, macroscopic effect.

The purpose of this experiment was to investigate the potential for quercetin and its metabolites to inhibit aggregation in the presence of plasma proteins, and therefore conditions were chosen to represent, as far as possible, the *in vivo* scenario. The incubation period was therefore increased for this assay compared to washed platelet aggregometry, from 5 minutes to 60 minutes. Reported values of time-to-peak quercetin plasma concentrations vary widely from 27 minutes to 3 hours depending on factors such as quercetin form administered (Olthof *et al.*, 2000; Graefe *et al.*, 2001; Hubbard *et al.*, 2004; Hubbard *et al.*, 2006; Moon *et al.*, 2008). Thus, 60 minutes was chosen to represent the peak plasma time, allowing for the theoretical accumulation of flavonoid in the plasma, and potentially inside the platelets. These assays were performed using the plate based aggregometry method, in order to allow useful comparisons between this and future high-throughput aggregometry data presented in Chapter 5.

PRP was incubated with quercetin, tamarixetin, isorhamnetin or vehicle control in a 96 well plate for 60 minutes at 37^{o}C on a stationary heated plate shaker. After this incubation period, collagen (5µg/mL) was added to wells and the plate was shaken at 1200rpm for 5 minutes at 37^{o}C. Absorption of light at a wavelength of 405nm was then measured using a plate reader and percentage aggregation was calculated using unstimulated and uninhibited samples as 0 and 100%, respectively.

Quercetin displayed a dose-dependent inhibitory profile, with significant inhibition of aggregation observed between 25-50μM. At higher concentrations the effect was potent, with ~55% reduction at 25μM and near complete (>90%) inhibition at 50μM (Figure 4-2A). Although a significant effect was not seen at the upper physiological range of 10μM, a trend towards decreased aggregation was noted. Tamarixetin inhibited with a similar profile to quercetin; however, a significant effect (32% reduction) on platelet aggregation was also seen at 10μM (Figure 4-2B). Interestingly, tamarixetin was more effective at lower concentrations, and slightly less potent at higher concentrations, when compared to quercetin. This is the same observation as was made in washed platelet aggregometry, with isorhamnetin (instead of tamarixetin) having increased effect over quercetin at lower concentrations. Indeed, the similarities do not end there, with isorhamnetin proving significantly less potent than both quercetin and tamarixetin (compared to the observation in Chapter 3 of tamarixetin proving significantly less potent than both quercetin and isorhamnetin). This reduced potency is dramatic, with only a 25% effect at 25μM and ~32% inhibition at 50μM (Figure 4-2C). Indeed, at 25 and 50μM, there is a statistically significant reduced potency of inhibition of aggregation by isorhamnetin compared to both quercetin and tamarixetin. This was an unexpected observation, in that it effectively switches tamarixetin and isorhamnetin in the inhibitory hierarchy observed in washed platelets; whereas in washed platelet assays it was isorhamnetin > quercetin > tamarixetin, in PRP it so far appears to be tamarixetin>quercetin>isorhamnetin. Overall, compared to washed platelet aggregometry (both LTA and plate-based aggregometry), quercetin and its metabolites were less potent in the inhibition of aggregation in PRP. Plasma proteins, therefore, clearly influence this process, as predicted due to high plasma protein binding. However, significant inhibitory effects can be seen as low as 10μM, with a trend to inhibition at 5μM; total flavonoid concentrations considered physiologically achievable.

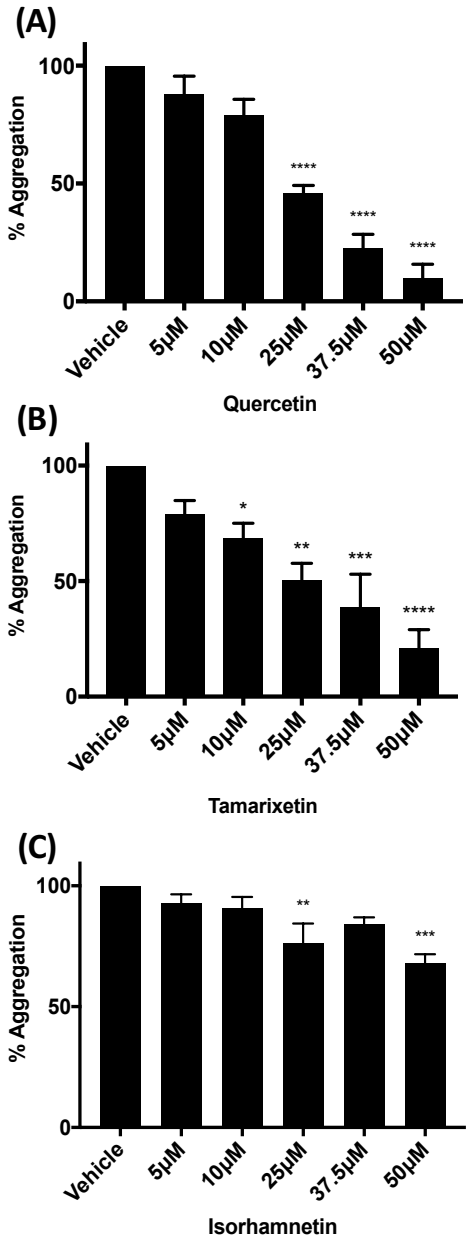

Figure 4-2 Quercetin and tamarixetin inhibit aggregation in PRP with higher potency than isorhamnetin

Platelet rich plasma (PRP) was incubated in a 96 well plate with quercetin (A), tamarixetin (B), isorhamnetin (C) or vehicle control (1% DMSO, v/v) for 60 minutes at 37°C on a heated plate shaker. Collagen (5μg/mL) was added to wells and the plate was shaken at 1200rpm for 5 minutes at 37°C. Absorption of 405nm light was then measured on a plate reader, and percentage aggregation calculated using unstimulated and uninhibited samples as 0 and 100%, respectively. Data represent percentage aggregation, normalised to the level of aggregation in the absence of flavonoid (vehicle). N=4, data represent mean ± SEM. Data analysed by one-way ANOVA with post-hoc Dunnett's test. *$p<0.05$, **$p<0.005$, ***$p<0.001$, ****$p<0.0001$ compared to vehicle control.

4.4 α-granule secretion and fibrinogen binding to integrin $\alpha_{IIb}\beta_3$ is less inhibited by flavonoids in the presence of plasma proteins compared to washed platelets

The secretion of granule contents and the interaction of fibrinogen with integrin $\alpha_{IIb}\beta_3$ are critical processes in the platelet activatory cascade. As shown in sections 3.3.2 and 3.4.1, quercetin and its metabolites tamarixetin and isorhamnetin are very effective inhibitors of these mechanisms in washed platelets, with over 90% inhibition of both P-Selectin exposure and fibrinogen binding by quercetin at 10μM. It was thus investigated how this inhibitory potency carried over into platelet rich plasma, and whether these mechanisms were as important for the anti-platelet effect of quercetin in the presence of plasma proteins.

Platelet rich plasma was incubated with flavonoid or vehicle control for 60 minutes at 30^{o}C in an incubation chamber. Anti-CD62 Cy5/PE-conjugated antibody or FITC conjugated anti-fibrinogen antibody was added to PRP samples, which were then stimulated with CRP-XL (1μg/mL) for 20 minutes. After this period, reactions were terminated by fixation with 0.2% paraformaldehyde and fluorescence measured by flow cytometry.

Initially, flavonoid concentrations up to 50μM were tested, as it was predicted that this level would be high enough to overcome any reduced effect caused by factors such as flavonoid binding to plasma proteins. This, however, was not the case, as seen in Figure 4-3. Unlike aggregation, quercetin inhibited P-Selectin exposure on the cell surface minimally, with a significant reduction of only 33% observed at 50μM (Figure 4-3A). Tamarixetin also had very little effect. A significant inhibition of 20% was observed at 1μM; the significance of this, however, is likely due to variation in the assay, as no significant inhibition was observed at any other tamarixetin concentrations tested (Figure 4-3B). Isorhamnetin also displayed no significant effect on P-Selectin exposure up to 50μM (Figure 4-3C).

Fibrinogen binding to integrin $\alpha_{IIb}\beta_3$ was inhibited significantly by quercetin at 20 and 50μM, with a 36 and 52% reduction respectively (Figure 4-3D). This effect at higher concentrations was not observed with tamarixetin or isorhamnetin (Figure 4-3E/F). These results displayed, therefore, that 50μM was perhaps not a sufficiently high concentration to overcome the influence of plasma proteins and other confounding factors perhaps present in plasma. Thus, the effect of quercetin at concentrations up to 200μM on CRP-XL (1μg/mL)-stimulated fibrinogen binding and P-Selectin exposure in PRP were investigated.

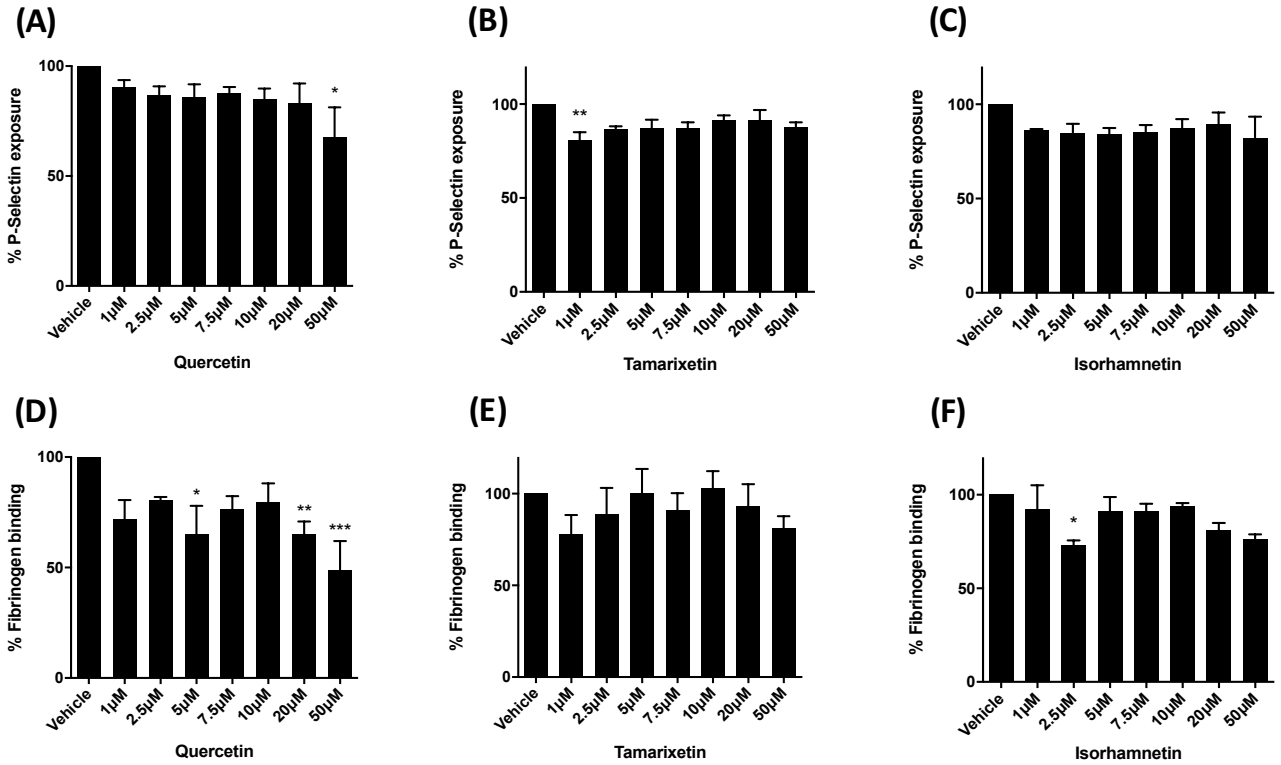

Figure 4-3 Quercetin, tamarixetin and isorhamnetin show little effect on P-Selectin exposure and fibrinogen binding in PRP up to 50μM

Platelet rich plasma (PRP) was incubated with quercetin (A,D), tamarixetin (B,E), isorhamnetin (C,F) or vehicle control (DMSO, 0.25% v/v) for 60 minutes, after which PE/Cy5-conjugated anti-human CD62P antibody or FITC-conjugated anti-human fibrinogen antibody was added to sample prior to stimulation for P-Selectin exposure or fibrinogen binding, respectively. Samples were then stimulated with CRP-XL (1μg/mL) for 20 minutes, after which they were fixed in 0.2% paraformaldehyde. P-Selectin exposure on the cell surface and fibrinogen binding were then measured by flow cytometry and data normalised to the levels of P-Selectin exposure or fibrinogen binding in the absence of flavonoid (vehicle). N=3, data represent mean ± SEM. *$p<0.05$, **$p<0.005$, ***$p<0.001$ compared to vehicle control, analysed by one way ANOVA with post-hoc Dunnett's test.

It must be recognised that 200μM is a supraphysiological concentration, considerably higher than could ever be achieved either through diet or supplementation. Nonetheless, to understand the effect that plasma proteins play in reducing the effects of quercetin on platelet α-granule secretion and fibrinogen binding, the use of these concentrations serves as a useful exercise (although due to the limitations of the physiological relevance of these high flavonoid levels, only quercetin was tested).

Quercetin inhibited significantly both P-Selectin exposure and fibrinogen binding at 150 and 200μM. Representative fluorescence histograms are shown in Figure 4-4A (P-Selectin exposure) and Figure 4-4D (fibrinogen binding). At 150μM, P-selectin exposure was inhibited 57%, with an almost complete effect (~95% inhibition) at 200μM (Figure 4-4B). Fibrinogen binding was affected to a greater degree, with ~80% reduction at 150μM and >98% effect at 200μM (Figure 4-4E). This is reflected in the observed IC_{50} values; 151 ± 8.1μM for P-Selectin exposure and 124 ± 19.4μM for fibrinogen binding (Figure 4-4C/F). Comparing these values to the IC_{50} values observed in washed platelets (Table 1), it becomes apparent that concentrations over an order of magnitude higher are required to achieve comparable inhibition in the presence of plasma proteins for these molecular processes. It may therefore be that an effect on both P-Selectin exposure and fibrinogen binding contribute less to the overall effect seen on aggregation in PRP than in washed platelets. This will be discussed further in section 4.7.

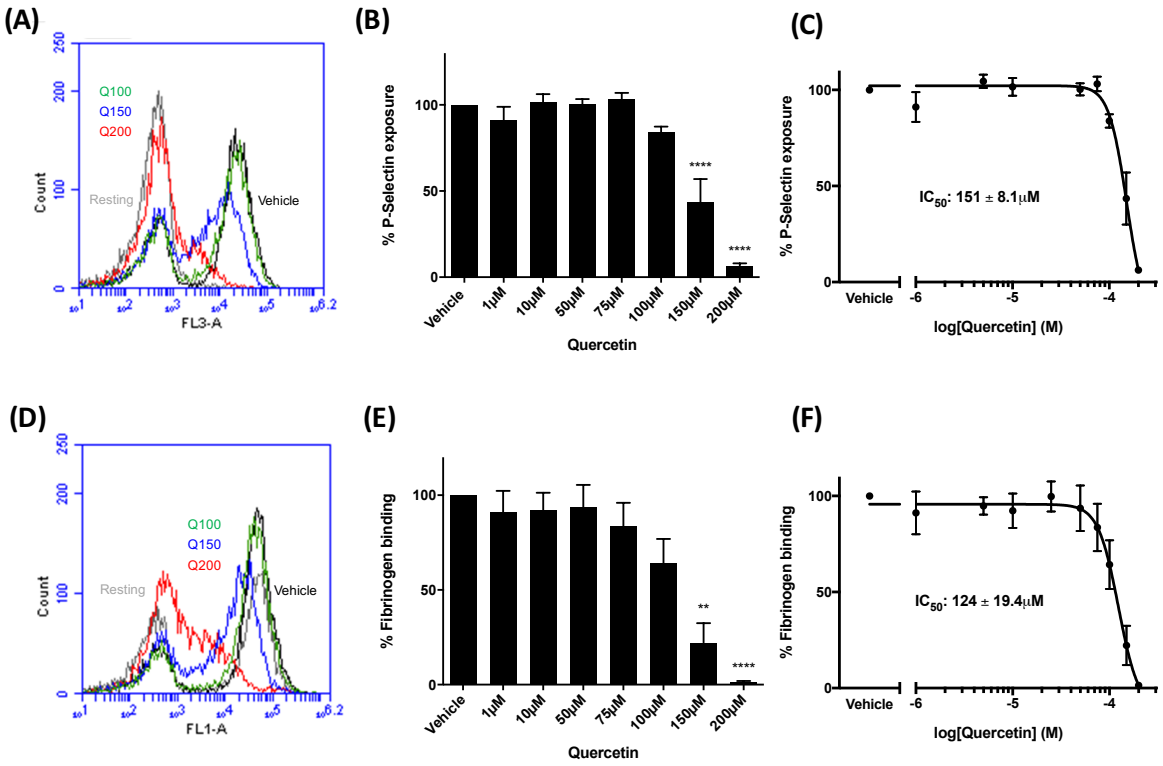

Figure 4-4 Effects on P-Selectin exposure and fibrinogen binding in PRP are obtained at concentrations above 100μM

Platelet rich plasma (PRP) was incubated with quercetin or vehicle control (DMSO, 0.25% v/v) for 60 minutes, after which PE/Cy5-conjugated anti-human CD62P antibody or FITC-conjugated anti-human fibrinogen antibody were added to samples prior to stimulation. Samples were then stimulated with CRP-XL (1μg/mL) for 20 minutes, after which they were fixed in 0.2% paraformaldehyde. P-Selectin exposure on the cell surface and fibrinogen binding were then measured by flow cytometry, with representative fluorescence histograms shown in (A) and (D), and data normalised to the levels of P-Selectin exposure (B) or fibrinogen binding (F) in the absence of quercetin (vehicle). Four parameter nonlinear regression curves were utilised to estimate the IC_{50} of quercetin in the inhibition of P-Selectin exposure (C) and fibrinogen binding (F). N=3, data represent mean ± SEM. **p<0.005, ****p<0.0001 compared to vehicle control, analysed by one-way ANOVA with post-hoc Dunnett's test. Q, quercetin.

4.5 Clot retraction is inhibited by quercetin and its methylated metabolites at physiological concentrations

The results from the previous section suggested a slightly increased potency for quercetin and its methylated metabolites in the modulation of inside-out integrin $\alpha_{IIb}\beta_3$ function compared to granule secretion. Some shared signalling proteins are involved in both aspects (inside-out and outside-in) of integrin signalling, and so it was hypothesised that outside-in signalling of integrin $\alpha_{IIb}\beta_3$ may also be affected by quercetin and its methylated metabolites. To measure this in PRP, clot retraction, a process driven by outside-in signalling, was measured. The cascade of events leading to the production of a thrombus involves both platelet activation, along with inside-out and outside-in integrin signalling, and the activation of the coagulation cascade, with associated production of thrombin and the development of a stable fibrin clot (Law *et al.*, 1999; Tucker *et al.*, 2012). Platelets are involved in both pathways, and are also key in the retraction of the clot. Integrin $\alpha_{IIb}\beta_3$ links fibrin outside the cell with the intracellular cytoskeleton, and allows platelets to contract the fibrin mesh to bring the wound edges together, expelling fluid plasma, stabilising and tightening the clot; indeed, $\alpha_{IIb}\beta_3$-driven contraction is observed in the stabilisation of platelet thrombi formed in the arterial circulation (Chen *et al.*, 1995; Schoenwaelder *et al.*, 1997; Tucker *et al.*, 2012; Cines *et al.*, 2014). Consequently, the investigation of the effect of flavonoids on clot retraction provides a useful insight into their effect on a physiological process involving both platelets as well as other factors such as the coagulation system, and provides some insight into their potential *in vivo* effects on a more complete system.

Platelet rich plasma was incubated with flavonoid or vehicle control for 60 minutes at 30^{o}C in an incubation chamber. 745µL of warmed modified Tyrodes-HEPES buffer was added into a test tube, along with 5µL red blood cells to allow visualisation of the clot. 50µL thrombin (final concentration 1U/mL) was added to stimulate clot formation, after which 200µL of vehicle or flavonoid-treated PRP was added to initiate the assay (flavonoid concentrations refer to the concentration added to PRP pre-dilution in tyrodes and initiation of the assay). A glass pipette was then immediately added into the

centre of each test tube, around which the clot would form, and samples were placed into an incubator chamber at 30°C. Clots were checked and photographed every 15 minutes, and the assay was terminated after 2 hours, at which time the vehicle clot would be expected to have retracted fully. Clots were then removed from the test tubes and transferred into pre-weighed microfuge tubes, and the remaining plasma was also transferred into separate pre-weighed microfuge tubes. Clots and plasma were then weighed and the individual microfuge tube weights subtracted to give absolute clot and plasma mass (mg). A decrease in plasma mass is used simply to confirm the corresponding clot weight increase and so plasma weight data is not shown here.

After the 2 hour time period, at which time vehicle clots had fully retracted, vehicle-treated clots weighed between 64 and 119 milligrams, with a mean mass of 90 milligrams (mg). Quercetin inhibited significantly clot retraction at 5 and 10μM, with an average clot weight of 346 and 474mg, respectively (Figure 4-5A). This represents an average ~300% increase in clot weight compared to vehicle control at 5μM quercetin. Tamarixetin inhibited significantly clot retraction at 2.5μM (average 250mg, 182% increase), 5μM (average 420mg, 377% increase) and 10μM (average 586mg, 579% increase) (Figure 4-5B). Isorhamnetin also inhibited significantly the process of clot retraction at 2.5, 5 and 10μM, with a maximal increase in clot weight of 440mg at 10μM, representing a ~400% increase in clot weight compared to vehicle control (Figure 4-5C). Representative images are shown in Figure 4-5D,E,F; it can be seen that, at 10μM, there is little to no retraction of clots at all. This implies the inhibition of integrin $\alpha_{IIb}\beta_3$ outside-in signalling as a key mechanism through which quercetin and its metabolites are able to display an anti-platelet effect at physiologically achievable concentrations in the presence of plasma proteins. Comparing average clot weights between quercetin, tamarixetin and isorhamnetin-treated samples (done with the same donors on the same day), it can be seen that there are minimal differences (<40mg) at lower concentrations. However, at 5 and 10μM, tamarixetin displays a trend towards reduced clot retraction compared to quercetin, with an average of 74mg and 112mg higher clot weights at 5 and 10μM, respectively. In addition to this, clot weights in quercetin-treated samples were slightly larger than isorhamnetin treated samples. This implies an inhibitory hierarchy of

tamarixetin > quercetin > isorhamnetin, and is in overall agreement with the observation in the PRP aggregometry data in section 4.3. This therefore adds data to the suggestion that the inhibitory potencies of tamarixetin and isorhamnetin are switched between the absence (washed platelets) and presence (PRP) of plasma proteins.

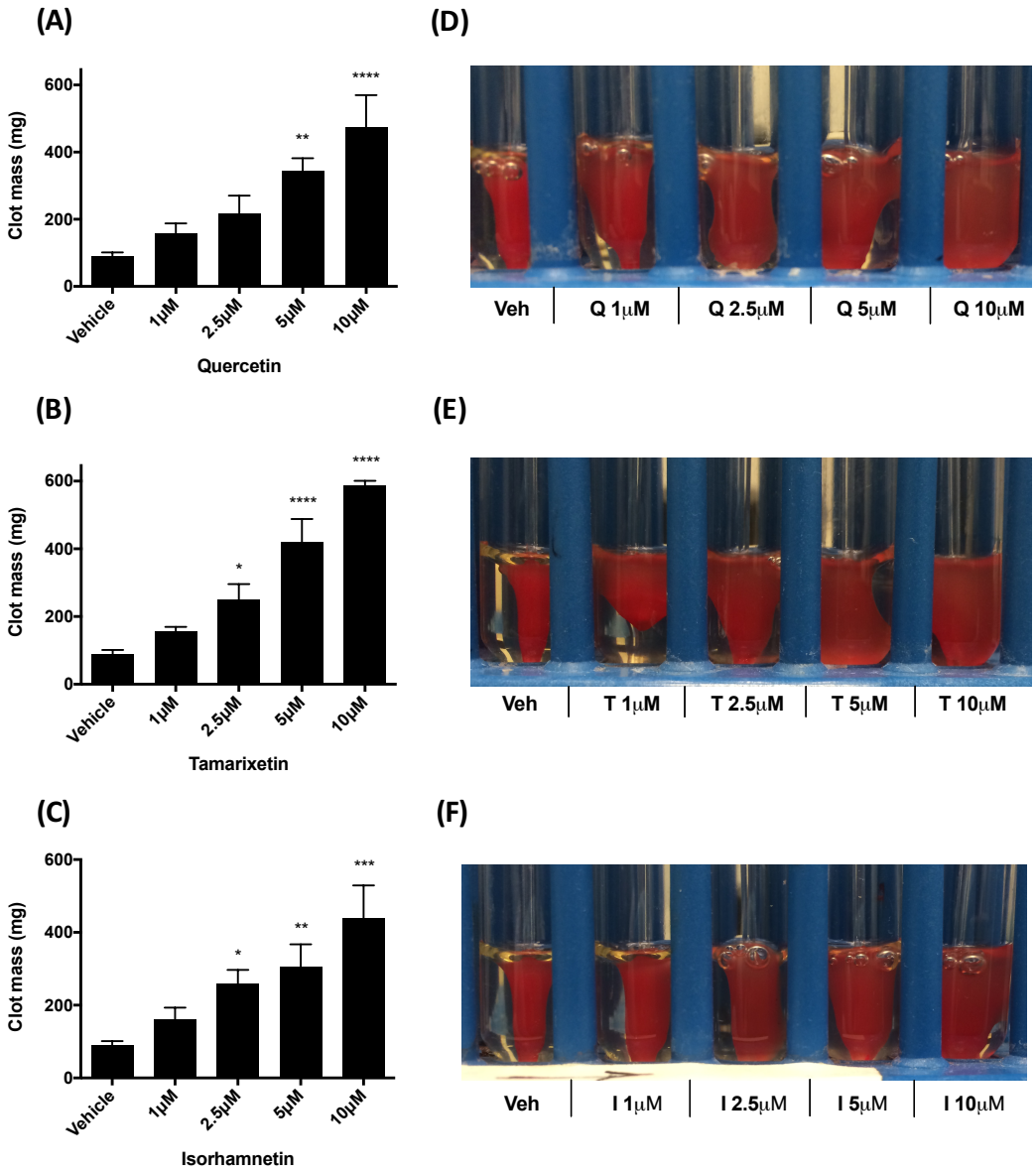

Figure 4-5 Quercetin, tamarixetin and isorhamnetin inhibit clot retraction

PRP (500µl) was incubated with quercetin (A/D), tamarixetin (B/E), isorhamnetin (C/F) or vehicle control (DMSO, 0.2% v/v) for 60 minutes at 30°C. 745µl warmed modified Tyrodes-HEPES buffer was added to test tubes, as well as 5µl red blood cells . Thrombin (1U/mL) was added to stimulate clot formation, after which 200µl treated PRP was added to initiate the assay. Glass pipettes were added for clots to form around, and samples placed in an incubation chamber at 30°C. The assay was terminated at 120 minutes after images were taken of samples, with representative images shown in D, E, and F. Clots were then weighed and these values plotted (A,B,C). N=4, data represent mean ± SEM. *p<0.05, **p<0.005, ***p<0.001, ****p<0.0001 compared to vehicle control, analysed by one-way ANOVA with post-hoc Dunnett's test. Q, quercetin; T, tamarixetin; I, Isorhamnetin

4.6 Quercetin, tamarixetin and isorhamnetin inhibit in vitro *thrombus formation in whole blood under arterial flow conditions at a high physiological concentration*

The results presented so far in this chapter demonstrate the ability of quercetin and its methylated metabolites to inhibit platelet function in the presence of plasma proteins. *In vivo,* the interactions between quercetin/metabolites and platelets happens in the matrix of whole blood. This adds another factor on top of plasma proteins: red blood cells. It has been shown that red blood cells accumulate quercetin through passive diffusion, with quercetin binding to haemoglobin (Fiorani *et al.*, 2003; Xi and Guo, 2007). This may therefore represent another mechanism through which the level of quercetin available to exert anti-platelet effects is reduced. It was thus important to investigate how quercetin, tamarixetin and isorhamnetin inhibited platelet function in whole blood. This was performed through an *in vitro* thrombus formation under flow assay, which measures the formation of thrombi on a collagen-coated surface under arterial flow conditions at a physiological shear rate. The inclusion of a physiological shear rate is also an important consideration; *in vivo,* interactions between GPIbα and vWF at high shear rates is crucial for platelet recruitment at the site of injury, and at shear rates below 600-900s^{-1}, integrin $\alpha_{IIb}\beta_3$:fibrinogen interactions can occur directly (with integrin $\alpha_{IIb}\beta_3$ also engaging vWF) (Savage *et al.*, 1996; Savage *et al.*, 1998; Nesbitt *et al.*, 2002; Nesbitt *et al.*, 2009). Indeed, at very high shear rates (>10,000s^{-1}), as may be present in severe atherosclerosis, platelets can become activated in the absence of activatory signals, and platelets exposed temporarily to high shear rates can become sensitised, activating much faster following exposure to low shear stress (Holme *et al.*, 1997; Sheriff *et al.*, 2010). The inclusion of these factors therefore enables this assay to represent well an *in vivo* scenario, with Roest *et al.* (2011) concluding that it allows good elucidation of arterial thrombotic mechanisms, comparing well and offering a good alternative to *in vivo* mouse models of thrombosis. It was thus investigated whether, and to what extent, quercetin, tamarixetin and isorhamnetin affected this thrombus formation under flow at a high physiologically achievable concentration of 10μM.

Physiological arterial shear stress has been reported to lie between 10 and 70 dynes/cm^2 (250 - 1750s^{-1}), and so a rate of 20dynes/cm^2 was chosen for this assay (Malek *et al.*, 1999; Papaioannou and Stefanadis, 2005; Chiu and Chien, 2011). This corresponds to a shear rate of 500s^{-1}, using the conversion described by Colman (2006). Citrated human whole blood was incubated with the lipophilic dye DiOC6 (3,3'Dihexyloxacarbocyanine iodide) at a concentration of 5μM for 1 hour at 30^{o}C to allow visualisation of platelets under the microscope. During this incubation, Vena8 BioChips were coated with type I collagen (100μg/mL) for one hour, after which excess collagen was washed through with modified Tyrodes-HEPES buffer. Whole blood was incubated with flavonoid (10μM) or vehicle control for 10 minutes at 30^{o}C prior to perfusion through the collagen-coated microfluidic channels at a shear stress of 20 dynes/cm^2. An incubation period of 10 minutes (as opposed to 60 minutes) was chosen for practicality. The microfluidic channel was observed on the 20X objective of a Nikon A1-R confocal microscope, with images captured every 1 second for 600 seconds. Fluorescence was excited at 488nm with an argon laser and emission detected at 500-520nm. Mean thrombus fluorescence intensity was calculated using NIS elements software.

Figure 4-6A shows the kinetics of the growing thrombus in vehicle treated whole blood. As blood flowed over collagen at a shear rate of 500s^{-1}, platelets bound and accumulated, developing thrombi, which was detected as an increase in the mean fluorescence intensity. The thrombi continued to develop over the 10-minute flow period, and the data were normalised so that vehicle represents 100% thrombus formation at the endpoint of the assay (normalisation was performed due to the variation in fluorescence intensity signal of samples between donors confounding analysis). As seen in Figure 4-6A, B and C, quercetin, tamarixetin and isorhamnetin inhibited the growth of the developing thrombi. Even from early time points, the mean fluorescence intensity was reduced; a significant reduction was observed from 210 seconds onward in quercetin and tamarixetin treated samples, with the growing thrombi never reaching the level of vehicle treated blood (Figure 4-6A/B). The formation of thrombi in isorhamnetin treated blood was inhibited significantly as early as 140 seconds, and again the

thrombi never reach levels of vehicle treated samples (Figure 4-6C). It can also be seen that tamarixetin-treated samples are inhibited most potently by the end of the assay. The representative images shown in Figure 4-6D showing the fluorescence at the end of the 10-minute period confirm this. The vehicle image shows large, bright thrombi, with the heavy accumulation of platelets and a large coverage of the channel. Quercetin and isorhamnetin-treated samples showed a reduced coverage and lower levels of fluorescence, as the developing thrombi have not grown to the same degree. Tamarixetin, however, clearly had the most effect on this process, with even fewer bright thrombi. Coverage of the channel can be seen but is limited and not characterised by the very bright, large thrombi seen in the vehicle channel, instead displaying smaller thrombi. The increased effect of tamarixetin over quercetin and isorhamnetin in the inhibition of *in vitro* thrombus formation under flow, whilst it did not reach statistical significance, is also demonstrated in Figure 4-7, in which the normalised mean fluorescence intensity values at the end of the 10-minute assay period are compared. Quercetin and isorhamnetin inhibited thrombus formation by an average of 39% and 41%, respectively, displaying almost identical potency; tamarixetin, on the other hand, reduced thrombus formation by 55% (Figure 4-7). This observation is in agreement with the clot retraction and PRP aggregometry data in respect to a trend towards increased potency of tamarixetin over quercetin and isorhamnetin in plasma (and now, indeed, in a whole blood, flowing system).

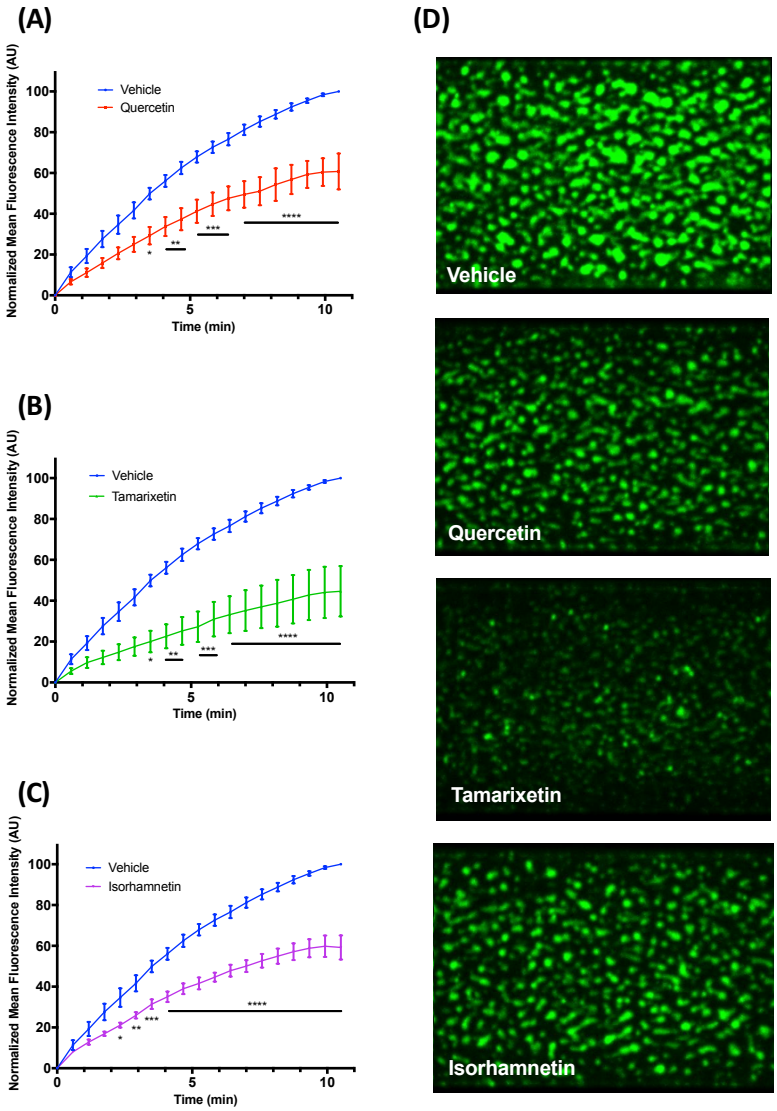

Figure 4-6 Quercetin, tamarixetin and isorhamnetin inhibit *in vitro* thrombus formation under flow

Citrated human whole blood was incubated with DioC6 lipophilic dye (5µM) for 1 hour at 30°C. Concurrently, Vena8 BioChip microfluidic channels were coated with collagen (type I, 100µg/mL) for one hour, and excess collagen washed through with modified Tyrodes-HEPES buffer. Whole blood was incubated with quercetin (A), tamarixetin (B), isorhamnetin (C) at a concentration of 10µM or vehicle control (DMSO, 0.2% v/v) for 10 minutes at 30°C prior to perfusion through channels at a shear rate of 20dyn/cm^2. Fluorescence was excited at 488nm with an argon laser and emission detected at 500-520nm. The channel was observed using a 20X objective on a Nikon A1-R confocal microscope, with images captured every second for 600s. Normalised mean thrombus fluorescence intensity (normalised to the level of mean fluorescence intensity in the absence of flavonoid (vehicle)) was calculated using NIS Elements software, and representative images at the assay endpoint are shown in (D). N=3, data represent mean ± SEM. *p<0.05, **p<0.005, ***p<0.001, ****p<0.0001 compared to vehicle control, analysed by two-way ANOVA with post-hoc Bonferroni correction.

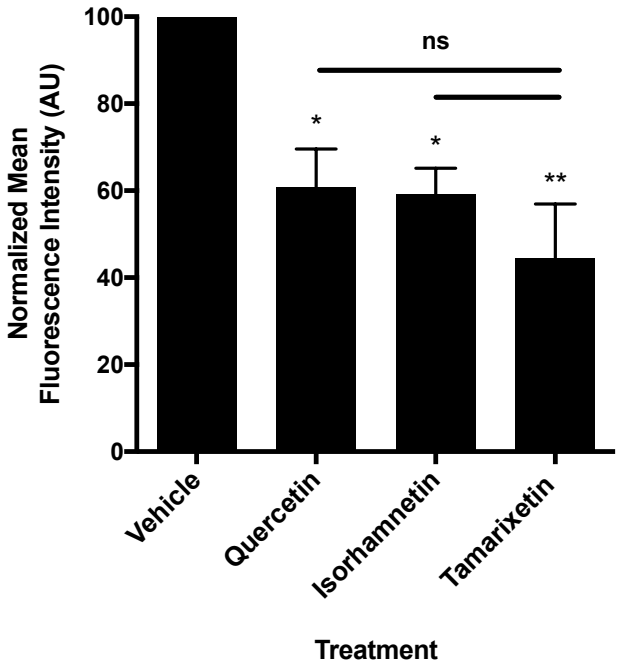

Figure 4-7 A trend is observed toward increased inhibition of *in vitro* thrombus formation under flow by tamarixetin

Citrated human whole blood was incubated with DioC6 lipophilic dye (5µM) for 1 hour at 30°C. Concurrently, Vena8 BioChip microfluidic channels were coated with collagen (type I, 100µg/mL) for one hour, and excess collagen washed through with modified Tyrodes-HEPES buffer. Whole blood was incubated with quercetin, tamarixetin, isorhamnetin or vehicle control (DMSO, 0.2% v/v) for 10 minutes at 30°C prior to perfusion through channels at a shear rate of 20dyn/cm^2. Fluorescence was excited at 488nm with an argon laser and emission detected at 500-520nm. The channel was observed using a 20X objective on a Nikon A1-R confocal microscope, with images in one focal plane captured every second for 600s. Data shows normalised mean fluorescence intensity taken at the endpoint of the assay, calculated using NIS Elements software. N=3, data represent mean ± SEM. *$p<0.05$, **$p<0.005$ compared to vehicle control, analysed by one-way ANOVA with post-hoc Dunnett's test. Ns, not significant.

4.7 Discussion of results presented in Chapter 4

The purpose of this chapter was twofold; firstly, to investigate the inhibitory ability of quercetin and its methylated metabolites in the presence of plasma proteins and in whole blood, and secondly, to identify any platelet necrotic or activatory effects caused by high, supraphysiological flavonoid concentrations. These aims were addressed through a flow cytometry study investigating potential toxicity at high quercetin concentrations, and then through a series of platelet functional experiments utilising platelet rich plasma and whole blood as the platelet-containing medium.

The high plasma protein-binding demonstrated by quercetin led to the hypothesis that higher concentrations would be needed to achieve inhibition comparable to the levels seen in the washed platelet work presented in Chapter 3, at least in the analysis of platelet function in suspension. Quercetin has displayed a degree of toxicity in other cell types, with LD_{50}s of 90.85μM, 61μM and 303μM in human lymphatic endothelial cells (HLECs), human umbilical vein endothelial cells (HUVECs) and TIG-1 cells (human lung embryonic fibroblasts), respectively (Matsuo *et al.*, 2005; Cao *et al.*, 2007). There is, however, no apparent work on quercetin toxicity in platelets. For this reason, it was investigated whether high quercetin concentrations of 100μM and 200μM could cause necrotic or activatory effects on platelets. This was investigated through P-Selectin exposure, fibrinogen binding to integrin $\alpha_{IIb}\beta_3$, annexin V binding to phosphatidylserine and surface GPIbα levels. There was no significant effect on any of these parameters at the highest concentration tested (200μM) and thus overall, these results suggest there are no significant adverse effects on platelets at quercetin concentrations up to 200μM, far beyond any physiologically achievable level. It was thus concluded that any effects of higher flavonoid concentrations were due to inhibition of platelet function, as opposed to an adverse effect on cell viability.

The primary function of platelets is to aggregate, and so to test the anti-platelet potential of quercetin and its methylated metabolites in the presence of plasma proteins, their ability to inhibit this key

function was tested. To allow direct comparison to the washed platelet aggregometry data in chapter 3 (section 3.2), aggregation was stimulated with the same agonist and concentration (collagen 5μg/mL); the only difference, therefore, would be the direct effect of plasma proteins (although it must be noted the differences in specific assay: LTA in washed platelets vs plate based aggregometry in PRP). Flavonoids have been shown to highly bind plasma proteins, and so higher concentrations were used here to investigate the concentrations required to overcome this effect (Boulton *et al.*, 1998; Kaldas *et al.*, 2005). Quercetin and its methylated metabolites were found to inhibit platelet aggregation in PRP, with a significant effect observed as low as 10μM with tamarixetin. In washed platelet assays, platelet aggregation was all but abolished at concentrations above 10μM, demonstrating, as predicted, a clear reduction (although not abolition) of inhibitory potency in the presence of plasma proteins. This reduced potency is in agreement with Pignatelli *et al.* (2006), who showed a lack of inhibitory potency of 1.25-20μM quercetin upon stimulation with collagen 7μg/mL. Other work from Mosawy *et al.* (2013a) has displayed anti-aggregatory effects of quercetin in PRP upon stimulation with collagen 5μg/mL, but at concentrations of 100μM. Thus, the work presented here demonstrates an increased potency of quercetin compared to previous reports; this is likely due to experimental differences e.g. the utilisation of the plate based aggregometry assay. An interesting observation of the data presented in section 4.3 is a switch in the inhibitory hierarchy presented in chapter 3; in the presence of plasma proteins, the order of potency appears to be tamarixetin>quercetin>isorhamnetin.

Work presented in Chapter 3 demonstrated that the inhibition of platelet aggregation by flavonoids is driven at least in part by an effect on granule secretion and fibrinogen:integrin $\alpha_{IIb}\beta_3$ interactions. As a result, it was hypothesised that the anti-aggregatory effects observed in PRP could also be driven by these mechanisms. The effect of quercetin, tamarixetin and isorhamnetin on P-Selectin exposure and fibrinogen binding to integrin $\alpha_{IIb}\beta_3$, as measures of α-granule secretion and integrin $\alpha_{IIb}\beta_3$ inside-out signalling respectively, were therefore investigated. Surprisingly, there was little effect on these processes across all concentrations tested, with consistent significant inhibitory effects observed only

in quercetin-treated samples at 20 and 50μM. Indeed, significant inhibitory effects were not observed in tamarixetin and isorhamnetin-treated samples even at these higher concentrations. This was unexpected, as work in washed platelets has shown these molecular processes to be more potently effected compared to the macroscopic process of aggregation. The same assay was therefore performed utilising quercetin concentrations up to 200μM; this resulted in full inhibition of P-Selectin exposure and fibrinogen binding, with IC_{50} values of 151μM and 124μM, respectively (very high, supraphysiological concentrations). Therefore, inhibition of aggregation in PRP could in part be through an effect on these mechanisms, but the high flavonoid levels needed perhaps imply primary importance through other pathways. The agonist used here must also be kept in mind; CRP-XL (1μg/mL) is a potent agonist, and its use is perhaps masking more subtle inhibitory effects. Compared to the flow cytometry data in Sections 3.3.2 and 3.4.1, it is clear that plasma proteins had a very large effect in dampening quercetin's response. Fibrinogen is a key plasma protein, with total protein concentrations of approximately 8.8μM (Lowe *et al.*, 2004). It has also been shown by Wright *et al.* (2010b), through a surface plasmon resonance assay, that quercetin and tamarixetin bind to fibrinogen. It may therefore be that in the presence of plasma proteins, the high fibrinogen level effectively 'sequesters' flavonoid, making it unavailable for entry into the cell and biological action within the platelet e.g. inhibition of key signalling proteins and processes such as calcium mobilisation and granule release as presented in Chapter 3. This could also potentially explain the low effect of quercetin on P-selectin exposure seen here. The binding of fibrinogen itself will, however, have potential inhibitory effects, discussed later in this section. Whether or not quercetin can bind integrin $\alpha_{IIb}\beta_3$ directly is uncertain; this could be the basis for future work.

The combined observation of an anti-aggregatory effect of quercetin and its metabolites in PRP and a slightly lower IC_{50} value for the inhibition of fibrinogen binding compared to P-Selectin exposure led to the hypothesis than integrin outside-in signalling may be effected. To test the effects of quercetin, tamarixetin and isorhamnetin on integrin $\alpha_{IIb}\beta_3$ outside-in signalling specifically in the presence of plasma proteins, a clot retraction assay was used. This measures the retraction of a thrombin-

stimulated clot over time by measuring end clot weight once a vehicle treated sample has fully retracted. This retraction of the fibrin mesh is driven by myosin-actin cytoskeletal interactions with fibrinogen through the bridge of integrin $\alpha_{IIb}\beta_3$ (Tucker *et al.*, 2012). Another advantage of this assay is that it incorporates the coagulation system; thrombin is heavily involved in the coagulation system, with evidence for roles in activating factors V, VIII and XI, as well as cleaving fibrinogen into fibrin to support the formation of a stable fibrin clot (Scheraga, 1958; Özge-Anwar *et al.*, 1965; Giddings and Bloom, 1975; Naito and Fujikawa, 1991; Crawley *et al.*, 2007). This assay therefore allows the effect of quercetin to be investigated in a more complex, inter-connected system. Quercetin, tamarixetin and isorhamnetin inhibited significantly the process of clot retraction at concentrations as low as 2.5μM; concentrations that are physiologically achievable through both supplementation and dietary modulation. Indeed, treatment with 10μM tamarixetin resulted in a large, 579% increase in clot weight compared to vehicle control. This displays a potent effect for quercetin and its methylated metabolites in the inhibition of integrin $\alpha_{IIb}\beta_3$ outside-in signalling, with the platelet unable to effectively contract the fibrin mesh.

This inhibition could be through a number of mechanisms. The initial binding of cytoskeletal myosin is driven by phosphorylation of the β3 integrin subunit, with downstream roles for Src-family kinases (SFKs) and PLCγ2 (Shattil *et al.*, 1998; Suzuki-Inoue *et al.*, 2007). It has been previously shown that quercetin can attenuate the activity of the Src-family kinases Fyn and Lyn, as well as inhibit collagen-stimulated PLCγ2 phosphorylation (Hubbard *et al.*, 2003; Wright *et al.*, 2010b). The involvement of tyrosine kinases in the transfer of contractile forces to fibrin polymers in the clot has been suggested by Schoenwaelder *et al.* (1994); total platelet tyrosine phosphorylation upon collagen-stimulation (90s stimulation with 25μg/mL collagen) has also been shown to be inhibited by ~20% at 20μM (Wright *et al.*, 2010b). There are thus numerous ways in which clot retraction could be affected by quercetin and its metabolites. Although clots did appear to form normally initially in flavonoid-treated samples, it must be considered that quercetin also has an effect on the coagulation system. A study by Choi *et al.* (2016) demonstrated an inhibitory effect of quercetin at >400μM on fibrin polymer formation, as

well as an inhibitory effect on the enzymatic activities of thrombin and factor Xa over a concentration range of 17-88μM. Another study by Guglielmone *et al.* (2002) displayed a prolonged activated partial thromboplastin time (APTT) and prothrombin time (PT) upon treatment with 1mM poly-sulphated quercetin forms. These studies have clear limitations in terms of use of high concentrations, but do demonstrate an anti-coagulant effect nonetheless. Quercetin conjugates that possess a 3-glycoside moiety (such as rutin and isoquercetin) have been shown to effectively inhibit protein disulphide isomerase (PDI), which has been shown to de-encrypt and thereby activate tissue factor, one of the key initiators of the coagulation process (Manukyan *et al.*, 2008; Jasuja *et al.*, 2012; Kiouptsi and Reinhardt, 2016). This could be one mechanism through which clot formation and retraction is inhibited *in vivo*. On a macroscopic scale, quercetin has displayed a protective effect against disseminated intravascular coagulation (DIC) in rabbits, showing the anticoagulant effect can translate into *in vivo* effects (Yu *et al.*, 2013). It may therefore be the case that these anti-coagulant mechanisms of quercetin were acting during the assay, combining with its anti-platelet effects or leading to the development of a 'weaker' clot, which could be retracted more easily. Consistent with the aggregation data presented in this chapter, a trend toward an inhibitory order of tamarixetin > quercetin > isorhamnetin was observed, implying that in the presence of plasma proteins (and therefore potentially *in vivo*), a 4' methyl group may result in an increased inhibitory potency compared to a B ring catechol moiety or a 3' methylation.

An anti-platelet effect of quercetin, tamarixetin and isorhamnetin in PRP is thus established, implicating an ability to overcome the effects of plasma proteins. The next step was to investigate quercetin and its metabolites' ability to inhibit platelet function in whole blood, the physiological medium in which it acts. This was tested through an *in vitro* thrombus formation under flow assay, in which flavonoid-treated whole blood was flowed through collagen-coated channels at a physiological shear rate. The use of whole blood and a shear rate representing physiological arterial levels combines to make the results of this assay a useful insight into the potential *in vivo* effect of compounds of interest. Due to the expense, both financially and temporally, of this assay, only one concentration of

each flavonoid was tested. 10μM was chosen to represent a high, yet potentially physiologically achievable concentration, as previously described; for example, a study by Hubbard *et al.* (2004) demonstrated that, upon consumption of a 300mg dose of quercetin-4'-O-β-D-glucoside, total plasma flavonoid levels reached a peak of 10.66μM. Quercetin and isorhamnetin inhibited the development of thrombi almost identically, with significant inhibition in thrombus growth observed from early time points up to the end of the assay. Tamarixetin displayed a trend (although not statistically significant) toward increased potency, reducing the size of thrombi greater than both quercetin and isorhamnetin (39 and 41% vs 55% inhibition).

Whilst the inhibition of the early stages of thrombus formation are likely explained to a large degree by the inhibition of collagen-stimulated platelet function and associated signalling events, the inhibition of the propagation phase of thrombus formation could be explained via different mechanisms. As demonstrated in Chapter 3, quercetin and its methylated metabolites potently inhibit platelet granule secretion. This is crucial to the positive feedback activatory loops characteristic of platelets; an inhibition of the release of pro-activatory molecules contained within granules could serve to dampen the propagation of thrombi. Another possible mechanism could be the interruption of GPVI:fibrin interactions and activatory mechanisms. A recent study by Alshehri *et. al.* (2015) identified fibrin as a novel ligand for GPVI, with evidence suggesting fibrin-mediated phosphorylation of FcRγ chain and Syk downstream of GPVI, and inhibited spreading on fibrin in platelets deficient in GPVI; these interactions are hypothesised to have roles in the growth and stability of thrombi. This is supported by a study from Mammadova-Bach *et al.* (2015), which suggests a role for GPVI:fibrin interactions in increased generation of thrombin and platelet recruitment to thrombi. Inhibition of this novel pathway by quercetin and its methylated metabolites is possible and could explain the sustained effects of these flavonoids on thrombus propagation; for example, it is shown in Chapter 6 of this study that quercetin, tamarixetin and isorhamnetin inhibit CRP-XL-stimulated Syk phosphorylation, with other studies also showing potent effects of quercetin on the phosphorylation of kinases downstream of GPVI (Hubbard *et al.,* 2003; Wright *et.al.,* 2010b).

Interestingly, inhibition of thrombus formation was stronger than the effect on PRP aggregometry. This could be for several methodological reasons; for example, the stirring of PRP versus the flow of whole blood, and the use of collagen in suspension versus static collagen adhered onto a channel. It could also, though, have a biological explanation. For example, quercetin is taken up into red blood cells through the binding of haemoglobin, and work has shown quercetin is able to inhibit the production of reactive oxygen species in these cells (Fiorani *et al.*, 2003; Henneberg *et al.*, 2013). Fiorani *et al.* (2003) have proposed that red blood cells may act as a flavonoid 'reservoir', with a key role for haemoglobin-bound quercetin in the plasma distribution of flavonoids. This group found that quercetin release from red blood cells was observed only when albumin was present, and that this was inhibited when this albumin was saturated with quercetin (Fiorani *et al.*, 2003). This was confirmed in the opposite direction, too, with red blood cells accumulating quercetin at increasing levels depending on the quercetin-saturation levels of the albumin (with increasing albumin quercetin concentration leading to more quercetin uptake into RBCs) (Fiorani *et al.*, 2003). The presence of red blood cells in this *in vitro* thrombus formation assay may therefore act to release quercetin from RBCs into the plasma once quercetin levels decreased, for example after being taken up by platelets, allowing further flavonoid:platelet interactions and uptake. This hypothesised mechanism could prove more potent over longer periods of time, for example over the hours in which quercetin is resident in plasma *in vivo*. Further work would be required to elucidate the validity of this hypothesis; for example, whole blood aggregometry could be utilised.

Previous work from Wright *et al.* (2013) has demonstrated the ability of quercetin and tamarixetin to inhibit thrombus formation *in vitro,* using a similar methodology. They studied the effects of these flavonoids, and found 5μM quercetin to be ineffective, with 5μM tamarixetin inhibiting only by 5%. Concentrations up to 200μM were tested, and found to inhibit thrombus formation by ~10% (Wright *et al.*, 2013). This difference in potency compared to the data presented here could represent the different methodologies used; for example, Wright *et al.* (2013) monitored thrombus formation only

for 5 minutes, and used a higher shear rate ($1000s^{-1}$); as discussed previously, shear rate is an important consideration. Differences in anti-thrombotic potency compared to the data presented here must therefore keep these differences in mind. There is agreement, however, in the fact that tamarixetin demonstrated a higher mean inhibition of thrombus formation than quercetin. This supports the inhibitory hierarchy observed throughout the results presented in this chapter; tamarixetin > quercetin > isorhamnetin.

The reason for this switch in the hierarchy between washed platelet assays and work in PRP and whole blood is not entirely clear. It could, in part, be explained by an observation by Wright *et al.* (2010b) regarding flavonoid binding to collagen and fibrinogen. They perfused flavonoids over immobilised collagen or fibrinogen and calculated affinities (K_D) from association and dissociation constants, and found that tamarixetin (1.06×10^{-6} M) bound collagen with a higher affinity than quercetin (3.62×10^{-6} M) (Wright *et al.*, 2010b). A very large difference was observed in fibrinogen binding affinity, with tamarixetin binding with picomolar affinity (6.15×10^{-10} M) compared to the micromolar affinity of quercetin (9.96×10^{-6} M) (Wright *et al.*, 2010b). They concluded that these affinities did not follow the observed inhibitory potencies, with quercetin proving more effective. However, the work conducted was in washed platelets, and thus agrees with the data presented in Chapter 3 of this study, which concludes that quercetin was more potent than tamarixetin. It may be that in the presence of plasma proteins and in whole blood (especially under shear stress), these differences in affinity become important. Tamarixetin binding to collagen with a slightly higher affinity may result in reduced platelet GPVI:collagen interactions compared to quercetin-treated samples, resulting in further inhibited activation. In addition to this, the great difference in fibrinogen binding affinity may result in a large difference between the scale of $\alpha_{IIb}\beta_3$:fibrinogen interactions, which may be particularly important under flow considering this interaction can occur directly in arterial shear conditions (Savage *et al.*, 1996; Nesbitt *et al.*, 2009). These hypotheses could, at least in part, explain the trend toward increased potency of tamarixetin in the inhibition of thrombus formation under flow. It could also explain the significantly increased efficacy of tamarixetin in the inhibition of aggregation and the larger average clot weights upon treatment with tamarixetin compared to quercetin and

isorhamnetin in clot retraction; two processes driven by fibrinogen:integrin interactions. It would be interesting to investigate the ability of quercetin to bind von Willebrand factor, with the implication of reduced ability to bind the GPIb/V/IX complex crucial to initial platelet adhesion at sites of injury. Another reason could be reduced plasma binding; indeed, bovine serum albumin binding constants are reduced 2-3 times upon methylation of the 4' hydroxyl residue (i.e. quercetin vs tamarixetin) (Andersen and Markham, 2007). Whether this carries through into human plasma, and the effect of 3'-methylation (as in isorhamnetin), could also be included in future work.

In summary, the results presented in this chapter demonstrate a reduced yet present anti-platelet effect of quercetin, tamarixetin and isorhamnetin in the presence of plasma proteins and in whole blood. Platelet aggregation was inhibited to a lesser degree than in washed platelets, with a further reduced potency in the inhibition of α-granule release and integrin $\alpha_{IIb}\beta_3$ inside-out signalling. Outside-in signalling of integrin $\alpha_{IIb}\beta_3$, measured through clot retraction, was affected at concentrations of flavonoid proven to be physiologically achievable. A measurement of platelet function in whole blood under flowing conditions also demonstrated significant effects of quercetin and its methylated metabolites, reducing the development of thrombi at a higher-end physiological concentration. This chapter therefore provides evidence for the potential of dietary or supplemental levels of plasma quercetin to exhibit anti-platelet effects in the presence of the antagonising factor of plasma proteins, and suggests some of the potential mechanisms through which these effects may occur. An inhibitory hierarchy of effect is observed that is the opposite to that seen in the washed platelet work demonstrated in chapter 3, implying that in plasma and whole blood, tamarixetin > quercetin > isorhamnetin, suggesting a 4'methyl group as key. The reason for this is not entirely clear, but is contemplated above, with suggestions to elucidate the true reasons discussed more in the 'Future Work' section of the general discussion. The next chapter will discuss the anti-platelet effect of novel quercetin formulations both *in vitro* and *in vivo,* in collaboration with industry, and will investigate the ability of quercetin and its metabolites to interact with aspirin to enhance anti-platelet effects.

5 – Novel quercetin formulations inhibit thrombus formation in vitro *and* in vivo*, and enhance the anti-platelet actions of aspirin*

5.1 – Novel quercetin formulations inhibit thrombus formation in vitro *and* in vivo, *and enhance the anti-platelet actions of aspirin*

Human studies have shown protective effects of quercetin against cardiovascular disease, with effects on associated biomarkers, with quercetin, upon consumption, reducing total and LDL cholesterol and both systolic and diastolic blood pressure in male smokers, reducing systolic blood pressure and oxidised LDL levels in overweight subjects, and reducing systolic and diastolic blood pressure in hypertensive subjects (Knekt *et al.*, 2002; Edwards *et al.*, 2007; Egert *et al.*, 2009; Lee *et al.*, 2011). This knowledge, combined with a potent *in vitro* anti-platelet effect displayed in numerous studies, has resulted in quercetin garnering attention as a potential anti-thrombotic supplement/pharmaceutical. In this chapter, four novel quercetin formulations (supplied by Quercegen Pharmaceuticals) have been investigated for their anti-platelet effects for the first time, as well as their anti-thrombotic ability *in vitro,* with one formulation tested in an *in vivo* model of arterial thrombosis, in order to understand and establish their potential as anti-thrombotic supplements / treatments. Aspirin is widely used as an anti-platelet medication, with millions of patients worldwide taking aspirin prophylactically on a daily basis or as a treatment (Hennekens *et al.*, 1997; Dai and Ge, 2012; Nansseu and Noubiap, 2015). It has been demonstrated that flavonoids can potentiate the inhibitory effects of aspirin; Crescente *et al.* (2009) found that a mixture containing resveratrol, quercetin and gallic acid (three polyphenols found in red wine) could potentiate the anti-platelet effects of aspirin, and Navarro-Nunez *et al.* (2008) concluded that apigenin could synergise with aspirin to inhibit platelet aggregation induced by arachidonic acid. This has also been investigated in a dietary setting; Zubair *et al.* (2011) demonstrated an increased bleeding time in participants upon consumption of both aspirin and flavonoid-rich dark chocolate, compared to aspirin alone.

An aim of this chapter, therefore, was to investigate the combined effects of aspirin with quercetin, its methylated metabolites or novel quercetin formulations on platelet aggregation, to establish whether any specific quercetin/metabolite-aspirin interactions exist, and the magnitude and nature of such

potential interactions. These interactions were also explored using a platelet function analyser in a whole blood assay, to understand how quercetin and its methylated metabolites inhibit platelet function in combination with aspirin in whole blood, in the presence of associated factors such as plasma proteins.

5.2 Aglycone-based quercetin formulations inhibit washed platelet aggregation, whereas isoquercetin-based formulations do not

The novel quercetin formulations to be investigated for anti-thrombotic potential had not before been tested for an effect on platelets; as such it was important to first understand if platelet aggregation was affected. The novel quercetin formulations to be investigated, supplied by Quercegen Pharmaceuticals, were as follows: QU995, a 99.5% pure form of quercetin aglycone, QB3C, a blend of QU995 and vitamins B3 and C (100g QU995, 24.8g ascorbic acid, 2g niacin (79% QU995, 19.5% ascorbic acid, 1.5% niacin)), IQC-950AN (isoquercetin, quercetin-3-O-glucoside) (herein referred to as 'isoquercetin'), and an isoquercetin blend with vitamins B3 and C (79% isoquercetin, 19.5% ascorbic acid, 1.5% niacin, herein referred to as 'isoblend'). These formulations are described in Table 5-1.

Interest in the 3-O-glucoside form of quercetin (isoquercetin) developed largely from the observation of Paulke *et al.* (2012) that, upon gavage of isoquercetin in rats, plasma and tissue quercetin metabolite levels were 2-5X higher than upon gavage with quercetin aglycone. Indeed, upon consumption of 500mg quercetin aglycone in humans, plasma levels reached a peak concentration of 0.77μM, whereas 500mg isoquercetin resulted in a peak plasma concentration of 3.45μM (internal communication with Quercegen Pharmaceuticals, work conducted by Stopa JD, Furie B, Flaumenhaft R and Zwicker J, 2013, Boston, USA). This is supported by previous observations from Hollman *et al.* (1995) and Hollman *et al.* (1997), who concluded that conjugation of quercetin with glucose dramatically enhances the absorption and bioavailability of quercetin compared to the aglycone as well as other, non-glucose glycosides such as rutin. This conclusion is supported by work from Graefe *et al.* (2001), who demonstrated plasma concentrations 7X higher upon consumption of quercetin-4'-O-glucoside compared to rutin (quercetin-3-O-rutinoside).

The addition of vitamins B3 and C to the formulations was based on the observation that these vitamins can inhibit the activity of cytochrome P450 (CYP) enzymes, with vitamin B3 inhibiting CYP2D6,

CYP3A4 and CYP2E1, and vitamin C shown to inhibit CYP2E proteins (Clarke *et al.*, 1996; Gaudineau and Auclair, 2004). Many studies have shown a role of cytochrome P450 enzymes in the metabolism of flavonoids including quercetin, primarily through oxidation and hydroxylation reactions, and so it was hypothesised (by our collaborator Dr. Mitsunori Ono of Quercegen Pharmaceuticals) that the competitive inhibition of these enzymes by vitamins B3 and C could lead to the maintenance of a higher and more maintained peak of quercetin in plasma, preventing the accumulation of the (largely) more inactive metabolites (Hodek *et al.*, 2002; Otake and Walle, 2002; Cermak, 2008; Cassidy and Minihane, 2017). It has also been shown that vitamin C can individually inhibit platelet function, with supplementation (260mg/day) in human subjects inhibiting significantly ADP-stimulated platelet aggregation and ATP secretion *ex vivo,* and it has also been hypothesised that plasma vitamin C can enhance the release of nitric oxide from polymorphonuclear leukocytes (PMNs) (Yang *et al.*, 1999; Raghavan *et al.*, 2003). Vitamin B3 also has anti-platelet effects; a study by Serebruany *et al.* (2010) demonstrated an inhibition of collagen and ADP-stimulated platelet aggregation upon *in vitro* addition of 0.3-3mM vitamin B3, and Norgard *et al.* (2016) concluded that supplementation with 1-2g vitamin B3 has a low, yet significant effect on platelet aggregation. These anti-aggregatory effects are far less pronounced than those achieved through addition of quercetin; however, they may be able to combine to increase anti-platelet effect.

As well as the individual effects of QU995 and isoquercetin, the effects of vitamins B3 and C in combination with quercetin/isoquercetin had not previously been investigated in platelets, and so in this study initial experiments focussed on the effect of QU995, QB3C, isoquercetin and isoblend on platelet aggregation, both with and without stimulation with collagen (5µg/mL), to elucidate any pro- or anti-aggregatory effects of these novel flavonoid formulations (whilst pro-aggregatory effects were unlikely, due to the untested nature of these formulations, it needed to be ensured).

QU995, QB3C, isoquercetin, isoblend or vehicle control (DMSO, 0.2% v/v) were added to washed platelets (2 x 10^8 cells/mL) and aggregation measured immediately for 5 minutes under stirring (1200rpm) conditions (for investigation into pro-aggregatory effect) or were added and incubated for

5 minutes at 37°C after 10s stirring, followed by stimulation with collagen (5μg/mL) for 5 minutes under stirring (1200rpm) conditions (to investigate anti-aggregatory effects). These aggregometry experiments were performed in an AggRAM optical aggregometer (Helena Biosciences Europe, Gateshead, UK), rather than the Chrono-Log optical aggregometer used in previous chapters. The functioning of the machine is identical, however it can run multiple samples simultaneously and requires smaller sample volumes. It outputs data as digital light transmission values approximately every 0.5 seconds, and percentage aggregation at 5 minutes was normalised to the level of aggregation in the absence of flavonoid (vehicle), taken as 0% in the absence of agonist, and 100% after stimulation with agonist.

Figure 5-1A/B shows aggregation traces output digitally upon conversion to percentage aggregation. Isoquercetin and isoblend did not cause any response when added at concentrations up to 50μM (Figure 5-1A/C). This concentration was chosen initially to match the highest level of quercetin aglycone used in the washed platelet aggregometry assays presented in chapter 3 (which represented a concentration beyond what was physiologically achievable through diet or supplementation). At the same high concentration, QU995 and QB3C did cause a significant aggregatory response (Figure 5-1A/C). This was, however, a very modest effect, with QU995 and QB3C causing an average of 3.5 and 7% aggregation, respectively. When the aggregation traces are viewed, as displayed in Figure 5-1A, it becomes particularly evident that these effects are not appreciable, and as such were not considered to be indicative of a serious, problematic pro-activatory effect (this was further confirmed by the observation of an anti-aggregatory effect upon collagen-stimulation, presented next).

Isoquercetin and isoblend did not inhibit collagen-stimulated aggregation (5μg/mL) at concentrations up to 50μM (Figure 5-1B/D). This could be due to numerous factors, including reduced cell permeability and reduced target enzyme inhibition, discussed in section 5.9. QU995 and QB3C inhibited significantly platelet aggregation at concentrations of 5μM and above. There was no significant difference between the level of inhibition achieved by QU995 and QB3C; this indicates

that, in washed platelets, the vitamin B3 and C additions are not enhancing the anti-platelet properties through a direct effect on the platelet (Figure 5-1D). This anti-activatory effect was also confirmed through flow cytometry, with QU995 and QB3C, but not isoquercetin or isoblend, inhibiting fibrinogen binding to integrin $\alpha_{IIb}\beta_3$ and P-selectin exposure (data not shown). Compared to quercetin aglycone studied in chapter 3 (section 3.2), QU995 at 5μM inhibited platelet aggregation significantly more ($p=0.001$), with a trend toward increased effect with QB3C also ($p=0.058$). This increase in inhibitory potency could reflect the increased purity of QU995 and QB3C, purported to have fewer or lower levels of contaminants than other quercetin preparations. However, this increased effect is not maintained at 10μM, where quercetin aglycone is significantly more potent than QU995 and QB3C (at this concentration, very high levels of inhibition (>80%) are achieved regardless, and so this difference may not be as critical).

Overall, these data suggest an inhibitory role for QU995 and QB3C, but not isoquercetin or isoblend, in the inhibition of the function of washed platelets.

Table 5-1 The composition of novel quercetin formulations used in Chapter 5

Quercetin formulation	Composition
QU995	99.5% pure quercetin aglycone
QB3C	A blend of • QU995 – 79% • Ascorbic acid (vitamin C) – 19.5% • Niacin (vitamin B3) – 1.5%
IQC950-AN (herein 'isoquercetin')	>95% pure isoquercetin (quercetin-3-glucoside)
Isoquercetin blend (herein 'isoblend')	A blend of • IQC950-AN – 79% • Ascorbic acid – 19.5% • Niacin – 1.5% Nb. In murine studies, contained 1mg folic acid per 1g isoblend (described in-text)

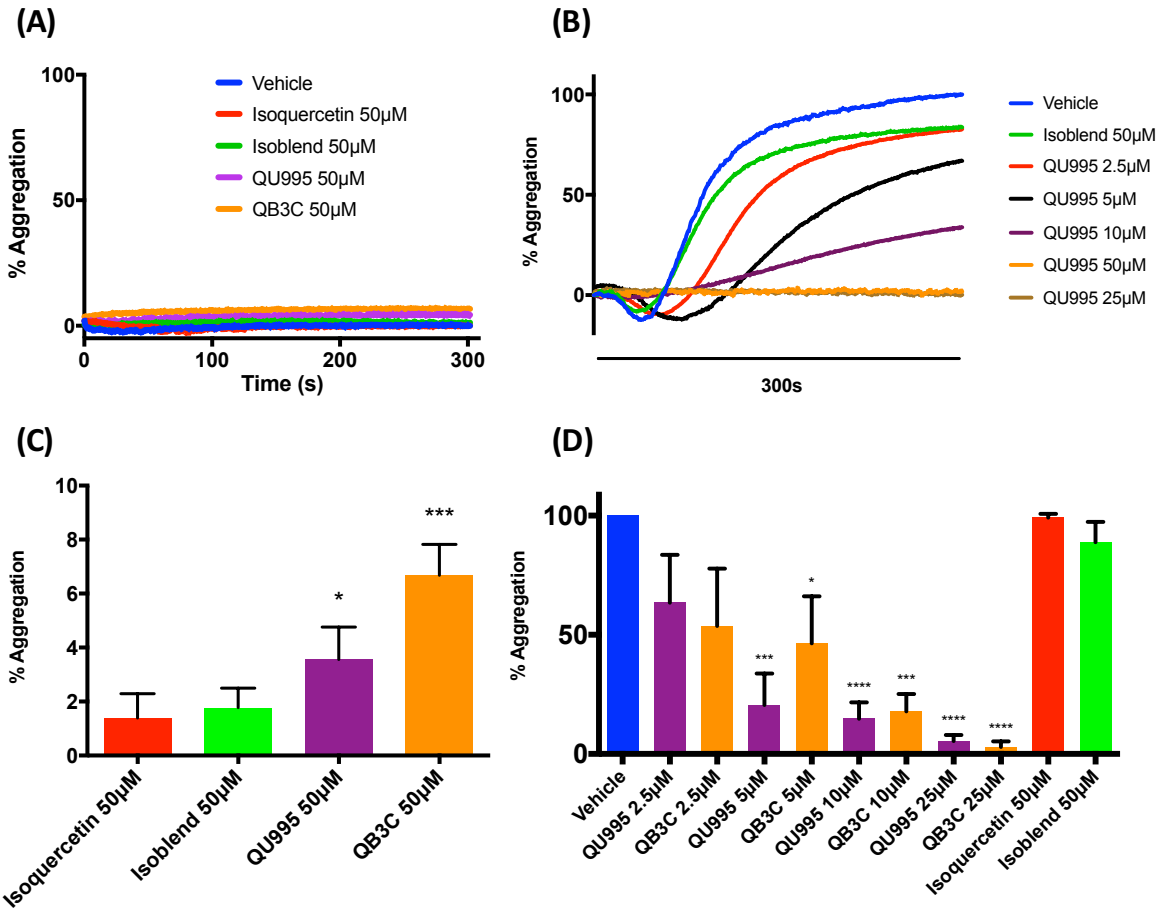

Figure 5-1 Novel quercetin aglycone-based formulations, but not isoquercetin-based formulations, inhibit collagen-stimulated washed platelet aggregation, and can cause mild platelet aggregation in the absence of agonist

QU995, QB3C, isoquercetin, isoblend or vehicle (DMSO, 0.4% v/v) were added to washed platelets (2 x 10^8 cells/mL) and aggregation immediately measured (A/C), or were added and incubated for 5 minutes (with 10 seconds stirring to mix) prior to addition of collagen (5µg/mL) (B/D) and aggregation measured for 5 minutes at 37ºC under constant stirring (1200rpm) conditions in an AggRAM platelet aggregometer. Percentage aggregation at 5 minutes was normalised to the level of aggregation in the absence of flavonoid (vehicle). N=4, data represent mean ± SEM. *p<0.05, ***p<0.001, ****p<0.0001 compared to vehicle control, analysed by one-way ANOVA with post-hoc Dunnett's test.

5.3 Novel quercetin formulations inhibit in vitro *thrombus formation under flow only at concentrations equivalent to high level supplementation*

5.3.1 No inhibitory effects are observed at demonstrated physiological concentrations

The demonstration of anti-aggregatory effects of novel quercetin formulations led to the hypothesis that they may have an effect on thrombus formation under flow. Analysis of this *in vitro* would allow the elucidation of any potential effects of these novel formulations in the presence of plasma proteins and red blood cells, in a flowing system. This is beneficial considering their potential as anti-thrombotic compounds; a demonstration of effect in this assay would indicate anti-platelet effects in whole blood. Another benefit of using the novel formulations in this assay is that it would inform the planned *in vivo* experimentation; it would indicate which novel formulation is most effective in whole blood, and give an indication as to the concentrations at which anti-thrombotic effects may be seen.

Initially, concentrations of 10μM were used, to allow comparison of the effects of the novel quercetin formulations with those of quercetin, tamarixetin and isorhamnetin presented in chapter 4 (section 4.6), which represented a high, physiologically achievable concentration. Conditions for the assay were kept the same, using a shear rate of $500s^{-1}$, representing a physiological arterial shear rate. Citrated human whole blood was incubated with DioC6 (5μM) for 1 hour at $30^{o}C$. During this, Vena8 BioChips were coated with type I collagen (100μg/mL) for one hour, after which excess collagen was washed through with modified Tyrodes-HEPES buffer. Whole blood was incubated with the novel quercetin formulations or vehicle control for 10 minutes at $30^{o}C$ (to match conditions in section 4.6) prior to perfusion through the collagen-coated microfluidic channels. Fluorescence was excited at 488nm with an argon laser and emission detected at 500-520nm. The microfluidic channel was observed using a 20X objective of a Nikon A1-R confocal microscope, with images captured every 1 second for 600 seconds. Mean thrombus fluorescence intensity was calculated using NIS elements software and normalised to the level of fluorescence at the end of the assay in the absence of flavonoid (vehicle).

None of the novel quercetin formulations (Table 5-1) inhibited thrombus formation under flow, as seen in Figure 5-2. Figure 5-2E shows representative images from the end of the assay; the vehicle sample displays large, bright thrombi that have developed over the 10 minute assay period, with flow in the direction from the top to the bottom of the image. The quercetin aglycone-based and isoquercetin-based formulations displayed similar growth of the thrombi throughout the assay (Figure 5-2A-D), and the end-point images show similar large thrombi covering most of the experimental channel. This was an unexpected result, particularly for QU995 and QB3C, considering quercetin aglycone, as shown in Figures 4-6 and 4-7, inhibited thrombus formation by an average of 39%. The reason for this is not entirely clear; however, quercetin aglycone, as noted in the previous section, was significantly more potent in the inhibition of platelet aggregation at 10μM compared to QU995 and QB3C. It may be that the reduced potency at this higher concentration is maintained in whole blood, and would offer an explanation for the results presented here. A lack of significant inhibitory effect for the isoquercetin-based formulations could represent reduced entry into the platelet or reduced target enzyme inhibition, as well as the fact that *in vitro,* isoquercetin will not be metabolised extensively, with metabolism *in vivo* perhaps liberating more potent "effector" metabolites. This is discussed further in section 5.9.

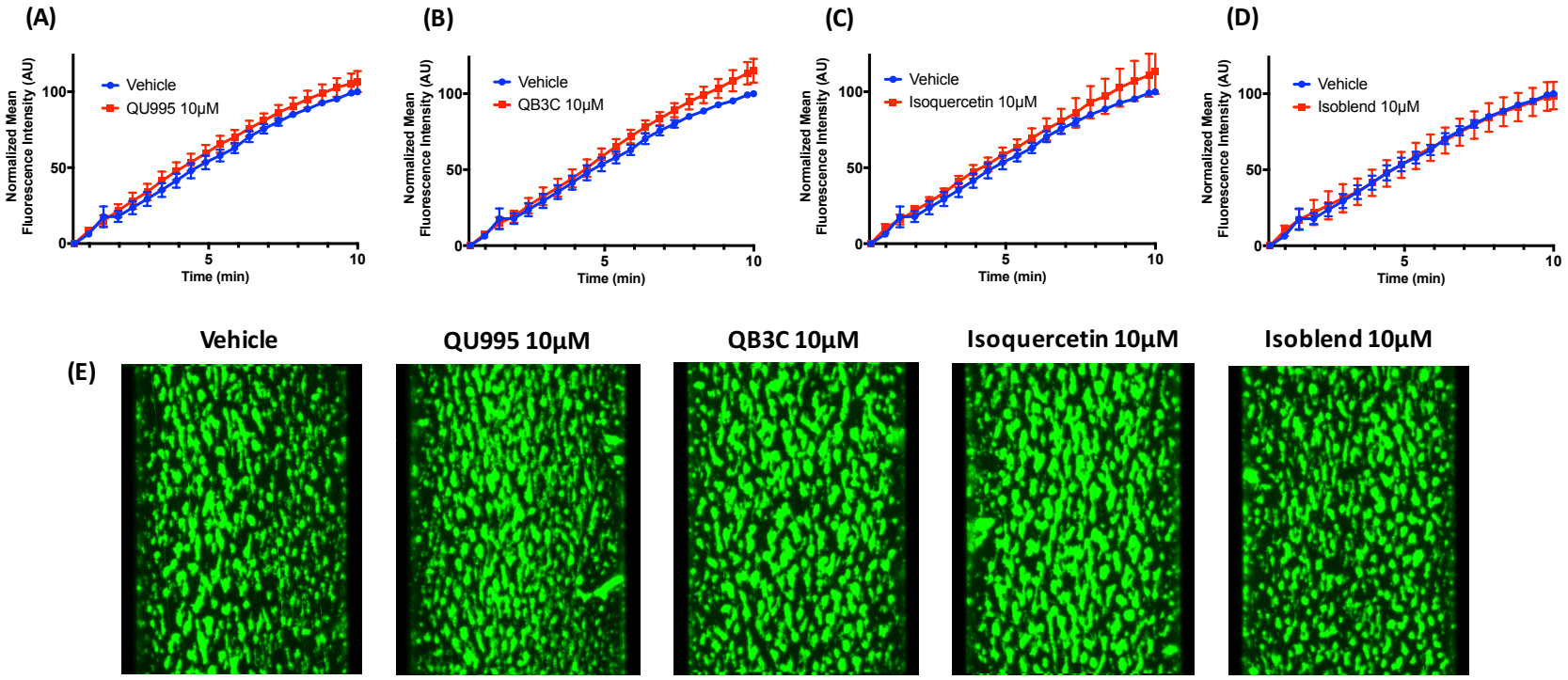

Figure 5-2 The novel quercetin formulations QU995, QB3C, isoquercetin and isoblend do not inhibit *in vitro* thrombus formation under flow at a concentration of 10µM

Citrated human whole blood was incubated with DioC6 lipophilic dye (5µM) for 1 hour at 30°C. Concurrently, Vena8 BioChip microfluidic channels were coated with collagen (type I, 100µg/mL) for one hour, and excess collagen washed through with modified Tyrodes-HEPES buffer. Whole blood was incubated with QU995 (A), QB3C (B), isoquercetin (C), isoblend (D) or vehicle control (DMSO, 0.2% v/v) for 10 minutes at 30°C prior to perfusion through channels at a shear rate of $500s^{-1}$. Fluorescence was excited at 488nm with an argon laser and emission detected at 500-520nm. The channel was observed using a 20X objective on a Nikon A1-R confocal microscope, with images captured every second for 600s. Mean thrombus fluorescence intensity, normalised to the level of fluorescence at the end of the assay in the absence of flavonoid (vehicle), was calculated using NIS Elements software, and representative images at the assay endpoint are shown in (E). N=4, data represent mean ± SEM, analysed by two-way ANOVA with post-hoc Bonferroni correction.

5.3.2 An investigation into the feasibility of novel quercetin formulations to inhibit **in vitro** *thrombus formation under flow*

Upon the conclusion that novel quercetin formulations were unable to inhibit thrombus formation *in vitro* at 10μM (a total concentration shown by Hubbard *et al.* (2004) to be physiologically achievable following supplementation with quercetin-4-O-β-D-glucoside), the next step was to investigate whether these formulations were able to inhibit this process even at higher, supraphysiological concentrations. This would enable an understanding of their overall inhibitory potency, as well as their feasibility to display an anti-platelet effect upon supplementation, which can result in higher concentrations of plasma quercetin than is achievable through diet alone. In addition, this use of higher concentrations would allow elucidation of the levels of quercetin that would be feasible to administer to mice in planned *in vivo* experimentation.

Internal communication with Quercegen Pharmaceuticals confirmed that, upon 50mg/kg supplementation in mice, QU995 and QB3C reached peak total quercetin plasma levels of approximately 5μM and 20μM (at 120 and 60 minutes), respectively, with isoquercetin and isoblend predicted to reach concentrations of approximately 17.5 and 70μM (at 2.5 hours and 1-2 hours), respectively. Preliminary work performed in this study concluded that, at 50mg/kg isoblend supplementation in mice, an inhibitory effect *in vivo* was not likely to be observed, and so a 200mg/kg supplementation protocol was planned. Whilst this represents a high dose, work conducted by Tamura *et al.* (2010) estimated a no adverse effect level (NOAEL) of 1% dietary concentration in male Wistar rats, corresponding to 542.4mg/kg/day for 52 weeks. A 200mg/kg supplementation protocol would result in approximate peak total quercetin plasma concentrations of 20μM, 80μM, 70μM and 280μM upon supplementation with QU995 (at approximately 1 hour), QB3C (at approximately 30 minutes), isoquercetin (at approximately 2.5 hours) and isoblend (at approximately 1-2 hours) respectively (internal communication with Quercegen pharmaceuticals). These concentrations were thus tested on

an *in vitro* thrombus formation under flow assay using human blood, in order to investigate which formulation would be optimal, based on greatest level of inhibition, for mouse *in vivo* experimentation.

Experimental methodology was kept identical to the previous section, the only differences being in the concentrations of flavonoid used. At the predicted peak plasma quercetin concentrations, formation of thrombi was inhibited significantly by all novel quercetin formulations (Figure 5-3A-D). QU995, QB3C and isoquercetin inhibited this process similarly, with average inhibition values of 43%, 42% and 43% at the 10 minute endpoint, respectively. This is an interesting observation considering the differing concentrations used; 20μM QU995, 80μM QB3C and 70μM isoquercetin. The work presented in section 4.6 revealed a 39% reduction in thrombus formation by quercetin aglycone at 10μM; it may therefore be that the effect of quercetin aglycone-based formulations reach a maximal inhibitory effect at this point. Another interesting finding is the equal potency of QB3C and isoquercetin at similar concentrations, as it was hypothesised that the glucose moiety would lead to reduced inhibitory effect. Isoblend inhibited significantly thrombus formation by an average of 72% (Figure 5-3D). This was a statistically significantly higher effect compared to QU995, QB3C and isoquercetin, as displayed in Figure 5-4. Whilst this is likely due to the higher concentration used, these reflected predicted plasma concentrations, and so the difference is an important finding. Testing the effect of 100μM+ concentrations of QU995 and QB3C could clarify this hypothesis.

Based on the above results, it was concluded that the analysis of thrombosis in mice would be explored using supplementation with isoblend 200mg/kg, as this was most potent in inhibiting thrombus formation *in vitro* at predicted peak plasma concentrations. These results demonstrate that perhaps lower concentrations could have been used, as the level of inhibition, especially with isoblend, was moderately high. However, it was unclear how an *in vitro* effect would translate into potency *in vivo*, and so a 200mg/kg dosage would be used. Lower concentrations could have been investigated to provide an insight into the inhibitory potential of these novel quercetin formulations at proposed human supplementation levels of 500mg – 2g; this is discussed further in section 5.9.

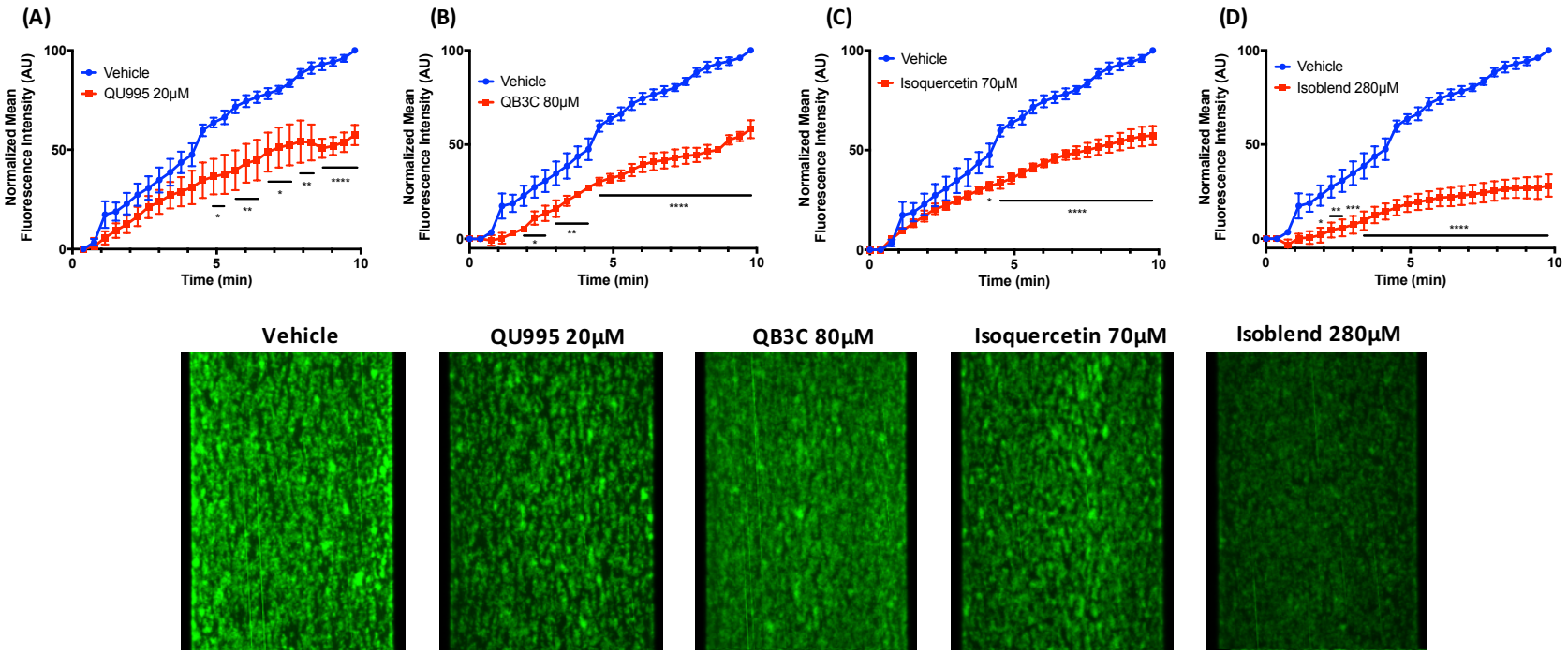

Figure 5-3 At predicted peak total quercetin plasma concentrations based upon 200mg/kg supplementation in mice, isoblend inhibits *in vitro* thrombus formation under flow in human blood most potently

Citrated human whole blood was incubated with DioC6 lipophilic dye (5μM) for 1 hour at 30°C. Concurrently, Vena8 BioChip microfluidic channels were coated with collagen (type I, 100μg/mL) for one hour, and excess collagen washed through with modified Tyrodes-HEPES buffer. Whole blood was incubated with QU995 (A), QB3C (B), isoquercetin (C) isoblend (D) or vehicle control (DMSO, 0.2% v/v) for 10 minutes at 30°C prior to perfusion through channels at a shear rate of $500s^{-1}$. Fluorescence was excited at 488nm with an argon laser and emission detected at 500-520nm. The channel was observed using a 20X objective on a Nikon A1-R confocal microscope, with images captured every second for 600s. Mean thrombus fluorescence intensity, normalised to the level of fluorescence at the end of the assay in the absence of flavonoid (vehicle), was calculated using NIS elements software, and representative images at the end of the assay endpoint are shown in (E). N=3, data represent mean ± SEM. *p<0.05, **p<0.005, ***p<0.001, ****p<0.0001 compared to vehicle control, analysed by two-way ANOVA with post-hoc Bonferroni correction.

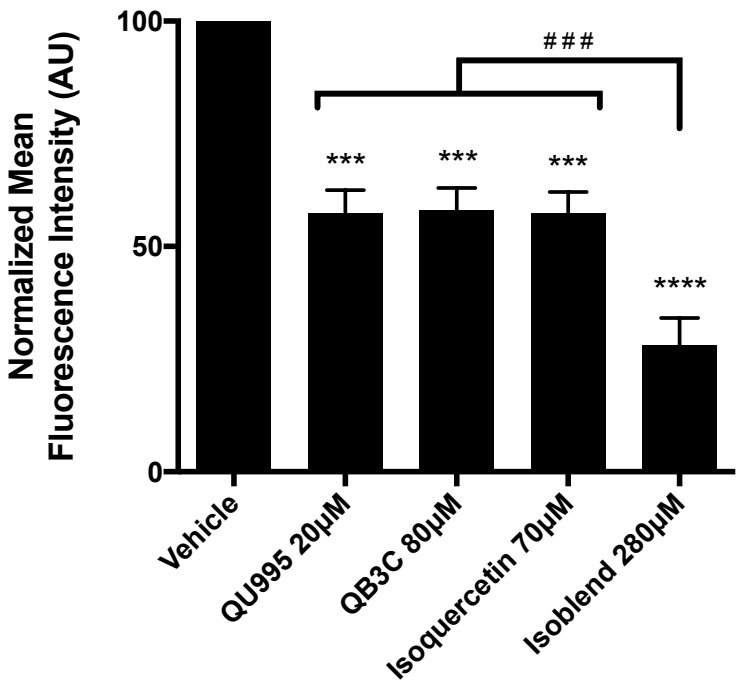

Figure 5-4 At predicted peak total quercetin plasma concentrations following 200mg/kg supplementation in mice, isoblend inhibits *in vitro* thrombus formation under flow in human blood significantly more than all other formulations

Citrated human whole blood was incubated with DioC6 lipophilic dye (5µM) for 1 hour at 30°C. Concurrently, Vena8 BioChip microfluidic channels were coated with collagen (type I, 100µg/mL) for one hour, and excess collagen washed through with modified Tyrodes-HEPES buffer. Whole blood was incubated with QU995, QB3C, isoquercetin, isoblend or vehicle control (DMSO, 0.2% v/v) for 10 minutes at 30°C prior to perfusion through channels at a shear rate of $500s^{-1}$. Fluorescence was excited at 488nm with an argon laser and emission detected at 500-520nm. The channel was observed using a 20X objective on a Nikon A1-R confocal microscope, with images captured every second for 600s. Mean thrombus fluorescence intensity, normalised to the level of fluorescence at the end of the assay in the absence of flavonoid (vehicle), was calculated using NIS elements software, and representative images at the end of the assay endpoint are shown in (E). N=3, data represent mean ± SEM. *p<0.05, **p<0.005, ***p<0.001, ****p<0.0001 compared to vehicle control, analysed by one-way ANOVA with post-hoc Dunnett's test. # # # p<0.001, compared to QU995, QB3C and Isoquercetin, analysed by unpaired t-tests.

5.4 Isoquercetin, the 3-O-glucoside of quercetin, inhibits thrombus formation in a murine model of arterial thrombosis

The work presented so far in this chapter resulted in the conclusion that isoblend (Table 5-1) was the novel quercetin formulation to be used in *in vivo* experimentation. In communication with Quercegen Pharmaceuticals, the potential benefit of adding folic acid, a synthetic form of folate (vitamin B9), into the isoblend formulation was discussed. This was for several reasons. Firstly, as well as being recognised as important to general health, folic acid has displayed beneficial anti-platelet and anti-CVD effects; Durand *et al.* (1996) demonstrated that a folate-deficient diet in rats led to an enhancement of ADP and thrombin-stimulated platelet aggregation, and Bechir *et al.* (2005) found that a single 5mg dose of folic acid was able to significantly enhance baroreceptor sensitivity in patients with hypertension. Indeed, a meta-analysis of studies by Wang *et al.* (2012b) concluded that dietary folate intake was inversely associated with risk of CHD, with the highest level of intake associated with a significantly reduced CHD risk (relative risk of 0.69). From a health perspective, supplementation with folic acid also has wide-ranging benefits, including the largely recognised benefit of reducing the rate of neural tube defects, and significantly reducing the risk of a neonate being small for gestational age (SGA) (De Wals *et al.*, 2007; Hodgetts *et al.*, 2015). The beneficial impact of folic acid is not solely reserved to birth-related effects; a study in severely depressed patients by Godfrey *et al.* (1990) demonstrated 15mg/day folic acid was able to improve symptom relief and social adaptation in patients more effectively than placebo control in addition to standard treatment. This is supported by a meta-analysis by Taylor *et al.* (2004), who concluded that adding folate supplementation to existing medication regimes reduced Hamilton Depression Rating Scale (HDRS) scores further than existing medication alone.

These were the reasons for the addition of folic acid to the supplement, and was what was made available to us for the murine study by Quercegen Pharmaceuticals. Preliminary work (not shown) had concluded that an equivalent of 100μg folic acid per gram of isoblend had no effect on *in vitro*

thrombus formation under flow in human blood compared to isoblend alone, whereas an equivalent of 1mg per gram displayed a trend towards an enhanced effect. Combined with the above knowledge, it was concluded that 1mg/g of folic acid would be added to isoblend for administration in murine studies. Studies investigating the anti-depressant potential of folic acid in humans found no safety issues or adverse effects at oral doses of 500μg, 15mg (methyltetrahydrofolate, the active form) and 50mg (methyltetrahydrofolate) (Godfrey *et al.*, 1990; Passeri *et al.*, 1993; Coppen and Bailey, 2000). This provides evidence for the safety of 1mg/g folic acid addition; indeed Canadian recommendations for folic acid intake in those with no health risks planning a pregnancy is daily supplementation with 0.4-1mg (Wilson *et al.*, 2007). Upon proposed isoblend doses of 1-2g, therefore, this addition of folic acid is likely safe.

The murine model of arterial thrombosis, described originally by Falati *et al.* (2002), measures the accumulation of fluorescently labelled platelets in a developing thrombus after injury to an arteriole of the cremaster muscle. The principle advantage to this assay compared to others presented in this study so far is its *in vivo* nature; as a result of this it gives an insight into how a compound of interest may affect thrombosis in a whole, living system, with considerations such as blood flow, blood pressure, metabolism etc.

C57BL/6 (C57 Black 6) mice were dosed twice per day, once in the morning (9am) and once in the afternoon (5pm), with 200mg/kg of isoblend containing 0.2mg/kg folic acid, or vehicle (distilled water containing 39mg/kg ascorbic acid, 3mg/kg niacin and 0.2mg/kg folic acid to allow elucidation of the effects of isoquercetin). This gavage was performed for a 48 or 72-hour period prior to initiation of the experiment, with one final dose on the morning of the experiment, 2.5 hours prior to initiation. This dosing regimen (once morning, once afternoon) was chosen to mimic a potential method of human supplemental consumption, and to investigate if repeated 'supplementation' resulted in anti-platelet effects. On the day of the experiment, mice were anesthetised, and the cremaster muscle of the testicle exteriorised. Connective tissue was removed, an incision was made, and the muscle was affixed over a glass slide as a single sheet, hydrated throughout with buffer. Platelets were labelled

with DyLight 649 anti-GPIbα antibody, after which the cremaster arteriole wall was injured using a Micropoint ablation laser unit. Thrombus formation was then observed, with images captured both prior to and after injury using a digital camera; multiple thrombi were formed per mouse. Due to the surgical expertise required for this work, data were obtained with substantial assistance from Dr. Parvathy Sasikumar. Images were then analysed in Slidebook software (version 6), with maximum fluorescence intensity of vehicle and isoblend-treated samples used to compare maximum thrombus size. Median fluorescence of all thrombi were also integrated and displayed as a line graph.

48 hours of isoblend supplementation resulted in a 43% reduction in maximum fluorescence intensity (Figure 5-5A). This is a useful measurement in that it gives the maximum levels of fluorescence reached over the entire assay, and so represents the largest size that the thrombus achieved. The kinetics of thrombus growth are also important, and can be seen in Figure 5-5B, which traces the median integrated fluorescence. Upon injury, the fluorescence in the vehicle sample rises rapidly, reaching a maximum at approximately 160 seconds, after which it gradually declines over the remainder of the 500s experimental period. After isoblend treatment, upon injury, fluorescence initially rises identically to the vehicle sample, but growth is not sustained, and fluorescence does not reach levels near that of vehicle-treated samples, remaining relatively low over the 500s time period. Although initial growth rates are similar, the thrombi quickly become unstable and break down and embolise; this instability is evident in the videos of the experiments, in which platelets in isoquercetin-treated thrombi consistently slough off and the thrombi cannot grow properly. This is reflected in Figure 5-5C, which displays representative images from the experiment. Pre-injury, no fluorescence can be seen. 30 seconds post injury, a thrombus has started to develop; in the vehicle sample this grows brighter and larger up to approximately 160 seconds as more platelets are incorporated. In the isoblend-treated samples, however, thrombi do not grow to this degree, with very little growth beyond the level seen at 30 seconds post-injury; instead the thrombus remains small over the time period measured (Figure 5-5C).

72 hours of isoblend supplementation resulted in a 41% reduction in maximum fluorescence intensity, representing a 41% reduction in maximum thrombus size (Figure 5-6A). Figure 5-6B shows that upon injury the median integrated fluorescence reaches its peak value earlier in the isoblend treated sample compared to vehicle, after which the thrombi break down and fluorescence levels reduce. Another smaller peak is observed, after which fluorescence gradually reduces to close to zero in the remaining time. Similar to Figure 5-5B, the vehicle sample here reaches a peak at approximately 170 seconds, after which the size of thrombi declines and fluorescence reduces over the remaining time. Figure 5-6C shows representative images from the experiments. At 30 seconds post-injury, the size of the thrombi are comparable between isoblend and vehicle treated mice (Figure 5-6C). However, after 60 seconds, whilst the vehicle-treated sample thrombus continues to grow, the thrombus in the isoblend treated mice has broken down completely or embolised, starting to form again only after 150 seconds (Figure 5-6C). This increased instability compared to 48-hour isoblend treatment is an interesting observation and could represent an increased effect of isoquercetin after longer supplementation periods. If platelets are inhibited to a greater degree, thrombi may be unstable and more prone to embolisation.

Figure 5-7 compares the effects of 48 and 72-hour isoblend treatment; there is no significant difference in maximum fluorescence intensity between the two. This implies the maximal inhibitory effect was reached by 48-hours; it could be worth experimenting with a 24 hour dosing period to see if effects are seen at this time, and to elucidate the minimal time/dosage with which an inhibitory effect can be seen.

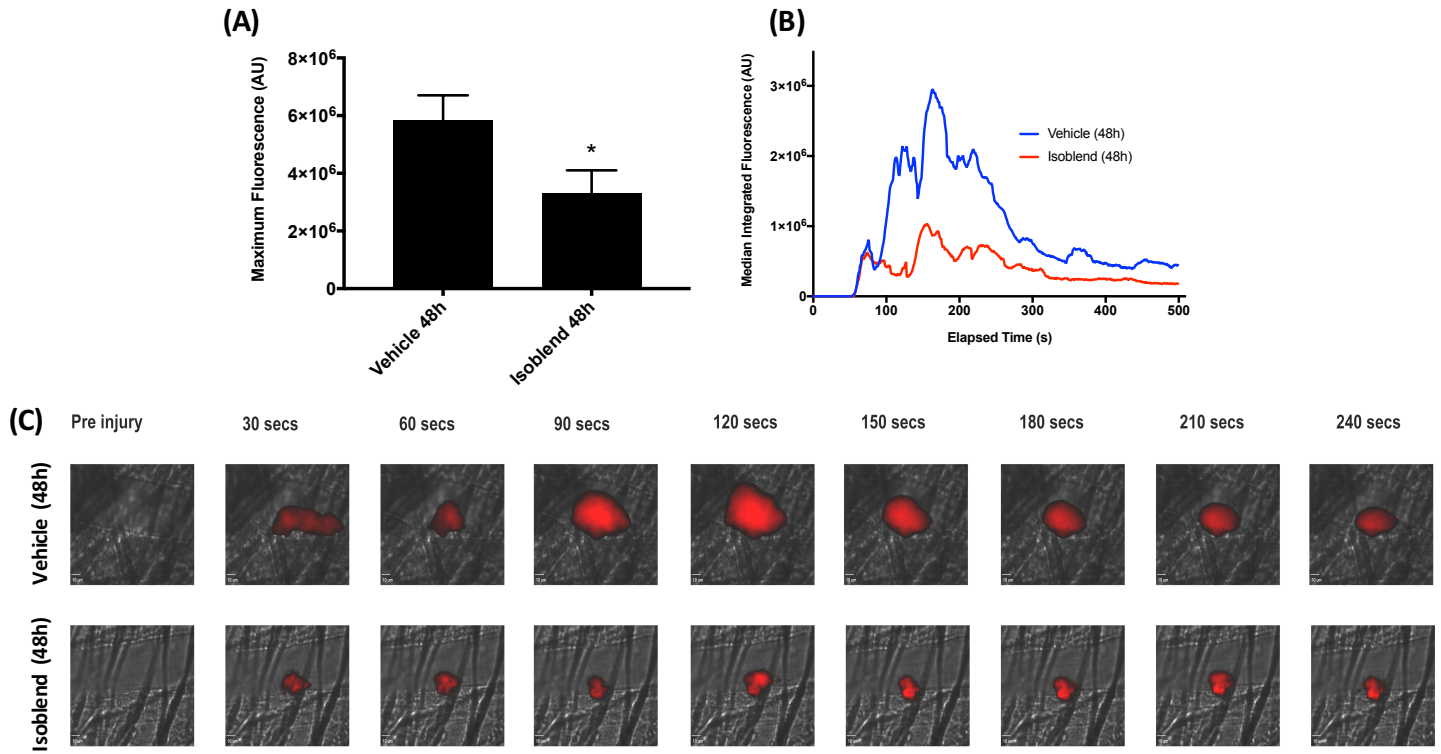

Figure 5-5 Isoblend inhibits laser-induced arterial thrombosis in mice after a 48-hour administration regime

C57BL/6 mice were dosed twice per day (9am and 5pm) with isoblend (200mg/kg containing 0.2mg/kg folic acid) or vehicle (distilled water, 39mg/kg ascorbic acid, 3mg/kg niacin, 0.2mg/kg folic acid) by gavage for 48 hours prior to the experiment, with one final dose administered on the morning of the experiment. 2.5 hours after the final dose, mice were anaesthetised by intraperitoneal injection of ketamine (125mg/kg), xylazine (12.5mg/kg) and atropine (0.25mg/kg), and anaesthesia was maintained with 5mg/kg pentobarbital through a carotid artery cannula as required. Platelets were labelled with DyLight 649 anti-GPIbα antibody and the cremaster muscle was exteriorised and affixed over a glass slide. Laser injury of a cremaster muscle arteriole wall was performed with a Micropoint ablation laser unit, and thrombus formation was observed using an Olympus BX61W1 microscope. Fluorescence and brightfield images were captured prior to and after injury with a Hamamatsu C9300 digital camera, and images were analysed to calculate fluorescence intensity of thrombi using Slidebook software (version 6). Maximum fluorescence of samples reached over the assay (A). Median integrated fluorescence values from all thrombi are shown in (B). Representative images from experiments at different time points are shown in (C); scale bars in bottom left of the images represent 10µm. N=4, with multiple thrombi per mouse. *$p<0.05$ compared to vehicle control, data in (A) represent mean ± SEM, analysed by unpaired t-test.

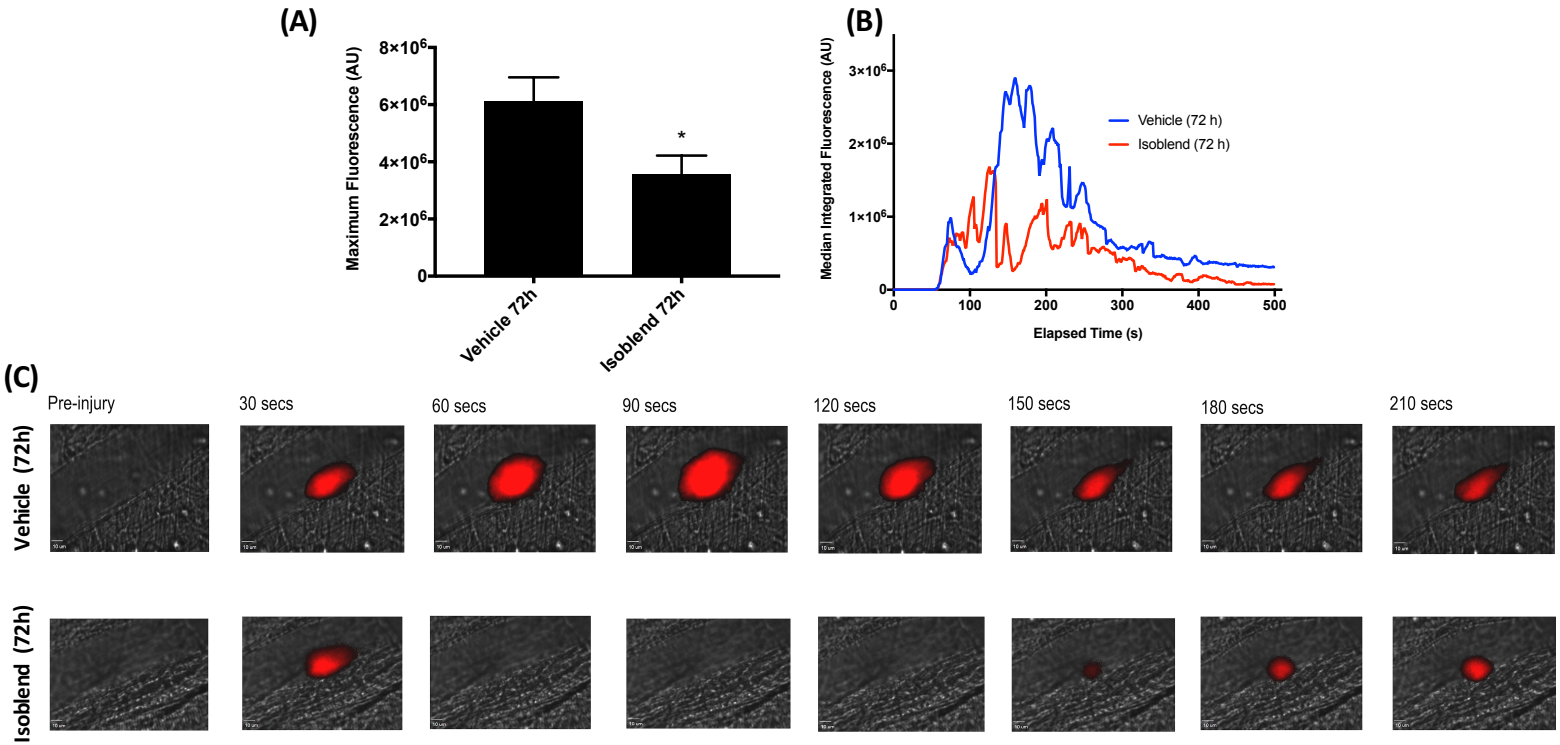

Figure 5-6 Isoblend inhibits laser-induced arterial thrombosis in mice after a 72-hour administration regime

C57BL/6 mice were dosed twice per day (9am and 5pm) with isoblend (200mg/kg containing 0.2mg/kg folic acid) or vehicle (distilled water, 39mg/kg ascorbic acid, 3mg/kg niacin, 0.2mg/kg folic acid) by gavage for 72 hours prior to the experiment, with one final dose administered on the morning of the experiment. 2.5 hours after the final dose, mice were anaesthetised by intraperitoneal injection of ketamine (125mg/kg), xylazine (12.5mg/kg) and atropine (0.25mg/kg), and anaesthesia was maintained with 5mg/kg pentobarbital through a carotid artery cannula as required. Platelets were labelled with DyLight 649 anti-GPIbα antibody and the cremaster muscle was exteriorised and affixed over a glass slide. Laser injury of a cremaster muscle arteriole wall was performed with a Micropoint ablation laser unit, and thrombus formation was observed using an Olympus BX61W1 microscope. Fluorescence and brightfield images were captured prior to and after injury with a Hamamatsu C9300 digital camera, and images were analysed to calculate fluorescence intensity of thrombi using Slidebook software (version 6). Maximum fluorescence of samples reached over the assay (A). Median integrated fluorescence values from all thrombi are shown in (B). Representative images from experiments at different time points are shown in (C); scale bars in bottom left of the images represent 10µm. N=4, with multiple thrombi per mouse. *$p<0.05$ compared to vehicle control, data in (A) represent mean ± SEM, analysed by unpaired t-test.

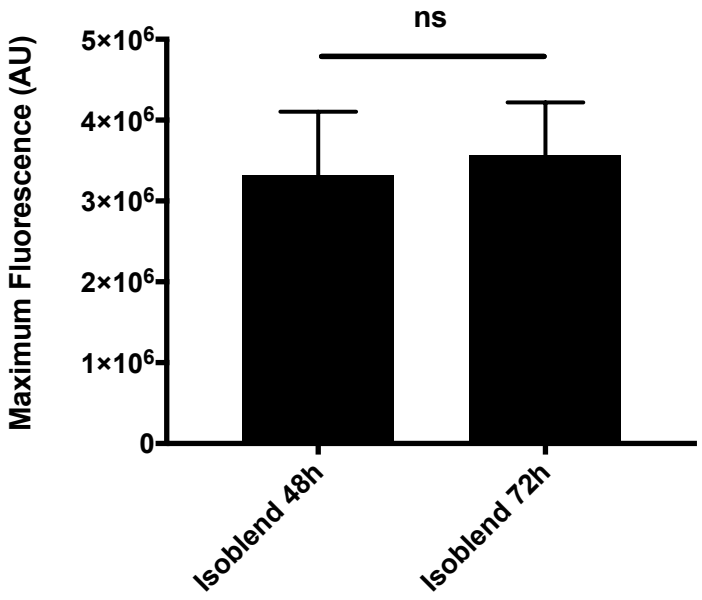

Figure 5-7 Peak inhibition of arterial thrombosis in mice is reached by 48 hours treatment

C57BL/6 mice were dosed twice per day (9am and 5pm) with isoblend (200mg/kg containing 0.2mg/kg folic acid) or vehicle (distilled water, 39mg/kg ascorbic acid, 3mg/kg niacin, 0.2mg/kg folic acid) by gavage for 48 or 72 hours prior to the experiment, with one final dose administered on the morning of the experiment. 2.5 hours after the final dose, mice were anaesthetised by intraperitoneal injection of ketamine (125mg/kg), xylazine (12.5mg/kg) and atropine (0.25mg/kg), and anaesthesia was maintained with 5mg/kg pentobarbital through a carotid artery cannula as required. Platelets were labelled with DyLight 649 anti-GPIbα antibody and the cremaster muscle was exteriorised and affixed over a glass slide. Laser injury of a cremaster muscle arteriole wall was performed with a Micropoint ablation laser unit, and thrombus formation was observed using an Olympus BX61W1 microscope. Fluorescence and brightfield images were captured prior to and after injury with a Hamamatsu C9300 digital camera, and images were analysed to calculate fluorescence intensity of thrombi using Slidebook software (version 6). Maximum fluorescence of samples reached over the assay. N=4, with multiple thrombi per mouse. Data represent mean ± SEM, analysed by unpaired t-test. Ns, not significant.

5.5 Quercetin, its methylated metabolites, and novel quercetin formulations significantly enhance the anti-platelet effect of aspirin in a more-than-additive manner

5.5.1 The effect of aspirin on platelet aggregation stimulated by varying concentrations of collagen

The antiplatelet effect of aspirin (acetylsalicylic acid) has long been recognised, with the proposition that aspirin is protective against coronary thrombosis first put forward by Craven (1950). Low dose aspirin, defined as doses between 75mg and 325mg per day, is now the most commonly used antiplatelet agent worldwide, largely due to its efficacy, low cost and accessibility (Lanas and Scheiman, 2007; Srivastava, 2010). It acts through acetylation of cyclooxygenase (COX), preventing the binding of arachidonic acid to COX and thus irreversibly inhibiting thromboxane formation in the platelet; the use of low dose aspirin allows maintenance of acceptable prostacyclin levels, a platelet inhibitor produced in endothelial cells, also via the actions of COX-1 (Burch *et al.*, 1978; Jaffe and Weksler, 1979; Schrör, 1997). The active form responsible for these antiplatelet effects is acetylsalicylic acid (ASA), with the metabolic product salicylic acid (SA) demonstrating far reduced or absent anti-platelet effects (Nitelius *et al.*, 1984; Rosenkranz *et al.*, 1986). A recent review by Guirguis-Blake *et al.* (2016) concluded that aspirin reduced non-fatal myocardial infarction risk (relative risk 0.78). In a meta-analysis of randomised trials by Baigent *et al.* (2009), aspirin use was associated with a reduction in serious vascular events (12%), non-fatal myocardial infarctions (20%) and total strokes (20%). This beneficial antiplatelet effect of aspirin has, however, been associated with adverse events; in the same meta-analysis by Baigent *et al.* (2009), aspirin use was associated with an increase in major gastrointestinal and extracranial bleeds. This risk of bleeding has also been demonstrated by McQuaid and Laine (2006), who in a meta-analysis found low dose aspirin to increase major bleeding risk by approximately 70%. It may therefore be of benefit to lower aspirin doses to try and prevent some of this bleeding risk.

One way in which this could be achieved is through co-administration of aspirin and flavonoids. Whilst interactions between flavonoids and aspirin have previously been demonstrated, very little has focussed on quercetin specifically, and there has been no investigation into the ability of quercetin's metabolites to interact with the anti-aggregatory effect of aspirin. This is important to elucidate, as the metabolites are the likely 'effectors' that will be acting on platelets in plasma. In this study, it was therefore investigated how quercetin, tamarixetin and isorhamnetin, as well as novel quercetin-based formulations, effect platelet aggregation in the presence of aspirin; this would allow elucidation of any interaction (additive, competitive or synergistic) between quercetin and its metabolites and aspirin in the inhibition of the key process of platelet aggregation.

The first step in this series of experiments was to define the effects of aspirin on collagen-stimulated washed platelet aggregation. Low doses of aspirin solution (75-100mg) result in a maximum plasma acetylsalicylic acid concentration of approximately 7.3μM, whilst analgesic doses between 325 and 600mg result in plasma concentrations of between 25 and 80μM (Seymour and Rawlins, 1982; Charman *et al.*, 1993; Dovizio *et al.*, 2012). Anti-inflammatory doses of 1.2g gave a maximum plasma concentration of approximately 144μM (Seymour and Rawlins, 1982). Maximal acetylsalicylic acid concentration also varies widely between the type of aspirin administered; tablet, chewable tablet, fast release formulations, etc. (Kanani *et al.*, 2015). Thus a concentration range of 5-500μM was chosen to investigate the effects of low concentrations as well as supraphysiological concentrations allowing the elucidation of a full range of effect and any saturation of effects that may occur. A range of collagen concentrations (1-10μg/mL) were used to stimulate platelet aggregation, in order to define the appropriate conditions in which any potential effects of quercetin and its metabolites on the effects of aspirin would not be masked by activation too strong or too weak.

Washed platelets (2×10^8 cells/mL) were incubated with aspirin or vehicle control in a 96 well plate for 60 minutes at 37^{o}C on a stationary heated plate shaker. An incubation period of 60 minutes was chosen for several reasons; firstly, it would allow comparison to the effects of aspirin and flavonoid

combinations in PRP, in which a 60 minute incubation period was chosen to represent the peak plasma concentration time (explained in section 4.3). Secondly, reported times to maximal (T_{max}) plasma acetylsalicylic acid concentrations have been reported between 30 minutes – 4 hours post-ingestion, and so in combination with the peak plasma flavonoid concentrations, a time point of 1 hour was chosen to reflect a T_{max} for aspirin (Sagar and Smyth, 1999; Jung *et al.*, 2013; Moore *et al.*, 2015). After this incubation period, collagen (1-10µg/mL) was added to wells and the plate was shaken at 1200rpm for 5 minutes at 37^{o}C. Absorption of 405nm light was then measured using a plate reader, and values converted to percentage aggregation using unstimulated and stimulated (uninhibited) samples to represent 0% and 100%, respectively.

Aspirin inhibited significantly platelet aggregation stimulated by collagen 1µg/mL between 10-500µM (Figure 5-8). The range of effect was narrow, with 10µM inhibiting aggregation by 56%, and 500µM causing 65% inhibition. These results demonstrate that upon stimulation with this low concentration of agonist, aspirin is able to effectively inhibit platelet aggregation at low concentrations. Upon stimulation with 2.5 and 5µg/mL collagen, there was no significant inhibition of aggregation observed at any concentration of aspirin. There was only significant inhibition of aggregation upon stimulation with 10µg/mL collagen at 500µM aspirin (Figure 5-8). This lack of significant effect may perhaps be explained by large inter-donor variability in response; it is widely recognised that individuals respond quite differently to aspirin, with a predicted 5-65% prevalence of 'aspirin resistance', defined as a reduced (to varying degrees) anti-platelet pharmacological effect upon aspirin consumption (Bhatt, 2004; Maree and Fitzgerald, 2007). Nonetheless, a trend toward reduced inhibition upon stronger agonist stimulation can be observed in Figure 5-8. From these results, it was concluded that collagen 5µg/mL would be used for experiments investigating flavonoid:aspirin combinations, as at this concentration it is likely that the strength of stimulation would not exaggerate or mask any effects. It was also decided that the aspirin concentration range would be altered to 0.5-500µM, as the lowest concentration tested here of 5µM had a relatively large effect.

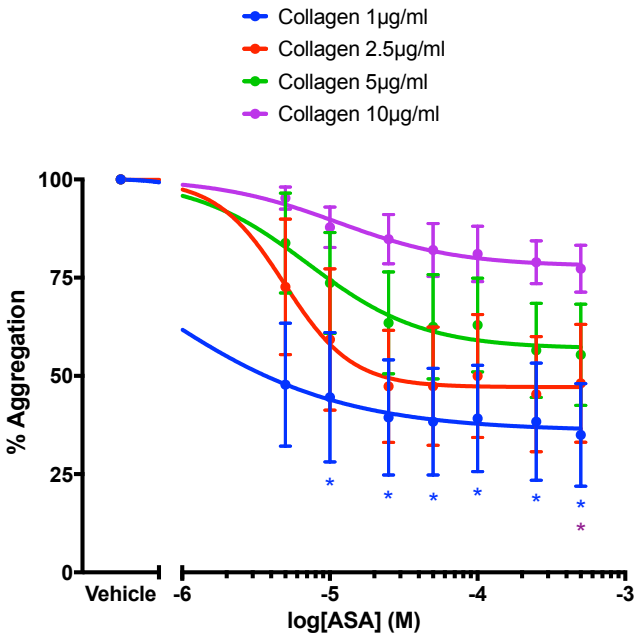

Figure 5-8 The effect of aspirin on collagen-stimulated washed platelet aggregation

Washed platelets (2 x 10^8 cells/mL) were incubated with aspirin or vehicle control (0.25% ethanol, v/v) for 60 minutes at 37ºC on a heated plate shaker. Collagen (1-10µg/mL) was added to wells and the plate was shaken at 1200rpm for 5 minutes at 37ºC. Absorption of 405nm light was then measured on a plate reader, and values converted to percentage aggregation using unstimulated and stimulated (uninhibited) samples to represent 0% and 100%, respectively. Data represent percentage aggregation, normalised to levels of aggregation in the absence of aspirin (vehicle). N=5, data represent mean ± SEM. *$p<0.05$ compared to vehicle control, analysed by one-way ANOVA with post-hoc Dunnett's test. Coloured stars refer to statistical significance against the agonist indicated by the same colour line in the legend.

5.5.2 Quercetin and its methylated metabolites significantly enhance the anti-platelet effect of aspirin in washed platelets

As stated previously, the interaction of quercetin and its methylated metabolites with aspirin in the inhibition of platelet function is unknown. The ability of quercetin, tamarixetin and isorhamnetin at physiologically achievable concentrations of 1-10μM to modify the anti-aggregatory effect of aspirin was therefore investigated. This work would initially be performed in washed platelets to establish the presence or absence of an interaction between the flavonoids and aspirin in a cleaner system in the absence of plasma proteins, with further work focussing on this interaction in whole blood.

Washed platelets (2 x 10^8 cells/mL) were incubated in a 96 well plate with aspirin ± quercetin, aspirin ± tamarixetin, aspirin ± isorhamnetin or vehicle control for 60 minutes at 37^{o}C on a heated plate shaker. Collagen (5μg/mL) was added to wells and the plate was shaken at 1200rpm for 5 minutes at 37^{o}C. Absorption of 405nm light was then measured on a plate reader, and values converted to percentage aggregation using unstimulated and stimulated (uninhibited) samples to represent 0% and 100%, respectively. Data were normalised to levels of aggregation in the absence of flavonoid (vehicle). Four parameter non-linear regression analyses were used to calculate IC_{50} values for each donor and were plotted together.

The blue lines in Figure 5-9 shows the inhibitory effect of aspirin alone on platelet aggregation; as aspirin concentration increases, the inhibition increased, with a significant inhibition at concentrations between 10-500μM. Red lines display the effect of flavonoid plus aspirin on platelet aggregation at the concentration shown in the graph. Blue stars indicate a significant difference between aspirin treatment alone and vehicle control, with black stars indicating a significant difference between aspirin treatment and aspirin plus flavonoid treatment. An “S” indicates a more-than-additive enhancement of inhibition of platelet aggregation upon treatment with flavonoid plus aspirin compared to the sum of effects of aspirin alone and flavonoid alone. In short, an “S” denotes a statistically significantly

greater effect of dual treatment compared to the individual effects of flavonoids and aspirin added together (as opposed to simply an additive effect of including another inhibitor of platelet function). This may be indicative of a synergistic interaction between aspirin and quercetin, tamarixetin and isorhamnetin; however, as described by Jarvis and Thompson (2013), the description of an interaction between two drugs as truly 'synergistic' holds significant analytical complexity, and so further work would be needed to conclude any more-than-additive enhancement as a truly synergistic interaction between the two mechanisms (Tallarida, 2011).

Quercetin plus aspirin treatment resulted in a significantly higher level of inhibition compared to aspirin alone at 2.5, 5 and 10μM quercetin; 1μM quercetin did not cause a significant increase in inhibition (Figure 5-9A-D). A more-than-additive enhancement of anti-platelet effect was observed at 2.5 and 5μM quercetin; dual treatment with 5μM quercetin plus 5μM or 10μM aspirin resulted in a significantly increased inhibitory effect on platelet aggregation compared to the sum of the individual effects of these compounds (Figure 5-C). This is an important observation, considering 5μM quercetin and 5μM aspirin lie within the reported physiological concentrations of both total quercetin and aspirin (upon low-dose treatment) described in previous sections. Indeed, treatment with 2.5μM quercetin and 5μM aspirin resulted in a 35% inhibition in aggregation, more than either 2.5μM quercetin or 5μM aspirin achieved alone (6.5% and 3.5% inhibition, respectively). No more-than-additive effects were observed at 10μM quercetin due to the high level of inhibition achieved by the flavonoid alone at this concentration (Figure 5-9D). Similar results were seen for tamarixetin; no significant effects of flavonoid plus aspirin were observed at 1μM tamarixetin, with more-than-additive effects upon treatment with 2.5μM tamarixetin plus 10μM aspirin and 5μM tamarixetin plus 10μM aspirin (Figure 5-9E-G). Again, levels of inhibition at 10μM tamarixetin were high and so no more than additive enhancement of the effects of aspirin were observed. Combinations of isorhamnetin plus aspirin followed the observed pattern; no significant effects of dual treatment were seen compared to aspirin alone at 1μM isorhamnetin (Figure 5-10A). At 2.5μM and 5μM isorhamnetin, dual treatment resulted in a more-than-additive effect compared to the sum of effects of aspirin alone and isorhamnetin alone

at both 5μM and 10μM aspirin, again lying within reported plasma aspirin concentrations upon low-dose use (Figure 5-10B/C). Treatment with 5μM aspirin alone resulted in 4% inhibition, and 5μM isorhamnetin alone inhibited platelet aggregation by 14%. Combining these two, however, resulted in a 59% reduction in aggregation. At 10μM isorhamnetin alone a high level of inhibition was observed, and so no more-than-additive effects were seen at this concentration (Figure 5-10D).

For each donor, IC_{50} values were calculated for the inhibition of aggregation by aspirin in the presence of all concentrations of quercetin, tamarixetin and isorhamnetin. These values were combined to investigate the ability of quercetin and its methylated metabolites to reduce the IC_{50} of aspirin in the inhibition of aggregation. Quercetin treatment reduced significantly the concentration of aspirin required to achieve 50% inhibition of aggregation at 2.5, 5 and 10μM (Figure 5-11A). The IC_{50} values were 10μM for aspirin alone, and 3.4, 3.1 and 1.1μM upon addition of quercetin at 2.5, 5 and 10μM, respectively. This therefore demonstrates the ability of quercetin at 10μM to reduce to IC_{50} of aspirin in the inhibition of aggregation by a whole order of magnitude. This could be of benefit in reducing aspirin concentrations required for anti-platelet effects in relation to associated issues such as gastric bleeding (although further work would be needed to determine that quercetin and its methylated metabolites themselves do not enhance bleeding). Tamarixetin also reduced significantly the IC_{50} value for the inhibition of platelet aggregation by aspirin at 2.5 and 10μM, with values of 5.4 and 0.5μM respectively, compared to the aspirin only IC_{50} value of 10μM (Figure 5-11B). Isorhamnetin displayed similar potency to quercetin, with 2.5, 5 and 10μM reducing significantly the IC_{50} value of aspirin (Figure 5-11C). Indeed, at 10μM isorhamnetin the IC_{50} value for aspirin was sub-micromolar, at 0.87μM. This demonstrates the ability of quercetin, tamarixetin and isorhamnetin to reduce the IC_{50} value of aspirin in the inhibition of washed platelet aggregation at concentrations as low as 2.5μM, a plasma concentration proven to be physiologically relevant (described in section 3.2). The only significant differences between potency in quercetin, tamarixetin and isorhamnetin was at 5μM, where quercetin and isorhamnetin reduced IC_{50} values for aspirin statistically significantly more than tamarixetin.

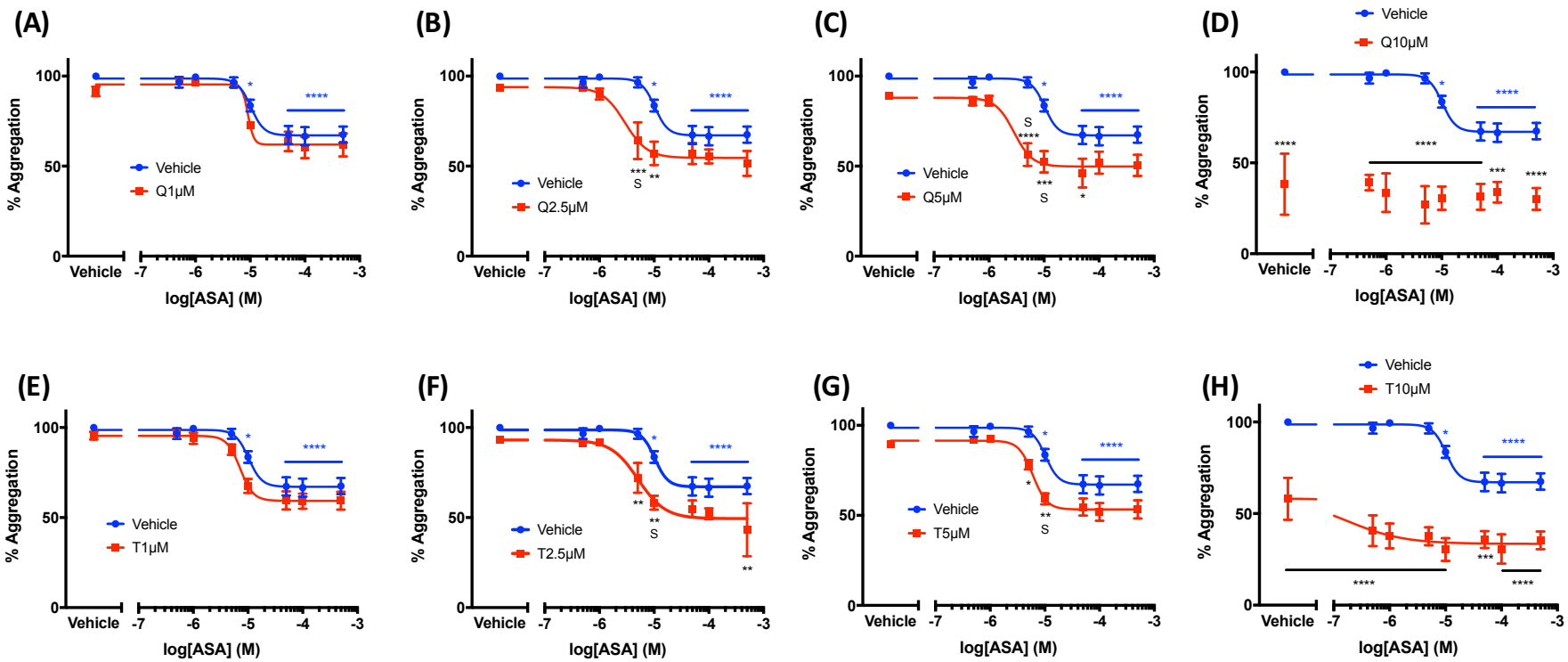

Figure 5-9 Quercetin and tamarixetin interact with aspirin to enhance anti-platelet effects in a more-than-additive manner

Washed platelets (2 x 10^8 cells/mL) were incubated in a 96 well plate with aspirin ± quercetin (A-D), aspirin ± tamarixetin (E-H) or vehicle control (0.25% ethanol + 0.5% DMSO, v/v) for 60 minutes at 37°C on a heated plate shaker. Collagen (5μg/mL) was added to wells and the plate was shaken at 1200rpm for 5 minutes at 37°C. Absorption of 405nm light was then measured on a plate reader, and values converted to percentage aggregation using unstimulated and stimulated (uninhibited) samples to represent 0% and 100%, respectively. Data represent percentage aggregation normalised to levels of aggregation in the absence of flavonoid (vehicle). N=4, data represent mean ± SEM. *p<0.05, **p<0.005, ***p<0.001, ****p<0.0001. Blue stars indicate a significant effect of aspirin compared to vehicle control, analysed by 1-way ANOVA with post-hoc Dunnett's test. Black stars indicate a significant effect of flavonoid plus aspirin compared to aspirin alone, analysed by 2-way ANOVA with post-hoc Dunnett's test. "S" indicates an enhanced effect of dual treatment compared to the combined effects of individual flavonoid and aspirin concentrations (p<0.05), analysed by Mann-Whitney U test. Q, quercetin; T, tamarixetin; ASA, acetylsalicylic acid (aspirin).

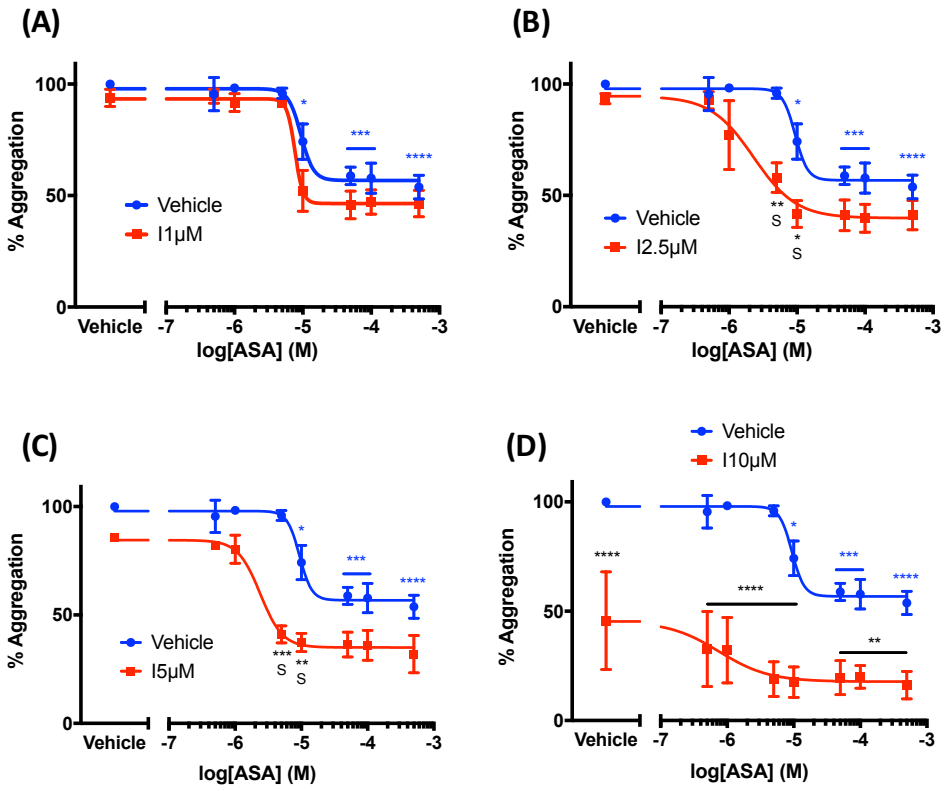

Figure 5-10 Isorhamnetin interacts with aspirin to enhance anti-platelet effects in a more-than-additive manner

Washed platelets (2 x 10^8 cells/mL) were incubated in a 96 well plate with aspirin ± isorhamnetin 1-10μM (A-D) or vehicle control (0.25% ethanol + 0.5% DMSO, v/v) for 60 minutes at 37°C on a heated plate shaker. Collagen (5μg/mL) was added to wells and the plate was shaken at 1200rpm for 5 minutes at 37°C. Absorption of 405nm light was then measured on a plate reader, and values converted to percentage aggregation using unstimulated and stimulated (uninhibited) samples to represent 0% and 100%, respectively. Data represent percentage aggregation normalised to levels of aggregation in the absence of flavonoid (vehicle). N=4, data represent mean ± SEM. *p<0.05, **p<0.005, ***p<0.001, ****p<0.0001. Blue stars indicate a significant effect of aspirin compared to vehicle control, analysed by 1-way ANOVA with post-hoc Dunnett's test. Black stars indicate a significant effect of flavonoid plus aspirin compared to aspirin alone, analysed by 2-way ANOVA with post-hoc Dunnett's test. "S" indicates an enhanced effect of dual treatment compared to the combined effects of individual flavonoid and aspirin concentrations (p<0.05), analysed by Mann-Whitney U test. Q, quercetin; T, tamarixetin; ASA, acetylsalicylic acid (aspirin).

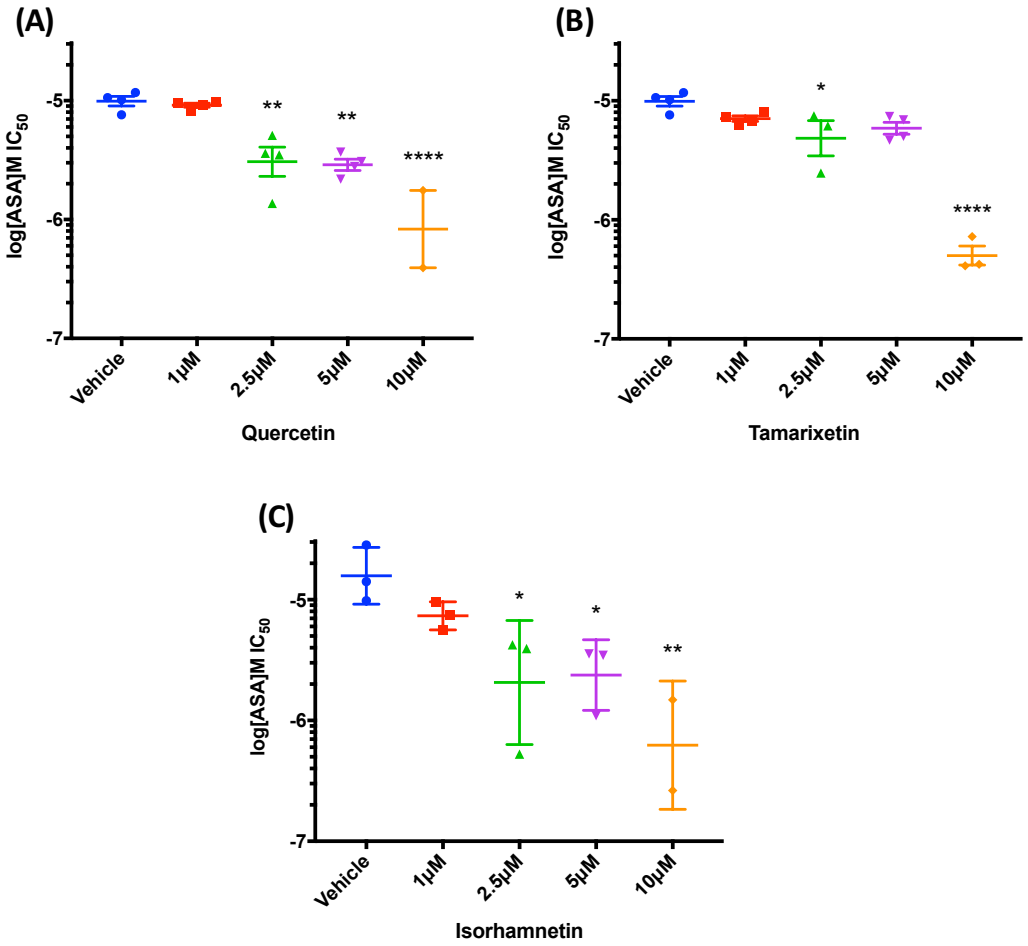

Figure 5-11 Quercetin, tamarixetin and isorhamnetin reduce significantly the IC_{50} of aspirin in the inhibition of collagen-stimulated washed platelet aggregation

Washed platelets (2 x 10^8 cells/mL) were incubated in a 96 well plate with aspirin ± quercetin (A), aspirin ± tamarixetin (B), aspirin ± isorhamnetin (C) or vehicle control (0.25% ethanol + 0.5% DMSO, v/v) for 60 minutes at 37°C on a heated plate shaker. Collagen (5µg/mL) was added to wells and the plate was shaken at 1200rpm for 5 minutes at 37°C. Absorption of 405nm light was then measured on a plate reader, and values converted to percentage aggregation using unstimulated and stimulated (uninhibited) samples to represent 0% and 100%, respectively. IC_{50} values for aspirin for individual donors were then calculated using four parameter non-linear regression analyses and plotted together. N=4, data represent mean ± SEM. *p<0.05, **p<0.005, ****p<0.0001 compared to vehicle control (i.e. aspirin-treatment only, no flavonoid), analysed by one-way ANOVA with post-hoc Dunnett's test.

5.5.3 Novel quercetin-aglycone based formulations significantly enhance the anti-platelet effect of aspirin in washed platelets in a more-than-additive manner

Since quercetin aglycone and its methylated metabolites were established to enhance the anti-platelet effects of aspirin in a more-than-additive manner, the effect of novel quercetin aglycone and isoquercetin-based formulations (Table 5-1) to interact with aspirin's anti-aggregatory effect were investigated. Again, concentrations of 1-10μM were used to reflect a physiologically attainable plasma quercetin concentration.

Washed platelets (2 x 10^8 cells/mL) were incubated in a 96 well plate with aspirin ± QU995, aspirin ± QB3C, aspirin ± isoquercetin, aspirin ± isoblend or vehicle control for 60 minutes at 37^{o}C on a heated plate shaker. Collagen (5μg/mL) was added to wells and the plate was shaken at 1200rpm for 5 minutes at 37^{o}C. Absorption of 405nm light was then measured on a plate reader, and values converted to percentage aggregation using unstimulated and stimulated (uninhibited) samples to represent 0% and 100%, respectively. Data were normalised to levels of aggregation in the absence of flavonoid (vehicle). Four parameter non-linear regression analyses were used to calculate IC_{50} values for each donor and were plotted together.

Similar to quercetin aglycone, QU995 and QB3C at 1μM displayed no more-than-additive effects with aspirin (Figure 5-12A/E). However, at 1μM QU995 and 10μM aspirin, there was significantly more inhibition than with aspirin alone, implying concentrations as low as 1μM of QU995 may enhance anti-platelet effect. Treatment with 2.5μM QU995, like tamarixetin and isorhamnetin, resulted in a more-than-additive enhancement of anti-platelet effect at an aspirin concentration of 10μM, and 5μM QU995 interacted with 5μM aspirin in a more than additive manner to dramatically enhance anti-aggregatory effects from 4% inhibition of aggregation with aspirin alone (and 26% inhibition with QU995 alone) to 62% inhibition upon treatment with both aspirin and QU995 (Figure 5-12B/C). There was no-more-than additive enhancement between QB3C 2.5μM and aspirin, but at 5μM QB3C such

an effect with aspirin was observed at 10μM ASA plus (Figure 5-12F/G). Unlike quercetin and its methylated metabolites, a more-than-additive enhancement of effect of QU995 and QB3C at 10μM and aspirin was observed; this was likely due to the low inhibitory effect of 10μM QB3C alone (Figure 5-12D/H).

Unlike QU995 and QB3C, isoquercetin-based formulations did not interact with aspirin to enhance anti-platelet effect in a more-than-additive manner. Isoquercetin treatment did result in an increased effect compared to aspirin alone (at varying aspirin concentrations) across all isoquercetin concentrations tested (Figure 5-13A-D); however, these interactions were merely additive, not more-than-additive (potentially indicative of synergy) as observed for QU995 and QB3C. This is an interesting observation considering that no concentration of isoquercetin alone inhibited platelet aggregation (indeed isoquercetin did not inhibit platelet aggregation up to 50μM, Figure 5-1); the ability of isoquercetin to increase significantly the anti-platelet effect of aspirin as low as 1μM (albeit not in a more-than-additive manner) is therefore important to note, implying interactions may occur even at very low concentrations of isoquercetin (Figure 5-13A). The magnitude of effect compared to quercetin and its methylated metabolites, and to quercetin aglycone-based formulations is, however, small. For example, treatment with 10μM aspirin resulted in 2.3% inhibition, and 5μM isoquercetin inhibited aggregation by 10%; the combined effect was only 20% inhibition (Figure 5-13C). Isoblend did not interact with aspirin, and did not enhance the anti-platelet effect at all, with no significant differences between aspirin alone and aspirin plus isoblend at any concentrations (Figure 5-13E-H).

QU995 treatment reduced significantly the concentration of aspirin required to achieve 50% inhibition of aggregation at 5 and 10μM (Figure 5-14). IC_{50} values reduced from 17.4μM in aspirin-only treated samples to 4.1μM and 0.7μM upon addition of QU995 at 5μM and 10μM, respectively (Figure 5-14A). Addition of QB3C only at 10μM lowered the IC_{50} for the inhibition of aggregation by aspirin, from 21μM to 0.8μM (Figure 5-14B). There were no significant differences between the IC_{50} values of aspirin in the inhibition of aggregation upon additional treatment with QU995 compared to QB3C

at 5 and 10μM, and no significant differences between the IC_{50} values of aspirin upon additional treatment of QU995 and QB3C compared to quercetin, tamarixetin or isorhamnetin (with the exception of quercetin aglycone reducing slightly the IC_{50} value more than QU995 at 5μM (with aspirin IC_{50} values of 2.9μM and 4μM for quercetin aglycone and QU995, respectively)). Overall, this suggests there are no large differences in potency between QU995, QB3C, quercetin, tamarixetin and isorhamnetin in the reduction of the concentration of aspirin required to achieve 50% inhibition of aggregation.

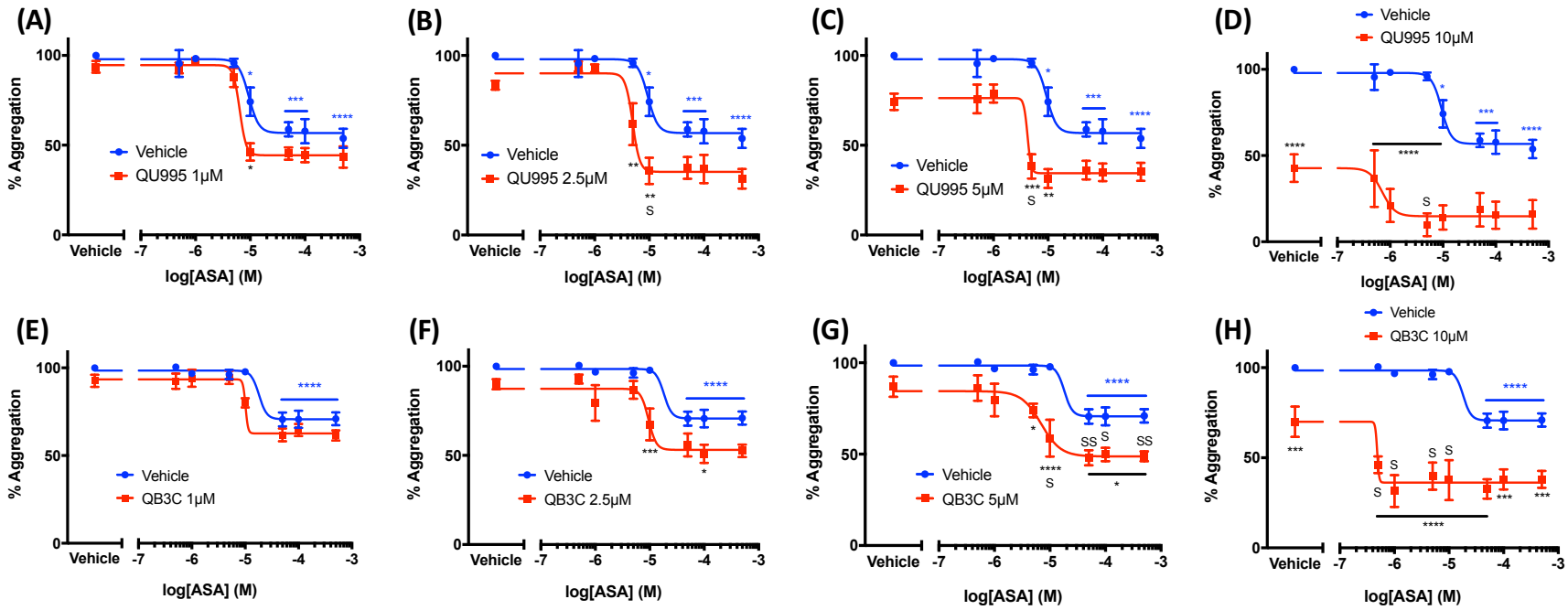

Figure 5-12 Novel quercetin aglycone-based formulations interact with aspirin to enhance anti-platelet effects in a more-than-additive manner

Washed platelets (2 x 10^8 cells/mL) were incubated in a 96-well plate with aspirin ± QU995 (A-D), aspirin ± QB3C (E-H) or vehicle control (0.25% ethanol + 0.5% DMSO, v/v) for 60 minutes at 37ºC on a heated plate shaker. Collagen (5μg/mL) was added to wells and the plate was shaken at 1200rpm for 5 minutes at 37ºC. Absorption of 405nm light was then measured on a plate reader, and values converted to percentage aggregation using unstimulated and stimulated (uninhibited) samples to represent 0% and 100%, respectively. Data represent percentage aggregation normalised to levels of aggregation in the absence of flavonoid (vehicle). N=3, data represent mean ± SEM. *p<0.05, **p<0.005, ***p<0.001, ****p<0.0001. Blue stars indicate a significant effect of aspirin compared to vehicle control, analysed by one-way ANOVA with post-hoc Dunnett's test. Black stars indicate a significant effect of flavonoid plus aspirin compared to aspirin alone, analysed by 2-way ANOVA with post-hoc Dunnett's test. "S" indicates an enhanced effect of dual treatment compared to the combined effects of individual flavonoid and aspirin concentrations ("S" p<0.05, "SS" p<0.005), analysed by Mann-Whitney U test. ASA, acetylsalicylic acid (aspirin).

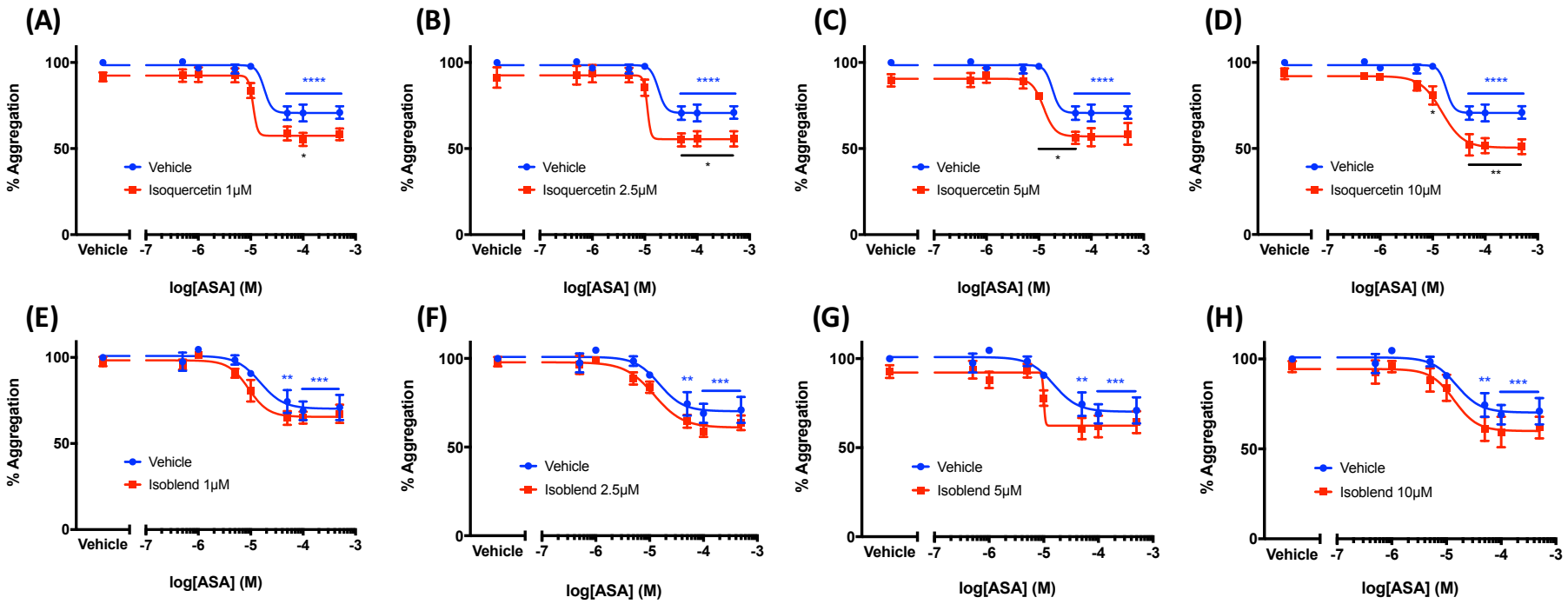

Figure 5-13 Novel isoquercetin-based formulations do not enhance the anti-platelet effects of aspirin in a more-than-additive manner in washed platelets

Washed platelets (2 x 10^8 cells/mL) were incubated in a 96-well plate with aspirin ± isoquercetin (A-D), aspirin ± isoblend (E-H) or vehicle control (0.25% ethanol + 0.5% DMSO, v/v) for 60 minutes at 37°C on a heated plate shaker. Collagen (5μg/mL) was added to wells and the plate was shaken at 1200rpm for 5 minutes at 37°C. Absorption of 405nm light was then measured on a plate reader, and values converted to percentage aggregation using unstimulated and stimulated (uninhibited) samples to represent 0% and 100%, respectively. Data represent percentage aggregation normalised to levels of aggregation in the absence of flavonoid (vehicle). N=3, data represent mean ± SEM. *p<0.05, **p<0.005, ***p<0.001, ****p<0.0001. Blue stars indicate a significant effect of aspirin compared to vehicle control, analysed by one-way ANOVA with post-hoc Dunnett's test. Black stars indicate a significant effect of flavonoid plus aspirin compared to aspirin alone, analysed by 2-way ANOVA with post-hoc Dunnett's test. ASA, acetylsalicylic acid (aspirin).

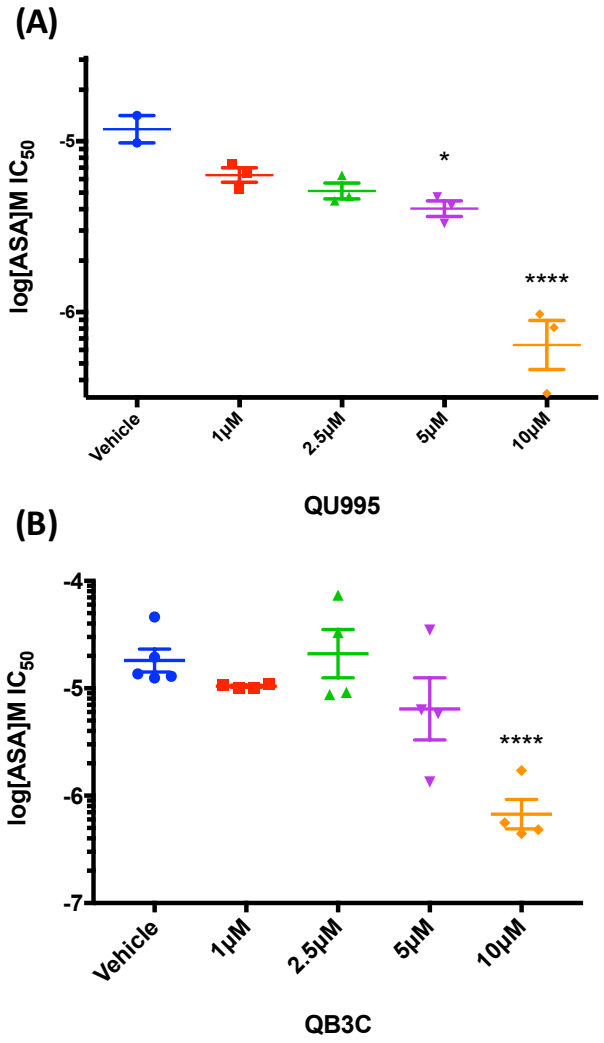

Figure 5-14 Novel quercetin aglycone-based formulations reduce significantly the IC_{50} of aspirin in the inhibition of collagen-stimulated washed platelet aggregation

Washed platelets (2 x 10^8 cells/mL) were incubated in a 96 well plate with aspirin ± QU995 (A), aspirin ± QB3C (B) or vehicle control (0.25% ethanol + 0.5% DMSO, v/v) for 60 minutes at 37°C on a heated plate shaker. Collagen (5μg/mL) was added to wells and the plate was shaken at 1200rpm for 5 minutes at 37°C. Absorption of 405nm light was then measured on a plate reader, and values converted to percentage aggregation using unstimulated and stimulated (uninhibited) samples to represent 0% and 100%, respectively. IC_{50} values for aspirin for individual donors were then calculated using four parameter non-linear regression analysis and plotted together. N=3, data represent mean ± SEM. *$p<0.05$, ****$p<0.0001$ compared to vehicle control (i.e. aspirin-treatment only, no flavonoid), analysed by one-way ANOVA with post-hoc Dunnett's test.

5.6 Quercetin enhances the anti-platelet effect of aspirin in a more-than-additive manner to prolong closure time in a platelet function analyser (PFA)-100 collagen/ADP platelet function test

This study has so far demonstrated more-than-additive interactions between quercetin and its methylated metabolites and aspirin in the inhibition of platelet aggregation in washed platelets. It was next investigated whether these interactions were maintained in a whole blood system, with the presence of interfering factors such as plasma proteins, which flavonoids bind to heavily (discussed in section 4.1). Due to the high number of samples required, utilising the *in vitro* thrombus formation under flow assay was not practical; instead platelet function in whole blood was here tested using a Platelet Function Analyser (PFA)-100 instrument, first described by Kundu *et al.* (1995). A widely used clinical tool for measuring platelet dysfunction, the PFA-100 simulates primary haemostasis by drawing anticoagulated blood through an aperture cut into a membrane coated with either collagen plus ADP (CADP) or collagen plus epinephrine (CEPI), contained within a disposable cartridge. The read-out is a 'closure time' (CT); that is, the time taken for the platelets to aggregate and block the aperture. A clear advantage of this methodology is its wide clinical use, with evidence for applications in screening for platelet disorders such as von Willebrand disorder, assessing primary haemostasis pre-surgery, and investigating sensitivity to, and monitoring of, anti-platelet medications such as aspirin (Favaloro, 2002; Franchini, 2005; Favaloro, 2008).

The platelet function analyser utilises whole blood, and so a flavonoid concentration of 10μM was used to reflect that used in the *in vitro* thrombus formation under flow assay. Preliminary work using the PFA-100 had shown this concentration to be appropriate. An aspirin concentration of 25μM was chosen for use in this assay based on preliminary work which indicated this concentration would allow sufficient elucidation of interactive effects of aspirin plus flavonoids without inhibiting excessively on its own. This preliminary work was done using the CADP cartridges, as aspirin is known to prolong significantly the closure time in the CEPI cartridges to the test limit (300s) but not the CADP cartridges.

Indeed, Chakroun *et al.* (2004) demonstrated that, in patients taking 75-250mg/d aspirin, in those who were 'good responders' to aspirin, closure time of the CEPI cartridge was consistently >300s.

Human citrated whole blood was incubated with quercetin, tamarixetin, isorhamnetin, aspirin, flavonoid-aspirin combinations or vehicle control for 60 minutes at 30^{o}C, after which the blood was added to the cartridge reservoir. Cartridges were loaded into the PFA-100 carousel and samples were then run. Running of samples is an automated process in which samples are assigned an ID, and the carousel is heated to 30^{o}C. Whole blood is then aspirated under vacuum through a capillary and through the aperture in the coated membrane. This aspiration occurs at a shear rate of between 5000-6000s^{-1}. It is important to note that this (unchangeable) shear rate is beyond the physiological arterial shear rate of 500s^{-1} (Glagov *et al.*, 1988; Malek *et al.*, 1999; Papaioannou and Stefanadis, 2005; Chiu and Chien, 2011). Indeed, it lies within reported shear rates of stenosed arteries, and is equal to ranges reported to be pathological (>5000s^{-1}) (Strony *et al.*, 1993; Casa *et al.*, 2015). Nonetheless, in severely stenosed coronary arteries (>75% diameter), Bark and Ku (2010) demonstrated using computational methods that shear rates could reach very high levels from 107,000 – 610,000s^{-1}, and so a shear rate of 5000-6000s^{-1} in this assay is not beyond what is pathologically physiologically relevant. Upon formation of a platelet aggregate that blocks the aperture, this is detected by the apparatus which terminates the assay and reports a closure time (CT). If closure has not occurred by 300s, the assay is terminated and a closure time of '>300' is reported. If this occurred, a value of 300s was reported. This is a limitation, in that high levels of inhibition are grouped into one category and so larger effects may be missed. This is discussed in section 5.7. Novel quercetin formulations were not tested here due to the expense of performing the assay, justified due to earlier observations (Section 5.5) that there is no significant difference between the effects of quercetin and the novel aglycone-based formulations in relation to their interaction with aspirin.

Individual treatment with quercetin, tamarixetin, isorhamnetin (10μM) and aspirin (25μM) did not prolong the closure time of the CADP cartridge (Figure 5-15A). However, dual treatment with quercetin and aspirin resulted in a significant prolongation of closure time, from 126s in vehicle treated

samples to 282s in quercetin plus aspirin treatment. Dual treatment with both aspirin and quercetin also resulted in a more-than-additive effect (282s) compared to individual treatment with quercetin (119s) and aspirin (130s) alone (Figure 5-15A). This more-than-additive enhancement of effect was not seen with dual treatment with tamarixetin plus aspirin or isorhamnetin plus aspirin; indeed these combinations did not significantly prolong closure time compared to vehicle control (Figure 5-15A). There was a trend towards prolongation of closure time, with average CT values of 231s and 233s for tamarixetin plus aspirin and isorhamnetin plus aspirin respectively, compared to the vehicle-treated average of 126s, and average tamarixetin-treated and isorhamnetin-treated closure times of 136s and 121s, respectively (Figure 5-15A). A lack of significance may perhaps be attributed to the large variability seen in this assay; this is a well-known limitation of the PFA-100, discussed in section 5.7. This may have been addressed by repeating the assay, but cost prevented this.

Similar to the CADP cartridges, quercetin, tamarixetin and isorhamnetin did not prolong significantly the closure time of the CEPI cartridge, with average closure times of 194s, 128s and 120s, respectively, compared to an average vehicle-treated CEPI closure time of 133s. Aspirin, however, prolonged the closure time significantly, with an average CT of 266s (Figure 5-15B). This is consistent with previously mentioned observations of highly prolonged CEPI closure times in patients taking aspirin (Chakroun *et al.*, 2004). Upon combination with aspirin, all flavonoids tested prolonged significantly the closure time of the CEPI cartridge (281s, 290s and 293s for quercetin, tamarixetin and isorhamnetin plus aspirin, respectively); however, this is more likely due to the high effect of aspirin than any significant flavonoid effect (i.e dual treatment had little effect beyond that of aspirin alone) (Figure 5-15B). Also due to the substantial effect of aspirin, no more-than-additive interactions between aspirin and flavonoids could be detected for prolongation of closure time in the CEPI cartridge.

Overall, these data provide evidence that quercetin interacts with aspirin in a more-than-additive (potentially synergistic) manner in whole blood to prolong the closure time of CADP cartridges;

further experimental repeats could elucidate whether the trend towards a prolongation in closure time in tamarixetin plus aspirin and isorhamnetin plus aspirin samples is a true effect.

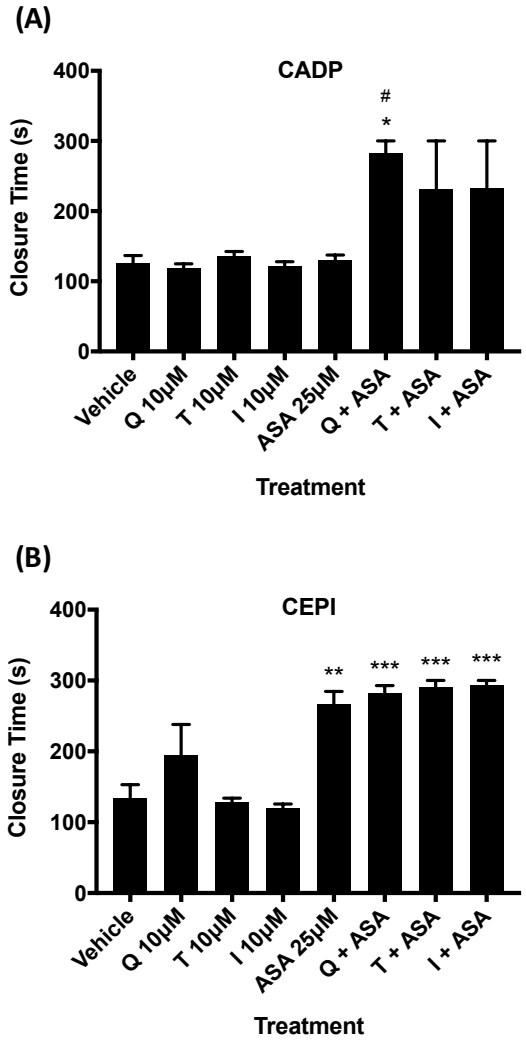

Figure 5-15 Quercetin interacts with aspirin to prolong closure time in a more-than-additive manner in collagen/ADP but not collagen/epinephrine cartridges in a platelet function analyser (PFA)-100

Whole blood was incubated with quercetin ± aspirin, tamarixetin ± aspirin, isorhamnetin ± aspirin, aspirin alone or vehicle control (0.1% DMSO + 0.1% ethanol) for 60 minutes at 30°C. Whole blood was loaded into the reservoir of CADP (A) and CEPI (B) cartridges and and samples were run through the PFA-100 in an automated process in which whole blood was aspirated through a capillary and through the coated membrane at 5000-6000s^{-1}. Upon blockage of the aperture, the assay was automatically terminated and closure time (s) was reported. N=3, data represent mean ± SEM of closure time (s) values. Stars represent a significant prolongation of closure time compared to closure time in the absence of flavonoid or aspirin (vehicle). *$p<0.05$, **$p<0.005$, *$p<0.001$, analysed by one-way ANOVA with post-hoc Dunnett's test. '#' represents an enhanced effect compared to the combined effects of the individual flavonoid and aspirin samples ($p<0.05$), analysed by paired t-test. CADP, collagen plus adenosine diphosphate; CEPI, collagen plus epinephrine; Q, quercetin; T, tamarixetin; I, isorhamnetin; ASA, acetylsalicylic acid (aspirin).

5.7 Discussion of results presented in Chapter 5

The purpose of this chapter was to elucidate the potential anti-platelet effects of novel quercetin formulations both *in vitro* and *in vivo*. This was initially tested through washed platelet aggregometry, and then through *in vitro* thrombus formation under flow assays and a murine laser injury model of arterial thrombosis. The novel quercetin formulations tested were QU995, a 99.5% pure quercetin aglycone, QB3C, a blend of QU995, ascorbic acid and niacin, IQC-950AN (isoquercetin, quercetin-3-O-glucoside), and isoblend (a blend of isoquercetin, ascorbic acid and niacin). Another aim was to investigate the interaction of these novel formulations, as well as quercetin and its methylated metabolites, with the anti-platelet effect of aspirin. This was achieved through use of a 96-well plate-based aggregometry assay, as well as through use of a platelet function analyser (PFA)-100 test.

As the primary function of platelets is to aggregate at the site of vessel injury, the effects of novel quercetin formulations were first tested in an aggregometry assay. They were tested with and without stimulation with collagen (5μg/mL); as these compounds had not been previously tested in platelets, it was important to investigate any effects in both resting and stimulated cells. Upon addition of flavonoid alone, QU995 and QB3C caused a low amount (3.5-7%) of aggregation; although significant, the low magnitude of effect was concluded not to represent an issue. Indeed, upon stimulation with collagen, QU995 and QB3C inhibited platelet aggregation. At 5μM, QU995 was significantly more potent than quercetin aglycone (presented in section 3.2); this may represent an increased potency due to increased purity of QU995. There were no significant differences between the inhibitory potency of QU995 and QB3C; this implies that any enhanced anti-platelet effects seen with the addition of ascorbic acid and niacin (present in QB3C and isoblend, see Table 5-1) are likely to be due to enhanced bioavailability as opposed to a direct anti-platelet effect of these vitamin additions. Isoquercetin-based formulations did not inhibit platelet aggregation up to 50μM. This is hypothesised to be for several reasons; firstly, Jasuja *et al.* (2012) have suggested that flavonoids with a 3-O-glycosidic linkage, as in isoquercetin, have impaired cell permeability. A lack of permeability would prevent isoquercetin

from entering the platelet and interacting with intracellular target enzymes, thus reducing its anti-platelet effect. It must be noted, however, that Wang *et al.* (2014b) have described isoquercetin as 'cell membrane permeable'. However, this was not proven experimentally, and so an investigation into the platelet membrane permeability of isoquercetin would be beneficial. Secondly, isoquercetin displays significantly reduced potency in the inhibition of the key platelet signalling protein phosphatidylinositol 3-kinase (PI3K) compared to quercetin in a kinase activity assay; indeed, 1μM quercetin aglycone inhibited PI3K activity by approximately 55%, whereas isoquercetin 1μM displayed no inhibition at all, with 100 and 70% inhibition of PI3K at 10μM quercetin and isoquercetin, respectively (Kong *et al.*, 2011). Thus, any isoquercetin able to accumulate in the cell may inhibit key protein kinases involved in activation less potently than quercetin aglycone. Experimentation investigating the inhibitory potency of isoquercetin on other key signalling proteins such as Syk and PLC activity and LAT phosphorylation could test this hypothesis.

As novel quercetin-aglycone based formulations inhibited washed platelet aggregation in a similar manner to quercetin, tamarixetin and isorhamnetin, it was hypothesised that they would also affect *in vitro* thrombus formation under flow in a similar way. This would allow an understanding of the effects of novel quercetin formulations on platelets in whole blood, and so the effect of 10μM QU995, QB3C, isoquercetin and isoblend were investigated, to allow direct comparison to the effects of quercetin and its methylated metabolites (presented in section 4.6). None of the novel quercetin formulations inhibited the formation of thrombi. This was expected for isoquercetin and isoblend, due to the aforementioned potential lack of cell permeability and reduced intracellular target enzyme inhibition. It was, however, unexpected for the aglycone-based QU995 and QB3C, as 10μM quercetin aglycone inhibited thrombus formation by 39% (Figure 4-6/7). As mentioned in section 5.2, quercetin aglycone had a significantly higher inhibitory effect on platelet aggregation at 10μM compared to QU995 and QB3C; this could partially explain the above observation but is unlikely to be a full explanation, the reason for which is unclear. As seen in the aggregometry data, addition of vitamins B3 and C did not enhance effects on thrombus formation here; this again implies that any increased

inhibitory effect conferred by their addition to be due to something other than a direct anti-platelet effect (e.g. improved bioavailability).

A lack of effect at 10μM led to the investigation of higher concentrations of novel quercetin formulations on thrombus formation under arterial flow conditions. Concentrations were tested based upon predicted plasma quercetin concentrations upon 200mg/kg supplementation in mice (based on internal communication with Quercegen Pharmaceuticals). This was for two reasons; firstly, higher concentrations used would allow an investigation into the overall feasibility of novel quercetin formulations to inhibit thrombus formation. Secondly, 200mg/kg was the planned dosage for future *in vivo* mouse experimentation, and so use of these concentrations would allow elucidation as to which novel quercetin formulation would be best suited to use in these experiments. This, it was predicted, would provide insight into whether aglycone-based formulations would be more inhibitory due to higher potency but lower bioavailability, or isoquercetin, with lower potency in washed platelets but a higher predicted bioavailability.

At predicted plasma concentrations upon 200mg/kg supplementation, all novel quercetin formulations inhibited significantly the process of thrombus formation under flow *in vitro*. Interestingly, there was no significant difference between the level of inhibition achieved by treatment with QU995 (20μM), QB3C (80μM) and isoquercetin (70μM). A lack of difference in inhibitory effect between QU995 and QB3C despite the widely differing concentrations could imply that a maximum inhibitory effect had been reached; indeed, QU995 and QB3C inhibited thrombus formation by 43% and 42% compared to a 39% effect of quercetin aglycone. This could be further investigated by testing the effects of higher concentrations of QU995 and QB3C, as well as increased concentrations of quercetin aglycone, on thrombus formation under flow *in vitro*.

A similar inhibitory effect between 80μM QB3C and 70μM isoquercetin was also unexpected, as it was hypothesised that, *in vitro*, isoquercetin would prove less potent, as was seen in the platelet

aggregometry data. One reason for the similar potencies of QB3C and isoquercetin may be that the reduced anti-platelet effect of a glucose moiety is balanced by the reduced serum albumin binding. Xiao *et al.* (2009) demonstrated that glycosylation of flavonoids reduced affinity for bovine serum albumin (BSA) by 1-3 orders of magnitude compared to their aglycone, and Liu *et al.* (2014) concluded that isoquercetin has a reduced affinity for BSA compared to quercetin, by an order of magnitude, due to alterations in hydrophobicity and steric hindrance. Isoblend (280μM) inhibited thrombus formation significantly more than QU995, QB3C and isoquercetin, inhibiting by 72% compared to 43% inhibition by isoquercetin. This is likely due to the higher concentration used, but these concentrations reflect predicted plasma concentrations, and so the differences in inhibition are important; it may also reflect an effect of the addition of vitamins B3 and C (although these are also present in QB3C, as described in Table 5-1).

This work allowed the conclusion that at predicted *in vivo* levels, isoblend would be the best novel quercetin formulation to use in planned *in vivo* thrombosis work. Due to the high level of inhibition achieved by isoblend, future work could focus on testing reduced concentrations of this novel formulation. It must be considered from this *in vitro* thrombus formation data, however, that addition of isoquercetin directly to whole blood *in vitro* is likely to result in direct inhibition of protein disulphide isomerase (PDI). Isoquercetin, and other flavonoids with a 3-O-glycosidic linkage, display an inhibitory effect on PDI activity, a thiol isomerase secreted by platelets and endothelial cells upon injury that is important in thrombus formation (Cho *et al.*, 2008; Jasuja *et al.*, 2012; Furie and Flaumenhaft, 2014; Stopa *et al.*, 2017). It has been shown that a glycoside moiety on the C ring, in position 3, results in effective inhibition of PDI activity, with quercetin-3-rutinoside inhibiting PDI by direct binding to its b'X domain, and inhibition of PDI activity also demonstrated by other 3-O-glycosides such as isoquercetin and hyperoside (quercetin-3-galactoside) (Jasuja *et al.*, 2012; Lin *et al.*, 2015). Mechanistically, Stopa *et al.* (2017) have demonstrated that isoquercetin inhibits platelet-dependent thrombin generation through blockade of activation of Factor Va, suggesting another mechanism through which anti-platelet effects may be exerted. *In vivo*, however, it is likely that orally

administered isoquercetin will be deconjugated and metabolised, and will not be found directly in the plasma, as discussed later.

Folic acid at a dose of 1mg folic acid per gram of isoblend was added to the dose given to mice during the *in vivo* study, as Quercegen pharmaceuticals had added this into their formulation. This was based upon communication with Quercegen pharmaceuticals (communication with Thomas Lines, 2016), and was for several reasons. Firstly, folic acid has demonstrated anti-platelet and anti-CVD effects, as well as being inversely associated with risk of CHD (Durand *et al.*, 1996; Bechir *et al.*, 2005; Wang *et al.*, 2012b). Secondly, folic acid has also demonstrated a range of other health benefits, including a decrease in neural tube defects in neonates, and benefits towards mental health such as improvement of depressive symptoms (Taylor *et al.*, 2004; De Wals *et al.*, 2007; Hodgetts *et al.*, 2015). As a supplement, inclusion of folic acid was therefore thought to represent an attractive addition in relation to public uptake of the supplement, on top of the benefits of isoquercetin. This addition was explored further in the present study by testing the effects of folic acid addition in a thrombus formation under flow assay *in vitro*, which demonstrated an enhanced anti-thrombotic effect of isoblend upon addition of 1mg folic acid per gram of isoblend (with no effect upon addition of 100μg/g)(data not shown). This enhancement of effect upon addition of folic acid was a novel observation, and was included in providing evidence for a patent application entitled 'Method for treating thrombotic disorders using quercetin-containing compositions' (US Patent and Trademark Office, App. No 13/272,508). As such, the isoblend used for murine studies contained 1mg folic acid per gram of isoblend.

The ability of isoblend (with added 1mg/g folic acid) to inhibit thrombosis *in vivo* was next investigated. For this, a murine laser injury model of thrombosis was used, which utilises a helium-neon laser to injure an arteriole wall in the mouse cremaster muscle and cause the development of a thrombus. This assay has several benefits, in that it is *in vivo* and so represents a true test of inhibitory potency of isoblend in a whole living organism, subject to all the positive and negative physiological regulatory mechanisms which a developing thrombus is subject to. Another advantage of this assay is

that isoblend was given orally by gavage; this allows for full absorption and metabolism of the flavonoid, and provides a test of the oral bioavailability of this novel quercetin formulation.

A dose of 200mg/kg was given for a 48 and 72-hour period; it was found that thrombosis was inhibited at both these time points, by 43% and 41%, respectively. Whilst the dose given was high, the results demonstrate a clear anti-thrombotic effect of isoblend, and prove for the first time that it is orally bioavailable. The anti-thrombotic effect of isoblend is in agreement with other studies which have displayed *in vivo* anti-thrombotic effects of different quercetin forms. A study by Liang *et al.* (2015) demonstrated the anti-thrombotic effect of pentamethylquercetin, a natural, poly-methylated form of quercetin; an intravenous dose of 20mg/kg improved significantly blood flow after ferric chloride injury, compared to vehicle control. The relatively lower dose used in this study compared to the data presented in this chapter may also provide evidence for the hypothesis that methylation can enhance the anti-platelet effect of quercetin. Indeed, Liang *et al.* (2015) demonstrated that a 20mg/kg pentamethylquercetin demonstrated a similar effect to 50mg/kg aspirin. It must be noted, however, that the method of administration was intravenous, and so the flavonoid was not subject to many of the metabolic changes that occur in the stomach and small intestine. Mosawy *et al.* (2013b) also demonstrated an anti-thrombotic effect of quercetin, with an intravenous bolus of quercetin aglycone (6mg/kg) better maintaining blood flow after ferric chloride injury than vehicle control. Again, the dose used was lower than presented here, but was given intravenously, with the direct infusion of the aglycone intravenously contrasting to the oral gavage of isoblend and associated metabolism and build up of metabolites in plasma presented here warranting a higher dose. Indeed, plasma quercetin levels after oral gavage of isoquercetin could provide an interesting comparison to levels after direct intravenous infusion of aglycone, and could form the basis for future work, in order to determine how plasma quercetin concentrations and metabolite identities compare after different methods of administration, and administration of different forms of quercetin.

Another 3-O glycoside of quercetin, quercetin-3-rutinoside, has also demonstrated anti-thrombotic actions *in vivo*, inhibiting thrombus formation after laser-induced injury after intravenous

administration of 0.1, 0.3 and 0.5mg/kg doses (Jasuja *et al.*, 2012). This conclusion is supported by Lin *et al.* (2015), who demonstrated complete inhibition of thrombus formation after infusion with 10μM quercetin-3-rutinoside. These are interesting results, in that a very high level of inhibition is seen with relatively low doses of quercetin-3-rutinoside. The large effect upon direct intravenous infusion of these 3-O-glycosylated forms imply that inhibition of PDI is a highly effective mechanism through which thrombus formation can be inhibited. Until recently, the mechanisms through which this occurred were largely unknown, and a number of potential mechanisms may be involved. For example, thiol isomerases such as PDI have been shown to bind and regulate the function of integrin $\alpha_{IIb}\beta_3$ and αvβ3 (Holbrook *et al.*, 2012; Mor-Cohen, 2016). A recent study by Bowley *et al.* (2017) has demonstrated that secreted PDI can reduce the disulphide bonds on plasma vitronectin, allowing it to bind integrin $\alpha_{IIb}\beta_3$ and integrin αvβ3. The result of this is the accumulation of vitronectin on the endothelium and in the platelet thrombus, promoting platelet recruitment to the thrombus and generation of fibrin. Bowley *et al.* (2017) demonstrated that inhibition of PDI by intravenous infusion of quercetin-3-rutinoside (0.5mg/kg, again a relatively low dose) prevents this accumulation of vitronectin and prevents the formation of a thrombus following injury. It may therefore be of benefit to investigate the prevention of metabolism (namely the de-glycosylation) of isoquercetin upon oral consumption, as this may result in effective PDI inhibition and a reduction in thrombus formation, more effective that the inhibition seen in the results presented here after metabolism of orally administered isoblend *in vivo*.

Future work should also focus on the identification of the active plasma metabolites upon oral isoquercetin consumption, to identify the *in vivo* 'effectors' upon oral consumption. A dose of 200mg/kg in this study allowed a mechanistic investigation into the feasibility of oral isoblend to inhibit thrombus formation *in vivo*. Having confirmed an inhibitory effect, further work could also focus on reducing the dose and frequency of dosing to find a minimum oral dose and minimal time of dosing that inhibits thrombosis.

The results presented in this study so far have demonstrated a potent anti-platelet effect of quercetin and its methylated metabolites, as well as their ability to inhibit thrombus formation *in vitro*. Novel quercetin formulations have been investigated and one, isoblend, is shown to inhibit thrombosis *in vivo*. These results introduce a key question: how important are these effects from a pharmacological perspective? Namely, what are the pharmacological implications with respect to anti-platelet drugs? It may be that quercetin and its metabolites interact with these agents, and the implications of this should be considered. This was initially investigated by examining the interaction between quercetin and its methylated metabolites, as well as novel quercetin formulations, with aspirin in the inhibition of platelet aggregation. Aspirin was chosen as it is the most widely used anti-platelet agent globally (Lanas and Scheiman, 2007; Srivastava, 2010). Aspirin use, however, is associated with adverse events such as gastric bleeding and intracranial bleeds (McQuaid and Laine, 2006; Baigent *et al.*, 2009). Studies have shown that reducing aspirin dose is beneficial in the prevention of these adverse events, with a reduction from >200mg to 75-100mg reducing adverse events without reducing anti-platelet efficacy (Peters *et al.*, 2003; Serebruany *et al.*, 2005; Huang *et al.*, 2011). However, even low-dose aspirin increases bleeding risk; a recent systematic review by García Rodríguez *et al.* (2016) demonstrated that even doses under 100mg resulted in increased upper gastrointestinal bleeding. Thus, further lowering of aspirin dose could be desirable, and if quercetin and its metabolites are able to interact with aspirin to enhance anti-platelet effect, this could be facilitated.

Quercetin, tamarixetin and isorhamnetin at 2.5 and 5μM interacted with aspirin at 5-10μM to inhibit platelet aggregation significantly more than their combined individual effects (i.e. in a more-than-additive manner). It is important to note that both the flavonoid and aspirin concentrations at which these more than additive effects are seen lie within reported plasma ranges, and therefore these interactions represent a physiologically relevant phenomenon. At concentrations between 1-10μM, quercetin, tamarixetin and isorhamnetin were also able to lower significantly the IC_{50} of aspirin in the inhibition of aggregation; at 10μM, this effect was over an order of magnitude. QU995 and QB3C had a similar effect, and also significantly lowered the IC_{50} values for aspirin at 5 and 10μM (QB3C at

10μM only). There were no significant differences between novel aglycone-based formulations and tamarixetin and isorhamnetin (with only one significant difference between quercetin and QU995), providing further evidence for a lack of difference in potency between quercetin, tamarixetin and isorhamnetin and novel quercetin-aglycone formulations in the inhibition of platelet function. These data therefore provide evidence of the potential for quercetin intake in lowering aspirin dose needed to achieve sufficient anti-platelet effect, and demonstrates for the first time a more-than-additive interaction between aspirin and the methylated metabolites of quercetin. Such interactions could imply a synergy between quercetin, tamarixetin and isorhamnetin and aspirin in the inhibition of platelet function. As discussed in Section 5.5.2, conclusively defining a synergistic interaction is complex, with various drug interaction models potentially used to define such a relationship, and requiring analytical methods such as isobolographic analysis; further work would therefore be needed to conclusively define a synergistic relationship (Tallarida, 2011; Jarvis and Thompson, 2013).

From another perspective, however, these interactions are potentially confounding variables in the current use of anti-platelet agents; one which we may benefit from controlling or at least one to which more attention should be paid, for example in respect to aspirin dosing and monitoring of flavonoid intake to avoid excessive anti-platelet effects and associated adverse effects such as bleeding. For example, a dietary study by Zubair *et al.* (2011) demonstrated that consumption of flavonoid-rich dark chocolate enhanced bleeding time in aspirin-treated volunteers, implying that haemostasis may be compromised if either flavonoid or aspirin levels are too high. The lowering of aspirin doses required upon flavonoid co-administration must therefore be tested further to ensure such events do not occur. From either perspective, it is an important issue to consider.

The interaction between quercetin and aspirin observed here is in agreement with other studies investigating the wider interactions between flavonoids and aspirin. Crescente *et al.* (2009) displayed the ability of a mixture of quercetin, resveratrol and gallic acid to potentiate the anti-aggregatory effect of aspirin, and (Navarro-Nunez *et al.*, 2008) demonstrated synergy between apigenin, a flavonoid structurally similar to quercetin, and aspirin in the inhibition of platelet aggregation. In some

individuals, aspirin does not inhibit the thromboxane A_2 pathway effectively, and Navarro-Nunez *et al.* (2008) suggest combined use of flavonoids and aspirin could be beneficial in this situation (Hankey and Eikelboom, 2006; Schwartz, 2011; Floyd and Ferro, 2014). The data presented in this study provide further evidence for the potential use of this suggestion.

Isoquercetin and isoblend did not interact with aspirin to enhance anti-platelet effect in a more-than-additive manner. This was expected due to the observed lack of inhibition by these formulations in washed platelet aggregation presented in section 5.2, and could be due to reduced cell permeability or lack of target enzyme inhibition discussed previously. However, isoquercetin plus aspirin treatment did display enhanced anti-aggregatory effect compared to aspirin alone, between 1-10μM isoquercetin. Thus even at low concentrations, isoquercetin, which displayed a much reduced potency in washed platelets compared to aglycone-based formulations, can interact with aspirin to increase anti-platelet effect. Although quercetin glucosides are not observed in plasma, these results nonetheless highlight the potential interactions between quercetin and aspirin (Sesink *et al.*, 2001).

The observation of more-than-additive, potentially synergistic effects between quercetin and its metabolites and aspirin in the inhibition of washed platelet aggregation led to the investigation of the potential for these interactions to be maintained in whole blood. This was investigated through a platelet function analyser (PFA) test, and not through *in vitro* thrombus formation under flow, due to the high sample numbers. There was no significant prolongation of closure time in both the CADP and CEPI cartridges after treatment of whole blood with individual flavonoids. This is consistent with data from Hollands *et al.* (2013), who concluded that a mix of quercetin metabolites at concentrations of 5, 20 and 100μM did not significantly prolong closure time in either cartridge type. Results from the CADP cartridges displayed a significant inhibition only upon dual treatment with quercetin plus aspirin, and this effect was more than additive compared to the combined individual effects of quercetin and aspirin alone. There were no such more-than-additive effects in the CEPI cartridge tests; this was due to the high effect of aspirin alone. A lack of significant prolongation of closure time in

the CADP cartridges (although there was a trend towards this) upon dual treatment with tamarixetin/aspirin and isorhamnetin/aspirin could be for several reasons. The high levels of plasma binding associated with the use of whole blood may have had an effect, as may the significantly higher shear rate (5000-6000s^{-1}) compared to the *in vitro* thrombus formation under flow assay (500s^{-1}). Another reason is that the experimental system does not allow for readouts above 300 seconds, and so any prolongation of closure time beyond this is obscured. However, these issues would also have effected quercetin-treated samples too. The sensitivity of this assay to confounding variables must also be considered; it has been shown that a wide range of variables such as blood group, smoking status, diet, age, platelet count and haematocrit can influence test results (Harrison *et al.*, 1999; Bock *et al.*, 1999; Pearson *et al.*, 2002; Hayward *et al.*, 2006; Paniccia *et al.*, 2015). Nonetheless, a more than additive interaction was observed between quercetin and aspirin in the prolongation of closure time, demonstrating that this significant enhancement of the effects of aspirin in the inhibition of platelet function by quercetin can be maintained in whole blood (at a physiologically relevant concentration - 10μM).

In summary, the results presented in this chapter demonstrate, for the first time, anti-platelet effects of novel quercetin formulations. Aglycone-based formulations were more effective than isoquercetin-based formulations in the inhibition of washed platelet function, with minimal differences between novel aglycone-based formulations and quercetin, tamarixetin and isorhamnetin. The addition of ascorbic acid and niacin, designed to enhance bioavailability, did not enhance anti-platelet effect when equal concentrations of flavonoid were used, and so any enhancement of effect *in vivo* is likely due to increased bioavailability. An anti-thrombotic effect of isoblend, a novel formulation containing isoquercetin, a 3-O-glucoside of quercetin, was demonstrated in mice, providing evidence of its oral bioavailability and anti-thrombotic effects after oral administration for the first time; future work will focus on elucidating plasma quercetin concentrations and the active metabolites upon consumption. A more-than-additive interaction between quercetin and its methylated metabolites and aspirin in the inhibition of washed platelet aggregation is also presented, with this potentially synergistic interaction maintained between quercetin and aspirin in a whole blood test of platelet function. This offers insight

into the lowering of aspirin treatment dosage with co-administration of flavonoids to potentially reduce bleeding complications.

Having investigated the anti-platelet effects and mechanisms of quercetin and its metabolites throughout the last three chapters, the next chapter discusses the development of mathematical modelling approaches to understand and predict the anti-platelet effects of quercetin and its methylated metabolites tamarixetin and isorhamnetin, and presents models of *in vitro* platelet aggregation. These approaches were utilised with an aim to describe the platelet activation and aggregation processes *in silico,* allowing the identification and prediction of the mechanisms of platelet inhibition by quercetin and its methylated metabolites, as well as further defining and describing the interactions between them and allowing future predictions of the effects of novel combinations *in silico*.

6 – Mathematical modelling of the effects of quercetin and its methylated metabolites on in vitro *platelet aggregation*

6.1 Mathematical modelling of the effects of quercetin and its methylated metabolites on in vitro *platelet aggregation*

Mathematical modelling of platelet systems alongside traditional laboratory experimentation is an increasingly utilised tool to understand and predict the mechanisms through which platelet function and signalling are regulated. Its use has been demonstrated on many occasions. A study by Dunster *et al.* (2015) used mathematical modelling approaches to predict the importance of the protein phosphatase T-cell ubiquitin ligand-2 (TULA-2) in the regulation of early GPVI signal transduction. On the macroscopic scale, numerous studies have used different approaches to model the development of thrombi and the deposition of platelets within them (Xu *et al.*, 2008; Leiderman and Fogelson, 2011; Xu *et al.*, 2011). As well as enhancing understanding of the normal physiological functioning of platelets, mathematical modelling approaches can also be used to study the effects of pharmacological agents on platelet function; Giaretta *et al.* (2015) modelled the effects of aspirin on the inactivation of platelet cyclo-oxygenase 1, and Yun *et al.* (2014) used mathematical modelling approaches to study the anti-platelet effects of clopidogrel. Several studies have been performed which investigated and modelled the pharmacokinetics of orally ingested quercetin; Graefe *et al.* (2001) investigated the effect of the sugar moiety on pharmacokinetic parameters including maximum plasma concentration (C_{max}) and time to maximal plasma concentration (T_{max}), and Chen *et al.* (2005) investigated and modelled the pharmacokinetics of quercetin aglycone in rats upon different routes of administration. Whilst these studies have provided useful insight into the metabolic fate of quercetin, no studies to date have mathematically modelled the effect of quercetin and its metabolites on platelet function. The aim of this chapter, therefore, was to use mathematical approaches to model the effects of quercetin and its methylated metabolites on *in vitro* platelet aggregation, individually and in combination, with an aim to examine their potential inhibitory synergy (inhibiting platelet function in a more-than-additive manner), as well as allow future *in silico* experimentation predicting the effects of novel quercetin/metabolite combinations and to build a base for the inclusion of further metabolites and pharmacological agents into the model to inform future *in vitro / in vivo* experimentation.

6.2 Mathematical modelling of platelet aggregation – Model A

6.2.1 Description of Model A

An ordinary differential equation (ODE) mathematical model was developed to understand the effects of quercetin and its methylated metabolites on collagen-stimulated platelet aggregation. Collagen was chosen here as it is the agonist which was used in aggregometry experimentation throughout the study, and would allow the mathematical models to be tested against this data. Model A incorporates three platelet populations: 'P_I', representing inactive platelets, 'P_A', representing activated platelets that have not yet been incorporated into an aggregate, and 'P_T', representing platelets that have been incorporated into a platelet aggregate. The P_A population of platelets were defined as activated when the key signalling proteins Spleen tyrosine kinase (Syk) and Linker for Activation of T cells (LAT) were phosphorylated upon stimulation with collagen. Their importance in GPVI signalling is discussed later. Figure 6-1 shows a network diagram describing the events of the model; upon stimulation with collagen, inactive platelets are activated at a rate of k_1. This is assumed to be a reversible reaction (with rate k_2), in that platelets can become inactive after being activated if they do not progress to a fully aggregated phenotype. Activated platelets will then aggregate at a rate of k_3; this is an irreversible reaction. The change over time in the populations of inactive platelets (equation 1.1), active platelets (equation 1.2) and aggregated platelets (equation 1.3) are as follows

$$\frac{dP_I}{dt} = -k_1 P_I + k_2 P_A \,, \qquad (1.1)$$

$$\frac{dP_A}{dt} = k_1 P_I - k_2 P_A - k_3 P_A \,, \qquad (1.2)$$

$$\frac{dP_T}{dt} = k_3 P_A \,, \qquad (1.3)$$

with

$$P_I(0) = P_{I0}, \qquad P_A(0) = 0, \qquad P_T(0) = 0 \qquad (1.4)$$

Initial conditions are displayed in (1.4); an initial inactive platelet density P_{I0} = 1x10^8 platelets per millilitre was chosen to represent the number of platelets used in a standard aggregometry assay, with the output normalised to 100% to allow for comparison to normalised *in vitro* platelet aggregometry data. Table 6-1 describes the variables of the model. The first-order dependence of the aggregation rate on the concentration of activated platelets is considered appropriate in this model, and has been utilised in previous studies; for example, Bell *et. al.* (1989) modelled aggregation using first order kinetics. From a biological perspective, this is also appropriate; a high concentration of activated platelets will result in strong positive feedback signals, and the aggregation of a high number of platelets. As the activated platelet concentration decreases, so will the number of platelets aggregating. This can be seen in light transmission aggregation traces shown in Figures 3-1 and 3-2; aggregation is initially rapid, with the rate slowing as time passes. The assumptions of Model A are: at resting state, all platelets are inactive; the agonist causes full platelet aggregation in the absence of flavonoid; the progression of a platelet from inactive to active is a reversible process and from activated to aggregated is an irreversible process; once flavonoid is introduced, it is available immediately and equally to all platelets, and is uncontaminated, and platelets are in the presence of equal levels of flavonoid throughout the experimental/modelling period. Upon model solving and simulation (using ode45, MATLAB (MathWorks, 2015)), Model A predicts the relative percentage of each population throughout the 300 second experimental period, allowing direct comparison to light transmission aggregometry data performed previously. Throughout the description of this model, the inactive platelet population, 'P_I', is not included in graphs; this population was not fitted to data and held less importance than the profiles of activation and aggregation to which the data was matched and the model was parameterised, describing only the reduction in inactive platelets as they activate and aggregate. Through comparison with experimental data the model was refined and parameterised, as described in Section 6.2.2.

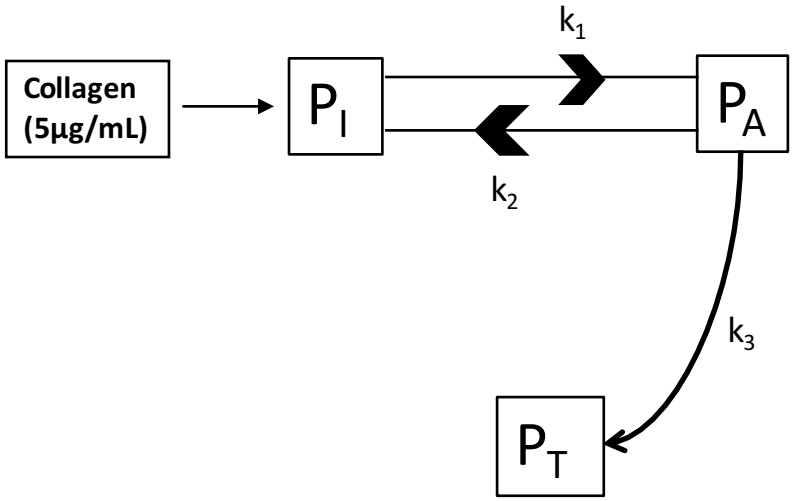

Figure 6-1 A network diagram for platelet aggregation Model A

A network diagram of Model A, with variables represented by square boxes, and the model parameters placed next to the associated arrow. Upon stimulation with collagen (5µg/mL), inactive platelets (P_I) become activated (P_A) in a reversible process. These activated platelets then become incorporated into an aggregate in an irreversible process, and are considered aggregated (P_T). A full description of the variables and parameters are found in Tables 6-1 and 6-2, respectively.

Table 6-1 Model A variables

Variable	Description	Units	Initial condition	Source
P_I	Inactive platelets	Percentage of total platelets	100	Estimated
P_A	Activated platelets	Percentage of total platelets	0	Estimated
P_T	Aggregated platelets	Percentage of total platelets	0	Estimated

6.2.2 Parameter estimation and fitting

The next step in the development of the platelet aggregation Model A was to estimate and fit parameters. These were fitted to the model profile of platelet activation and aggregation in the absence of any flavonoid; that is, in uninhibited collagen-stimulated samples. All three parameters (k_1, k_2 and k_3) were initially arbitrarily set at a value of $5x10^{-2}$ s^{-1}; from this, the parameters were fitted to experimental platelet aggregometry data. This was done by utilising the vehicle-treated samples from the light transmission aggregometry (LTA) data presented in Chapter 3 – these samples represented washed platelet aggregation in the absence of flavonoid. Assuming 100% aggregation at the end of the assay, these aggregation traces were analysed and percentage aggregation at specific time points (0, 26, 39, 52, 78, 104, 195, 300s) calculated in order to compare to the kinetics of aggregation predicted by Model A. The platelet aggregometer used in these *in vitro* experiments outputs optical density, and so a direct relationship between the percentage aggregation calculated from the aggregation traces, and percentage aggregation output by the model simulations is considered appropriate. Parameter fitting here was done by eye, and was considered a best fit when the model predictions matched the data closely and bisected the LTA data points, presented as mean ± standard deviation. Performing this fitting analysis resulted in best fit parameters of $4.5x10^{-2}$ s^{-1} for k_1, k_2 and k_3, with Model A output compared to LTA data in Figure 6-2, and the parameters and their best fit values for Model A described in Table 6-2. An analysis was performed to investigate the sensitivity of the model to changes in parameter values whilst the aggregation profile remained within the in vitro aggregometry data error bars. Changing the value of one parameter at a time in a local sensitivity analysis, these minimum and maximum values are also described in Table 6-2. Alteration of k_1 and k_3 parameters gave an identical effect on the aggregation profile, with differences only in the inactivated and activated populations; the aggregation profile of the model remained within error bars of in vitro data between values of $3.5–5.5x10^{-2}$ s^{-1} for both k_1 and k_3. Alteration of the value of k_2 was found to be less relevant to data fitting, with values between $2.5\text{-}6.5x10^{-2}$ s^{-1} resulting in an aggregation profile within the error bars of the in vitro aggregation data. These are interesting observations and imply that the rate at which platelets are activated from an inactive state and the rate at which platelets aggregate

from an active state are equally contributory and sensitive to the whole aggregatory process, with the rate at which platelets become inactive from an active state being less contributory and therefore less sensitive to change. The next step in the development of Model A was to model the effects of quercetin, tamarixetin and isorhamnetin on platelet aggregation.

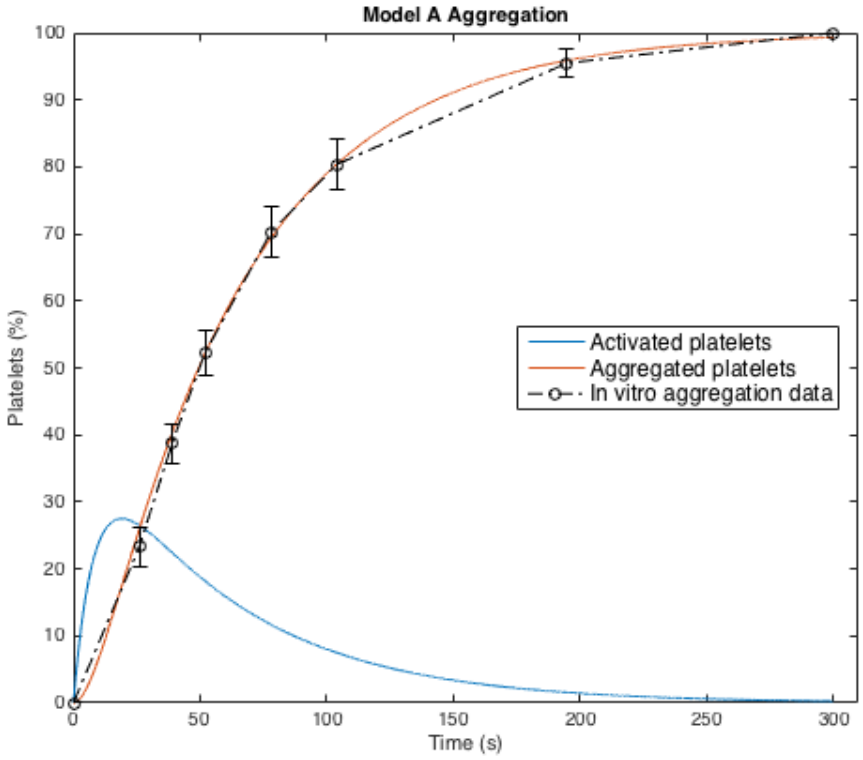

Figure 6-2 Model A aggregation profile compared to *in vitro* collagen-stimulated aggregometry data

The Model A profile of platelet aggregation (solid orange line) compared to experimental *in vitro* collagen (5µg/mL) stimulated platelet aggregometry data (dot-dashed black line with circles). The model accurately describes the kinetics of platelet aggregation across the 300 second experimental period, with the model profile dissecting the error bars of the aggregometry data. *In vitro* aggregation data is presented as mean ± standard deviation, N=9 donors. Model simulations (solid lines) use parameter values described in Table 6-2.

Table 6-2 A summary of Model A parameters. The descriptions, units and values of parameters used in simulations of Model A in the absence of flavonoid.

Parameter	Description	Units	Values		
			Best fit	Minimum fit	Maximum fit
k_1	Rate of platelet activation	s^{-1}	$4.5x10^{-2}$	$3.5x10^{-2}$	$5.5x10^{-2}$
k_2	Rate of platelet inactivation	s^{-1}	$4.5x10^{-2}$	$3.5x10^{-2}$	$5.5x10^{-2}$
k_3	Rate of platelet aggregation	s^{-1}	$4.5x10^{-2}$	$2.5x10^{-2}$	$6.5x10^{-2}$

6.2.3 Modelling the effects of quercetin and its methylated metabolites on platelet aggregation

The next step in the development of Model A was to model the effects of quercetin, tamarixetin and isorhamnetin on platelet activation and aggregation. It is well known that, upon stimulation of platelets through GPVI, quercetin and its metabolites inhibit total tyrosine phosphorylation as well as the tyrosine phosphorylation of key signalling proteins including phospholipase Cγ2, Syk, LAT, and Src-family kinases (Hubbard *et al.*, 2004; Hubbard *et al.*, 2006; Wright *et al.*, 2010b). From the data presented in Chapter 3 it was concluded that quercetin, tamarixetin and isorhamnetin inhibit platelet aggregation. It is therefore unlikely that one component of Model A (activation and aggregation) will be inhibited when another is not, and so in the initial fitting of the effects of flavonoids on platelet aggregation, the values of k_1 and k_3 were modified equally. It is also less biologically plausible that flavonoids would increase the rate of inactivation of activated platelets, instead inhibiting the initial activation or aggregation, and so combined with observation of the reduced relevance of k_2 in the previous section, k_2 remained constant at 4.5×10^{-2} s^{-1} throughout. Through a fit by eye process, k_1 and k_3 values were altered to fit the profile of aggregation seen in the light transmission aggregometry data, at all concentrations of quercetin, tamarixetin and isorhamnetin, using the same methodology of calculating percentage aggregation at specific time points as in Section 6.2.2. The same fitting criteria were used, in that the model aggregation profile must fit within the error bars of the *in vitro* aggregometry data. The values for this fitting process are shown in Table 6-3, with an intermediate flavonoid concentration of 5μM chosen to display graphically the model profiles compared to *in vitro* data (Figure 6-3). One of the key observations is that the k_1 and k_3 values for quercetin are equal to uninhibited samples at 1μM, but much lower than tamarixetin and isorhamnetin at 7.5μM; this reflects the lower and higher levels of inhibition of aggregation seen at these concentrations, respectively when compared to the methylated metabolites. Quercetin-3-glucuronide, which proved significantly less potent in the inhibition of platelet function, was also modelled; parameter values were much higher compared to quercetin and its methylated metabolites (Table 6-3/Figure 6-3D).

Table 6-3 Model A parameter values for the inhibition of platelet aggregation by quercetin, tamarixetin and isorhamnetin. For specific flavonoids and concentrations, the k_1 and k_3 values that simulated a profile of aggregation that matched in vitro aggregation data are presented.

Flavonoid	Concentration (µM)	k_1 value (s^{-1})	k_3 value (s^{-1})
Quercetin	1	$4.5x10^{-2}$	$4.5x10^{-2}$
	5	$2x10^{-2}$	$2x10^{-2}$
	7.5	$2.8x10^{-3}$	$2.8x10^{-3}$
	10	$4x10^{-3}$	$4x10^{-3}$
	20	$4x10^{-3}$	$4x10^{-3}$
Tamarixetin	1	$2.75x10^{-2}$	$2.75x10^{-2}$
	5	$1.85x10^{-2}$	$1.85x10^{-2}$
	7.5	$1.21x10^{-2}$	$1.21x10^{-2}$
	10	$1x10^{-2}$	$1x10^{-2}$
	20	$4x10^{-3}$	$4x10^{-3}$
Isorhamnetin	1	$2.5x10^{-2}$	$2.5x10^{-2}$
	5	$1.5x10^{-2}$	$1.5x10^{-2}$
	7.5	$1.18x10^{-2}$	$1.18x10^{-2}$
	10	$9x10^{-3}$	$9x10^{-3}$
	20	$6.5x10^{-3}$	$6.5x10^{-3}$
Quercetin-3-glucuronide	50	$2.5x10^{-2}$	$2.5x10^{-2}$
	100	$2.3x10^{-2}$	$2.3x10^{-2}$
	150	$1.6x10^{-2}$	$1.6x10^{-2}$
	200	$1.33x10^{-2}$	$1.33x10^{-2}$

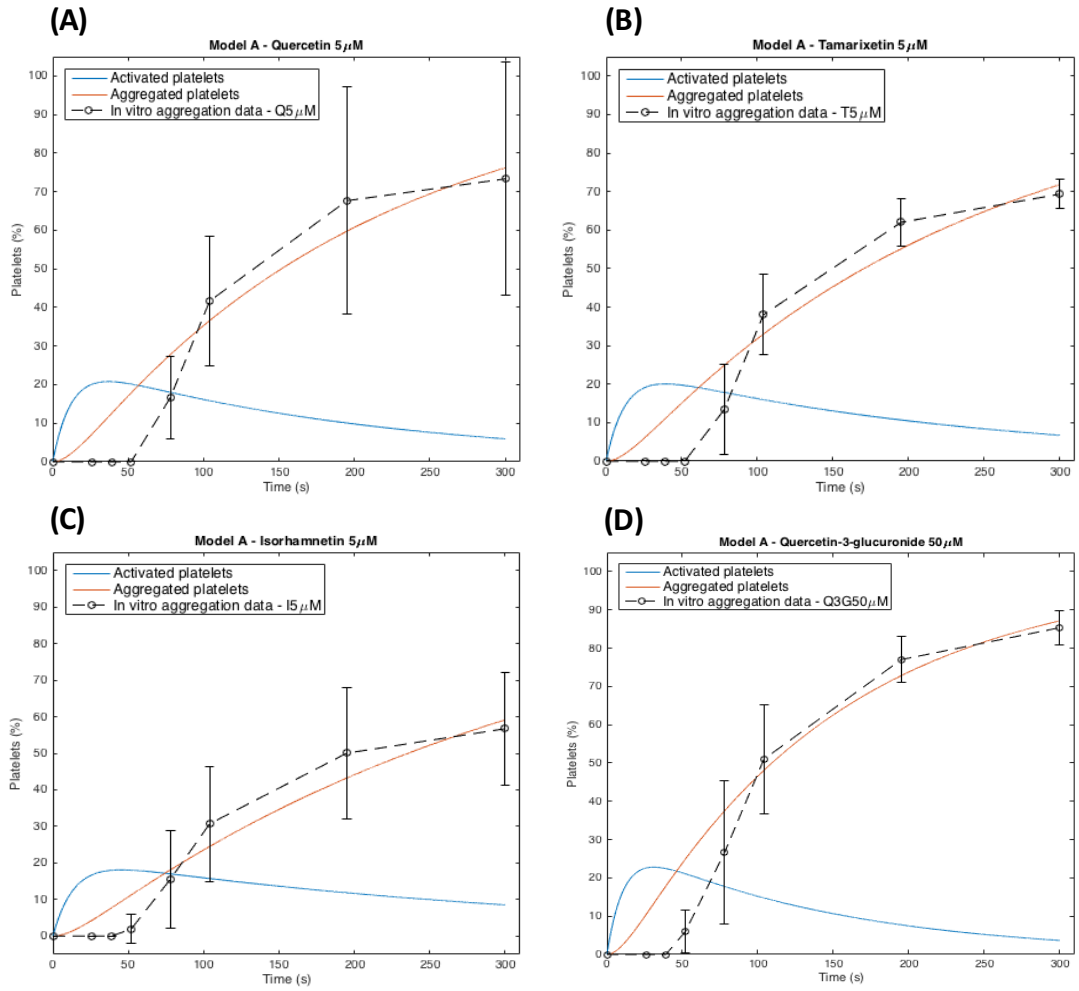

Figure 6-3 Model A aggregation profiles compared to *in vitro* collagen-stimulated aggregometry data inhibited by flavonoids

The Model A profiles of platelet aggregation (solid orange lines) compared to experimental *in vitro* collagen (5μg/mL) stimulated platelet aggregometry data inhibited with quercetin 5μM (A), tamarixetin 5μM (B), isorhamnetin 5μM (C), or quercetin-3-glucuronide 50μM (D) (dashed black lines with circles). The model largely accurately describes the kinetics of platelet aggregation across the 300 second experimental period. *In vitro* aggregation data is presented as mean ± standard deviation, as percentage aggregation normalised to the level of aggregation in the absence of flavonoid (vehicle), N=3 per flavonoid. Model simulations (solid lines) use parameter values described in Table 6-3. Q, Quercetin; T, Tamarixetin; I, Isorhamnetin; Q3G, Quercetin-3-glucuronide.

6.2.4 The effects of quercetin, tamarixetin and isorhamnetin on CRP-XL stimulated platelet signalling

Model A was able to accurately describe the profile of aggregation in vehicle-treated and flavonoid-treated samples, but the activation line was not matched to data. It was therefore investigated how *in vitro* data could match the profile of activation predicted by Model A. As mentioned above, reducing k_1 values resulted in the same profile of aggregation as reducing k_3 by an equal amount, but there was a difference in the activation profiles predicted by these different conditions. An *in vitro* investigation into the rate of activation of platelets upon GPVI-stimulation would therefore allow an elucidation of the rate and extent of platelet activation and the model could then be fitted to this data to understand the relative importance and contribution of k_1 (rate of activation) and k_3 (rate of aggregation) in the platelet aggregatory process and the ways in which these rates are differentially affected upon inhibition by quercetin, tamarixetin and isorhamnetin.

As discussed in Section 3.3.2, P-selectin is a transmembrane adhesion receptor found in α-granules, which upon activation of the platelet, becomes exposed on the cell membrane and functions in leukocyte recruitment (Koedam *et al.*, 1992; Blair and Flaumenhaft, 2009). α-granules are rapidly released upon stimulation of platelets through GPVI; indeed, a study by Jonnalagadda *et al.* (2012) found platelet factor 4 (PF4, a cytokine found in α-granules) was released upon stimulation with convulxin (a GPVI-specific agonist derived from the venom of the Tropical Rattlesnake) within seconds. It was thus investigated whether P-Selectin exposure on the cell surface could be used as an appropriate marker for activation, to be incorporated into Model A. This was investigated through a flow cytometry assay, stimulating platelets with CRP-XL (1μg/mL) and measuring P-Selectin exposure at 5 second intervals from 0-60 seconds, and then every 30 seconds up to 300s. This resulted in increasing P-Selectin exposure levels after every time point, with levels rising, up to 300s (data not shown). Thus, this did not give the transient peak in activation predicted by the model, and so another approach was used.

The phosphorylation of signalling proteins in platelets upon GPVI stimulation is crucial to the propagation of the activatory signal; two such proteins involved in signalling proximal to GPVI are spleen tyrosine kinase (Syk) and linker for activation of T cells (LAT) (Asselin *et al.*, 1997; Pasquet *et al.*, 1999a; Watson *et al.*, 2005; Spalton *et al.*, 2009). Upon stimulation with convulxin or CRP-XL, Syk and LAT are phosphorylated on tyrosine residues; studies by Buitrago *et al.* (2013) and Dunster *et al.* (2015) have shown that this phosphorylation is transient, with a peak in phosphorylation levels between 30-60 seconds and then a reduction in phosphorylation levels as the platelet activation and aggregation process continues. This transient peak led to the hypothesis that phosphorylation of Syk and LAT could be used as a representation of platelet activation to use in Model A, matching the model-predicted rise and transient peak in activation. The temporal profiles of Syk (phosphotyrosines 525+526, in the activation loop of Syk) and LAT (phosphotyrosine 200) phosphorylation following stimulation of washed platelets with CRP-XL (1μg/mL) at time points between 0-300s was therefore investigated, and compared to the activation profile predicted by Model A. Quercetin and its methylated metabolite tamarixetin have been shown to inhibit collagen-stimulated total tyrosine phosphorylation, as well as specifically Syk, PLCγ2 and LAT phosphorylation (Hubbard *et al.*, 2003; Wright *et al.*, 2010b). These studies, however, utilised only one time point, and so in this study the effect of quercetin, tamarixetin and isorhamnetin on Syk and LAT phosphorylation at defined time points between 0-300s was also investigated, to compare to the profiles of activation predicted by Model A upon inhibition by flavonoids.

Washed human platelets (4×10^8 cells/mL) were incubated with quercetin, tamarixetin, isorhamnetin at 7.5μM or vehicle control for 5 minutes at 37^{o}C, prior to addition of collagen-related peptide (cross linked) (CRP-XL, 1μg/mL), with aggregation monitored for 0, 5, 15, 20, 25, 30, 40, 60, 90 or 300 seconds, after which samples were immediately lysed in 6X reducing sample buffer. CRP-XL was used as the agonist here to avoid using the high concentrations of collagen required to achieve an appropriate signal in immunoblotting samples, and the associated increase in flavonoid concentration

that may have to have been utilised. A flavonoid concentration of 7.5μM was chosen here as it represents an intermediate concentration used in the aggregometry assays, and is a concentration at which there was intermediate inhibition of aggregation (for tamarixetin and isorhamnetin). Due to the high number of samples (because of the high-temporal nature of the experiment), only one concentration of each flavonoid could feasibly be tested. Samples were boiled at 95^{o}C for 3 minutes at stored at -20^{o}C until use. On the day of use, samples were again heated to 95^{o}C for 3 minutes, and then separated by SDS-PAGE using 4-20% gradient protein gels for 45 minutes at a constant voltage of 150V. After separation by SDS-PAGE, proteins were transferred onto a PVDF membrane by semi-dry western blotting, performed at 15V for 2 hours. Membranes were removed and blocked with a bovine serum albumin (BSA, 2% w/v) solution for 1 hour at room temperature to prevent non-specific antibody binding, after which primary antibodies diluted 1:1000 in a 2% (w/v) solution of BSA were added to the membranes, which were incubated overnight at 4^{o}C. Primary antibodies were anti-Syk phosphotyrosine 525+526 rabbit polyclonal antibody, anti-LAT phosphotyrosine 200 rabbit monoclonal antibody, or anti-β3 integrin (N-20) goat polyclonal antibody as a loading control. Primary antibodies were removed and membranes washed three times for 10 minutes in TBS-T buffer, and secondary antibodies added in a 1:4000 dilution in a 1% BSA (w/v) solution, incubated for 1 hour in the dark at room temperature. PVDF membranes were washed again in TBS-T buffer (3 x 5 minutes), and were scanned using a Typhoon Trio fluorescence imager, with levels of fluorescence of individual Syk and LAT bands normalised to loading controls.

Upon stimulation with CRP-XL (1μg/mL), both Syk and LAT phosphorylation peaked at 40 seconds. This can be seen in Figure 6-4A and D with phosphorylation in vehicle-treated platelets (blue lines) rising rapidly up to 40s. After this, phosphorylation levels decrease up to 90 seconds in vehicle-treated samples at a similar rate to which they initially rose, and from 90-300 seconds phosphorylation levels remain at a relatively low level. Quercetin inhibited significantly the phosphorylation of Syk between 15-40 seconds, with 74% inhibition of phosphorylation at 15 seconds, and 63% inhibition at 40 seconds. The peak level of phosphorylation was delayed upon quercetin treatment, reaching a peak at

60 seconds, and the peak levels of phosphorylation were reduced significantly (51% reduction) compared to vehicle control (Figure 6-4A). Tamarixetin inhibited significantly the phosphorylation of Syk between 20-40 seconds, with 75% inhibition of phosphorylation at 20 seconds and 64% inhibition at 40 seconds (Figure 6-4B). As with quercetin, the peak phosphorylation was delayed upon tamarixetin treatment compared to vehicle control, with a peak phosphorylation level at 90 seconds (Figure 6-4B). However, there was no significant difference between peak phosphorylation levels of tamarixetin and vehicle-treated samples. Similar to quercetin, isorhamnetin inhibited the phosphorylation of Syk at the earlier time points, and as the vehicle-treated Syk phosphorylation levels declined after the peak, flavonoid-treated phosphorylation levels rose to match these. Isorhamnetin-treated phosphorylation levels were inhibited significantly compared to vehicle control between 20-40 seconds; phosphorylation was inhibited 85% at 20 seconds and 81% at 40 seconds (Figure 6-4C). The peak phosphorylation was also delayed upon isorhamnetin treatment, with peak levels at 90 seconds; this peak phosphorylation was significantly lower than the vehicle peak (53% inhibition), and was at similar levels to the vehicle treated samples' basal levels between 90 and 300s (Figure 6-4C). Representative blot images for Syk Y525+526 phosphorylation are shown in Figure 6-5A,C,E,G.

Quercetin also inhibited the CRP-XL stimulated tyrosine phosphorylation of LAT, in a similar manner to the inhibition of Syk tyrosine phosphorylation; peak phosphorylation was delayed from 40 to 60 seconds. A significant inhibition of phosphorylation was achieved between 25 and 40 seconds, with 91% and 83% inhibition at these time points, respectively (Figure 6-4D). There was no significant different in peak levels of phosphorylation of LAT between vehicle and quercetin, tamarixetin or isorhamnetin; this is likely largely due to the large standard error values in these experiments. Tamarixetin treatment delayed the peak in phosphorylation to 100 seconds, with significant inhibition of LAT phosphorylation between 30 and 40 seconds, with 91% and 89% inhibition, respectively (Figure 6-4E). As seen in Figure 6-4F, isorhamnetin potently inhibited phosphorylation of LAT, with levels remaining below vehicle-treated levels throughout the 300 second experimental period. Indeed, levels of phosphorylation in isorhamnetin-treated samples remained below the basal level seen in vehicle-treated samples between 100-300 seconds. Significant inhibition was achieved between 25

and 40 seconds, with 93% and 91% inhibition at 25s and 40s, respectively (Figure 6-4E). Representative blot images for LAT Y200 phosphorylation are shown in Figure 6-5B,D,F,H (Nb. Due to membrane smudging and slight sample bleeding into adjacent (empty) wells there is a larger gap between molecular weight marker and sample bands in Figure 6-5H; the time labels are, however, in the correct place).

Overall, quercetin, tamarixetin and isorhamnetin effectively inhibited the phosphorylation of Syk and LAT, with the kinetics of phosphorylation displaying a transient peak that could be utilised to inform the development of Model A.

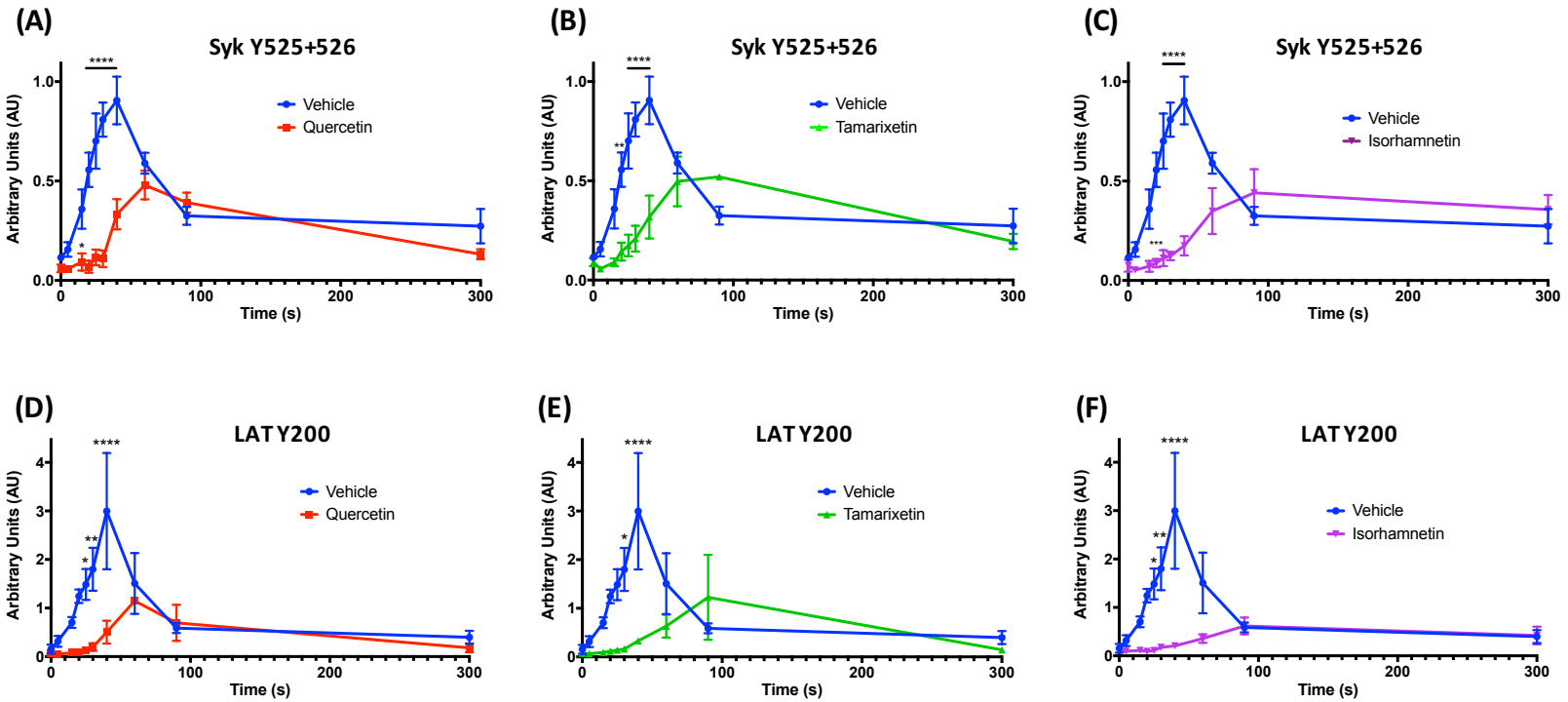

Figure 6-4 Quercetin and its methylated metabolites tamarixetin and isorhamnetin inhibit the phosphorylation of Syk Y525+526 and LAT Y200

Washed human platelets (4 x 10^8 cells/mL) were incubated with quercetin (A/D), tamarixetin (B/E), isorhamnetin (C/F) or vehicle control (DMSO, 0.4% v/v) for 5 minutes at 37°C prior to addition of Collagen-Related Peptide Cross-Linked (CRP-XL, 1µg/mL). Aggregation was allowed to occur for 0, 5, 15, 20, 25, 30, 40, 60, 90 or 300 seconds at 37°C under constant stirring conditions, after which samples immediately were lysed in 6X reducing sample buffer. Proteins were separated by SDS-PAGE for 45 minutes at a constant voltage of 150V, and transferred onto PVDF membranes by semi-dry western blotting for 2 hours at 15V. Membranes were blocked with 2% (w/v) BSA for 1 hour, and incubated overnight with primary antibody; anti-Syk phospho-tyrosine 525+526 rabbit polyclonal antibody (A/B/C), anti-LAT phosphotyrosine 200 rabbit monoclonal antibody (D/E/F), or anti-β3 integrin (N-20) goat polyclonal antibody as a loading control. The PVDF membranes were washed with TBS-T buffer and secondary antibody incubated for 1 hour; Alexa Fluor 647 donkey anti-rabbit polyclonal antibody or Alexa Fluor 488 donkey anti-goat polyclonal antibody. PVDF membranes were again washed with TBS-T buffer and scanned using a Typhoon Trio fluorescence imager. Levels of fluorescence of individual bands were normalised to loading controls. N=3, data represent mean ± SEM. *p<0.05, **p<0.005, ****p<0.0001 compared to vehicle control, analysed by two-way ANOVA with post-hoc Bonferroni correction. Syk, Spleen tyrosine kinase; LAT, Linker for activation of T cells; SDS-PAGE, sodium dodecyl sulphate polyacrylamide gel electrophoresis; PVDF, polyvinylidene fluoride; BSA, bovine serum albumin.

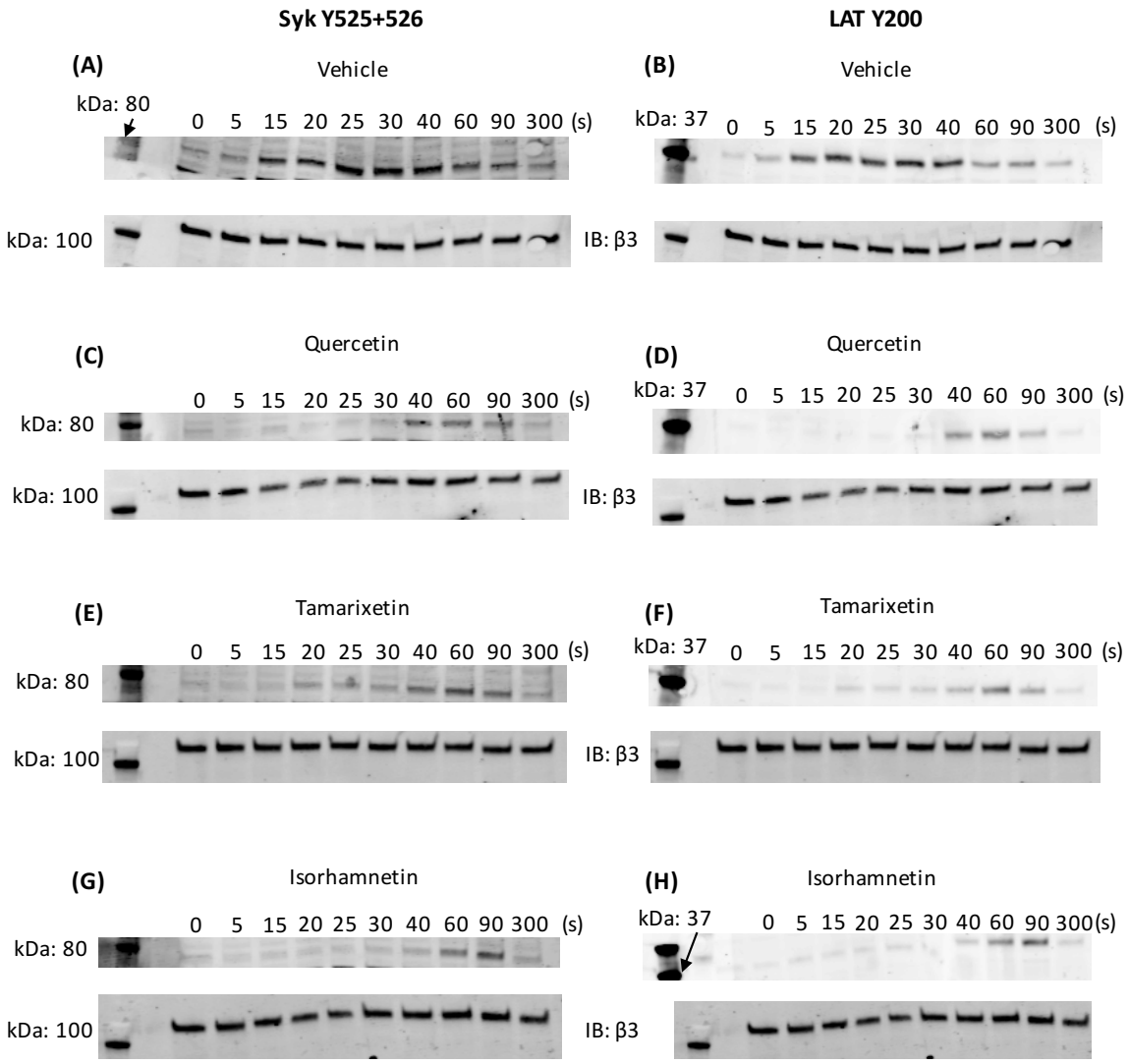

Figure 6-5 Representative blots showing quercetin and its methylated metabolites tamarixetin and isorhamnetin inhibit the phosphorylation of Syk Y525+526 and LAT Y200

Washed human platelets (4 x 10^8 cells/mL) were incubated with quercetin (C/D), tamarixetin (E/F), isorhamnetin (G/H) or vehicle control (DMSO, 0.4% v/v (A/B)) for 5 minutes at 37°C prior to addition of Collagen-Related Peptide Cross-Linked (CRP-XL, 1µg/mL). Aggregation was allowed to occur for 0, 5, 15, 20, 25, 30, 40, 60, 90 or 300 seconds at 37°C under constant stirring conditions, after which samples immediately were lysed in 6X reducing sample buffer. Proteins were separated by SDS-PAGE for 45 minutes at a constant voltage of 150V, and transferred onto PVDF membranes by semi-dry western blotting for 2 hours at 15V. Membranes were blocked with 2% (w/v) BSA for 1 hour, and incubated overnight with primary antibody; anti-Syk phospho-tyrosine 525+526 rabbit polyclonal antibody (A/C/E/G), anti-LAT phosphotyrosine 200 rabbit monoclonal antibody (DB/D/F/H), or anti-β3 integrin (N-20) goat polyclonal antibody as a loading control. The PVDF membranes were washed with TBS-T buffer and secondary antibody incubated for 1 hour; Alexa Fluor 647 donkey anti-rabbit polyclonal antibody or Alexa Fluor 488 donkey anti-goat polyclonal antibody. PVDF membranes were again washed with TBS-T buffer and scanned using a Typhoon Trio fluorescence imager. Levels of fluorescence of individual bands were normalised to loading controls. Syk, Spleen tyrosine kinase; LAT, Linker for activation of T cells; SDS-PAGE, sodium dodecyl sulphate polyacrylamide gel electrophoresis; PVDF, polyvinylidene fluoride; BSA, bovine serum albumin, IB; immunoblot.

6.2.5 Incorporation of Syk and LAT phosphorylation data into Model A

As seen in Figure 6-4, there is a transient peak in phosphorylation of Syk and LAT following stimulation of washed platelets with CRP-XL (1μg/mL), with a peak at 40 seconds followed by a decrease in phosphorylation levels over the remaining period. The profile of platelet activation was therefore fitted to Model A simultaneously with fitting the Model A-predicted profile of aggregation to *in vitro* aggregometry data. This was done for vehicle-treated, as well as quercetin, tamarixetin and isorhamnetin-treated samples, to give a best-fit series of k_1 and k_3 values. This would allow the elucidation of the relative importance of the rate of activation (k_1) and the rate of aggregation (k_3) to the overall platelet activatory process, and their inhibition by quercetin and its methylated metabolites.

Gaining the best fit of the vehicle-treated data by eye gave the profiles of aggregation and activation displayed in Figure 6-6. The profile of aggregation fits very well across all time points, with the model accurately predicting the kinetics of platelet aggregation from 0-300 seconds. The activation profile predicted by the model is initially too fast, with the model profile rising faster than the Syk and LAT phosphorylation data from 0-25 seconds. This is represented by the earlier predicted peak phosphorylation time of 19 seconds compared to 40 seconds shown in the data. From 30 seconds onwards, though, the profile of activation predicted by Model A lies within the error bars of the data. Altering the parameters of the model to slow the rate of activation resulted in no improvement to the model-data fit; instead this slightly earlier predicted activation peak is considered a limitation of Model A. Whilst platelet signalling is a rapid process, the model cannot simulate the complexities of this initial biological cascade, thus predicting a faster rate; this is likely the reason for this discrepancy between model simulation and *in vitro* data. Thus, the best fit parameters in the absence of flavonoids are 4.5×10^{-2} s^{-1} for k_1, k_2 and k_3, as stated in Table 6-4.

The concurrent fitting of flavonoid-inhibited aggregation and activation data allowed the best-fit parameters for flavonoid-treated platelet function in Model A to be elucidated, along with the relative contributions of k_1 (inactive platelets to activated platelets) and k_3 (active platelets to aggregated

platelets) to the overall platelet activatory process, something which is hard to achieve simultaneously in the same *in vitro* platelet assay, which typically either investigate a single measure of activation or aggregation. These parameter outputs from Model A therefore give a useful insight into the way in which flavonoids may be differentially inhibiting the processes involved in platelet function. The fitting of quercetin (7.5μM) treated aggregation and activation data to Model A gives the profiles shown in Figure 6-7A. Due to the high level of inhibition of aggregation seen at this concentration of quercetin (which the model matches well) compared to tamarixetin and isorhamnetin, the profile of activation predicted by the model does not reach the transient peak shown in the data, instead rising to a low level of approximately 6.3% after 100 seconds and remaining above 6% throughout the remaining period. Thus, the model predicts a later peak than the data suggests here. Nonetheless, the model profile of aggregation lies within the error bars of the data at all time points (excluding at 20 seconds). Model profiles obtained from fitting Model A to activation and aggregation upon treatment with tamarixetin (7.5μM) faithfully represent the aggregation data, with the activation profile reaching a peak earlier, at 51 seconds compared to 90s in the data (Figure 6-7B). This is the same as seen in the vehicle-treated samples; delaying the activation peak reduced aggregation to beyond acceptable limits. Much the same is seen when fitting the isorhamnetin data to Model A; aggregation is faithfully represented, and a peak in activation is also observed at 51 seconds, earlier than the 90s peak observed in the data (Figure 6-7C). Similar to vehicle-treated platelets, isorhamnetin-treated platelets display much reduced activation compared to the model at earlier time points, catching up to model predictions at 60 seconds. This is an interesting observation; the model predicts earlier peak activation for tamarixetin and isorhamnetin-treated platelets than the data shows, and later activation for quercetin. This is likely due to the higher levels of aggregation achieved after treatment with the methylated metabolites compared to quercetin aglycone at the concentration used here.

The best fit parameters elucidated above are displayed in Table 6-4, and offer insight into the relative contributions of inhibiting activation and aggregation. Upon quercetin (7.5μM) treatment, both k_1 and k_3 rates are reduced by over an order of magnitude compared to vehicle control. This implies that both

activation and aggregation are strongly affected, which is in agreement with the data presented in this study; indeed at 7.5μM quercetin, aggregation was abolished (Figure 6-7A). The lower k_3 value compared to the k_1 value nevertheless results in the prediction from Model A that, upon quercetin treatment, the aggregation of platelets is inhibited more than their initial activation. This is a novel prediction, the potential testing of which is discussed later in this chapter. Upon tamarixetin or isorhamnetin treatment, the rate of platelet activation (k_1) is also reduced by nearly an order of magnitude, but the rate of aggregation (k_3) is not affected to this degree. This implies that aggregation is much less potently affected upon treatment with 7.5μM tamarixetin or isorhamnetin compared to quercetin, which the data confirms to be true; there is a statistically significant difference between the levels of aggregation achieved when comparing quercetin treatment to either tamarixetin or isorhamnetin treatment at 7.5μM. The similar best fit k_1 rates imply that there may be no significant difference between the rate of platelet activation upon treatment with quercetin or its methylated metabolites; although the data collected was not temporally resolute enough to compare rates, there is no significant difference between the levels of peak phosphorylation upon treatment with quercetin, tamarixetin or isorhamnetin at 7.5μM. The lower k_1 compared to k_3 values for tamarixetin and isorhamnetin treatment is in contrast to quercetin, and predicts that the inhibition of initial platelet activation is more potently affected than the aggregation of platelets by tamarixetin and isorhamnetin. Again, this is a novel prediction, and is discussed later in this chapter.

One limitation of this model is that the flavonoids are not having a 'direct' effect; rather, the rate parameters k_1 and k_3 were changed to represent inhibition by quercetin and its metabolites. Whilst this formed an appropriate starting point, the next step in the development of the aggregation model was to specifically include terms describing the direct inhibition of activation and aggregation by specific concentrations of quercetin and its methylated metabolites themselves; this is presented in the next section.

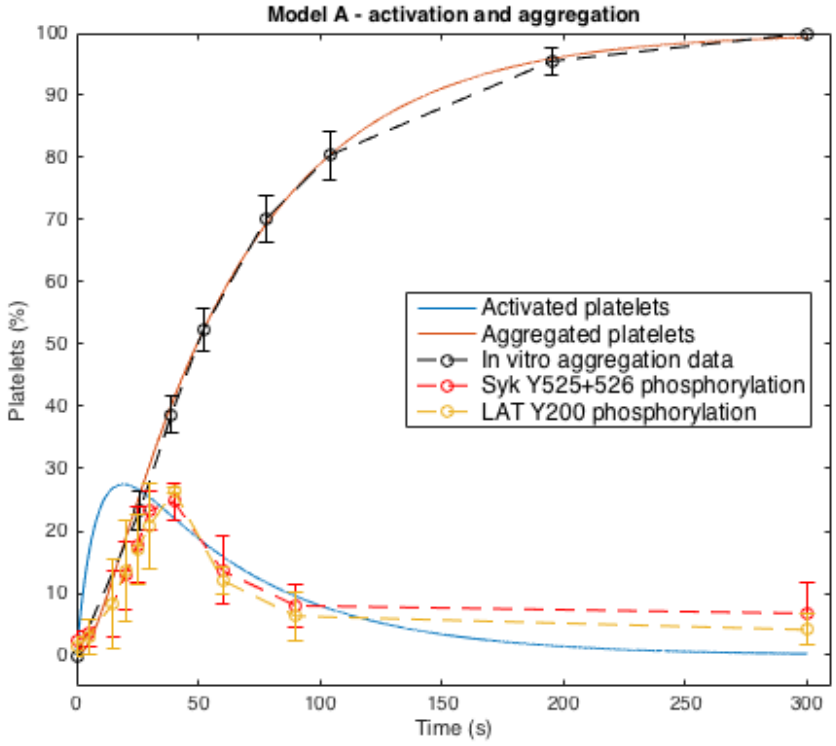

Figure 6-6 Model A aggregation and activation profiles compared to *in vitro* collagen-stimulated aggregometry data and *in vitro* Syk and LAT phosphorylation data

The Model A profile of platelet aggregation (solid orange line) compared to experimental *in vitro* collagen (5µg/mL) stimulated platelet aggregometry data (dashed black line with circles), as well as the Model A profile of activation (solid blue line) compared to *in vitro* CRP-XL (1µg/mL) stimulated Syk tyrosine 525+526 (dashed red line with circles) and LAT tyrosine 200 (dashed yellow line with circles) phosphorylation data. The model accurately describes the kinetics of platelet aggregation, and from 30 seconds onwards also accurately describes the kinetics of platelet activation defined by the protein phosphorylation. Between 5-25 seconds, the model predicts activation at a faster rate – this is a limitation discussed in the text. *In vitro* aggregation data is presented as mean ± standard deviation, N=9. *In vitro* protein phosphorylation data is presented as mean ± standard deviation, N=3. Model simulations (solid lines) use parameter values described in Table 6-4. Syk, Spleen tyrosine kinase; LAT, linker for activation of T cells; Y, tyrosine.

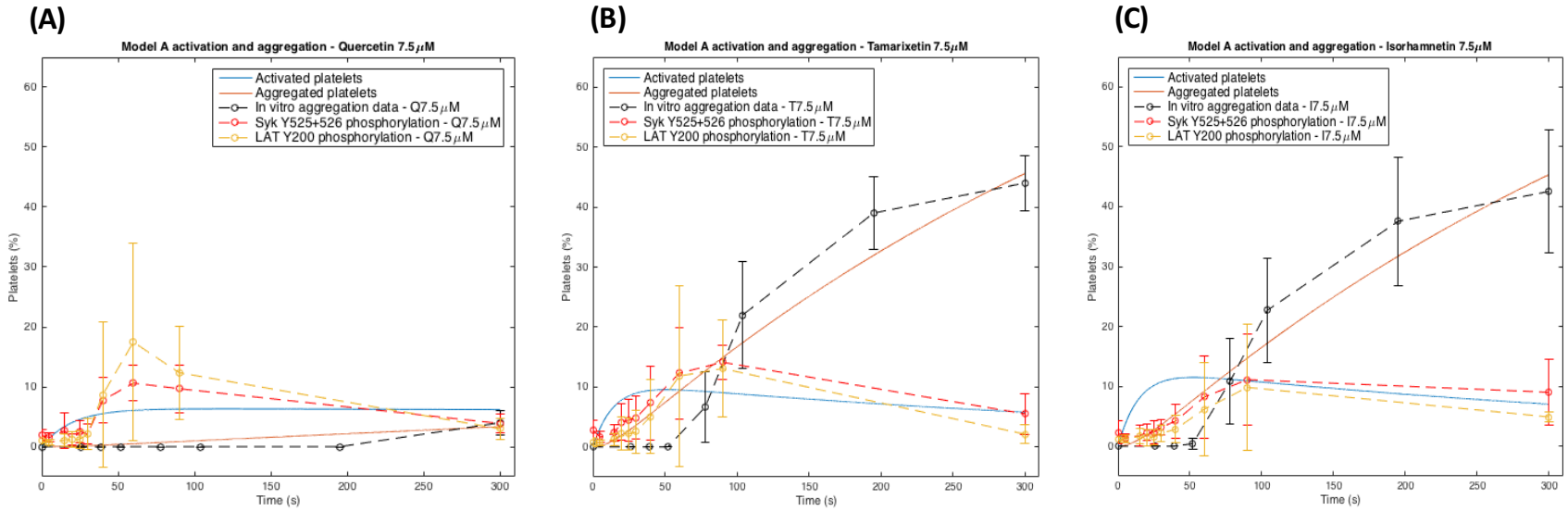

Figure 6-7 Profiles obtained from fitting Model A to *in vitro* Syk and LAT phosphorylation and platelet aggregation data inhibited by flavonoids

Model profiles of activation and aggregation (blue and orange solid lines) obtained by fitting Model A to experimental Syk and LAT phosphorylation (red and yellow dashed lines with circles) and platelet aggregation (dashed black lines with circles) upon treatment with quercetin 7.5μM (A) accurately represent the general profile of activation and aggregation, but are unable to fully achieve the transient peak in activation observed by the data and the subsequent drop in levels of activation. Nonetheless, profiles remain within error bars. Model profiles from fitting Model A to activation and aggregation upon treatment with tamarixetin 7.5μM (B) faithfully represent the aggregation and activation data, with the model demonstrating an earlier activation peak. The same is seen when fitting Model A to experimental data upon treatment with isorhamnetin 7.5μM (C); a faithful fit to the aggregation data with an earlier activation peak in the model profile. *In vitro* aggregation data is presented as mean ± standard deviation, as percentage aggregation normalised to the level of aggregation in the absence of flavonoid (vehicle), N=3 per flavonoid. Experimental phosphorylation data presented here is the mean ± standard deviation, with levels of phosphorylation normalised to loading controls, N=3. Model simulations (solid lines) obtained here by fitting the model to experimental data gave the parameter values described in Table 6-4. Syk, spleen tyrosine kinase; LAT, linker for activation of T cells; Y, tyrosine; Q, quercetin; T, tamarixetin; I, isorhamnetin.

Table 6-4 Best fit Model A parameter values for the inhibition of platelet activation and aggregation by quercetin, tamarixetin and isorhamnetin (7.5µM). The values displayed here represent the best fit values after simultaneously fitting Model A profiles of activation and aggregation to *in vitro* CRP-XL (1µg/mL) stimulated Syk and LAT phosphorylation data, and *in vitro* collagen stimulated (5µg/mL) platelet aggregation data.

Flavonoid	k_1 best fit value (s^{-1})	k_3 best fit value (s^{-1})
Vehicle	$4.5x10^{-2}$	$4.5x10^{-2}$
Quercetin 7.5µM	$3.2x10^{-3}$	$1.9x10^{-3}$
Tamarixetin 7.5µM	$7.5x10^{-3}$	$2x10^{-2}$
Isorhamnetin 7.5µM	$8.75x10^{-3}$	$1.65x10^{-2}$

6.3 Mathematical modelling of platelet aggregation – FLavonoid AGGregation (FLAGG) model

6.3.1 Description of the FLAGG model

The next step in the development of a model of the effects of flavonoids on platelet aggregation was to alter the equations to introduce specific terms describing the concentrations of quercetin, tamarixetin and isorhamnetin as well as describing their direct effects on the platelet aggregation process. This would form a step up from Model A, which modelled the inhibitory effects of flavonoids simply by changing the parameter rates affecting activation and aggregation. Whilst Model A did give useful information and predictions, the development of this next model, the FLavonoid AGGregation (FLAGG) model, would allow simulations of the effects of one, two or three flavonoids simultaneously, at any combination of concentrations. As quercetin, tamarixetin and isorhamnetin are the flavonoids used throughout this study, the modelling of all three simultaneously would allow novel predictions, and inform the development of a pharmacokinetic/pharmacokinetic model presented later in this Chapter.

An ODE mathematical model was developed to describe the direct, concentration-dependent inhibition of collagen-stimulated platelet activation and aggregation by quercetin, tamarixetin and isorhamnetin, alone and in combination. Collagen was again chosen as the agonist to allow direct comparison to *in vitro* data. The populations incorporated into the model are the same as Model A – inactive platelets (P_I), activated platelets (P_A) and aggregated platelets (P_T), as these populations were considered to represent well the activatory and aggregatory process. As such, the network diagram shown in Figure 6-1 also represents the FLAGG model (with the addition of flavonoids specifically inhibiting the rates k_1 and k_3), with Table 6-1 describing the FLAGG model variables as well as the variables of Model A. Multiple new parameters were included in this model; Q, TR and I represent the concentrations of quercetin, tamarixetin and isorhamnetin, respectively, and K_{XQ}, K_{XTR}, K_{XI}, K_{YQ}, K_{YTR} and K_{YI} represent constants of inhibition of platelet activation (K_X) and aggregation (K_Y) by the

indicated flavonoids. These new parameters are described fully in Table 6-5. The units of k_1, k_2 and k_3 change in the FLAGG model depending on the number of flavonoids present: s^{-1} in the absence of flavonoid, μM/s with one flavonoid, $\mu M^2/s$ with two flavonoids, and $\mu M^3/s$ with three flavonoids. The equations for the FLAGG model include a multiplicative interaction between quercetin, tamarixetin and isorhamnetin, and are as follows

$$\frac{dP_I}{dt} = \frac{-k_1 P_I}{(K_{XQ} + Q)(K_{XTR} + TR)(K_{XI} + I)} + k_2 P_A \,, \qquad (2.1)$$

$$\frac{dP_A}{dt} = \frac{k_1 P_I}{(K_{XQ} + Q)(K_{XTR} + TR)(K_{XI} + I)} - \frac{k_3 P_A}{(K_{YQ} + Q)(K_{YTR} + TR)(K_{YI} + I)} - k_2 P_A, \qquad (2.2)$$

$$\frac{dP_T}{dt} = \frac{k_3 P_A}{(K_{YQ} + Q)(K_{YTR} + TR)(K_{YI} + I)} \,, \qquad (2.3)$$

with

$$P_I(0) = P_{I0}, \qquad P_A(0) = 0, \qquad P_T(0) = 0 \,, \qquad (2.4)$$

where equation (2.1) describes the change over time in the number of inactive platelets, equation (2.2) describes the change over time in the number of activated platelets, and equation (2.3) describes the change over time in the number of aggregated platelets. An initial inactive platelet density $P_{I0} = 1\text{x}10^8$ platelets per milliliter was used, as in Model A, to represent the number of platelets in a standard aggregometry assay, with the output normalised to 100% to allow for comparison to normalised *in vitro* platelet aggregometry data. The equations describe a multiplicative nature of effect upon addition of multiple flavonoids, as opposed to an additive effect. This was done primarily because aggregometry data presented in Section 3.6.1 (Figure 3-15) demonstrated a more-than-additive, potentially synergistic effect upon addition of certain combinations of quercetin and its metabolites, and so it was thought that an additive model may not accurately describe the magnitude of inhibitory

effects. An additive model (not shown) was developed and tested, but proved less accurate in matching the *in vitro* data than the multiplicative model presented here. Indeed, this is a finding in itself; that the mathematical model most representative of the data concludes a multiplicative, potentially synergistic (i.e. more-than-additive) interaction between quercetin and its methylated metabolites, supported by the data presented in Section 3.6.1, is a significant output of the modelling process (discussed more in Section 6.4). The assumptions of the FLAGG model are: at resting state, all platelets are inactive; the agonist causes full platelet aggregation in the absence of flavonoid; the progression of a platelet from inactive to activated is a reversible process and from activated to aggregated is an irreversible process; once flavonoid is introduced, it is available immediately and equally to all platelets, and is uncontaminated, and platelets are in the presence of equal levels of flavonoid throughout the experimental/modelling period. Upon model solving and simulation (using ode45, MATLAB (MathWorks, 2015)), the FLAGG model predicts the relative percentage of each population (inactive, activated and aggregated) throughout the 300 second experimental period, allowing direct comparison to light transmission aggregometry data performed previously, as well as comparison to the end-point (300s) plate-based aggregometry data for multiple flavonoids presented in Section 3.6.1. In solving the model, when simulating that a certain flavonoid was absent, the terms describing it were removed, such that only the parameter values describing the flavonoids present in the simulated 'sample' were included. The first aim of the FLAGG model was to match simulations of the effects of individual concentrations of quercetin, tamarixetin and isorhamnetin to the *in vitro* light transmission aggregometry data, as was done for Model A in Section 6.2.3.

Table 6-5 A summary of FLAGG model parameters. The units of k_1, k_2 and k_3 change depending on the number of flavonoids present (s^{-1} in the absence of flavonoid, μM/s with one flavonoid, $\mu M^2/s$ with two flavonoids, and $\mu M^3/s$ with three flavonoids).

Parameter	Description	Units
k_1	Rate of platelet activation	μM^3 / s
k_2	Rate of platelet inactivation	μM^3 / s
k_3	Rate of platelet aggregation	μM^3 / s
Q	Quercetin concentration	μM
TR	Tamarixetin concentration	μM
I	Isorhamnetin concentration	μM
K_{XQ}	Constant of inhibition of activation by quercetin	μM
K_{XTR}	Constant of inhibition of activation by tamarixetin	μM
K_{XI}	Constant of inhibition of activation by isorhamnetin	μM
K_{YQ}	Constant of inhibition of aggregation by quercetin	μM
K_{YTR}	Constant of inhibition of aggregation by tamarixetin	μM
K_{YI}	Constant of inhibition of aggregation by isorhamnetin	μM

6.3.2 FLAGG model – modelling individual flavonoid effects

In the case of untreated platelets, when all three flavonoids are absent (as is the case in a vehicle-treated sample *in vitro*), the equations, and subsequently the parameters values, are the same as the vehicle-treated conditions of Model A; that is, $4.5x10^{-2}$ s^{-1}. Figure 6-6 therefore also represents the model profiles and best fit of *in vitro* data in the simulation of the FLAGG model under vehicle-treated conditions. The next step in the development of the FLAGG model was to fit the parameters to *in vitro* light transmission aggregometry data and *in vitro* Syk and LAT phosphorylation data, and investigate whether the parameters from these fits were also appropriate to describe the levels of aggregation achieved upon addition of other individual flavonoid concentrations.

Due to the introduction of flavonoid concentrations and the multiplicative interaction between these, the values of the rates k_1, k_2 and k_3 upon addition of one, two or three flavonoids must be altered accordingly. Upon addition of one flavonoid, this gave values of k_1, k_2 and k_3 of $4.5x10^{-1}$ μM/s. These values (as well as the K_X and K_Y values) stay constant over individual flavonoid concentrations, unlike Model A (where these rate values changed to represent inhibition by flavonoids), as individual terms have now been introduced to describe flavonoid concentration; inhibition of aggregation is now a direct function of flavonoid concentration. FLAGG model simulations were run, comparing the model profiles to *in vitro* 7.5μM flavonoid-treated activation and aggregation data simultaneously to gain the best fit. Fitting was done by eye as described previously, ensuring the model profiles matched the data and lay within the error bars of the *in vitro* data as much as possible. Performing this fitting analysis resulted in the best fit parameters described in Table 6-6. The profile of platelet activation predicted by the FLAGG model was inhibited more dramatically at lower flavonoid concentrations compared to the Model A profile of activation. It was not possible to elucidate the true level of inhibition of activation at these lower concentrations due to the time required for such further high-throughput experimentation, and so the constants of inhibition of activation (K_X) and aggregation (K_Y) were kept

the same in this model. Overall, as can be seen in Table 6-6, fitting the FLAGG model to *in vitro* activation and aggregation data gave similar K_X and K_Y values for all three flavonoids.

The activation and aggregation model profiles from the FLAGG model are compared with *in vitro* data in Figure 6-8. As can be seen in Figure 6-8A, the profile of activation predicted by the model reaches a very rapid peak (10s), earlier than the *in vitro* data (60s), and levels of phosphorylation are also lower. However, between 40 and 300s the model profile of activation lies within the error bars of the data. The aggregation profile predicted by the model upon treatment with 7.5μM quercetin is far above that seen *in vitro* – a predicted 57% aggregation compared to the observed 4% aggregation. This is the largest outlier seen across the FLAGG model's individual flavonoid effect predictions, and is likely due to the fact that this concentration of quercetin (7.5μM) caused a very high level of inhibition compared to the concentration tested below it (5μM). There is a large jump in inhibition from quercetin 5μM treatment (27% inhibition) to quercetin 7.5μM treatment (96% inhibition) that is hard to incorporate into this model. With Model A, the rate of aggregation could specifically be altered to achieve a profile of aggregation matching the data, but these rates cannot be altered in the FLAGG model, instead remaining constant. Nevertheless, in matching the data to the FLAGG model across all individual quercetin concentrations, the model values presented in Table 6-6 provided the best fit overall. The model profile of activation predicted upon treatment with 7.5μM tamarixetin also displays an earlier and lower peak, again at 10 seconds, compared to a 90s peak shown by *in vitro* data (Figure 6-8B). Similar to Model A, however, delaying the model peak resulted in vastly reduced platelet aggregation, beyond the error bars of the *in vitro* data, and so was considered inappropriate. However, from 20-300s the model profile of activation fits the data, and the model largely fits within the error bars of the aggregation data (later aggregation data points, especially endpoint, were given more weighting in the fitting process as the final percentage of aggregation is the key value), with the largest outlier (at tamarixetin 20μM) being only 8% out. The profile of activation predicted upon isorhamnetin 7.5μM treatment is similar to quercetin and tamarixetin treatment, with a peak at 11 seconds compared to the 90s peak in the data (Figure 6-8C). Similar to quercetin, however, from 40-300 seconds the

model profile of activation lies within the error bars of the *in vitro* data. The model profile of aggregation also faithfully represents the *in vitro* aggregometry data at intermediate and later time points, and at all concentrations of isorhamnetin, model profiles of aggregation simulated from the parameter values shown in Table 6-6 accurately represented *in vitro* aggregation data. It can be seen in Figure 6-8 that aggregation can be delayed by flavonoids (dashed black lines), with aggregation starting at a time point beyond zero seconds; this is something that the FLAGG model cannot predict, instead faithfully representing the percentage inhibition after 300 seconds, and is the reason why at earlier time points the model profile of aggregation does not always match the *in vitro* data.

Now that the FLAGG model had been parameterised and the model fitted to the effects of individual flavonoids on platelet activation and aggregation, the next step was to utilise the multiple flavonoid plate-based aggregometry data from Chapter 3 (Section 3.6.1) to allow development of the model to simulate the effects of flavonoid combinations on platelet aggregation.

Table 6-6 Best fit FLAGG model parameter values for the inhibition of platelet activation and aggregation by individual flavonoids. The best fit parameter values for inhibition by individual flavonoids, obtained by simultaneously fitting the FLAGG model profiles of activation and aggregation to *in vitro* CRP-XL (1µg/mL) stimulated Syk and LAT phosphorylation data, and *in vitro* collagen (5µg/mL) stimulated platelet aggregation data. N/A indicates the parameter has no role under the specified conditions.

Flavonoid	k_1 **(µM/s)**	k_2 **(µM/s)**	k_3 **(µM/s)**	K_X **(µM)**	K_Y **(µM)**
Vehicle	4.5×10^{-2}	4.5×10^{-2}	4.5×10^{-2}	N/A	N/A
Quercetin	4.5×10^{-1}	4.5×10^{-1}	4.5×10^{-1}	4.2	4.2
Tamarixetin	4.5×10^{-1}	4.5×10^{-1}	4.5×10^{-1}	5.9	5.9
Isorhamnetin	4.5×10^{-1}	4.5×10^{-1}	4.5×10^{-1}	6.5	6.5

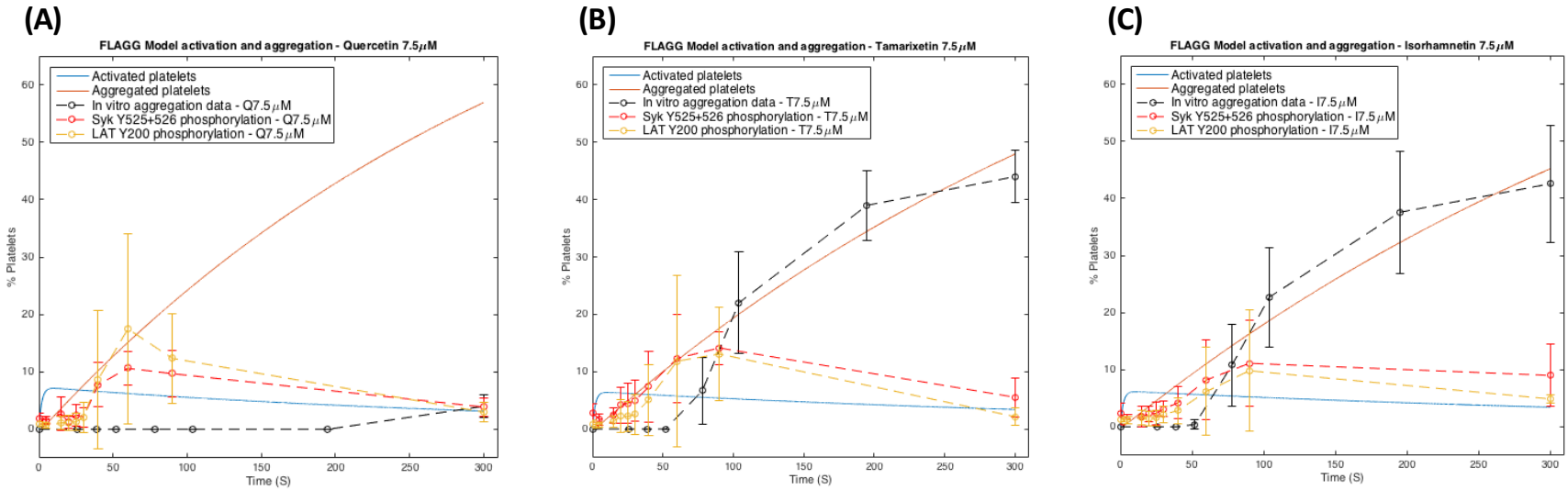

Figure 6-8 Profiles obtained from fitting the FLAGG model to *in vitro* Syk and LAT phosphorylation and platelet aggregation data

The model profile of activation (solid blue line) obtained by fitting the FLAGG model to experimental Syk and LAT phosphorylation (red and yellow dashed lines with circles) and platelet aggregation data (dashed black line with circles) upon treatment with quercetin 7.5μM (A) represents the general profile of activation, fitting within the error bars of later time points. The model profile of aggregation, however, rises far beyond the *in vitro* data (discussed in text). Model profiles obtained from fitting the FLAGG model to activation and aggregation data upon treatment with tamarixetin 7.5μM (B) faithfully represent the data, with predicted activation and aggregation profiles lying largely within the error bars. The same is seen when fitting Model A to experimental data upon treatment with isorhamnetin 7.5μM (C), with faithful fits to both activation and aggregation data, lying largely within the error bars. All three simulations predict an earlier peak in activation compared to the data. *In vitro* aggregation data is presented as mean ± standard deviation, as percentage aggregation normalised to the level of aggregation in the absence of flavonoid (vehicle), N=3 per flavonoid. Experimental phosphorylation data presented here is the mean ± standard deviation, with levels of phosphorylation normalised to loading controls, N=3. Model simulations (solid lines) obtained here by fitting the model to experimental data gave the parameter values described in Table 6-6. Syk, spleen tyrosine kinase; LAT, linker for activation of T cells; Y, tyrosine; Q, quercetin; T, tamarixetin; I, isorhamnetin.

6.3.3 FLAGG model – modelling the effects of dual flavonoid treatment

After parameterisation of the FLAGG model to *in vitro* data describing the effects of individual flavonoid concentrations, the next step was to utilise plate-based aggregometry data to test the FLAGG model's capability to predict the effects of multiple flavonoids added simultaneously; this is important as *in vivo* there will be many metabolites of quercetin (as well as potentially the aglycone) in plasma. The first step in this was to investigate how the FLAGG model parameters predicted the effects of dual flavonoid treatment.

This was done through use of the *in vitro* plate based aggregometry data presented in Section 3.6.1. This assay allowed for the simultaneous testing of many flavonoid concentration combinations; a limitation of this, however, is that it is an endpoint only assay, with no data gathered as to the kinetics of platelet aggregation over the 300s experimental period. As such, there is only one data point to fit the effects of multiple flavonoids in the FLAGG model to. This is a limitation of the fitting process, and is discussed more at the end of the chapter. As was the case from no flavonoid to one being present, moving the model from one to two-flavonoid treatment required another change in the rates of k_1, k_2 and k_3. As was done previously, they were initially multiplied by 10 to give rates of $4.5\mu M^2/s$, and simulations were run to see if these rates, combined with the inhibition constants determined in the previous section, accurately predicted the levels of aggregation observed *in vitro* upon dual flavonoid treatment. The use of this rate ($4.5\mu M^2/s$) combined with the calculated inhibition constants consistently predicted higher levels of inhibition than seen in the *in vitro* data. As a result, the k_1, k_2 and k_3 rates were altered to match the model profiles of aggregation to *in vitro* dual-flavonoid inhibited platelet aggregation, with rates of $9.25\mu M^2/s^{-1}$ providing an overall best fit to the data; these values are summarised in Table 6-7. With the rates altered to $9.25\mu M^2/s^{-1}$, the simulations of quercetin + tamarixetin and quercetin + isorhamnetin combinations fitted the data well, with the endpoints from the model largely fitting within the error bars of the *in vitro* data (Figure 6-9A/B show examples of dual 5μM treatment); there were several outliers where the model profile of aggregation predicts 1-

5% above or below the error bar, and one outlier (quercetin 1μM + tamarixetin 5μM) which predicted approximately 20% less aggregation than the *in vitro* data observed. The observation that most simulations from the model, in which the interaction between flavonoids is defined as multiplicative (not additive), fit within the error bars of the *in vitro* data suggests that the interaction between these flavonoids is indeed more-than-additive (potentially synergistic), as opposed to merely additive. An interesting observation is that the FLAGG model predicted very low levels of platelet activation upon dual treatment with these flavonoid combinations – approximately 1% activation. Combined with the accuracy of the model in predicting levels of aggregation, this novel prediction could warrant further investigation in the future; no work has been done so far investigating the effects of quercetin/metabolite combinations on platelet signalling. The FLAGG model was unable to accurately predict the effects of isorhamnetin + tamarixetin combinations on platelet aggregation, consistently predicting a higher level of inhibition (ranging from 7-40% increased inhibition) compared to the *in vitro* data (Figure 6-9C). This is due to the different nature of the *in vitro* interaction between these metabolites, compared to quercetin + tamarixetin and quercetin + isorhamnetin – as seen in Figure 3-15, no more-than-additive effects on platelet aggregation were observed using this combination, with a general low level of effect. The reason for this is unclear, and due to the nature of the FLAGG model, it was unable to account for this. This is thus a limitation of the model and further *in vitro* work investigating this combination is thus required. The effects of these flavonoid combinations of the kinetics of platelet aggregation (as opposed to endpoint-only data) obtained through light transmission aggregometry could overcome the data limitations and allow better model fitting; this is discussed in Section 6.4.

The FLAGG model is therefore now capable of predicting the effects of any combination of concentrations of quercetin + tamarixetin and quercetin + isorhamnetin, but not tamarixetin + isorhamnetin, on aggregation. However, *in vivo* there will be more complex combinations than this, and so the next step was to model the effects of the simultaneous addition of quercetin, tamarixetin and isorhamnetin on platelet aggregation.

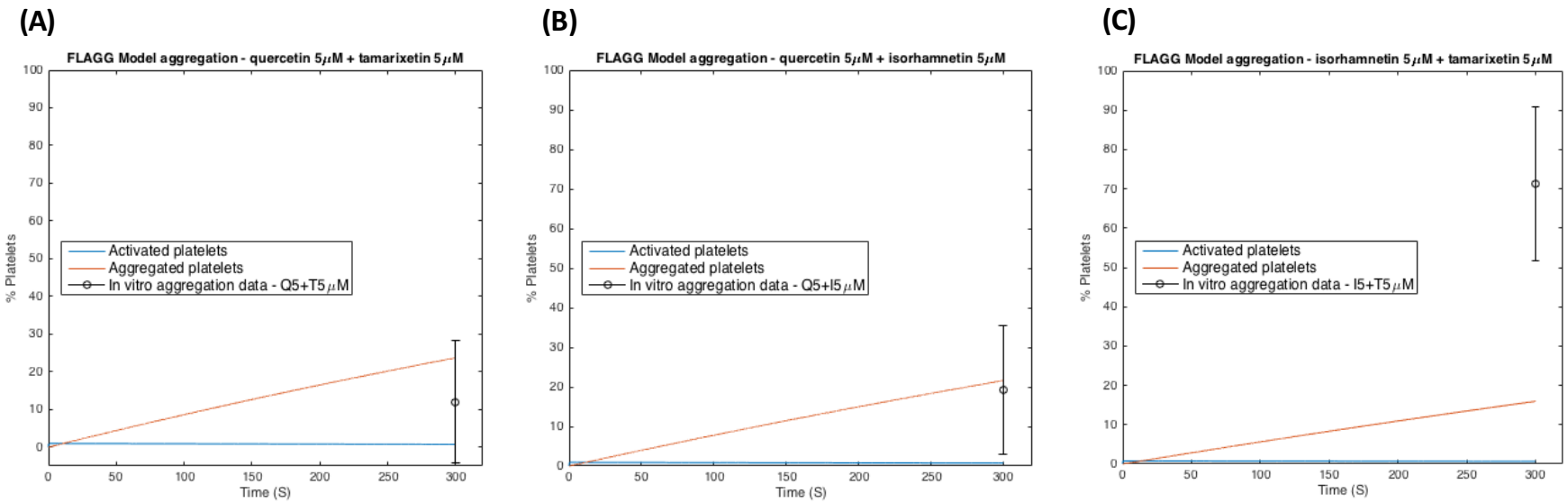

Figure 6-9 Best fit FLAGG model profiles of aggregation compared to *in vitro* plate-based aggregation data of dual-flavonoid (5μM) treatment

Model profiles of aggregation (solid orange lines) obtained by fitting the FLAGG model to endpoint-only experimental plate-based aggregation data upon treatment with two flavonoids – quercetin + tamarixetin (A), quercetin + isorhamnetin (B), and isorhamnetin + tamarixetin (C). The model accurately represents the level of aggregation achieved upon dual treatment with quercetin + tamarixetin (A) and quercetin + isorhamnetin (B), but is unable to accurately match the levels of aggregation observed *in vitro* after dual isorhamnetin + tamarixetin treatment, due to the different nature of the interaction between the two methylated metabolites. *In vitro* plate-based aggregation data is presented as mean ± standard deviation, as percentage aggregation normalised to the level of aggregation in the absence of flavonoids (vehicle), N=5 per flavonoid combination. Model simulations (solid lines) obtained here by fitting the model to experimental data gave the parameter values described in Table 6-7. Q, quercetin; T, tamarixetin; I, isorhamnetin.

6.3.4 FLAGG model – modelling triple flavonoid treatment

This study has primarily utilised quercetin and its methylated metabolites tamarixetin and isorhamnetin, and so the final step in the development of the FLAGG model was to incorporate and model the effects of platelet aggregation upon treatment with all three flavonoids. Whilst this does not represent the complexity of metabolites observed *in vivo*, it represents the maximum complexity of flavonoid combinations that data has been collected for in this study, and so provides a useful starting point for the building of a model of platelet aggregation incorporating many of quercetin's *in vivo* metabolites.

The values of k_1, k_2 and k_3 were again modified due to the addition of another flavonoid (i.e. triple-flavonoid treatment). Multiplying the two-flavonoid treatment rates by 10 (as was initially tested from one to dual-flavonoid treatment) and simulating the model with the previously defined flavonoid inhibition constants resulted in the model consistently predicting an increased inhibitory potency than was observed in the *in vitro* aggregation data. The k_1, k_2 and k_3 rates were therefore altered to match the model profiles of aggregation to *in vitro* triple-flavonoid inhibited platelet aggregation, with rates of $350\mu M^3/s$ providing an overall best fit to the data; these values are summarised in Table 6-7. With these altered rates and the previously elucidated inhibition constants, the model profiles of aggregation matched well to the *in vitro* data at 1μM and 2.5μM triple-flavonoid treatment (Figure 6-10). At 5μM triple treatment, the model predicted slightly more aggregation (7.6%) than was seen *in vitro* (<1%), where aggregation was abolished; however, the model still predicted a very low, sub-10% level of aggregation, and so this was considered acceptable (Figure 6-10). Lowering the k_1, k_2 and k_3 rates to match this data point would also result in the model profile of aggregation falling outside of the error bars at 2.5μM and 1μM triple-flavonoid treatment, which was considered an unacceptable compromise.

The FLAGG model is therefore now capable of predicting the levels of platelet activation and aggregation *in vitro* upon addition of quercetin, tamarixetin and isorhamnetin at any concentration and in any combination (except for tamarixetin + isorhamnetin as previously described). A limitation of this, however, is that it only accounts for quercetin aglycone and two of its methylated metabolites. Whilst these are important, *in vivo*, there will be many other metabolites (e.g. sulphated and glucuronidated). Limited data has been gather for the effect of quercetin-3-glucuronide on platelet aggregation in this study; however, such high (supraphysiological) concentrations were required for inhibition (approximately 50% inhibition at 200μM) that including this metabolite in the FLAGG model was not a priority. The FLAGG model represents a step forward from Model A in that it introduced specific parameters to directly describe the effects of flavonoids (i.e. inhibition of aggregation is now a direct function of flavonoid concentration), and can now predict the effect of flavonoid combinations on platelet activation and aggregation *in vitro*. The extension of this model to include the anti-platelet effects of, and interactions between, other metabolites and indeed other pharmacological agents is discussed in Section 6.4.

Table 6-7 Best fit FLAGG model parameter values for the inhibition of platelet aggregation by individual flavonoids, as well as by dual and triple flavonoid treatments. The best fit parameter values for inhibition by individual flavonoids, obtained by simultaneously fitting the FLAGG model profiles of activation and aggregation to *in vitro* CRP-XL (1µg/mL) stimulated Syk and LAT phosphorylation data, and *in vitro* collagen (5µg/mL) stimulated platelet aggregation data, as well as the best fit parameter values for inhibition of aggregation by combinations of two and three flavonoids, obtained by fitting the FLAGG model to *in vitro* collagen (5µg/mL) stimulated plate-based platelet aggregation data. N/A indicates the parameter has no role under the specified conditions. 'No fit' refers to the lack of matching between *in vitro* data and model predictions of the effects of tamarixetin + isorhamnetin combinations, discussed in-text.

Flavonoid(s)	k_1 †	k_2 †	k_3 †	K_X (µM)	K_Y (µM)
Vehicle	4.5×10^{-2}	4.5×10^{-2}	4.5×10^{-2}	N/A	N/A
Quercetin	4.5×10^{-1}	4.5×10^{-1}	4.5×10^{-1}	4.2	4.2
Tamarixetin	4.5×10^{-1}	4.5×10^{-1}	4.5×10^{-1}	5.9	5.9
Isorhamnetin	4.5×10^{-1}	4.5×10^{-1}	4.5×10^{-1}	6.5	6.5
Quercetin + Tamarixetin	9.25	9.25	9.25	K_{XQ} = 4.2 K_{XTR} = 5.9	K_{YQ} = 4.2 K_{YTR} = 5.9
Quercetin + Isorhamnetin	9.25	9.25	9.25	K_{XQ} = 4.2 K_{XI} = 6.5	K_{YQ} = 4.2 K_{YI} = 6.5
Isorhamnetin + Tamarixetin	No fit	No fit	No fit	K_{XI} = 6.5 K_{XTR} = 5.9	K_{YI} = 6.5 K_{YTR} = 5.9
Quercetin + Tamarixetin + Isorhamnetin	350	350	350	K_{XQ} = 4.2 K_{XTR} = 5.9 K_{XI} = 6.5	K_{YQ} = 4.2 K_{YTR} = 5.9 K_{YI} = 6.5

† The units for k_1, k_2 and k_3 are: s^{-1} with no flavonoid, µM/s with one flavonoid present, $\mu M^2/s$ with two flavonoids present, and $\mu M^3/s$ with three flavonoids present.

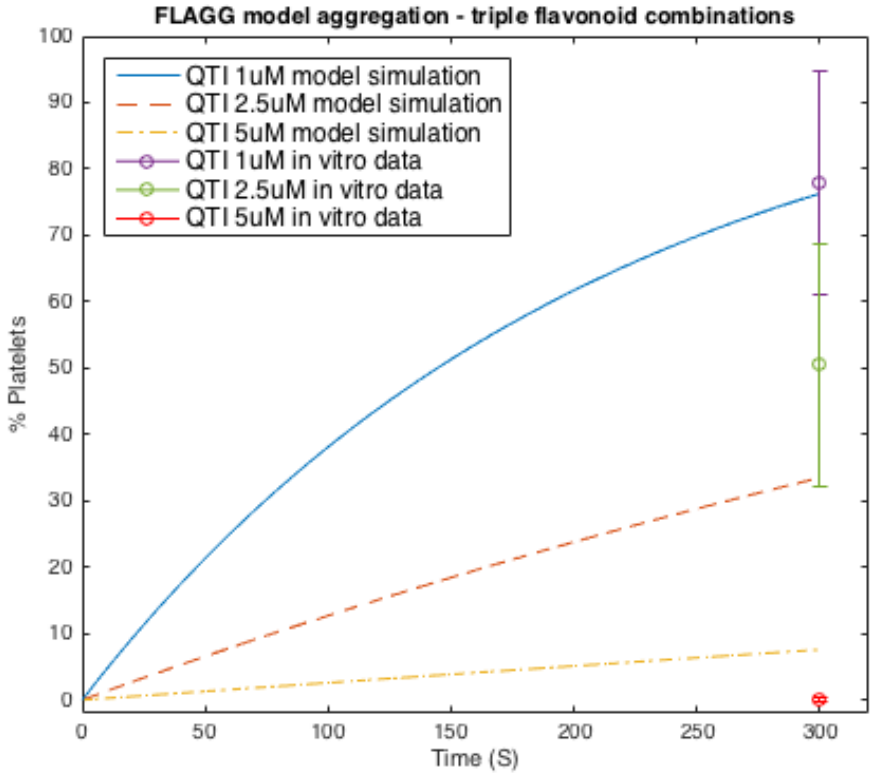

Figure 6-10 Best fit FLAGG model profiles of aggregation compared to *in vitro* plate-based aggregation data of triple-flavonoid treatment

FLAGG model profiles of aggregation obtained by fitting the model to endpoint-only experimental plate-based aggregation data upon treatment with quercetin + tamarixetin + isorhamnetin (QTI) at 1 µM (solid blue line), 2.5 µM (orange dashed line) and 5 µM (yellow dash-dot line). The end-point data values are shown on the right side of the graph for comparison. The model predicts the effect of QTI 1 µM treatment and QTI 2.5 µM treatment, with the end-point of the simulations lying within the error bars. The model profile of aggregation upon QTI 5 µM treatment is slightly above the *in vitro* data point; however, aggregation is still sub-10%, and altering parameters more to match it would move QTI 1 µM and QTI 2.5 µM simulations out of the error bars, so was accepted as a compromise. *In vitro* plate-based aggregation data is presented as the mean ± standard deviation, as percentage aggregation normalised to the level of aggregation in the absence of flavonoids (vehicle), N=5 per flavonoid combination. Model simulations obtained here by fitting the model to experimental data gave the parameter values described in Table 6-7. QTI, quercetin + tamarixetin + isorhamnetin.

6.4 Discussion of results presented in Chapter 6

The aim of this chapter was to use mathematical approaches to model the effects of quercetin and its methylated metabolites on *in vitro* platelet aggregation, individually and in combination, with an aim to examine their potential inhibitory interactions, as well as to inform future *in silico* and *in vitro* experimentation. This was achieved through the development of two ODE mathematical models, Model A and the FLAGG model, which were developed and parameterised using *in vitro* data gathered in this study.

Model A was a relatively simple mathematical model simulating *in vitro* washed platelet activation and aggregation. It contained three variables – inactive platelets (P_I), activated platelets (P_A) and aggregated platelets (P_T). Inactive platelets were activated at rate k_1, in a reversible reaction (with rate k_2). Activated platelets then became aggregated in an irreversible reaction with rate k_3. The simulation of inhibition of activation and aggregation was achieved through altering these rate parameters, as opposed to the inclusion of specific terms describing the effects of flavonoids (as in the FLAGG model). Initial fitting of the model to *in vitro* aggregometry data revealed a gap in the data – namely, no data had been gathered to accurately model the profile of activation. Thus, *in vitro* signalling experiments were carried out, investigating the effects of quercetin, tamarixetin and isorhamnetin (7.5μM) on CRP-XL (1μg/mL) stimulated Syk (spleen tyrosine kinase) tyrosine 525+526 and LAT (linker for activation of T cells) tyrosine 200 phosphorylation. Quercetin, tamarixetin and isorhamnetin inhibited significantly the phosphorylation of both Syk and LAT, as well as delaying peak phosphorylation. The inhibition of Syk and LAT phosphorylation by quercetin and tamarixetin is in agreement with data by Wright *et al.* (2010b), who observed inhibition of collagen (25μg/mL) stimulated total tyrosine, Syk, PLCγ2 and LAT phosphorylation after 90s upon treatment with 20μM flavonoid. The utilisation of many time points in the data presented here allowed accurate fitting of the model to the *in vitro* data, and the effects of isorhamnetin on Syk and LAT phosphorylation are novel observations. Simultaneous fitting of Model A profiles of activation and aggregation to the *in*

vitro Syk and LAT phosphorylation data and *in vitro* aggregometry data allowed the elucidation of k_1 and k_3 values that best represented the inhibition of activation and aggregation by quercetin, tamarixetin and isorhamnetin. Overall, the fitting process was successful, with Model A simulations matching well the *in vitro* data.

The best fit parameter values ascertained above gave novel predictions regarding the relative contributions of the inhibition of activation and aggregation in the overall anti-platelet effect of quercetin and its methylated metabolites. Upon quercetin treatment, the values of k_1 and k_3 were both reduced by over an order of magnitude compared to vehicle-treated platelets. The value of k_3 (representing the transition of platelets from an activated to an aggregated state) was lower than the value for k_1 (from inactive platelet to activated platelet), implying that the aggregation of platelets is more strongly inhibited by quercetin than their initial activation. Upon tamarixetin or isorhamnetin treatment, however, this observation is reversed; the k_1 value was lower than the k_3 value, predicting that the initial activation of platelets was more effected than their aggregation. These are novel predictions, in that Model A predicts a difference in the primary inhibitory mechanism of quercetin (inhibition of aggregation) compared to its methylated metabolites (inhibition of initial activation). Future *in vitro* experimentation and incorporation of this into Model A could elucidate whether this is a general consequence of quercetin metabolism, and the implications of this observation *in vivo*, where metabolites are thought to be the primary 'effectors', must be considered.

In Model A, flavonoids did not directly affect platelet aggregation; rather the values of the rates k_1, k_2 and k_3 were altered to represent inhibition. As a result of this, the model was limited to modelling the effect of one flavonoid at a time. The FLAGG model was therefore formulated, in which inhibition of platelet activation and aggregation was a direct function of flavonoid concentration. The FLAGG model was an ODE mathematical model utilising the same three variables as Model A (P_I, P_A and P_T), with the inclusion of new parameters to specify the direct inhibition of activation and aggregation by flavonoids, allowing the simulation of the inhibitory effects of one, two or three flavonoids simultaneously. Using *in vitro* aggregometry and Syk and LAT phosphorylation data gathered in this

study, the model was first fitted to individual flavonoid concentration data, allowing values for the constants of inhibition (K_X and K_Y parameters) to be determined. The effects of dual and triple-flavonoid concentrations were then simulated, and fitted to the plate-based aggregometry data presented in Section 3.6.1. This fitting process led to the observation that a model in which the interaction between flavonoids was multiplicative (as described in equations (2.1) to (2.3)) fitted the data more accurately than a model in which the interactions were additive. Thus, a model defining flavonoid interactions as multiplicative (i.e. potentially synergistic) provided a better fit to the dual and triple-flavonoid treatment data overall than a model defining the interactions as additive. This supports the data presented in Section 3.6.1, and provides further evidence that quercetin and its metabolites can inhibit platelet aggregation in a more-than-additive manner. The effect of dual tamarixetin + isorhamnetin treatment could not be fitted to the model due to lack of inhibitory effect of this combination, described in Section 3.6.1.

A limitation of the *in vitro* data used in the dual and triple-flavonoid treatment model fitting process must be acknowledged here, in that the data was end-point only (i.e. one measurement of aggregation at the end of the 300s assay). This was due to the high number of samples required to investigate the effects of dual and triple-flavonoid combinations at different concentrations; this made plate-based aggregometry a more attractive option in this investigation compared to light transmission aggregometry (LTA). As a result, the model simulations for dual and flavonoid triple-treatment could only be fitted to one data point, which is of limited use. Future work could therefore focus on light transmission aggregometry experimentation on the effect of dual and triple-flavonoid combinations on collagen (5μg/mL)-stimulated platelet aggregation, as well as on the CRP-XL (1μg/mL) phosphorylation of Syk and LAT over a 300s time course, as the model predicted activation would be very low (approximately 1%) upon dual and triple flavonoid treatment. This would allow fitting of the FLAGG model to the kinetics of aggregation as well as provide more information on the unexpected interaction between tamarixetin and isorhamnetin. Future work (discussed in Chapter 8) could also focus on the incorporation of more quercetin metabolites into the FLAGG model. For example, sulphated metabolites of quercetin such as quercetin-3'-O-sulphate have been identified in plasma

upon quercetin administration, and a study by Wright *et al.* (2010b) demonstrated an anti-aggregatory effect of this metabolite with similar potency to tamarixetin (Jones *et al.*, 2004; Crozier *et al.*, 2008; Wright *et al.*, 2010b). Inclusion of this data into the FLAGG model could therefore allow novel simulations to predict the interaction of this metabolite with quercetin and its methylated metabolites with respect to anti-aggregatory effect, which could be compared against future *in vitro* aggregation data. This would allow further validation of the model and inform future *in vitro* experimentation, providing insight into which flavonoid combinations may be particularly effective and worth pursuing in further *in vitro* / *in vivo* experimentation. This could be extended to include interactions between quercetin and other flavonoids/polyphenols, and quercetin and pharmacological agents such as aspirin, as the model is theoretically able to incorporate any inhibitor of platelet function (discussed in Chapter 8). For example, Pignatelli *et al.* (2000) demonstrated that quercetin and catechin can synergise in the inhibition of platelet function, and Crescente *et al.* (2009) demonstrated an interactive effect of a combination of resveratrol, quercetin and gallic acid and aspirin in the inhibition of platelet aggregation; an interaction between quercetin/tamarixetin/isorhamnetin and aspirin is also observed in Section 5.5.2. The incorporation of these data into the FLAGG model could also inform further *in vitro* experimentation, as well as highlighting interactions worth investigating in *in vivo* experimentation.

The models presented in this chapter focussed on the modelling of *in vitro* platelet activation and platelet aggregation, using data from washed platelet assays in parameterisation and model fitting. This is useful in the analysis of platelet function and its inhibition by flavonoids in a 'clean' system; *in vivo*, however, platelets act in the medium of whole blood (with associated plasma proteins and red blood cells), and upon activation are incorporated into a thrombus. Data from this study has also focussed on platelets in whole blood, and on the development of thrombi after flavonoid treatment, in the form of *in vitro* thrombus formation under flow assays presented in Chapter 4, Section 4.6. This data was therefore utilised in the development of a mathematical model of the effects of quercetin, tamarixetin and isorhamnetin on thrombus formation, individually and in combination, as well as

incorporation of this into a pharmacokinetic/pharmacodynamic (PKPD) model of quercetin metabolism and anti-thrombotic function, presented in Chapter 7.

7 – A pharmacokinetic/pharmacodynamic model of quercetin metabolism and anti-thrombotic effect

7.1 A pharmacokinetic/pharmacodynamic model of quercetin metabolism and anti-thrombotic effect

The mathematical models presented in Chapter 6 provided accurate representations of the washed platelet aggregation process *in vitro,* and its inhibition by quercetin and its methylated metabolites. However, *in vivo*, platelets circulate in the medium of whole blood, with the associated plasma proteins and red blood cells. As described in Chapter 4, quercetin has been shown to bind extensively to plasma proteins, with up to approximately 99% of circulating quercetin binding to human serum albumin, which translates into a reduced anti-platelet effect in plasma (Boulton *et al.*, 1998; Kaldas *et al.*, 2005; Raghavendra and Naidu, 2009). As well as this, *in vivo*, platelets are incorporated into a thrombus, with associated red blood cells and fibrin mesh, as opposed to simply a platelet aggregate. *In vitro* thrombus formation under flow data gathered in this study overcomes some of these limitations, in that flavonoid-treated whole blood was flowed over a collagen-coated surface at an arterial shear rate. The first aim of this chapter was to utilise this data to develop a mathematical model of *in vivo* thrombus formation. There are several examples in the literature of the mathematical modelling of this process; Xu *et al.* (2008) developed a multiscale model of thrombus formation, incorporating factors such as blood plasma, platelet activation, and blood flow dynamics, and Leiderman and Fogelson (2011) developed a spatial-temporal model of thrombus formation incorporating platelet aggregation and coagulation, including complex interactions such as biochemical coagulation reactions, platelet activation and the effects of blood flow on the developing thrombus and vice versa. Due to the complexity of these models, however, the effects of platelet antagonists were not investigated. The aim of this chapter was therefore to develop a model of thrombus formation, and investigate the effects of quercetin and its methylated metabolites on this process using *in vitro* data gathered in this study.

One of the assumptions of the models presented in Chapter 6 is a static flavonoid concentration. Whilst this represents well the situation *in vitro,* this is not the case *in vivo*, where flavonoid metabolism and elimination result in dynamic flavonoid/metabolite plasma concentrations. Another aim of this chapter

was therefore to develop the mathematical model of thrombus formation into a pharmacokinetic/pharmacodynamic model of quercetin metabolism, elimination and anti-thrombotic effect. Numerous studies have investigated the pharmacokinetics of quercetin; for example, Hubbard *et al.* (2004) measured plasma quercetin, tamarixetin and isorhamnetin concentrations over 32 hours after human supplementation with 150mg and 300mg doses of quercetin 4'-O-β-D-glucoside, with peak quercetin values of 4.66 and 9.72μM, respectively, and Graefe *et al.* (2001) measured peak total quercetin concentrations after administration of different glycoside forms of quercetin. Several studies have also mathematically modelled the pharmacokinetics of quercetin. Moon *et al.* (2008) developed a pharmacokinetic model of quercetin and its metabolites incorporating enterohepatic recirculation, and informed it through a human supplementation study, whilst Chen *et al.* (2005) modelled the pharmacokinetics of quercetin and its combined sulphate and glucuronide metabolites in rats. Mathematical models and biological data of quercetin pharmacokinetics have, however, not been linked to the *in vitro* or mathematically modelled anti-thrombotic effects of quercetin; another aim of this chapter was therefore to utilise these studies and *in vitro* data gathered in this study in the development of a pharmacokinetic/pharmacodynamic (PK/PD) model describing the metabolism, elimination and anti-thrombotic effect of quercetin, with an aim to run *in silico* trials investigating the effects of different dose regimens as well as the effects of altering pharmacokinetics to potentially enhance anti-thrombotic effect.

7.2 Mathematical modelling of thrombus formation – FLAvonoid Thrombus (FLAT) model

7.2.1 Description of the FLAT model

As mentioned previously, whilst the platelet aggregation models presented in Chapter 6 provided a useful insight into the mechanistic effects of quercetin and its methylated metabolites on platelet activation and aggregation, *in vivo* platelets circulate in the medium of whole blood, and are incorporated into a thrombus upon vessel injury. The next step was therefore to mathematically model the flavonoids' effects on the thrombus formation process.

An ODE mathematical model was developed to describe the effects of quercetin, tamarixetin and isorhamnetin, individually and in combination, on the formation of a thrombus under arterial flow conditions. This would utilise the *in vitro* thrombus formation under flow assay data presented in Section 4.6, and thus the model represents the formation of a thrombus upon flow of blood at a shear rate of $500s^{-1}$ over a surface coated with collagen (100μg/mL). This is referred to as the FLAT model and it contains only one variable – '*T*', which represents the approximate size (μL) of an occluding thrombus in the left anterior descending (LAD) coronary artery. This artery forms the primary blood supply to the interventricular septum, as well as supplying blood to the left ventricle (Villa *et al.*, 2016). This artery was chosen due to its involvement in disease; the LAD artery is one of the most commonly involved arteries in coronary artery disease (Wasilewski *et al.*, 2015). Indeed, as well as being one of the most commonly occluded coronary arteries, occlusion in this artery often leads to highly fatal myocardial infarctions, leading to it being colloquially referred to as the 'widow-maker' artery (Fadem, 2007; Topol and Califf, 2007; Lewis, 2012). In calculating the volume of a thrombus in this artery, the diameter was taken as 2.8mm; this was based on a study by Dodge *et al.* (1992), who demonstrated an average proximal LAD coronary artery diameter of 3.7mm and an average distal diameter of 1.9mm. Thus, an average of 2.8mm was taken. This is in approximate agreement with a study by Zhang *et al.* (2011a), who demonstrated average diameters of 3.92mm and 2.1mm at the origin and distal ends of

the artery, respectively. The volume of the thrombus, assuming it is spherical, was thus calculated as follows

$$\text{Volume} = \frac{4}{3}\pi r^3 = \frac{4}{3}\pi((1.4\ X\ 10^{-3})^3) = 1.149\ X\ 10^{-8}\ m^3 = 11.49\mu L\ ,$$

with this figure matched to the *in vitro* thrombus formation under flow assay data presented in Section 4.6 (described in Section 7.2.2). Figure 7-1 shows a network diagram describing the events of the model; upon flow of blood over collagen (100μg/mL), a thrombus grows at rate k_T. This thrombus growth is inhibited by quercetin (Q), tamarixetin (T_R) and isorhamnetin (I) at rates k_{TQ}, k_{TTR} and k_{TI}, respectively, with concentrations input as a constant in the model. A term is also included to describe the natural breakdown of the thrombus, d_T. The change over time in T, the thrombus size, is thus

$$\frac{dT}{dt} = k_T - k_{TQ}QT - k_{TT_R}T_RT - k_{TI}IT - d_TT\ , \qquad (3.1)$$

with

$$T(0) = 0\ , \qquad (3.2)$$

where equation (3.1) describes the change in the volume (μL) of the thrombus over time. An initial value for T of 0 (equation 3.2) represents a lack of thrombus until initiation, representing the initial quiescent state. Table 7-1 describes the single variable used in the FLAT model. The assumptions of the FLAT model are: at resting state (i.e. in the initial conditions of the model) there is zero thrombus, the growth of the thrombus occurs at a constant rate (i.e. k_T), the thrombogenic substance (collagen 100μg/mL) is available at this concentration throughout the experiment, flavonoid is available at the full concentration throughout the experimental period and is uncontaminated, natural thrombus breakdown occurs at a constant rate throughout the experimental period (d_T), the inhibition of thrombus formation by flavonoids occurs at a constant rate (k_{TQ}, k_{TTR} and k_{TI}) (parameters of this model are described in Table 7-2). Another assumption of this model is that, through data conversion to

thrombus size in a coronary artery, the model represents an *in vivo* thrombogenic event. Upon model solving and simulation (using ode45, MATLAB (MathWorks, 2015)), the FLAT model predicts the thrombus size (μL) over the 10 minute experimental period; a 10 minute period was chosen to allow direct comparison to, and parameterisation using, the *in vitro* thrombus formation under flow data presented in Section 4.6. Through comparison with this experimental data the model was refined and parameterised, as described in Section 7.2.3.

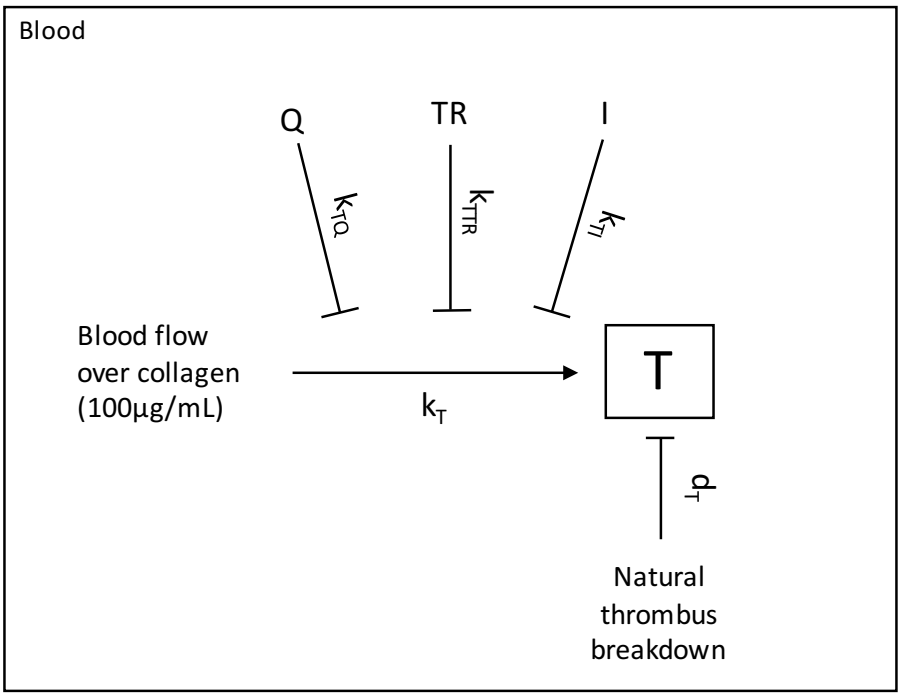

Figure 7-1 A network diagram for the FLAT model

A network diagram of the FLAT model, with the only variable of thrombus size represented by '*T*', and the model parameters placed next to the appropriate arrow. Upon flow of blood over collagen (100µg/mL), a thrombus will develop (*T*) in an irreversible process at rate k_T, which is inhibited by quercetin (*Q*), tamarixetin (*TR*), and isorhamnetin (*I*), at the rates indicated in the diagram. The thrombus is also subject to natural (i.e. not due to inhibitors) breakdown, represented by rate d_T. A full description of the variables and parameters are found in Tables 7-1 and 7-2, respectively.

Table 7-1 A description of the single FLAT model variable

Variable	Description	Units	Initial condition	Source
T	Thrombus size	Microliters (μL)	0	Estimated

7.2.2 Parameter estimation and fitting of the FLAT model

The next step in the development of the FLAT model was to estimate and fit the parameters. Due to a lack of comprehensive *in vivo* data, FLAT model simulations were fitted to the *in vitro* thrombus formation under flow data presented in Section 4.6 with some modification; the fluorescence data gathered from thrombus formation *in vitro* experimentation was converted to thrombus size according to the thrombus volume calculated above, with fluorescence values in the absence of flavonoid (i.e. vehicle) *in vitro* considered as 100% (uninhibited) thrombus volume, i.e. 11.49μL. In short, the data was converted from normalised mean fluorescence intensity to thrombus size, by dividing the data to give 11.49 (μL) at the 600s endpoint in vehicle-treated samples (treated as 100% thrombus formation) and converting the flavonoid treated data according to this. This allowed the percentage inhibition by flavonoids to remain at the same level whilst converting the data to values that could be used to fit the model to, and were assumed to represent a thrombogenic scenario *in vivo*. The standard deviation values were also converted accordingly, and this data is used throughout when comparing FLAT model simulations to *in vitro* experimental data. To gather data *in vitro* or *in vivo* of actual thrombus size was not feasible, and therefore the use of the converted *in vitro* data is a limitation of this model.

The value of k_T was arbitrarily set to 5×10^{-2} s^{-1}, and was initially tested without the inclusion of a term describing the natural (i.e. not due to flavonoid) breakdown of the thrombus. The simulation of this model resulted in linear growth of the thrombus, which the *in vitro* data did not represent; instead there is an initial period of slightly faster growth, which then slows slightly towards the end, which can be seen in Figure 7-2. As a result of this, a term was introduced to describe the natural breakdown of the thrombus, d_T, which can be seen acting on the developing thrombus in equation (3.1). The introduction of this term is considered appropriate as it is observed in the *in vitro* thrombus formation under flow and *in vivo* thrombosis data presented in this study that during the development of thrombi in vehicle-treated conditions, platelets build up in the thrombi but can also slough off, with the thrombi reaching an approximate maximal size; *in vitro* experimentation showed that this approximate maximal size

can be relatively stable over time. The introduction of a natural breakdown term, d_T, is also supported by the literature, which describes thrombus breakdown as a key mechanism through which thrombus size may be limited *in vivo* (Ciccone, 2015). The introduction of this term gave kinetics of thrombus formation which more closely matched the data, and so the model profile of thrombus formation was fitted to the *in vitro* vehicle-treated data. This fitting process was done by eye, matching the model simulation profile as closely as possible to the data, dissecting the error bars, with the simultaneous modification of the values of k_T and d_T to get the best fit. This fitting process gave the best fit values of 3.288×10^{-2} s^{-1} for k_T and 2×10^{-3} s^{-1} for d_T; natural thrombus breakdown therefore occurs at a rate around one order of magnitude lower than the growth of the thrombus (summarised in Table 7-2). The best fit model profile of thrombus formation is compared to the data in Figure 7-2. Modelling the effects of quercetin, tamarixetin and isorhamnetin individually on thrombus formation was the next step in the development of the FLAT model.

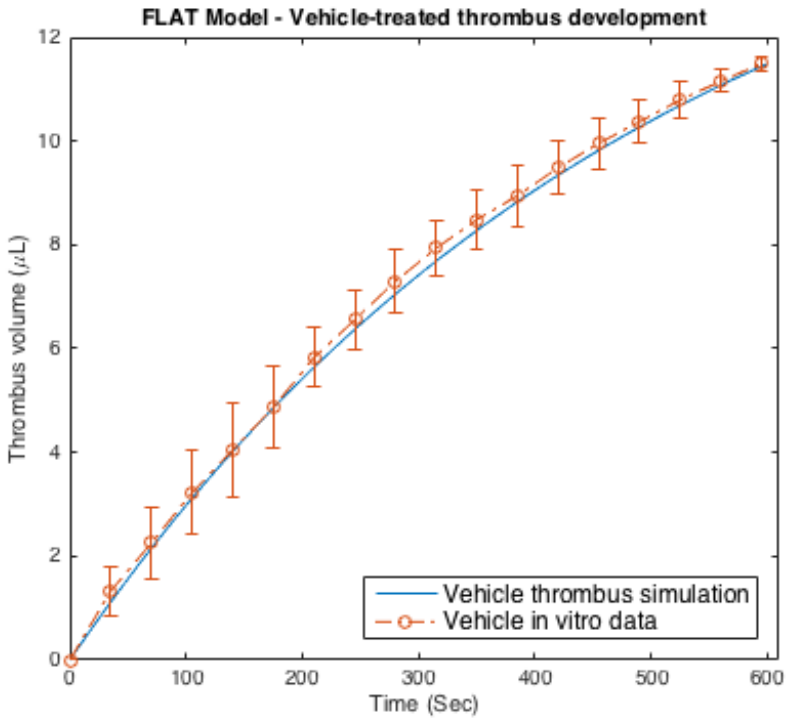

Figure 7-2 FLAT model thrombus formation profile compared to *in vitro* thrombus formation under flow data

The FLAT model profile of thrombus formation (solid blue line) compared to experimental *in vitro* thrombus formation under flow data (blood flow at $500s^{-1}$ over collagen 100µg/mL)(orange dash-dot line). The model accurately describes the kinetics of thrombus formation across the 600s experimental period, with the model profile dissecting the error bars of the *in vitro* data. *In vitro* thrombus formation under flow data is presented as mean ± standard deviation, converted as described in Section 6.4.2, N=3. The model simulation uses parameter values described in Table 7-2.

7.2.3 Modelling the effects of quercetin, tamarixetin and isorhamnetin in the FLAT model

Now that the vehicle-treated profile of thrombus formation in the FLAT model had been fitted to *in vitro* data, the effects of quercetin and its methylated metabolites were modelled. This was done through the same process as fitting the vehicle-treated data, fitting by eye to the individual flavonoid-treated *in vitro* data, converted as described in Section 7.2.3. Inputting a value of 10μM into the individual Q, T or I parameters, the rates of inhibition (k_{TQ}, k_{TTR} and k_{TI}) were initially arbitrarily set at $0.05(\mu Ms)^{-1}$, and lowered to fit to the data. A limitation here is that due to the high cost (both financially and temporally) of performing the *in vitro* thrombus formation under flow assay, data was only gathered for one concentration - 10μM – chosen to represent a high physiologically achievable concentration. Initially, fitting was performed by altering only the rates of inhibition (keeping k_T and d_T the same as in vehicle-treated samples); however, this resulted in a relatively poor fit to the data, with the model simulating thrombi initially forming faster than the data, and slowing toward the end, falling below the endpoint values of the data. It was thus hypothesised that removal of the natural breakdown rate (i.e. $d_T = 0$) may fix this. This was tested and found to be the case; when k_T was altered to account for the absence of d_T (i.e. linear growth to an endpoint of 11.49μL), alteration of the values of k_{TQ} ($1.8\text{x}10^{-4}$ $(\mu Ms)^{-1}$), k_{TTR} ($3.16\text{x}10^{-4}$ $(\mu Ms)^{-1}$) and k_{TI} ($1.82\text{x}10^{-4}$ $(\mu Ms)^{-1}$) allowed a close fit to the data. These best fit values are summarised in Table 7-2, with FLAT best fit model profiles compared to the *in vitro* data in Figure 7-3. Thus, in this model, it can be assumed that natural decay is an important factor in the absence of flavonoid; when flavonoid is present, however, its effects greatly exceed the effect of natural thrombus breakdown, which is thus neglected (at least at the relatively high concentration of 10μM). The similarity of the k_{TQ} and k_{TI} values reflect the fact that the levels of inhibition achieved by these flavonoids was very similar; 39 and 41% average inhibition of thrombus formation, respectively. The higher (effectively double) value of k_{TTR} represents the higher level of inhibition *in vitro* by tamarixetin – an average of 55% inhibition of thrombus formation.

The FLAT model, at this stage, could now predict the effect of any individual concentration of quercetin, tamarixetin and isorhamnetin on thrombus formation, as well as predict the effects of combinations of quercetin and its methylated metabolites. The prioritisation of the development of the PKPD model, and the cost of performing the *in vitro* thrombus formation assay, prevented testing of any of these predictions.

One observation from the FLAT model, as well as from the *in vitro* data, is that the thrombi do not appear to reach a plateau at the 600 second experimental endpoint, instead continuing to increase in size. The FLAT model was therefore altered to model thrombus formation over a 1 hour period, in order to investigate the potential for true inhibition versus merely a delay in thrombus formation by quercetin and its methylated metabolites.

Table 7-2 FLAT model parameters and their best fit values. A description of the parameters of the FLAT model, their units, and their best fit values for the modelling of thrombus formation and its inhibition by quercetin, tamarixetin and isorhamnetin. Best fit values were obtained by fitting the FLAT model profiles of thrombus growth to *in vitro* thrombus formation under flow data as described in Section 7.2.3. N/A indicates the lack of best fit for the flavonoid concentrations, as they can take any value in the model.

Parameter	Description	Units	Best fit value
k_T	Thrombus growth rate	s^{-1}	3.288×10^{-2} without flavonoid
			1.915×10^{-2} with flavonoid
d_T	Thrombus breakdown rate	s^{-1}	2×10^{-3} without flavonoid
			0 with flavonoid
Q	Quercetin concentration	μM	N/A
TR	Tamarixetin concentration	μM	N/A
I	Isorhamnetin concentration	μM	N/A
k_{TQ}	Rate of inhibition of thrombus growth by quercetin	$(\mu Ms)^{-1}$	1.8×10^{-4}
k_{TTR}	Rate of inhibition of thrombus growth by tamarixetin	$(\mu Ms)^{-1}$	3.16×10^{-4}
k_{TI}	Rate of inhibition of thrombus growth by isorhamnetin	$(\mu Ms)^{-1}$	1.82×10^{-4}

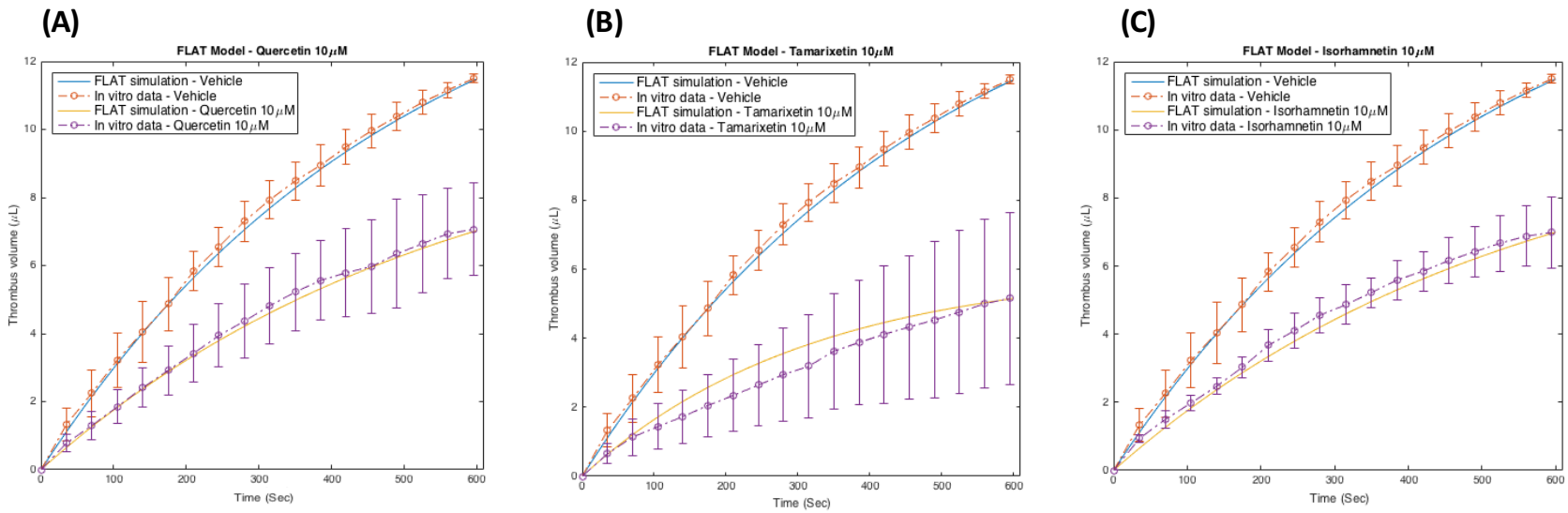

Figure 7-3 FLAT model thrombus formation profiles compared to *in vitro* thrombus formation under flow data inhibited by flavonoids

The FLAT model profiles of thrombus formation (yellow solid lines) compared to experimental *in vitro* thrombus formation under flow data inhibited by quercetin (A), tamarixetin (B) and isorhamnetin (C) (dash-dot purple lines with circles). The FLAT model profile of vehicle-treated thrombus formation (solid blue line) and vehicle-treated *in vitro* data (orange dash-dot line) are included for reference. The model accurately describes the kinetics of thrombus formation across the entire 600 second experimental period, with model simulations of flavonoid-inhibited thrombus formation (as well as vehicle-treated thrombus formation) consistently passing through the error bars of the *in vitro* data. *In vitro* thrombus formation under flow data is presented as mean ± standard deviation, converted as described in Section 6.4.2, N=3. Model simulations (solid lines) use parameter values described in Table 7-2.

7.2.4 Modelling the effects of quercetin and its methylated metabolites on thrombus formation over an extended period

The observation from the FLAT model and from the *in vitro* data that thrombi continue to increase in size up to 600 seconds led to the modification of the FLAT model to simulate thrombus formation over an extended period of one hour. All parameter values were kept the same as in Table 7-2; the only change was the time over which the simulations were run. Up to 10 minutes, therefore, the simulations match the data as shown in Figure 7-3, with the profiles of thrombus formation from 11-60 minutes providing novel predictions.

Running the FLAT model to simulate thrombus formation over a period of 1 hour gives the profiles shown in Figure 7-4. At 60 minutes, the vehicle-treated thrombus has a predicted volume of 16.43μL, implying that, at the 10-minute experimental period, only 70% of thrombus formation has occurred (again, it must be kept in mind the conversion from normalised mean fluorescence intensity). This could be tested in future work through the running of an *in vitro* thrombus formation under flow assay over a 60-minute period and comparing thrombi development from 10 to 60 minutes. Treating the 16.43μL as 100% thrombus size, at 60 minutes, quercetin, isorhamnetin and tamarixetin (10μM) inhibit thrombus formation by 35%, 36% and 63%, respectively. This is compared to the *in vitro* data which, after 10 minutes, displayed 39%, 41% and 55% inhibition by quercetin, isorhamnetin and tamarixetin, respectively. Thus, the model predicts relatively similar levels of inhibition over 1 hour compared to 10 minutes, with slightly less inhibition by quercetin and isorhamnetin as the thrombi continue to grow from 10 to 60 minutes. The model predicts an increased inhibition by tamarixetin over 60 minutes compared to 10 minutes (8% more inhibition); this is due to the vehicle-treated thrombi continuing to grow over the 60-minute period (with a peak of 16.44μL at 68 minutes), whereas tamarixetin-treated thrombi reach a peak size of 6.06μL at 49 minutes. Whilst peak thrombus sizes are reached after 60 minutes for vehicle, quercetin and isorhamnetin-treated samples, the difference between peak size and size at 60 minutes is 0.01-0.02μL, and so simulation over 60 minutes is

considered sufficient. These novel predictions could be tested via *in vitro* thrombus formation under flow assay experimentation over a 60-minute period. However, this is not particularly feasible due to the nature of the assay, and therefore demonstrates an advantage of mathematical modelling; the *in silico* investigation into a biological phenomenon that does not easily facilitate *in vitro* 'wet' experimentation. One limitation of this model is that it was developed according to, and was fitted to, thrombus formation data gathered *in vitro,* not *in vivo. In vivo* data has been gathered in this study, and is presented in Section 5.4. The data presented in Figures 5-5 and 5-6 show that overall, in vehicle-treated thrombi, thrombi reach a peak size (represented by the median integrated fluorescence (AU)) between approximately 150-175 seconds, and then decrease in size over the remainder of the experimental period as platelets slough off the thrombi and the thrombus contracts. The *in vivo* data agree with the *in vitro* data, however, in that treatment with flavonoid reduces the maximal thrombi size. Limited *in vivo* data prevented the development of a model fitted to this data, and so future work could focus on increased *in vivo* experimentation and the subsequent development of a new model.

The ability of the FLAT model to now simulate thrombus formation over 1 hour led to *in silico* experimentation; as an example, an investigation into the effects of quercetin and tamarixetin on thrombus formation at 5μM, individually and in combination. The results of this *in silico* experiment is displayed in Figure 7-5. At 10 minutes, the time point used in *in vitro* thrombus formation under flow experimentation, quercetin would appear inhibitory, with 23% inhibition at 10 minutes. However, at the 60-minute endpoint, quercetin 5μM treatment is not inhibitory, displaying a 24% increase in thrombus size compared to vehicle control. This increase in thrombus size, as opposed to merely 0% inhibition, could imply that at lower flavonoid concentrations the contribution of natural thrombus breakdown (d_T) to overall thrombus size is not completely neglected, as it is the parameter of natural thrombus breakdown that limits the size of the vehicle-treated thrombi. At 10 minutes, tamarixetin 5μM inhibits thrombus formation by 35%, and at the 60-minute simulation endpoint, inhibits by 26%. Thus, the model predicts that overall, at 5μM, tamarixetin is inhibitory whereas quercetin is not. Whilst this was not tested *in vitro,* it can be compared to data in the literature; this is examined in the

discussion section of this Chapter. Dual treatment with quercetin and tamarixetin at 5μM was predicted by the FLAT model to inhibit thrombus formation at 60 minutes by 53%; a more than additive, potentially synergistic effect when considering the individual effects of quercetin and tamarixetin predicted by the FLAT model. A more-than-additive effect of dual treatment with quercetin and isorhamnetin at 5μM each is also predicted by the FLAT model; individually, 5μM quercetin or isorhamnetin do not inhibit thrombus formation, but when combined, 36% inhibition is predicted at 60 minutes. Thus, a more than additive, potentially synergistic interaction between quercetin and tamarixetin, and quercetin and isorhamnetin, is observed in *in vitro* plate based aggregometry data as well as being represented in the FLAGG model (as described in Section 6.3), and is also predicted by the FLAT model. Dual treatment with isorhamnetin and tamarixetin is not considered here due to a lack of a more-than-additive interaction in the FLAGG model. Another use of the FLAT model is to predict the minimal individual concentrations of quercetin and isorhamnetin that would have an inhibitory effect on thrombus formation, as, unlike tamarixetin, they are not predicted to be inhibitory at 5μM. These individual minimal inhibitory concentrations are predicted to be 6.4μM for both quercetin and isorhamnetin (with a minimal inhibitory concentration prediction of 3.7μM for tamarixetin); these predictions could be tested in future work.

The work presented in this Chapter so far has described a model of thrombus formation *in vivo* (FLAT model), which has been parameterised and fitted to *in vitro* data gathered in this study. This model can simulate the effects of quercetin, tamarixetin and isorhamnetin, individually and in combination, at any concentrations, on thrombus formation. The next step in the development of the mathematical modelling work was to modify this model to account for the *in vivo* metabolism of quercetin. This was done through the addition of new terms and equations to describe quercetin administration, metabolism and elimination, leading to the development of a pharmacokinetic/pharmacodynamic (PK/PD) model of quercetin's anti-thrombotic effect, presented next.

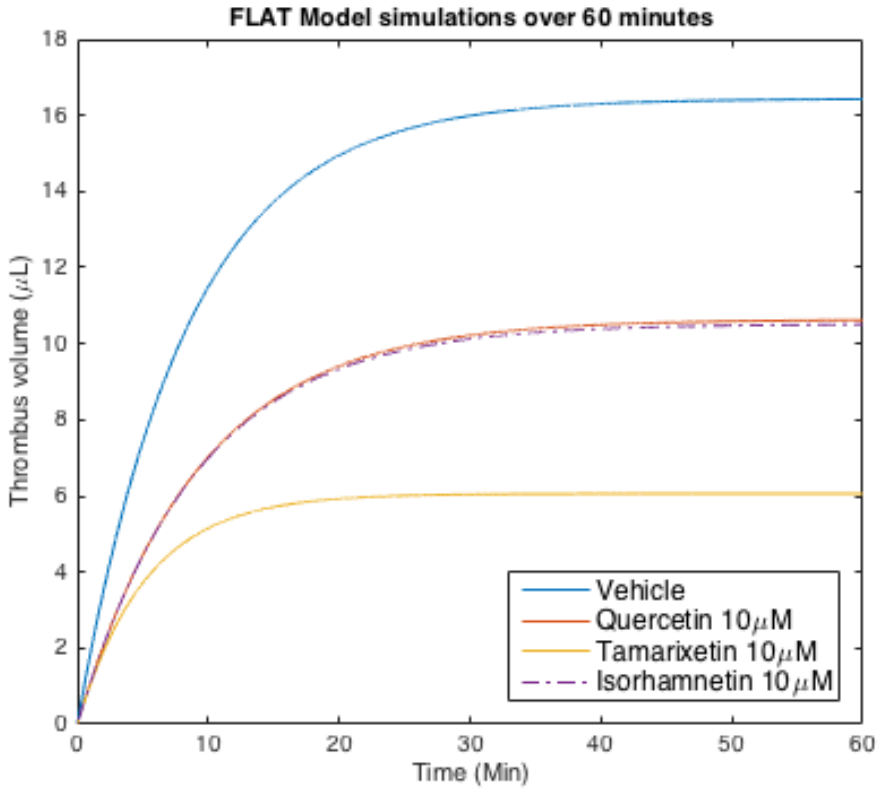

Figure 7-4 FLAT model simulations for the inhibition of thrombus formation by quercetin and its methylated metabolites at 10µM over one hour

The FLAT model profiles of thrombus formation after the extension of the model to simulate thrombus formation over a 60 minute period. The vehicle-treated thrombus (solid blue line) continues to grow marginally over and past the 60 minute period, as do the quercetin and isorhamnetin-treated thrombi (solid orange line and dash-dot purple line, respectively). The tamarixetin-treated thrombus, however, reaches a peak size of 6.06µL at 49 minutes. At 60 minutes, this translates into 35%, 36% and 63% inhibition by quercetin, isorhamnetin and tamarixetin, respectively.

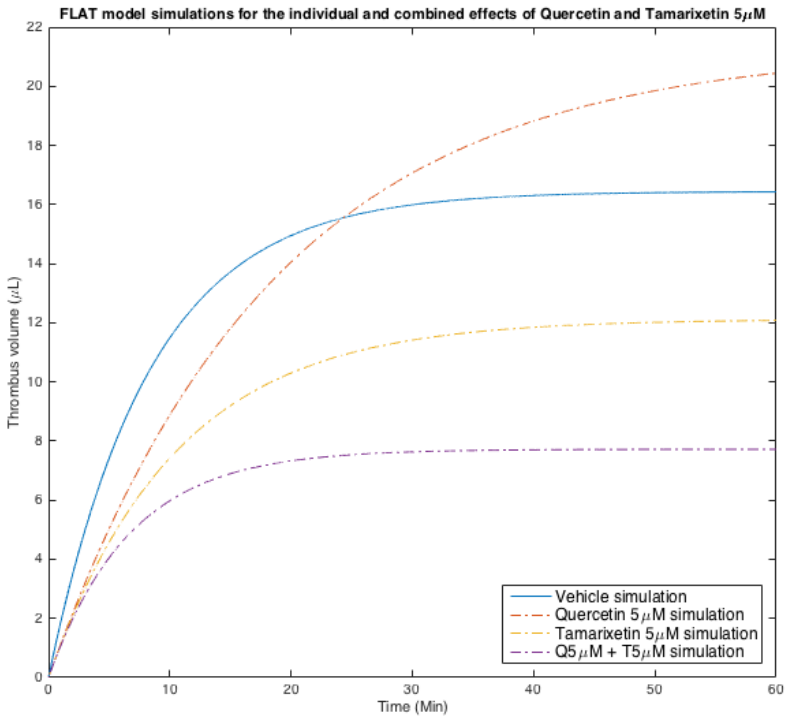

Figure 7-5 FLAT model simulations for the inhibition of thrombus formation by quercetin and tamarixetin, individually and in combination, at 5μM

The FLAT model was modified to simulate thrombus formation over one hour as described in Section 6.4.4, and the effects of quercetin 5μM (orange dash-dot line), tamarixetin 5μM (yellow dash-dot line) and quercetin + tamarixetin (5μM each flavonoid, purple dash-dot line) were compared to vehicle-treated thrombi (solid blue line). At 10 minutes, the *in vitro* experimentation time point, all treatments would appear inhibitory. Over 60 minutes, however, the model predicts that treatment with quercetin 5μM would not inhibit thrombus formation, whilst tamarixetin and quercetin + tamarixetin would prove inhibitory. Dual treatment with quercetin + tamarixetin is predicted to have a synergistic effect on the inhibition of thrombus formation, discussed in the text. Model simulations presented here used parameter values described in Table 7-2. Q, quercetin; T, tamarixetin.

7.3 A pharmacokinetic/pharmacodynamic model of the anti-thrombotic effect of quercetin

7.3.1 Description of the PK/PD model

The FLAT model presented above represents an accurate, data-fitted model of thrombus formation *in vivo*. One limitation of this, however, is that the flavonoid concentrations are assumed to be static; *in vivo,* they will be dynamic due to metabolism and elimination processes. The FLAT model was therefore developed into a pharmacokinetic/pharmacodynamic (PK/PD) model describing the administration, metabolism and elimination of quercetin and the associated dynamic anti-thrombotic effects. This was modelled over a time scale of one week, to represent a prolonged period of quercetin supplementation.

The ODE describing thrombus formation and its inhibition by quercetin, tamarixetin and isorhamnetin was kept the same in this model as it was in the FLAT model. As such, equation (3.1) describes this process (reiterated below (equation (4.4)) for clarity). The PK/PD model therefore also represents the formation of a thrombus under arterial flow ($500s^{-1}$ shear rate) conditions. The variable '*T'* again represents the thrombus size. This was combined with the incorporation of ODEs describing the pharmacokinetics of quercetin; a quercetin dose is introduced at specified time points (through a term, *W*) in the model, and metabolism and elimination occurs as described in the equations below. A network diagram describing the events of the model is shown in Figure 7-1 (as thrombus formation and its inhibition by flavonoid occurs as in the FLAT model): upon flow of blood over collagen (100μg/mL), a thrombus grows at rate k_T. This thrombus growth is inhibited by quercetin, tamarixetin and isorhamnetin at rates k_{TQ}, k_{TTR} and k_{TI}, respectively, with the concentrations of these flavonoids defined by the processes of metabolism of quercetin (which is introduced at defined time points in the model) to tamarixetin and isorhamnetin (m_{TR} and m_{TI}, respectively), as well as the elimination of quercetin, tamarixetin and isorhamnetin (u_Q, u_{TR} and u_I, respectively). The PK/PD model thus adds three new variables; 'Q', the concentration of quercetin, 'T_R', the concentration of tamarixetin, and 'I',

the concentration of isorhamnetin in blood. A term is also included to describe the natural breakdown of the thrombus, d_T. The change over time in Q, T_R, I and T are thus

$$\frac{dQ}{dt} = -m_{T_R}Q - m_I Q - u_Q Q + W \ , \qquad (4.1)$$

$$\frac{dT_R}{dt} = m_{T_R}Q - \ u_{T_R}T_R \ , \qquad (4.2)$$

$$\frac{dI}{dt} = m_I Q - \ u_I I \ , \qquad (4.3)$$

$$\frac{dT}{dt} = k_T - k_{TQ}QT - k_{TT_R}T_R T - k_{TI}IT - d_T T \ , \qquad (4.4)$$

with

$$Q(0) = \ Q_0, \qquad T_R(0) = \ 0, \qquad I(0) = 0, \qquad T(0) = 0 \ , \qquad (4.5)$$

where W is the source of quercetin, which is given by

$$W = \begin{cases} 0, & 0 \le t < t_1 \\ W_0, & t_1 \le t < t_2 \\ 0, & t_2 \le t < t_3 \end{cases} \qquad (4.6)$$

where W is the source of quercetin (μM) introduced at specified time points. Equations (4.1-4.3) describe the change over time in the concentrations of quercetin, tamarixetin and isorhamnetin (μM), respectively, and equation (4.4) describes the change over time in the thrombus volume (μL). Equation (4.5) describes the initial conditions of the model, where $Q(0) = Q_0$, with Q_0 being determined by W, the source of quercetin, described in equation (4.6). In this model, therefore, quercetin addition is described through a source term (W), with quercetin introduced at specific time points, not as an initial condition (which is the focus of future development of the model). Equations describing the absorption

of quercetin into the blood from other compartments (e.g. small intestine) were not included in this model due to the time constraints of adding another compartment and associated equations to the model; future work will focus on including these. Table 7-3 describes the variables of the PK/PD model. The assumptions of the PK/PD model are: at resting state (i.e. in the initial conditions of the model) there is zero thrombus, the growth of the thrombus occurs at a constant rate (i.e. k_T), flavonoid is uncontaminated, natural thrombus breakdown occurs at a constant rate throughout the experimental period (d_T), the inhibition of thrombus formation by flavonoids occurs at a constant rate (k_{TQ}, k_{TTR} and k_{TI}) (proportional to flavonoid concentration), metabolism and elimination of flavonoids occurs at a constant rate (proportional to flavonoid concentration), introduction of flavonoid in the model results in immediate metabolism of quercetin-4'-O-β-D-glucoside (discussed in Section 7.3.2) and availability of quercetin in the blood to inhibit thrombus formation. Another assumption of this model is that, through the use of the equation describing thrombus formation from the FLAT model (equation 4.4), the model represents an *in vivo* thrombogenic event. There are several assumptions regarding the flavonoids themselves; many studies in the literature have measured plasma quercetin after hydrolysis, and so conjugates such as sulphates and glucuronides are not accounted for, instead included in this total figure. It is therefore assumed that the 'Q' population in this model represents the total plasma quercetin, including these conjugates, and that they will act with the anti-platelet potency of quercetin aglycone. Further development of this model combined with increasing sensitivity and improved standards for metabolite analysis can account for these metabolites, with further *in vitro* work elucidating their anti-platelet effect to separate out their contributions in the PK/PD model. The same assumption is made for isorhamnetin and tamarixetin. Upon model solving and simulation (using ode45, MATLAB (MathWorks, 2015)), the PK/PD model predicts the concentrations of quercetin, tamarixetin and isorhamnetin over time, as well as thrombus size upon initiation of thrombus growth. Through comparison with *in vitro* data and the literature, the model was parameterised, as described in Section 7.3.2.

Table 7-3 A description of the PK/PD model variables

Variable	Description	Units	Initial condition	Source
T	Thrombus size	Microliters (μL)	0	Estimated
Q	Quercetin concentration	Micromolar (μM)	0	Estimated
T_R	Tamarixetin concentration	Micromolar (μM)	0	Estimated
I	Isorhamnetin concentration	Micromolar (μM)	0	Estimated

7.3.2 Parameter estimation and fitting

The next step in the development of the PK/PD model was to estimate and fit the parameters. The rate of thrombus growth (k_T) and natural thrombus breakdown (d_T) in the absence of flavonoid were known from parameterisation of the FLAT model. Pharmacokinetic parameters were fit primarily to the study by Hubbard *et al.* (2004). This study measured the plasma quercetin, tamarixetin and isorhamnetin concentrations in volunteers over a 32-hour period following ingestion of either 150mg or 300mg of quercetin-4'-O-β-D-glucoside supplement. Parameter fitting to this study's data was done primarily due to the fact that quercetin, tamarixetin and isorhamnetin are the three primary flavonoids used in the work presented here, and the levels of these flavonoids were quantified by Hubbard *et al.* (2004). Upon supplementation with 150mg and 300mg quercetin-4'-O-β-D-glucoside, plasma quercetin concentrations reach peak values (C_{max}) of 4.66 and 9.72μM, respectively. This was rounded to 5 and 10μM for the sake of simplicity. Therefore, throughout the PK/PD model presented here, a 5μM dose corresponds to a 150mg dose and a 10μM dose corresponds to a 300mg dose of quercetin-4'-O-β-D-glucoside, etc. For the sake of simplicity, doses are referred to as μM per day (μM/d).

The predicted profiles of metabolite accumulation and elimination from the PK/PD model were primarily fitted to the data from the above study, which observed a tamarixetin C_{max} of 0.54μM after 45 minutes and an isorhamnetin C_{max} of 0.44μM at 30 minutes, after 300mg supplementation (10μM total quercetin). During this fitting process, the observation from Graefe *et al.* (2001) that the total isorhamnetin concentration (the methylated metabolite, after conjugate hydrolysis) was approximately one-tenth that of quercetin was also considered. Thus, a peak tamarixetin and isorhamnetin concentration of one tenth to one twentieth of peak quercetin concentration was considered appropriate. The value of u_Q, the rate of quercetin elimination, was set to zero. This was due to an observation by Chen *et al.* (2005), who observed in pharmacokinetic studies that the loss of quercetin is primarily through metabolism, with less than 1% excreted in urine and bile. Indeed, in their pharmacokinetic study, the excretion of unchanged quercetin was assumed to equal zero, and that assumption is also

made here (with the parameter kept in the model to allow future experimentation altering this parameter if required). This data fitting process resulted in parameter values stated in Table 7-4, with the pharmacokinetics of a 10μM quercetin dose shown in Figure 7-6; quercetin levels peak immediately at 10μM, with tamarixetin reaching a C_{max} of 0.93μM at 45.5 minutes, and isorhamnetin reaching a C_{max} of 0.86μM at 32 minutes.

The values for the parameters describing thrombus formation and inhibition in the presence of flavonoids was initially kept the same as in the FLAT model (Table 7-2), with the natural thrombus breakdown term removed when flavonoids were present. However, upon simulation of the PK/PD model, it became clear that this natural thrombus breakdown parameter needed to be included. As can be seen in Figure 7-5, at lower flavonoid concentrations, the size of the thrombus can continue to increase up to and beyond the 1 hour time-point. It was hypothesised previously (in Section 7.2.4) that at lower flavonoid concentrations, the contribution of natural thrombus breakdown (d_T) to overall thrombus size is not completely neglected, as it is the parameter of natural thrombus breakdown that limits the size of the vehicle-treated thrombi. When flavonoid concentrations in the PK/PD model were lowered as metabolism and elimination occurred (beginning at below approximately 3.8μM total flavonoid), the thrombus grew far beyond feasible limits, and so the model was re-fitted to include natural decay in the presence of flavonoids. This was done through fitting the *in vitro* thrombus formation under flow data to the FLAT model, keeping $k_T = 3.288 \times 10^{-2}\ s^{-1}$ and $d_T = 2 \times 10^{-3}\ s^{-1}$ (the values in the absence of flavonoids); this gave the k_T, d_T, k_{TQ}, k_{TTR} and k_{TI} parameter values stated in Table 7-4. Thus, the maximum thrombus size in the PK/PD model was set to the maximum, steady state size reached in the absence of flavonoids (with the associated assumption that flavonoid treatment could not increase thrombus size). The PK/PD model could now be used to investigate the effects of different quercetin dosing regimens as well as the effects of altering pharmacokinetics to potentially enhance the anti-thrombotic effect.

Table 7-4 PK/PD model parameters and their best fit values. A description of the parameters of the PK/PD model, their units, and their best fit values. Best fit values were obtained by fitting the PK/PD model pharmacokinetic profiles of tamarixetin and isorhamnetin to the study by Hubbard *et. al.* (2004), and fitting thrombus formation and inhibition parameters to *in vitro* thrombus formation under flow data, as described in Section 7.3.2

Parameter	Description	Units	Best fit value
m_{TR}	Rate of metabolic conversion of quercetin to tamarixetin	s^{-1}	9.5×10^{-5}
m_I	Rate of metabolic conversion of quercetin to isorhamnetin	s^{-1}	1.35×10^{-4}
u_Q	Rate of quercetin elimination	s^{-1}	0
u_{TR}	Rate of tamarixetin elimination	s^{-1}	5.4×10^{-4}
u_I	Rate of isorhamnetin elimination	s^{-1}	1×10^{-3}
k_T	Rate of thrombus growth	s^{-1}	3.288×10^{-2}
d_T	Rate of natural thrombus breakdown	s^{-1}	2×10^{-3}
k_{TQ}	Rate of inhibition of thrombus growth by quercetin	$(\mu Ms)^{-1}$	2.3×10^{-4}
k_{TTR}	Rate of inhibition of thrombus growth by tamarixetin	$(\mu Ms)^{-1}$	4.25×10^{-4}
k_{TI}	Rate of inhibition of thrombus growth by isorhamnetin	$(\mu Ms)^{-1}$	2.375×10^{-4}

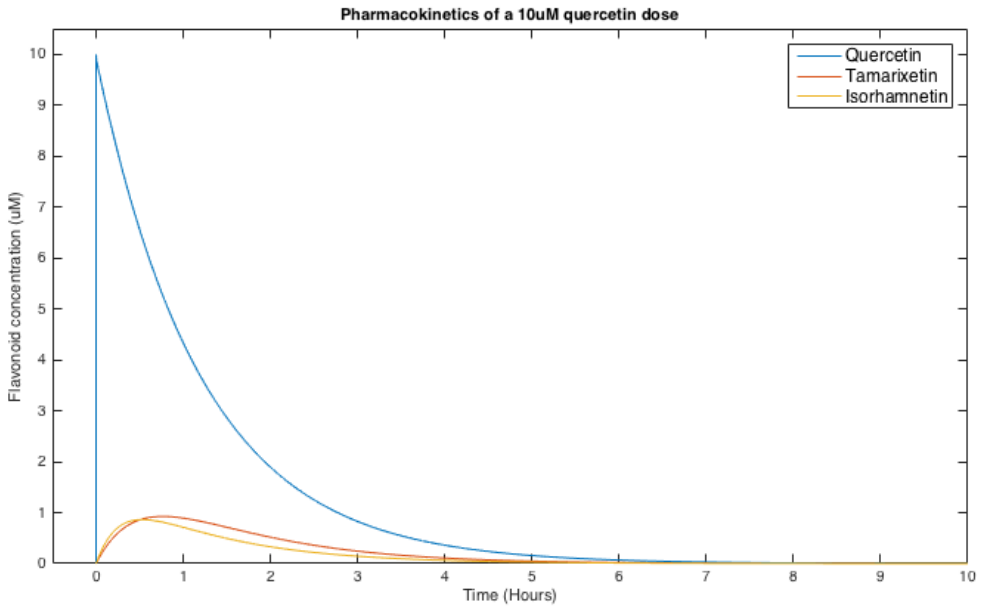

Figure 7-6 Pharmacokinetics of a 10µM quercetin dose in the PK/PD model

The pharmacokinetic fate of a quercetin dose (10µM) in the PK/PD model. Quercetin levels (blue line) immediately reach C_{max} (10µM) after the dose is administered in the model, reaching a low, near-zero 'basal' level (defined here as <0.05µM) at 384 minutes. Tamarixetin levels achieve a C_{max} of 0.93µM at 45.5 minutes, reaching a basal level at 298 minutes. Isorhamnetin (yellow line) achieves a C_{max} of 0.86µM at 32 minutes, reaching a basal level at 257 minutes.

7.3.3 PK/PD model simulations of once-per-day quercetin dosing regimens under normal flavonoid metabolic conditions

Now that the PK/PD model was parameterised and fitted, the next step was to run *in silico* experiments simulating different quercetin dosing regimens, to investigate which dose and which dosing frequency resulted in optimal anti-thrombotic effect.

Initially, a simple dosing regimen of once per day was investigated, with thrombus formation arbitrarily initiated in the PK/PD model at the beginning of day 2. Doses of 5, 10, 20 and 50μM per day were simulated, corresponding to daily quercetin-4'-O-β-D-glucoside supplementation of 150, 300, 600 and 1500mg, respectively. A phase 1 study by Ferry *et al.* (1996) demonstrated a lack of toxicity with intravenous quercetin doses up to approximately 2.5g, with an approximately 3.5g resulting in renal toxicity. Thus, doses under 2.5g were considered acceptable here. It must be noted, however, that these doses were administered at weekly intervals; the safety and tolerance of daily doses at this level must therefore be investigated in future work. Figure 7-7 shows the results of these simulations. Figure 7-7A shows the pharmacokinetics of daily quercetin dosing over a week-long period; as can be seen, the maximum concentration of quercetin differs slightly over the different days, with a range of 10.12μM on day 1, to 9.279μM on day 3. This is a limitation due to the temporal resolution of the running of the model simulations with quercetin being introduced according to the source term *W*. However, the C_{max} values from day to day are unlikely to be identical *in vivo*, with factors such as intestinal microbiota and concomitant drugs affecting the absorption and metabolism process, and with other factors such as diet also potentially affecting plasma concentrations (Beatty *et al.*, 2000; Erlund *et al.*, 2006; Wu *et al.*, 2011; Nishimuro *et al.*, 2015; Marin *et al.*, 2015). This was thus considered acceptable, and could be representative of these factors. Introduction of quercetin doses as an initial condition in the model is the basis of further model development. As can be seen in Figure 7-7B, in the absence of flavonoid treatment, the thrombus is initiated at the beginning of day 2 and rapidly grows to a maximum size (16.44μL, the max thrombus size described in Section 7.2.4),

remaining at this size for the remainder of the simulation period. *In vivo,* upon reaching a maximum size, the thrombus would break down over time; this is observed in the *in vivo* data presented in Section 5.4. This is therefore a limitation of this model which could be solved in future iterations upon production of more comprehensive *in vivo* data.

The modelling of the formation of one thrombus over a week-long period allowed a 'snapshot' to be taken at any point to compare flavonoid concentration to inhibition of thrombus formation; future work could also focus on initiating multiple thrombotic events. Upon treatment with 5, 10, 20 and 50μM per day, thrombus formation can be seen to be delayed; however, thrombi eventually reach maximum size, as quercetin is metabolised, and the metabolites are eliminated (Figure 7-7B). This can be seen when comparing the pharmacokinetic (PK) model profile to the pharmacodynamic (PD) model profile; as quercetin and metabolite concentrations lower to zero, the thrombus grows to maximum size. Upon introduction of another quercetin dose, the size of the thrombus dramatically reduces, as the growth rate of the thrombus (k_T) is dwarfed by the inhibition by the flavonoids, and the change over time in thrombus size becomes a negative figure. Biologically, this could represent the breakdown, embolism, or sloughing off of platelets from the thrombus, with an associated reduction in thrombus size. Indeed, this thrombus instability was observed in Section 5.4, with isoquercetin appearing to increase thrombus instability in an *in vivo* model of arterial thrombosis. This translates to a maximal inhibitory potency at these time-points of 36, 51, 69 and 85% inhibition. Therefore, whilst during certain time periods thrombus formation would appear to be inhibited, the thrombi grew to maximum size upon treatment with these quercetin regimens, which were only able to (dose-dependently) delay thrombus formation. This raises an important consideration with respect to ex vivo studies of platelet function; whilst platelet function or thrombus formation *ex vivo* may appear inhibited at certain time points, at others there may be no effect; this highlights the importance of choosing a wide range of sampling points to account for the peaks and lows of plasma quercetin/metabolite concentration upon supplementation, to ensure anti-thrombotic effects are not overstated or indeed missed.

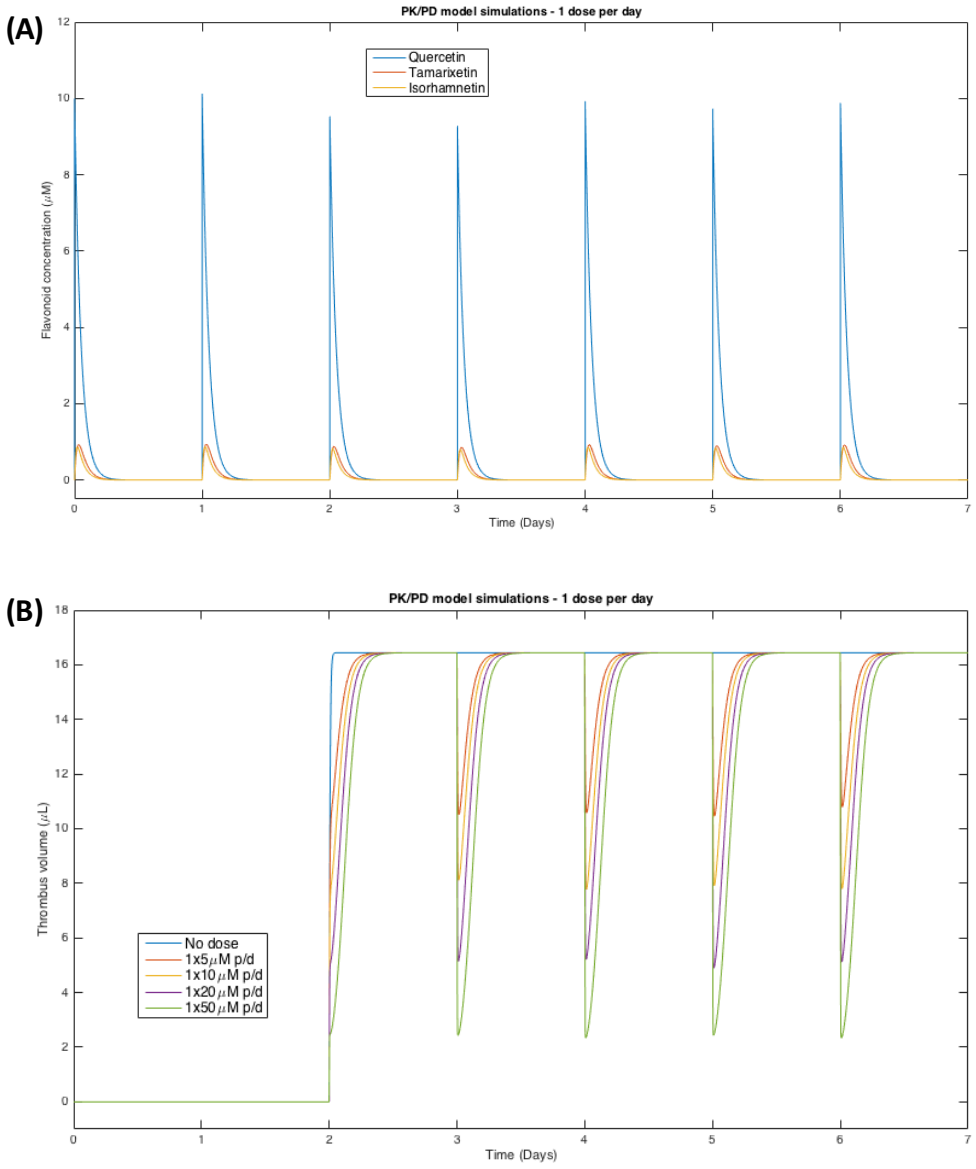

Figure 7-7 PK/PD model predictions of the anti-thrombotic effect of once per day doses of 5, 10, 20 and 50µM quercetin

The pharmacokinetics of quercetin after once per day doses of 10µM are shown in (A) as an example, and to allow comparison of quercetin (blue line), tamarixetin (orange line) and isorhamnetin (yellow line) levels with anti-thrombotic effect. The anti-thrombotic effect of once per day doses of 5µM (orange line), 10µM (yellow line), 20µM (purple line) and 50µM (green line), compared to thrombus formation in the absence of flavonoid (blue line) is shown in (B). None of the quercetin doses were able to inhibit maximum thrombus size, only delaying the formation of the thrombus. Introduction of quercetin doses from day 3 onwards reduced thrombus size initially in a dose-dependent manner, as described in the text, with thrombi growing again to maximum size. Model simulations used parameter values stated in Table 7-4. p/d, per day.

7.3.4 PK/PD model simulations of three and five-per-day quercetin dosing regimens under normal flavonoid metabolic conditions

A lack of overall anti-thrombotic effect upon once-per-day quercetin doses up to 50μM led to the hypothesis that increasing the dosing frequency may be of benefit; the effects of quercetin doses from 5-30μM, taken three times per day (corresponding to 3x150mg – 3x900mg p/d), were therefore investigated. A 3x30μM per day regimen would correspond to a total daily dose of 2.7g of quercetin, and as such may prove unsafe. However, the simulations were included here as an exercise to investigate the feasibility of inhibition upon these dosing regimens; if dosage regimens approach toxicity levels it will be stated in-text.

The results of this simulation are displayed in Figure 7-8. Upon three-per-day treatment of 5-20μM (spaced 8 hours apart), there was delay in thrombus formation; as quercetin and metabolite levels reduced, similar to the results presented in Figure 7-7, the thrombus increased in size and grew to the levels in the absence of flavonoid treatment. As seen in Figure 7-8A, despite the increased dosing frequency, quercetin levels were still able to reach basal levels before another dose was administered; this lack of flavonoid accumulation results in the lack of overall anti-thrombotic effect observed in Figure 7-8B. As a result of the increased dosing frequency, the time at which thrombi remain at maximum size is reduced compared to a once-per-day dosing regimen. Nevertheless, thrombi do grow to the maximal size in the absence of flavonoid dosing (i.e. 16.44μL), and therefore a true anti-thrombotic effect is not achieved; this is defined as an inhibition of maximum thrombus size across the entire simulation period. A 3x30μM treatment regimen resulted in such an effect; the range of inhibition (defined as the minimal and maximal percentage inhibition achieved by the treatment compared to thrombus formation without flavonoid dosing) was 1-78% (Figure 7-8B). This treatment regime therefore inhibited thrombus formation across the entire week-long simulation, as can be seen by the green line in Figure 7-8B. However, a minimal effect of 1% is very low, and a 3x30μM regimen

corresponds to a near-toxic level. The effects of reducing the dose but increasing the number of doses per day was therefore investigated.

A five-per-day dosing regimen was next simulated, to investigate whether reducing the dose but increasing the dose frequency would result in the retention of quercetin above basal levels across the simulation period; that is, whether plasma quercetin levels from one dose would be above zero at the time of administration of the next dose. This was hypothesised to be the most likely method to enhance anti-thrombotic effect, as the loss of quercetin to metabolism to levels effectively equalling zero was observed to be the mechanism through which anti-thrombotic efficacy is lost. The potential adherence to a five times per day dosing regimen must be considered; Brown and Bussell (2011) concluded that adherence to a medication regimen dropped approximately 10% per additional daily dose. 5 doses per day at 5μM and 10μM per dose were simulated, corresponding to a total daily intake of 750mg and 1.5g, respectively. 5x5μM doses per day resulted in successful inhibition of thrombus formation across the week-long simulation, with a 2% reduction in maximum thrombus size, and a maximum inhibitory potency of 36% (Figure 7-9B). 5x10μM doses per day displayed a similar inhibitory profile, with maximum thrombus size inhibited by 4% and a maximum inhibitory potency of 52% (Figure 7-9B). These treatment regimens therefore resulted in very low to moderate inhibition over the entire simulation. This inhibition of maximum thrombus size (16.44μL in the untreated thrombus) is attributable to the retention of quercetin above basal levels due to the increased dosing frequency; it can be seen in Figure 7-9A that quercetin from one dose is retained at a level of 0.18-0.19μM (after 10μM dose) at the point of the administration of the next dose (i.e. when a quercetin dose is administered, quercetin from the previous dose remains). This adds evidence to the hypothesis that this retention of quercetin is likely key to achieve anti-thrombotic effect over the entire simulation period.

Under normal metabolic conditions, therefore, 5x10μM doses per day is predicted to be the most effective anti-thrombotic dosing regimen of quercetin. Increasing the dosing frequency above this was

considered unrealistic and therefore not tested, and whilst 3x30μM doses per day offered a wider range of inhibitory effect, the dose was near toxicity levels and thus not considered. The levels of inhibition achieved by this 'best' regimen was, however, not substantial across the entire simulation period. It was therefore investigated whether altering the pharmacokinetic parameters of quercetin could enhance anti-thrombotic effect.

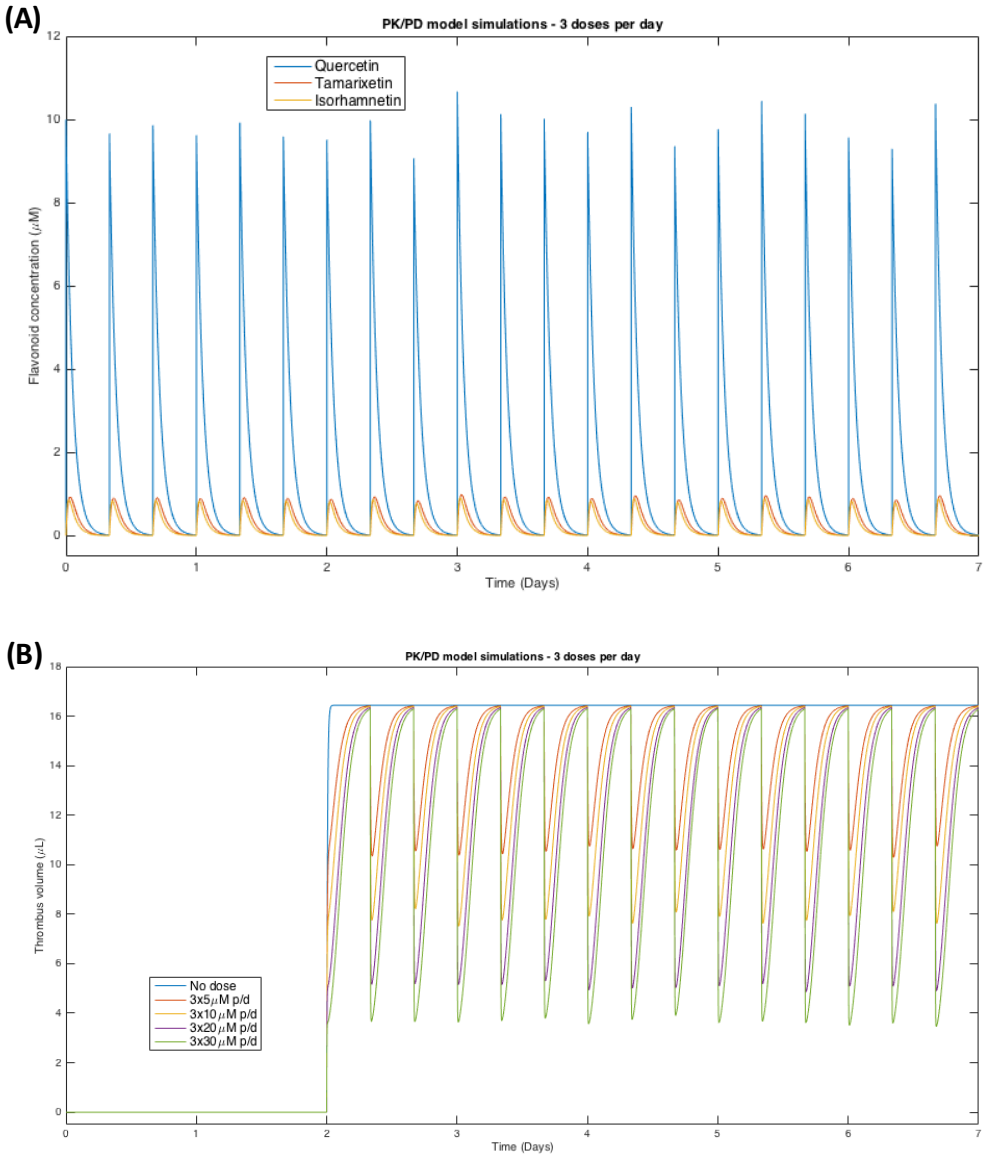

Figure 7-8 PK/PD model predictions of the anti-thrombotic effect of three-per-day doses of 5, 10, 20 and 30μM quercetin

The pharmacokinetics of quercetin after three-per-day doses of 10μM are shown in (A) as an example, and to allow comparison of quercetin (blue line), tamarixetin (orange line) and isorhamnetin (yellow line) levels with anti-thrombotic effect. The anti-thrombotic effect of thrice per day doses of 5μM (orange line), 10μM (yellow line), 20μM (purple line) and 30μM (green line), compared to thrombus formation in the absence of flavonoid (blue line) is shown in (B). 5-20μM doses were unable to inhibit maximum thrombus size, only delaying the formation of the thrombus. Introduction of quercetin doses reduced thrombus size initially in a dose-dependent manner, with thrombi growing again to maximum size. 30μM treatment resulted in 1% inhibition of maximum thrombus size. Model simulations used parameter values stated in Table 7-4. p/d, per day.

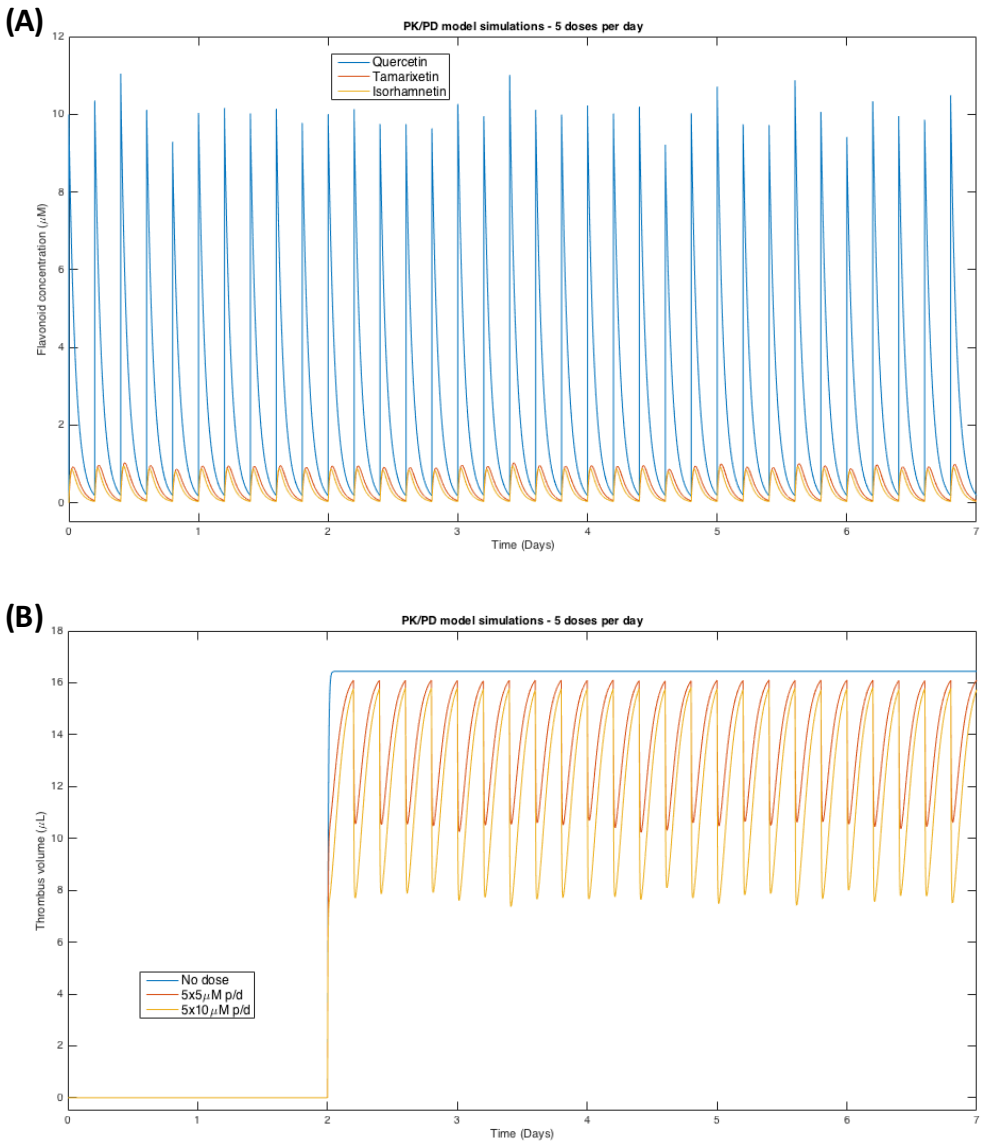

Figure 7-9 PK/PD model predictions of the anti-thrombotic effect of five-per-day doses of 5 and 10μM quercetin

The pharmacokinetics of quercetin after five-per-day doses of 10μM are shown in (A) as an example, and to allow comparison of quercetin (blue line), tamarixetin (orange line) and isorhamnetin (yellow line) levels with anti-thrombotic effect. It can be seen in (A) that in this dosing regimen, quercetin is retained (at 0.18-0.19μM) from one dose at the time another dose is administered. The anti-thrombotic effect of five per day doses of 5μM (orange line) and 10μM (yellow line), compared to thrombus formation in the absence of flavonoid (blue line) is shown in (B). Introduction of quercetin doses reduced thrombus size in a dose-dependent manner, with 5μM and 10μM treatment also resulting in 2 and 4% inhibition of maximum thrombus size. Model simulations used parameter values stated in Table 7-4. p/d, per day.

7.3.5 Altering the pharmacokinetics of quercetin results in enhanced anti-thrombotic efficacy

Model simulations described in the previous section demonstrated that retaining a quercetin concentration non-zero during the entire simulation period is key to achieving constant anti-thrombotic effect. Chapter 5 of this study discusses the potential for slowing/inhibiting the metabolism of quercetin by co-administration of quercetin glucosides with vitamins B3 (niacin) and C (ascorbic acid), leading to the potential for higher plasma quercetin concentrations being retained over a longer period of time. This hypothesis requires biological testing to confirm; however, the development of the PK/PD model allows simulations to be performed to give insight into the potential effects of slowing quercetin metabolism (through this or other mechanisms) on anti-thrombotic effect.

Simulations were first performed investigating the effect of dividing the metabolic terms of the PK/PD model, m_{TR} and m_I, by 2 (to give $m_{TR} = 4.75 \times 10^{-5}\ s^{-1}$ and $m_I = 6.75 \times 10^{-5}\ s^{-1}$). Simulating a quercetin dosing regimen of once per day at 5, 10, 20 and 50μM resulted in no inhibition of thrombus formation. However, dosing 3 times per day with 5, 10 or 20μM (corresponding to 450, 900 and 1800mg per day, respectively) resulted in an anti-thrombotic effect being achieved across the entire simulation period (not shown). A 3x5μM per day regimen resulted in inhibition of maximum thrombus size by 3%, with a maximum inhibition of 36% seen immediately after each dose is administered as the thrombus reduces in size as explained previously. The higher dose of 3x20μM per day resulted in an 11% reduction in maximum thrombus size, with a maximal inhibitory effect of 70%. Whilst the reduction in maximum thrombus size compared to no dose is relatively low upon these dosing regimens, under normal metabolic conditions these regimens were not effective in reducing maximum thrombus size at all; this therefore shows the potential effectiveness of slowing metabolism in the enhancement of anti-thrombotic effect, and is an important, novel conclusion from the PK/PD model. As a result of this observation from the model, the metabolic rates in the model were slowed even further, and similar dosing regimens were again simulated.

Dividing the rates of metabolism, m_{TR} and m_I, by 5 gave the parameter values described in Table 7-5. These were used for all subsequent simulations; the metabolic rates were the only parameter values altered. The effects of this retardation of metabolism was first investigated by simulating the effects of 1 dose per day at 5-50μM (i.e. 150mg – 1.5g quercetin-4'-O-β-D-glucoside). This dosing regimen gave an inhibitory phenotype across all doses tested, including at the lower 5μM dose, ranging from an inhibition of maximum thrombus size of 1-11% upon 5 and 50μM quercetin dosing, respectively (Figure 7-10B). Anti-thrombotic effects were maintained across the entire simulation period; as can be seen in Figure 7-10B, thrombus size was inhibited by 1-36% upon 5μM treatment, and by 11-85% upon 50μM treatment. The pharmacokinetic model profiles from this simulation are shown in Figure 7-10A, taking a 10μM dose as an example. The model profiles show that slowing the metabolism of quercetin results in minimum quercetin concentrations of 0.18μM, as the quercetin from one dose is not fully metabolised before another dose is administered. Another benefit of slowing metabolism shown by the model profiles in Figure 7-10A is the presence of relatively higher quercetin levels across all time, as the downward curve of quercetin levels (due to its metabolism) is less steep. This results in higher quercetin levels available to inhibit thrombus formation across the entire simulation period compared to those seen under normal metabolic conditions. Lower metabolite concentrations are observed as a result of altering the metabolic parameters, as metabolites build up more slowly and are eliminated, reaching peak levels of between 0.24-0.46μM (Figure 7-10A). However, it is hypothesised that the benefits of the raised and sustained quercetin levels far outweigh this potential disadvantage, demonstrated in the improved anti-thrombotic effect. These simulations demonstrate that a once per day dose of quercetin can be inhibitory if metabolism is slowed; as discussed previously, a lower number of doses per day is likely to increase adherence to dosing regimen. This is discussed more in Section 7.4.

Table 7-5 PK/PD model parameter values used for simulations when quercetin metabolism was slowed 5X

Parameter	Description	Units	Best fit value
m_{TR}	Rate of metabolic conversion of quercetin to tamarixetin	s^{-1}	$1.9x10^{-5}$
m_I	Rate of metabolic conversion of quercetin to isorhamnetin	s^{-1}	$2.7x10^{-5}$
u_Q	Rate of quercetin elimination	s^{-1}	0
u_{TR}	Rate of tamarixetin elimination	s^{-1}	$5.4x10^{-4}$
u_I	Rate of isorhamnetin elimination	s^{-1}	$1x10^{-3}$
k_T	Rate of thrombus growth	s^{-1}	$3.288x10^{-2}$
d_T	Rate of natural thrombus breakdown	s^{-1}	$2x10^{-3}$
k_{TQ}	Rate of inhibition of thrombus growth by quercetin	$(\mu Ms)^{-1}$	$2.3x10^{-4}$
k_{TTR}	Rate of inhibition of thrombus growth by tamarixetin	$(\mu Ms)^{-1}$	$4.25x10^{-4}$
k_{TI}	Rate of inhibition of thrombus growth by isorhamnetin	$(\mu Ms)^{-1}$	$2.375x10^{-4}$

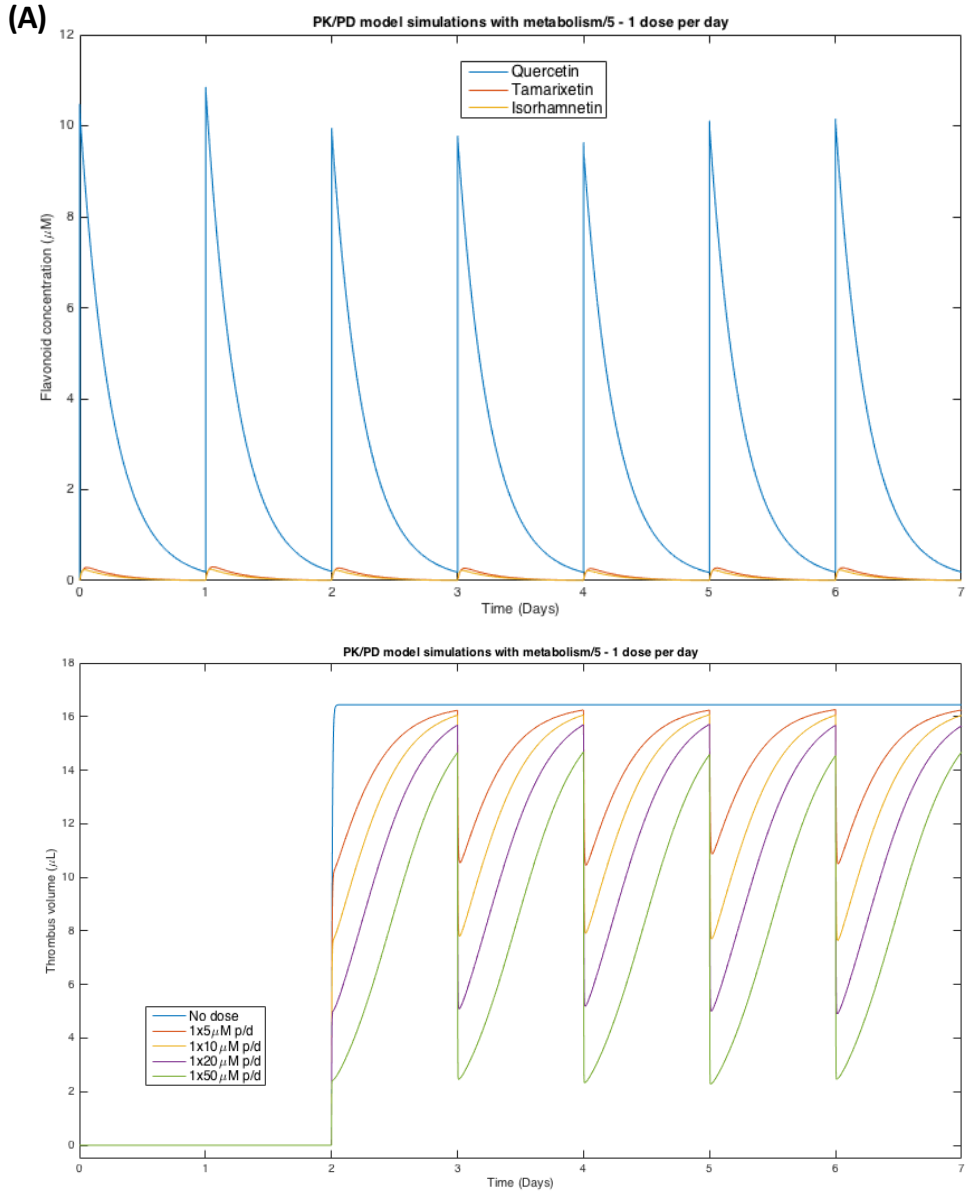

Figure 7-10 PK/PD model predictions of the anti-thrombotic effect of once-per-day doses of 5, 10, 20 and 50μM quercetin when quercetin metabolism is slowed 5X

The pharmacokinetics of quercetin after once-per-day doses of 10μM when metabolism is slowed 5X are shown in (A) as an example, and to allow comparison of quercetin (blue line), tamarixetin (orange line) and isorhamnetin (yellow line) levels with anti-thrombotic effect. It can be seen in (A) that slowing metabolism results in quercetin being retained (at 0.18-0.2μM) from one dose at the time another dose is administered. Slowing of metabolism also results in relatively higher quercetin doses across all time periods, discussed in-text. The anti-thrombotic effect of one dose per day of 5μM (orange line), 10μM (yellow line), 20μM (purple line) and 50μM (green line) compared to thrombus formation in the absence of flavonoid (blue line) is shown in (B). Introduction of quercetin doses reduced thrombus size in a dose-dependent manner, with all treatments resulting in inhibition of maximum thrombus size. Model simulations used parameter values stated in Table 7-5. p/d, per day.

A dosing regimen of three doses per day demonstrated anti-thrombotic effect under normal metabolic conditions upon 3x30μM, and when metabolic rates were divided by 2, this dosing regimen was effective at doses as low as 3x5μM. The potential anti-thrombotic effect of three doses of quercetin per day under conditions in which metabolism was slowed by 5X was therefore investigated. Dosing regimens of 3x5, 3x10 and 3x20μM per day were simulated, corresponding to 450, 900 and 1800mg per day. 3x30μM doses were not investigated here due to the near toxicity of this dose (2.7g). As seen in Figure 7-11B, these dosing regimens under the slowed metabolic conditions resulted in effective anti-thrombotic action across the entire simulation period, even at the lowest dose. Maximum thrombus size was inhibited by 19, 31 and 47% upon 5, 10 and 20μM doses, respectively, with a range of inhibition of 19-44%, 31-61% and 47-76% for these three dosing regimens (Figure 7-11B). Therefore, even at the point of maximum thrombus size, these dosing regimens provide relatively high inhibitory effects. Figure 7-11A shows the pharmacokinetics of quercetin 10μM doses from this simulation; the increased frequency of dosing, combined with the retarded metabolism, allowed significant accumulation of quercetin to occur, which drives the inhibitory phenotype. This accumulation of quercetin resulted in the lowest concentration observed across the week-long simulation of 2.7μM (upon 10μM dosing). This higher basal level of quercetin, whilst beneficial on its own, also results in higher plasma quercetin concentration upon administration of another dose on top of these increased basal levels, with concentrations reaching up to 16μM (Figure 7-11A). 5x per day dosing regimens were not tested here, due to the efficacy of 3x per day regimens and the assumption that a 5 times per-day regimen would result in far reduced adherence (discussed in Section 7.4). Overall, therefore, assuming the possibility of the retardation of quercetin metabolism, the recommended dosing regimen for quercetin to achieve consistent anti-thrombotic effect is 3x20μM per day, corresponding to 1.8g quercetin-4'-O-β-D-glucoside per day. The safety of this dose could be elucidated in further work; if these levels prove unsafe, a recommended dosing regimen (again with retarded metabolism) would be 3x10μM per day. This corresponds to a total of 900mg quercetin-4'-O-β-D-glucoside per day, which is likely tolerable and safe (discussed in Section 7.4.).

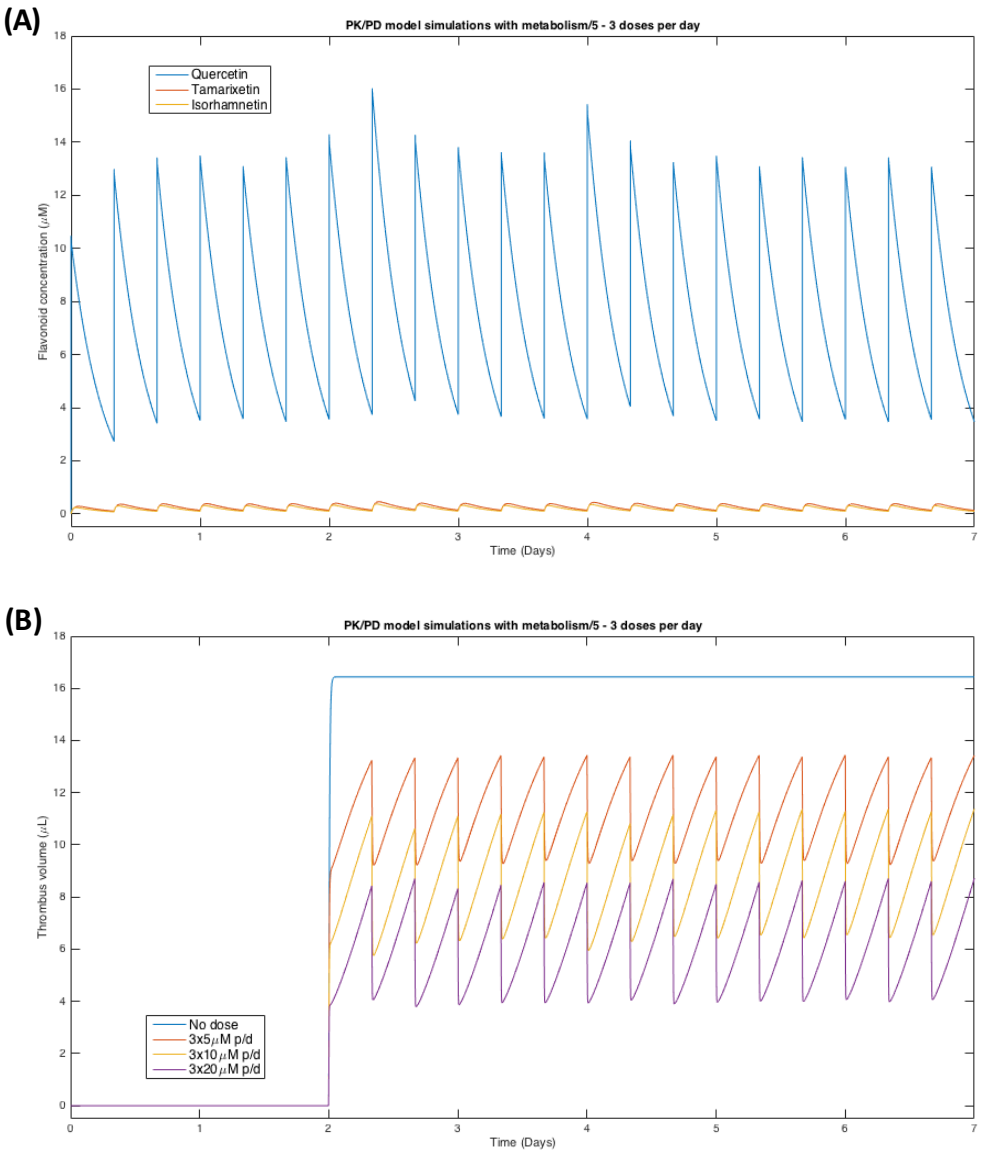

Figure 7-11 PK/PD model predictions of the anti-thrombotic effect of three-per-day doses of 5, 10 and 20μM quercetin when quercetin metabolism is slowed 5X.

The pharmacokinetics of quercetin after three-per-day doses of 10μM when metabolism is slowed 5X are shown in (A) as an example, and to allow comparison of quercetin (blue line), tamarixetin (orange line) and isorhamnetin (yellow line) levels with anti-thrombotic effect. It can be seen in (A) that slowing metabolism results in quercetin being retained from one dose at the time another dose is administered, with plasma quercetin never dropping below 2.7μM here. Slowing of metabolism also results in relatively higher quercetin doses across all time periods, discussed in-text. The anti-thrombotic effect of three doses per day of 5μM (orange line), 10μM (yellow line) and 20μM (purple line) compared to thrombus formation in the absence of flavonoid (blue line) is shown in (B). Introduction of quercetin doses reduced thrombus size in a dose-dependent manner, with all treatments resulting in high levels of inhibition of maximum thrombus size compared to other PK/PD model simulations, with 19, 31 and 47% inhibition of maximum thrombus size upon 3x5, 3x10 and 3x20μM p/d treatment, respectively. Model simulations used parameter values stated in Table 7-5. p/d, per day.

Now that an optimal dosing regimen under altered metabolic conditions had been established, the effects of perturbations in the dosing regimen were investigated; namely, how would the antithrombotic effect be altered if an entire day's doses were missed or if only half doses were taken for a day? A dose of 3x10μM per day with metabolism slowed 5X were chosen for these simulations to allow comparison to the pharmacokinetics of other presented simulations, and because this is the minimum recommended dosing regimen discussed above.

Figure 7-12 shows the results of these simulations. The orange solid line shows the antithrombotic effect of consistent 3x10μM per day dosing with the slowed metabolism; an anti-thrombotic effect is observed over the entire week-long simulation period. If half doses are taken on day 3, the plasma quercetin levels reduce accordingly, with a minimum level observed of 1.8μM (upon 3x10μM dosing, to allow comparison to other PK simulations in this Chapter, and as 3x10μM is the minimum recommended dose as stated above) (Figure 7-12A). This retention of a relatively high basal level of quercetin results in a consistent anti-thrombotic effect upon half-dosing on day three, with the inhibition of maximum thrombus size now reaching 19%, compared to a 31% inhibition of maximum thrombus size upon full dosing (Figure 7-12B). If no doses are administered on day 3, however, then even with the slowed metabolism, quercetin levels drop to a low of 0.07μM over day 3, which is associated with an inhibition of maximum thrombus size of only 1%. Thus, these simulations conclude that if half doses were taken for one day, there is retention of some anti-thrombotic effect, but if doses are missed for an entire day, then the anti-thrombotic effects are effectively lost.

The effects of speeding up the metabolism of quercetin was next investigated to examine the effects this would have on the pharmacokinetics and anti-thrombotic action. This was investigated due to the observation that, *in vitro,* tamarixetin displayed a trend toward an increased inhibitory effect in the thrombus formation under flow assay (Figure 4-6, Section 4.6), with isorhamnetin displaying similar potency to quercetin. The enhancement of metabolism (m_{TR} and m_I multiplied by 5) resulted in peak metabolite concentrations between 2 and 2.5μM. This, however, did not result in a sustained anti-

thrombotic effect due to rapid loss of quercetin through metabolism and the elimination of metabolites, which was complete (i.e. quercetin and metabolite concentrations <0.05μM) after 156 minutes.

In conclusion, the PK/PD model described above can predict the pharmacokinetics of quercetin supplementation at any concentration and frequency of dose, over any period of time, as well as predict the pharmacodynamic, anti-thrombotic effects of such supplementation, with thrombus formation initiated at any time-point. One such novel prediction, shown by the simulations presented in this Chapter, is that, under normal metabolic conditions (i.e. the rates of metabolism are those matched to literature data as described in Section 7.3.2), one dose per day is unable to inhibit thrombus formation over the entire week-long period, able only to delay the process. Under normal metabolic rates, the PK/PD model simulations predict an optimal dosing regimen of 5x10μM per day, corresponding to a total intake of 1.5g quercetin-4'-O-β-D-glucoside per day. This high frequency of dosing was shown by the model to be the most feasible way to achieve consistent anti-thrombotic effect under normal metabolic conditions. Thus, the PK/PD model demonstrated the importance of both the size of the dose and the frequency of administration. Another novel prediction from this model is that slowing the metabolism of quercetin offers an effective way to enhance the anti-thrombotic effect. Upon slowing the metabolism of quercetin in the model by 2X and 5X, the optimal dosing regimen was 3x10-20μM per day, corresponding to a daily intake of 0.9-1.8g quercetin-4'-O-β-D-glucoside per day; these dosing regimens resulted in effective anti-thrombotic action over the entire week-long simulation period. This dosing regimen also resulted in the maintenance of an anti-thrombotic phenotype if only half-doses were taken on one day, demonstrating the efficacy of this regimen. The predictions from this PK/PD model could be tested and refined through human supplementation studies, discussed in Section 7.4.

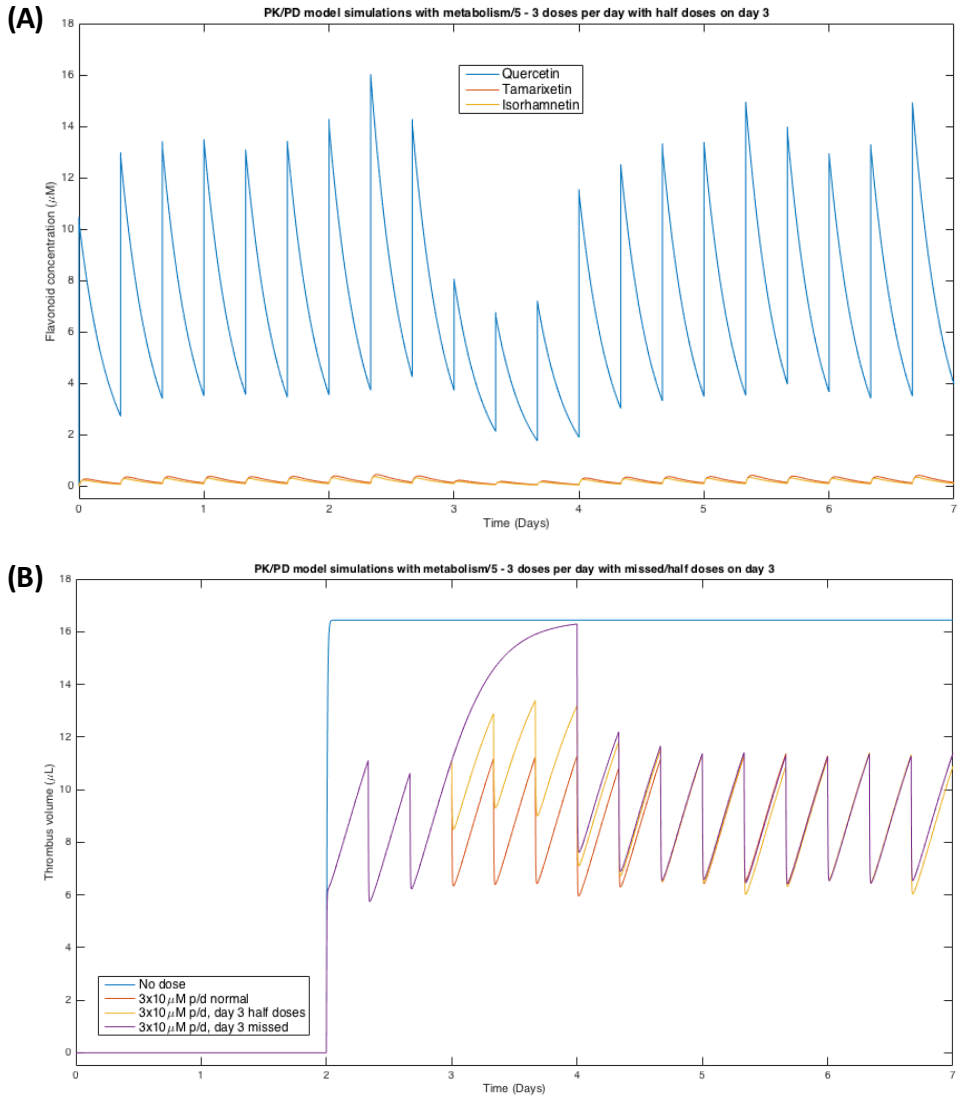

Figure 7-12 PK/PD model predictions of the anti-thrombotic effect of three-per-day doses of 10 µM quercetin when quercetin metabolism is slowed 5X, with zero and half-doses on day 3

The pharmacokinetics of quercetin after three-per day doses of 10 µM when metabolism is slowed 5X, with half doses (5 µM) on day three, are shown in (A). It can be seen that taking only half doses on day 3 results in a drop in plasma quercetin levels during this day; a minimum level of 1.8 µM is observed. Plasma quercetin levels then recover by the end of day 4, as full doses are again taken. The anti-thrombotic effect of three doses per day of 10 µM with all doses administered (orange line), half doses on day 3 (yellow line) and no doses on day 3 (purple line), compared to thrombus formation in the absence of flavonoid (blue line). If all doses are missed on day three, thrombus size grows continuously until the first dose is taken on day 4, resulting in only a 1% inhibition of maximum thrombus size. If half doses are taken on day 3, thrombus size is less inhibited than upon full dosing, inhibiting maximum thrombus size by 19% compared to 31%. Nonetheless, an anti-thrombotic effect is maintained across the entire week-long simulation period. Thrombus formation profiles in the day 3 half (yellow line) and no-dose (purple line) simulations return to normal by the end of day 4. p/d, per day.

7.4 Discussion of results presented in Chapter 7

The first aim of this chapter was to develop a mathematical model of thrombus formation *in vivo*, utilising *in vitro* thrombus formation under flow assay data gathered in this study, with an aim to predict the effects of different concentrations and combinations of quercetin, isorhamnetin and tamarixetin. *In vivo*, quercetin and metabolite concentrations are dynamic due to metabolism and elimination, and so another aim of this chapter was to incorporate this thrombus formation model into a pharmacokinetic/pharmacodynamic model of quercetin metabolism, elimination and anti-thrombotic effect. This model could then be used to perform *in silico* trials investigating the effects of different dosing regimens of quercetin on anti-thrombotic action, as well as altering the pharmacokinetics of quercetin to potentially enhance anti-thrombotic efficacy.

The FLAT model was an ODE model containing only one variable – T – representing thrombus size. The thrombus grew at a constant rate, k_T, and was inhibited by quercetin, tamarixetin and isorhamnetin at rates k_{TQ}, k_{TTR} and k_I, respectively. This model was fitted to *in vitro* thrombus formation under flow data, an assay performed in whole blood under arterial shear conditions (Section 4.6). This *in vitro* data was converted to represent thrombus size in the left anterior descending (LAD) artery, as described in Section 7.2.2. Model simulations of thrombus formation in the absence of flavonoid resulted in linear growth of the thrombus, which did not match the *in vitro* data, and so a term describing the natural breakdown of the thrombus, d_T, was included. Alteration of k_T and d_T values resulted in a good model fit to the data. Fitting of the FLAT model to the flavonoid-treated data was limited; due to the cost of performing the *in vitro* assay, only one concentration (10μM, chosen to represent a high physiological concentration) was used. Future work could focus on gathering data for more flavonoid concentrations in this assay, which could further validate the model. Nevertheless, setting of the natural breakdown (d_T) parameter to zero with associated k_{TQ}, k_{TTR} and k_{TI} values gave the best fit to the flavonoid-treated data. This led to the novel prediction from the FLAT model that when flavonoid is present, its effects greatly exceed the effect of natural thrombus breakdown, which

is thus neglected (at least at the relatively high concentration of 10μM). The best-fit values of k_{TQ} and k_{TI} from the fitting process were very similar, representing the similar biological effect of these two flavonoids. The best-fit value of k_{TTR} was much higher, representing the trend toward increased inhibition by this metabolite observed in the *in vitro* data. The FLAT model, at this stage in its development, can predict the effect of any combination of quercetin, tamarixetin and isorhamnetin, at any concentrations, on thrombus formation over the 10-minute simulation period, and is thus an effective model of the *in vitro* thrombus formation under flow assay. An advantage of the simplicity of the model is that effectively any inhibitor could be added into the model, with *in vitro* experimentation able to inform parameterisation as well as validate any predictions.

It was observed from the FLAT model simulations that thrombi continued to grow and increase in size up to the 10-minute simulation period, i.e. they did not reach a maximum, steady-state size. The FLAT model was therefore modified to simulate thrombus formation over a 1-hour period. Simulating the formation of a thrombus in the absence of flavonoids over an hour resulted in a steady state being reached; these results showed that, at 10 minutes, only 70% maximum thrombus size was reached. The effects of 10μM quercetin, tamarixetin and isorhamnetin were thus investigated over this time period; similar levels of inhibition were seen at 10 minutes and an hour. This implies that the *in vitro* thrombus formation under flow experimentation endpoint of 10 minutes is appropriate, with little need to extend it beyond this, and shows the data was good for use in model parameterisation; further experimentation utilising this assay, run over an hour, could test this hypothesis. One limitation of the FLAT model is that *in vitro* data is used to represent an *in vivo* process; future *in vivo* murine experimentation could be utilised, with the data from this used to develop a more representative model of *in vivo* thrombus formation.

Now that the FLAT model could be used in a predictive capacity, the effects of quercetin and tamarixetin at 5μM, individually and in combination, were simulated. Whilst quercetin and tamarixetin at concentrations of 5μM were not tested *in vitro,* a study by Wright *et al.* (2013) did

investigate the effects of these concentrations on the same assay. A comparison between the data from the data from Wright *et al.* (2013) and FLAT model predictions could therefore be performed. It must be noted, however, the difference in some experimental conditions; experiments were performed for 5 minutes (as opposed to 10 minutes) and at a shear rate of $1000s^{-1}$ (as opposed to $500s^{-1}$). At the 5-minute endpoint, Wright *et al.* (2013) demonstrated a lack of inhibition by quercetin at 5μM, with a zero to approximately minus 3% inhibitory effect. Tamarixetin, on the other hand, inhibited thrombus formation by approximately 5-9%. The FLAT model predicted an inhibitory effect of both quercetin (32%) and tamarixetin (38%) at 5μM at 5 minutes, and thus the FLAT model predicted a higher level of inhibition at this time-point. These differences could be explained at least partially by the difference in shear rate used; higher shear rates can lead to increased levels of platelet activation, as discussed in Section 4.6. An interesting observation is that, at the 60-minute endpoint of the simulation, the FLAT model is roughly in agreement with the data from Wright *et al.* (2013), in that quercetin did not inhibit (-24.4% inhibition), whereas tamarixetin did (26% inhibition). Whilst the magnitude of effects are different, this could, at least in part, be attributed to the aforementioned differences in experimental conditions. Further *in vitro* work could elucidate the accuracy of FLAT model predictions at 5, 10 and 60 minutes.

Another key way in which the FLAT model could be developed is through *in vitro* experimentation, and incorporation into the model of the effects of other quercetin metabolites such as sulphated metabolites. For example, as stated in Section 6.4, sulphated metabolites such a quercetin-3'-O-sulphate have been identified in plasma, with Wright *et al.* (2010b) demonstrating a similar anti-aggregatory effect of this metabolite to tamarixetin (Jones *et al.*, 2004; Crozier *et al.*, 2008). An investigation of the effect of metabolites such as these on *in vitro* thrombus formation under flow would be novel observations in themselves, and would also allow the development of the FLAT model to include more *in vivo* metabolites of quercetin; this would also contribute to the improvement of the PK/PD model, discussed below.

As mentioned above, an advantage of the FLAT model is its ability to effectively incorporate any inhibitor, so long as data has been acquired regarding its anti-thrombotic effect in the *in vitro* thrombus formation under flow assay. The FLAT model could therefore be developed to incorporate the effects of pharmacological agents such as aspirin and ADP antagonists (e.g. clopidogrel, discussed in Chapter 8), with future experimentation performed to investigate the anti-thrombotic effects of these anti-platelet agents under the specific assay conditions described in the present study, with the data incorporated into the FLAT model, allowing simulation of the anti-thrombotic effects of combined flavonoid/anti-platelet drug treatment, which could be tested to further validate the model. This would build on the data presented in Chapter 5 regarding the interaction between quercetin/tamarixetin/isorhamnetin and aspirin, and could allow predictions as to which combinations, at which concentrations, may be particularly efficacious and worth pursuing in further *in vitro/in vivo* experiments. Indeed, this could be extended to the incorporation of other dietary polyphenols; for example, Pignatelli *et al.* (2000) demonstrated interactions between quercetin and catechin, a polyphenol found in fruits, teas and chocolate, in the enhancement of anti-platelet effect (Lakenbrink *et al.*, 2000; Manach *et al.*, 2004; Gottumukkala *et al.*, 2014). This, combined with pharmacokinetic data, could lead to the development of a detailed model of thrombus formation and its inhibition by natural as well as pharmacological inhibitors of platelet function, discussed in Chapter 8.

The flavonoid concentrations in the FLAT model were static, whereas *in vivo* they are dynamic, and so a pharmacokinetic/pharmacodynamic model was next developed, describing the administration, metabolism and elimination of quercetin, as well as the dynamic anti-thrombotic effects associated with this. The ODE describing thrombus formation from the FLAT model was utilised in the PK/PD model to describe the same process, and this was combined with the incorporation of ODEs describing the pharmacokinetics of quercetin; quercetin was introduced and metabolised into tamarixetin and isorhamnetin, which were then eliminated. As such, three new variables were included as well as T (thrombus size variable) from the FLAT model; Q, T_R and I, representing quercetin, tamarixetin and isorhamnetin concentration respectively. The time-scale of the model was also changed to one week, to allow for simulation of extended quercetin dosing.

One limitation of this model is that it does not include an absorption rate for quercetin and the methylated metabolites; instead quercetin is introduced immediately, with the full dose available at the point of administration to inhibit thrombus formation. This introduction of equations describing absorption (with the addition of associated compartment(s)) is a primary goal of the future development of this model. Several pharmacokinetic studies have described the absorption of quercetin and metabolites, with Olthof *et al.* (2000) demonstrating peak total quercetin concentrations at 27 minutes after quercetin-4-glucoside supplementation, and Graefe *et al.* (2001) observing a peak total quercetin concentration at 42 minutes post-supplementation with quercetin-4'-O-glucoside. Hubbard *et al.* (2004), the data from which was used in the fitting and parameterisation of the model, observed a total plasma quercetin t_{max} of 30 minutes. The t_{max} of total plasma quercetin is thus relatively quick, and over the week-long timescale of the PK/PD model, not accounting for absorption of quercetin may not therefore have a large impact on the model simulations presented in this Chapter. Future iterations of this model will elucidate this.

The pharmacokinetic simulations of the model were largely fitted to data from Hubbard *et al.* (2004) as described in Section 7.3.2, resulting in tamarixetin and isorhamnetin peaks at the times observed in this study. This was combined with data from Graefe *et al.* (2001), who observed that, after quercetin-4'-O-glucoside supplementation, the total isorhamnetin concentration (the methylated metabolite, after conjugate hydrolysis) was approximately one-tenth that of quercetin. Thus, a peak tamarixetin and isorhamnetin concentration of one tenth to one twentieth of peak quercetin concentration was considered appropriate. Upon completion of the fitting process, the addition of 10μM quercetin resulted in simulated peak tamarixetin and isorhamnetin concentrations of 0.93 and 0.86μM, at 45.5 and 32 minutes, respectively. Future work could focus on gathering pharmacokinetic data directly, as opposed to fitting to the literature, with the results of a human supplementation pharmacokinetic study with quercetin-4'-O-β-D-glucoside or isoquercetin being used to fit the PK model simulations to.

Fitting of the pharmacodynamic data to the PK/PD model demonstrated that in this model, unlike the FLAT model, the parameter of natural decay could not be set to zero when flavonoid was present. When flavonoid concentrations were low (due to metabolism and elimination), due to a lack of natural decay limiting the thrombus growth, thrombi grew to sizes vastly above the maximum size of the thrombus in the absence of flavonoids, which was assumed to represent the maximum size that a thrombus could grow (i.e. flavonoids would only ever inhibit, not potentiate, the process of thrombus formation). This interesting observation was missed in FLAT model simulations due to static flavonoid concentrations and the much shorter time scale (10 minutes to one hour vs. one week), although it was hypothesised in Section 7.2.4 that at lower flavonoid concentrations, the contribution of natural thrombus breakdown (d_T) to overall thrombus size may not be completely neglected. The pharmacodynamic section of the PK/PD model was thus reparameterised, with k_{TQ}, k_{TTR} and k_{TI} values re-fitted using the FLAT model, keeping k_T and d_T at the same values they were in the absence of flavonoids; this still gave an overall good fit to the *in vitro* thrombus formation under flow data. The PK/PD model could now be used to run *in silico* trials of different doses and different dosing regimens to investigate which gave the best anti-thrombotic effect.

Simulations were first run under normal metabolic conditions. It was found that once per day doses of quercetin would not result in a consistent anti-thrombotic effect; whilst thrombus formation was delayed when quercetin levels were high, as quercetin was metabolised and the metabolites were eliminated the anti-thrombotic effect was lost, with thrombi growing to the same maximum size as in the absence of flavonoid. This result demonstrated the importance of choosing appropriate time points in human studies; whilst platelet function or thrombus formation *ex vivo* may appear inhibited at certain time points, at others there may be no effect. This could result in anti-thrombotic/anti-platelet effect being missed or overstated.

Three-per-day quercetin dosing regimens were also largely unable to fully inhibit thrombus formation, again only delaying the time to reach maximum thrombus size. A small anti-thrombotic effect across the entire week-long simulation period was observed upon 3x30μM dosing, with a 1% inhibition in

maximum thrombus size. However, this dose corresponds to 2.7g quercetin-4'-O-β-D-glucoside per day (matched to data from Hubbard *et al.* (2004) as described in Section 7.3.2); a study by Ferry *et al.* (1996) concluded that 3g of quercetin (given intravenously) resulted in a toxic response, and so this level of supplementation was considered inappropriate. The potential anti-thrombotic effect of five doses per day (10μM per dose) were next investigated, and found to result in basal quercetin levels of 0.18-0.19μM, i.e. at this dosing regimen, not all quercetin from one dose is lost to metabolism and subsequent elimination before another dose is given. This resulted in an anti-thrombotic effect across the entire week-long period (with a 4% inhibition in maximum thrombus size, and a maximal inhibitory potency of 52%). This retention of quercetin above 0 at all time appears to be key for an overall anti-thrombotic effect across the entire simulation period. Under normal metabolic conditions, therefore, the optimal dosing regimen is predicted by the PK/PD model to be 5x10μM doses per day, corresponding to 5x 300mg quercetin-4'-O-β-D-glucoside supplements per day.

The predicted efficacy of this dosing regimen could be tested in a human supplementation study; through the utilisation of sampling time-points predicted by the model to result in minimum and maximum anti-thrombotic effect, with PK data as well as *in vitro* thrombus formation under flow assay performed at these time-points. A dosing regimen of 5x per day, however, is unlikely to have a high level of adherence; it has been shown that increasing dose frequency reduces adherence (Schroeder *et al.*, 2004; Brown and Bussell, 2011). A systematic review by Claxton *et al.* (2001) investigating medication compliance concluded average compliance of a once daily dose was 79%, which dropped to 69, 65 and 51% upon increasing dose frequency to 2, 3 and 4 doses per day. Thus, a 5x per day dosing regimen is unlikely to have good compliance. This fact, along with the observation of a minimal anti-thrombotic effect (only 4% inhibition of maximum thrombus size), led to the investigation of the effects of altering the pharmacokinetic parameters of quercetin metabolism to enhance anti-thrombotic effect and reduce the required dosing frequency.

Data presented in Chapter 5 discussed the potential of inhibiting/slowing the metabolism of quercetin through the co-administration of niacin (vitamin B3) and ascorbic acid (vitamin C). These vitamins have been shown to inhibit the activity of cytochrome P450 enzymes, which many studies have shown are involved in the metabolism of flavonoids including quercetin (Clarke *et al.*, 1996; Hodek *et al.*, 2002; Otake and Walle, 2002; Gaudineau and Auclair, 2004; Cermak, 2008; Cassidy and Minihane, 2017). It was therefore hypothesised that competitive inhibition of these enzymes by niacin and ascorbic acid could lead to the maintenance of higher and more maintained plasma quercetin peaks. The retention of quercetin above zero levels from one dose to the next was shown by the PK/PD model to be of critical importance in maintaining a consistent anti-thrombotic effect, and so the effects of slowing quercetin metabolism in the PK/PD model were investigated. Slowing the metabolism 2X (i.e. dividing m_{TR} and m_I by 2) resulted in an enhancement of anti-thrombotic effect, and so metabolism was slowed 5X. This retardation of quercetin metabolism by 5X dramatically enhanced the anti-thrombotic effect; one dose per day as low as 5μM now demonstrated an anti-thrombotic effect across the entire simulation period. This was due to the increased retention of quercetin from one dose to the next; by the time of administration of another quercetin dose, quercetin from the previous dose had yet to be metabolised, and so plasma quercetin levels were raised even further. The downward slope of quercetin due to its metabolism was also less steep, which resulted in relatively higher plasma quercetin levels across the entire simulation period compared to normal metabolic conditions. This anti-thrombotic effect of once-per-day doses is beneficial when considering the increased compliance of this dosing regimen discussed above.

The effects of three doses per day under the slowed metabolic conditions were next simulated, and resulted in the best overall anti-thrombotic effects of all simulations, at 3x5, 3x10 and 3x20μM per day. It was also found that if half doses were taken for a day (3x5μM on day 3 instead of 3x10μM), an anti-thrombotic effect was maintained, and so at this dosing regimen the system is somewhat resistant to perturbations. One of the key outputs from the PK/PD model is therefore that the best potential (and feasible in terms of dose size) anti-thrombotic effect is achieved upon 3x10 – 3x20μM

per day, when metabolism is slowed 5X. This dosing regimen corresponds to 900mg (3x10μM) – 1.8g (3x20μM) quercetin-4'-O-β-D-glucoside per day. A study by Ferry *et al.* (1996) demonstrated the safety of an approximately 2.5g once-weekly intravenous dose of quercetin, and a recent study by Stopa *et al.* (2017) demonstrated the safety of a one-time, 1g dose of isoquercetin, and so these recommended dosing regimens (especially 3x10μM) are likely safe, with future work key to confirming this, especially given the potential quercetin accumulation due to retarded metabolism. Interesting to note is a current clinical trial investigating the effect of isoquercetin on cancer associated thrombosis (clinicaltrials.gov identification number NCT02195232). This trial is investigating the effects of 500mg – 1g daily isoquercetin on cancer associated thrombosis. The tolerability/toxicity of isoquercetin is also a primary outcome of the trial, which will be interesting given the similarity of this dose (1g isoquercetin (quercetin-3-O-glucoside)/day) to the predicted recommended dose from the PK/PD model (900mg-1.8g quercetin-4'-O-β-D-glucoside per day).

The hypothesis that slowed metabolism is beneficial, and indeed could be key, to the anti-thrombotic effect of quercetin, could be examined in a human supplementation study (discussed in Chapter 8) comparing the pharmacokinetics and pharmacodynamics (through *ex vivo* thrombus formation assays) of isoquercetin and isoblend, compounds introduced in Chapter 5. Pharmacokinetic investigations from this supplementation study would examine whether isoblend (with the additions of niacin and ascorbic acid potentially retarding metabolism) resulted in a sustained plasma quercetin peak, and higher peak plasma concentrations compared to isoquercetin alone. Pharmacodynamic investigations from this study would investigate whether anti-thrombotic effect is more potent or is maintained for a longer period of time upon isoblend supplementation compared to isoquercetin. Limited investigations have been performed regarding this in the literature; a recent study by Stopa *et al.* (2017) investigated the pharmacokinetics of isoquercetin and isoblend upon one 1g dose, and observed no significant differences, although a trend towards higher peak quercetin concentrations can be seen upon addition of niacin and ascorbic acid. More investigation is therefore required, to elucidate pharmacokinetic differences upon multiple dosing regimens, and to investigate potential anti-thrombotic effect *ex vivo*.

As well as this, other ways to potentially retard metabolism, such as co-administration of quercetin with other inhibitors of CYP, as well as inhibitors of phase-2 metabolism (e.g. inhibitors of uridine diphosphoglucuronosyl transferases (UGTs) and sulphotransferases (SULTs)) could also be investigated, although the potential for off-target effects of this must also be considered.

This hypothesised inhibition of metabolism could also lead to increased plasma quercetin aglycone concentrations, as the conjugation and metabolism reactions are theoretically inhibited. This would make the '*Q*' variable in the PK/PD model more representative of the aglycone itself, as it is currently assumed to represent the total plasma quercetin, including conjugates such as sulphated and glucuronidated forms, as described in Section 7.3.1. Indeed, this current representation of '*Q*' as also including quercetin conjugates is a key aim of the further development of the PK/PD model. Through the development of improved identification techniques and standards over time, the separation of total plasma quercetin into its constituent metabolites is increasingly possible. For example, a study by Lee *et al.* (2012b) developed a mass spectrometry method for the measurement of individual quercetin metabolites; this methodology does not rely on enzymatic cleavage of conjugate products, and as such was able to identify metabolites including quercetin glucuronide, quercetin diglucuronide and methylquercetin diglucuronide. Human supplementation studies combined with pharmacokinetic analysis coupled with such techniques could lead to the development of very detailed metabolite profiles; once plasma concentrations for these metabolites have been elucidated, *in vitro* assays investigating their anti-platelet and anti-thrombotic effect could be utilised, and allow their incorporation into the FLAGG, FLAT and ultimately, PK/PD models. This could be combined with the incorporation of the effects of anti-platelet agents and other dietary polyphenols (as well as their interactions with quercetin) into the PK/PD model as discussed above (with pharmacokinetic data for anti-platelet pharmacological agents widely available), allowing the simulation and prediction of the optimal dynamic anti-thrombotic effects of different quercetin supplementation regimens, accounting for detailed quercetin metabolism as well as the presence of, and interaction of quercetin and its metabolites with anti-platelet agents and other dietary polyphenols, informing further *in vitro* and *in vivo* experimentation, as well as potential human studies.

8 – General discussion

8.1 General discussion

Flavonoids are a class of polyphenols found in plants; they are the most common of plant phenolic compounds, with over 9000 identified. Flavonoids have long been known to demonstrate biological effects in humans, with the observation in 1936 that extracts from Hungarian red pepper increased capillary wall permeability (Rusznyak and Szent-Gyorgyi, 1936). From these observations, interests in flavonoids grew, and the most common dietary flavonoid, quercetin, has now demonstrated anti-CVD effects in many studies upon supplementation; reduced total and LDL cholesterol, increased HDL cholesterol, decreased systolic and diastolic blood pressure, and decreased blood glucose concentrations (Edwards *et al.*, 2007; Lee *et al.*, 2011; Serban *et al.*, 2016). Indeed, cohort studies have demonstrated a reduced relative risk (RR) of CHD and fatal CVD upon high flavonol intake, and a reduced RR of ischemic heart disease specifically upon high quercetin intake (Hertog *et al.*, 1995; Knekt *et al.*, 2002; McCullough *et al.*, 2012; Wang *et al.*, 2014a). These cardio-protective effects of flavonols and quercetin are thought, at least in part, to be due to the anti-platelet effects of quercetin.

The hypothesis of this study was as follows; quercetin inhibits thrombosis through anti-platelet mechanisms, the efficacy of which are modulated by its metabolism, and can be mathematically modelled to predict inhibitory mechanisms, interactions, and optimal dosing regimens. The methylated metabolites tamarixetin and isorhamnetin maintain anti-platelet effects in platelet rich plasma and whole blood, and interact with aspirin to enhance anti-platelet effects.

To investigate this hypothesis, the anti-platelet efficacy of quercetin, tamarixetin and isorhamnetin in washed platelets were first examined, as well as the mechanisms through which these flavonoids inhibited platelet function.

8.1.1 Metabolism of quercetin can enhance or reduce anti-platelet effect

Quercetin has been shown to inhibit washed platelet function in a range of studies; quercetin inhibits platelet aggregation stimulated by collagen, thrombin and ADP, as well as inhibiting collagen-stimulated dense granule secretion and integrin $\alpha_{IIb}\beta_3$ activation, and collagen-stimulated tyrosine phosphorylation of downstream proteins such as Syk, PLCγ2 and LAT (Pignatelli *et al.*, 2000; Hubbard *et al.*, 2003; Oh *et al.*, 2012). A consistent issue with these studies, however, is the use of high, supraphysiological concentrations of quercetin, as well as the sole use of quercetin aglycone, the presence of which, as discussed in Section 1.7.2.4, was historically a point of some controversy (with low levels now detected in plasma due to improved analytical techniques and, as discussed in Section 3.8, proven roles for the aglycone in the vasculature) (Sesink *et al.*, 2001; Chen *et al.*, 2005). In addition to this, as discussed throughout Section 1.7.2, upon consumption, quercetin is extensively metabolised; the anti-platelet effects of these metabolites are not well characterised.

Significantly less is known about the effects of quercetin's metabolites on platelet function, and so initial work in this study focussed on determining the anti-platelet effects of more physiologically relevant concentrations of quercetin, as well as the anti-platelet efficacy of two identified plasma methylated metabolites, tamarixetin and isorhamnetin, and one plasma glucuronidated metabolite, quercetin-3-glucuronide (Ueno *et al.*, 1983; Manach *et al.*, 1997; Moon *et al.*, 2001; Guo *et al.*, 2014). Investigations focussed on the effect of metabolism/conjugation on anti-platelet efficacy in washed platelets, and the mechanisms through which quercetin and its metabolites inhibited platelet function.

Quercetin and its methylated metabolites tamarixetin and isorhamnetin were found to inhibit platelet aggregation, granule secretion and fibrinogen binding to integrin $\alpha_{IIb}\beta_3$ (integrin inside-out signalling) at physiologically achievable concentrations, with an inhibitory potency of isorhamnetin > quercetin > tamarixetin. This is an important observation as it suggests that methylation may enhance or reduce the anti-platelet efficacy of quercetin. Data from Wright *et al.* (2010b) support this; they observed a

reduction in the inhibition of aggregation and dense granule secretion when comparing tamarixetin to quercetin. Granule secretion is a critical early event to drive the positive feedback mechanisms characteristic of platelet activation; inhibition of both dense and α-granule secretion results in reduced positive feedback driven through the contents of these granules, such as ADP, vWF, fibrinogen, serotonin and coagulation factors, therefore leading to dampened platelet activation.

Quercetin-3-glucuronide required concentrations an order of magnitude higher to achieve comparable levels of inhibition. It is hypothesised that this could be due to cell impermeability, or may be due to a general decreased inhibitory potency of this metabolite, for example through decreased kinase inhibitory potency; indeed, the kinase inhibitory activity of quercetin-3-glucuronide is largely unknown, and could be further tested in a cell-free system to elucidate if this metabolite is less potent compared to quercetin and its methylated metabolites. Due to the lack of inhibitory potency, work on quercetin-3-glucuronide was discontinued.

There may, however, be a role for this metabolite in the inhibition of platelet function *in vivo*, through either the inhibition of extracellular targets or its deconjugation to quercetin aglycone. Recent work has demonstrated the key role of extracellular protein disulphide isomerase (PDI) in thrombus formation, with PDI inhibition proving an effective anti-thrombotic mechanism (Jasuja *et al.*, 2012; Kim *et al.*, 2013; Lin *et al.*, 2015). Jasuja *et al.* (2012) have demonstrated the potential for PDI inhibitors as anti-thrombotics, and observed that quercetin forms with a 3-O-glycoside inhibit PDI activity. Thus, quercetin-3-glucuronide may preferentially inhibit extracellular PDI activity during thrombus formation; this is supported by evidence from Stopa *et al.* (2017), who demonstrated an IC_{50} for PDI inhibition by quercetin-3-glucuronide of 8.5μM. This is compared to an IC_{50} of 2.5μM for isoquercetin, a quercetin glycoside discussed later. It has also been hypothesised by Menendez *et al.* (2011) that quercetin-3-glucuronide may act as a quercetin 'carrier' in plasma, which becomes deconjugated in target tissues, largely through the actions of the enzyme β-glucuronidase, liberating quercetin aglycone as an effector. This is supported by evidence from Kawai *et al.* (2008), who

demonstrated the uptake and deconjugation of quercetin-3-glucuronide by murine macrophages, which also acted to methylate the liberated aglycone. It is hypothesised here that platelets may also take up quercetin-3-glucuronide, and, inside the platelet this may be deconjugated by platelet β-glucuronidase. Evidence for the metabolism of quercetin in platelets already exists, with Wright *et al.* (2010a) suggesting platelet-mediated metabolism of quercetin aglycone to tamarixetin by catechol-*O*-methyltransferase (COMT). This may provide a novel pathway through which quercetin aglycone accumulates in platelets.

As well as integrin $\alpha_{IIb}\beta_3$ inside-out signalling, quercetin and its metabolites also inhibited integrin outside-in signalling, as measured by an inhibition of platelet spreading on fibrinogen. This inhibition of the bi-directional signalling of the integrin key to platelet adhesion and aggregation is likely one of the key mechanisms through which platelet function is inhibited by these flavonoids, and is supported by Oh *et al.* (2012), who observed a reduction in fibrinogen binding to integrin $\alpha_{IIb}\beta_3$ upon quercetin treatment (Cosemans *et al.*, 2008). Intracellular calcium mobilisation lies upstream in the activatory process, with rapid (under 1 second) changes in cytosolic calcium crucial to integrin activation (Brass and Joseph, 1985; Sage and Rink, 1986). The CRP-XL stimulated mobilisation of calcium was inhibited by quercetin, tamarixetin and isorhamnetin as low as 1μM; again, isorhamnetin proved significantly more potent than quercetin, indicating a 3' methyl group as important in the inhibition of platelet function by quercetin and its metabolites, in contrast to Wright *et al.* (2010b), who suggested a B ring catechol moiety as important to anti-platelet potency. The inhibition of calcium mobilisation, which lies upstream of granule secretion, integrin activation and aggregation, indicates that the inhibitory effects of quercetin and its methylated metabolites occur early in the GPVI activation pathway. This was confirmed by data presented in Chapter 6, which presents the inhibition of Syk and LAT tyrosine phosphorylation by quercetin, tamarixetin and isorhamnetin, demonstrating that both methylated metabolites of quercetin also inhibit these early signalling events. The inhibition of such early signalling events downstream of GPVI likely explains the functional inhibition of collagen/CRP-XL stimulated calcium mobilisation, granule secretion and, ultimately, aggregation. This is in

agreement with data from Hubbard *et al.* (2004), which demonstrated the *ex vivo* inhibition of tyrosine phosphorylation of PLCγ2, an enzyme crucial in driving calcium mobilisation, upon consumption of quercetin-4-O-β-D-glucoside. Just how far upstream the GPVI pathway of activation quercetin acts requires further investigation; Hubbard *et al.* (2003) demonstrated an inhibition of collagen-stimulated FcRγ-chain phosphorylation, an early step in the GPVI activation pathway. Indeed, platelet adhesion and spreading on CRP-XL was inhibited by quercetin, tamarixetin and isorhamnetin, which may point to an effect on GPVI dimerization and/or clustering, which are key events in activation through this receptor (Poulter *et al.*, 2017).

The inhibition of activatory mechanisms downstream of GPVI by quercetin and its methylated metabolites tamarixetin and isorhamnetin is now well characterised; *in vivo*, however, there are many other activatory pathways through which soluble agonists such as ADP, thrombin and thromboxane A_2 act, to further drive the activatory process and lead to the development of stable aggregates. Quercetin, tamarixetin and isorhamnetin also inhibited platelet aggregation stimulated by these agonists (with U46619, a thromboxane mimetic, used in place of TXA_2) at physiologically achievable concentrations. Whilst the mechanisms of inhibition and the underlying signalling proteins effected were not elucidated in this study, the broad inhibitory effect on all of these pathways is likely due to the general kinase-inhibitory activity of quercetin. Many studies have demonstrated this kinase inhibition by quercetin, with evidence for the inhibition of PI3K, SFKs, ERK, Akt, Syk, Fyn, PLCγ2, mitogen-activated protein kinases (MAPKs) and glycogen synthase kinase 3-beta (GSK3β); indeed, quercetin has been shown to inhibit the activity of approximately 100 kinases (Wright *et al.*, 2010b; Boly *et al.*, 2011; Russo *et al.*, 2014b; Wright *et al.*, 2015). Thus, the initial signalling and functional activatory processes through platelet interaction with collagen are inhibited by quercetin and its methylated metabolites, and any subsequent activation that does occur via soluble agonist binding (which is itself inhibited through inhibition of calcium mobilisation and subsequent granule release) is also affected, leading to the potent inhibition of platelet function via the inhibition of multiple

platelet pathways. This is supported by data from Mosawy *et al.* (2013a), who observed an inhibition of arachidonic acid and ADP-induced platelet aggregation by quercetin.

In addition to this, it is shown here that quercetin, tamarixetin and isorhamnetin can act additively, and at some higher concentrations, more than additively, in the inhibition of platelet aggregation. *In vivo*, multiple metabolites will be present in the plasma at any given time, and so these interactions warrant further investigation, as well as the inclusion of other metabolites, such as sulphated and glucuronidated conjugates. These interactions at sub-micromolar concentrations may explain, at least in part, the anti-platelet effects of quercetin observed despite the sometimes low bioavailability. This hypothesis is supported by evidence from Pignatelli *et al.* (2000) that concentrations of quercetin and catechin that were not individually inhibitory, when combined, resulted in a significant, synergistic inhibition of platelet function. Indeed, quercetin has demonstrated synergistic interactions with other plant compounds, with sulforaphane (a bioactive compound in vegetables) synergising with quercetin in the inhibition of the replication of pancreatic cancer stem cells (Srivastava *et al.* (2011)). Such interactions may be general to flavonoids as a whole; for example, Harasstani *et al.* (2010) demonstrated flavonoid synergy with respect to anti-inflammatory effects, observing a particular interaction between kaempferol and chrysin. Williamson (2001) hypothesises that such interactions may underpin the biological efficacy observed despite low doses; in extension to this, such interactions may explain the anti-platelet and anti-CVD effects observed upon flavonoid/quercetin intake despite sometimes relatively low plasma concentrations.

8.1.2 A significant anti-platelet effect is maintained in platelet rich plasma and whole blood

Having elucidated the mechanisms through which platelet function is inhibited by quercetin and its methylated metabolites, and established that metabolism can enhance or reduce effects, the translation of the anti-platelet efficacy of quercetin, tamarixetin and isorhamnetin from washed platelets to platelet rich plasma and whole blood was next investigated.

Quercetin is known to bind heavily to plasma proteins, with up to 99% of circulating quercetin bound to human serum albumin (Boulton *et al.*, 1998; Kaldas *et al.*, 2005). It was therefore hypothesised that significantly increased concentrations would be required to achieve comparable levels of inhibition to that seen in washed platelets. The effects of such high concentrations of quercetin on platelets was not known; it is shown in this study that at concentrations up to 200μM, there were no significant effects on fibrinogen binding, P-selectin exposure, annexin V binding to phosphatidylserine, and surface GPIbα levels. This indicates that any inhibition of platelet function seen in PRP in this study is due to anti-platelet effects, as opposed to any adverse effect on cell viability.

Collagen-stimulated platelet aggregation in PRP was inhibited by quercetin, tamarixetin and isorhamnetin at higher concentrations compared to in washed platelets, with significant inhibition observed only at 10μM plus for tamarixetin, and 25μM plus for quercetin and isorhamnetin, indicating plasma proteins in a reduced inhibitory potency. This is in agreement with Pignatelli *et al.* (2006), who observed quercetin concentrations between 1.25 and 20μM were unable to inhibit collagen-stimulated aggregation. The high plasma binding of other dietary flavonoids has also been demonstrated, with Vaiyapuri *et al.* (2013) observing reduced anti-platelet effects of the flavonoid tangeretin in PRP compared to washed platelets. Nonetheless, it demonstrates an increased potency compared to a study from Mosawy *et al.* (2013a), who observed inhibition of collagen-stimulated PRP aggregation only at 100μM quercetin. The increased potency observed here is consistent with the washed platelet data, which demonstrated lower IC_{50} values in the inhibition of aggregation compared to previous studies (Hubbard *et al.*, 2003). Interestingly, tamarixetin was significantly more potent compared to isorhamnetin, whereas in the washed platelet data, this inhibitory hierarchy was reversed.

The inhibition of integrin $\alpha_{IIb}\beta_3$ activation and α-granule release was dramatically reduced in PRP compared to washed platelets, with minimal effects at up to 20μM, indicating plasma proteins in a reduced effect against these parameters of activation. It may be that inhibition of platelet function in PRP occurs more through the inhibition of other pathways. A confounding factor here could be the

abundance of fibrinogen in plasma. Quercetin and tamarixetin have been shown to bind to fibrinogen as well as collagen; this could either sequester them away from the platelet resulting in a lack of inhibition, or interfere with fibrinogen- and collagen-platelet interactions and cause an inhibitory phenotype (Wright *et al.*, 2010b). Future work is needed to elucidate this.

Through a clot retraction assay, integrin $\alpha_{IIb}\beta_3$ outside-in signalling in PRP was found to be affected to a greater extent than inside-out signalling, with inhibitory effects observed as low as 2.5μM, a concentration physiologically achievable through diet or supplementation (Hubbard *et al.*, 2004; Hubbard *et al.*, 2006; Stopa *et al.*, 2017). It is hypothesised that the mechanism of inhibition of clot retraction could additionally be via the inhibition of Src-family kinases and PLCγ2, kinases with a role in clot retraction that quercetin has been shown previously to inhibit (Shattil *et al.*, 1998; Suzuki-Inoue *et al.*, 2007; Wright *et al.*, 2010b). As well as this, the involvement of the coagulation cascade in the clot retraction assay introduces several other potential mechanisms; namely, the inhibition of aspects of the coagulation cascade by quercetin. Quercetin has been shown to inhibit the enzymatic activity of thrombin and factor Xa, as well as prolonging activated partial thromboplastin time and prothrombin time (Guglielmone *et al.*, 2002; Manukyan *et al.*, 2008; Choi *et al.*, 2016). It is hypothesised that the inhibition of extracellular PDI by quercetin-3-glucuronide could also inhibit the coagulation cascade, due to the involvement of PDI in activating tissue factor (Manukyan *et al.*, 2008). The increased potency of quercetin and its metabolites in an assay also involving the coagulation system (clot retraction) compared to platelet function alone (i.e. PRP aggregometry, fibrinogen binding and P-selectin exposure) could indicate that the anti-platelet and anti-coagulant actions of quercetin and its metabolites combine *in vivo* to inhibit thrombosis. Indeed, a recent study by Choi *et al.* (2016) demonstrated *ex vivo* and *in vivo* anti-coagulant effects of quercetin and isoquercetin (20mg/kg) following intravenous and intraperitoneal flavonoid administration, providing evidence to potentially support this hypothesis. Similar to the aggregometry data in PRP, a trend for an inhibitory hierarchy of tamarixetin > quercetin > isorhamnetin was observed, indicating a 4'-methyl group in an increased anti-platelet efficacy in PRP compared to a 3'-methyl group or B ring catechol moiety.

The effects of quercetin and its methylated metabolites on *in vitro* thrombus formation under flow were next investigated, an assay that utilises whole blood under arterial flow conditions. At 10μM there was potent inhibition of thrombus formation, supporting the clot retraction data in the inhibition of platelet function in the presence of plasma proteins at physiologically achievable concentrations. It is speculated here that there may also be a role for red blood cells in the effects of the flavonoids in this assay; as discussed in Section 4.7, flavonoids are taken up into red blood cells through binding haemoglobin, with enhanced uptake when plasma concentrations are high, and are released from RBCs, with enhanced release when plasma quercetin concentrations reduce (for example, upon platelet uptake) (Fiorani *et al.*, 2003). This 'reservoir', as suggested by Fiorani *et al.* (2003), may provide a mechanism whereby plasma quercetin concentrations are maintained, allowing prolonged platelet:flavonoid interactions.

Quercetin and isorhamnetin inhibited thrombus formation with similar magnitudes, and again a trend was observed toward increased inhibition with tamarixetin. This in agreement with data from Wright *et al.* (2013), who observed an increased inhibition of thrombus formation by tamarixetin compared to quercetin. This increased effect of tamarixetin compared to quercetin could be for several reasons. Firstly, it has been demonstrated that tamarixetin binds collagen and fibrinogen, particularly fibrinogen, with a much high affinity compared to quercetin (Wright *et al.*, 2010b). This binding could interfere with the interactions of these ligands with platelets, thereby hindering platelet activation and aggregation, especially under flow conditions; structural studies investigating the nature of this binding need to be undertaken to investigate this hypothesis. In a similar investigative line, the ability of quercetin to bind other adhesive ligands such as vWF could also be explored (the importance of which is particularly high under flowing conditions), as well as the potentially disruptive nature of this binding. Another mechanism for the increased potency of tamarixetin over quercetin could also be due reduced albumin binding by tamarixetin; a study by Andersen and Markham (2007) observed a 2-3X reduction in binding constants to bovine serum albumin upon methylation of quercetin at the 4' hydroxyl residue. Future experimentation could confirm this in human plasma, as well as investigating

the effects of 3' methylation (i.e. isorhamnetin). It is hypothesised that the enhanced potency of tamarixetin observed in PRP and whole blood is not due to an increased direct anti-platelet effect, but rather an increase in bioavailability or platelet ligand binding, or other as yet unknown mechanism, as tamarixetin did not prove more potent in the inhibition of washed platelet function compared to quercetin and isorhamnetin.

8.1.3 A novel isoquercetin formulation inhibits thrombosis in vivo

Having established inhibitory effects of quercetin and its methylated metabolites in PRP and whole blood *in vitro*, investigations were planned to test the potential inhibitory effect of quercetin on an *in vivo* murine laser injury model of thrombosis. However, an opportunity arose for the investigation into the anti-platelet effects of four novel quercetin formulations (summarised in Table 5-1), produced and supplied by a pharmaceutical company. The specific potential anti-platelet effects of these novel formulations had not been tested, and are presented here for the first time.

Quercetin aglycone based formulations inhibited collagen-stimulated platelet aggregation in a similar manner to quercetin aglycone, whereas isoquercetin-based formulations were unable to inhibit aggregation up to 50μM. This lack of effect of isoquercetin may be due to a lack of cell permeability and/or due to less potent inhibition of intracellular target enzymes (Kong *et al.*, 2011; Jasuja *et al.*, 2012). As suggested previously, isoquercetin and isoblend, with a 3-glucoside moiety, may inhibit thrombus formation primarily through inhibiting the activity of PDI; whilst PDI plays a role in platelet aggregation (as demonstrated by reduced aggregation in PDI-deficient platelets), it may be that isoquercetin-mediated inhibition of other *in vivo* mechanisms, such as inhibition of endothelial-derived PDI, drives the inhibitory phenotype (Jasuja *et al.*, 2010; Kim *et al.*, 2013). In addition to this, it is speculated that the benefits of isoquercetin over quercetin aglycone-based formulations lie largely in the enhanced bioavailability that they confer, with glucosides of quercetin displaying increased absorption compared to quercetin aglycone; it is also hypothesised that the addition of vitamins B3

and C to the formulations could lead to retarded metabolism and enhanced plasma quercetin through, for example, inhibition of cytochrome p450 enzymes, as discussed in Chapter 5 (Hollman *et al.*, 1995; Clarke *et al.*, 1996; Gaudineau and Auclair, 2004).

This led to the investigation of the effect of novel quercetin formulations on thrombus formation in an *in vitro* thrombus formation under flow assay. At a concentration of 10μM, no significant inhibitory effects were observed. For aglycone-based formulations, the reason for this was unclear. However, for isoquercetin based formulations, this was unsurprising, based on a lack of effect on platelet aggregation. It is hypothesised that a lack of inhibition in this assay could be due to reasons stated above; namely a lack of *in vivo* mechanisms in this *in vitro* assay through which isoquercetin may act, or a lack of cell permeability and reduced intracellular target inhibition.

In order to define which novel quercetin-based formulation to use in *in vivo* assays, their effects at predicted plasma concentrations upon oral supplementation with 200mg/kg, the planned *in vivo* dose, were tested on the same assay. Isoblend proved the most potent; whilst this is likely due to the higher concentration used, this reflects the higher predicted plasma concentrations upon its use compared to other formulations, and so reflects an important difference. Thus, isoblend was selected for investigation of anti-thrombotic effect *in vivo.* It is important to note that any inhibition achieved in this *in vitro* assay through inhibition of PDI by isoquercetin is unlikely to be as significant *in vivo,* where, during absorption, the glucoside moieties implied in PDI inhibition are cleaved. However, as mentioned previously in this section, quercetin-3-glucuronide is a plasma metabolite that inhibits PDI activity, with evidence from Flaumenhaft (2013) and (Stopa *et al.*, 2017) supporting this. In addition, for oral administration, glycosylated quercetin forms were considered best due to the enhanced absorption of these compared to quercetin aglycone. Communication with Quercegen Pharmaceuticals resulted in the addition of folic acid to isoblend for use *in vivo*. An inverse association between folic acid with CHD has been observed, as have other health benefits of folic acid, such as alleviation of mental health symptoms; it was thought that this addition would therefore encourage uptake of the supplement, and Quercegen pharmaceuticals therefore added this to their formulation (Durand *et al.*,

1996; Taylor *et al.*, 2004; Wang *et al.*, 2012b). Experiments with folic acid added to isoblend to ensure a lack of adverse effect interestingly displayed a trend toward increased inhibition of thrombus formation *in vitro* compared to isoblend alone. The mechanisms behind this are not clear, and the only known interaction between flavonoids and folic acid is the *in vitro* observation of the inhibition by flavonoids of enzymes involved in folate uptake (although in a human pilot study investigating this, no significant differences were noted), with no direct evidence for quercetin specifically (Alemdaroglu *et al.*, 2007; Alemdaroglu *et al.*, 2008; Augustin *et al.*, 2009). Thus, the isoblend used in murine studies contained added folic acid.

In a murine laser injury model of thrombosis, isoblend inhibited thrombosis, with 43 and 41% inhibition of maximum thrombus size after 48 and 72 hours, respectively. This was achieved after a relatively high dose of 200mg/kg, over extended dosing periods of 48 and 72 hours (with dosing morning and evening). Nonetheless, it demonstrates the oral bioavailability of the novel quercetin formulation isoblend, and provides initial evidence for the potential of isoblend as an antithrombotic. Several previous studies have demonstrated *in vivo* anti-thrombotic effects of various quercetin derivatives, including pentamethylquercetin, quercetin aglycone, and quercetin-3-rutinoside (Jasuja *et al.*, 2012; Mosawy *et al.*, 2013b; Lin *et al.*, 2015; Liang *et al.*, 2015). However, these studies all administered quercetin intravenously, and the presence of the administered forms in plasma is unlikely to be realistic upon oral consumption of quercetin. The work presented here is the first study demonstrating a direct anti-thrombotic effect in mice following oral administration (via gavage) of quercetin, specifically isoquercetin.

The mechanism underlying this inhibition is important to elucidate; a direct isoquercetin-mediated inhibition of PDI is unlikely due to cleavage of the glucoside moiety during absorption, although an inhibition of PDI by glucuronidated metabolites could play a role, as shown by Stopa *et al.* (2017), discussed earlier. If the inhibition of PDI proves to be an important mechanism, investigations into preventing the de-glycosylation of isoquercetin during absorption and metabolism could prove useful, especially considering the increased potency of isoquercetin compared to quercetin-3-glucuronide in

the inhibition of PDI activity (IC_{50} values of 2.5μM and 8.5μM, respectively) (Stopa *et al.*, 2017). The predicted enhanced bioavailability of quercetin upon isoblend supplementation, as opposed to quercetin aglycone supplementation, could also be responsible for the anti-thrombotic effect upon isoblend supplementation; a pharmacokinetic study in mice comparing plasma quercetin and metabolite concentrations upon oral gavage with quercetin aglycone and isoblend is required to answer this question, and would also allow the identification of the active metabolites responsible for anti-platelet effects. In addition to this, a pharmacokinetic study comparing plasma concentrations following isoquercetin and isoblend administration could confirm or refute the hypothesis of enhanced plasma quercetin (i.e. retarded metabolism) with the addition of vitamins B3 and C. It may also be the case that in a complete *in vivo* system, as in the murine laser injury model, isoquercetin-mediated effects other than anti-platelet effects may occur. The anti-coagulant of effects of quercetin have already been discussed; however, quercetin has also been demonstrated to enhance nitric oxide and cyclic AMP production in endothelial cells, two key negative regulators of platelet function (Huk *et al.*, 1998; Sanchez *et al.*, 2006; Li *et al.*, 2012). All these mechanisms could combine to result in an anti-thrombotic effect of isoquercetin *in vivo*.

8.1.4 Quercetin and its methylated metabolites interact with aspirin to enhance anti-platelet effect

The observation of anti-thrombotic effects of quercetin *in vitro* and *in vivo* posed an interesting question; namely, what are the implications of these effects from a pharmacological perspective, specifically in relation to anti-platelet drugs? It was hypothesised that quercetin and its metabolites may interact with aspirin to modulate platelet function. Investigations focussed on aspirin, as the most widely used anti-platelet agent (Diener, 2006).

As aspirin use is associated with adverse events such as gastric bleeding, if the dose required could be lowered by simultaneous use of quercetin, this could be beneficial (McQuaid and Laine, 2006; Baigent *et al.*, 2009). Quercetin, tamarixetin and isorhamnetin, as well as novel quercetin aglycone-based

formulations (but not isoquercetin-based formulations), significantly enhanced the anti-platelet effects (inhibition of collagen-stimulated washed platelet aggregation) of aspirin in a more than additive manner; i.e., there was a statistically significantly greater effect of dual treatment (aspirin + flavonoid) compared to the individual effects added together. Importantly, these interactions occurred at physiologically achievable quercetin concentrations. Indeed, IC_{50} values for the inhibition of platelet aggregation by aspirin were significantly lowered by flavonoid concentrations as low as 1μM. This data supports the observations from Crescente *et al.* (2009) and Navarro-Nunez *et al.* (2008) that flavonoids can enhance the anti-platelet effects of aspirin, and, for the first time, describes a specific quercetin-aspirin interaction, as well as an interaction between aspirin and the methylated metabolites of quercetin in the enhancement of anti-platelet effect. Indeed, in a whole blood assay of platelet function, quercetin plus aspirin treatment also resulted in a more-than-additive enhancement of anti-platelet effect, providing evidence that this interaction can be maintained in whole blood. Whether this interaction can lower the risk of problem bleeding is critical to establish, and is discussed in Section 8.2. A recent study by Choi *et al.* (2016) demonstrated a mild increase in tail bleeding times upon treatment with 20mg/kg quercetin or isoquercetin, with no haemorrhage observed after a subcutaneous injection. However, flavonoid was administered intravenously, and so plasma concentrations were likely much higher than after oral administration; the effects upon oral administration, as well as the effects of simultaneous isoquercetin and aspirin administration (with a view to lowering the required concentrations of both), must be established.

The mechanisms underlying the interaction between quercetin and its methylated metabolites and aspirin were not investigated, but are thought to be through inhibition of multiple signalling pathways. Aspirin irreversibly inhibits platelet cyclooxygenase-1 (COX-1), resulting in the blockade of platelet thromboxane A_2 production. As a result, platelet activation through the thromboxane A_2 pathway is limited, and activation through the other pathways becomes crucial; however, through quercetin's broad general kinase activity, these pathways are also potently inhibited, with this study demonstrating the inhibition of collagen, ADP and thrombin-stimulated pathways (as well as the thromboxane A_2 pathway itself), resulting in a strong inhibition of platelet aggregation. In addition to this, quercetin

may also affect the metabolism and therefore plasma concentration of aspirin. Aspirin, acetylsalicylic acid, has potent anti-platelet effects, and is metabolised to salicylic acid, which demonstrates far reduced potency (Nitelius *et al.*, 1984; Rosenkranz *et al.*, 1986). Indeed, the metabolism of aspirin has been demonstrated to limit COX inhibition in patients (Clarke *et al.*, 1991). Aspirin is metabolised by cytochrome P450 (CYP) 2C9, UDP-glucuronosyltransferase 1A6 (UGT1A6), and N-acetyl transferase 2 (NAT2) (Palikhe *et al.*, 2011). A study by Si *et al.* (2009) demonstrated that quercetin inhibits CYP2C9 via substrate binding site interaction, and Mohamed and Frye (2011) observed a weak inhibition of UGT1A6 by cranberry extract, a fruit rich in quercetin. However, quercetin has also been shown to enhance the activity of NAT2 (Chen *et al.*, 2009). The balance between the inhibition and activation of aspirin metabolism by quercetin is unclear, but could lead to increased or retained plasma aspirin concentrations. Overall, the interaction between quercetin, its metabolites and aspirin may prove useful in lowering the aspirin concentrations required to achieve sufficient platelet inhibition, and may be beneficial in patients in which aspirin does not effectively inhibit TXA_2 production (Hankey and Eikelboom, 2006; Schwartz, 2011; Floyd and Ferro, 2014).

8.1.5 Mathematical modelling of the anti-platelet effects of quercetin and its metabolites identifies inhibitory mechanisms and interactions, with optimal doses for anti-thrombotic effect predicted in a pharmacokinetic/pharmacodynamic model

Having investigated in detail the *in vitro* anti-platelet effects of quercetin and its methylated metabolites, as well as their interaction with aspirin, and the *in vivo* effect of isoquercetin, development of the work next focussed on mathematical modelling approaches, with a view to further understanding and predicting the anti-platelet effects of quercetin, tamarixetin and isorhamnetin, as well as developing a pharmacokinetic/pharmacodynamic model of quercetin administration, metabolism and antithrombotic effect. Initial work focussed on the modelling of platelet activation and aggregation, and its inhibition by quercetin, tamarixetin and isorhamnetin.

Platelet aggregation Model A simulated inhibition by flavonoids through the alteration of rate parameters. This model included platelet activation and aggregation, and was fit to *in vitro* aggregation (light transmission aggregometry) and activation (Syk and LAT phosphorylation) data. The best fit values for this, with the relative values of k_1 (from inactive to activated) and k_3 (from activated to aggregated), resulted in novel predictions; namely a difference in the primary inhibitory mechanism, with quercetin aglycone primarily inhibiting aggregation (from an activated state), and the methylated metabolites primarily inhibiting the initial activation (from an inactive state). This could be a general consequence of quercetin metabolism; future work incorporating more metabolites could clarify this. Due to prioritising further modelling work, however, this was not explored further in this study.

Platelet aggregation Model A relied on altering the parameters (k_1, k_2 and k_3) to simulate platelet inhibition, and so the model was developed to make inhibition of activation and aggregation a direct function of flavonoid concentration in the FLAGG (FLavonoid AGGregation) model, which introduced specific terms describing the inhibition of platelet activation and aggregation by flavonoids (K_X and K_Y constants of inhibition, as well as Q, TR and I, describing flavonoid concentration). This also allowed simulation of the effects of quercetin and its methylated metabolites simultaneously, which was fit to plate-based aggregometry data. The model best fit the data when the equations describing the interactions between quercetin, tamarixetin and isorhamnetin were multiplicative instead of additive; this provides further evidence, in addition to data presented in Chapter 3, that quercetin and its metabolites may act together in a more-than-additive manner to inhibit platelet function. The *in vitro* data used in model fitting was endpoint only, however, and so kinetic data for this through light transmission aggregometry experimentation would allow the model to be fit to more extensive, temporally resolute data. Inclusion of more *in vivo* metabolites of quercetin is key to the improvement of this model (as well as the PK/PD model, discussed later); *in vitro* data for the anti-activatory and anti-aggregatory effects of, for example, quercetin-3'-sulphate and quercetin-3-glucuronide, could be gathered; indeed, quercetin-3'-sulphate has been demonstrated to inhibit platelet aggregation (Wright *et al.*, 2010b). This would build a more extensive profile of the *in vitro* inhibitory effects of quercetin's plasma metabolites, for which data is lacking, as well as allow *in silico*

predictions of the interactions of these metabolites with quercetin, tamarixetin and isorhamnetin. Pharmacological agents such as aspirin could also be included; together, this could allow the FLAGG model to simulate the anti-platelet efficacy of novel combinations of quercetin, metabolites and anti-platelet agents and predict which may be worth pursuing in further *in vitro* or *in vivo* experimentation.

Further mathematical modelling work focussed on the development of a model of *in vivo* thrombus formation, the FLAT model. This was fit to *in vitro* thrombus formation under flow data, and allowed the prediction of the effects of any combination of quercetin, tamarixetin and isorhamnetin at any concentrations. A novel prediction from the model is that, at higher flavonoid concentrations, the effects of flavonoids greatly exceed the effect of natural thrombus breakdown, which is thus neglected in the model. Extension of the model simulation period from 10 minutes to 1 hour resulted in similar profiles of inhibition by quercetin and its methylated metabolites. One advantage of the FLAT model is that it can easily incorporate any inhibitor of platelet function, and the predictions from the model are relatively easily testable; development of this model will therefore include gathering *in vitro* data for other *in vivo* quercetin plasma metabolites as well as pharmacological anti-platelet agents, and their incorporation into the model. This inclusion of other metabolites, such as quercetin-3'-sulphate, and pharmacological agents such as aspirin and clopidogrel, would allow *in silico* experimentation and predictions as to which combinations may be particularly efficacious, and start to build answers to the questions posed in this study regarding the implications of flavonoid-flavonoid and flavonoid-anti-platelet drug interactions on anti-thrombotic action.

In vivo, upon oral intake, plasma flavonoid concentrations are dynamic due to metabolism and elimination, and so a pharmacokinetic/pharmacodynamic (PK/PD) model was developed describing the metabolism, elimination and dynamic anti-thrombotic actions of quercetin. This PK/PD model used the thrombus formation parameter described in the FLAT model, with the inclusion of equations describing the pharmacokinetics of quercetin, fitting the model to PK data from Hubbard *et al.* (2004) and Graefe *et al.* (2001). Development of this model allowed simulation of the anti-thrombotic efficacy of any quercetin dose, with any dosing frequency/regimen, over any period of time, with

thrombus formation initiated at any chosen time. Simulations were first run under normal metabolic conditions, and it was found that once per day dosing could not achieve a consistent antithrombotic effect, instead only delaying thrombus formation. Three doses per day resulted in minimal anti-thrombotic effect; a 5X per day dosing regimen was optimal, even with lower overall daily doses compared to 3X per day, demonstrating the importance not only of dose, but of the frequency with which they are taken. The PK/PD model is based upon dosing with quercetin-4-O-β-D-glucoside, as opposed to isoquercetin, as this glucoside has shown to result (albeit across different studies) in enhanced plasma quercetin concentrations (Hubbard *et al.*, 2004; Stopa *et al.*, 2017). Future work could therefore investigate the different bioavailability of these glucosides in a pharmacokinetic human supplementation study. Isoquercetin was used for *in vivo* experimentation in this study due to the commercial production and availability, as well as the more extensive safety data and its potential in development as a novel antithrombotic.

The addition of vitamins B3 and C are hypothesised to retard the metabolism of quercetin through inhibition of cytochrome P450 enzymes, and there may be the potential to modify the metabolism of quercetin in other ways (Clarke *et al.*, 1996; Hodek *et al.*, 2002; Gaudineau and Auclair, 2004). This may result in higher plasma quercetin, and lower metabolite concentrations, which may prove beneficial in anti-thrombotic effect. The usefulness of the PK/PD model was demonstrated here, in that it could be used to simulate this retardation of metabolism *in silico*. Slowing metabolism by 5X had a dramatic effect, with one dose per day as low as 5μM demonstrating consistent anti-thrombotic effects across the week-long simulation period. Three doses per day, with metabolism slowed 5X, proved the most beneficial of all simulated dosing regimens, with the PK/PD model predicting 3x10μM – 3x20μM per day as the optimal dosing regimens for consistent anti-thrombotic effect. This regimen was even resistant to perturbations such as half doses being taken for a day. This corresponds to a dose of 900mg – 1.8g per day; it is speculated that this would be a safe dose based on observations by Ferry *et al.* (1996) of the safety of a once per week intravenous dose of 2.5g quercetin, and from Stopa *et al.* (2017), who recently noted the safety of a one-off 1g oral dose of isoquercetin. Specific

trials would be needed to validate this, though, as less human data has been gathered for quercetin-4-O-β-D-glucoside compared to isoquercetin in relation to safety as a potential commercial human supplement.

Thus, overall, the PK/PD model was used to predict an optimal dosing regimen to maintain anti-thrombotic effect, with the novel prediction that slowing quercetin metabolism is key to attaining consistent and potent effects. Future work regarding this model could focus on the inclusion of equations and compartments describing quercetin absorption; a lack of absorption equations in the current iteration, however, are not thought to be of particular concern, due to the speed of quercetin absorption (peak plasma quercetin observed between 27-42 minutes after oral intake) compared to the week-long model simulations (Olthof *et al.*, 2000; Graefe *et al.*, 2001; Hubbard *et al.*, 2004). In addition, development will also focus on incorporating more plasma metabolites of quercetin, as well as pharmacological agents into the model, allowing the anti-thrombotic effects of quercetin supplementation to be predicted *in silico* in a truly representative scenario accounting for the multitude of flavonoid-flavonoid and flavonoid-drug interactions.

8.2 Future directions

The work performed in this study has described the mechanisms through which the methylated metabolites of quercetin, as well as the aglycone itself, inhibit platelet function, as well as providing evidence for effects in PRP and whole blood, and of an interaction of quercetin and its metabolites with aspirin. There are, however, several questions remaining regarding the actions of other plasma metabolites, as well as the pharmacological implications of the quercetin-aspirin interaction.

Further *in vitro* work focussing on the anti-platelet efficacy and mechanisms of other plasma quercetin metabolites such as quercetin-3-sulphate and quercetin-3-glucuronide will enable the construction of a full profile of the anti-platelet effects of quercetin and its metabolites, combining washed platelet, PRP and whole blood assays, particularly *in vitro* thrombus formation under flow assays, and this data could be included in the mathematical models presented in this study. In addition to this, *in vitro* thrombus formation studies investigating the interaction between quercetin/tamarixetin/isorhamnetin and aspirin, as well as between these flavonoids and other anti-platelet agents such as clopidogrel, will allow elucidation of interactions potentially important from a clinical perspective.

Identification of the underlying mechanism responsible for the trend toward the increased inhibitory potency of tamarixetin compared to quercetin and isorhamnetin in the presence of plasma proteins is also important, especially from the implication of metabolism potentially enhancing anti-platelet effect. Initial investigations will focus on the differences in human serum albumin binding affinity of quercetin, tamarixetin and isorhamnetin, as well as their binding to adhesive ligands such as vWF.

The investigation of potential *in vivo* interactions between quercetin and aspirin in the inhibition of thrombosis is of key importance; one important way in which this could be explored is through the murine model of thrombosis described in Chapter 5. Simultaneous administration of isoblend and aspirin, in comparison to individual dosing with each, could allow the elucidation of any *in vivo*

interaction between the orally bioavailable isoblend and aspirin. These experiments, combined with the identification of the active plasma metabolites upon isoblend consumption, could also lead to an investigation into the reduction of isoblend doses to more physiologically relevant levels that models feasible human supplementation, and into the anti-thrombotic effects achieved in mice upon reduced aspirin dose co-administered with isoblend. Combined with tail bleeding assays following the same treatments, this will allow an investigation into the anti-thrombotic potential of isoblend plus aspirin dual treatment whilst discovering if haemostasis is maintained or compromised, and whether lowering aspirin doses with simultaneous isoblend administration lowers the risk of problem bleeding.

In addition to this, Crescente *et al.* (2017) have very recently described the production of a platelet COX-1 knockout mouse. They cite the differences in aspirin pharmacokinetics in mice and humans as a significant blockade to effective investigation of human low-dose aspirin effects in mice, and propose these platelet $COX1^{-/-}$ mice as a murine model of human low-dose aspirin treatment. As one of the hypothesised benefits of isoquercetin in the present study is to potentially reduce aspirin concentration required to achieve anti-platelet effect, it would be very interesting to investigate the effect of isoblend treatment on thrombosis (through the laser injury model) and haemostasis (through tail bleeding assay) in these mice.

To investigate the presence and magnitude of an interaction between quercetin and aspirin *in vivo*, a human interventional study could also be performed, investigating the effect of acute isoblend, aspirin, and combined isoblend plus aspirin supplementation on platelet function *ex vivo*, through plate-based PRP aggregation utilising a panel of agonists, as well as through measurement of platelet function in whole blood through use of the platelet function analyser (PFA). A key benefit of this approach is that it allows full metabolism of isoquercetin in humans *in vivo*, and thus the *ex vivo* platelet functional assays would provide a true insight into the potential effect of isoblend (as well as combined isoblend and aspirin treatment) to achieve anti-platelet effects in humans upon supplementation, and could inform the progression of supplement development and dosing, as well as giving an insight into the true potential for reducing aspirin doses in humans whilst maintaining anti-platelet effect. *Ex vivo*

analyses would also enable the identification of plasma quercetin concentrations and the identity of the specific plasma metabolites and concentrations upon human isoquercetin consumption (which could then be tested for specific anti-platelet effects *in vitro*). Indeed, this human study was planned and ethical approval gained, and was due to take place. However, due to funding complications at the last minute, it could not be performed.

All the above data could be incorporated into the existing mathematical models of platelet aggregation and thrombus formation, as well as the PK/PD model. The pharmacokinetic data from the human study could be utilised to re-parameterise the PK parameters, with novel *in vitro, ex vivo* and *in vivo* data combining to inform the pharmacodynamic parameters, including addition of more quercetin metabolites. Including all this data regarding quercetin and its metabolites into the PK/PD model, as well as data describing the anti-activatory, anti-aggregatory and anti-thrombotic actions of anti-platelet agents such as aspirin and clopidogrel and their interactions with quercetin and its metabolites (as well as data on their pharmacokinetics which is readily available in the literature), will allow *in silico* experimentation investigating and identifying optimal quercetin and anti-platelet agent concentrations and combinations. This could inform future *in vitro* and *in vivo* experimentation in the field, as well as future human studies to test predictions and allow further development of the models.

8.3 Conclusions

The data presented in this study provide evidence that metabolism of quercetin into its methylated metabolites can enhance or reduce anti-platelet effects, and has identified some of the activatory mechanisms and pathways that tamarixetin and isorhamnetin (as well as quercetin aglycone) act upon. Quercetin, tamarixetin and isorhamnetin inhibit collagen-stimulated platelet function early in the activatory pathway, and also act to inhibit platelet aggregation stimulated by soluble agonists. In addition to this, it is shown that quercetin and its metabolites can interact with aspirin to enhance anti-platelet effect. It is also demonstrated that the methylated metabolites maintain significant anti-platelet and *in vitro* anti-thrombotic efficacy in platelet rich plasma and whole blood.

The anti-platelet effects of four novel quercetin formulations are presented here for the first time, as are the oral bioavailability and *in vivo* anti-thrombotic effect of an isoquercetin-based formulation. Mathematical modelling approaches have been utilised to develop a pharmacokinetic/pharmacodynamic model of the anti-thrombotic actions of quercetin, with *in silico* experimentation predicting optimal dosing regimens.

In conclusion, this study provides further strong evidence for the anti-platelet and anti-thrombotic potential of quercetin and its metabolites, as well as identifying an interaction with aspirin. This strengthens the argument that the anti-CVD effects observed upon flavonoid consumption may, at least in part, be due to the quercetin-mediated inhibition of platelet function, and highlights quercetin as a potential dietary anti-platelet agent or supplement worth further investigation.

References

Abdel-Lateif, K., Bogusz, D. & Hocher, V. (2012). The role of flavonoids in the establishment of plant roots endosymbioses with arbuscular mycorrhiza fungi, rhizobia and Frankia bacteria. *Plant Signal. Behav.,* **7**, 636-641.

Akbiyik, F., Ray, D. M., Gettings, K. F., Blumberg, N., Francis, C. W. & Phipps, R. P. (2004). Human bone marrow megakaryocytes and platelets express PPARgamma, and PPARgamma agonists blunt platelet release of CD40 ligand and thromboxanes. *Blood,* **104**, 1361-8.

Alemdaroglu, N. C., Dietz, U., Wolffram, S., Spahn-Langguth, H. & Langguth, P. (2008). Influence of green and black tea on folic acid pharmacokinetics in healthy volunteers: potential risk of diminished folic acid bioavailability. *Biopharm. Drug Dispos.,* **29**, 335-48.

Alemdaroglu, N. C., Wolffram, S., Boissel, J. P., Closs, E., Spahn-Langguth, H. & Langguth, P. (2007). Inhibition of folic acid uptake by catechins and tea extracts in Caco-2 cells. *Planta Med.,* **73**, 27-32.

Alevriadou, B. R., Moake, J. L., Turner, N. A., Ruggeri, Z. M., Folie, B. J., Phillips, M. D., Schreiber, A. B., Hrinda, M. E. & McIntire, L. V. (1993). Real-time analysis of shear-dependent thrombus formation and its blockade by inhibitors of von Willebrand factor binding to platelets. *Blood,* **81**, 1263-76.

Ali, F. Y., Davidson, S. J., Moraes, L. A., Traves, S. L., Paul-Clark, M., Bishop-Bailey, D., Warner, T. D. & Mitchell, J. A. (2006). Role of nuclear receptor signaling in platelets: antithrombotic effects of PPARbeta. *FASEB J.,* **20**, 326-8.

Alshehri, O.M., Hughes, C.E., Montague, S., Watson, S.K., Frampton, J., Bender, M. & Watson, S.P. (2015). Fibrin activates GPVI in human and mouse platelets. *Blood.,* **126**, 1601-08.

Altschuler, D. & Lapetina, E. G. (1993). Mutational analysis of the cAMP-dependent protein kinase-mediated phosphorylation site of Rap1b. *J. Biol. Chem.,* **268**, 7527-31.

Amaretti, A., Raimondi, S., Leonardi, A., Quartieri, A. & Rossi, M. (2015). Hydrolysis of the Rutinose-Conjugates Flavonoids Rutin and Hesperidin by the Gut Microbiota and Bifidobacteria. *Nutrients,* **7**, 2788-2800.

Anand David, A. V., Arulmoli, R. & Parasuraman, S. (2016). Overviews of Biological Importance of Quercetin: A Bioactive Flavonoid. *Pharmacogn Rev.,* **10**, 84-89.

Andersen, O. M. & Markham, K. R. (2007). *Flavonoids: Chemistry, Biochemistry and Applications.* Florida, USA: CRC Press.

Andrews, R. K. & Berndt, M. C. (2004). Platelet physiology and thrombosis. *Thromb. Res.,* **114**, 447-53.

Andrews, R. K., Munday, A. D., Mitchell, C. A. & Berndt, M. C. (2001). Interaction of calmodulin with the cytoplasmic domain of the platelet membrane glycoprotein Ib-IX-V complex. *Blood,* **98**, 681-7.

Antonin, W., Fasshauer, D., Becker, S., Jahn, R. & Schneider, T. R. (2002). Crystal structure of the endosomal SNARE complex reveals common structural principles of all SNAREs. *Nat. Struct. Mol. Biol.,* **9**, 107-111.

Anzenbacher, P. & Zanger, U.M. (2012). Metabolism of drugs and other xenobiotics. Hoboken, NJ: John Wiley & Sons, pp. 557.

Ariëns, R. (2013). Fibrin (ogen) and thrombotic disease. *J. Thromb. Haemost.,* **11**, 294-305.

Arthur, J. F., Gardiner, E. E., Matzaris, M., Taylor, S. G., Wijeyewickrema, L., Ozaki, Y., Kahn, M. L., Andrews, R. K. & Berndt, M. C. (2005). Glycoprotein VI is associated with GPIb-IX-V on the membrane of resting and activated platelets. *Thromb. Haemost.,* **93**, 716-23.

Arthur, W. T., Petch, L. A. & Burridge, K. (2000). Integrin engagement suppresses RhoA activity via a c-Src-dependent mechanism. *Curr. Biol.,* **10**, 719-22.

Asazuma, N., Wilde, J. I., Berlanga, O., Leduc, M., Leo, A., Schweighoffer, E., Tybulewicz, V., Bon, C., Liu, S. K., McGlade, C. J., Schraven, B. & Watson, S. P. (2000). Interaction of linker for activation of T cells with multiple adapter proteins in platelets activated by the glycoprotein VI-selective ligand, convulxin. *J. Biol. Chem.,* **275**, 33427-34.

Asselin, J., Gibbins, J. M., Achison, M., Lee, Y. H., Morton, L. F., Farndale, R. W., Barnes, M. J. & Watson, S. P. (1997). A collagen-like peptide stimulates tyrosine phosphorylation of syk and phospholipase C gamma2 in platelets independent of the integrin alpha2beta1. *Blood,* **89**, 1235-42.

Atkinson, B. T., Ellmeier, W. & Watson, S. P. (2003). Tec regulates platelet activation by GPVI in the absence of Btk. *Blood,* **102**, 3592-9.

Augustin, K., Frank, J., Augustin, S., Langguth, P., Ohrvik, V., Witthoft, C. M., Rimbach, G. & Wolffram, S. (2009). Greeen tea extracts lower serum folates in rats at very high dietary concentrations only and do not affect plasma folates in a human pilot study. *J. Physiol. Pharmacol.,* **60**, 103-8.

Azuma, K., Ippoushi, K., Ito, H., Higashio, H. & Terao, J. (2002). Combination of lipids and emulsifiers enhances the absorption of orally administered quercetin in rats. *J. Agric. Food Chem.,* **50**, 1706-12.

Baigent, C., Blackwell, L., Collins, R., Emberson, J., Godwin, J., Peto, R., Buring, J., Hennekens, C., Kearney, P., Meade, T., Patrono, C., Roncaglioni, M. C. & Zanchetti, A. (2009). Aspirin in the primary and secondary prevention of vascular disease: collaborative meta-analysis of individual participant data from randomised trials. *Lancet,* **373**, 1849-60.

Balsinde, J., Winstead, M. V. & Dennis, E. A. (2002). Phospholipase A(2) regulation of arachidonic acid mobilization. *FEBS Lett.,* **531**, 2-6.

Bark, D. & Ku, D. (2010). Wall shear over high degree stenoses pertinent to atherothrombosis. *J Biomech.,* **43**, 2970-2977.

Barnes, M. J. & Farndale, R. W. (1999). Collagens and atherosclerosis. *Exp. Gerontol.,* **34**, 513-25.

Barrett, N. E., Holbrook, L., Jones, S., Kaiser, W. J., Moraes, L. A., Rana, R., Sage, T., Stanley, R. G., Tucker, K. L., Wright, B. & Gibbins, J. M. (2008). Future innovations in anti-platelet therapies. *Br. J. Pharmacol.,* **154**, 918-39.

Baumgartner, H. R. & Haudenschild, C. (1972). Adhesion of platelets to subendothelium. *Ann. N. Y. Acad. Sci.,* **201**, 22-36.

Beatty, E. R., O'Reilly, J. D., England, T. G., McAnlis, G. T., Young, I. S., Geissler, C. A., Sanders, T. A. & Wiseman, H. (2000). Effect of dietary quercetin on oxidative DNA damage in healthy human subjects. *Br. J. Nutr.,* **84**, 919-25.

Bechir, M., Enseleit, F., Chenevard, R., Muntwyler, J., Luscher, T. F. & Noll, G. (2005). Folic Acid improves baroreceptor sensitivity in hypertension. *J. Cardiovasc. Pharmacol.,* **45**, 44-8.

Beck, F., Geiger, J., Gambaryan, S., Veit, J., Vaudel, M., Nollau, P., Kohlbacher, O., Martens, L., Walter, U., Sickmann, A. & Zahedi, R. P. (2014). Time-resolved characterization of cAMP/PKA-dependent signaling reveals that platelet inhibition is a concerted process involving multiple signaling pathways. *Blood,* **123**, e1-e10.

Bednar, F., Kroupa, J., Ondrakova, M., Osmancik, P., Kopa, M. & Motovska, Z. (2016). Antiplatelet efficacy of P2Y12 inhibitors (prasugrel, ticagrelor, clopidogrel) in patients treated with mild therapeutic hypothermia after cardiac arrest due to acute myocardial infarction. *J. Thromb. Thrombolysis,* **41**, 549-55.

Behnke, O. (1967). Electron microscopic observations on the membrane systems of the rat blood platelet. *Anat. Rec.,* **158**, 121-137.

Bennett, J. S. (2005). Structure and function of the platelet integrin alphaIIbbeta3. *J. Clin. Invest.,* **115**, 3363-9.

Beretz, A., Cazenave, J. P. & Anton, R. (1982). Inhibition of aggregation and secretion of human platelets by quercetin and other flavonoids: structure-activity relationships. *Agents Actions,* **12**, 382-7.

Berger, G., Masse, J. M. & Cramer, E. M. (1996). Alpha-granule membrane mirrors the platelet plasma membrane and contains the glycoproteins Ib, IX, and V. *Blood,* **87**, 1385-95.

Bergmeier, W., Piffath, C. L., Cheng, G., Dole, V. S., Zhang, Y., von Andrian, U. H. & Wagner, D. D. (2004a). Tumor necrosis factor-alpha-converting enzyme (ADAM17) mediates GPIbalpha shedding from platelets in vitro and in vivo. *Circ. Res.,* **95**, 677-83.

Bergmeier, W., Rabie, T., Strehl, A., Piffath, C. L., Prostredna, M., Wagner, D. D. & Nieswandt, B. (2004b). GPVI down-regulation in murine platelets through metalloproteinase-dependent shedding. *Thromb. Haemost.,* **91**, 951-958.

Berndt, M. C., Shen, Y., Dopheide, S. M., Gardiner, E. E. & Andrews, R. K. (2001). The vascular biology of the glycoprotein Ib-IX-V complex. *Thromb. Haemost.,* **86**, 178-88.

Bhatt, D. L. (2004). Aspirin resistance: more than just a laboratory curiosity. *J. Am. Coll. Cardiol.,* **43**, 1127-1129.

Bhatt , D. L., Stone , G. W., Mahaffey , K. W., Gibson , C. M., Steg , P. G., Hamm , C. W., Price , M. J., Leonardi , S., Gallup , D., Bramucci , E., Radke , P. W., Widimský , P., Tousek , F., Tauth , J., Spriggs , D., McLaurin , B. T., Angiolillo , D. J., Généreux , P., Liu , T., Prats , J., Todd , M., Skerjanec , S., White , H. D. & Harrington , R. A. (2013). Effect of Platelet Inhibition with Cangrelor during PCI on Ischemic Events. *N. Engl. J. Med.,* **368**, 1303-1313.

Bieger, J., Cermak, R., Blank, R., de Boer, V. C., Hollman, P. C., Kamphues, J. & Wolffram, S. (2008). Tissue distribution of quercetin in pigs after long-term dietary supplementation. *J. Nutr.,* **138**, 1417-20.

Bizzozero, J. (1882). Ueber einen neuen Fornnbestandteil des Blutes und dessen Rolle bei der Thrombose und Blutgerinnung. *Virchows Arch. Pathol. Anat. Physiol. Klin. Med.,* **90**, 261-332.

Blair, P. & Flaumenhaft, R. (2009). Platelet α–granules: Basic biology and clinical correlates. *Blood Rev.,* **23**, 177-189.

Bock, M., De Haan, J., Beck, K. H., Gutensohn, K., Hertfelder, H. J., Karger, R., Heim, M. U., Beeser, H., Weber, D. & Kretschmer, V. (1999). Standardization of the PFA-100(R) platelet function test in 105 mmol/l buffered citrate: effect of gender, smoking, and oral contraceptives. *Br. J. Haematol.,* **106**, 898-904.

Boly, R., Gras, T., Lamkami, T., Guissou, P., Serteyn, D., Kiss, R. & Dubois, J. (2011). Quercetin inhibits a large panel of kinases implicated in cancer cell biology. *Int. J. Oncol.,* **38**, 833-42.

Bonnefoy, A., Hantgan, R., Legrand, C. & Frojmovic, M. M. (2001). A model of platelet aggregation involving multiple interactions of thrombospondin-1, fibrinogen, and GPIIbIIIa receptor. *J. Biol. Chem.,* **276**, 5605-12.

Bootman, M. D., Rietdorf, K., Collins, T., Walker, S. & Sanderson, M. (2013). Ca2+-sensitive fluorescent dyes and intracellular Ca2+ imaging. *Cold Spring Harb. Protoc.,* **2013**, 83-99.

Boots, A. W., Haenen, G. R. & Bast, A. (2008). Health effects of quercetin: from antioxidant to nutraceutical. *Eur. J. Pharmacol.,* **585**, 325-37.

Born, G. V. R. (1962). Aggregation of blood platelets by adenosine diphosphate and its reversal. *Nature,* **194**, 927-929.

Boulton, D. W., Walle, U. K. & Walle, T. (1998). Extensive binding of the bioflavonoid quercetin to human plasma proteins. *J. Pharm. Pharmacol.,* **50**, 243-9.

Bowley, S. R., Fang, C., Merrill-Skoloff, G., Furie, B. C. & Furie, B. (2017). Protein disulfide isomerase secretion following vascular injury initiates a regulatory pathway for thrombus formation. *Nat. Commun.,* **8**, 14151.

Boylan, B., Gao, C., Rathore, V., Gill, J. C., Newman, D. K. & Newman, P. J. (2008). Identification of FcgammaRIIa as the ITAM-bearing receptor mediating alphaIIbbeta3 outside-in integrin signaling in human platelets. *Blood,* **112**, 2780-6.

Braidot, E., Zancani, M., Petrussa, E., Peresson, C., Bertolini, A., Patui, S., Macrì, F. & Vianello, A. (2008). Transport and accumulation of flavonoids in grapevine (Vitis vinifera L.). *Plant Signal. Behav.,* **3**, 626-632.

Brass, L. F. & Joseph, S. K. (1985). A role for inositol triphosphate in intracellular Ca2+ mobilization and granule secretion in platelets. *J. Biol. Chem.,* **260**, 15172-9.

Bray, P. F., Mathias, R. A., Faraday, N., Yanek, L. R., Fallin, M. D., Herrera-Galeano, J. E., Wilson, A. F., Becker, L. C. & Becker, D. M. (2007). Heritability of platelet function in families with premature coronary artery disease. *J. Thromb. Haemost.,* **5**, 1617-23.

Breen, M.E. & Soellner, M.B. (2015). Small molecule substrate phosphorylation site inhibitors of protein kinases: approaches and challenges. *ACS Chem. Biol.,* **10**, 175-89.

Brown, M. T. & Bussell, J. K. (2011). Medication Adherence: WHO Cares? *Mayo Clin. Proc.,* **86**, 304-314.

Buensuceso, C., de Virgilio, M. & Shattil, S. J. (2003). Detection of integrin alpha IIbbeta 3 clustering in living cells. *J. Biol. Chem.,* **278**, 15217-24.

Buensuceso, C. S., Obergfell, A., Soriani, A., Eto, K., Kiosses, W. B., Arias-Salgado, E. G., Kawakami, T. & Shattil, S. J. (2005). Regulation of outside-in signaling in platelets by integrin-associated protein kinase C beta. *J. Biol. Chem.,* **280**, 644-53.

Buitrago, L., Bhavanasi, D., Dangelmaier, C., Manne, B. K., Badolia, R., Borgognone, A., Tsygankov, A. Y., McKenzie, S. E. & Kunapuli, S. P. (2013). Tyrosine phosphorylation on spleen tyrosine kinase (Syk) is differentially regulated in human and murine platelets by protein kinase C isoforms. *J. Biol. Chem.,* **288**, 29160-9.

Burch, J. W., Stanford, N. & Majerus, P. W. (1978). Inhibition of platelet prostaglandin synthetase by oral aspirin. *J. Clin. Invest.,* **61**, 314-9.

Butt, E., Abel, K., Krieger, M., Palm, D., Hoppe, V., Hoppe, J. & Walter, U. (1994). cAMP- and cGMP-dependent protein kinase phosphorylation sites of the focal adhesion vasodilator-stimulated phosphoprotein (VASP) in vitro and in intact human platelets. *J. Biol. Chem.,* **269**, 14509-17.

Bye, A. P., Unsworth, A. J. & Gibbins, J. M. (2016). Platelet signaling: a complex interplay between inhibitory and activatory networks. *J. Thromb. Haemost.,* **14**, 918-930.

Cai, X., Fang, Z., Dou, J., Yu, A. & Zhai, G. (2013). Bioavailability of quercetin: problems and promises. *Curr. Med. Chem.,* **20**, 2572-82.

Calderwood, D. A. (2015). The Rap1-RIAM pathway prefers β2 integrins. *Blood,* **126**, 2658-2659.

Campbell, I. D. & Humphries, M. J. (2011). Integrin structure, activation, and interactions. *Cold Spring Harb. Perspect. Biol.,* **3**, a004994.

Cao, X.-G., Li, X.-X., Bao, Y.-Z., Xing, N.-Z. & Chen, Y. (2007). Responses of Human Lens Epithelial Cells to Quercetin and DMSO. *Invest. Ophthalmol. Vis. Sci.,* **48**, 3714-3718.

Casa, L. D. C., Deaton, D. H. & Ku, D. N. (2015). Role of high shear rate in thrombosis. *J. Vasc. Surg.,* **61**, 1068-1080.

Cassidy, A. & Minihane, A.-M. (2017). The role of metabolism (and the microbiome) in defining the clinical efficacy of dietary flavonoids. *Am. J. Clin. Nutr.,* **105**, 10-22.

Celik, H. & Arinc, E. (2010). Evaluation of the protective effects of quercetin, rutin, naringenin, resveratrol and trolox against idarubicin-induced DNA damage. *J. Pharm. Pharm. Sci.,* **13**, 231-41.

Cermak, R. (2008). Effect of dietary flavonoids on pathways involved in drug metabolism. *Expert Opin. Drug Metab. Toxicol.,* **4**, 17-35.

Chakroun, T., Gerotziafas, G., Robert, F., Lecrubier, C., Samama, M. M., Hatmi, M. & Elalamy, I. (2004). In vitro aspirin resistance detected by PFA-100 closure time: pivotal role of plasma von Willebrand factor. *Br. J. Haematol.,* **124**, 80-5.

Chan, H., Moore, J.C., Finch, C.N., Warkentin, T.E. & Kelton, J.G. (2003). The IgG subclasses of platelet-associated autoantibodies directed against platelet glycoproteins IIb/IIIa in patients with idiopathic thrombocytopenic purpura. *Br J Haematol.,* **122**, 818-24.

Charman, W. N., Charman, S. A., Monkhouse, D. C., Frisbee, S. E., Lockhart, E. A., Weisman, S. & Fitzgerald, G. A. (1993). Biopharmaceutical characterisation of a low-dose (75 mg) controlled-release aspirin formulation. *Br. J. Clin. Pharmacol.,* **36**, 470-3.

Chen, J., De, S., Damron, D. S., Chen, W. S., Hay, N. & Byzova, T. V. (2004). Impaired platelet responses to thrombin and collagen in AKT-1–deficient mice. *Blood,* **104**, 1703-1710.

Chen, J., Diacovo, T. G., Grenache, D. G., Santoro, S. A. & Zutter, M. M. (2002). The α(2) Integrin Subunit-Deficient Mouse : A Multifaceted Phenotype Including Defects of Branching Morphogenesis and Hemostasis. *Am. J. Pathol.,* **161**, 337-344.

Chen, X., Li, D., Hu, Y., Jin, M., Zhou, L., Peng, K. & Zheng, H. (2011). Simultaneous determination of 3,3',4',5,7-pentamethylquercetin and its possible metabolite 3,3',4',7-tetramethylquercetin in dog plasma by liquid chromatography-tandem mass spectrometry and its application to preclinical pharmacokinetic study. *J. Chromatogr. B Analyt. Technol. Biomed. Life Sci.,* **879**, 2339-44.

Chen, X., Yin, O. Q. P., Zuo, Z. & Chow, M. S. S. (2005). Pharmacokinetics and Modeling of Quercetin and Metabolites. *Pharm. Res.,* **22**, 892-901.

Chen, Y. & Deuster, P. (2009). Comparison of quercetin and dihydroquercetin: antioxidant-independent actions on erythrocyte and platelet membrane. *Chem. Biol. Interact.,* **182**, 7-12.

Chen, Y., Xiao, P., Ou-Yang, D. S., Fan, L., Guo, D., Wang, Y. N., Han, Y., Tu, J. H., Zhou, G., Huang, Y. F. & Zhou, H. H. (2009). Simultaneous action of the flavonoid quercetin on cytochrome P450 (CYP) 1A2, CYP2A6, N-acetyltransferase and xanthine oxidase activity in healthy volunteers. *Clin. Exp. Pharmacol. Physiol.,* **36**, 828-33.

Chen, Y. P., O'Toole, T. E., Leong, L., Liu, B. Q., Diaz-Gonzalez, F. & Ginsberg, M. H. (1995). Beta 3 integrin-mediated fibrin clot retraction by nucleated cells: differing behavior of alpha IIb beta 3 and alpha v beta 3. *Blood,* **86**, 2606-15.

Chen, Z., Zheng, S., Li, L. & Jiang, H. (2014). Metabolism of flavonoids in human: a comprehensive review. *Curr. Drug Metab.,* **15**, 48-61.

Cheng, H-C., Qi, R.Z., Paudel, H. & Zhu, H-J. (2011). Regulation and function of protein kinases and phosphatases. *Enzyme Res.,* **2011**, ePub.

Chiu, J.-J. & Chien, S. (2011). Effects of Disturbed Flow on Vascular Endothelium: Pathophysiological Basis and Clinical Perspectives. *Physiol. Rev.,* **91**, 327-87.

Cho, J., Furie, B. C., Coughlin, S. R. & Furie, B. (2008). A critical role for extracellular protein disulfide isomerase during thrombus formation in mice. *J. Clin. Invest.,* **118**, 1123-31.

Choi, J. H., Kim, K. J. & Kim, S. (2016). Comparative Effect of Quercetin and Quercetin-3-O-beta-d-Glucoside on Fibrin Polymers, Blood Clots, and in Rodent Models. *J. Biochem. Mol. Toxicol.,* **30**, 548-558.

Chondrogianni, N., Kapeta, S., Chinou, I., Vassilatou, K., Papassideri, I. & Gonos, E. S. (2010). Anti-ageing and rejuvenating effects of quercetin. *Exp. Gerontol.,* **45**, 763-71.

Ciccone, C. D. (2015). *Pharmacology in Rehabilitation.* Philadelphia, USA: F. A. Davis Company.

Cicmil, M., Thomas, J. M., Leduc, M., Bon, C. & Gibbins, J. M. (2002). Platelet endothelial cell adhesion molecule-1 signaling inhibits the activation of human platelets. *Blood,* **99**, 137-44.

Cicmil, M., Thomas, J. M., Sage, T., Barry, F. A., Leduc, M., Bon, C. & Gibbins, J. M. (2000). Collagen, Convulxin, and Thrombin Stimulate Aggregation-independent Tyrosine

Phosphorylation of CD31 in Platelets. Evidence for the involvement of Src family kinases. *J. Biol. Chem.,* **275**, 27339-27347.

Ciferri, S., Emiliani, C., Guglielmini, G., Orlacchio, A., Nenci, G. G. & Gresele, P. (2000). Platelets release their lysosomal content in vivo in humans upon activation. *Thromb. Haemost.,* **83**, 157-64.

Cines, D. B., Lebedeva, T., Nagaswami, C., Hayes, V., Massefski, W., Litvinov, R. I., Rauova, L., Lowery, T. J. & Weisel, J. W. (2014). Clot contraction: compression of erythrocytes into tightly packed polyhedra and redistribution of platelets and fibrin. *Blood,* **123**, 1596-603.

Clarke, J., Snelling, J., Ioannides, C., Flatt, P. R. & Barnett, C. R. (1996). Effect of vitamin C supplementation on hepatic cytochrome P450 mixed-function oxidase activity in streptozotocin-diabetic rats. *Toxicol. Lett.,* **89**, 249-56.

Clarke, R. J., Mayo, G., Price, P. & FitzGerald, G. A. (1991). Suppression of thromboxane A2 but not of systemic prostacyclin by controlled-release aspirin. *N. Engl. J. Med.,* **325**, 1137-41.

Claxton, A. J., Cramer, J. & Pierce, C. (2001). A systematic review of the associations between dose regimens and medication compliance. *Clin. Ther.,* **23**, 1296-310.

Clemetson, J. M., Polgar, J., Magnenat, E., Wells, T. N. & Clemetson, K. J. (1999). The platelet collagen receptor glycoprotein VI is a member of the immunoglobulin superfamily closely related to FcalphaR and the natural killer receptors. *J. Biol. Chem.,* **274**, 29019-24.

Cole, V., Staton, J., Eikelboom, J., Hankey, G., Yi, Q., Shen, Y., Berndt, M. & Baker, R. (2003). Collagen platelet receptor polymorphisms integrin α2β1 C807T and GPVI Q317L and risk of ischemic stroke. *J. Thromb. Haemost.,* **1**, 963-970.

Colman, R. W. (2006). *Hemostasis and thrombosis: basic principles and clinical practice.* Philadelphia, USA: Lippincott Williams & Wilkins.

Coppen, A. & Bailey, J. (2000). Enhancement of the antidepressant action of fluoxetine by folic acid: a randomised, placebo controlled trial. *J. Affect. Disord.,* **60**, 121-30.

Cosemans, J. M., Iserbyt, B. F., Deckmyn, H. & Heemskerk, J. W. (2008). Multiple ways to switch platelet integrins on and off. *J. Thromb. Haemost.,* **6**, 1253-1261.

Coughlin, S. R. (2000). Thrombin signalling and protease-activated receptors. *Nature,* **407**, 258-64.

Cozzi, M. R., Guglielmini, G., Battiston, M., Momi, S., Lombardi, E., Miller, E. C., De Zanet, D., Mazzucato, M., Gresele, P. & De Marco, L. (2015). Visualization of nitric oxide production by individual platelets during adhesion in flowing blood. *Blood,* **125**, 697-705.

Cramer, E. M., Berger, G. & Berndt, M. C. (1994). Platelet alpha-granule and plasma membrane share two new components: CD9 and PECAM-1. *Blood,* **84**, 1722-30.

Craven, L. L. (1950). Acetylsalicylic acid, possible preventive of coronary thrombosis. *Ann. West. Med. Surg.,* **4**, 95.

Crawley, J. T., Zanardelli, S., Chion, C. K. & Lane, D. A. (2007). The central role of thrombin in hemostasis. *J. Thromb. Haemost.,* **5 Suppl 1**, 95-101.

Crescente, M., Armstrong, P. C., Chan, M. V., Edin, M. L., Lih, F. B., Jiao, J., Gaston-Massuet, C., Cottrell, G. S., Kirkby, N. S., Mitchell, J. A., Zeldin, D. C., Herschman, H. R. & Warner, T. D. (2017). Platelet cox-1 knockout mouse as a model of the effects of aspirin in the cardiovascular system. *Heart,* **103**, A108.

Crescente, M., Jessen, G., Momi, S., Holtje, H. D., Gresele, P., Cerletti, C. & de Gaetano, G. (2009). Interactions of gallic acid, resveratrol, quercetin and aspirin at the platelet cyclooxygenase-1 level. Functional and modelling studies. *Thromb. Haemost.,* **102**, 336-46.

Crespy, V., Morand, C., Besson, C., Cotelle, N., Vezin, H., Demigne, C. & Remesy, C. (2003). The splanchnic metabolism of flavonoids highly differed according to the nature of the compound. *Am. J. Physiol. Gastrointest. Liver Physiol.,* **284**, G980-8.

Crespy, V., Morand, C., Besson, C., Manach, C., Demigne, C. & Remesy, C. (2002). Quercetin, but not its glycosides, is absorbed from the rat stomach. *J. Agric. Food Chem.,* **50**, 618-621.

Crespy, V., Morand, C., Manach, C., Besson, C., Demigne, C. & Remesy, C. (1999). Part of quercetin absorbed in the small intestine is conjugated and further secreted in the intestinal lumen. *Am. J. Physiol.,* **277**, G120-6.

Crow, A.R. & Lazarus, A.H. (2003). Role of Fcgamma receptors in the pathogenesis and treatment of idiopathic thrombocytopenic purpura. *J Pediatr Hematol Oncol.,* **25**, S14-18.

Crozier, A., Clifford, M. N. & Ashihara, H. (2008). *Plant Secondary Metabolites: Occurrence, Structure and Role in the Human Diet.* Oxford, UK: Blackwell Publishing.

Cruz, M. A., Chen, J., Whitelock, J. L., Morales, L. D. & Lopez, J. A. (2005). The platelet glycoprotein Ib-von Willebrand factor interaction activates the collagen receptor alpha2beta1 to bind collagen: activation-dependent conformational change of the alpha2-I domain. *Blood,* **105**, 1986-91.

Cutler, L., Rodan, G. & Feinstein, M. B. (1978). Cytochemical localization of adenylate cyclase and of calcium ion, magnesium ion-activated ATPases in the dense tubular system of human blood platelets. *Biochim. Biophys. Acta,* **542**, 357-71.

D'Souza, L. & Glueck, H. I. (1977). Measurement of nucleotide pools in platelets using high pressure liquid chromatography. *Thromb. Haemost.,* **38**, 990-1001.

D'Andrea, G., Chetta, M. & Margaglione, M. (2009). Inherited platelet disorders: thrombocytopenias and thrombocytopathies. *Blood Transfusion,* **7**, 278-292.

Dai, Y. & Ge, J. (2012). Clinical Use of Aspirin in Treatment and Prevention of Cardiovascular Disease. *Thrombosis,* **2012**, 245037.

Dangel, O., Mergia, E., Karlisch, K., Groneberg, D., Koesling, D. & Friebe, A. (2010). Nitric oxide-sensitive guanylyl cyclase is the only nitric oxide receptor mediating platelet inhibition. *J. Thromb. Haemost.,* **8**, 1343-1352.

Daniel, J. L., Dangelmaier, C. & Smith, J. B. (1994). Evidence for a role for tyrosine phosphorylation of phospholipase Cγ2 in collagen-induced platelet cytosolic calcium mobilization. *Biochem. J.,* **302**, 617-622.

Davì , G. & Patrono , C. (2007). Platelet Activation and Atherothrombosis. *N. Engl. J. Med.,* **357**, 2482-2494.

Day, A. J., Cañada, F. J., Díaz, J. C., Kroon, P. A., Mclauchlan, R., Faulds, C. B., Plumb, G. W., Morgan, M. R. & Williamson, G. (2000). Dietary flavonoid and isoflavone glycosides are hydrolysed by the lactase site of lactase phlorizin hydrolase. *FEBS Lett.,* **468**, 166-170.

Day, A. J., DuPont, M. S., Ridley, S., Rhodes, M., Rhodes, M. J., Morgan, M. R. & Williamson, G. (1998). Deglycosylation of flavonoid and isoflavonoid glycosides by human small intestine and liver β-glucosidase activity. *FEBS Lett.,* **436**, 71-75.

Day, A. J., Gee, J. M., DuPont, M. S., Johnson, I. T. & Williamson, G. (2003). Absorption of quercetin-3-glucoside and quercetin-4'-glucoside in the rat small intestine: the role of lactase phlorizin hydrolase and the sodium-dependent glucose transporter. *Biochem. Pharmacol.,* **65**, 1199-206.

Day, A. J., Mellon, F., Barron, D., Sarrazin, G., Morgan, M. R. A. & Williamson, G. (2001). Human metabolism of dietary flavonoids: Identification of plasma metabolites of quercetin. *Free Radic. Res.,* **35**, 941-952.

De Candia, E., Hall, S. W., Rutella, S., Landolfi, R., Andrews, R. K. & De Cristofaro, R. (2001). Binding of Thrombin to Glycoprotein Ib Accelerates the Hydrolysis of Par-1 on Intact Platelets. *J. Biol. Chem.,* **276**, 4692-4698.

de Lorgeril, M., Salen, P., Martin, J. L., Monjaud, I., Delaye, J. & Mamelle, N. (1999). Mediterranean diet, traditional risk factors, and the rate of cardiovascular complications after myocardial infarction: final report of the Lyon Diet Heart Study. *Circulation,* **99**, 779-85.

De Luca, G., Barberi, I., Ruggeri, P. & Di Giorgio, R. (1976). Catechol-O-methyl transferase activity in the individual human platelet populations. *Ital. J. Biochem.,* **25**, 213-218.

de Sauvage, F. J., Hass, P. E., Spencer, S. D., Malloy, B. E., Gurney, A. L., Spencer, S. A., Darbonne, W. C., Henzel, W. J., Wong, S. C., Kuang, W. J. & et al. (1994). Stimulation of megakaryocytopoiesis and thrombopoiesis by the c-Mpl ligand. *Nature,* **369**, 533-8.

de Vet, E. C., Aguado, B. & Campbell, R. D. (2001). G6b, a novel immunoglobulin superfamily member encoded in the human major histocompatibility complex, interacts with SHP-1 and SHP-2. *J. Biol. Chem.,* **276**, 42070-6.

De Wals, P., Tairou, F., Van Allen, M. I., Uh, S. H., Lowry, R. B., Sibbald, B., Evans, J. A., Van den Hof, M. C., Zimmer, P., Crowley, M., Fernandez, B., Lee, N. S. & Niyonsenga, T. (2007). Reduction in neural-tube defects after folic acid fortification in Canada. *N. Engl. J. Med.,* **357**, 135-42.

del Valle, J. C., Buide, M. L., Casimiro-Soriguer, I., Whittall, J. B. & Narbona, E. (2015). On flavonoid accumulation in different plant parts: variation patterns among individuals and populations in the shore campion (Silene littorea). *Front. Plant Sci.,* **6**, 939

Depeint, F., Gee, J. M., Williamson, G. & Johnson, I. T. (2002). Evidence for consistent patterns between flavonoid structures and cellular activities. *Proc. Nutr. Soc.,* **61**, 97-103.

DeSesso, J. M. & Jacobson, C. F. (2001). Anatomical and physiological parameters affecting gastrointestinal absorption in humans and rats. *Food Chem. Toxicol.,* **39**, 209-28.

Diener, H. C. (2006). Secondary stroke prevention with antiplatelet drugs: have we reached the ceiling? *Int. J. Stroke,* **1**, 4-8.

Djellas, Y., Manganello, J. M., Antonakis, K. & Le Breton, G. C. (1999). Identification of Galpha13 as one of the G-proteins that couple to human platelet thromboxane A2 receptors. *J. Biol. Chem.,* **274**, 14325-30.

Dodge, J. T., Jr., Brown, B. G., Bolson, E. L. & Dodge, H. T. (1992). Lumen diameter of normal human coronary arteries. Influence of age, sex, anatomic variation, and left ventricular hypertrophy or dilation. *Circulation,* **86**, 232-46.

Dohlman, H. G., Caron, M. G. & Lefkowitz, R. J. (1987). A family of receptors coupled to guanine nucleotide regulatory proteins. *Biochemistry,* **26**, 2657-2664.

Dovizio, M., Tacconelli, S., Sostres, C., Ricciotti, E. & Patrignani, P. (2012). Mechanistic and pharmacological issues of aspirin as an anticancer agent. *Pharmaceuticals (Basel),* **5**, 1346-71.

Du, X., Beutler, L., Ruan, C., Castaldi, P. A. & Berndt, M. C. (1987). Glycoprotein Ib and glycoprotein IX are fully complexed in the intact platelet membrane. *Blood,* **69**, 1524-7.

Duman, J. G. & Forte, J. G. (2003). What is the role of SNARE proteins in membrane fusion? *Am. J. Physiol. Cell Physiol.,* **285**, C237-49.

Dunster, J. L., Mazet, F., Fry, M. J., Gibbins, J. M. & Tindall, M. J. (2015). Regulation of Early Steps of GPVI Signal Transduction by Phosphatases: A Systems Biology Approach. *PLoS Comput. Biol.,* **11**, e1004589.

Durand, P., Prost, M. & Blache, D. (1996). Pro-thrombotic effects of a folic acid deficient diet in rat platelets and macrophages related to elevated homocysteine and decreased n-3 polyunsaturated fatty acids. *Atherosclerosis,* **121**, 231-43.

Dutta-Roy, A. K. & Sinha, A. K. (1987). Purification and properties of prostaglandin E1/prostacyclin receptor of human blood platelets. *J. Biol. Chem.,* **262**, 12685-91.

Dütting, S., Bender, M. & Nieswandt, B. (2012). Platelet GPVI: a target for antithrombotic therapy?! *Trends Pharmacol. Sci.,* **33**, 583-590.

Ebbeling, L., Robertson, C., McNicol, A. & Gerrard, J. M. (1992). Rapid ultrastructural changes in the dense tubular system following platelet activation. *Blood,* **80**, 718-23.

Edelstein, L. C., Simon, L. M., Lindsay, C. R., Kong, X., Teruel-Montoya, R., Tourdot, B. E., Chen, E. S., Ma, L., Coughlin, S., Nieman, M., Holinstat, M., Shaw, C. A. & Bray, P. F. (2014). Common variants in the human platelet PAR4 thrombin receptor alter platelet function and differ by race. *Blood,* **124**, 3450-8.

Edelstein, L. C., Simon, L. M., Montoya, R. T., Holinstat, M., Chen, E. S., Bergeron, A., Kong, X., Nagalla, S., Mohandas, N., Cohen, D. E., Dong, J. F., Shaw, C. & Bray, P. F. (2013). Racial differences in human platelet PAR4 reactivity reflect expression of PCTP and miR-376c. *Nat. Med.,* **19**, 1609-16.

Edwards, R. L., Lyon, T., Litwin, S. E., Rabovsky, A., Symons, J. D. & Jalili, T. (2007). Quercetin reduces blood pressure in hypertensive subjects. *J. Nutr.,* **137**, 2405-11.

Egert, S., Bosy-Westphal, A., Seiberl, J., Kurbitz, C., Settler, U., Plachta-Danielzik, S., Wagner, A. E., Frank, J., Schrezenmeir, J., Rimbach, G., Wolffram, S. & Muller, M. J. (2009). Quercetin reduces systolic blood pressure and plasma oxidised low-density lipoprotein concentrations in overweight subjects with a high-cardiovascular disease risk phenotype: a double-blinded, placebo-controlled cross-over study. *Br. J. Nutr.,* **102**, 1065-74.

Egert, S., Wolffram, S., Bosy-Westphal, A., Boesch-Saadatmandi, C., Wagner, A. E., Frank, J., Rimbach, G. & Mueller, M. J. (2008). Daily quercetin supplementation dose-dependently increases plasma quercetin concentrations in healthy humans. *J. Nutr.,* **138**, 1615-21.

Elyamany, G., Alzahrani, A. M. & Bukhary, E. (2014). Cancer-Associated Thrombosis: An Overview. *Clin. Med. Insights Oncol.,* **8**, 129-137.

Emsley, J., Cruz, M., Handin, R. & Liddington, R. (1998). Crystal structure of the von Willebrand Factor A1 domain and implications for the binding of platelet glycoprotein Ib. *J. Biol. Chem.,* **273**, 10396-401.

Emsley, J., Knight, C. G., Farndale, R. W., Barnes, M. J. & Liddington, R. C. (2000). Structural basis of collagen recognition by integrin alpha2beta1. *Cell,* **101**, 47-56.

EPIC-Investigators (1994). Use of a Monoclonal Antibody Directed against the Platelet Glycoprotein IIb/IIIa Receptor in High-Risk Coronary Angioplasty. *N. Engl. J. Med.,* **330**, 956-961.

Erlund, I., Freese, R., Marniemi, J., Hakala, P. & Alfthan, G. (2006). Bioavailability of quercetin from berries and the diet. *Nutr. Cancer,* **54**, 13-7.

Escolar, G. & White, J. G. (1991). The platelet open canalicular system: a final common pathway. *Blood Cells,* **17**, 467-95.

Esmon, C. T. & Jackson, C. M. (1974). The conversion of prothrombin to thrombin. III. The factor Xa-catalyzed activation of prothrombin. *J. Biol. Chem.,* **249**, 7782-90.

Estruch, R., Ros, E., Salas-Salvadó, J., Covas, M.-I., Corella, D., Arós, F., Gómez-Gracia, E., Ruiz-Gutiérrez, V., Fiol, M., Lapetra, J., Lamuela-Raventos, R. M., Serra-Majem, L., Pintó, X., Basora, J., Muñoz, M. A., Sorlí, J. V., Martínez, J. A. & Martínez-González, M. A. (2013). Primary Prevention of Cardiovascular Disease with a Mediterranean Diet. *N. Engl. J. Med.,* **368**, 1279-1290.

Ezumi, Y., Shindoh, K., Tsuji, M. & Takayama, H. (1998). Physical and functional association of the Src family kinases Fyn and Lyn with the collagen receptor glycoprotein VI-Fc receptor gamma chain complex on human platelets. *J. Exp. Med.,* **188**, 267-76.

Fabre, J. E., Nguyen, M., Latour, A., Keifer, J. A., Audoly, L. P., Coffman, T. M. & Koller, B. H. (1999). Decreased platelet aggregation, increased bleeding time and resistance to thromboembolism in P2Y1-deficient mice. *Nat. Med.,* **5**, 1199-202.

Fadem, B. (2007). *High-yield Comprehensive USMLE Step 1 Review.* Philadelphia, USA: Lippincott Williams & Wilkins.

Fadok, V. A., Voelker, D. R., Campbell, P. A., Cohen, J. J., Bratton, D. L. & Henson, P. M. (1992). Exposure of phosphatidylserine on the surface of apoptotic lymphocytes triggers specific recognition and removal by macrophages. *J. Immunol.,* **148**, 2207-16.

Falati, S., Edmead, C. E. & Poole, A. W. (1999). Glycoprotein Ib-V-IX, a receptor for von Willebrand factor, couples physically and functionally to the Fc receptor gamma-chain, Fyn, and Lyn to activate human platelets. *Blood,* **94**, 1648-56.

Falati, S., Gross, P., Merrill-Skoloff, G., Furie, B. C. & Furie, B. (2002). Real-time in vivo imaging of platelets, tissue factor and fibrin during arterial thrombus formation in the mouse. *Nat. Med.,* **8**, 1175-1180.

Falati, S., Patil, S., Gross, P. L., Stapleton, M., Merrill-Skoloff, G., Barrett, N. E., Pixton, K. L., Weiler, H., Cooley, B., Newman, D. K., Newman, P. J., Furie, B. C., Furie, B. & Gibbins, J. M. (2006). Platelet PECAM-1 inhibits thrombus formation in vivo. *Blood,* **107**, 535-541.

Falet, H., Barkalow, K. L., Pivniouk, V. I., Barnes, M. J., Geha, R. S. & Hartwig, J. H. (2000). Roles of SLP-76, phosphoinositide 3-kinase, and gelsolin in the platelet shape changes initiated by the collagen receptor GPVI/FcR gamma-chain complex. *Blood,* **96**, 3786-92.

Farndale, R. W., Slatter, D. A., Siljander, P. R. & Jarvis, G. E. (2007). Platelet receptor recognition and cross-talk in collagen-induced activation of platelets. *J. Thromb. Haemost.,* **5 Suppl 1**, 220-9.

Favaloro, E. J. (2002). Clinical application of the PFA-100. *Curr. Opin. Hematol.,* **9**, 407-415.

Favaloro, E. J. (2008). Clinical utility of the PFA-100. *Semin. Thromb. Hemost.,* **34**, 709-33.

Feijge, M. A. H., Ansink, K., Vanschoonbeek, K. & Heemskerk, J. W. M. (2004). Control of platelet activation by cyclic AMP turnover and cyclic nucleotide phosphodiesterase type-3. *Biochem. Pharmacol.,* **67**, 1559-1567.

Feinman, R. D., Lubowsky, J., Charo, I. & Zabinski, M. P. (1977). The lumi-aggregometer: a new instrument for simultaneous measurement of secretion and aggregation by platelets. *J. Lab. Clin. Med.,* **90**, 125-9.

Feng, S., Christodoulides, N., Reséndiz, J. C., Berndt, M. C. & Kroll, M. H. (2000). Cytoplasmic domains of GpIbα and GpIbβ regulate 14-3-3ζ binding to GpIb/IX/V. *Blood,* **95**, 551-557.

Ferry, D. R., Smith, A., Malkhandi, J., Fyfe, D. W., deTakats, P. G., Anderson, D., Baker, J. & Kerr, D. J. (1996). Phase I clinical trial of the flavonoid quercetin: pharmacokinetics and evidence for in vivo tyrosine kinase inhibition. *Clin. Cancer Res.,* **2**, 659-68.

Fiorani, M., Accorsi, A. & Cantoni, O. (2003). Human red blood cells as a natural flavonoid reservoir. *Free Radic. Res.,* **37**, 1331-8.

FitzGerald, G. A. (1991). Mechanisms of platelet activation: thromboxane A2 as an amplifying signal for other agonists. *Am. J. Cardiol.,* **68**, 11b-15b.

Flaumenhaft, R. (2013). Protein disulfide isomerase as an antithrombotic target. *Trends Cardiovasc. Med.,* **23**, 264-268.

Flaumenhaft, R., Croce, K., Chen, E., Furie, B. & Furie, B. C. (1999). Proteins of the exocytotic core complex mediate platelet alpha-granule secretion. Roles of vesicle-associated membrane protein, SNAP-23, and syntaxin 4. *J. Biol. Chem.,* **274**, 2492-501.

Flevaris, P., Stojanovic, A., Gong, H., Chishti, A., Welch, E. & Du, X. (2007). A molecular switch that controls cell spreading and retraction. *J. Cell Biol.,* **179**, 553-65.

Floras, J. S., Aylward, P. E., Victor, R. G., Mark, A. L. & Abboud, F. M. (1988). Epinephrine facilitates neurogenic vasoconstriction in humans. *J. Clin. Invest.,* **81**, 1265-1274.

Floyd, C. N. & Ferro, A. (2014). Mechanisms of aspirin resistance. *Pharmacol. Ther.,* **141**, 69-78.

Fogelson, A. L. & Wang, N. T. (1996). Platelet dense-granule centralization and the persistence of ADP secretion. *Am. J. Physiol.,* **270**, H1131-40.

Förstermann, U. & Sessa, W. C. (2012). Nitric oxide synthases: regulation and function. *Eur. Heart J.,* **33**, 829-837.

Foster, C. J., Prosser, D. M., Agans, J. M., Zhai, Y., Smith, M. D., Lachowicz, J. E., Zhang, F. L., Gustafson, E., Monsma, F. J., Jr., Wiekowski, M. T., Abbondanzo, S. J., Cook, D. N., Bayne, M. L., Lira, S. A. & Chintala, M. S. (2001). Molecular identification and characterization of the platelet ADP receptor targeted by thienopyridine antithrombotic drugs. *J. Clin. Invest.,* **107**, 1591-8.

Fox, J. E. (1994). Shedding of adhesion receptors from the surface of activated platelets. *Blood Coagul. Fibrinolysis,* **5**, 291-304.

Franchini, M. (2005). The platelet function analuzer (PFA-100): an update on its clinical use. *Clin. Lab.,* **51**, 367-372.

Francis, S. H., Blount, M. A., Zoraghi, R. & Corbin, J. D. (2005). Molecular properties of mammalian proteins that interact with cGMP: protein kinases, cation channels, phosphodiesterases, and multi-drug anion transporters. *Front. Biosci.,* **10**, 2097-117.

Fredriksson, R. & Schiöth, H. B. (2005). The repertoire of G-protein–coupled receptors in fully sequenced genomes. *Mol. Pharmacol.,* **67**, 1414-1425.

Friebe, A. & Koesling, D. (2009). The function of NO-sensitive guanylyl cyclase: What we can learn from genetic mouse models. *Nitric Oxide,* **21**, 149-156.

Fukuda, K., Doggett, T., Laurenzi, I. J., Liddington, R. C. & Diacovo, T. G. (2005). The snake venom protein botrocetin acts as a biological brace to promote dysfunctional platelet aggregation. *Nat. Struct. Mol. Biol.,* **12**, 152-159.

Furie, B. & Flaumenhaft, R. (2014). Thiol isomerases in thrombus formation. *Circ. Res.,* **114**, 1162-1173.

Furie , B. & Furie , B. C. (2008). Mechanisms of Thrombus Formation. *N. Engl. J. Med.,* **359**, 938-949.

Gaarder, A., Jonsen, J., Laland, S., Hellem, A. & Owren, P. A. (1961). Adenosine diphosphate in red cells as a factor in the adhesiveness of human blood platelets. *Nature,* **192**, 531-2.

Gambaryan, S. & Tsikas, D. (2015). A review and discussion of platelet nitric oxide and nitric oxide synthase: do blood platelets produce nitric oxide from L-arginine or nitrite? *Amino Acids,* **47**, 1779-93.

Garcia, A., Kim, S., Bhavaraju, K., Schoenwaelder, S. M. & Kunapuli, S. P. (2010). Role of phosphoinositide 3-kinase beta in platelet aggregation and thromboxane A2 generation mediated by Gi signalling pathways. *Biochem. J.,* **429**, 369-77.

García Rodríguez, L. A., Martín-Pérez, M., Hennekens, C. H., Rothwell, P. M. & Lanas, A. (2016). Bleeding Risk with Long-Term Low-Dose Aspirin: A Systematic Review of Observational Studies. *PLoS One,* **11**, e0160046.

Gardiner, E. E., Karunakaran, D., Shen, Y., Arthur, J. F., Andrews, R. K. & Berndt, M. C. (2007). Controlled shedding of platelet glycoprotein (GP)VI and GPIb-IX-V by ADAM family metalloproteinases. *J. Thromb. Haemost.,* **5**, 1530-7.

Gaudineau, C. & Auclair, K. (2004). Inhibition of human P450 enzymes by nicotinic acid and nicotinamide. *Biochem. Biophys. Res. Commun.,* **317**, 950-6.

Gaziano, T. A., Bitton, A., Anand, S., Abrahams-Gessel, S. & Murphy, A. (2010). Growing Epidemic of Coronary Heart Disease in Low- and Middle-Income Countries. *Curr. Probl. Cardiol.,* **35**, 72-115.

Gear, A. R. & Burke, D. (1982). Thrombin-induced secretion of serotonin from platelets can occur in seconds. *Blood,* **60**, 1231-4.

Gee, J. M., DuPont, M. S., Rhodes, M. J. & Johnson, I. T. (1998). Quercetin glucosides interact with the intestinal glucose transport pathway. *Free Radic. Biol. Med.,* **25**, 19-25.

Genetta, T. B. & Mauro, V. F. (1996). Abciximab: a new antiaggregant used in angioplasty. *Ann. Pharmacother.,* **30**, 251-7.

George, J. N., Caen, J. P. & Nurden, A. T. (1990). Glanzmann's thrombasthenia: the spectrum of clinical disease. *Blood,* **75**, 1383-95.

Gerrard, J. M., White, J. G. & Peterson, D. A. (1978). The platelet dense tubular system: its relationship to prostaglandin synthesis and calcium flux. *Thromb. Haemost.,* **40**, 224-31.

Giaretta, A., Rocca, B., Di Camillo, B., Toffolo, G. M. & Patrono, C. (2015). An in silico model of aspirin-iduced inactivation of platelet and Megakaryocyte Cyclooxygenase-1. *Clin. Ther.,* **37**, e102.

Gibbins, J. M., Okuma, M., Farndale, R., Barnes, M. & Watson, S. P. (1997). Glycoprotein VI is the collagen receptor in platelets which underlies tyrosine phosphorylation of the Fc receptor γ-chain. *FEBS Lett.,* **413**, 255-259.

Giddings, J. C. & Bloom, A. L. (1975). Factor-V activation by thrombin and its role in prothrombin conversion. *Br. J. Haematol.,* **29**, 349-64.

Gilbert, G. E., Sims, P. J., Wiedmer, T., Furie, B., Furie, B. C. & Shattil, S. J. (1991). Platelet-derived microparticles express high affinity receptors for factor VIII. *J. Biol. Chem.,* **266**, 17261-8.

Giles, C. (1981). The platelet count and mean platelet volume. *Br. J. Haematol.,* **48**, 31-7.

Gilio, K., Munnix, I. C., Mangin, P., Cosemans, J. M., Feijge, M. A., van der Meijden, P. E., Olieslagers, S., Chrzanowska-Wodnicka, M. B., Lillian, R., Schoenwaelder, S., Koyasu, S., Sage, S. O., Jackson, S. P. & Heemskerk, J. W. (2009). Non-redundant roles of phosphoinositide 3-kinase isoforms alpha and beta in glycoprotein VI-induced platelet signaling and thrombus formation. *J. Biol. Chem.,* **284**, 33750-62.

Ginsberg, M. H., Xiaoping, D., O'Toole, T. E., Loftus, J. C. & Plow, E. F. (1993). Platelet integrins. *Thromb. Haemost.,* **70**, 87-93.

Gitz, E., Koopman, C. D., Giannas, A., Koekman, C. A., van den Heuvel, D. J., Deckmyn, H., Akkerman, J.-W. N., Gerritsen, H. C. & Urbanus, R. T. (2013). Platelet interaction with von Willebrand factor is enhanced by shear-induced clustering of glycoprotein Ibα. *Haematologica,* **98**, 1810-1818.

Glagov, S., Zarins, C., Giddens, D. & Ku, D. (1988). Hemodynamics and atherosclerosis. Insights and perspectives gained from studies of human arteries. *Arch. Pathol. Lab. Med.,* **112**, 1018-1031.

Glanzmann, E. (1918). Hereditare hamorrhagische thrombasthenie. Ein beitrag zur pathologie der blutplattchen. *J Kinderkranken,* **88**, 113-141.

Glossmann, H., Presek, P. & Eigenbrodt, E. (1981). Quercetin inhibits tyrosine phosphorylation by the cyclic nucleotide-independent, transforming protein kinase, pp60src. *Naunyn Schmiedebergs Arch. Pharmacol.,* **317**, 100-102.

Godfrey, P. S., Toone, B. K., Carney, M. W., Flynn, T. G., Bottiglieri, T., Laundy, M., Chanarin, I. & Reynolds, E. H. (1990). Enhancement of recovery from psychiatric illness by methylfolate. *Lancet,* **336**, 392-5.

Goggs, R., Harper, M. T., Pope, R. J., Savage, J. S., Williams, C. M., Mundell, S. J., Heesom, K. J., Bass, M., Mellor, H. & Poole, A. W. (2013). RhoG protein regulates platelet granule secretion and thrombus formation in mice. *J. Biol. Chem.,* **288**, 34217-29.

Golebiewska, E. M., Harper, M. T., Williams, C. M., Savage, J. S., Goggs, R., Fischer von Mollard, G. & Poole, A. W. (2015). Syntaxin 8 regulates platelet dense granule secretion, aggregation, and thrombus stability. *J. Biol. Chem.,* **290**, 1536-45.

Golebiewska, E. M. & Poole, A. W. (2015). Platelet secretion: From haemostasis to wound healing and beyond. *Blood Rev.,* **29**, 153-162.

Gong, H., Shen, B., Flevaris, P., Chow, C., Lam, S. C., Voyno-Yasenetskaya, T. A., Kozasa, T. & Du, X. (2010). G protein subunit Galpha13 binds to integrin alphaIIbbeta3 and mediates integrin "outside-in" signaling. *Science,* **327**, 340-3.

Gorman, R. R., Bunting, S. & Miller, O. V. (1977). Modulation of human platelet adenylate cyclase by prostacyclin (PGX). *Prostaglandins,* **13**, 377-88.

Gormaz, J. G., Quintremil, S. & Rodrigo, R. (2015). Cardiovascular Disease: A Target for the Pharmacological Effects of Quercetin. *Curr. Top. Med. Chem.,* **15**, 1735-42.

Gottumukkala, R. V. S. S., Nadimpalli, N., Sukala, K. & Subbaraju, G. V. (2014). Determination of Catechin and Epicatechin Content in Chocolates by High-Performance Liquid Chromatography. *Int. Sch. Res. Notices,* **2014**, 628196.

Graefe, E. U., Wittig, J., Mueller, S., Riethling, A. K., Uehleke, B., Drewelow, B., Pforte, H., Jacobasch, G., Derendorf, H. & Veit, M. (2001). Pharmacokinetics and bioavailability of quercetin glycosides in humans. *J. Clin. Pharmacol.,* **41**, 492-9.

Graf, B. A., Ameho, C., Dolnikowski, G. G., Milbury, P. E., Chen, C. Y. & Blumberg, J. B. (2006). Rat gastrointestinal tissues metabolize quercetin. *J. Nutr.,* **136**, 39-44.

Graf, B. A., Mullen, W., Caldwell, S. T., Hartley, R. C., Duthie, G. G., Lean, M. E., Crozier, A. & Edwards, C. A. (2005). Disposition and metabolism of [2-14C]quercetin-4'-glucoside in rats. *Drug Metab. Dispos.,* **33**, 1036-43.

Grewal, P. K., Uchiyama, S., Ditto, D., Varki, N., Le, D. T., Nizet, V. & Marth, J. D. (2008). The Ashwell receptor mitigates the lethal coagulopathy of sepsis. *Nat. Med.,* **14**, 648-55.

Gross, B. S., Melford, S. K. & Watson, S. P. (1999). Evidence that phospholipase C-gamma2 interacts with SLP-76, Syk, Lyn, LAT and the Fc receptor gamma-chain after stimulation of the collagen receptor glycoprotein VI in human platelets. *Eur. J. Biochem.,* **263**, 612-23.

Grosse, J., Braun, A., Varga-Szabo, D., Beyersdorf, N., Schneider, B., Zeitlmann, L., Hanke, P., Schropp, P., Muhlstedt, S., Zorn, C., Huber, M., Schmittwolf, C., Jagla, W., Yu, P., Kerkau, T., Schulze, H., Nehls, M. & Nieswandt, B. (2007). An EF hand mutation in Stim1 causes premature platelet activation and bleeding in mice. *J. Clin. Invest.,* **117**, 3540-50.

Grozovsky, R., Hoffmeister, K.M. & Falet, H. (2010). Novel clearance mechanisms of platelets. *Curr Opin Hematol.,* **17**, 585-89.

Grozovsky, R., Giannini, S., Falet, H. & Hoffmeister, K. M. (2015). Novel mechanisms of platelet clearance and thrombopoietin regulation. *Curr. Opin. Hematol.,* **22**, 445-451.

Grucza, R. A., Futterer, K., Chan, A. C. & Waksman, G. (1999). Thermodynamic study of the binding of the tandem-SH2 domain of the Syk kinase to a dually phosphorylated ITAM peptide: evidence for two conformers. *Biochemistry,* **38**, 5024-33.

Gryglewski, R. J., Dembinska-Kiec, A. & Korbut, R. (1978). A possible role of thromboxane A2 (TXA2) and prostacyclin (PGI2) in circulation. *Acta Biol. Med. Ger.,* **37**, 715-23.

Grynkiewicz, G., Poenie, M. & Tsien, R. Y. (1985). A new generation of Ca2+ indicators with greatly improved fluorescence properties. *J. Biol. Chem.,* **260**, 3440-50.

Guerrero, J. A., Navarro-Nuñez, L., Lozano, M. L., Martínez, C., Vicente, V., Gibbins, J. M. & Rivera, J. (2007). Flavonoids inhibit the platelet TxA(2) signalling pathway and antagonize

TxA(2) receptors (TP) in platelets and smooth muscle cells. *Br. J. Clin. Pharmacol.,* **64**, 133-44.

Gugler, R., Leschik, M. & Dengler, H. J. (1975). Disposition of quercetin in man after single oral and intravenous doses. *Eur. J. Clin. Pharmacol.,* **9**, 229-34.

Guglielmone, H. A., Agnese, A. M., Nunez Montoya, S. C. & Cabrera, J. L. (2002). Anticoagulant effect and action mechanism of sulphated flavonoids from Flaveria bidentis. *Thromb. Res.,* **105**, 183-8.

Guidetti, G., Bernardi, B., Consonni, A., Rizzo, P., Gruppi, C., Balduini, C. & Torti, M. (2009). Integrin α2β1 induces phosphorylation-dependent and phosphorylation-independent activation of phospholipase Cγ2 in platelets: role of Src kinase and Rac GTPase. *J. Thromb. Haemost.,* **7**, 1200-1206.

Guillemette, G., Balla, T., Baukal, A. & Catt, K. (1988). Characterization of inositol 1, 4, 5-trisphosphate receptors and calcium mobilization in a hepatic plasma membrane fraction. *J. Biol. Chem.,* **263**, 4541-4548.

Guirguis-Blake, J. M., Evans, C. V., Senger, C. A., O'Connor, E. A. & Whitlock, E. P. (2016). Aspirin for the Primary Prevention of Cardiovascular Events: A Systematic Evidence Review for the U.S. Preventive Services Task Force. *Ann. Intern. Med.,* **164**, 804-13.

Guo, Y., Mah, E. & Bruno, R. S. (2014). Quercetin bioavailability is associated with inadequate plasma vitamin C status and greater plasma endotoxin in adults. *Nutrition,* **30**, 1279-86.

Gurbel, P. A., Kuliopulos, A. & Tantry, U. S. (2015). G-Protein–Coupled Receptors Signaling Pathways in New Antiplatelet Drug Development. *Arterioscler. Thromb. Vasc. Biol.,* **35**, 500-512.

Gurney, A. L., Carver-Moore, K., de Sauvage, F. J. & Moore, M. W. (1994). Thrombocytopenia in c-mpl-deficient mice. *Science,* **265**, 1445-1448.

Gyulkhandanyan, A. V., Mutlu, A., Freedman, J. & Leytin, V. (2012). Markers of platelet apoptosis: methodology and applications. *J. Thromb. Thrombolysis,* **33**, 397-411.

Habib, A., FitzGerald, G. A. & Maclouf, J. (1999). Phosphorylation of the thromboxane receptor alpha, the predominant isoform expressed in human platelets. *J. Biol. Chem.,* **274**, 2645-51.

Halbwirth, H. (2010). The creation and physiological relevance of divergent hydroxylation patterns in the flavonoid pathway. *Int. J. Mol. Sci.,* **11**, 595-621.

Hamberg, M., Svensson, J. & Samuelsson, B. (1975). Thromboxanes: a new group of biologically active compounds derived from prostaglandin endoperoxides. *Proc. Natl. Acad. Sci. U. S. A.,* **72**, 2994-2998.

Hamilton, J. R., Cornelissen, I. & Coughlin, S. R. (2004). Impaired hemostasis and protection against thrombosis in protease-activated receptor 4-deficient mice is due to lack of thrombin signaling in platelets. *J. Thromb. Haemost.,* **2**, 1429-1435.

Han, J., Lim, C. J., Watanabe, N., Soriani, A., Ratnikov, B., Calderwood, D. A., Puzon-McLaughlin, W., Lafuente, E. M., Boussiotis, V. A., Shattil, S. J. & Ginsberg, M. H. (2006). Reconstructing and deconstructing agonist-induced activation of integrin alphaIIbbeta3. *Curr. Biol.,* **16**, 1796-806.

Hankey, G. J. & Eikelboom, J. W. (2006). Aspirin resistance. *Lancet,* **367**, 606-17.

Harasstani, O. A., Moin, S., Tham, C. L., Liew, C. Y., Ismail, N., Rajajendram, R., Harith, H. H., Zakaria, Z. A., Mohamad, A. S., Sulaiman, M. R. & Israf, D. A. (2010). Flavonoid combinations cause synergistic inhibition of proinflammatory mediator secretion from lipopolysaccharide-induced RAW 264.7 cells. *Inflamm. Res.,* **59**, 711-21.

Harbury, P. A. B. (1998). Springs and zippers: coiled coils in SNARE-mediated membrane fusion. *Structure,* **6**, 1487-1491.

Hardy, A. R., Conley, P. B., Luo, J., Benovic, J. L., Poole, A. W. & Mundell, S. J. (2005). P2Y1 and P2Y12 receptors for ADP desensitize by distinct kinase-dependent mechanisms. *Blood,* **105**, 3552-60.

Harnly, J. M., Doherty, R. F., Beecher, G. R., Holden, J. M., Haytowitz, D. B., Bhagwat, S. & Gebhardt, S. (2006). Flavonoid Content of U.S. Fruits, Vegetables, and Nuts. *J. Agric. Food Chem.,* **54**, 9966-9977.

Harrison, P. & Cramer, E. M. (1993). Platelet alpha-granules. *Blood Rev.,* **7**, 52-62.

Harrison, P., Robinson, M. S., Mackie, I. J., Joseph, J., McDonald, S. J., Liesner, R., Savidge, G. F., Pasi, J. & Machin, S. J. (1999). Performance of the platelet function analyser PFA-100 in testing abnormalities of primary haemostasis. *Blood Coagul. Fibrinolysis,* **10**, 25-31.

Hartwig, J. H. (1992). Mechanisms of actin rearrangements mediating platelet activation. *J. Cell Biol.,* **118**, 1421-42.

Harwood, M., Danielewska-Nikiel, B., Borzelleca, J., Flamm, G., Williams, G. & Lines, T. (2007). A critical review of the data related to the safety of quercetin and lack of evidence of in vivo toxicity, including lack of genotoxic/carcinogenic properties. *Food Chem. Toxicol.,* **45**, 2179-2205.

Haslam, R. J., Dickinson, N. T. & Jang, E. K. (1999). Cyclic nucleotides and phosphodiesterases in platelets. *Thromb. Haemost.,* **82**, 412-23.

Hassock, S. R., Zhu, M. X., Trost, C., Flockerzi, V. & Authi, K. S. (2002). Expression and role of TRPC proteins in human platelets: evidence that TRPC6 forms the store-independent calcium entry channel. *Blood,* **100**, 2801-11.

Hathaway, D. R. & Adelstein, R. S. (1979). Human platelet myosin light chain kinase requires the calcium-binding protein calmodulin for activity. *Proc. Natl. Acad. Sci. U. S. A.,* **76**, 1653-7.

Hayward, C. P. M., Harrison, P., Cattaneo, M., Ortel, T. L., Rao, A. K., The Platelet Physiology Subcommittee Of The, S., Standardization Committee Of The International Society On, T. & Haemostasis (2006). Platelet function analyzer (PFA)-100® closure time in the evaluation of platelet disorders and platelet function. *J. Thromb. Haemost.,* **4**, 312-319.

Hechler, B., Leon, C., Vial, C., Vigne, P., Frelin, C., Cazenave, J. P. & Gachet, C. (1998). The P2Y1 receptor is necessary for adenosine 5'-diphosphate-induced platelet aggregation. *Blood,* **92**, 152-9.

Heemskerk, J. W., Bevers, E. M. & Lindhout, T. (2002). Platelet activation and blood coagulation. *Thromb. Haemost.,* **88**, 186-93.

Hendler, S. & Rorvik, D. M. (2009). *PDR for nutritional supplements.* New Jersey, USA: Thomson PDR.

Henneberg, R., Otuki, M. F., Furman, A. E. F., Hermann, P., Nascimento, A. J. d. & Leonart, M. S. S. (2013). Protective effect of flavonoids against reactive oxygen species production in sickle cell anemia patients treated with hydroxyurea. *Brazilian Journal of Hematology and Hemotherapy,* **35**, 52-55.

Hennekens, C. H., Dyken, M. L. & Fuster, V. (1997). Aspirin as a therapeutic agent in cardiovascular disease: a statement for healthcare professionals from the American Heart Association. *Circulation,* **96**, 2751-3.

Hertog, M. G., Kromhout, D., Aravanis, C., Blackburn, H., Buzina, R., Fidanza, F., Giampaoli, S., Jansen, A., Menotti, A., Nedeljkovic, S. & et al. (1995). Flavonoid intake and long-term risk of coronary heart disease and cancer in the seven countries study. *Arch. Intern. Med.,* **155**, 381-6.

Hertog, M. G., Sweetnam, P. M., Fehily, A. M., Elwood, P. C. & Kromhout, D. (1997). Antioxidant flavonols and ischemic heart disease in a Welsh population of men: the Caerphilly Study. *Am. J. Clin. Nutr.,* **65**, 1489-94.

Hibasami, H., Mitani, A., Katsuzaki, H., Imai, K., Yoshioka, K. & Komiya, T. (2005). Isolation of five types of flavonol from seabuckthorn (Hippophae rhamnoides) and induction of apoptosis by some of the flavonols in human promyelotic leukemia HL-60 cells. *Int. J. Mol. Med.,* **15**, 805-9.

Hirai, I., Okuno, M., Katsuma, R., Arita, N., Tachibana, M. & Yamamoto, Y. (2010). Characterisation of anti-Staphylococcus aureus activity of quercetin. *Int. J. Food Sci. Technol.,* **45**, 1250-1254.

Hirata, M., Hayashi, Y., Ushikubi, F., Yokota, Y., Kageyama, R., Nakanishi, S. & Narumiya, S. (1991). Cloning and expression of cDNA for a human thromboxane A2 receptor. *Nature,* **349**, 617-620.

Hirota, S., Nishioka, T., Shimoda, T., Miura, K., Ansai, T. & Takahama, U. (2001). Quercetin glucosides are hydrolyzed to quercetin in human oral cavity to participate in peroxidase-dependent scavenging of hydrogen peroxide. *Food Sci. Technol. Res.,* **7**, 239-245.

Hodek, P., Trefil, P. & Stiborova, M. (2002). Flavonoids-potent and versatile biologically active compounds interacting with cytochromes P450. *Chem. Biol. Interact.,* **139**, 1-21.

Hodgetts, V. A., Morris, R. K., Francis, A., Gardosi, J. & Ismail, K. M. (2015). Effectiveness of folic acid supplementation in pregnancy on reducing the risk of small-for-gestational age neonates: a population study, systematic review and meta-analysis. *BJOG,* **122**, 478-90.

Hodivala-Dilke, K. M., McHugh, K. P., Tsakiris, D. A., Rayburn, H., Crowley, D., Ullman-Cullere, M., Ross, F. P., Coller, B. S., Teitelbaum, S. & Hynes, R. O. (1999). Beta3-integrin-deficient mice are a model for Glanzmann thrombasthenia showing placental defects and reduced survival. *J. Clin. Invest.,* **103**, 229-38.

Holbrook, L. M., Sasikumar, P., Stanley, R. G., Simmonds, A. D., Bicknell, A. B. & Gibbins, J. M. (2012). The platelet-surface thiol isomerase enzyme ERp57 modulates platelet function. *J. Thromb. Haemost.,* **10**, 278-288.

Hollands, W. J., Saha, S., Hayran, O., Boyko, N., Glibetic, M., Konic-Ristic, A., Jorjadze, M. & Kroon, P. A. (2013). Lack of effect of bioactive-rich extracts of pomegranate, persimmon, nettle, dill, kale and Sideritis and isolated bioactives on platelet function. *J. Sci. Food Agric.,* **93**, 3588-3594.

Hollman, P. C., de Vries, J. H., van Leeuwen, S. D., Mengelers, M. J. & Katan, M. B. (1995). Absorption of dietary quercetin glycosides and quercetin in healthy ileostomy volunteers. *Am. J. Clin. Nutr.,* **62**, 1276-82.

Hollman, P. C., Geelen, A. & Kromhout, D. (2010). Dietary flavonol intake may lower stroke risk in men and women. *J. Nutr.,* **140**, 600-604.

Hollman, P. C., van Trijp, J. M., Buysman, M. N., van der Gaag, M. S., Mengelers, M. J., de Vries, J. H. & Katan, M. B. (1997). Relative bioavailability of the antioxidant flavonoid quercetin from various foods in man. *FEBS Lett.,* **418**, 152-6.

Hollman, P. C. H. (2004). Absorption, Bioavailability, and Metabolism of Flavonoids. *Pharm. Biol.,* **42**, 74-83.

Hollopeter, G., Jantzen, H. M., Vincent, D., Li, G., England, L., Ramakrishnan, V., Yang, R. B., Nurden, P., Nurden, A., Julius, D. & Conley, P. B. (2001). Identification of the platelet ADP receptor targeted by antithrombotic drugs. *Nature,* **409**, 202-7.

Holme, P. A., Orvim, U., Hamers, M. J., Solum, N. O., Brosstad, F. R., Barstad, R. M. & Sakariassen, K. S. (1997). Shear-induced platelet activation and platelet microparticle formation at blood flow conditions as in arteries with a severe stenosis. *Arterioscler. Thromb. Vasc. Biol.,* **17**, 646-53.

Howell, W. H. & Donahue, D. D. (1937). The production of blood platelets in the lungs. *J. Exp. Med.,* **65**, 177-203.

Huang, C., Chen, Y., Zhou, T. & Chen, G. (2009). Sulfation of dietary flavonoids by human sulfotransferases. *Xenobiotica,* **39**, 312-322.

Huang, E. M. & Detwiler, T. C. (1981). Characteristics of the synergistic actions of platelet agonists. *Blood,* **57**, 685-91.

Huang, E. S., Strate, L. L., Ho, W. W., Lee, S. S. & Chan, A. T. (2011). Long Term Use of Aspirin and the Risk of Gastrointestinal Bleeding. *Am. J. Med.,* **124**, 426-433.

Huang, N., Lou, M., Liu, H., Avila, C. & Ma, Y. (2016a). Identification of a potent small molecule capable of regulating polyploidization, megakaryocyte maturation, and platelet production. *J. Hematol. Oncol.,* **9**, 136.

Huang, X., Yao, J., Zhao, Y., Xie, D., Jiang, X. & Xu, Z. (2016b). Efficient Rutin and Quercetin Biosynthesis through Flavonoids-Related Gene Expression in Fagopyrum tataricum Gaertn. Hairy Root Cultures with UV-B Irradiation. *Front. Plant Sci.,* **7**, eCollection 2016.

Hubbard, G. P., Stevens, J. M., Cicmil, M., Sage, T., Jordan, P. A., Williams, C. M., Lovegrove, J. A. & Gibbins, J. M. (2003). Quercetin inhibits collagen-stimulated platelet activation through inhibition of multiple components of the glycoprotein VI signaling pathway. *J. Thromb. Haemost.,* **1**, 1079-88.

Hubbard, G. P., Wolffram, S., de Vos, R., Bovy, A., Gibbins, J. M. & Lovegrove, J. A. (2006). Ingestion of onion soup high in quercetin inhibits platelet aggregation and essential components of the collagen-stimulated platelet activation pathway in man: a pilot study. *Br. J. Nutr.,* **96**, 482-8.

Hubbard, G. P., Wolffram, S., Lovegrove, J. A. & Gibbins, J. M. (2004). Ingestion of quercetin inhibits platelet aggregation and essential components of the collagen-stimulated platelet activation pathway in humans. *J. Thromb. Haemost.,* **2**, 2138-45.

Hughes, C. E., Auger, J. M., McGlade, J., Eble, J. A., Pearce, A. C. & Watson, S. P. (2008). Differential roles for the adapters Gads and LAT in platelet activation by GPVI and CLEC-2. *J. Thromb. Haemost.,* **6**, 2152-2159.

Hughes, P. E., Diaz-Gonzalez, F., Leong, L., Wu, C., McDonald, J. A., Shattil, S. J. & Ginsberg, M. H. (1996). Breaking the integrin hinge. A defined structural constraint regulates integrin signaling. *J. Biol. Chem.,* **271**, 6571-4.

Huk, I., Brovkovych, V., Nanobash Vili, J., Weigel, G., Neumayer, C., Partyka, L., Patton, S. & Malinski, T. (1998). Bioflavonoid quercetin scavenges superoxide and increases nitric oxide concentration in ischaemia-reperfusion injury: an experimental study. *Br. J. Surg.,* **85**, 1080-5.

Hung, D. T., Wong, Y. H., Vu, T. K. & Coughlin, S. R. (1992). The cloned platelet thrombin receptor couples to at least two distinct effectors to stimulate phosphoinositide hydrolysis and inhibit adenylyl cyclase. *J. Biol. Chem.,* **267**, 20831-4.

Ignarro, L. J., Buga, G. M., Wood, K. S., Byrns, R. E. & Chaudhuri, G. (1987). Endothelium-derived relaxing factor produced and released from artery and vein is nitric oxide. *Proc. Natl. Acad. Sci. U. S. A.,* **84**, 9265-9.

Inoue, O., Suzuki-Inoue, K., Dean, W. L., Frampton, J. & Watson, S. P. (2003). Integrin α2β1 mediates outside-in regulation of platelet spreading on collagen through activation of Src kinases and PLCγ2. *J. Cell Biol.,* **160**, 769-780.

Ioku, K., Pongpiriyadacha, Y., Konishi, Y., Takei, Y., Nakatani, N. & Terao, J. (1998). β-Glucosidase activity in the rat small intestine toward quercetin monoglucosides. *Biosci. Biotechnol. Biochem.,* **62**, 1428-1431.

Italiano, J. E. & Battinelli, E. M. (2009). Selective sorting of alpha-granule proteins. *Journal of thrombosis and haemostasis : J Thromb Haemost,* **7**, 173-176.

Italiano, J. E., Jr., Richardson, J. L., Patel-Hett, S., Battinelli, E., Zaslavsky, A., Short, S., Ryeom, S., Folkman, J. & Klement, G. L. (2008). Angiogenesis is regulated by a novel mechanism: pro- and antiangiogenic proteins are organized into separate platelet alpha granules and differentially released. *Blood,* **111**, 1227-33.

Jaffe, E. A., Hoyer, L. W. & Nachman, R. L. (1974). Synthesis of von Willebrand factor by cultured human endothelial cells. *Proc. Natl. Acad. Sci. U. S. A.,* **71**, 1906-9.

Jaffe, E. A. & Weksler, B. B. (1979). Recovery of Endothelial Cell Prostacyclin Production after Inhibition by Low Doses of Aspirin. *J. Clin. Invest.,* **63**, 532-535.

Jantzen, H. M., Gousset, L., Bhaskar, V., Vincent, D., Tai, A., Reynolds, E. E. & Conley, P. B. (1999). Evidence for two distinct G-protein-coupled ADP receptors mediating platelet activation. *Thromb. Haemost.,* **81**, 111-7.

Jantzen, H. M., Milstone, D. S., Gousset, L., Conley, P. B. & Mortensen, R. M. (2001). Impaired activation of murine platelets lacking G alpha(i2). *J. Clin. Invest.,* **108**, 477-83.

Jardín, I., López, J. J., Redondo, P. C., Salido, G. M. & Rosado, J. A. (2009). Store-operated Ca2+ entry is sensitive to the extracellular Ca2+ concentration through plasma membrane STIM1. *Biochim. Biophys. Acta,* **1793**, 1614-1622.

Jarvis, G. E. & Thompson, A. J. (2013). A golden approach to ion channel inhibition. *Trends Pharmacol. Sci.,* **34**, 481-488.

Jasuja, R., Furie, B. & Furie, B. C. (2010). Endothelium-derived but not platelet-derived protein disulfide isomerase is required for thrombus formation in vivo. *Blood,* **116**, 4665-74.

Jasuja, R., Passam, F. H., Kennedy, D. R., Kim, S. H., van Hessem, L., Lin, L., Bowley, S. R., Joshi, S. S., Dilks, J. R., Furie, B., Furie, B. C. & Flaumenhaft, R. (2012). Protein disulfide isomerase inhibitors constitute a new class of antithrombotic agents. *J. Clin. invest.,* **122**, 2104-2113.

Jenkins, A. L., Nannizzi-Alaimo, L., Silver, D., Sellers, J. R., Ginsberg, M. H., Law, D. A. & Phillips, D. R. (1998). Tyrosine phosphorylation of the beta3 cytoplasmic domain mediates integrin-cytoskeletal interactions. *J. Biol. Chem.,* **273**, 13878-85.

Jin, J., Daniel, J. L. & Kunapuli, S. P. (1998). Molecular basis for ADP-induced platelet activation. II. The P2Y1 receptor mediates ADP-induced intracellular calcium mobilization and shape change in platelets. *J. Biol. Chem.,* **273**, 2030-4.

Jin, J. & Kunapuli, S. P. (1998). Coactivation of two different G protein-coupled receptors is essential for ADP-induced platelet aggregation. *Proc. Natl. Acad. Sci. U. S. A.,* **95**, 8070-4.

Jokinen, J., Dadu, E., Nykvist, P., Kapyla, J., White, D. J., Ivaska, J., Vehvilainen, P., Reunanen, H., Larjava, H., Hakkinen, L. & Heino, J. (2004). Integrin-mediated cell adhesion to type I collagen fibrils. *J. Biol. Chem.,* **279**, 31956-63.

Jones, C. I., Garner, S. F., Moraes, L. A., Kaiser, W. J., Rankin, A., Ouwehand, W. H., Goodall, A. H. & Gibbins, J. M. (2009). PECAM-1 expression and activity negatively regulate multiple platelet signaling pathways. *FEBS Lett.,* **583**, 3618-24.

Jones, C. I., Sage, T., Moraes, L. A., Vaiyapuri, S., Hussain, U., Tucker, K. L., Barrett, N. E. & Gibbins, J. M. (2014). Platelet endothelial cell adhesion molecule-1 inhibits platelet response to thrombin and von Willebrand factor by regulating the internalization of glycoprotein Ib via AKT/glycogen synthase kinase-3/dynamin and integrin alphaIIbbeta3. *Arterioscler. Thromb. Vasc. Biol.,* **34**, 1968-76.

Jones, D. J., Lamb, J. H., Verschoyle, R. D., Howells, L. M., Butterworth, M., Lim, C. K., Ferry, D., Farmer, P. B. & Gescher, A. J. (2004). Characterisation of metabolites of the putative cancer chemopreventive agent quercetin and their effect on cyclo-oxygenase activity. *Br. J. Cancer,* **91**, 1213-9.

Jonnalagadda, D., Izu, L. T. & Whiteheart, S. W. (2012). Platelet secretion is kinetically heterogeneous in an agonist-responsive manner. *Blood,* **120**, 5209-16.

Josefsson, E. C., White, M. J., Dowling, M. R. & Kile, B. T. (2012). Platelet life span and apoptosis. *Methods Mol. Biol.,* **788**, 59-71.

Judd, B. A., Myung, P. S., Obergfell, A., Myers, E. E., Cheng, A. M., Watson, S. P., Pear, W. S., Allman, D., Shattil, S. J. & Koretzky, G. A. (2002). Differential Requirement for LAT and SLP-76 in GPVI versus T Cell Receptor Signaling. *J. Exp. Med.,* **195**, 705-717.

Jung, J. A., Kim, T.-E., Kim, J.-R., Kim, M.-J., Huh, W., Park, K.-M., Lee, S.-Y. & Ko, J.-W. (2013). The Pharmacokinetics and Safety of a Fixed-Dose Combination of Acetylsalicylic Acid and Clopidogrel Compared With the Concurrent Administration of Acetylsalicylic

Acid and Clopidogrel in Healthy Subjects: A Randomized, Open-Label, 2-Sequence, 2-Period, Single-Dose Crossover Study. *Clin. Ther.,* **35**, 985-994.

Junt, T., Schulze, H., Chen, Z., Massberg, S., Goerge, T., Krueger, A., Wagner, D. D., Graf, T., Italiano, J. E., Jr., Shivdasani, R. A. & von Andrian, U. H. (2007). Dynamic visualization of thrombopoiesis within bone marrow. *Science,* **317**, 1767-70.

Jurk, K., Clemetson, K. J., de Groot, P. G., Brodde, M. F., Steiner, M., Savion, N., Varon, D., Sixma, J. J., Van Aken, H. & Kehrel, B. E. (2003). Thrombospondin-1 mediates platelet adhesion at high shear via glycoprotein Ib (GPIb): an alternative/backup mechanism to von Willebrand factor. *FASEB J.,* **17**, 1490-2.

Kahn, M. L., Nakanishi-Matsui, M., Shapiro, M. J., Ishihara, H. & Coughlin, S. R. (1999). Protease-activated receptors 1 and 4 mediate activation of human platelets by thrombin. *J. Clin. Invest.,* **103**, 879-87.

Kaldas, M. I., Walle, U. K., van der Woude, H., McMillan, J. M. & Walle, T. (2005). Covalent binding of the flavonoid quercetin to human serum albumin. *J. Agric. Food Chem.,* **53**, 4194-7.

Kanani, K., Gatoulis, S. & Voelker, M. (2015). Influence of differing analgesic formulations of aspirin on pharmacokinetic parameters. *Pharmaceutics,* **7**, 188-198.

Kaplan, J.E. & Saba, T.M. (1978). Platelet removal from the circulation by the liver and spleen. *Am J Physiol.,* **235**, H314-20.

Karshovska, E., Zhao, Z., Blanchet, X., Schmitt, M. M., Bidzhekov, K., Soehnlein, O., von Hundelshausen, P., Mattheij, N. J., Cosemans, J. M., Megens, R. T., Koeppel, T. A., Schober, A., Hackeng, T. M., Weber, C. & Koenen, R. R. (2015). Hyperreactivity of junctional adhesion molecule A-deficient platelets accelerates atherosclerosis in hyperlipidemic mice. *Circ. Res.,* **116**, 587-99.

Kashino, Y., Murota, K., Matsuda, N., Tomotake, M., Hamano, T., Mukai, R. & Terao, J. (2015). Effect of Processed Onions on the Plasma Concentration of Quercetin in Rats and Humans. *J. Food Sci.,* **80**, H2597-602.

Kasirer-Friede, A., Cozzi, M. R., Mazzucato, M., De Marco, L., Ruggeri, Z. M. & Shattil, S. J. (2004). Signaling through GP Ib-IX-V activates alpha IIb beta 3 independently of other receptors. *Blood,* **103**, 3403-11.

Katsanos, K., Spiliopoulos, S., Saha, P., Diamantopoulos, A., Karunanithy, N., Krokidis, M., Modarai, B. & Karnabatidis, D. (2015). Comparative Efficacy and Safety of Different Antiplatelet Agents for Prevention of Major Cardiovascular Events and Leg Amputations in Patients with Peripheral Arterial Disease: A Systematic Review and Network Meta-Analysis. *PLoS One,* **10**, e0135692.

Katsuki, S., Arnold, W., Mittal, C. & Murad, F. (1977). Stimulation of guanylate cyclase by sodium nitroprusside, nitroglycerin and nitric oxide in various tissue preparations and comparison to the effects of sodium azide and hydroxylamine. *J. Cyclic Nucleotide Res.,* **3**, 23-35.

Kauffenstein, G., Bergmeier, W., Eckly, A., Ohlmann, P., Leon, C., Cazenave, J. P., Nieswandt, B. & Gachet, C. (2001). The P2Y(12) receptor induces platelet aggregation through weak activation of the alpha(IIb)beta(3) integrin--a phosphoinositide 3-kinase-dependent mechanism. *FEBS Lett.,* **505**, 281-90.

Kaufman, R. M., Airo, R., Pollack, S. & Crosby, W. H. (1965). Circulating megakaryocytes and platelet release in the lung. *Blood,* **26**, 720-31.

Kaushansky, K., Lichtman, M. A., Prchal, J., Levi, M. M., Press, O. W., Burns, L. J. & Caligiuri, M. (2015). *Williams Hematology*. New York, USA: McGraw-Hill Education.

Kaushansky, K., Lok, S., Holly, R. D., Broudy, V. C., Lin, N., Bailey, M. C., Forstrom, J. W., Buddle, M. M., Oort, P. J. & Hagen, F. S. (1994). Promotion of megakaryocyte progenitor expansion and differentiation by the c-Mpl ligand thrombopoietin. *Nature,* **369**, 568-571.

Kawai, Y., Nishikawa, T., Shiba, Y., Saito, S., Murota, K., Shibata, N., Kobayashi, M., Kanayama, M., Uchida, K. & Terao, J. (2008). Macrophage as a target of quercetin glucuronides in human atherosclerotic arteries: implication in the anti-atherosclerotic mechanism of dietary flavonoids. *J. Biol. Chem.,* **283**, 9424-9434.

Keularts, I. M., van Gorp, R. M., Feijge, M. A., Vuist, W. M. & Heemskerk, J. W. (2000). alpha(2A)-adrenergic receptor stimulation potentiates calcium release in platelets by modulating cAMP levels. *J. Biol. Chem.,* **275**, 1763-72.

Keuren, J. F. W., Wielders, S. J. H., Ulrichts, H., Hackeng, T., Heemskerk, J. W. M., Deckmyn, H., Bevers, E. M. & Lindhout, T. (2005). Synergistic Effect of Thrombin on Collagen-Induced Platelet Procoagulant Activity Is Mediated Through Protease-Activated Receptor-1. *Arterioscler. Thromb. Vasc. Biol.,* **25**, 1499-1505.

Khan, F., Vaillancourt, C. & Bourjeily, G. (2017). Diagnosis and management of deep vein thrombosis in pregnancy. *BMJ,* **357**.

Kim, K., Hahm, E., Li, J., Holbrook, L. M., Sasikumar, P., Stanley, R. G., Ushio-Fukai, M., Gibbins, J. M. & Cho, J. (2013). Platelet protein disulfide isomerase is required for thrombus formation but not for hemostasis in mice. *Blood,* **122**, 1052-61.

Kim, S., Foster, C., Lecchi, A., Quinton, T. M., Prosser, D. M., Jin, J., Cattaneo, M. & Kunapuli, S. P. (2002). Protease-activated receptors 1 and 4 do not stimulate G(i) signaling pathways in the absence of secreted ADP and cause human platelet aggregation independently of G(i) signaling. *Blood,* **99**, 3629-36.

Kiouptsi, K. & Reinhardt, C. (2016). Protein disulfide-isomerase - a trigger of tissue factor-dependent thrombosis. *Clin. Hemorheol. Microcirc.,* **64**, 279-286.

Klages, B., Brandt, U., Simon, M. I., Schultz, G. & Offermanns, S. (1999). Activation of G12/G13 results in shape change and Rho/Rho-kinase-mediated myosin light chain phosphorylation in mouse platelets. *J. Cell Biol.,* **144**, 745-54.

Kleuss, C., Raw, A. S., Lee, E., Sprang, S. R. & Gilman, A. G. (1994). Mechanism of GTP hydrolysis by G-protein alpha subunits. *Proc. Natl. Acad. Sci. U. S. A.,* **91**, 9828-9831.

Knekt, P., Kumpulainen, J., Jarvinen, R., Rissanen, H., Heliovaara, M., Reunanen, A., Hakulinen, T. & Aromaa, A. (2002). Flavonoid intake and risk of chronic diseases. *Am. J. Clin. Nutr.,* **76**, 560-8.

Knezevic, I., Borg, C. & Le Breton, G. C. (1993). Identification of Gq as one of the G-proteins which copurify with human platelet thromboxane A2/prostaglandin H2 receptors. *J. Biol. Chem.,* **268**, 26011-7.

Knight, C. G., Morton, L. F., Onley, D. J., Peachey, A. R., Ichinohe, T., Okuma, M., Farndale, R. W. & Barnes, M. J. (1999). Collagen-platelet interaction: Gly-Pro-Hyp is uniquely specific for platelet Gp VI and mediates platelet activation by collagen. *Cardiovasc. Res.,* **41**, 450-7.

Knighton, D.R., Zheng, J.H., Ten Eyck, L.F., Ashford, V.A., Xuong, N.H., Taylor, S.S. & Sowadski, J.M. (1991). Crystal structure of the catalytic subunit of cyclic adenosine monophosphate-dependent protein kinase. *Science,* **253**, 407-14.

Kobayashi, T., Tahara, Y., Matsumoto, M., Iguchi, M., Sano, H., Murayama, T., Arai, H., Oida, H., Yurugi-Kobayashi, T., Yamashita, J. K., Katagiri, H., Majima, M., Yokode, M., Kita, T. & Narumiya, S. (2004). Roles of thromboxane A(2) and prostacyclin in the development of atherosclerosis in apoE-deficient mice. *J. Clin. Invest.,* **114**, 784-94.

Koedam, J. A., Cramer, E. M., Briend, E., Furie, B., Furie, B. C. & Wagner, D. D. (1992). P-selectin, a granule membrane protein of platelets and endothelial cells, follows the regulated secretory pathway in AtT-20 cells. *J. Cell Biol.,* **116**, 617-25.

Koes, R. E., Quattrocchio, F. & Mol, J. N. M. (1994). The flavonoid biosynthetic pathway in plants: Function and evolution. *Bioessays,* **16**, 123-132.

Kong, C. H., Zhao, H., Xu, X. H., Wang, P. & Gu, Y. (2007). Activity and allelopathy of soil of flavone o-glycosides from rice. *J. Agric. Food Chem.,* **55**, 6007-12.

Kong, D., Zhang, Y., Yamori, T., Duan, H. & Jin, M. (2011). Inhibitory activity of flavonoids against class I phosphatidylinositol 3-kinase isoforms. *Molecules,* **16**, 5159-67.

Konopatskaya, O., Matthews, S. A., Harper, M. T., Gilio, K., Cosemans, J. M., Williams, C. M., Navarro, M. N., Carter, D. A., Heemskerk, J. W., Leitges, M., Cantrell, D. & Poole, A. W. (2011). Protein kinase C mediates platelet secretion and thrombus formation through protein kinase D2. *Blood,* **118**, 416-24.

Kozasa, T., Jiang, X., Hart, M. J., Sternweis, P. M., Singer, W. D., Gilman, A. G., Bollag, G. & Sternweis, P. C. (1998). p115 RhoGEF, a GTPase activating protein for Galpha12 and Galpha13. *Science,* **280**, 2109-11.

Krebs, E.G. & Beavo J.A. (1979). Phosphorylation-dephosphorylation of enzymes. *Annu. Rev. Biochem.,* **48**, 923-59.

Krishnaswamy, S. (2013). The Transition of Prothrombin to Thrombin. *J. Thromb. Haemost.,* **11**, 265-276.

Kühne, T., Blanchette, V., Buchanan, G.R., Ramenghi, U., Donato, H., Tamminga, R.Y., Rischewski, J., Berchtold, W., Imbach, P. & Intercontinental Childhood ITP Study Group. (2007). Splenectomy in children with idiopathic thrombocytopenic purpura: A prospective study of 134 children from the Intercontinental Childhood ITP Study Group. *Pediatr Blood Cancer.,* **49**, 829-834.

Kuijpers, M. J., Schulte, V., Bergmeier, W., Lindhout, T., Brakebusch, C., Offermanns, S., Fassler, R., Heemskerk, J. W. & Nieswandt, B. (2003). Complementary roles of glycoprotein VI and alpha2beta1 integrin in collagen-induced thrombus formation in flowing whole blood ex vivo. *FASEB J.,* **17**, 685-7.

Kumar, S. & Pandey, A. K. (2013). Chemistry and Biological Activities of Flavonoids: An Overview. *Sci. World J.,* **2013**, 16.

Kundu, S. K., Heilmann, E. J., Sio, R., Garcia, C., Davidson, R. M. & Ostgaard, R. A. (1995). Description of an in vitro platelet function analyzer--PFA-100. *Semin. Thromb. Hemost.,* **21 Suppl 2**, 106-12.

Kunicki, T. J., Nugent, D. J., Staats, S. J., Orchekowski, R. P., Wayner, E. A. & Carter, W. G. (1988). The human fibroblast class II extracellular matrix receptor mediates platelet adhesion to collagen and is identical to the platelet glycoprotein Ia-IIa complex. *J. Biol. Chem.,* **263**, 4516-4519.

Kwak, J.-H., Seo, J. M., Kim, N.-H., Arasu, M. V., Kim, S., Yoon, M. K. & Kim, S.-J. (2017). Variation of quercetin glycoside derivatives in three onion (Allium cepa L.) varieties. *Saudi J. Biol. Sci.,* **24**, 1387-1391.

Laemmli, U. K. (1970). Cleavage of Structural Proteins during the Assembly of the Head of Bacteriophage T4. *Nature,* **227**, 680-685.

Lafuente, E. M., van Puijenbroek, A. A. F. L., Krause, M., Carman, C. V., Freeman, G. J., Berezovskaya, A., Constantine, E., Springer, T. A., Gertler, F. B. & Boussiotis, V. A. (2004). RIAM, an Ena/VASP and Profilin Ligand, Interacts with Rap1-GTP and Mediates Rap1-Induced Adhesion. *Dev. Cell,* **7**, 585-595.

Lagarrigue, F., Kim, C. & Ginsberg, M. H. (2016). The Rap1-RIAM-talin axis of integrin activation and blood cell function. *Blood,* **128**, 479-487.

Lakenbrink, C., Lapczynski, S., Maiwald, B. & Engelhardt, U. H. (2000). Flavonoids and other polyphenols in consumer brews of tea and other caffeinated beverages. *J. Agric. Food Chem.,* **48**, 2848-2852.

Lanas, A. & Scheiman, J. (2007). Low-dose aspirin and upper gastrointestinal damage: epidemiology, prevention and treatment. *Curr. Med. Res. Opin.,* **23**, 163-73.

Landolfi, R., Mower, R. L. & Steiner, M. (1984). Modification of platelet function and arachidonic acid metabolism by bioflavonoids. Structure-activity relations. *Biochem. Pharmacol.,* **33**, 1525-30.

Lanza, F., Beretz, A., Stierle, A., Hanau, D., Kubina, M. & Cazenave, J. P. (1988). Epinephrine potentiates human platelet activation but is not an aggregating agent. *Am. J. Physiol.,* **255**, H1276-88.

Law, D. A., DeGuzman, F. R., Heiser, P., Ministri-Madrid, K., Killeen, N. & Phillips, D. R. (1999). Integrin cytoplasmic tyrosine motif is required for outside-in alphaIIbbeta3 signalling and platelet function. *Nature,* **401**, 808-11.

Lee, D., Fong, Karen P., King, Michael R., Brass, Lawrence F. & Hammer, Daniel A. (2012a). Differential Dynamics of Platelet Contact and Spreading. *Biophys. J.,* **102**, 472-482.

Lee, H. S., Lim, C. J., Puzon-McLaughlin, W., Shattil, S. J. & Ginsberg, M. H. (2009). RIAM activates integrins by linking talin to ras GTPase membrane-targeting sequences. *J. Biol. Chem.,* **284**, 5119-27.

Lee, J., Ebeler, S. E., Zweigenbaum, J. A. & Mitchell, A. E. (2012b). UHPLC-(ESI)QTOF MS/MS Profiling of Quercetin Metabolites in Human Plasma Postconsumption of Applesauce Enriched with Apple Peel and Onion. *J. Agric. Food Chem.,* **60**, 8510-8520.

Lee, K.-H., Park, E., Lee, H.-J., Kim, M.-O., Cha, Y.-J., Kim, J.-M., Lee, H. & Shin, M.-J. (2011). Effects of daily quercetin-rich supplementation on cardiometabolic risks in male smokers. *Nutr. Res. Pract.,* **5**, 28-33.

Lefrançais, E., Ortiz-Muñoz, G., Caudrillier, A., Mallavia, B., Liu, F., Sayah, D. M., Thornton, E. E., Headley, M. B., David, T., Coughlin, S. R., Krummel, M. F., Leavitt, A. D., Passegué, E. & Looney, M. R. (2017). The lung is a site of platelet biogenesis and a reservoir for haematopoietic progenitors. *Nature,* **544**, 105-109.

Leger, A. J., Jacques, S. L., Badar, J., Kaneider, N. C., Derian, C. K., Andrade-Gordon, P., Covic, L. & Kuliopulos, A. (2006). Blocking the protease-activated receptor 1-4 heterodimer in platelet-mediated thrombosis. *Circulation,* **113**, 1244-54.

Leiderman, K. & Fogelson, A. L. (2011). Grow with the flow: a spatial-temporal model of platelet deposition and blood coagulation under flow. *Math. Med. Biol.,* **28**, 47-84.

Lentz, B. R. (2003). Exposure of platelet membrane phosphatidylserine regulates blood coagulation. *Prog. Lipid Res.,* **42**, 423-38.

Leo, L., Di Paola, J., Judd, B. A., Koretzky, G. A. & Lentz, S. R. (2002). Role of the adapter protein SLP-76 in GPVI-dependent platelet procoagulant responses to collagen. *Blood,* **100**, 2839-44.

Leonard, E., Yan, Y. & Koffas, M. A. (2006). Functional expression of a P450 flavonoid hydroxylase for the biosynthesis of plant-specific hydroxylated flavonols in Escherichia coli. *Metab Eng,* **8**, 172-81.

Leopoldt, D., Hanck, T., Exner, T., Maier, U., Wetzker, R. & Nurnberg, B. (1998). Gbetagamma stimulates phosphoinositide 3-kinase-gamma by direct interaction with two domains of the catalytic p110 subunit. *J. Biol. Chem.,* **273**, 7024-9.

Lerner, D. J., Chen, M., Tram, T. & Coughlin, S. R. (1996). Agonist recognition by proteinase-activated receptor 2 and thrombin receptor. Importance of extracellular loop interactions for receptor function. *J. Biol. Chem.,* **271**, 13943-7.

Lesser, S., Cermak, R. & Wolffram, S. (2004). Bioavailability of quercetin in pigs is influenced by the dietary fat content. *J. Nutr.,* **134**, 1508-11.

Lesser, S. & Wolffram, S. (2006). Oral bioavailability of the flavonol quercetin - a review. *Curr. Top. Neutraceutical Res.,* **4**, 239-256.

Letan, A. (1966). The Relation of Structure to Antioxidant Activity of Quercetin and Some of Its Derivatives I. Primary Activity. *J. Food Sci.,* **31**, 518-523.

Levine, R. F., Eldor, A., Shoff, P. K., Kirwin, S., Tenza, D. & Cramer, E. M. (1993). Circulating megakaryocytes: delivery of large numbers of intact, mature megakaryocytes to the lungs. *Eur. J. Haematol.,* **51**, 233-46.

Lewis, K. M. (2012). *Multiple Lead ECGs: A Practical Analysis of Arrhythmias.* Boston, USA: Cengage Learning.

Leytin, V. (2012). Apoptosis in the anucleate platelet. *Blood Rev.,* **26**, 51-63.

Li, P. G., Sun, L., Han, X., Ling, S., Gan, W. T. & Xu, J. W. (2012). Quercetin induces rapid eNOS phosphorylation and vasodilation by an Akt-independent and PKA-dependent mechanism. *Pharmacology,* **89**, 220-8.

Li, X. & Cong, H. (2009). Platelet-Derived Microparticles and the Potential of Glycoprotein IIb/IIIa Antagonists in Treating Acute Coronary Syndrome. *Tex. Heart Inst. J.,* **36**, 134-139.

Li, Z., Delaney, M. K., O'Brien, K. A. & Du, X. (2010). Signaling during platelet adhesion and activation. *Arterioscler. Thromb. Vasc. Biol.,* **30**, 2341-9.

Li, Z., Zhang, G., Le Breton, G. C., Gao, X., Malik, A. B. & Du, X. (2003). Two waves of platelet secretion induced by thromboxane A2 receptor and a critical role for phosphoinositide 3-kinases. *J. Biol. Chem.,* **278**, 30725-31.

Lian, L., Wang, Y., Draznin, J., Eslin, D., Bennett, J. S., Poncz, M., Wu, D. & Abrams, C. S. (2005). The relative role of PLCβ and PI3Kγ in platelet activation. *Blood,* **106**, 110-117.

Liang, M.-L., Da, X.-W., He, A.-D., Yao, G.-Q., Xie, W., Liu, G., Xiang, J.-Z. & Ming, Z.-Y. (2015). Pentamethylquercetin (PMQ) reduces thrombus formation by inhibiting platelet function. *Sci. Rep.,* **5**, 11142.

Lin, L., Gopal, S., Sharda, A., Passam, F., Bowley, S. R., Stopa, J., Xue, G., Yuan, C., Furie, B. C., Flaumenhaft, R., Huang, M. & Furie, B. (2015). Quercetin-3-rutinoside Inhibits Protein Disulfide Isomerase by Binding to Its b′x Domain. *J. Biol. Chem.,* **290**, 23543-23552.

Liou, J., Kim, M. L., Heo, W. D., Jones, J. T., Myers, J. W., Ferrell, J. E., Jr. & Meyer, T. (2005). STIM is a Ca2+ sensor essential for Ca2+-store-depletion-triggered Ca2+ influx. *Curr. Biol.,* **15**, 1235-41.

Liu, L., Gao, C., Yao, P. & Gong, Z. (2015). Quercetin Alleviates High-Fat Diet-Induced Oxidized Low-Density Lipoprotein Accumulation in the Liver: Implication for Autophagy Regulation. *BioMed Res. Int.,* **2015**, 9.

Liu, S., Guo, C., Guo, Y., Yu, H., Greenaway, F. & Sun, M.-Z. (2014). Comparative Binding Affinities of Flavonoid Phytochemicals with Bovine Serum Albumin. *Iran J. Pharm. Res.,* **13**, 1019-1028.

Lordkipanidzé, M., Lowe, G. C., Kirkby, N. S., Chan, M. V., Lundberg, M. H., Morgan, N. V., Bem, D., Nisar, S. P., Leo, V. C., Jones, M. L., Mundell, S. J., Daly, M. E., Mumford, A. D., Warner, T. D., Watson, S. P., Watson, S. P., Mumford, A. D., Mundell, S. J., Gissen, P., Daly, M. E., Lester, W., Clark, J., Williams, M., Motwani, J., Marshall, D., Nyatanga, P., Mann, P., Kirwan, J., Wilde, J., Dunkley, T., Greenway, A., Makris, M., Pavord, S., Dattani, R., Grimley, G. D. C., Stokley, S., Astwood, E., Chang, C., Foros, M., Trower, L., Thachil, J., Hay, C., Pike, G., Will, A., Grainger, J., Foulkes, M., Fareh, M., Talks, K., Biss, T., Kesteven, P., Hanley, J., Vowles, J., Basey, L., Barnes, M., Collins, P., Rayment, R., Alikhan, R., Morris, A. G. R., Mansell, D., Toh, C. H., Martlew, V., Murphy, E., Lachmann, R., Rose, P., Chapman, O., Lokare, A., Marshall, K., Khan, N., Keeling, D., Giangrande, P., Austin, S., Bevan, D. & Alamelu, J. (2014). Characterization of multiple platelet activation pathways in patients with bleeding as a high-throughput screening option: use of 96-well Optimul assay. *Blood,* **123**, e11-e22.

Lova, P., Paganini, S., Hirsch, E., Barberis, L., Wymann, M., Sinigaglia, F., Balduini, C. & Torti, M. (2003). A selective role for phosphatidylinositol 3,4,5-trisphosphate in the Gi-dependent activation of platelet Rap1B. *J. Biol. Chem.,* **278**, 131-8.

Lowe, G. D., Rumley, A. & Mackie, I. J. (2004). Plasma fibrinogen. *Ann. Clin. Biochem.,* **41**, 430-40.

Lozoya, X., Meckes, M., Abou-Zaid, M., Tortoriello, J., Nozzolillo, C. & Arnason, J. T. (1994). Quercetin glycosides in Psidium guajava L. leaves and determination of a spasmolytic principle. *Arch. Med. Res.,* **25**, 11-5.

Luo, B. H., Takagi, J. & Springer, T. A. (2004). Locking the beta3 integrin I-like domain into high and low affinity conformations with disulfides. *J. Biol. Chem.,* **279**, 10215-21.

Luo, S. Z., Mo, X., Afshar-Kharghan, V., Srinivasan, S., Lopez, J. A. & Li, R. (2007). Glycoprotein Ibalpha forms disulfide bonds with 2 glycoprotein Ibbeta subunits in the resting platelet. *Blood,* **109**, 603-9.

Ma, Y. Q., Qin, J. & Plow, E. F. (2007). Platelet integrin alpha(IIb)beta(3): activation mechanisms. *J. Thromb. Haemost.,* **5**, 1345-52.

Maalik, A., Khan, F. A., Mumtaz, A., Mehmood, A., Azhar, S., Atif, M., Karim, S., Altaf, Y. & Tariq, I. (2014). Pharmacological applications of quercetin and its derivatives: a short review. *Trop. J. Pharm. Res.,* **13**, 1561-1566.

Macaulay, I. C., Tijssen, M. R., Thijssen-Timmer, D. C., Gusnanto, A., Steward, M., Burns, P., Langford, C. F., Ellis, P. D., Dudbridge, F., Zwaginga, J. J., Watkins, N. A., van der Schoot, C. E. & Ouwehand, W. H. (2007). Comparative gene expression profiling of in vitro differentiated megakaryocytes and erythroblasts identifies novel activatory and inhibitory platelet membrane proteins. *Blood,* **109**, 3260-9.

Machlus, K. R., Thon, J. N. & Italiano, J. E., Jr. (2014). Interpreting the developmental dance of the megakaryocyte: a review of the cellular and molecular processes mediating platelet formation. *Br. J. Haematol.,* **165**, 227-36.

Maeda, N., Kawasaki, T., Nakade, S., Yokota, N., Taguchi, T., Kasai, M. & Mikoshiba, K. (1991). Structural and functional characterization of inositol 1,4,5-trisphosphate receptor channel from mouse cerebellum. *J. Biol. Chem.,* **266**, 1109-16.

Malek, A. M., Alper, S. L. & Izumo, S. (1999). Hemodynamic shear stress and its role in atherosclerosis. *JAMA,* **282**, 2035-42.

Mammadova-Bach, E., Ollivier, V., Loyau, S., Schaff, M., Dumont, B., Favier, R., Freyburger, G., Latger-Cannard, V., Nieswandt, B., Gachet, C., Mangin, P.H. & Jandrot-Perrus, M. (2015). Platelet glycoprotein VI binds to polymerized fibrin and promotes thrombin generation. *Blood.,* **126**, 683-91.

Manach, C., Morand, C., Crespy, V., Demigne, C., Texier, O., Regerat, F. & Remesy, C. (1998). Quercetin is recovered in human plasma as conjugated derivatives which retain antioxidant properties. *FEBS Lett.,* **426**, 331-6.

Manach, C., Morand, C., Demigne, C., Texier, O., Regerat, F. & Remesy, C. (1997). Bioavailability of rutin and quercetin in rats. *FEBS Lett.,* **409**, 12-6.

Manach, C., Scalbert, A., Morand, C., Rémésy, C. & Jiménez, L. (2004). Polyphenols: food sources and bioavailability. *Am J Clin Nutr,* **79**, 727-747.

Manukyan, D., von Bruehl, M. L., Massberg, S. & Engelmann, B. (2008). Protein disulfide isomerase as a trigger for tissue factor-dependent fibrin generation. *Thromb. Res.,* **122 Suppl 1**, S19-22.

Maree, A. O. & Fitzgerald, D. J. (2007). Variable Platelet Response to Aspirin and Clopidogrel in Atherothrombotic Disease. *Circulation,* **115**, 2196-2207.

Marin, L., Miguelez, E. M., Villar, C. J. & Lombo, F. (2015). Bioavailability of Dietary Polyphenols and Gut Microbiota Metabolism: Antimicrobial Properties. *BioMed Res. Int.,* **2015**, 905215.

Martel, V., Racaud-Sultan, C., Dupe, S., Marie, C., Paulhe, F., Galmiche, A., Block, M. R. & Albiges-Rizo, C. (2001). Conformation, localization, and integrin binding of talin depend on its interaction with phosphoinositides. *J. Biol. Chem.,* **276**, 21217-27.

Martin, J. F., Trowbridge, E. A., Salmon, G. L. & Slater, D. N. (1982). The relationship between platelet and megakaryocyte volumes. *Thromb. Res.,* **28**, 447-59.

Mason, K. D., Carpinelli, M. R., Fletcher, J. I., Collinge, J. E., Hilton, A. A., Ellis, S., Kelly, P. N., Ekert, P. G., Metcalf, D., Roberts, A. W., Huang, D. C. & Kile, B. T. (2007). Programmed anuclear cell death delimits platelet life span. *Cell,* **128**, 1173-86.

MathWorks (2015). MATLAB, Release 2015b. The MathWorks. Natick, Massachusetts, United States.

Matsukawa, N., Matsumoto, M. & Hara, H. (2009). High biliary excretion levels of quercetin metabolites after administration of a quercetin glycoside in conscious bile duct cannulated rats. *Biosci. Biotechnol. Biochem.,* **73**, 1863-1865.

Matsuo, M., Sasaki, N., Saga, K. & Kaneko, T. (2005). Cytotoxicity of flavonoids toward cultured normal human cells. *Biol. Pharm. Bull.,* **28**, 253-9.

Maynard, D. M., Heijnen, H. F., Horne, M. K., White, J. G. & Gahl, W. A. (2007). Proteomic analysis of platelet alpha-granules using mass spectrometry. *J. Thromb. Haemost.,* **5**, 1945-55.

McCullough, M. L., Peterson, J. J., Patel, R., Jacques, P. F., Shah, R. & Dwyer, J. T. (2012). Flavonoid intake and cardiovascular disease mortality in a prospective cohort of US adults. *Am J Clin Nutr,* **95**, 454-464.

McElroy, W. D. (1947). The Energy Source for Bioluminescence in an Isolated System. *Proc. Natl. Acad. Sci. U. S. A.,* **33**, 342-345.

McNicol, A. & Gerrard, J. M. (1993). Post-receptor events associated with thrombin-induced platelet activation. *Blood Coagul. Fibrinolysis,* **4**, 975-91.

McQuaid, K. R. & Laine, L. (2006). Systematic review and meta-analysis of adverse events of low-dose aspirin and clopidogrel in randomized controlled trials. *Am. J. Med.,* **119**, 624-38.

Menendez, C., Dueñas, M., Galindo, P., González-Manzano, S., Jimenez, R., Moreno, L., Zarzuelo, M. J., Rodríguez-Gómez, I., Duarte, J., Santos-Buelga, C. & Perez-Vizcaino, F. (2011). Vascular deconjugation of quercetin glucuronide: The flavonoid paradox revealed? *Mol. Nutr. Food Res.,* **55**, 1780-1790.

Meskin, M. S., Bidlack, W. R., Davies, A. J., Lewis, D. S. & Randolph, R. K. (2003). *Phytochemicals: Mechanisms of Action.* Florida, USA: CRC Press.

Meyers, K. M., Holmsen, H. & Seachord, C. L. (1982). Comparative study of platelet dense granule constituents. *Am. J. Physiol.,* **243**, R454-61.

Mierziak, J., Kostyn, K. & Kulma, A. (2014). Flavonoids as important molecules of plant interactions with the environment. *Molecules,* **19**, 16240-16265.

Millward, T.A., Zolnierowicz, S. & Hemmings, B.A. (1999). Regulation of protein kinase cascades by protein phosphatase 2A. *Trends Biochem. Sci.,* **24**, 186-91.

Mitchell, J. A. & Warner, T. D. (1999). Cyclo-oxygenase-2: pharmacology, physiology, biochemistry and relevance to NSAID therapy. *Br. J. Pharmacol.,* **128**, 1121-1132.

Mohamed, M.-E. F. & Frye, R. F. (2011). Inhibitory Effects of Commonly Used Herbal Extracts on UDP-Glucuronosyltransferase 1A4, 1A6, and 1A9 Enzyme Activities. *Drug Metab. Dispos.,* **39**, 1522-1528.

Moncada, S., Higgs, E. A. & Vane, J. R. (1977). Human arterial and venous tissues generate prostacyclin (prostaglandin x), a potent inhibitor of platelet aggregation. *Lancet,* **1**, 18-20.

Moon, J.-H., Tsushida, T., Nakahara, K. & Terao, J. (2001). Identification of quercetin 3-O-β-D-glucuronide as an antioxidative metabolite in rat plasma after oral administration of quercetin. *Free Radic. Biol. Med.,* **30**, 1274-1285.

Moon, Y. J., Wang, L., DiCenzo, R. & Morris, M. E. (2008). Quercetin pharmacokinetics in humans. *Biopharm. Drug Dispos.,* **29**, 205-17.

Moore, R. A., Derry, S., Wiffen, P. J. & Straube, S. (2015). Effects of food on pharmacokinetics of immediate release oral formulations of aspirin, dipyrone, paracetamol and NSAIDs - a systematic review. *Br. J. Clin. Pharmacol.,* **80**, 381-8.

Mor-Cohen, R. (2016). Disulfide Bonds as Regulators of Integrin Function in Thrombosis and Hemostasis. *Antioxid. Redox Signal.,* **24**, 16-31.

Moraes, L. A., Barrett, N. E., Jones, C. I., Holbrook, L. M., Spyridon, M., Sage, T., Newman, D. K. & Gibbins, J. M. (2010). Platelet endothelial cell adhesion molecule-1 regulates collagen-stimulated platelet function by modulating the association of phosphatidylinositol 3-kinase with Grb-2-associated binding protein-1 and linker for activation of T cells. *J. Thromb. Haemost.,* **8**, 2530-41.

Moraes, L. A., Paul-Clark, M. J., Rickman, A., Flower, R. J., Goulding, N. J. & Perretti, M. (2005). Ligand-specific glucocorticoid receptor activation in human platelets. *Blood,* **106**, 4167-75.

Moraes, L. A., Swales, K. E., Wray, J. A., Damazo, A., Gibbins, J. M., Warner, T. D. & Bishop-Bailey, D. (2007). Nongenomic signaling of the retinoid X receptor through binding and inhibiting Gq in human platelets. *Blood,* **109**, 3741-4.

Morand, C., Manach, C., Crespy, V. & Remesy, C. (2000). Respective bioavailability of quercetin aglycone and its glycosides in a rat model. *Biofactors,* **12**, 169-74.

Mori, J., Pearce, A. C., Spalton, J. C., Grygielska, B., Eble, J. A., Tomlinson, M. G., Senis, Y. A. & Watson, S. P. (2008). G6b-B Inhibits Constitutive and Agonist-induced Signaling by Glycoprotein VI and CLEC-2. *J. Biol. Chem.,* **283**, 35419-35427.

Moroi, M., Jung, S. M., Shinmyozu, K., Tomiyama, Y., Ordinas, A. & Diaz-Ricart, M. (1996). Analysis of platelet adhesion to a collagen-coated surface under flow conditions: the involvement of glycoprotein VI in the platelet adhesion. *Blood,* **88**, 2081-92.

Morton, L. F., Hargreaves, P. G., Farndale, R. W., Young, R. D. & Barnes, M. J. (1995). Integrin alpha 2 beta 1-independent activation of platelets by simple collagen-like peptides: collagen tertiary (triple-helical) and quaternary (polymeric) structures are sufficient alone for alpha 2 beta 1-independent platelet reactivity. *Biochem. J.,* **306 (Pt 2)**, 337-44.

Mosawy, S., Jackson, D. E., Woodman, O. L. & Linden, M. D. (2013a). Inhibition of platelet-mediated arterial thrombosis and platelet granule exocytosis by 3',4'-dihydroxyflavonol and quercetin. *Platelets,* **24**, 594-604.

Mosawy, S., Jackson, D. E., Woodman, O. L. & Linden, M. D. (2013b). Treatment with quercetin and 3′,4′-dihydroxyflavonol inhibits platelet function and reduces thrombus formation in vivo. *J. Thromb. Thrombolysis,* **36**, 50-57.

Moser, M., Nieswandt, B., Ussar, S., Pozgajova, M. & Fassler, R. (2008). Kindlin-3 is essential for integrin activation and platelet aggregation. *Nat. Med.,* **14**, 325-330.

Mullen, W., Edwards, C. A. & Crozier, A. (2006). Absorption, excretion and metabolite profiling of methyl-, glucuronyl-, glucosyl-and sulpho-conjugates of quercetin in human plasma and urine after ingestion of onions. *Br. J. Nutr.,* **96**, 107-116.

Mullen, W., Graf, B. A., Caldwell, S. T., Hartley, R. C., Duthie, G. G., Edwards, C. A., Lean, M. E. J. & Crozier, A. (2002). Determination of Flavonol Metabolites in Plasma and Tissues of Rats by HPLC−Radiocounting and Tandem Mass Spectrometry Following Oral Ingestion of [2-14C]Quercetin-4‘-glucoside. *J. Agric. Food Chem.,* **50**, 6902-6909.

Mundell, S. J., Jones, M. L., Hardy, A. R., Barton, J. F., Beaucourt, S. M., Conley, P. B. & Poole, A. W. (2006). Distinct roles for protein kinase C isoforms in regulating platelet purinergic receptor function. *Mol. Pharmacol.,* **70**, 1132-42.

Munnix, I., Gilio, K., Siljander, P., Raynal, N., Feijge, M., Hackeng, T., Deckmyn, H., Smethurst, P., Farndale, R. & Heemskerk, J. (2008). Collagen-mimetic peptides mediate flow-dependent thrombus formation by high-or low-affinity binding of integrin α2β1 and glycoprotein VI. *J. Thromb. Haemost.,* **6**, 2132-2142.

Murga, C., Laguinge, L., Wetzker, R., Cuadrado, A. & Gutkind, J. S. (1998). Activation of Akt/protein kinase B by G protein-coupled receptors. A role for alpha and beta gamma subunits of heterotrimeric G proteins acting through phosphatidylinositol-3-OH kinasegamma. *J. Biol. Chem.,* **273**, 19080-5.

Murota, K. & Terao, J. (2005). Quercetin appears in the lymph of unanesthetized rats as its phase II metabolites after administered into the stomach. *FEBS Lett.,* **579**, 5343-6.

Naik, M. U., Caplan, J. L. & Naik, U. P. (2014). Junctional adhesion molecule-A suppresses platelet integrin alphaIIbbeta3 signaling by recruiting Csk to the integrin-c-Src complex. *Blood,* **123**, 1393-402.

Naik, M. U., Stalker, T. J., Brass, L. F. & Naik, U. P. (2012). JAM-A protects from thrombosis by suppressing integrin alphaIIbbeta3-dependent outside-in signaling in platelets. *Blood,* **119**, 3352-60.

Nair, M. P. N., Saiyed, Z. M., Gandhi, N. H. & Ramchand, C. N. (2009). The flavonoid, quercetin, inhibits HIV-1 infection in normal peripheral blood mononuclear cells. *Am. J. Infect. Dis.,* **5**, 135-141.

Naito, K. & Fujikawa, K. (1991). Activation of human blood coagulation factor XI independent of factor XII. Factor XI is activated by thrombin and factor XIa in the presence of negatively charged surfaces. *J. Biol. Chem.,* **266**, 7353-8.

Nakamura, T., Murota, K., Kumamoto, S., Misumi, K., Bando, N., Ikushiro, S., Takahashi, N., Sekido, K., Kato, Y. & Terao, J. (2014). Plasma metabolites of dietary flavonoids after combination meal consumption with onion and tofu in humans. *Mol. Nutr. Food Res.,* **58**, 310-317.

Nakashima, S., Banno, Y. & Nozawa, Y. (1997). Platelet Phospholipases C and D. *In:* von Bruchhausen, F. & Walter, U. (eds.) *Platelets and Their Factors.* Berlin, Heidelberg: Springer Berlin Heidelberg.

Nanevicz, T., Ishii, M., Wang, L., Chen, M., Chen, J., Turck, C. W., Cohen, F. E. & Coughlin, S. R. (1995). Mechanisms of thrombin receptor agonist specificity. Chimeric receptors and complementary mutations identify an agonist recognition site. *J. Biol. Chem.,* **270**, 21619-25.

Nansseu, J. R. N. & Noubiap, J. J. N. (2015). Aspirin for primary prevention of cardiovascular disease. *Thromb J.,* **13**, 38.

Nasdala, I., Wolburg-Buchholz, K., Wolburg, H., Kuhn, A., Ebnet, K., Brachtendorf, G., Samulowitz, U., Kuster, B., Engelhardt, B., Vestweber, D. & Butz, S. (2002). A transmembrane tight junction protein selectively expressed on endothelial cells and platelets. *J. Biol. Chem.,* **277**, 16294-303.

Navarro-Núñez, L., Lozano, M. L., Martínez, C., Vicente, V. & Rivera, J. (2010). Effect of quercetin on platelet spreading on collagen and fibrinogen and on multiple platelet kinases. *Fitoterapia,* **81**, 75-80.

Navarro-Nunez, L., Lozano, M. L., Palomo, M., Martinez, C., Vicente, V., Castillo, J., Benavente-Garcia, O., Diaz-Ricart, M., Escolar, G. & Rivera, J. (2008). Apigenin inhibits platelet adhesion and thrombus formation and synergizes with aspirin in the suppression of the arachidonic acid pathway. *J. Agric. Food Chem.,* **56**, 2970-6.

Navarro-Núñez, L., Rivera, J., Guerrero, J. A., Martínez, C., Vicente, V. & Lozano, M. L. (2009). Differential effects of quercetin, apigenin and genistein on signalling pathways of protease-activated receptors PAR(1) and PAR(4) in platelets. *Br. J. Pharmacol.,* **158**, 1548-1556.

Negrescu, E. V., de Quintana, K. L. & Siess, W. (1995). Platelet shape change induced by thrombin receptor activation. Rapid stimulation of tyrosine phosphorylation of novel protein substrates through an integrin- and Ca(2+)-independent mechanism. *J. Biol. Chem.,* **270**, 1057-61.

Nemeth, K. & Piskula, M. (2007). Food content, processing, absorption and metabolism of onion flavonoids. *Crit. Rev. Food Sci. Nutr.,* **47**, 397-409.

Nemeth, K., Plumb, G. W., Berrin, J. G., Juge, N., Jacob, R., Naim, H. Y., Williamson, G., Swallow, D. M. & Kroon, P. A. (2003). Deglycosylation by small intestinal epithelial cell beta-glucosidases is a critical step in the absorption and metabolism of dietary flavonoid glycosides in humans. *Eur. J. Nutr.,* **42**, 29-42.

Nesbitt, W. S., Kulkarni, S., Giuliano, S., Goncalves, I., Dopheide, S. M., Yap, C. L., Harper, I. S., Salem, H. H. & Jackson, S. P. (2002). Distinct glycoprotein Ib/V/IX and integrin αIIbβ3-dependent calcium signals cooperatively regulate platelet adhesion under flow. *J. Biol. Chem.,* **277**, 2965-2972.

Nesbitt, W. S., Westein, E., Tovar-Lopez, F. J., Tolouei, E., Mitchell, A., Fu, J., Carberry, J., Fouras, A. & Jackson, S. P. (2009). A shear gradient-dependent platelet aggregation mechanism drives thrombus formation. *Nat. Med.,* **15**, 665-673.

Neumann, F.-J., Hochholzer, W., Pogatsa-Murray, G., Schömig, A. & Gawaz, M. (2001). Antiplatelet effects of abciximab, tirofiban and eptifibatide in patients undergoing coronary stenting. *J. Am. Coll. Cardiol.,* **37**, 1323.

Newland, S. A., Macaulay, I. C., Floto, A. R., de Vet, E. C., Ouwehand, W. H., Watkins, N. A., Lyons, P. A. & Campbell, D. R. (2007). The novel inhibitory receptor G6B is expressed on the surface of platelets and attenuates platelet function in vitro. *Blood,* **109**, 4806-9.

Newman, K. D., Williams, L. T., Bishopric, N. H. & Lefkowitz, R. J. (1978). Identification of α-Adrenergic Receptors in Human Platelets by [(3)H]Dihydroergocryptine Binding. *J. Clin. Invest.,* **61**, 395-402.

Nieswandt, B. & Watson, S. P. (2003). Platelet-collagen interaction: is GPVI the central receptor? *Blood,* **102**, 449-61.

Nieuwland, R., Van Willigen, G. & Akkerman, J. W. (1993). 4,4'-Di-isothiocyanatostilbene-2,2'-disulphonic acid ('DIDS') activates protein kinase C and Na+/H+ exchange in human platelets via alpha 2A-adrenergic receptors. *Biochem. J.,* **293 (Pt 2)**, 523-30.

Nishimura, T., Yamamoto, T., Komuro, Y. & Hara, Y. (1995). Antiplatelet functions of a stable prostacyclin analog, SM-10906 are exerted by its inhibitory effect on inositol 1,4,5-trisphosphate production and cytosolic Ca++ increase in rat platelets stimulated by thrombin. *Thromb. Res.,* **79**, 307-17.

Nishimuro, H., Ohnishi, H., Sato, M., Ohnishi-Kameyama, M., Matsunaga, I., Naito, S., Ippoushi, K., Oike, H., Nagata, T., Akasaka, H., Saitoh, S., Shimamoto, K. & Kobori, M. (2015). Estimated Daily Intake and Seasonal Food Sources of Quercetin in Japan. *Nutrients,* **7**, 2345-2358.

Nitelius, E., Brantmark, B., Fredholm, B., Hedner, U., Plym Forshell, G., Wåhlin-Boll, E. & Melander, A. (1984). Actions and interactions of acetylsalicylic acid, salicylic acid and diflunisal on platelet aggregation. *Eur. J. Clin. Pharmacol.,* **27**, 165-168.

Norgard, N. B., Bacon, N. R. & Agosti, M. (2016). Oral Administration of Sustained Release Niacin Inhibits Platelet Aggregation. *Curr. Clin. Pharmacol.,* **11**, 43-6.

Nurden, A. T. (2006). Glanzmann thrombasthenia. *Orphanet J. Rare Dis.,* **1**, 10.

Nuyttens, B. P., Thijs, T., Deckmyn, H. & Broos, K. (2011). Platelet adhesion to collagen. *Thromb. Res.,* **127 Suppl 2**, S26-9.

O'Leary, K. A., Day, A. J., Needs, P. W., Mellon, F. A., O'Brien, N. M. & Williamson, G. (2003). Metabolism of quercetin-7- and quercetin-3-glucuronides by an in vitro hepatic model: the role of human beta-glucuronidase, sulfotransferase, catechol-O-methyltransferase and multi-resistant protein 2 (MRP2) in flavonoid metabolism. *Biochem. Pharmacol.,* **65**, 479-91.

Obergfell, A., Eto, K., Mocsai, A., Buensuceso, C., Moores, S. L., Brugge, J. S., Lowell, C. A. & Shattil, S. J. (2002). Coordinate interactions of Csk, Src, and Syk kinases with [alpha]IIb[beta]3 initiate integrin signaling to the cytoskeleton. *J. Cell Biol.,* **157**, 265-75.

Offermanns, S. (2006). Activation of platelet function through G protein-coupled receptors. *Circ. Res.,* **99**, 1293-304.

Offermanns, S., Laugwitz, K. L., Spicher, K. & Schultz, G. (1994). G proteins of the G12 family are activated via thromboxane A2 and thrombin receptors in human platelets. *Proc. Natl. Acad. Sci. U. S. A.,* **91**, 504-508.

Oh, W. J., Endale, M., Park, S.-C., Cho, J. Y. & Rhee, M. H. (2012). Dual Roles of Quercetin in Platelets: Phosphoinositide-3-Kinase and MAP Kinases Inhibition, and cAMP-Dependent Vasodilator-Stimulated Phosphoprotein Stimulation. *Evid. Based Complement. Alternat. Med.,* **2012**, 485262.

Ohlmann, P., Laugwitz, K. L., Nurnberg, B., Spicher, K., Schultz, G., Cazenave, J. P. & Gachet, C. (1995). The human platelet ADP receptor activates Gi2 proteins. *Biochem. J.,* **312 (Pt 3)**, 775-9.

Ohto, H., Maeda, H., Shibata, Y., Chen, R.-F., Ozaki, Y., Higashihara, M., Takeuchi, A. & Tohyama, H. (1985). A novel leukocyte differentiation antigen: two monoclonal antibodies TM2 and TM3 define a 120-kd molecule present on neutrophils, monocytes, platelets, and activated lymphoblasts. *Blood,* **66**, 873-881.

Oldham, W. M. & Hamm, H. E. (2008). Heterotrimeric G protein activation by G-protein-coupled receptors. *Nat. Rev. Mol. Cell Biol.,* **9**, 60-71.

Olthof, M. R., Hollman, P. C., Vree, T. B. & Katan, M. B. (2000). Bioavailabilities of quercetin-3-glucoside and quercetin-4'-glucoside do not differ in humans. *J. Nutr.,* **130**, 1200-3.

Otake, Y. & Walle, T. (2002). Oxidation of the flavonoids galangin and kaempferide by human liver microsomes and CYP1A1, CYP1A2, and CYP2C9. *Drug Metab. Dispos.,* **30**, 103-5.

Otsuka, F., Yasuda, S., Noguchi, T. & Ishibashi-Ueda, H. (2016). Pathology of coronary atherosclerosis and thrombosis. *Cardiovasc Diagn Ther.,* **6**, 396-408.

Ozaki, Y., Suzuki-Inoue, K. & Inoue, O. (2013). Platelet receptors activated via mulitmerization: glycoprotein VI, GPIb-IX-V, and CLEC-2. *J. Thromb. Haemost.,* **11 Suppl 1**, 330-9.

Özge-Anwar, A., Connell, G. & Mustard, J. (1965). The activation of factor VIII by thrombin. *Blood,* **26**, 500-509.

Palikhe, N. S., Kim, S.-H., Nam, Y. H., Ye, Y.-M. & Park, H.-S. (2011). Polymorphisms of Aspirin-Metabolizing Enzymes CYP2C9, NAT2 and UGT1A6 in Aspirin-Intolerant Urticaria. *Allergy Asthma Immunol. Res.,* **3**, 273-276.

Pandey, K. B. & Rizvi, S. I. (2009). Plant polyphenols as dietary antioxidants in human health and disease. *Oxid. Med. Cell. Longev.,* **2**, 270-278.

Paniccia, R., Priora, R., Alessandrello Liotta, A. & Abbate, R. (2015). Platelet function tests: a comparative review. *Vasc Health Risk Manag.,* **11**, 133-148.

Papaioannou, T. G. & Stefanadis, C. (2005). Vascular wall shear stress: basic principles and methods. *Hellenic J. Cardiol.,* **46**, 9-15.

Park, T. K., Song, Y. B., Ahn, J., Carriere, K. C., Hahn, J.-Y., Yang, J. H., Choi, S.-H., Choi, J.-H., Lee, S. H. & Gwon, H.-C. (2016). Clopidogrel Versus Aspirin as an Antiplatelet

Monotherapy After 12-Month Dual-Antiplatelet Therapy in the Era of Drug-Eluting Stents. *Circ. Cardiovasc. Interv.,* **9**, e002816.

Pasquet, J.-M., Gross, B., Quek, L., Asazuma, N., Zhang, W., Sommers, C. L., Schweighoffer, E., Tybulewicz, V., Judd, B., Lee, J. R., Koretzky, G., Love, P. E., Samelson, L. E. & Watson, S. P. (1999a). LAT Is Required for Tyrosine Phosphorylation of Phospholipase Cγ2 and Platelet Activation by the Collagen Receptor GPVI. *Mol. Cell. Biol.,* **19**, 8326-8334.

Pasquet, J. M., Bobe, R., Gross, B., Gratacap, M. P., Tomlinson, M. G., Payrastre, B. & Watson, S. P. (1999b). A collagen-related peptide regulates phospholipase Cgamma2 via phosphatidylinositol 3-kinase in human platelets. *Biochem. J.,* **342 (Pt 1)**, 171-7.

Passeri, M., Cucinotta, D., Abate, G., Senin, U., Ventura, A., Stramba Badiale, M., Diana, R., La Greca, P. & Le Grazie, C. (1993). Oral 5'-methyltetrahydrofolic acid in senile organic mental disorders with depression: results of a double-blind multicenter study. *Aging (Milano),* **5**, 63-71.

Patel, S. R., Hartwig, J. H. & Italiano, J. E. (2005). The biogenesis of platelets from megakaryocyte proplatelets. *J. Clin. Invest.,* **115**, 3348-3354.

Patschke, L. & Grisebach, H. (1968). Biosynthesis of flavonoids—XVI. *Phytochemistry,* **7**, 235-237.

Paul, B. Z., Jin, J. & Kunapuli, S. P. (1999). Molecular mechanism of thromboxane A(2)-induced platelet aggregation. Essential role for p2t(ac) and alpha(2a) receptors. *J. Biol. Chem.,* **274**, 29108-14.

Paulke, A., Eckert, G. P., Schubert-Zsilavecz, M. & Wurglics, M. (2012). Isoquercitrin provides better bioavailability than quercetin: comparison of quercetin metabolites in body tissue and brain sections after six days administration of isoquercitrin and quercetin. *Pharmazie,* **67**, 991-6.

Pearce, A. C., Senis, Y. A., Billadeau, D. D., Turner, M., Watson, S. P. & Vigorito, E. (2004). Vav1 and Vav3 Have Critical but Redundant Roles in Mediating Platelet Activation by Collagen. *J. Biol. Chem.,* **279**, 53955-53962.

Pearson, D. A., Paglieroni, T. G., Rein, D., Wun, T., Schramm, D. D., Wang, J. F., Holt, R. R., Gosselin, R., Schmitz, H. H. & Keen, C. L. (2002). The effects of flavanol-rich cocoa and aspirin on ex vivo platelet function. *Thromb. Res.,* **106**, 191-7.

Peters, R. J. G., Mehta, S. R., Fox, K. A. A., Zhao, F., Lewis, B. S., Kopecky, S. L., Diaz, R., Commerford, P. J., Valentin, V. & Yusuf, S. (2003). Effects of Aspirin Dose When Used Alone or in Combination With Clopidogrel in Patients With Acute Coronary Syndromes. Observations From the Clopidogrel in Unstable angina to prevent Recurrent Events (CURE) Study. *Circulation*, **108**, 1682-1687.

Peyvandi, F., Garagiola, I. & Baronciani, L. (2011). Role of von Willebrand factor in the haemostasis. *Blood Transfusion,* **9**, s3-s8.

Pignatelli, P., Di Santo, S., Buchetti, B., Sanguigni, V., Brunelli, A. & Violi, F. (2006). Polyphenols enhance platelet nitric oxide by inhibiting protein kinase C-dependent NADPH oxidase activation: effect on platelet recruitment. *FASEB J.,* **20**, 1082-9.

Pignatelli, P., Pulcinelli, F. M., Celestini, A., Lenti, L., Ghiselli, A., Gazzaniga, P. P. & Violi, F. (2000). The flavonoids quercetin and catechin synergistically inhibit platelet function by antagonizing the intracellular production of hydrogen peroxide. *Am. J. Clin. Nutr.,* **72**, 1150-5.

Pinheiro, P. F. & Justino, G. C. (2012). Structural analysis of flavonoids and related compounds-a review of spectroscopic applications. *Phytochemicals-A Global Perspective of Their Role in Nutrition and Health.* Rijeka, Croatia: InTech.

Podoplelova, N. A., Sveshnikova, A. N., Kotova, Y. N., Eckly, A., Receveur, N., Nechipurenko, D. Y., Obydennyi, S. I., Kireev, II, Gachet, C., Ataullakhanov, F. I., Mangin, P. H. & Panteleev, M. A. (2016). Coagulation factors bound to procoagulant platelets concentrate in cap structures to promote clotting. *Blood,* **128**, 1745-55.

Polanowska-Grabowska, R., Simon, C. G., Jr. & Gear, A. R. (1999). Platelet adhesion to collagen type I, collagen type IV, von Willebrand factor, fibronectin, laminin and fibrinogen: rapid kinetics under shear. *Thromb. Haemost.,* **81**, 118-23.

Polasek, J. (2005). Platelet secretory granules or secretory lysosomes? *Platelets,* **16**, 500-501.

Polgar, J. & Reed, G. L. (1999). A critical role for N-ethylmaleimide-sensitive fusion protein (NSF) in platelet granule secretion. *Blood,* **94**, 1313-8.

Poulter, N. S., Pollitt, A. Y., Owen, D. M., Gardiner, E. E., Andrews, R. K., Shimizu, H., Ishikawa, D., Bihan, D., Farndale, R. W., Moroi, M., Watson, S. P. & Jung, S. M. (2017). Clustering of glycoprotein VI (GPVI) dimers upon adhesion to collagen as a mechanism to regulate GPVI signaling in platelets. *J. Thromb. Haemost.,* **15**, 549-564.

Pozgajova, M., Sachs, U. J., Hein, L. & Nieswandt, B. (2006). Reduced thrombus stability in mice lacking the alpha2A-adrenergic receptor. *Blood,* **108**, 510-4.

Prakriya, M. & Lewis, R. S. (2015). Store-Operated Calcium Channels. *Physiol. Rev.,* **95**, 1383.

PRISM-PLUS-Investigators (1998). Inhibition of the Platelet Glycoprotein IIb/IIIa Receptor with Tirofiban in Unstable Angina and Non–Q-Wave Myocardial Infarction. *N. Engl. J. Med.,* **338**, 1488-1497.

Pulcinelli, F. M., Ciampa, M. T., Favilla, M., Pignatelli, P., Riondino, S. & Gazzaniga, P. P. (1999). Concomitant activation of Gi protein-coupled receptor and protein kinase C or phospholipase C is required for platelet aggregation. *FEBS Lett.,* **460**, 37-40.

PURSUIT-Investigators (1998). Inhibition of Platelet Glycoprotein IIb/IIIa with Eptifibatide in Patients with Acute Coronary Syndromes. *N. Engl. J. Med.,* **339**, 436-443.

Quek, L. S., Bolen, J. & Watson, S. P. (1998). A role for Bruton's tyrosine kinase (Btk) in platelet activation by collagen. *Curr. Biol.,* **8**, 1137-40.

Quek, L. S., Pasquet, J. M., Hers, I., Cornall, R., Knight, G., Barnes, M., Hibbs, M. L., Dunn, A. R., Lowell, C. A. & Watson, S. P. (2000). Fyn and Lyn phosphorylate the Fc receptor gamma chain downstream of glycoprotein VI in murine platelets, and Lyn regulates a novel feedback pathway. *Blood,* **96**, 4246-53.

Quinn, M., Fitzgerald, D. & Cox, D. (2007). *Platelet Function: Assessment, Diagnosis, and Treatment.* New York, USA: Humana Press.

Quinton, T. M., Kim, S., Dangelmaier, C., Dorsam, R. T., Jin, J., Daniel, J. L. & Kunapuli, S. P. (2002). Protein kinase C- and calcium-regulated pathways independently synergize with Gi pathways in agonist-induced fibrinogen receptor activation. *Biochem. J.,* **368**, 535-543.

Radomski, M. W., Palmer, R. M. & Moncada, S. (1987a). Comparative pharmacology of endothelium-derived relaxing factor, nitric oxide and prostacyclin in platelets. *Br. J. Pharmacol.,* **92**, 181-7.

Radomski, M. W., Palmer, R. M. & Moncada, S. (1987b). The role of nitric oxide and cGMP in platelet adhesion to vascular endothelium. *Biochem. Biophys. Res. Commun.,* **148**, 1482-9.

Raghavan, S. A. V., Sharma, P. & Dikshit, M. (2003). Role of ascorbic acid in the modulation of inhibition of platelet aggregation by polymorphonuclear leukocytes. *Thromb. Res.,* **110**, 117-126.

Raghavendra, R. H. & Naidu, K. A. (2009). Spice active principles as the inhibitors of human platelet aggregation and thromboxane biosynthesis. *Prostaglandins Leukot. Essent. Fatty Acids,* **81**, 73-78.

Rathore, V., Stapleton, M. A., Hillery, C. A., Montgomery, R. R., Nichols, T. C., Merricks, E. P., Newman, D. K. & Newman, P. J. (2003). PECAM-1 negatively regulates GPIb/V/IX signaling in murine platelets. *Blood,* **102**, 3658-64.

Raychowdhury, M. K., Yukawa, M., Collins, L. J., McGrail, S. H., Kent, K. C. & Ware, J. A. (1995). Alternative splicing produces a divergent cytoplasmic tail in the human endothelial thromboxane A2 receptor. *J. Biol. Chem.,* **270**, 7011.

Razi, M. S., Butt, I. F., Aslam, M., Hameed, W., Ashraf, R. & Effendi, S. (2005). Dose response relationships of different reagents for platelet aggregation. *Pak J Physiol,* **1**, 1-2.

Razi, M. S., Hameed, W., Habib, S. S., Aslam, M. & Ashraf, R. (2009). Synergism between collagen-adenosine diphosphate and collagen-epinephrine in platelets' aggregation: different dose response relationships. *J. Pak. Med. Assoc.,* **59**, 368-71.

Rechner, A. R., Smith, M. A., Kuhnle, G., Gibson, G. R., Debnam, E. S., Srai, S. K., Moore, K. P. & Rice-Evans, C. A. (2004). Colonic metabolism of dietary polyphenols: influence of structure on microbial fermentation products. *Free Radic. Biol. Med.,* **36**, 212-25.

Reiner, S., Ziegler, N., Leon, C., Lorenz, K., von Hayn, K., Gachet, C., Lohse, M. J. & Hoffmann, C. (2009). beta-Arrestin-2 interaction and internalization of the human P2Y1 receptor are dependent on C-terminal phosphorylation sites. *Mol. Pharmacol.,* **76**, 1162-71.

Reppschlager, K., Gosselin, J., Dangelmaier, C. A., Thomas, D. H., Carpino, N., McKenzie, S. E., Kunapuli, S. P. & Tsygankov, A. Y. (2016). TULA-2 Protein Phosphatase Suppresses Activation of Syk through the GPVI Platelet Receptor for Collagen by Dephosphorylating Tyr(P)346, a Regulatory Site of Syk. *J. Biol. Chem.,* **291**, 22427-22441.

Rhee, S. G. (2001). Regulation of phosphoinositide-specific phospholipase C. *Annu. Rev. Biochem.,* **70**, 281-312.

Ricard-Blum, S. (2011). The Collagen Family. *Cold Spring Harb. Perspect. Biol.,* **3**, a004978.

Richardson, J. L., Shivdasani, R. A., Boers, C., Hartwig, J. H. & Italiano, J. E. (2005). Mechanisms of organelle transport and capture along proplatelets during platelet production. *Blood,* **106**, 4066-4075.

Rocha, D. S., de Souza, S. K., Onsten, T. G. H., da Silva, R. S. M. & Frizzo, M. E. (2014). A simple method to quantify glycogen from human platelets. *J. Cytol. Histol.,* **5**, 217.

Roest, M., Reininger, A., Zwaginga, J. J., King, M. R. & Heemskerk, J. W. (2011). Flow chamber-based assays to measure thrombus formation in vitro: requirements for standardization. *J. Thromb. Haemost.,* **9**, 2322-4.

Rosenkranz, B., Fischer, C., Meese, C. O. & Frölich, J. C. (1986). Effects of salicylic and acetylsalicylic acid alone and in combination on platelet aggregation and prostanoid synthesis in man. *Br. J. Clin. Pharmacol.,* **21**, 309-317.

Russo, G. L., Russo, M. & Spagnuolo, C. (2014a). The pleiotropic flavonoid quercetin: from its metabolism to the inhibition of protein kinases in chronic lymphocytic leukemia. *Food Funct.,* **5**, 2393-2401.

Russo, G. L., Russo, M., Spagnuolo, C., Tedesco, I., Bilotto, S., Iannitti, R. & Palumbo, R. (2014b). Quercetin: A Pleiotropic Kinase Inhibitor Against Cancer. *In:* Zappia, V., Panico, S., Russo, G. L., Budillon, A. & Della Ragione, F. (eds.) *Advances in Nutrition and Cancer.* Berlin, Heidelberg: Springer Berlin Heidelberg.

Rusznyak, S. & Szent-Gyorgyi, A. (1936). Vitamin P: flavonols as vitamins. *Nature,* **138**.

Sagar, K. A. & Smyth, M. R. (1999). A comparative bioavailability study of different aspirin formulations using on-line multidimensional chromatography. *J. Pharm. Biomed. Anal.,* **21**, 383-92.

Sage, S., Yamoah, E. & Heemskerk, J. (2000). The roles of P2X1and P2T ACreceptors in ADP-evoked calcium signalling in human platelets. *Cell Calcium,* **28**, 119-126.

Sage, S. O. & Rink, T. J. (1986). Kinetic differences between thrombin-induced and ADP-induced calcium influx and release from internal stores in fura-2 loaded human platelets. *Biochem. Biophys. Res. Commun.,* **136**, 1124-1129.

Sanchez, M., Galisteo, M., Vera, R., Villar, I. C., Zarzuelo, A., Tamargo, J., Perez-Vizcaino, F. & Duarte, J. (2006). Quercetin downregulates NADPH oxidase, increases eNOS activity and prevents endothelial dysfunction in spontaneously hypertensive rats. *J. Hypertens.,* **24**, 75-84.

Sánchez-Cortés, J. & Mrksich, M. (2009). The Platelet Integrin αIIbβ3 Binds to the RGD and AGD Motifs in Fibrinogen. *Chem. Biol.,* **16**, 990-1000.

Sandler, S.G. (2000). The spleen and splenectomy in immune (idiopathic) thrombocytopenic purpura. *Semin Hematol.,* **37**, Suppl 1, 10-12.

Sandmann, R. & Koster, S. (2016). Topographic Cues Reveal Two Distinct Spreading Mechanisms in Blood Platelets. *Sci. Rep.,* **6**, 22357.

Savage, B., Almus-Jacobs, F. & Ruggeri, Z. M. (1998). Specific synergy of multiple substrate-receptor interactions in platelet thrombus formation under flow. *Cell,* **94**, 657-66.

Savage, B., Saldivar, E. & Ruggeri, Z. M. (1996). Initiation of platelet adhesion by arrest onto fibrinogen or translocation on von Willebrand factor. *Cell,* **84**, 289-97.

Savage, B., Sixma, J. J. & Ruggeri, Z. M. (2002). Functional self-association of von Willebrand factor during platelet adhesion under flow. *Proc Natl Acad Sci,* **99**, 425-430.

Savi, P., Labouret, C., Delesque, N., Guette, F., Lupker, J. & Herbert, J. M. (2001). P2y(12), a new platelet ADP receptor, target of clopidogrel. *Biochem. Biophys. Res. Commun.,* **283**, 379-83.

Scheraga, H. A. (1958). Thrombin and its interaction with fibrinogen. *Ann. N. Y. Acad. Sci.,* **75**, 189-194.

Schoenwaelder, S. M., Jackson, S. P., Yuan, Y., Teasdale, M. S., Salem, H. H. & Mitchell, C. A. (1994). Tyrosine kinases regulate the cytoskeletal attachment of integrin alpha IIb beta 3 (platelet glycoprotein IIb/IIIa) and the cellular retraction of fibrin polymers. *J. Biol. Chem.,* **269**, 32479-87.

Schoenwaelder, S. M., Yuan, Y., Cooray, P., Salem, H. H. & Jackson, S. P. (1997). Calpain cleavage of focal adhesion proteins regulates the cytoskeletal attachment of integrin αIIbβ3 (platelet glycoprotein IIb/IIIa) and the cellular retraction of fibrin clots. *J. Biol. Chem.,* **272**, 1694-1702.

Schoenwaelder, S. M., Yuan, Y., Josefsson, E. C., White, M. J., Yao, Y., Mason, K. D., O'Reilly, L. A., Henley, K. J., Ono, A., Hsiao, S., Willcox, A., Roberts, A. W., Huang, D. C., Salem, H. H., Kile, B. T. & Jackson, S. P. (2009). Two distinct pathways regulate platelet phosphatidylserine exposure and procoagulant function. *Blood,* **114**, 663-6.

Schroeder, K., Fahey, T. & Ebrahim, S. (2004). How can we improve adherence to blood pressure-lowering medication in ambulatory care? Systematic review of randomized controlled trials. *Arch. Intern. Med.,* **164**, 722-32.

Schrör, K. (1997). Aspirin and platelets: the antiplatelet action of aspirin and its role in thrombosis treatment and prophylaxis. *Semin. Thromb. Hemost.,* **23**, 349-356.

Schrör, K. (2016). *Acetylsalicylic Acid.* New Jersey, USA: John Wiley & Sons.

Schultze, M. (1865). Ein heizbarer Objecttisch und seine Verwendung bei Untersuchungen des Blutes. *Archiv für mikroskopische Anatomie,* **1**, 1-42.

Schulze, H., Korpal, M., Hurov, J., Kim, S.-W., Zhang, J., Cantley, L. C., Graf, T. & Shivdasani, R. A. (2006). Characterization of the megakaryocyte demarcation membrane system and its role in thrombopoiesis. *Blood,* **107**, 3868-3875.

Schwartz, K. A. (2011). Aspirin Resistance: A Clinical Review Focused on the Most Common Cause, Noncompliance. *The Neurohospitalist,* **1**, 94-103.

Sehgal, S. & Storrie, B. (2007). Evidence that differential packaging of the major platelet granule proteins von Willebrand factor and fibrinogen can support their differential release. *J. Thromb. Haemost.,* **5**, 2009-16.

Selway, J. W. (1986). Antiviral activity of flavones and flavans. *Prog. Clin. Biol. Res.,* **213**, 521-36.

Senis, Y. A., Tomlinson, M. G., Ellison, S., Mazharian, A., Lim, J., Zhao, Y., Kornerup, K. N., Auger, J. M., Thomas, S. G., Dhanjal, T., Kalia, N., Zhu, J. W., Weiss, A. & Watson, S. P. (2009). The tyrosine phosphatase CD148 is an essential positive regulator of platelet activation and thrombosis. *Blood,* **113**, 4942-54.

Senis, Y. A., Tomlinson, M. G., Garcia, A., Dumon, S., Heath, V. L., Herbert, J., Cobbold, S. P., Spalton, J. C., Ayman, S., Antrobus, R., Zitzmann, N., Bicknell, R., Frampton, J., Authi, K. S., Martin, A., Wakelam, M. J. & Watson, S. P. (2007). A comprehensive proteomics and genomics analysis reveals novel transmembrane proteins in human platelets and mouse megakaryocytes including G6b-B, a novel immunoreceptor tyrosine-based inhibitory motif protein. *Mol. Cell. Proteomics,* **6**, 548-64.

Serban, M. C., Sahebkar, A., Zanchetti, A., Mikhailidis, D. P., Howard, G., Antal, D., Andrica, F., Ahmed, A., Aronow, W. S., Muntner, P., Lip, G. Y. H., Graham, I., Wong, N., Rysz, J. & Banach, M. (2016). Effects of Quercetin on Blood Pressure: A Systematic Review and Meta-Analysis of Randomized Controlled Trials. *J. Am. Heart. Assoc.,* **5**, e002713.

Serebruany, V., Malinin, A., Aradi, D., Kuliczkowski, W., Norgard, N. B. & Boden, W. E. (2010). The in vitro effects of niacin on platelet biomarkers in human volunteers. *Thromb. Haemost.,* **104**, 311-17.

Serebruany, V. L., Steinhubl, S. R., Berger, P. B., Malinin, A. I., Baggish, J. S., Bhatt, D. L. & Topol, E. J. (2005). Analysis of Risk of Bleeding Complications After Different Doses of

Aspirin in 192,036 Patients Enrolled in 31 Randomized Controlled Trials. *Am. J. Cardiol.,* **95**, 1218-1222.

Sesink, A. L., O'Leary, K. A. & Hollman, P. C. (2001). Quercetin glucuronides but not glucosides are present in human plasma after consumption of quercetin-3-glucoside or quercetin-4'-glucoside. *J. Nutr.,* **131**, 1938-41.

Sesso, H. D., Gaziano, J. M., Liu, S. & Buring, J. E. (2003). Flavonoid intake and the risk of cardiovascular disease in women. *Am. J. Clin. Nutr.,* **77**, 1400-8.

Seymour, R. A. & Rawlins, M. D. (1982). Efficacy and pharmacokinetics of aspirin in post-operative dental pain. *Br. J. Clin. Pharmacol.,* **13**, 807-10.

Shattil, S. J. & Brass, L. F. (1987). Induction of the fibrinogen receptor on human platelets by intracellular mediators. *J. Biol. Chem.,* **262**, 992-1000.

Shattil, S. J., Kashiwagi, H. & Pampori, N. (1998). Integrin signaling: the platelet paradigm. *Blood,* **91**, 2645-57.

Shattil, S. J. & Newman, P. J. (2004). Integrins: dynamic scaffolds for adhesion and signaling in platelets. *Blood,* **104**, 1606-15.

Shen, B., Zhao, X., O/'Brien, K. A., Stojanovic-Terpo, A., Delaney, M. K., Kim, K., Cho, J., Lam, S. C. T. & Du, X. (2013). A directional switch of integrin signalling and a new anti-thrombotic strategy. *Nature,* **503**, 131-135.

Sheriff, J., Bluestein, D., Girdhar, G. & Jesty, J. (2010). High-Shear Stress Sensitizes Platelets to Subsequent Low-Shear Conditions. *Ann. Biomed. Eng.,* **38**, 1442-1450.

Shimizu, M., Li, J., Inoue, J. & Sato, R. (2015). Quercetin represses apolipoprotein B expression by inhibiting the transcriptional activity of C/EBPbeta. *PLoS One,* **10**, e0121784.

Shin, E.-K., Park, H., Noh, J.-Y., Lim, K.-M. & Chung, J.-H. (2017). Platelet Shape Changes and Cytoskeleton Dynamics as Novel Therapeutic Targets for Anti-Thrombotic Drugs. *Biomol. Ther. (Seoul),* **25**, 223-230.

Shirakawa, R., Higashi, T., Tabuchi, A., Yoshioka, A., Nishioka, H., Fukuda, M., Kita, T. & Horiuchi, H. (2004). Munc13-4 is a GTP-Rab27-binding protein regulating dense core granule secretion in platelets. *J. Biol. Chem.,* **279**, 10730-7.

Shrimpton, C. N., Borthakur, G., Larrucea, S., Cruz, M. A., Dong, J. F. & Lopez, J. A. (2002). Localization of the adhesion receptor glycoprotein Ib-IX-V complex to lipid rafts is required for platelet adhesion and activation. *J. Exp. Med.,* **196**, 1057-66.

Si, D., Wang, Y., Zhou, Y. H., Guo, Y., Wang, J., Zhou, H., Li, Z. S. & Fawcett, J. P. (2009). Mechanism of CYP2C9 inhibition by flavones and flavonols. *Drug Metab. Dispos.,* **37**, 629-34.

Siljander, P. R.-M., Hamaia, S., Peachey, A. R., Slatter, D. A., Smethurst, P. A., Ouwehand, W. H., Knight, C. G. & Farndale, R. W. (2004). Integrin Activation State Determines Selectivity for Novel Recognition Sites in Fibrillar Collagens. *J. Biol. Chem.,* **279**, 47763-47772.

Sim, X., Poncz, M., Gadue, P. & French, D. L. (2016). Understanding platelet generation from megakaryocytes: implications for in vitro–derived platelets. *Blood,* **127**, 1227-1233.

Simmonds, M. S. & Stevenson, P. C. (2001). Effects of isoflavonoids from Cicer on larvae of Heliocoverpa armigera. *J. Chem. Ecol.,* **27**, 965-977.

Sims, P. J., Faioni, E. M., Wiedmer, T. & Shattil, S. J. (1988). Complement proteins C5b-9 cause release of membrane vesicles from the platelet surface that are enriched in the membrane receptor for coagulation factor Va and express prothrombinase activity. *J. Biol. Chem.,* **263**, 18205-12.

Sinauridze, E. I., Kireev, D. A., Popenko, N. Y., Pichugin, A. V., Panteleev, M. A., Krymskaya, O. V. & Ataullakhanov, F. I. (2007). Platelet microparticle membranes have 50- to 100-fold higher specific procoagulant activity than activated platelets. *Thromb. Haemost.,* **97**, 425-34.

Smethurst, P. A., Onley, D. J., Jarvis, G. E., O'Connor, M. N., Knight, C. G., Herr, A. B., Ouwehand, W. H. & Farndale, R. W. (2007). Structural basis for the platelet-collagen interaction. The smallest motif within collagen that recognizes and activates platelet glycoprotein VI contains two Glycine-Proline-Hydroxyproline triplets. *J. Biol. Chem.,* **282**, 1296-1304.

Smith, S. K. & Limbird, L. E. (1981). Solubilization of human platelet alpha-adrenergic receptors: evidence that agonist occupancy of the receptor stabilizes receptor--effector interactions. *Proc. Natl. Acad. Sci.,* **78**, 4026-4030.

Smolenski, A. (2012). Novel roles of cAMP/cGMP-dependent signaling in platelets. *J. Thromb. Haemost.,* **10**, 167-76.

Sollner, T., Whiteheart, S. W., Brunner, M., Erdjument-Bromage, H., Geromanos, S., Tempst, P. & Rothman, J. E. (1993). SNAP receptors implicated in vesicle targeting and fusion. *Nature,* **362**, 318-24.

Sondek, J., Bohm, A., Lambright, D. G., Hamm, H. E. & Sigler, P. B. (1996). Crystal structure of a G-protein beta gamma dimer at 2.1A resolution. *Nature,* **379**, 369-74.

Spalton, J. C., Mori, J., Pollitt, A. Y., Hughes, C. E., Eble, J. A. & Watson, S. P. (2009). The novel Syk inhibitor R406 reveals mechanistic differences in the initiation of GPVI and CLEC-2 signaling in platelets. *J. Thromb. Haemost.,* **7**, 1192-9.

Srivastava, P. (2010). Optimization of antiplatelet/antithrombotic therapy for secondary stroke prevention. *Ann. Indian Acad. Neurol.,* **13**, 6-13.

Srivastava, R. K., Tang, S.-N., Zhu, W., Meeker, D. & Shankar, S. (2011). Sulforaphane synergizes with quercetin to inhibit self-renewal capacity of pancreatic cancer stem cells. *Front. Biosci. (Elite Ed.),* **3**, 515-528.

Srivastava, S., Somasagara, R. R., Hegde, M., Nishana, M., Tadi, S. K., Srivastava, M., Choudhary, B. & Raghavan, S. C. (2016). Quercetin, a Natural Flavonoid Interacts with DNA, Arrests Cell Cycle and Causes Tumor Regression by Activating Mitochondrial Pathway of Apoptosis. *Sci. Rep.,* **6**, 24049.

Stahlhut, S. G., Siedler, S., Malla, S., Harrison, S. J., Maury, J., Neves, A. R. & Forster, J. (2015). Assembly of a novel biosynthetic pathway for production of the plant flavonoid fisetin in Escherichia coli. *Metab. Eng.,* **31**, 84-93.

Stalker, T. J., Wu, J., Morgans, A., Traxler, E. A., Wang, L., Chatterjee, M. S., Lee, D., Quertermous, T., Hall, R. A., Hammer, D. A., Diamond, S. L. & Brass, L. F. (2009). Endothelial cell specific adhesion molecule (ESAM) localizes to platelet–platelet contacts and regulates thrombus formation in vivo. *J. Thromb. Haemost.,* **7**, 1886-1896.

Stathopulos, P. B., Zheng, L., Li, G. Y., Plevin, M. J. & Ikura, M. (2008). Structural and mechanistic insights into STIM1-mediated initiation of store-operated calcium entry. *Cell,* **135**, 110-22.

Steen, V. M., Holmsen, H. & Aarbakke, G. (1993). The platelet-stimulating effect of adrenaline through alpha 2-adrenergic receptors requires simultaneous activation by a true stimulatory platelet agonist. Evidence that adrenaline per se does not induce human platelet activation in vitro. *Thromb. Haemost.,* **70**, 506-13.

Stefanini, L. & Bergmeier, W. (2010). CalDAG-GEFI and platelet activation. *Platelets,* **21**, 239-243.

Stefanini, L., Roden, R. C. & Bergmeier, W. (2009). CalDAG-GEFI is at the nexus of calcium-dependent platelet activation. *Blood,* **114**, 2506-14.

Stenberg, P. E., Shuman, M. A., Levine, S. P. & Bainton, D. F. (1984). Redistribution of alpha-granules and their contents in thrombin-stimulated platelets. *J. Cell. Biol.,* **98**, 748-760.

Stopa, J. D., Neuberg, D., Puligandla, M., Furie, B., Flaumenhaft, R. & Zwicker, J. I. (2017). Protein disulfide isomerase inhibition blocks thrombin generation in humans by interfering with platelet factor V activation. *JCI Insight,* **2**, e89373.

Stramentinoli, G., Gualano, M., Algeri, S., de Gaetano, G. & Rossi, E. C. (1978). Catechol-o-methyl transferase (COMT) in human and rat platelets. *Thromb. Haemost.,* **39**, 238-9.

Stritt, S., Wolf, K., Lorenz, V., Vögtle, T., Gupta, S., Bösl, M. R. & Nieswandt, B. (2014). Rap1-GTP-interacting adaptor molecule (RIAM) is dispensable for platelet integrin activation and function in mice. *Blood*.

Strony, J., Beaudoin, A., Brands, D. & Adelman, B. (1993). Analysis of shear stress and hemodynamic factors in a model of coronary artery stenosis and thrombosis. *Am. J. Physiol.,* **265**, H1787-1796.

Stuart, M. J., Murphy, S. & Oski, F. A. (1975). A Simple Nonradioisotope Technic for the Determination of Platelet Life-Span. *N. Engl. J. Med.,* **292**, 1310-1313.

Subramanian, H., Walter, U. & Gambaryan, S. (2013). Differential regulation of platelet inhibition by cGMP- and cAMP-dependent protein kinases. *BMC Pharmacol. Toxicol.,* **14**, P69.

Sudhof, T. C. & Rothman, J. E. (2009). Membrane fusion: grappling with SNARE and SM proteins. *Science,* **323**, 474-7.

Sun, J., Williams, J., Yan, H. C., Amin, K. M., Albelda, S. M. & DeLisser, H. M. (1996a). Platelet endothelial cell adhesion molecule-1 (PECAM-1) homophilic adhesion is mediated by immunoglobulin-like domains 1 and 2 and depends on the cytoplasmic domain and the level of surface expression. *J. Biol. Chem.,* **271**, 18561-70.

Sun, Q. H., DeLisser, H. M., Zukowski, M. M., Paddock, C., Albelda, S. M. & Newman, P. J. (1996b). Individually distinct Ig homology domains in PECAM-1 regulate homophilic binding and modulate receptor affinity. *J. Biol. Chem.,* **271**, 11090-8.

Suzuki-Inoue, K., Hughes, C. E., Inoue, O., Kaneko, M., Cuyun-Lira, O., Takafuta, T., Watson, S. P. & Ozaki, Y. (2007). Involvement of Src kinases and PLCgamma2 in clot retraction. *Thromb. Res.,* **120**, 251-8.

Suzuki-Inoue, K., Yatomi, Y., Asazuma, N., Kainoh, M., Tanaka, T., Satoh, K. & Ozaki, Y. (2001). Rac, a small guanosine triphosphate-binding protein, and p21-activated kinase are activated during platelet spreading on collagen-coated surfaces: roles of integrin alpha(2)beta(1). *Blood,* **98**, 3708-16.

Tabashnik, B. E. (1987). Plant secondary compounds as oviposition deterrents for cabbage butterfly, Pieris rapae (Lepidoptera: Pieridae). *J. Chem. Ecol.,* **13**, 309-316.

Takagi, J., Petre, B. M., Walz, T. & Springer, T. A. (2002). Global conformational rearrangements in integrin extracellular domains in outside-in and inside-out signaling. *Cell,* **110**, 599-11.

Takahama, U., Hirota, S., Nishioka, T. & Yoshitama, K. (2002). Oxidation of quercetin by salivary components I. Salivary peroxidase-dependent oxidation of quercetin and characterization of the oxidation products. *Food Sci. Technol. Res.,* **8**, 148-153.

Tallarida, R. J. (2011). Quantitative Methods for Assessing Drug Synergism. *Genes Cancer,* **2**, 1003-1008.

Tamura, T., Mitsumori, K., Muto, S., Kasahara, H., Kobayashi, S., Okuhara, Y., Hayashi, M., Nagasawa, T., Onozato, T. & Kuroda, J. (2010). Fifty-two week chronic toxicity of enzymatically decomposed rutin in Wistar rats. *Food Chem. Toxicol.,* **48**, 2312-8.

Tapas, A. R., Sakarkar, D. & Kakde, R. (2008). Flavonoids as nutraceuticals: a review. *Trop. J. Pharm. Res.,* **7**, 1089-1099.

Tattini, M., Galardi, C., Pinelli, P., Massai, R., Remorini, D. & Agati, G. (2004). Differential accumulation of flavonoids and hydroxycinnamates in leaves of Ligustrum vulgare under excess light and drought stress. *New Phytol.,* **163**, 547-561.

Taussig, R., Iniguez-Lluhi, J. A. & Gilman, A. G. (1993). Inhibition of adenylyl cyclase by Gi alpha. *Science,* **261**, 218-21.

Taylor, M. J., Carney, S. M., Goodwin, G. M. & Geddes, J. R. (2004). Folate for depressive disorders: systematic review and meta-analysis of randomized controlled trials. *J. Psycho. Pharmacol.,* **18**, 251-6.

Tazawa, R., Green, E. D., Ohashi, K., Wu, K. K. & Wang, L.-H. (1996). Characterization of the Complete Genomic Structure of Human Thromboxane Synthase Gene and Functional Analysis of Its Promoter. *Arch. Biochem. Biophys.,* **334**, 349-356.

Testa, L., Biondi Zoccai, G. G. L., Valgimigli, M., Latini, R. A., Pizzocri, S., Lanotte, S., Laudisa, M. L., Brambilla, N., Ward, M. R., Figtree, G. A., Bedogni, F. & Bhindi, R. (2010). Current Concepts on Antiplatelet Therapy: Focus on the Novel Thienopyridine and Non-Thienopyridine Agents. *Adv. Hematol.,* **2010**, 595934.

Thilakarathna, S. H. & Rupasinghe, H. P. V. (2013). Flavonoid Bioavailability and Attempts for Bioavailability Enhancement. *Nutrients,* **5**, 3367-3387.

Thomas, D. W., Mannon, R. B., Mannon, P. J., Latour, A., Oliver, J. A., Hoffman, M., Smithies, O., Koller, B. H. & Coffman, T. M. (1998). Coagulation defects and altered hemodynamic responses in mice lacking receptors for thromboxane A2. *J. Clin. Invest.,* **102**, 1994-2001.

Thon, J. N., Montalvo, A., Patel-Hett, S., Devine, M. T., Richardson, J. L., Ehrlicher, A., Larson, M. K., Hoffmeister, K., Hartwig, J. H. & Italiano, J. E. (2010). Cytoskeletal mechanics of proplatelet maturation and platelet release. *J. Cell Biol.,* **191**, 861-874.

Tolhurst, G., Carter, R. N., Amisten, S., Holdich, J. P., Erlinge, D. & Mahaut-Smith, M. P. (2008). Expression profiling and electrophysiological studies suggest a major role for Orai1 in the store-operated Ca2+ influx pathway of platelets and megakaryocytes. *Platelets,* **19**, 308-13.

Topol, E. J. & Califf, R. M. (2007). *Textbook of Cardiovascular Medicine.* Philadelphia, USA: Lippincott Williams & Wilkins.

Townsend, N., Bhatnagar, P., Wilkins, E. & Wickramasinghe, K. (2015). Cardiovascular disease statistics 2015. *In:* Dicks, E. (ed.) *Cardiovascular disease statistics.* London: British Heart Foundation.

Treutter, D. (2005). Significance of flavonoids in plant resistance and enhancement of their biosynthesis. *Plant Biol. (Stuttg.),* **7**, 581-91.

Tsimogiannis, D., Samiotaki, M., Panayotou, G. & Oreopoulou, V. (2007). Characterization of flavonoid subgroups and hydroxy substitution by HPLC-MS/MS. *Molecules,* **12**, 593-606.

Tucker, K. L., Sage, T. & Gibbins, J. M. (2012). Clot retraction. *Methods Mol. Biol.,* **788**, 101-7.

Ueno, I., Nakano, N. & Hirono, I. (1983). Metabolic fate of [14C] quercetin in the ACI rat. *Jpn. J. Exp. Med.,* **53**, 41-50.

Ulmer, T. S., Calderwood, D. A., Ginsberg, M. H. & Campbell, I. D. (2003). Domain-specific interactions of talin with the membrane-proximal region of the integrin beta3 subunit. *Biochemistry,* **42**, 8307-12.

Unsworth, A. J., Flora, G. D., Sasikumar, P., Bye, A. P., Sage, T., Kriek, N., Crescente, M. & Gibbins, J. M. (2017a). RXR Ligands Negatively Regulate Thrombosis and Hemostasis. *Arterioscler. Thromb. Vasc. Biol.,* **37**, 812-822.

Unsworth, A. J., Kriek, N., Bye, A. P., Naran, K., Sage, T., Flora, G. D. & Gibbins, J. M. (2017b). PPARγ agonists negatively regulate αIIbβ3 integrin outside-in signaling and platelet function through up-regulation of protein kinase A activity. *J. Thromb. Haemost.,* **15**, 356-369.

Vaiyapuri, S., Ali, M. S., Moraes, L. A., Sage, T., Lewis, K. R., Jones, C. I. & Gibbins, J. M. (2013). Tangeretin Regulates Platelet Function Through Inhibition of Phosphoinositide 3-Kinase and Cyclic Nucleotide Signaling. *Arterioscler. Thromb. Vasc. Biol.,* **33**, 2740-2749.

van Duynhoven, J., Vaughan, E. E., Jacobs, D. M., Kemperman, R. A., van Velzen, E. J., Gross, G., Roger, L. C., Possemiers, S., Smilde, A. K., Dore, J., Westerhuis, J. A. & Van de Wiele, T. (2011). Metabolic fate of polyphenols in the human superorganism. *Proc. Natl. Acad. Sci. U. S. A.,* **108 Suppl 1**, 4531-8.

Varga-Szabo, D., Braun, A. & Nieswandt, B. (2009). Calcium signaling in platelets. *J. Thromb. Haemost.,* **7**, 1057-1066.

Varga-Szabo, D., Pleines, I. & Nieswandt, B. (2008). Cell adhesion mechanisms in platelets. *Arterioscler. Thromb. Vasc. Biol.,* **28**, 403-12.

Vemana, H. P., Karim, Z. A., Conlon, C. & Khasawneh, F. T. (2015). A critical role for the transient receptor potential channel type 6 in human platelet activation. *PLoS One,* **10**, e0125764.

Verrall, S., Ishii, M., Chen, M., Wang, L., Tram, T. & Coughlin, S. R. (1997). The thrombin receptor second cytoplasmic loop confers coupling to Gq-like G proteins in chimeric receptors. Additional evidence for a common transmembrane signaling and G protein coupling mechanism in G protein-coupled receptors. *J. Biol. Chem.,* **272**, 6898-902.

Vial, C., Hechler, B., Leon, C., Cazenave, J. & Gachet, C. (1997). Presence of P2X1 purinoceptors in human platelets and megakaryoblastic cell lines. *Thromb. Haemost.,* **78**, 1500-1504.

Vig, M., Peinelt, C., Beck, A., Koomoa, D. L., Rabah, D., Koblan-Huberson, M., Kraft, S., Turner, H., Fleig, A., Penner, R. & Kinet, J. P. (2006). CRACM1 is a plasma membrane protein essential for store-operated Ca2+ entry. *Science,* **312**, 1220-3.

Villa, A. D. M., Sammut, E., Nair, A., Rajani, R., Bonamini, R. & Chiribiri, A. (2016). Coronary artery anomalies overview: The normal and the abnormal. *World J. Radiol.,* **8**, 537-555.

Vlahos, C. J., Matter, W. F., Hui, K. Y. & Brown, R. F. (1994). A specific inhibitor of phosphatidylinositol 3-kinase, 2-(4-morpholinyl)-8-phenyl-4H-1-benzopyran-4-one (LY294002). *J. Biol. Chem.,* **269**, 5241-8.

Vu, T.-K. H., Hung, D. T., Wheaton, V. I. & Coughlin, S. R. (1991). Molecular cloning of a functional thrombin receptor reveals a novel proteolytic mechanism of receptor activation. *Cell,* **64**, 1057-1068.

Vulpetti, A. & Bosotti, R. (2004). Sequence and structural analysis of kinase ATP pocket residues. *Farmaco.,* **59**, 759-65.

Wagner, C. L., Mascelli, M. A., Neblock, D. S., Weisman, H. F., Coller, B. S. & Jordan, R. E. (1996). Analysis of GPIIb/IIIa receptor number by quantification of 7E3 binding to human platelets. *Blood,* **88**, 907-14.

Walgren, R. A., Karnaky, K. J., Lindenmayer, G. E. & Walle, T. (2000). Efflux of dietary flavonoid quercetin 4′-β-glucoside across human intestinal Caco-2 cell monolayers by apical multidrug resistance-associated protein-2. *J. Pharmacol. Exp. Ther.,* **294**, 830-836.

Walker, E.H., Pacold, M.E., Perisic, O., Stephens, L., Hawkins, P.T., Wymann, M.P. & Williams, R.L. (2000). Structural determinants of phosphoinositide 3-kinase inhibition by wortmannin, LY294002, quercetin, myricetin, and staurosporine. *Mol. Cell,* **6**, 909-19.

Wall, M. E., Francis, S. H., Corbin, J. D., Grimes, K., Richie-Jannetta, R., Kotera, J., Macdonald, B. A., Gibson, R. R. & Trewhella, J. (2003). Mechanisms associated with cGMP binding and activation of cGMP-dependent protein kinase. *Proc. Natl. Acad. Sci.,* **100**, 2380-2385.

Walle, T. (2004). Absorption and metabolism of flavonoids. *Free Radic. Biol. Med.,* **36**, 829-37.

Walle, T., Walle, U. K. & Halushka, P. V. (2001). Carbon dioxide is the major metabolite of quercetin in humans. *J. Nutr.,* **131**, 2648-2652.

Wang, X., Ouyang, Y. Y., Liu, J. & Zhao, G. (2014a). Flavonoid intake and risk of CVD: a systematic review and meta-analysis of prospective cohort studies. *Br. J. Nutr.,* **111**, 1-11.

Wang, X., Schröder, H. C., Feng, Q., Diehl-Seifert, B., Grebenjuk, V. A. & Müller, W. E. G. (2014b). Isoquercitrin and polyphosphate co-enhance mineralization of human osteoblast-like SaOS-2 cells via separate activation of two RUNX2 cofactors AFT6 and Ets1. *Biochem. Pharmacol.,* **89**, 413-421.

Wang, Z. & Cole, P.A. (2014). Catalytic mechanisms and regulation of protein kinases. *Methods Enzymol.,* **548**, 1-21.

Wang, Z.-M., Nie, Z.-L., Zhou, B., Lian, X.-Q., Zhao, H., Gao, W., Wang, Y.-S., Jia, E.-Z., Wang, L.-S. & Yang, Z.-J. (2012a). Flavonols intake and the risk of coronary heart disease: a meta-analysis of cohort studies. *Atherosclerosis,* **222**, 270-273.

Wang, Z. M., Zhou, B., Nie, Z. L., Gao, W., Wang, Y. S., Zhao, H., Zhu, J., Yan, J. J., Yang, Z. J. & Wang, L. S. (2012b). Folate and risk of coronary heart disease: A meta-analysis of prospective studies. *Nutr. Metab. Cardiovasc. Dis.,* **22**, 890-899.

Ware, J. A., Johnson, P. C., Smith, M. & Salzman, E. W. (1986). Effect of common agonists on cytoplasmic ionized calcium concentration in platelets. Measurement with 2-methyl-6-methoxy 8-nitroquinoline (quin2) and aequorin. *J. Clin. Invest.,* **77**, 878-86.

Wasilewski, J., Niedziela, J., Osadnik, T., Duszańska, A., Sraga, W., Desperak, P., Myga-Porosiło, J., Jackowska, Z., Nowakowski, A. & Głowacki, J. (2015). Predominant location of coronary artery atherosclerosis in the left anterior descending artery. The impact of septal perforators and the myocardial bridging effect. *Polish Journal of Cardio-Thoracic Surgery,* **12**, 379-385.

Watson, S. P., Auger, J. M., McCarty, O. J. & Pearce, A. C. (2005). GPVI and integrin alphaIIb beta3 signaling in platelets. *J. Thromb. Haemost.,* **3**, 1752-62.

Webster, G., Jain, V., Davey, M., Gough, C., Vasse, J., Denarie, J. & Cocking, E. (1998). The flavonoid naringenin stimulates the intercellular colonization of wheat roots by Azorhizobium caulinodans. *Plant Cell Environ.,* **21**, 373-383.

Weidenbörner, M. & Jha, H. (1993). Antifungal activity of flavonoids in relation to degree of hydroxylation, methoxylation and glycosidation. *In:* International Symposium on Natural Phenols in Plant Resistance 381, Weihenstephan, Germany. 702-709.

Weisshaar, B. & Jenkins, G. I. (1998). Phenylpropanoid biosynthesis and its regulation. *Curr. Opin. Plant Biol.,* **1**, 251-257.

Weljie, A. M., Hwang, P. M. & Vogel, H. J. (2002). Solution structures of the cytoplasmic tail complex from platelet integrin αIIb-and β3-subunits. *Proc. Natl. Acad. Sci.,* **99**, 5878-5883.

Wencel-Drake, J. D., Plow, E. F., Kunicki, T. J., Woods, V. L., Keller, D. M. & Ginsberg, M. H. (1986). Localization of internal pools of membrane glycoproteins involved in platelet adhesive responses. *Am. J. Pathol.,* **124**, 324-34.

Weston, L. A. & Mathesius, U. (2013). Flavonoids: their structure, biosynthesis and role in the rhizosphere, including allelopathy. *J. Chem. Ecol.,* **39**, 283-297.

White, J. G. (1972). Interaction of Membrane Systems in Blood Platelets. *Am. J. Pathol.,* **66**, 295-312.

Wiley, J. S., Kuchibhotla, J., Shaller, C. C. & Colman, R. W. (1976). Potassium uptake and release by human blood platelets. *Blood,* **48**, 185-97.

Williams, C. A. & Grayer, R. J. (2004). Anthocyanins and other flavonoids. *Nat. Prod. Rep.,* **21**, 539-573.

Williamson, D., Pikovski, I., Cranmer, S. L., Mangin, P., Mistry, N., Domagala, T., Chehab, S., Lanza, F., Salem, H. H. & Jackson, S. P. (2002). Interaction between Platelet Glycoprotein Ibα and Filamin-1 Is Essential for Glycoprotein Ib/IX Receptor Anchorage at High Shear. *J. Biol. Chem.,* **277**, 2151-2159.

Williamson, E. M. (2001). Synergy and other interactions in phytomedicines. *Phytomedicine,* **8**, 401-409.

Williamson, G., Day, A., Plumb, G. & Couteau, D. (2000). *Human metabolic pathways of dietary flavonoids and cinnamates.* London, England: Portland Press Limited.

Wilson, R. D., Johnson, J. A., Wyatt, P., Allen, V., Gagnon, A., Langlois, S., Blight, C., Audibert, F., Desilets, V., Brock, J. A., Koren, G., Goh, Y. I., Nguyen, P. & Kapur, B. (2007). Pre-conceptional vitamin/folic acid supplementation 2007: the use of folic acid in combination with a multivitamin supplement for the prevention of neural tube defects and other congenital anomalies. *J. Obstet. Gynaecol. Can.,* **29**, 1003-26.

Wolffram, S., Blöck, M. & Ader, P. (2002). Quercetin-3-glucoside is transported by the glucose carrier SGLT1 across the brush border membrane of rat small intestine. *J. Nutr.,* **132**, 630-635.

Wong, C., Liu, Y., Yip, J., Chand, R., Wee, J. L., Oates, L., Nieswandt, B., Reheman, A., Ni, H., Beauchemin, N. & Jackson, D. E. (2009). CEACAM1 negatively regulates platelet-collagen interactions and thrombus growth in vitro and in vivo. *Blood,* **113**, 1818-28.

Wong, Y. H., Conklin, B. R. & Bourne, H. R. (1992). Gz-mediated hormonal inhibition of cyclic AMP accumulation. *Science,* **255**, 339-42.

Woodside, D. G., Obergfell, A., Leng, L., Wilsbacher, J. L., Miranti, C. K., Brugge, J. S., Shattil, S. J. & Ginsberg, M. H. (2001). Activation of Syk protein tyrosine kinase through interaction with integrin beta cytoplasmic domains. *Curr. Biol.,* **11**, 1799-804.

Woronowicz, K., Dilks, J. R., Rozenvayn, N., Dowal, L., Blair, P. S., Peters, C. G., Woronowicz, L. & Flaumenhaft, R. (2010). The Platelet Actin Cytoskeleton Associates with SNAREs and Participates in α-Granule Secretion. *Biochemistry,* **49**, 4533-4542.

Woulfe, D., Jiang, H., Mortensen, R., Yang, J. & Brass, L. F. (2002). Activation of Rap1B by G(i) family members in platelets. *J. Biol. Chem.,* **277**, 23382-90.

Woulfe, D. S. (2005). Platelet G protein-coupled receptors in hemostasis and thrombosis. *J. Thromb. Haemost.,* **3**, 2193-2200.

Wright, B., Gibson, T., Spencer, J., Lovegrove, J. A. & Gibbins, J. M. (2010a). Platelet-Mediated Metabolism of the Common Dietary Flavonoid, Quercetin. *PLoS One,* **5**, e9673.

Wright, B., Moraes, L. A., Kemp, C. F., Mullen, W., Crozier, A., Lovegrove, J. A. & Gibbins, J. M. (2010b). A structural basis for the inhibition of collagen-stimulated platelet function by quercetin and structurally related flavonoids. *Br. J. Pharmacol.,* **159**, 1312-1325.

Wright, B., Spencer, J. P. E., Lovegrove, J. A. & Gibbins, J. M. (2013). Flavonoid inhibitory pharmacodynamics on platelet function in physiological environments. *Food Funct.,* **4**, 1803-1810.

Wright, B., Watson, K. A., McGuffin, L. J., Lovegrove, J. A. & Gibbins, J. M. (2015). GRID and docking analyses reveal a molecular basis for flavonoid inhibition of Src family kinase activity. *J. Nutr. Biochem.,* **26**, 1156-1165.

Wu, B., Kulkarni, K., Basu, S., Zhang, S. & Hu, M. (2011). First-pass metabolism via UDP-glucuronosyltransferase: a barrier to oral bioavailability of phenolics. *J. Pharm. Sci.,* **100**, 3655-3681.

Wu, T., Zang, X., He, M., Pan, S. & Xu, X. (2013). Structure–activity relationship of flavonoids on their anti-Escherichia coli activity and inhibition of DNA gyrase. *J. Agric. Food Chem.,* **61**, 8185-8190.

Wu, W., Li, R., Li, X., He, J., Jiang, S., Liu, S. & Yang, J. (2016). Quercetin as an Antiviral Agent Inhibits Influenza A Virus (IAV) Entry. *Viruses,* **8**, E6.

Wu, Y., Asazuma, N., Satoh, K., Yatomi, Y., Takafuta, T., Berndt, M. C. & Ozaki, Y. (2003). Interaction between von Willebrand factor and glycoprotein Ib activates Src kinase in human platelets: role of phosphoinositide 3-kinase. *Blood,* **101**, 3469-76.

Wu, Y., Suzuki-Inoue, K., Satoh, K., Asazuma, N., Yatomi, Y., Berndt, M. C. & Ozaki, Y. (2001). Role of Fc receptor gamma-chain in platelet glycoprotein Ib-mediated signaling. *Blood,* **97**, 3836-45.

Xi, J. & Guo, R. (2007). Interactions between flavonoids and hemoglobin in lecithin liposomes. *Int. J. Biol. Macromol.,* **40**, 305-11.

Xiao, J., Cao, H., Wang, Y., Zhao, J. & Wei, X. (2009). Glycosylation of dietary flavonoids decreases the affinities for plasma protein. *J. Agric. Food Chem.,* **57**, 6642-8.

Xu, W.-f., Andersen, H., Whitmore, T. E., Presnell, S. R., Yee, D. P., Ching, A., Gilbert, T., Davie, E. W. & Foster, D. C. (1998). Cloning and characterization of human protease-activated receptor 4. *Proc. Natl. Acad. Sci.,* **95**, 6642-6646.

Xu, Z., Chen, N., Kamocka, M. M., Rosen, E. D. & Alber, M. (2008). A multiscale model of thrombus development. *J. R. Soc. Interface,* **5**, 705-722.

Xu, Z., Chen, N., Shadden, S. C., Marsden, J. E., Kamocka, M. M., Rosen, E. D. & Alber, M. (2009). Study of blood flow impact on growth of thrombi using a multiscale model. *Soft Matter,* **5**, 769-779.

Xu, Z., Kamocka, M., Alber, M. & Rosen, E. D. (2011). Computational approaches to studying thrombus development. *Arterioscler. Thromb. Vasc. Biol.,* **31**, 500-5.

Xu, Z., Lioi, J., Mu, J., Kamocka, M. M., Liu, X., Chen, D. Z., Rosen, E. D. & Alber, M. (2010). A multiscale model of venous thrombus formation with surface-mediated control of blood coagulation cascade. *Biophys. J.,* **98**, 1723-1732.

Yacoub, D., Théorêt, J.-F., Villeneuve, L., Abou-Saleh, H., Mourad, W., Allen, B. G. & Merhi, Y. (2006). Essential role of protein kinase Cδ in platelet signaling, αIIbβ3 activation, and thromboxane A2 release. *J. Biol. Chem.,* **281**, 30024-30035.

Yan, B., Calderwood, D. A., Yaspan, B. & Ginsberg, M. H. (2001). Calpain cleavage promotes talin binding to the beta 3 integrin cytoplasmic domain. *J. Biol. Chem.,* **276**, 28164-70.

Yang, J., Wu, J., Jiang, H., Mortensen, R., Austin, S., Manning, D. R., Woulfe, D. & Brass, L. F. (2002). Signaling through Gi family members in platelets. Redundancy and specificity in the regulation of adenylyl cyclase and other effectors. *J. Biol. Chem.,* **277**, 46035-42.

Yang, J., Wu, J., Kowalska, M. A., Dalvi, A., Prevost, N., O'Brien, P. J., Manning, D., Poncz, M., Lucki, I., Blendy, J. A. & Brass, L. F. (2000). Loss of signaling through the G protein, Gz, results in abnormal platelet activation and altered responses to psychoactive drugs. *Proc. Natl. Acad. Sci. U. S. A.,* **97**, 9984-9.

Yang, M., Collis, C. S., Kelly, M., Diplock, A. T. & Rice-Evans, C. (1999). Do iron and vitamin C co-supplementation influence platelet function or LDL oxidizability in healthy volunteers? *Eur. J. Clin. Nutr.,* **53**, 367-74.

Yu, P. X., Zhou, Q. J., Zhu, W. W., Wu, Y. H., Wu, L. C., Lin, X., Chen, M. H. & Qiu, B. T. (2013). Effects of quercetin on LPS-induced disseminated intravascular coagulation (DIC) in rabbits. *Thromb. Res.,* **131**, e270-3.

Yun, H. Y., Kang, W., Lee, B. Y., Park, S., Yoon, Y. R., Yeul Ma, J. & Kwon, K. I. (2014). Semi-mechanistic modelling and simulation of inhibition of platelet aggregation by antiplatelet agents. *Basic Clin. Pharmacol. Toxicol.,* **115**, 352-9.

Zappia, V., Panico, S., Russo, G.L., Budillon, A. & Ragione F.D. (2013). Advances in Nutrition and Cancer (Volume 159 of Cancer Treatmenr and Research). Berlin: Springer Science & Business Media, pp. 195.

Zhang, L., Orban, M., Lorenz, M., Barocke, V., Braun, D., Urtz, N., Schulz, C., von Bruhl, M. L., Tirniceriu, A., Gaertner, F., Proia, R. L., Graf, T., Bolz, S. S., Montanez, E., Prinz, M., Muller, A., von Baumgarten, L., Billich, A., Sixt, M., Fassler, R., von Andrian, U. H., Junt, T. & Massberg, S. (2012). A novel role of sphingosine 1-phosphate receptor S1pr1 in mouse thrombopoiesis. *J. Exp. Med.,* **209**, 2165-81.

Zhang, L. R., Xu, D. S., Liu, X. C., Wu, X. S., Ying, Y. N., Dong, Z., Sun, F. W., Yang, P. P. & Li, X. (2011a). Coronary artery lumen diameter and bifurcation angle derived from CT

coronary angiographic image in healthy people. *Chinese Journal of Cardiovascular Diseases,* **39**, 1117-23.

Zhang, M., Swarts, S. G., Yin, L., Liu, C., Tian, Y., Cao, Y., Swarts, M., Yang, S., Zhang, S. B., Zhang, K., Ju, S., Olek, D. J., Jr., Schwartz, L., Keng, P. C., Howell, R., Zhang, L. & Okunieff, P. (2011b). Antioxidant properties of quercetin. *Adv. Exp. Med. Biol.,* **701**, 283-9.

Zhang, S. L., Yu, Y., Roos, J., Kozak, J. A., Deerinck, T. J., Ellisman, M. H., Stauderman, K. A. & Cahalan, M. D. (2005). STIM1 is a Ca2+ sensor that activates CRAC channels and migrates from the Ca2+ store to the plasma membrane. *Nature,* **437**, 902-905.

Zharikov, S. & Shiva, S. (2013). Platelet mitochondrial function: from regulation of thrombosis to biomarker of disease. *Biochem. Soc. Trans.,* **41**, 118-23.

Zheng, S. Y., Li, Y., Jiang, D., Zhao, J. & Ge, J. F. (2012). Anticancer effect and apoptosis induction by quercetin in the human lung cancer cell line A-549. *Mol Med Rep,* **5**, 822-6.

Zhou, J., Fang, L., Liao, J., Li, L., Yao, W., Xiong, Z. & Zhou, X. (2017). Investigation of the anti-cancer effect of quercetin on HepG2 cells in vivo. *PLoS One,* **12**, e0172838.

Zimmet, J. & Ravid, K. (2000). Polyploidy: occurrence in nature, mechanisms, and significance for the megakaryocyte-platelet system. *Exp. Hematol.,* **28**, 3-16.

Zubair, M. H., Zubair, M. H., Zubair, M. N., Zubair, M. M., Aftab, T. & Asad, F. (2011). Augmentation of anti-platelet effects of aspirin. *J. Pak. Med. Assoc.,* **61**, 304-7.